Land Use/ Land Cover Change and Urban Growth Modelling Using Geo-spatial Techniques and Cellular Automata

Ph.D. Thesis

by

Ankita Saxena

(2015RCE9020)

DEPARTMENT OF CIVIL ENGINEERING
MALAVIYA NATIONAL INSTITUTE OF TECHNOLOGY
JAIPUR JLN MARG, JAIPUR-302017 (INDIA)

JANUARY, 2019

Land Use/ Land Cover Change and Urban Growth Modelling Using Geo-spatial Techniques and Cellular Automata

Submitted in
fulfillment of the requirements for the degree of

Doctor of Philosophy

by

Ankita Saxena
(2015RCE9020)

Under Supervision of

Prof. Mahesh Kumar Jat

DEPARTMENT OF CIVIL ENGINEERING
MALAVIYA NATIONAL INSTITUTE OF TECHNOLOGY
JAIPUR JLN MARG, JAIPUR-302017 (INDIA)

JANUARY, 2019

This thesis is dedicated to my parents...

DECLARATION

I, **Ankita Saxena,** declare that this Ph.D. thesis entitled **"Land Use/ Land Cover Change and Urban Growth Modelling Using Geo-spatial Techniques and Cellular Automata"** and the work presented in it, are my own. I further declare that:

- This work has been done while in candidature for Ph.D. degree at MNIT Jaipur.
- Where I have consulted the published work of others, the same has been clearly attributed.
- Where I have quoted from the work of others, the source has been given, with the exception of such quotations; this thesis is entirely my own work.
- I have acknowledged all main sources of help.

Place: Jaipur
Date:

Ms. Ankita Saxena
2015RCE9020
Department of Civil Engineering
M.N.I.T Jaipur, India

CERTIFICATE

This is to certify that the thesis entitled **"Land Use/ Land Cover Change and Urban Growth Modelling Using Geo-spatial Techniques and Cellular Automata"** is being submitted by **Ms. Ankita Saxena (College Id: 2015RCE9020)** to the **Malaviya National Institute of Technology Jaipur** for the award of the degree of **Doctor of Philosophy** is a bonafide record of original research work carried out by her. She has worked under my guidance and supervision and has fulfilled the requirement for the submission of this thesis, which has reached the requisite standards.

The thesis embodies the original work done by her and has not been carried out earlier to the best of my knowledge and belief.

Date:

Dr. Mahesh Kumar Jat
Professor & Head
Department of Civil Engineering
MNIT Jaipur

ABSTRACT

Land use/ land cover (LULC) changes and urbanization are the natural and human-induced temporal land transformations and conversion processes, which are taking place under the influence of different natural and anthropogenic drivers. Increase in population, industrialization, migration of people from rural areas to urban areas in search of better livelihood, facilities and employment lead to urbanization. Therefore, to meet out the development needs of such an ever-increasing population in urban areas, more and more LULC conversion has to take place into urban land use class. Urban land use class can be defined as developed land (impervious /semi-impervious cover), and includes residential as well as commercial and industrial land uses that result in a developed or built landscape. LULC conversion and especially urbanization affects terrestrial ecosystems, causing ecological disturbances, habitat loss, fragmentation and interaction with other components of global change leading to many undesirable consequences. Therefore, LULC change & urban growth monitoring, assessment and modelling are very necessary and vital for optimal land use planning, generation of different developmental scenarios, a comparison of the pros & cons of different land use policy decisions, making adequate future provisions of urban services, estimation of resource requirements for development needs in different scenarios, impact assessment and identification of adaptations for adverse consequences related to climate, urban heat islands, ecological disturbances, and the hydrological cycle.

Urban growth modelling is a tool to quantify and analyze urban growth and its patterns, to better understand the dynamics of urban systems, to develop hypotheses (to be tested empirically) and to predict urban growth in different scenarios. There are a variety of approaches and methods available for the assessment, monitoring, and modelling of LULC changes and urban growth. However, Cellular Automata based approaches have been found to be promising. The CA-based SLEUTH model is a popular model, calibrated and tested extensively throughout the world, however, it has limitations and research issues which need to be further studied. Therefore, in the presented research an attempt has been made to understand the sensitivity of SLEUTH with respect to a few important model parameters/ constants. Efforts have been made to improve the SLEUTH by incorporating an additional land suitability decision rule which explains the influence of a few important urbanization drivers, in the simulation process. Also, efforts have been made to develop a

new version i.e., SLEUTH-Density which is capable of estimating the urban intensity or built-up density. Further, the performance of improved versions of the model has been tested through a demonstration of the application of the model for Ajmer urban fringes.

The present study includes GIS database creation, development of improved versions of the SLEUTH model to simulate urban growth more realistically and to estimate built-up density. The suitable GIS database at required spatial and temporal resolutions has been created to extract input parameters for parameterization of the SLEUTH model. The base version of SLEUTH with default parameter/ constant settings was conceptualized for the selected study area, successfully calibrated and urban growth was simulated for up to the year 2040. Various limitations of the model were shown, which include overestimation of urban areas at some places, inability to capture fragmented growth especially of smaller size development and different urban forms leading to lower accuracy and more false positives and negatives. Possible reasons of the lower performance of the available SLEUTH model have been identified as unsuitable values of a few model constants and parameters for which model sensitivity was not tested earlier and non-inclusion of important urbanization explanatory variables in the urban growth simulation process. To address these issues, first, model sensitivity for selected critical model constants/ parameters has been tested using an iterative procedure. The optimal values of selected constant/ parameters with respect to optimal model fitness measure (i.e. OSM), goodness of fit metrics, spatial and statistical measures and accuracy assessment are obtained as; 1.3, 0.10, 0.90, and 1.25 for *boom, bust, critical low and critical high* respectively, the *diffusive value parameter* with 0.0055, the 60 *no. of Monte Carlo runs*, a range of 15-19 for *critical slope, game of life rule* with 1 cell in neighborhood and extended Moore Neighborhood of 12 cell size. Performance has been found to be better with the optimal values of model constants/parameters obtained from the sensitivity analysis. The model currently simulated LULC changes and urban growth using only historical urban area, road, exclusions and slope in the decision making of urbanisation. In the present study, a newer version of the model i.e., SLEUTH-Suitability has been developed to include an additional land suitability decision rule in the simulation process. The land suitability decision variable layer has been developed to include the influence of few important urbanization drivers/ explanatory variables using the Analytical Hierarchy Process (AHP) method of Multi-Criteria Evaluation (MCE) techniques. Suitable method/algorithms have been developed and integrated with the existing model. Optimal weights (AHP) for the different urbanization explanatory variables were achieved from the sensitivity analysis of SLEUTH-Suitability

with respect to different combinations of weights. Optimum weights corresponding to acceptable model performance in comparison with the actual urban area have been found to as 44.7 for the slope, 5.06 for the distance from bus and railway stations, hospitals & recreational places and 20.05 for the distance from the main roads and land. The SLEUTH accuracy was found to improve from 79% in the case of base SLEUTH with default parameters to 80% (SLEUTH with optimum parameters) to 83% with SLEUTH-Suitability with respect to more than 100 randomly selected test pixels. Performance of improved versions has also been validated from the ground truthing and significant improvement in accuracy has been observed from the base SLEUTH model (56 %) to 68% for SLEUTH-Suitability.

Another version of SLEUTH i.e. SLEUTH-Density has been developed which is capable of capturing and prediction of the urban intensity or built-up density. The new algorithm has been developed and the code of the model is modified to include the density estimation algorithm. The built-up density was successfully validated with the field data and various statistical and other metrics of built-up density estimation. Performance and accuracy of built-up density estimated from SLEUTH-Density have been found to be satisfactory. The R^2 value of 0.79 has been found from the relationship between normalized simulated built-up density and observed no. of floors of built-up features and the accuracy was found to be 75%.

The present research has been found to be successful in addressing the research questions and in meeting the research objectives. The model application has been demonstrated successfully for simulating the urban growth and built-up density for a heterogeneous urban area i.e., Ajmer fringe.

Keywords: Urban Growth, Land Use/ Land Cover, SLEUTH, Cellular Automata, Geo-spatial.

ACKNOWLEDGEMENT

First of all, I would like to thank Almighty God for all the blessings. Completion of this doctoral dissertation was possible with the support of several people without their help and support, it would have been a difficult one.

I would like to express my sincere gratitude to my Supervisor Prof. Mahesh Kumar Jat for his constant support, encouragement, and guidance throughout my Ph.D. work. I truly feel that the motivation and inspiration which I have got from him cannot be expressed in words. Keeping patience during a tough time, curiosity, passion, learning ability, research motivation and keep going in life are such qualities which made a deep impact on my life and I truly appreciate that. In his guidance, the journey has been a great experience and I relished all the moments of either success or struggle.

I would like to express my sincere thanks to Prof. Keith Clarke and Dr. Kanthakumar for their help and useful suggestions during my Ph.D.

I would like to thank Prof. Mahender Choudhary and Prof. Sudhir Kumar for their critics and motivation, which helped me in many ways during my Ph.D.

I would also like to pay my sincere thanks to my DREC members, Prof. Urmila Brighu, Prof. Gunwant Sharma, Dr. Sumit Khandelwal, Dr, Sanjay Batter and Dr. Satish Pripalia for their valuable suggestions and encouragement during my Ph.D.

I would like to thank Dr. Shuchi Mala for her kind help, love, support, and togetherness during my Ph.D. Your valuable time given during my research struggle was really a great help and I heartily appreciate that.

I would like to thank Dr. Surendra Pratap Singh for his support and friendly nature which was very helpful for releasing stress sometimes.

I would like to thank Ms. Arjita Saxena for her support and help during my Ph.D. work and I also enjoyed the company in the office with you.

I would like to thank my dear friend Ms. Kusum Joshi for her motivation and your zeal to follow your dreams in life is remarkable and you inspired me in many ways.

I would like to thank my sweet friend SE Reenu Palawat for her love, care, support, and togetherness.

I would like to thank Mr. Shiv Chadha, Ms. Manisha Choudhary, Mr. Devendra Choudhary, Mr. Nitish Dholakhandi, Mr. JG Rao, Mr. Deepak Prajapat for their help and support.

I would like to thank Mr. Sachin Shekhawat for his valuable support when I was stuck at some point during my Ph.D.

I would like to thank Ms. Poonam Shekhawat and Mr. Mohit Bhandari for their support and togetherness during my Ph.D.

I would like to thank Mr. Rajendra and other non-teaching staff who helped me during my Ph.D. in many ways.

I would like to thank Mrs. Sharda Choudhary for her love, support, and care. You are just like my own family and the days spent with you have been a beautiful and memorable time during my Ph.D.

I would like to thank my two loving sweetheart Ms. Bharti and Ms. Niharika for their pure heart and love which always made me mesmerized and it was enough to make me happy even when I was ever sad.

I would like to thank Mrs. Archna Srivastava, Dr. Harish Srivastava and Mr. Umesh Sinha for their kind help and motivation.

I would like to thank Mr. Ramesh Chandra Sharma for his constant motivation during my Ph.D.

I would like to thank all in my beautiful family, my mother (Mrs. Meenu Saxena), father (Mr. Pradeep Kumar Saxena), younger brother (Mr. Swastik Saxena), elder sister (Ms. Kirti Saxena) and Mr. Ashish Chauhan (jiju) for their endless love, support, care and motivation.

I would like to thank all known/ unknown who might have missed unintentionally from this acknowledgment, but really, your existence would have been very useful during my Ph.D.

Table of Contents

List of Figures

List of Tables

ABBREVIATIONS USED

CA	Cellular Automata
GIS	Geographic Information System
IRS	Indian Remote Sensing
LCD	Land Cover Deltatron
LULC	Land use/ Land Cover
LISS	Linear Imaging Self-Scanning Sensors
MC	Monte Carlo
OG	Organic Growth
PCA	Principal Component Analysis
PCC	Post Classification Comparison
POP	Population of urban pixels
PAN	Panchromatic
PAN	Panchromatic
RT	Road Influenced Growth
RS	Remote Sensing
RS1	Resourcesat 1
RS2	Resourcesat 2
SA	Simulating Annealing
SNG	Spontaneous Neighborhood Growth
SDG	Spontaneous Diffusive Growth
SDC	Spreading Centre Growth
UGM	Urban Growth Model

CHAPTER 1
INTRODUCTION

1.1. Prologue

Land use/ land cover (LULC) changes are the natural and human-induced temporal land transformations and conversion processes, which are taking place under the influence of different natural and anthropogenic drivers. According to the Food and Agriculture Organization of United Nations[1], Land use describes how the human being uses the land. Land cover is the observed (bio) physical cover on the Earth surface. In a natural and strict sense, the land cover can be confined to describe forest, vegetation, ocean etc.

Various land cover classes like a forest, vegetation, open land, aquaculture, water bodies, and many others transforming into the built-up, open, agriculture, recreational areas etc. over the time is called land use/ land cover (LULC) change. Significant land cover conversions include the conversion of forest and open/waste land into agriculture, open areas, and built-up/semi-built-up land use classes. Impervious cover is a well-accepted indicator of urbanization (Wilson et al., 2003).

Geographically, conversion of different LULC classes into built-up/semi-built-up areas may also be called urban growth which means expansion of built-up areas primarily for catering to the needs of human beings. Such a conversion is one of the significant and largest conversion, as a result of ever-increasing urbanization due to an increase in population, industrialization, migration of people from rural areas to urban areas in search of better livelihood, facilities, and employment. Therefore, to meet out the development needs of such an ever-increasing population in urban areas, more and more LULC conversion has to take place into the urban land use class. The urban land use class can be defined as developed land (impervious /semi-impervious cover), and includes residential as well as commercial and industrial land uses that result in a developed or built landscape. The built-up landscape can also be referred to as urban growth or sometimes urban sprawl. Urban sprawl can be referred to a type of land-consumptive pattern of urban development (Wilson et al., 2003).

Such an ever increasing land use change and urbanization are causes of social and environmental challenges (Martellozzo and Clarke, 2011) affecting adversely natural

[1] http://www.fao.org/docrep/003/x0596e/x0596e01e.htm

resources including land, water, vegetation (Pingle et al., 2014; Jat et al., 2008), public services (Carruthers and Ulfarsson, 2003), public health (Ewing et al., 2003), hydrological cycle (Jat et al., 2008), water availability (Srinivasan et al., 2013) and climate (Ewing et al., 2008, Pingle et al., 2014). More and more people are under the risk of such possible adverse impacts of LULC change and urbanization i.e., conversion of pervious surfaces into impervious in the form of developed land because of higher density of population in urban areas. Such adverse impacts are more pronounced and significant due to urbanization as compared to other land cover changes relatively.

Accurate, consistent and timely assessment of urbanization and city growth are critical for assessing current and future needs with respect to urban growth and for setting policy priorities to promote inclusive and equitable urban & rural development. The urban growth assessment and prediction can provide critical information to the local authorities and other stakeholders to take appropriate decisions related to land use planning and development (Weber and Puissant, 2003). Assessment, modelling, and prediction of urbanization is a very active topic of research and discussion in the recent past, being one of the major land use change phenomena and have very profound effects on human beings as discussed above (Wilson et al., 2003; Syphard et al., 2011; Akin et al., 2014; Jat et al., 2017). Research on the causes and processes of LULC changes has been identified as one of the ten most important and challenging research areas in landscape ecology (Wu and Hobbs, 2002).

Urban growth is a very complex and dynamical process associated with landscape change driving forces such as environment, politics, socio-economic aspects, geography and many others that affect urban areas at multiple spatial and temporal scales (Akin et al., 2014). The spatial and temporal components of urbanization can be identified through modelling (Goldstein et al., 2005). LULC change modelling is the process of identifying changes in the state of land classes in the same geographical area at different time periods. Urban growth modelling is a tool to quantify and analyze urban growth and its patterns, to better understand the dynamics of urban systems, to develop hypotheses (to be tested empirically) and to predict urban growth and future scenarios.

A variety of approaches and methods have been developed for the assessment, monitoring and modelling of LULC changes and urban growth, which includes Machine-Learning and Statistical, Cellular Automata, Sector-based Economic, Spatially Disaggregate Economic, Agent-based and Hybrid approaches. Different approaches have their own framework to handle different type of drivers, variables, suitability, and

capability to handle complexity. There is no absolute agreement among users and the research community about the most appropriate approach. However, Cellular Automata based approaches have been found to be promising in modelling of LULC changes & urban growth, which is very much evident from the number of applications reported in the literature in recent past (Agarwal et al., 2002, Chaudhuri and Clarke, 2013; Jat et al., 2017; Saxena and Jat, 2018). In the recent past, many LULC changes & urban growth models have been developed and reported, which are capable of modelling this phenomenon at different spatial & temporal scales with different complexities like SLEUTH, DINIMICA, PLM, CLUE, CUF, LUCAS, CURBA UrbanSim etc. These models are developed based on one or more approaches listed above. Detailed review about these models can be found in Agarwal et al. (2002), Silva and Wu (2012) and NRC (2015).

The SLEUTH model has been found to be a promising LULC change and urban growth model based on research interest from the research community and the number of applications reported from different countries. The SLEUTH urban growth model is a Cellular Automata based model and an acronym for the six required data inputs that include; slope, land use, excluded zones, urban extent, transportation, and hillshade. To date, SLEUTH has been applied world-wide to a variety of International urban regions for various type of applications (Akin et al., 2014; Saxena et al., 2016; Jat et al., 2017; Clarke, 2017; Jat and Saxena, 2018; Saxena and Jat, 2018).

Therefore, LULC change & urban growth monitoring, assessment and modelling are very necessary and vital for optimal land use planning, generation of different developmental scenarios, a comparison of the pros & cons of different land use policy decisions, making adequate future provisions of urban services, estimation of resource requirements for development needs in different scenarios, impact assessment and identification of adaptations for adverse consequences related to climate, urban heat islands, ecological disturbances, and the hydrological cycle.

The proposed research is aimed to understand and study the LULC change and urbanization processes, drivers & mechanism of urban growth, different modelling approaches & models to develop an improved version of the SLEUTH model which is suitable in simulating the realistic urban growth and its prediction, considering selected drivers & variables.

1.2. LULC Change and Urban Growth

1.2.1. LULC change and urbanization processes

Urban is a synonym of developed land which includes residential, industrial and commercial land uses which results in built-up activities or features. Urban growth can be classified into three categories i.e. *infill, expansion, and outlying*. Different types of urban growth and responsible drivers have been shown in Figure 1.1. O*utlying growth* further can be classified into an *isolated*, *linear branch*, and *clustered branch* growth (Wilson et al., 2003). Here, distance and neighborhood variables play an important role in determining which kind of growth will take place.

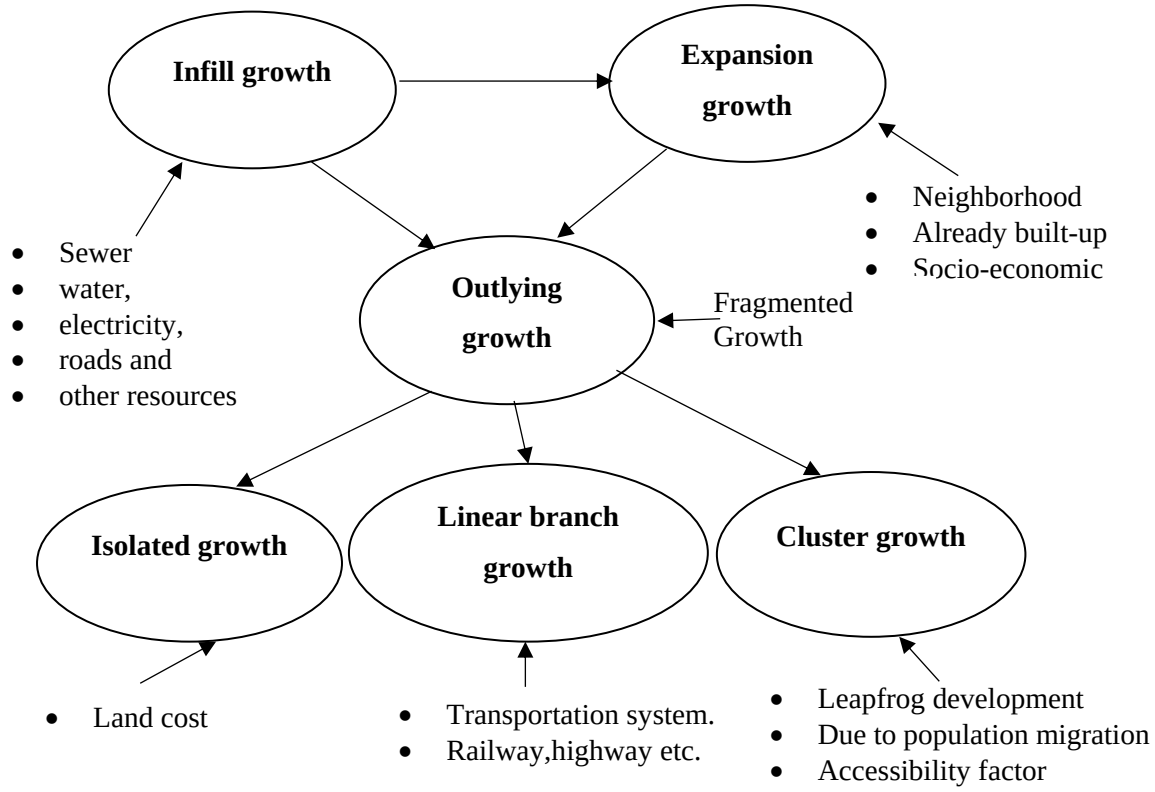

Figure 1.1: Urban growth processes and drivers (Wilson et al., 2003)

The urban growth processes can be defined in terms of landscape transformation (which include fragmentation, reduction of non-developed land) and the development of urban patches (Wilson et al., 2003). *Infill growth* is defined as a non-urban pixel is transformed into urban land use as a function of multiple drivers such as public facilities (sewer, water, roads, and other resources etc.) in already developed areas. *Infill growth* promotes urbanization at those places which are less developed and 40 % of the area has already developed (Wilson et al., 2003). An *expansion growth* is a type of growth when undeveloped pixel being transformed into urban land use, where not more than 40% of

surrounded pixels are already urban. *Expansion growth* is also called fringe development. Land development in a unidirectional form can be called *edge growth*. *Outlying growth* is the by-product of *infill growth* and *expansion growth*. As the development takes place, the land cost will increase along with a reduction in open land and people start migrating to city outskirts which are known as fringe (Wilson et al., 2003). The *Isolated growth* is a very first phase of *outlying growth* which begins when people start being attracted toward the outskirts of the city because of reduced land cost. Then *linear branch growth* takes place along the transportation facilities i.e., road and railway. Urban *growth clusters* will start forming with an increase in accessibility after the development of transportation facilities triggering population migration which leads to *fragmented* and *leapfrog* development. *Leapfrog* development is a sort of cluster development which is called a discontinuous settlement (Wilson et al., 2003) (Figure 1.1).

1.2.2. LULC change and urbanization drivers

Urbanization is a very complex, dynamic, heterogeneous and stochastic process, where multiple factors are in play (Akin et al., 2014). LULC change and urban growth is a function of different explanatory variables/drivers such as neighborhood, proximity, demographic, socio-economic, institutional, suitability, biophysical, and site-specific variables. Neighborhood variables, are such that a person would be more interested in constructing his/her house on the basis of neighboring conditions like near residential areas, city center etc. Proximity drivers like distance to market, distance to road, distance to hospitals, distance to railways, distance to highways, distance to schools etc. are the factors which everyone considers while making a choice about development. Demographic drivers include population and related variables which creates demand for development. Socio-economic variables like land cost, time to travel, opportunity cost, tradition, status, education etc. influences the decision of development and also decides neighborhood. An institutional variable may comprise the decision taken by managerial authorities of or relating to the construction which takes place nearby to the already established industries and institutions. Suitability variable are land suitability for construction of a particular type of development like residential, industrial or agriculture etc. Economic variables like land tenure, farm size, income may be important factors contributing to the LULC change and urbanization. Climatic drivers like climatic variability and life zones are the factors which one considers while building their houses or businesses. Bio-Physical drivers like topography, elevation, slopes, soil types, altitude are considered while making a decision

of development and construction (especially in disaster-prone areas) and Restriction variables or site-specific variables may comprise a prohibited area for development such as a reserved forest, green belt, historical place, airport area etc. A list of urbanization explanatory variables is presented in Table 1.1.

Table 1.1: LULC and urban growth explanatory variables

S. no.	Category of the explanatory variable	LULC change & urban growth driver/explanatory variables
1	Economic variables	1. Land tenure 2. Farm size 3. Distance to market 4. Industrial activities
2	Demographic variables	1. Population density 2. Annual Income 3. Occupational characteristics 4. Cultural preferences
3	Neighborhood variables	1. Distance to city center 2. Distance from important facilities like railway station, school, hospital, Airport 3. Distance from recreation facilities 4. Distance from important roads
4	Climatic & hydrological variables	1. Water availability 2. Meteorological variables 3. Groundwater quality and status
5	Biophysical variables	1. Topographical elevation & slope 2. Soil type 3. Water bodies
6	Social & political variables	1. Literacy 2. Public sector investment in road and infrastructure 3. Land ownership rights 4. Land use zoning
7	Site specific variables	1. Proximity variables

1.3. Urbanization and its Consequences

Globally, more people are living in urban areas as compared to rural areas. As per an estimate, 54 percent of the world's population was residing in urban areas in the year 2014 (UNO, 2014). In the year 1950, 30 percent of the world's population was urban, and by the year 2050, 66 percent of the world's population is projected to be urban (UNO, 2014). India

has also experienced rapid urbanization in the last 60 years. In the year 1951, there were only 5 cities having a population of more than 1.0 million and only 41 cities greater than 0.10 million population. In the year 2011, there are 3 cities with a population of more than 10 million and 53 cities with a population greater than 1.0 million. As per an estimate by the year 2031, there will be more than 6 cities in India with a population of more than 10 million (IIHS, 2011).

Population growth is directly proportional to the growth in built-up activities which leads to land cover changes into impervious built-up/semi built-up areas. Built-up areas in major Indian cities have increased by 10% to 100% in a decade (IIHS, 2011). Such a rapid urbanization and LULC conversions have significant consequences on the surroundings and environment.

On the positive side of consequences, the process of urbanization historically has been associated with other important economic and social transformations, which have brought greater geographic mobility, lower fertility, longer life expectancy, and population aging. Urban areas are important drivers of development and poverty reduction in both urban and rural areas, as they concentrate much of the national economic activity, government, commerce, and transportation, and provide crucial links with rural areas, between cities, and across international borders. Urban living is often associated with higher levels of literacy and education, better health, greater access to social services, and enhanced opportunities for cultural and political participation.

On the negative side of consequences, rapid and unplanned urban growth threatens sustainable development, when the necessary infrastructure is not developed or when policies are not implemented to ensure that the benefits of urban life are equitably shared. Today, despite the comparative advantage of cities, urban areas are more unequal than rural areas and hundreds of millions of the world's urban poor live in sub-standard conditions. In some cities, unplanned or inadequately managed urban expansion leads to rapid sprawl, pollution, and environmental degradation, together with unsustainable production and consumption patterns. The urban growth is generally uncontrolled and not planned in a proper way, therefore, negative consequences override the positive ones. Specific adverse consequences of urbanization (Portugali and Benenson, 1995; Waddell, 2002; Wilson et al., 2003; Weber and Puissant, 2003; Syphard et al., 2011; Lambin and Meyfroidt, 2011; Sankhala and Singh, 2014) are as follows:

1. LULC changes & urbanization affect local, regional, and global climate processes. Choices about LULC patterns have affected and will continue to affect our

vulnerability to the effects of climate change like an increase in temperature, Urban Heat Island (UHI), heat waves and health consequences.

2. Ecological disturbances. Urban sprawl decreases the amount of agriculture, forests, and water. Open space breaks up into small chunks which disrupt the habitat. Loss of farmland causes not only loss of agricultural land but also fresh food sources, species diversity, and habitat,
3. The disparity in wealth occurs and there are differences between the development of urban areas (like metropolises) and the suburbs (like towns),
4. Change in the hydrological regime,
5. Reduction in forest and vegetation,
6. Increase in pollution, and
7. The increased infrastructure and public services cost.

1.4. The Necessity of Urban Growth Assessment and Modelling

The principal advantage of simulation & modelling is that experiments are cheaper, faster and safer on silicon than in reality (Clarke, 2014). This is important for urbanization. We are not prepared and unwilling to build entire experimental urban areas, make daily or annual adjustment to land use policies, investment decisions, transportation networks or socio-economic activities. Once an urban area is built, it is reality and further experiments are not possible. However, without much disturbances and expenses digital urban areas can be created through simulation and modelling and different land use policies and impacts can be investigated. Through modelling and simulation of urban areas can explain the behavior of explanatory variables, forecast future and discover new structures, forms, and processes (Mills, 2000; Clarke, 2014a). Urban areas are also the center of cultural & social pathology, disease & crime, cure and learning. Therefore, we need to model and simulate every aspect of urban areas to make better decisions related to optimal land use planning, infrastructure development, and to arrive at infrastructure investment estimates and environmental sustainability. Various LULC change and urban growth modelling approaches have been developed and reported in the recent past to address following questions;

1. Which environmental, social and other variables contribute most to an explanation of land use/ land cover changes and urban growth — why?
2. Prominent locations of change — where?

3. The rate at which land use change and urban growth are taking place — how much?
4. What would be the future pattern of land use/ land cover change and urban growth— when?

Accurate, consistent and timely assessment of urbanization and city growth are critical for assessing current and future needs of resources with respect to urban growth and for setting policy priorities to promote inclusive and equitable urban and rural development. Specific requirements of urban growth assessment and modelling are discussed in detail below.

Climate change studies: Urban growth simulation and modelling are required to ascertain the impact of LULC change & urban growth on climate regime and to select optimal adaptation strategies for reducing the harmful effects of possible change in micro-climate and urban heat islands.

Land use policy making: Government authorities and Municipalities can use modelling and simulation of urban areas to arrive at optimum and suitable land use policies targeting decided development goals. Also, urban growth modelling can help in generating consequences of different land use policy decisions.

Infrastructure development: For determining the requirement of infrastructure and public services for which urban growth assessment and prediction is necessary.

Investment decisions: Investment requirement for the different types of developmental works in urban areas can be made only after having accurate information about expansion and growth of urban areas temporally.

Natural Resources Planning and Optimum Utilization: Urban growth monitoring and modelling can help in estimating the requirement of natural resources and further their optimum development & use, which lead to optimum utilization of natural resources and development of sustainable cities.

Sustainable planning: How the urbanization is taking place, what are the patterns of urban growth, which area is getting more urbanized, which area is less urbanized, urban density and growth rate of any particular area etc. are the prominent issues and crucial for sustainable development planning of any city which can be effectively assessed and understand by urban growth modelling.

1.5. Role of Geospatial Technologies

Geospatial technologies and methods like remote sensing, geographical information systems (GIS), satellite-based positioning solutions and terrestrial scanning techniques

have opened a new era for geospatial data collection, data storage, manipulation, analysis of geospatial information and modelling of different processes and phenomena related to different areas especially for the phenomenon which has an association with the earth surface and geography. These technologies have provided a system for storing & retrieving a large volume of spatial data and to bring them to a common reference, scale, and format. They have helped in incorporating the spatial influences in the analysis of different problems, which is otherwise not possible. These techniques have also helped in incorporating the spatial and temporal variabilities of different input variables in modelling and analysis of a variety of problems and helped in reducing the uncertainties. LULC change and urban growth assessment and modelling are geo-spatial phenomena and many of their drivers are also geographical in nature. Therefore, geospatial technologies have a very critical role in spatial data capturing, geo-referencing, integration of data from diverse sources and parameterization of LULC change and urban growth models.

1.6. Problem Statement

A variety of approaches and methods have been developed for the assessment, monitoring, and modelling of LULC changes and urban growth. Different approaches have their own framework to handle different type of drivers, variables, suitability, and capability to handle complexity. There is no absolute agreement among users and the research community about the most appropriate approach. The CA-based SLEUTH model is a robust LULC change and urban growth model successfully calibrated and tested extensively throughout the world and largely explored through sensitivity tests (Candau, 2002; Dietzel and Clarke, 2004a; Goldstein et al., 2005; NRC, 2015; Saxena and Jat, 2018). Unresolved issues and problems in modelling of urban growth using SLEUTH have been examined and highlighted by Clarke (2008a, 2008b, 2014), Jantz et al. (2010) and Houet et al., (2016). Different aspects of SLEUTH have been investigated and how its limitations/problems have been resolved in the last 20 years are discussed in Chapter 2. However, many research challenges still remained unresolved which need to be further studied and explored.

1. SLEUTH is a very computationally intensive (Clarke, 2007, 2008, 2014; Houet et al., 2016) model.
2. SLEUTH does not consider many socio-economic variables in the modelling of urban growth like land cost, cost of land conversion and other economic variables, which affects land use decisions. The lack of socio-economic and demographic data in the

modelling leads to the model's inability to capture the real world processes successfully, which in turn results in increased uncertainty of the predicted maps of the distant future (Chaudhuri and Clarke, 2015).

3. Different authors have tried to incorporate the other important explanatory variables in the modelling of the urban growth using different approaches, which include multi-criteria based weighing, logistic regression, empirical relationships and through calculating transition probabilities (Wu and Webster, 1998; Weber and Puissant, 2003; Aspinall, 2004; Mahiny and Clarke, 2012). SLEUTH does not consider a few neighborhood and proximity variables which affect the decision of individuals for land use and urbanization like distances from important facilities in urban areas like the city center, airport, railway line and distance from important roads. Also, SLEUTH does not consider human behavioral explanatory variables in urban growth modelling. However, these variables have not been incorporated into the SLEUTH model framework except in the exclusion layer while forecasting growth for scenario generation (Mahiny and Clarke, 2012).
4. SLEUTH has not been able to capture the fragmented urban growth of smaller size built-up units, which is a common type of development in developing countries. It has been shown that refining spatial resolution increases model sensitivity to local conditions (Silva and Clarke, 2002). Therefore, the research question that what is the appropriate spatial resolution of input data to capture the different forms and structure of urban development having different built unit sizes needs to be investigated.
5. SLEUTH uses historical land use data to calibrate the model, where it matches the land use category at individual pixels with observed status, however, it does not consider the form and structure of built-up form/development in calibration and validation.
6. SLEUTH calibration has a limitation of scale sensitivity i.e., how well do the model results cross spatial scales (Jantz and Goetz, 2005; Clarke, 2014), temporal sensitivity i.e., sensitive is the model to the length, frequency, and irregularity of the spacing of time-slices used both as input data and output and sequencing i.e., does the model updates annually, once, synchronously in space or asynchronously in space (Clarke, 2014; Houet et al., 2016).
7. SLEUTH is also sensitive to the level of aggregation i.e., the model uses a hierarchical land use classification are the model results at the higher level of aggregation better than those at a lower level? (Dietzel and Clarke, 2006; Clarke, 2014),

8. SLEUTH is a stochastic model and its performance is a function of its computational pseudo-random number generator (Van Neil and Laffin, 2003),
9. Model is also not capable of explaining the influence of biophysical variables except the slope in modelling of urban growth.
10. The model is sensitive to temporal and spatial scale and it is not capable of determining the interior structure of cities, nor is it capable of creating urban density estimates within them.
11. Various studies used the Monte Carlo method to estimate the uncertainty of models' performances. Model accuracy not only depends on models' performance but on the uncertainty of input data, urban history and accuracy of reference maps (Caglioni et al., 2006; Gazulis and Clarke, 2006; Clarke et al., 2007; Chaudhuri and Clarke, 2014). There is an accounting for, but no explicit model of uncertainty in the SLEUTH model (Clarke, 2014).
12. The clusters of the settlements at places, where highways intersect, for example, was not programmed into the model but happened anyway (Clarke, 2014).
13. SLEUTH does not consider land use demand attributes (population density, incomes, employment potential, land prices etc.) in urban growth modelling.
14. Unexplored dimensions of SLEUTH include more use of visualization on the model results, what constants might have been variables (like self-modification model parameters), exactly how changes in transportation impact growth, how dynamic probabilities of land use change could be included and how the model's assumptions about topographic slopes are.
15. SLEUTH does not have answers for time, a change propagation "wave" takes to get from any point in the model space to the most distant places (Clarke, 2014; Houet et al., 2016).
16. SLEUTH is developed as a path dependent model as it mimics the historical trends and then forecasts the growth. SLEUTH assumes the same number and type of driving factors and their fixed influence during calibration and forecasting. However, urban systems are dynamic and may not be stationary. New drivers may come into force or their influence can change with respect to time (Mas et al., 2012; Houet et al., 2016).
17. SLEUTH has not been further tested extensively so far for simulating different types of urban development in different countries having different socio-economic, cultural and human behavioral characteristics as suggested by Kumar et al. (2011) that SLEUTH

needs to be improved to simulate the urban growth in developing country conditions like India.

18. What will be the effect of different sets of data resolution on the land use/ land cover change analysis? What data resolution set would be appropriate for a particular situation/ scenario like India where the growth is fragmented?

Therefore, it can be concluded from the above discussion that, many research issues and challenges still need to be addressed for accurate urban growth assessment, modelling, and prediction. Many approaches and models are available which are based on different assumptions, require different input parameters, have different suitability and are appropriate for particular spatial & temporal resolutions, consider different change drivers & processes and use different methods to model & predict the LULC change and urban growth. Many models developed and reported in the literature have not been tested for different socio-economic and geographical settings and the sensitivity of their parameters has not been evaluated so far. The following research questions have been formulated based on the research issues discussed above-

- ✓ What are the important urbanization drivers and explanatory variables of urban growth?
- ✓ How is the performance of the SLEUTH model in simulating the urban growth of cities/ towns or urban areas having socio-economic conditions of developing countries like India?
- ✓ What is the SLEUTH model sensitivity with respect to different model constants and parameters?
- ✓ How the performance of the SLEUTH model can be improved by incorporating other urbanization explanatory variables in the simulation process?
- ✓ How built-up density/ urban intensity/density can be estimated and modelled?

Therefore, in the presented research an attempt has been made to understand and study the LULC change and urbanization processes, drivers & mechanism of urban growth, different modelling approaches & models. Efforts have been made to develop an improved version of SLEUTH i.e., SLEUTH-Suitability, which is capable of simulating realistic urban growth considering the influence of additional urban growth explanatory variables (land suitability). An effort has also been made to improve and enhance the performance & capabilities of the SLEUTH model by examining its sensitivity to different model parameters and constants. Also, efforts have been made to develop a new version of the

model i.e., SLEUTH-Density to estimate the urban intensity or built-up density. Further, model performance and application have been demonstrated through modelling and prediction of urban growth for Ajmer urban fringes.

1.7. Objectives

The proposed research is aimed to understand and study the LULC change and urbanization processes, drivers & mechanism of urban growth, different modelling approaches and models to develop an appropriate model which is capable in simulating the realistic urban growth, considering selected drivers. An effort will be made to improve and enhance the performance and capabilities of CA-based SLEUTH model by examining its sensitivity to different model variables & constants, which has not been examined so far and by estimating the built-up density. Further, model performance and application will be demonstrated through modelling and prediction of urban growth for a selected urban area. Specific objectives of the proposed research are –

- Review of the present state of knowledge of LULC change and urban growth modelling approaches and models,
- Collection of suitable data with suitable spatial and temporal resolution required for parameterization, calibration, and validation of CA-based SLEUTH Model,
- Creation of GIS database for the urbanization explanatory variables used as input data for the SLEUTH model for the selected area,
- Conceptualization, calibration, and validation of the SLEUTH model for the selected area,
- Development of methods and techniques to improve the performance of the SLEUTH model to address the issues related to built-up density, parameter sensitivity, and the inclusion of important explanatory variables in urban growth simulation.
- Comparative analysis of SLEUTH performance in modelling & prediction of urban growth before and after improvements.
- Demonstration of the application of CA-based improved SLEUTH model for the selected real urban area.

1.8. The Scope of the Work

Above mentioned research objectives have been achieved through steps given below;

i. Literature review to understand the present state of knowledge, and to find out the research issues & challenges in LULC change, urban growth assessment and modelling,

ii. Collection of spatial and non-spatial data from different sources required for parameterization of SLEUTH,

iii. Preparation of land use/ land cover maps for different years through digital image processing of multi-spectral satellite images of different years,

iv. Creation of GIS database for required explanatory variables of urban growth,

v. Conceptualizations and parameterization of CA-based SLEUTH model,

vi. Calibration of a model for the base case with existing SLEUTH model for the test case study area,

vii. Sensitivity analysis of a model for the selected model input variables and constants like the *cellular neighborhood, diffusive value parameter, a game of life rule* threshold *value, critical slope and self-modification parameters* etc.,

viii. Development of additional capability in the SLEUTH to estimate urban/ built-up density,

ix. Development of improved version of SLEUTH model by incorporating selected explanatory variables (if possible) into the algorithm to improve the performance of the model in simulating realistic urban growth,

x. Comparison of model performance before and after improvements in simulating the urban growth of the selected area,

xi. Demonstration of the application of improved SLEUTH model for simulating the urban growth of a real urban area.

1.9. Material and Tools to be Used

Following tools and data has been used to achieve the stated objective.

1. Multi-spectral remote sensing images for a number of years for the selected study area
2. Survey of India toposheets
3. Secondary data related to biophysical variables of the selected study area
4. Demographic and socio-economic data

Following tools will be used in the proposed research –

- ERDAS Imagine and ArcGIS

- SLEUTH Model

1.10. Organization of Thesis

The above mentioned objectives for the proposed research have been organized into ten chapters. The contents of each chapter are briefly described below:

Chapter 2 presents the literature review to understand the present state of knowledge related to LULC change & urban growth modelling approaches, issues and challenges.

Chapter 3 describes the profile of the study area which was selected to demonstrate the application of present research work. The collection of spatial and non-spatial data from different sources required for parameterization of SLEUTH in achieving the different objectives have been included in this chapter. The salient details of the input data have been described. Processing of input data and preparation of land use/ land cover maps for different years through satellite images have been described here. Creation of a GIS database for required explanatory variables of urban growth and preparation of various thematic layers required for the parametrization of the model has been presented in this chapter.

Chapter 4 is devoted to the detailed methodology for fulfilling the individual objective of present research. Methodology for conceptualizations and parameterization of CA-based SLEUTH model, calibration of the base model with default model parameters, sensitivity analysis of crucial parameters of the SLEUTH model, development of SLEUTH-Density and SLEUTH-Suitability have been discussed. Further, the methodology used to compare the performance of different versions of the model has also been presented in this Chapter.

Chapter 5 deals with the sensitivity analysis of a model for selected model parameters and constants like *self-modification constants, critical slope coefficient, cellular neighborhood, Monte Carlo iterations, a game of life rules*, etc.

Chapter 6 presents the development of the SLEUTH-Density model which is capable of simulating the built-up density. Development of a built-up density algorithm, development of programming code and its integration with the existing SLEUTH code, program testing, and demonstration of application have been discussed in the chapter.

Chapter 7 presents the development of SLEUTH-Suitability model which includes the development of the algorithm, programming code and its integration with the existing SLEUTH code, program testing, and demonstration of application have been discussed in

the chapter. Derivation of land suitability decision variable using the AHP method of MCE technique has also been discussed in this chapter.

Chapter 8 describes the comparison of model performance before and after improvements in simulating the urban growth of the selected area. Demonstration of the application of the improved SLEUTH model for simulating the urban growth of a real urban area has also been presented in this chapter.

Chapter 9 presents conclusions drawn from the present research work along with limitations of the study and future scope of the work.

CHAPTER 2
LITERATURE REVIEW

2.1 Prologue

Land use/ land cover change and urbanization are one of the most important anthropogenic processes affecting terrestrial ecosystems, causing ecological disturbances, habitat loss, fragmentation and interaction with other components of global change (Syphard et al., 2005, 2011). More and more people are under the risk of such possible adverse impacts of LULC change and urbanization i.e., conversion of pervious surfaces into impervious in the form of developed land because of higher density of population in urban areas. Such adverse impacts are more pronounced and significant due to urbanization as compared to other land cover changes relatively. Urbanization is a very complex, dynamic, heterogeneous and stochastic process, where multiple factors are in play (Akin et al., 2014). Accurate monitoring, assessment, and prediction of such LULC transformations are very necessary to deal with their adverse consequences. LULC and urban growth monitoring, assessment and modelling are very necessary and vital for optimum land use planning, generation of different development scenarios, estimation of resource requirements for development needs in different scenarios, impact assessment and identification of adaptations for adverse consequences related to climate, urban heat islands, ecological disturbances, and the hydrological cycle.

A number of approaches and methods have been developed for the assessment, monitoring and modelling of LULC changes and urban growth which include Machine-Learning, Statistical, Cellular, Sector-based Economic, Spatially Disaggregate Economic, Agent-based and Hybrid approaches. Different approaches have their own framework to handle different types of drivers, variables, suitability and capability to handle complexity. There is no absolute agreement among users and the research community about the most appropriate approach. This chapter is aimed to understand and study the LULC change and urbanization processes, drivers & mechanism of urban growth, different modelling approaches & models to develop an appropriate model suitable in simulating realistic urban growth and its prediction by considering selected drivers in different socio-economic conditions. Different issues and aspects related to LULC change and urban growth modelling have been discussed in the form of representative case studies. First of all

different LULC change assessment & modelling approaches were discussed and their comparison has been made to ascertain different research issues. Then salient features of different type of models available to deal with LULC change and the urban growth phenomenon have been presented. Further, a detailed review has been done to ascertain the present state of the knowledge and research issues with respect to different aspects of LULC change and urban growth like Land use/ Land Cover Change and Urban growth, land use/ land cover change and urban growth drivers, cellular automata based modelling and land use/ land cover change assessment using remote sensing.

2.2 LULC Change & Urban Growth Assessment & Modelling

2.2.1 LULC change and urban growth modelling approaches

Various LULC change and urban growth modelling approaches have been developed and reported in the recent past, which aimed to address the following questions;

1. Which environmental, social and other variables contribute most to an explanation of land use/ land cover changes and urban growth — why?
2. Prominent locations of getting change — where?
3. The rate at which land use change and urban growth are taking place — how much?
4. What would be the future pattern of land use/ land cover change and urban growth— when?

The standard LULC change and urban growth modelling approaches have been reviewed and reported in the literature extensively (Agarwal et al., 2002; NRC, 2015). Various approaches to LULC change as classified by the NRC (NRC, 2015) are –

2.2.1.1 Machine-learning and statistical approaches

Such approaches use observations of past land use/ land cover changes to calibrate parametric or non-parametric relationships between those changes and spatially and temporally specific predictors (Brown et al., 2000; Millington et al., 2007; Carlson et al., 2000; Ray and Pijanowski, 2010).

2.2.1.2 Cellular automata based approaches

CA-based approaches integrate land use/ land cover suitability maps with neighborhood effects and information about the amounts of change expected to project future LULC changes (Wolfram, 1984, 1986; White and Engelen, 1993; Clarke et al., 1997; Clarke and

Gaydos, 1998; Wu and Webester, 1998; Batty, 2000; Verburg et al., 2002; Clarke, 2014; Clarke, 2017, 2018).

2.2.1.3 Sector-based economic approach

Sector-based economic approaches use partial and general equilibrium structural models to represent supply and demand for land by economic sectors within regions based on overall economic activity and trade (van Tongeren et al., 2001; Hertel et al., 2009; Palatnik and Roson, 2009; van der Werf and Peterson, 2009; NRC, 2015).

2.2.1.4 Spatially disaggregated economic approaches

Spatially disaggregated economic approaches involve development of structural or reduced form econometric models to identify the causal relationships influencing the spatial equilibrium in land systems (Bockstael, 1996; Chomitz and Gray, 1995; Nelson and Hellerstein, 1997; Irwin and Bockstael, 2002; Towe et al., 2008; Lewis et al., 2009; Lewis, 2010; Newburn and Berck, 2011; Wrenn and Irwin, 2012; NRC, 2015).

2.2.1.5 Agent-based approaches

Agent-based approaches simulate the decisions and actions of heterogeneous land-change actors that interact with each other and the land surface to make changes in the land system (Schelling, 1971; Parker et al., 2003, 2004; Gimblett, 2002; Brown, 2006; Niazi and Hussain, 2011; Hatna and Benenson, 2012; Clarke, 2014).

2.2.1.6 Hybrid approaches

Hybrid approaches encompass applications that include different approaches into a single model or modelling framework (Hilbert and Ostendorf, 2001; Li and Yeh, 2002; Hurtt et al., 2006, 2011; NRC, 2015). The first five approaches are arranged roughly in order from least to most focussed on processes. The approaches that rely on data about land-change patterns, including Machine Learning and Statistical, and Cellular, tend to use land cover information from satellite imagery and relationships based on observed changes in the past. These approaches are useful for projecting observed LULC changes over short periods into the future but often have limited ability to evaluate conditions not observed in the past. The more process-based approaches, such as Sector-Based Economic, Spatially Disaggregate Economic, and Agent-Based approaches, make greater use of social science information about land-change processes. These approaches provide more realistic representations of the processes of change that can be used to evaluate a wider range of alternative futures,

but their calibration and validation is more challenging and may provide only qualitative information about possible future LULC change outcomes (Agarwal et al., 2002; Brown et al., 2000; NRC, 2015). Machine Learning & Statistical and Cellular Automata based modelling approaches are most suitable for problem identification because they lack the richer structural detail about the process needed to evaluate the effects of changes in policy structure, they are easy to implement and can provide valuable descriptions and projections of patterns and trends. Agent-Based and Structural Economic approaches are useful for intervention design because they provide a means for exploring interactions in the land system and for assessing the possible effects of policies or decisions based on predictions. Once policies or decisions have been implemented, the after-effects of these implementations can be evaluated using reduced-form econometric models that compare observable outcomes either before and after the intervention or in an intervention area and a comparable location. Understanding the underlying structures, assumptions, and data requirements of different modelling approaches are critical for understanding their applicability for various scientific and decision-making purposes. Generalized characteristics of different above-mentioned modelling approaches have been compared and discussed in Table 2.1.

2.3 Land Use/Land Cover Change and Urban Growth Models

A variety of LULC change and urban growth models have been available and reported in the literature based on one or more approaches as discussed above. A detailed review of different LULC change and urban growth can be found in Lambin et al. (2000), Silva and Wu (2012); Gaunt and Jackson (2003), Lambin et al. (2000), Chang (2006), Clarke (2014), and NRC (2015). LULC change and urban growth models have been classified into different categories based on their capability, suitability and used modelling approach as presented in Table 2.2. In a study, Matthews et al. (2007) presented the complete review of different agent-based models suitable in modelling of LULC change and urban growth. The main advantages of this modelling approach are; individual decision-making entities capability and interaction among variables that make this approach more realistic and robust in nature. Different ABLUM's (Agent-Based Land use Models) such as LUCITA, FLORES, GEOLP, SHADOC, SLUDGE, MEJAN, CORMAS, LUCIM etc. are there. Pontius et al. (2008) have also analyzed the 13 modelling applications using different models by comparing actual with modeled outputs.

Table 2.1: Generalized characteristics of different modelling approaches

Modelling Approach	**Pattern/ Process**	**Land cover, Land use**	**Key Assumptions**	**Typical Data Requirements**	**Recommended Uses**
Machine Learning and Statistical	Pattern	Land cover	Strong stationarity	LC maps from at least two-time points Some number of maps of predictor variable(s)	Make forecasts of land cover patterns under stationarity, Extrapolating past patterns
Cellular		Land cover and land use	Stationarity, Strong spatial control and/or interaction, No market interactions	A land LULC map at some point in time, some number of maps of the predictor variable(s)	Forecast land cover patterns, Evaluate changes in spatial controls without market feedbacks
Spatially Disaggregated Economic Models		Land cover	Utility or profit Maximization, Price and/or spatial Equilibrium, Heterogeneous agents sometimes specified	Data on LC at one or more point(s) in time; Economic and biophysical variables that influence land demand and supply; any other required instrumental variables	Reduced-form models: Identify the causal effect of key variables on land change outcomes Structural models: Simulate effects of policy changes on land market outcomes, including changes in prices and land use patterns
Sector-Based Economic Models	Process	Land cover	Heterogeneous agents sometimes specified, Utility or profit Maximization, Price equilibrium Representative agents	Economic variables that influence aggregate demand and supply including prices of commodities and values of trade at a regional or country scale	Forecast aggregate land changes under a variety of market-based changes that can affect demand and supply
Agent-Based Models		Land cover and land use	Usually heterogeneous Agents, Variable interactions among agents	Data describing characteristics of agents, Qualitative or quantitative data on decision processes, Data on land use or land cover at some point(s) in time	Explore land change processes, often under stylized conditions; Explore the effects of exogenous change on a system, where it has not happened; Explore future scenarios where past patterns may be poor indicators of future outcomes

Table 2.2: Classification of LULC change and urban growth models
(Source Lambin et al., 2000)

What is already known on LUCC	**What one needs to know on LUCC**	**Model category**	**Modelling approach**
Where and when in the past	When in the future (short-term)	Stochastic	Transition probability models
	Why in the past (proximate causes) Where in the future (short-term)	Empirical, statistical	Multivariate statistical modelling, Spatial statistical (GIS-based) models
Where, when and why in the past	When in the future (long-term) When and where in the future (long-term)	Process-based, mechanistic	Behavioral models and dynamic simulation models, Dynamic spatial simulation models
	Why in the future (underlying causes) Why in the future (underlying causes; scenarios)	Analytical, agent-based, economic	Generalized von Thünen models, Deterministic and stochastic, optimization models

Out of 13, 12 applications were found to have errors in modelling results. The study explained that validation is a very important phase for any modelling application. In the present study, a detailed comparison of different models using different approaches has been presented in ANNEXURE I.

Further, the important LULC changes and urban growth models have been discussed in subsequent sections.

1. Empirical Statistical Models
2. Stochastic Models
3. Optimization Models
4. Dynamic Process Based Simulation Models
5. Cellular Automata based Models
6. Integrated Model

2.3.1 Empirical statistical models

Empirical, statistical approaches are used to establish a relationship between LULC change or urban growth and their explanatory variables. Relationships are derived empirically by

fitting statistical data to assess LULC change and urban growth explicitly. The multivariate analysis builds the relationship between explanatory variables of LULC change for potential contributions of empirically-derived growth rates. Multiple linear regression, logistic regression, multinomial regression, logit regression etc. are the popular techniques used for this purpose. The statistical relationship does not establish a significant causal relationship. The regression model that fits well for the coefficient ranges may poorly perform outside that region, therefore, models cannot be used for long-term predictions. This type of approach is better suited for analyzing land use change and urban growth patterns on the basis of historical data only, no further dynamism is considered, in most studies, this is not valid. Some of the empirically fitted models are PLM, CLUE, CLUE-CR, and DINAMICA (Wang and Zhang, 2001; Verburg et al., 2006; Mas et al., 2012; Xu et al., 2013; NRC, 2015).

2.3.2 Stochastic models

LULC change and urbanization is a very complex process, heterogeneous and stochastic in nature. Such stochastic modelling approaches mainly incorporates transitional probabilities for each cell of land use/ land cover / urban growth and the decision of transition are based on a stochastic variable e.g. random number. The transition probabilities are measured by some statistical means, which determine changes from one LULC class to another. Such approaches are useful for top-down relationship based applications where impact assessment is an issue of concern. Effect of one variable on the phenomenon based relationship can be effectively developed by such approaches. Transition probability-based approaches are limited to their application as an intensification of LULC change cannot be determined by the method because it is purely based on recent past data only. However, for incorporating intensification into stochastic models some efforts have been made such as spatial diffusion models, which do appear to be effective on land use change intensification. Some of the empirically fitted models are CURBA, LUCUS, SimLand, and CUF (Landis et al., 1998; Landis and Zhang, 1998; Berry et al., 1994, 1996; Irwin et al., 2001; Silva and Wu, 2012; NRC, 2015).

2.3.3 Optimization based models

Optimization techniques are used to determine the optimum combination of explanatory variables and their value ranges to explain the LULC and urban growth phenomenon. Optimization techniques like linear and non-linear programming apply at the general

equilibrium, micro scale & macro scale and generally incorporated into economic models. In various applications such as a parcel of land given with its attributes and location then highest earned rent can be estimated using this approach. This modelling approach allows investigating the influence of various policies on LULC change and urban growth. It can be used for land allocation for optimal crop production. This modelling approach may suffer from the discretional definition of objective functions and non-optimal and ambiguous behavior of people such as differences in values, culture, and attitude. However, at a generalized level, this can be underestimated but are likely to be significant as one looks at small or fine scale LULC change processes. FASOM is an optimization-based model (Alig et al., 1997).

2.3.4 Dynamic (process-based) simulation models

These models are based on the interaction of socio-economic and biophysical processes. Change in LULC patterns with time and space is determined by these processes. The dynamic process-based simulation models incorporate the interaction among all components to develop a spatially explicit dynamic system. The complex aggregate system is formed by combining small chunks of analysis using differential equations. The prior understanding among variables is developed before simulation. This modelling approach is more powerful in establishing the relationship among variables and simulating the dynamic behavior of the system. The relationship cannot be built into the system in a straightforward way. For analyzing LULC change and urban growth it is complex as numerous interactions among variables take place. PRISM is an example of a process-based model (Alberti and Waddell, 2000; NRC, 2015).

2.3.5 Cellular automata based models

Cellular automata (CA) is a cell-based framework which includes cell states, transition rules, finite discrete cells, and neighborhood. CA-based models are very effective for addressing LULC change and especially urban growth. Urban growth is a dynamic and complex phenomenon and CA includes the capability to model a complex phenomenon in an easy and effective manner. It is difficult to simulate human behavior which is a very important variable which can be simulated using CA only. The integration of CA and Agent-based methods would be an effective approach in the field of LULC change and urban growth modelling. DUEM, CVCA, LOV, SLEUTH and LUSD are the examples of cellular automata based models (Clarke et al., 1997; Clarke and Gaydos, 1998, Batty et al.,

1997; White, R. and Engelen, 2000; Silva, 2003; Silva et al., 2008; Kumar et al., 2011; Clarke, 2017, 2018).

2.3.6 Integrated models

Above discussion gives a straight forward classification of the various types of LULC and urban growth modelling approaches. The recent advancement includes the integration of more than one approaches for providing added attributes to the LULC change and urban growth modelling. Such modelling approaches are used where spatially explicit interaction and dynamic behavior including long-term prediction is required. It is very complex to hybrid two different modelling approaches for a large landscape as a number of interactions hugely increases. LUSD, SimLand, UrbanSim are integrated models (He et al., 2005, 2006; Wu, 1998; Waddell, 2000, 2002; Waddell et al., 2003; Duthie et al., 2007; Hepinstall et al., 2008; Wang et al., 2011; NRC, 2015).

The detailed review of the literature has been done for below-mentioned classes with the help of representative reported case studies

i. Land use/ land cover change and urban growth assessment,
ii. Land use/ land cover change and urban growth drivers
iii. Cellular Automata based LULC change and urban growth modelling
iv. Land use/ land cover change using remote sensing

2.4 Land Use/ Land Cover Change and Urban Growth Assessment

Gottmann (1957) explained the geography of megalopolis cities in detail by considering various social aspects of the present time. The urbanization has been increased especially in bigger and metropolitan cities in last few decades which tends to increase the number of industries, organizations, institutions, and hospitals. The study was found useful in improving the management of the complex process of urbanization.

Lambin et al. (2001) discussed the opportunities and constraints derived by local as well as national markets and policies with respect to the LULC change and urban growth. The global forces become the main determinants of land-use change and economic opportunities.

Shen et al. (2001) discussed that an effective urban land use and regional planning are essential for the development of society.

Couclelis et al. (2005) discussed various approaches, methods, and techniques to model urban growth such as agent-based, cellular automata, rule-based, neural network and logit modelling methods are available. Authors outlined the need for urban growth monitoring and modelling and found it to be very useful in the planning of urban land use scenarios, resources, land use, and budget and policy making etc.

Jabareen (2006) analyzed different forms of sustainable urban growth along with models and theoretical concepts. A compact city, Neo-traditional development, Eco-city, Urban containment are the sustainable urban forms which have been discussed in this study. Moreover, compactness, sustainable transport, density, mixed land use, diversity, passive solar design, and greening are considered design concepts or urbanization drivers.

Chu et al. (2010) have presented two empirical simulation methods such as ANN and Logistic Regression and used them to simulate land use change by incorporating ANN and Logistic regression in the CLUE-S i.e. Logistic CLUE-S and ANN CLUE-S models to predict the land use changes. The authors have also discussed various modelling approaches to land use change such as stochastic models, optimization models, dynamic process-based simulation model, cellular automata and empirical- statistical model. The authors have validated model results with respect to the landscape metrics and kappa coefficients. The study reveals that the ANN CLUE-S has a higher probability of generating accurate simulation and results are more accurate as compared to the Logistic CLUE-S model. Also, the urbanization demand was estimated in two ways i.e. CA-based SLEUTH model and Markov chain method. The study shows that CA-based SLEUTH model is more appropriate to calculate demand which further leads to the prediction of land use change using CLUE-S. In further research, a number of land use change models in place of SLEUTH and Markov model can be integrated to improve the performances of CLUE-S.

Lambin and Meyfroidt (2011) stated that economic globalization combined with the looming global land scarcity increases the complexity of future pathways of land use change. Predictions of the expected land use impact of national policies have become more uncertain. The study analyze the land use change impacts on the environmental ecosystem, climate change, and global warming.

Gould et al. (2012) provide a comprehensive review of land use, land cover, population dynamics, and land-cover change processes. Population density and land use/ land cover change have been correlated to understand the complex phenomenon of urbanization.

Rimal (2012) utilized GIS and Remote Sensing techniques to figure out the transition of land use classes. Change detection has been analyzed using different satellite imagery. A post classification comparison method was used to analyze the change detection. Lang (2012) explained the understanding of urban resilience in the perspective of socio-economic crisis by urban change and determined it as a completely theoretical process of understanding.

Chaudhuri and Clarke (2015) coupled the land use and road networks on the spatiotemporal dynamics of land use changes. The effect of road networks on land use change was analyzed using graph theory indices method. The comparative analysis of the overall results for Pordenone and Gorizia revealed that an unstable and vulnerable political environment in the historical past of an urban area does make a difference in the development of the road network and in land use change over time.

Price et al. (2015) analyzed the urban sprawl effects i.e. urban heat island (UHI). The study reveals that due to excessive urban growth, the urban heat island effect is increasing.

Qin et al. (2015) determined the 3D urban morphology by using geo-spatial techniques. The weighted average height of the buildings, volume of buildings, 3D expansion intensity and 3D fractal dimension were used to quantify the 3D urban morphology.

Van Vliet et al. (2016) found that statistical analysis and automated procedures are the two most common calibration approaches in LULC change modelling, while expert knowledge, manual calibration, and transfer of parameters from other applications are less frequently used.

2.5 Land Use/ Land Cover Change and Urban Growth Drivers

Schelling (1971) explained that urbanization is a complex phenomenon to understand and depends on many variables such as transportation, facilities, social factors, and economic factors.

Clark (1991) has refined the understanding of residential preferences and find out that neighborhood is one of the major explanatory variables. However, neighborhood possesses

some empirical phenomena like racial preferences, choices, and patterns. Survey analysis towards such issues have been plotted on curves and Clark analyzed the preferences and choices of residents. Authors have suggested a study of some more exploratory variables for analyzing residential choices.

Knox (1991) has explained the relationship between landscape change with economic and socio-cultural change. The integration of land use and transportation models has been done to analyze the impacts of land use on transport by considering various driving factors. Some deriving forces such as human behavior (how people will change with their location and mobility according to land use policy, transportation costs etc.) were included in the decision making of the model. The human-induced decisions are implemented by using mathematical and logit based models.

Serneels (2001) incorporated multiple driving forces of LULC change using the multiple logistic regression method in the simulation process. The study is able to determine the effect of various driving forces such as distance to road, distance to market, distance to river, population density, slope, elevation, intercept, soil suitability, distance to water, distance to village etc. on LULC change. However, LULC change predictions have not been done in the study.

Veldkamp and Lambin (2001) discussed the contributing factors of urban growth like biophysical factors such as slope, soil type, and altitude. Socio-economic drivers were also found to be playing an important role in LULC change e.g. international environment treaty such as the Kyoto protocol may drive significant changes in determining land use land cover change. However, incorporating socioeconomic and political drivers into LULC change assessment may be hampered by a lack of spatially explicit data.

Kok (2001) analyzed the influence of urbanization drivers on LULC change and urbanization. Influence of a number of drivers was studied and presented which includes the influence of population density, distance to city, distance to roads; bio-physical drivers such as topography, elevation, slopes, soil types; climatic drivers such as climatic variability, life zones; political drivers such as land redistribution programs park protection, subsidy system; economic variables such as land tenure, farm size, income, distance to market; social drivers such as tradition, status, education; miscellaneous drivers such as diseases, civil war; physical conditions like topography, slope, soil, and rivers in the valley; public service accessibility: services available to the desired location such as,

transportation, electricity, education, drinking water, health services, commercial services, waste disposal, open spaces and recreation facilities; economic opportunities: high paying jobs, business opportunities in tourism, finance industry, education, health, wholesale and retails; land market: local people, land broker and real estate developers; population growth: high population influx; political situation; plans and policies: effectiveness of zoning, land reforms, land pooling, guided land development, economic and investment plans. Few drivers have been found to have significance as compared to others.

Serra et al. (2008) assessed the LULC change as a function of biophysical and human factors. A logistic regression method has been studying the influence of different drivers as independent variables. Data from various sources were used for modelling, calibration, and validation of an urban growth model. Effect of different bio-physical, social and infrastructure driving factors (digital elevation model, slope map in percentage, distance to rivers, distance to industrial estates, distances to five urban centers. distances to highways and major roads, distances to the ring road, distances to feeder roads, distances to existing built-up surfaces and annual population growth rate) on the LULC change and urban growth was studied. To check the effect of each variable, the weight of evidence method has been used. Model results were validated using overlaying analysis and FOM (figure of merit) ratio.

Bürgi and Turner (2002) have explored the contribution of various causative factors in changing the LULC. A multivariate linear regression method has been used with three abiotic and two socio-economic variables. The effect and importance of different driving factors for the study area have been determined. The study may be useful for analyzing anthropogenic relationships with cultural landscape change.

Park et al. (2012) examined the role of topographic, geographic and social environment factors in urbanization. The Frequency Ratio (FR), Analytical Hierarchy Process (AHP) and Logistic Regression models (LR) have been used to quantify the effect of urbanization drivers into LULC change and urban growth. Also, future prediction for urban growth has been done. All three methods showed similar accuracy in urban growth simulation.

Gharbia et al. (2016) analyzed LULC change using an integrated approach of CA and GIS. The study incorporates biophysical factors such as slope, proximity, population density, transportation and distance to the main road into the assessment process. The suitability maps were generated in the form of a restricted layer. Influence of urbanization drivers was

considered in the form of weights which were calculated by overlaying different maps on LULC maps. Nearest neighbor transition rules were also used in the study. Also, validation has been done by calculating kappa coefficients and overlaying the simulated maps over the actual land use maps.

2.6 Cellular Automata based LULC Change and Urban Growth Modelling

Wolfram (1984) stated that cellular automata is a very effective approach to modelling and simulating the behavior of changing patterns in various fields. The simulation includes the transition states of each cell at the end of every time state and the transition is determined by neighborhood states of each cell. However, its complexity increases with the increase in the size of cellular automata.

White and Engelen (1993) discussed the evolution of simulation of fractals of urban areas using DLA (disaggregated land analysis) and CA. The CA is very much efficient in producing the real pattern of complex urban dynamics as complexity is a necessary behavior of cities.

Batty and Xie (1994) stated that cities should be understood in terms of their local properties. The more local characteristics are involved the better the understanding of cities would be. This idea illustrates that local characteristics / variables of cities such as distance to roads, distance to city center and neighborhood would lead to the understanding of the global phenomenon. The CA provides insights into simulating the urban systems rather an alternative approach, it was used to represent cities as cells in this study for the very first time. The game of life rule was used in making a decision of state transition of cells. The study elaborates the performance of cellular automata in land use change modelling and also how the game of life proceeds for capturing urban patterns. Some issues related to urban growth simulation were flagged out in this study such as; it is important to understand the urban system at their local scale first to completely portray the global pattern of the urban system. But, it is very unlikely to include local scale phenomena into the study. Therefore, the value of this approach lies in focusing our attention on the understanding of urban patterns at a different scale. Also, the urban automata were in the form of undeveloped and developed, only two cell states and many states and extensions are needed to embrace into the urban CA.

Portugali and Benenson (1995) claimed the city as a complex, open and self-organized structure described on a cell space. The central property of a self-organizing system is uncontrollable by any of the factors such as economic, social and political.

Clarke et al. (1996) described the extension of traditional cellular automata into self-modifying cellular automata for urban growth simulation. Self-modification rules of cellular automata allow incorporating other growth influential variables into the model such as economic growth variable and global average temperature. Animation, description, and prediction strategies were used to analyze urban growth. The animation is used to analyze regional urban change, further which helped in analyzing natural and human-induced urban growth influencing factors. Model replications produced during the calibration phase have been used in predicting future urban growth. Self-modifying CA has made this study more valuable as now the S curve growth could be analyzed which was not possible in traditional CA.

Batty et al. (1997) described the origin of cellular automata and game of life theory. CA and game of life theory were successfully implemented in an urban system using computational technologies. The game of life theory was first given by Von Neumann.

Batty (1997) conceptualized the urban system simulation and replaced the mathematical model by the rule-based model. After knowing the relationship between cells and urban state transition, the first time urban system was implemented on a cell basis using cellular automata. A generic form of cellular automata for the urban system was described including a cell's neighborhood, transition rules, and cell's state. Some issues were flagged out such as; spatial interaction is important to understand the real and possible patterns of urban change. Also, it is important to understand the relationship between fractal dimension and density. Dimension and density both are different terms and produce different urban patterns. Fractals are basically identified by fragmented and outskirts growth and density indicate growth around urban centers.

Batty and Xie (1997) stated that understanding of the urban system is not only about simulating real patterns of urban phenomenon however, it is also about identifying potential or possible patterns of urban growth. This study includes the analysis of different urban forms using cellular automata. Aerial and linear growth models were separately developed for the urban system and then combined for getting integrated urban forms. The elementary urban automata were developed which included neighborhood game of life rule and

transportation networking link into the model. A road pixel was identified near an urban pixel randomly and neighboring pixels of that road pixel were analyzed for possible conversion of state of that neighboring pixel. The elementary urban automata are very much similar to the SLEUTH model developed by Clarke et al. (1997) but some extensions were embraced in the SLEUTH model. The transportation network was included in the form of weights to analyze possible urban growth near road side areas. The slope in percentage layer was included for providing topographic suitability factor into the model. Land use maps were used for providing land use change (for non- urban classes as well), the exclusion layer for providing restrictions on cells for not being transitioned into another class. Moreover, five growth coefficients i.e. diffusion, breed, spread, road gravity, and slope resistance were used in making decisions of a cell's state change. Although, the idea of SLEUTH was first conceptualized by elementary urban automata only.

Clarke et al. (1997) presented cellular automata based urban growth model to analyze human-induced land use transformation. The urban growth model (SLEUTH) uses five growth controlling factors; diffusion, breed, dispersive, road influenced and slope resistant coefficient. Urban growth has been simulated through four growth rules; spontaneous, diffusive, organic and road influenced growth rules. In addition to these, the second level of growth rules called self-modification rules are also used to control the linear and exponential growth behavior of the model was included into the model.

Takeyama and Couclelis (1997) introduced the concept of spatial dynamics by integrating GIS and CA with geo-algebra. The technique provided useful static, dynamic behavior into the modeling framework. Also, it proved effective in forming the complex spatial dynamics behavior of urban dynamics. The additional features such as multi-layer interactions and the inclusion of external input map layers can be consistently incorporated into map dynamics. An interactive map dynamics opens up the possibility of integrating into GIS new kinds of phenomena and behaviors such as design, learning, and gaming.

Park and Wagner (1997) have coupled CA with GIS to provide an increased ability for dynamic spatial modelling in GIS. GIS suffer from poor handling of dynamic spatial modelling and temporal dimension.

Wagner (1997) explained the limitation of GIS that it cannot handle temporal dimensional behavior and many numbers of variables. So, by integrating GIS with CA these limitations

can be overcome. Since GIS and CA have many similarities so, transition rules, neighborhood rules etc. can be implemented easily.

White et al. (1997) specified that cellular automata are able to give a complex spatially detailed representation. The study is able to produce real patterns of urban growth and sensitivity analysis (by varying the number of iterations.) shows the reproducibility of the outcomes. Site characteristics, transportation network etc. variables were introduced into the study.

Clarke and Gaydos (1998) have calibrated and predicted the urban growth of two study areas; San Francisco Bay area and Washington D.C./Baltimore using SLEUTH. The spatial and statistical measures were computed and compared for these areas. Pearson's r-squared for urban pixels, Pearson's r-squared for urban edges, Pearson's r square for urban clusters and LeeSallee shape index were computed for statistical analysis and validation of calibration and urban growth prediction.

Wu (1998) developed a prototype of a simulation model, SimLand, based on cellular automata (CA), multi-criteria evaluation (MCE) and integrated with GIS to simulate land conversion in the urban-rural fringe. In the study, MCE is not used to provide an optional solution to the land allocation problem, rather, it is used to mimic how land development potential is evaluated via the tradeoff of multiple developmental factors. A method, analytical hierarchy process (AHP) of MCE, is used to derive behavior-oriented rules of transition in CA. Simulation schemes of the model were a projection of land demand, identification of development factors, and preparation of development preference.

Brown et al. (2000) included the Markovian transition probability method to simulate the historical trend. To simulate more realistically it is important to include restrictions on grid cells. But the Markovian method assumes that the system is spatially and temporally static. This study attempts to include socio-economic and bio-physical restrictions on grid cells as land use change is spatially and temporally dynamic in nature. Also, it leads to a more realistic simulation and prediction of urban change.

Silva and Clarke (2002) calibrated the SLEUTH for two Portuguese cities; Lisbon and Porto and demonstrated the detailed and exhaustive calibration process to improve the performance of SLEUTH. Major findings of the study were, first, up to what extent the resolution for spatial data be improved, second, how we can improve the accuracy of spatial

data which is a major part of a SLEUTH calibration process that will definitely improve the performance of the urban growth model. Increasing the number of Monte Carlo simulations will make the model more sensitive to local conditions. Additionally, narrowing down the coefficient ranges may fit the spatial data to model data in a more realistic way. Third, cluster computing would also be a good approach for reducing computation time.

Wu (2002) has demonstrated the use of stochastic cellular automata to determine the rural-urban land conversion. The initial probability of land use change simulation has been driven by observed sequential land use simulation data. Furthermore, initial probability has been updated dynamically by incorporating local characteristics of land use in the form of strength of neighborhood development. Consequently, integration of global- static and local-dynamic factors have been used to produce a more realistic pattern of landscape change.

Xiang and Clarke (2003) explained that scenario building is a major part of land use planning which leads to the sustainable planning of a city.

Dietzel and Clarke (2004a) have shown the robustness of the SLEUTH model for urban growth simulation and LULC change analysis. The study shows that the SLEUTH model replicates the land use patterns in a better way both spatially and temporally. In this study, the LULC change has been handled by Deltatron model.

Dietzel and Clarke (2004b) have investigated the effect of the spatial resolution of the input data sets on SLEUTH calibration and urban growth prediction. SLEUTH was parameterized, calibrated and growth was predicted and compared with input data of three spatial resolution. No significant difference has been observed in SLEUTH calibration and prediction performance except computational time, more time is required with finer resolution data.

Solecki et al. (2004) analyzed the impact of LULC change on climate using the cellular automata based SLEUTH model. First of all, UGM and LCDM model of SLEUTH was calibrated and validated for the study area then some modifications into the source code were made to analyze the change on climate in term of surface albedo and soil factors.

Herold et al. (2005) have described the role of spatial metrics in the field of land use change and urban growth modelling by integrating remote sensing and spatial metrics together.

The study shows that spatial metrics are very helpful in analyzing the spatial and temporal change of urban growth quantitatively. Also, it is utilized in the calibration and validation of the urban model. The hybrid approach of remote sensing, spatial metrics, and urban growth modelling is very promising in analyzing urban growth and LULC change. However, it is in its early phase, depends on the accuracy of spatial metrics so, further improvements will be required in the future. Also, the present research is needed to be tested for different geographical scales.

Jantz et al. (2005) discussed the influence of spatial resolution and geographical extent on urban growth using the CA SLEUTH model. A detailed sensitivity analysis was carried out by simulating the effect of varying the cell size on urban patterns and growth. The resampled input data at different resolution (45m, 90m, 180m, and 360m) were used for exhaustive calibration and sensitivity testing. The study concluded that urban growth is affected by spatial resolution.

Xian and Crane (2005) presented the use of sub-pixel imperviousness for land use change simulation. Sub-pixel imperviousness provides the spatial heterogeneous characteristics of land use change. This was later used in SLEUTH model to simulate the urban growth pattern in a more realistic way for future prediction of urban growth.

Dietzel et al. (2005) provided empirical evidence to the dynamism of urbanization using landscape metrics calculated using FRAGSTATS. Also, results were compared with the results of the SLEUTH urban growth model.

Goldstein et al. (2005) attempted to measure the optimal number of Monte Carlo iterations required for SLEUTH model calibration. The two metrics used for measuring the change in performance of model calibration for a different number of Monte Carlo iterations i.e. OSM (Optimal SLEUTH Metrics) and MCAWS derived diversity metrics. The exhaustive analysis of Monte Carlo runs for the calibration phase of the SLEUTH model reveals that 10 to 25 number of Monte Carlo runs would be required for the optimal calibration of the SLEUTH model.

Syphard et al. (2005) have forecasted the effects of urban growth on habitat pattern in southern California. The principal drivers of land use change considered in the study were population growth and economic expansion. The CA model has been calibrated using historical growth and urban growth was predicted for three urban growth scenarios from

2000 to 2050 with development prohibited on slopes greater than 25%, 30%, and 60% slope.

Batty (2005) demonstrated the inclusion of agents and cells in simulating the patterns of city change in different modelling approaches. The study comprises a thorough review of different modelling approaches at different scales such as mesoscale, micro, and macro scale. The three driving factors were considered most important for identifying potential change i.e. employment, distance, and population. The study revealed that CA and agent-based models are capable of implementing fully policy-based applications which are very limited in present time. Also, as the scale gets finer the number of agents and cells eventually increases which somehow increases the complexity of the model. The biggest problem common in all models is their lack of parsimonious nature. The richness of input data makes the calibration phase complex and prediction accuracy on the basis of past simulation is hard to validate.

Caglioni et al. (2006) have investigated the sensitivity of parameters used in the SLEUTH model such as the diffusion coefficient, breed coefficient, spread coefficient, slope resistant and road gravity coefficient. The study performs the sensitivity analysis of SLEUTH model parameters by increasing and lowering the values of parameters to analyze the effect on landscape change. The study reveals that diffusion, breed, and spread are interrelated with each other. So, the individual performance of each growth type is difficult to interpret and therefore, only the reproduction of overall growth complexity can be observed. It shows that an increase in the spread coefficient by keeping lower values of breed and diffusion coefficients leads to forming high growth clusters. On the other side, by increasing the breed coefficient urban growth increases exponentially and linear growth takes place. Increasing diffusion value also leads to an increase in growth similar to the increased breed coefficient but with a lower rate. Road coefficients lead to the growth along road side areas. Self-modification growth rule is embedded into the model to control the linear and exponential growth.

Li and Liu (2006) introduced an extended method of cellular automata (CA). Rule-based CA has been widely used to simulate urban growth. But there is a limitation in rule-based CA that it is unable to include local characteristics for a large complex region. For overcoming this limitation of rule-based CA an extended form of rule-based CA has been proposed in the present study i.e. Case-based Reasoning (CBR). The commonly used k-NN

algorithm of CBR has been modified to include the location factor which reflects the spatial variation in transition rules.

Dietzel and Clarke (2006a) have worked on two types of model for calibrating and predicting urban growth. Calibration of urban growth was done by using urban/ non-urban classed data model and generated metrics which were used to predict urban growth. On the other side, calibration of urban growth was done using a disaggregating land use classed data model and by generating statistical metrics which were used to predict urban growth. The study shows a large difference in the statistical metrics calculated for the two different models. Also, there is much difference between both urban areas calculated from the two models. The reason for this huge difference in an urban area could be; in urban/ non-urban classed model urban is spreading outwardly from the existing urban centers or urban edges while in disaggregated land use model, the non-urban area is classified into various classes. So, there is a huge probability of transforming disaggregated classes into urban areas.

Dietzel and Clarke (2006b) studied the model performance using the SLEUTH model with different operating systems such as Linux, Solaris, and windows. The study shows that the model is computationally efficient in Linux and Windows environment as compared to its native UNIX/ Solaris environment as faster processors are available in Windows/ Linux.

Gazulis and Clarke (2006) have investigated the performance of the SLEUTH model for its data independency and growth behavior. The temporal sensitivity, data sensitivity, and effects of resolutions are highly recommended for future research.

Clarke et al. (2007) presented a review of SLEUTH model applications for different cities worldwide and shared the different issues and challenges. This include; SLEUTH is a portable model which is globally acceptable as it has been applied in various continents and nations already. Increasing the spatial resolution of input dataset leads to more promising results and makes the model more sensitive towards local characteristics. Applying multistage brute force calibration is helpful for determining best fit coefficient values. Also, the parameters derived from the model can be compared with other model parameters which may lead to the foundation for understanding a complex growth system. SLEUTH can be coupled to combine different applications on the same platform. Moreover, it can be used to provide exploratory visualization. An important step was taken towards improving the computational time by Silva and Clarke, (2002). The study suggests that multi-dimensional sensitivity testing would be needed to analyze the performance of

SLEUTH in the near future. Moreover, issues related to the number of Monte Carlo iteration and robust sensitivity testing of input dataset scale, number of input data layers, parameters ranges, and different parameters like critical slope etc. would be required in the future.

Dietzel and Clarke (2007) presented a composite goodness of fit landscape metric i.e., OSM (Optimal SLEUTH Metric) judging the calibration performance of SLEUTH. The seven metrics were decided by plotting the relationship curve, the metrics with higher influence were chosen to combine with OSM. Fmatch was also included with OSM in case of land use change modelling.

Hu and Lo (2007) compared the performance of a logistic regression based LULC change method and the CA-based SLEUTH model. The logistic regression is not temporally explicit and does not determine when the urban growth will take place. Authors have concluded that a specific resolution dataset is not able to produce all information about heterogeneous growth.

Clarke (2008a) discussed the LULC change mapping using the SLEUTH model. SLEUTH has two modules i.e. UGM (urban growth model) and LCD (Land cover Deltatron model). The author has presented the various applications of the model. The study explains why LCD has not been widely applied in contrast to UGM in various applications. Performance of LCD module was examined by testing its performance with respect to two data sets. The LCD produced linear transition matrix which further needs to produce non-linear behavior as well. Also, inaccurate maps, misclassification and inconsistencies with the class definition is a serious problem of LCD.

Clarke (2008b) has described the cellular automata approach for land use change modelling. The extended CA has been recently developed in various application of land use change modelling. The study reveals that cellular automata can be integrated with agent-based modelling to improve the functionality and prominent outcomes.

Silva et al. (2008) integrated an ecological model with SLEUTH to investigate sustainable urban growth scenarios. CVCA is countervailing cellular automata model. It uses a set of landscape ecological strategies to counteract the urban growth at good to grow areas. The CVCA model requires the same input files as the SLEUTH model such as slope, land use, urban, transportation, and hillshade and excluded map. However, the excluded map is

different from the SLEUTH as the area is not restricted here to get urbanized as in SLEUTH model but the meaning is different here in CVCA. The outputs of CVCA are the same as in SLEUTH model but four more output classes are generated in CVCA such as protective, offensive, defensive, opportunistic and let it grow that matches five landscape planning strategies.

Fan et al. (2008) presented a study of LULC change analysis and prediction using GIS and remote sensing. The study includes the use of multi-temporal satellite data which is classified into a number of land use classes then change detection from the base image is performed using a post-classification comparison method. Markov chain modelling was used to determine the transition probabilities of land use change classes, which assumes some predetermined stochastic variables. The Markov chain based modelling approach has some limitations like it does not consider exogenous and endogenous variables.

Wu et al. (2009) analyzed the performance of the SLEUTH model with respect to three different methods i.e. ROC (Relative Operating Characteristic) method, Multiple Resolution Budget method, and landscape metrics. The study reveals that there are much fewer limitations of the SLEUTH model in the prediction of urban growth. First, the model is more focused on simulating edge growth and limiting the ability of simulating other urban growth. Second, the model is very time consuming and a different number of Monte Carlo simulations produces different statistical metrics which leads to different ranges set for the start step stop values for the calibration. Third, the metrics selection and deciding ranges for the simulation is user dependent which can falsify the prediction of urban growth. Fourth, it does not incorporate other driving factors of urban growth such as socio-economic factors which can improve the performance and real forecasting of urban growth.

Guan and Clarke (2010) developed a general purpose pRPL with any arbitrary neighborhood algorithm to parallelize raster processing so that non-specialist GIScientists can use SLEUTH for urban growth simulation. pRPL accepts multilayer algorithms which are common in geospatial applications nowadays. pRPL includes multiple data-decomposition methods for users which enables raster processing less time taking by reducing communication overhead among processors. A parallel geographic CA model pSLEUTH using pRPL was developed to show the usability of pRPL in raster processing of a model. The study reveals that pSLEUTH greatly reduced computational time of the previous version of SLEUTH.

Irwin (2010) presented a review of different LULC change and urban growth modelling approaches (such as CA, agent-based modelling etc.). The study explains that it would be beneficial if one focus on individual behavior of land use change for small run equilibrium rather long-run equilibrium and should relax the assumption of equilibrium and yet retain the correspondence between individual location and aggregate economic outlet.

Nong and Du (2011) simulated the urban growth using a logistic regression model and compared the performance with the logistic regression-based model. The authors have concluded that the logistic regression method is much more efficient while conducting urban growth modelling for a county-based area rather for a wide area.

Kumar et al. (2011) simulated the urban growth for an Indian city CA-based SLEUTH model. The study reveals that SLEUTH is an appropriate model for coarse resolution data as well in Indian conditions. Also, the study suggests the minor changes to the SLEUTH model to improve the performance in the Indian context.

Syphard et al. (2011) tested the sensitivity of different sources of input data for SLEUTH model calibration which may often contribute to the uncertainty in the prediction. Also, varying temporal resolution contributes to the differences in projected rates of development. The SLEUTH model was calibrated for two different sources of the input dataset. The parameter ranges have been found to be different from two different source data. The study revealed that the model is sensitive to the sources of datasets, class aggregation, and class definition. The study was not able to conclude which one source of input dataset gives better results. The study explains that model might be sensitive to the spatial resolution of input dataset also.

Mahiny and Clarke (2012) introduced the concept of multi-criteria evaluation (MCE) to include multiple land suitability factors into the SLEUTH model in the form of the exclusion layer. The land suitability was derived as a function of 15 explanatory variables such as slope, aspect, pedology, geology, proximity to rivers and water-bodies, proximity to roads, proximity to town edges, land use or land cover, distance to geological faults, forest density, distance to protected areas, underground water depth, distance to villages and industrial sites, climate classification, minimum and maximum temperature and elevation. The MCE weighted scheme takes into account for deciding fuzzy weights (0-1) for each cell of a raster layer. The suitability layer then combined with the exclusion layer and weights were stretched between 1and 100 and the model simulated the land use change

and urban growth. The results were compared with landscape metrics for the validation of model output, for which both with and without MCE suitability layer were considered.

Wu et al. (2012) studied the performance of the size of the neighborhood considered while simulating the urban growth using SLEUTH. Nowadays, spatial scale for land use change analysis has been a major issue of concern. The study was done to determine the effect of neighborhood configuration characteristics and spatial scale on land use change analysis this study has been made. Cellular automata is a prominently used method for analyzing land use change. Different neighborhood configurations were tested for the land use change analysis such as Moore neighborhood, linear neighborhood, planner neighborhood, ribbon neighborhood etc. of different cell sizes (3*3, 4*4 etc.). The study revealed that as the size of CA neighborhood increases, the accuracy of land use changes analysis increases although computational complexity also increases. In the future, the SLEUTH model can be tested for different neighborhood configurations.

Feng and Liu (2013) attempted to simulate LULC change using CA with the heuristic approach of simulation. The simulated annealing (SA) with CA has been integrated to provide dynamic optimization of the CA transition rules. In this approach, an objective function was constructed to form theoretical accumulated disagreement between simulated and actual land use change. The difference between simulated and actual land use change is minimized by using the SA method. SA optimization tool is developed in MATLAB and incorporated CA simulation in GIS as well to give an integrated SACA tool for simulation of land use change. The typical CA is based on a logistic regression model which was later compared with SACA, the study reveals that SACA is more accurate as compared to logistic CA.

Chaudhuri and Clarke (2013) presented a detailed review of SLEUTH applications up to the year 2005. The technical modifications and versions of SLEUTH have been discussed.

Riccioli et al. (2013) used the CA model for finding out the wine production areas. The study determines that there are three kinds of CA model i.e. deterministic CA, stochastic CA, and probabilistic CA.

García et al. (2013) revealed that a large number of parameters are required to introduce the neighborhood effect in the CA-based LULC change and urban growth modelling applications which makes the CA model less flexible. This study proposes a more flexible

CA model by reducing the number of parameters required for the neighborhood effect by introducing a Genetic Algorithm (GA) into the urban CA model.

Akın et al. (2014) explored the sensitivity of the SLEUTH calibration process with respect to different exclusion layers. The classification of satellite imagery was performed using object-oriented methods. Three exclusion layers of different weights were incorporated (1) no restriction, water body was excluded, (2) complete exclusion of water body, green belt and 250m buffer around water body, (3) weighted exclusion for each green belt class. The urban potential cells can be calculated by using some weights incorporated into the probability and a series of spatial variables can be included in the cellular automata. The study revealed that if these rules are used then it will affect the model prediction results.

Clarke (2014b) discussed different aspects of LULC change and urban growth modelling using two approaches i.e. agent-based and cellular automata based modelling. The author has concluded that agent-based models are effective where behavioral processes need to be considered more prominently in the simulation process. On the other side, the cellular automata based method uses the neighborhood as an exploratory variable essentially. ABMs have the potential to integrate multiple models with similar computational methods and dealing with irregular shapes and for preserving heterogeneity across space and time. CA models are applicable to spatially distributed areas (such as diffusive and spread) where some predefined inputs and variables are required, also, scale, extent, geometry and time frame are strictly decided well before the basic behavior of the system starts. ABMs start with no prior input data, past data and system knowledge are absent. ABM based applications are more exploratory than CA-based methods.

Deep and Saklani (2014) analyzed the urban growth pattern using LULC change detection. Furthermore, CA- Markov model has been used to predict urban growth for the future.

Liao et al. (2014) presented a study based on the simulation of LULC change using cellular automata techniques. The transition rules have been determined using CA with Particle Swarm Optimization (PSO) techniques. The traditional CA is not able to include a neighborhood decay factor and optimal values for transition rules so, transition rules were optimized by incorporating a neighbor decay function with PSO algorithm. The study concluded that the results of PSO-NDCA are far efficient and accurate as compared to PSO-CA.

Li et al. (2014) have assessed urban growth and LULC change using the CA-based method. Also, sensitivity analysis of CA transition rules, time steps and stochastic perturbation in a stepwise comparison were done to explore the performance of transition rules in different conditions. The study revealed that the transition rules are the core component of urban CA modelling. Also, the ensemble method (i.e. CART) is a feasible method to improve the performance of urban modelling using CA. In addition, to include the vertical growth phenomenon into LULC change a GIS-based CA model along with linguistic approach has been used in the study. A number of spatial variables in the model for determining the distribution of buildings in space and time have been used. Al-sharif and Pradhan (2014) presented the results of a LULC change study using Markov-CA based model. Markov modelling has been done to determine the land use transition probabilities and change area. Further, Markov-CA integrated model has been used to predict the land use change.

Chaudhuri and Clarke (2014) assessed the accuracy of predicted land use change over a period. Model accuracy was assessed using three methods such as; kappa statistics, kappa simulation, and allocation disagreement and location disagreement. The study revealed that prediction accuracy not only depends on models' performance but on the uncertainty of input data, urban history, and the accuracy of reference maps.

Nouri et al. (2014) demonstrated the application of an integrated approach i.e. CA- Markov for urban growth monitoring and prediction. The study overcomes the limitation of a Markovian model of not incorporating spatial knowledge using cellular automata. The temporal changes were determined by calculating transition probability using a Markov model which was later used in cellular automata for the simulation of land use change. The study is very much effective in simulating the land use changes for the future which has been validated by sample urban growth comparison of observed and modelled land use changes.

Jantz et al. (2014) studied the role of different exclusion/ attraction layers in assessing the impacts of urban growth in different scenarios like uncertainty related to population and employment forecasts. In addition to these, we can incorporate the other growth influential factors into the SLEUTH model.

Yagoub and Al Bizreh (2014) presented a study of LULC changes analysis using Markov-CA modelling. Markov model has been used to assess transition probability and CA has been used for prediction of LULC change.

Li et al. (2015) presented an integrated approach to an ensemble of urban CA models to improve the performance of a single model. The logistic regression based CA has been used first to create an uncertainty map for land use change. Furthermore, CART and ANN-based models have been used to improve the performances of land use transition rules. Consequently, a self-adaptive k-NN (k nearest neighbor algorithm) has been used to refine the transition rules more accurately. Thereafter, final integrated transition rules were used to simulate land use change for the study area.

Lu et al. (2015) presented a study of LULC change analysis using a vector based cellular automata method. The vector-based CA approach eliminates the scale sensitivity issues related to spatial data. The study reveals that vector-based CA is more accurate as compared to raster-based CA in simulating land use change when compared with real land use data.

Han et al. (2015) predicted urban growth using the cellular automata based SLEUTH model. The model was calibrated and predicted for the year 2050 using two scenarios i.e. historical growth scenario and compact growth scenario. In the historical growth scenario, urban growth was simulated using the historical trend of urban areas. In the second i.e. compact growth scenario urban growth was simulated and predicted by reducing the spread and road gravity coefficient to 50% and then simulation was performed. Afterward, a comparison between both the scenarios was performed.

Houet et al. (2016) developed a CA-based SLEUTH model which is able to produce trend breaking future scenario results and follows the non-path dependent approach. This latest version of SLEUTH introduced a new parameter i.e. land demand into the model which was calculated from a user-defined scenario file or external model. The model provides improved performance in the field of land use change modelling.

Clarke, (2017) presented a new version of SLEUTH i.e., SLEUTH-GA in which brute force calibration method was replaced with a genetic algorithm (GA). The model was calibrated successfully and calibration performance from both the algorithms GA as well as the brute force was compared. GA based calibration has used very less computational time as compared to the brute force method.

Jat and Saxena (2018) demonstrated the application of SLEUTH in deriving sustainable land use policies. Different types of targeted sustainability objectives were included in the exclusion layer and corresponding urban growth scenarios were generated.

Saxena and Jat (2018) presented a comparative study of calibration performance of brute force and GA based methods in simulating the urban growth of Ajmer city (India) in term of computational time required and ability to capture a different type of urban growths. Urban growth predicted from both methods was also compared to ascertain the change in model behavior from two different calibration methods. GA based calibration method has been found to be better in term of few aspects like computational efficiency, better goodness of fit landscape metrics and accuracy in term of hit-miss- false alarm.

2.7 Land Use/ Land Cover Change Using Remote Sensing

Singh (1998) compared the remote sensing based LULC change detection techniques. Performance of thresholding, digital change detection techniques (like univariate image differencing), image regression, image rationing, vegetation index differencing, Principal Component Analysis (PCA), Post Classification Comparison (PCC), direct multi-date classification, change vector analysis, background subtraction and other methods like Kolmogrov Smirnov test LULC change detection techniques have been analyzed. The study gives an overview of all the change detection outputs obtained from various change detection methods. But, there is a lack of quantitative and spatial assessment of land use change as no visual interpretation has been done in this study. Also, there should be a measure of accuracies obtained by all the methods of change detection so it would be better to judge the suitable method of change detection for the respective study area.

Turner et al. (1989) analyzed the land use change pattern on different spatial scales using Shannon's diversity index, dominance (D) and Contagion (C) methods.

Prakash and Gupta (1998) gave a study on LULC change detection by using different image processing techniques. As for detecting vegetation NDVI differencing method is used. Band ratioing and image differencing methods were also applied for the assessment of change detection for all the land use classes using different years satellite imagery.

Different authors like Su (1998), Jaiswal et al. (1999) , Jha et al. (2000), López et al. (2001), Ryavec (2001), Bisht and Kothyari (2001), Gautam et al. (2002), Wilson et al. (2003), and Bajracharya et al. (2010) presented the role of GIS in urban growth simulation and LULC change assessment. How urban growth modelling can be integrated with GIS or GIS can be embedded in urban growth modelling has been discussed. Various issues like spatiotemporal scalability limitations have also been discussed.

Lambin et al. (2000) compared different land use change modelling approaches and the best approach for the prediction of land use change intensification have been identified. The dynamic process-based modelling approach seems better to predict the land use change intensification. Although, stochastic and optimization approaches may be useful to incorporate the decision making of land use change.

Irwin and Geoghegan (2001) presented the theory, data, and methods of explicit economic interaction models of land use change detection. The study revealed the variables which can be incorporated for understanding the land use change phenomenon in a better way. The authors have concluded that a benefit of structural economic models is to model human behavior directly into the land use change model rather than the consequences of human behavior. Spatially explicit LULC change models were classified into three broad categories; simulation, estimation, and hybrid. Many of the simulation models found that the cellular automata approach based model lies in a category of a mathematical model in which behavior of the system is determined by some predefined set of deterministic and probabilistic growth rules which decide the state of each cell. The state of the cell in time t+1 is dependent on the state of that cell in time t, this condition is not true for vice-versa.

Zhang et al. (2002) proposed a new method of the structural method using road density in combination with spectral bands for reducing the spectral confusion among built-up and non-built-up areas. The road density information was extracted from the Gradient Direction Profile Analysis (GDPA). The GDPA algorithm has been found to be useful in creating another spectral band for the road layer and then integrating with other spectral bands so that spectral confusion can later be reduced while doing LULC change detection. Spectral structural post-classification comparison (SSPCC) and spectral structural image differencing (SSID) methods were used and compared with change detection using the spectral only method. The proposed method SSPCC was found to be an efficient method for reducing the spectral confusion. This study revealed that the built-up can be better extracted from this method which can be further used in urban growth simulations.

Petit and Lambin (2002) revealed that the integration of data leads to better analysis of the landscape pattern but there is some discrepancy in the results of different methods. Like, change detection results using data integration methods are far different from the change detection results estimated before the data integration. Also, after data integration, it is not

possible to analyze landscape pattern at the same resolution. Moreover, data integration using older data may often lead to coarser resolution data.

Petrov and Sugumaran (2005) used an integrated approach of CA and Markov model to investigate the losses in agriculture filed due to urbanization. Also, the future prediction has been done to analyze the losses that may occur in near future due to rampantly growing urbanization.

Dietzel et al. (2005) determined the spatiotemporal urban dynamics and validated through landscape metrics such as the index of contagion, the mean nearest neighbor distance, urban patch density, and edge density. The study also analyzed the diffusive and coalescence growth patterns using these metrics. The study suggests that spatial dynamics factor is a crucial one in determining the urban dynamics which must be incorporated in future research.

Jat et al. (2008) analyzed urban sprawl using Shannon's entropy, patchiness, urban density and landscape metrics. Quantification and pattern analysis have also been done using remote sensing and landscape metrics. Future studies can be done by incorporating more metrics.

Beekhuizen and Clarke (2010) presented a geo-computational approach for satellite image classification. This approach aims to improve classification accuracy and revealed the uncertain areas. The classification was performed by different methods such as image texture and band ratioing. For each land use, class probability maps were prepared. By selecting the land use class with the highest class probability for each pixel, a hard classification was performed. Also, corresponding probabilities in a separate map were stored indicating the spatial uncertainty in the hard classification. By combining the uncertainty map and hard classification probability based land use map spatial uncertainty was quantified. The technique was tested for both the images of ASTER and Landsat 5.

Otukei and Blaschke (2010) performed LULC change analysis using GIS and Remote sensing. The maximum likelihood classification (MLC), Support Vector Machine (SVM) and Decision Tree (DT) have been used for image classification and compared. Also, decision tree (DT) method was introduced for the first time for the assessment of land use change which shows faster results as compared to other methods. DT provides the freedom of statistical data distribution assumptions which make it more reliable. The accuracy of

DT was compared with the results of MLC and SVM and found to be 86%. Huang et al. (2010) demonstrated the use of Support Vector Machine tools (SVMs) for analyzing the LULC change. SVM uses a quadratic programming problem for classification of land use classes. For removing classification errors and including non-linearity and complexity of classification a kernel was also used. The SVMs proves its effectiveness in the field of land use change and prediction analysis by comparing it with logistic regression methods.

Pandey et al. (2013) presented a study to examine the vertical growth aspect using Cartosat I stereo pair satellite data and a DEM for the study area. The vertical urban growth has been examined by comparing horizontal urban sprawl with high-density contours and slopying terrains. However, the study is not validated with any of the recognized methods which can be improved in further studies.

Mao et al. (2013) analyzed LULC change using CA. Especially impacts of land use change on ecology has been analyzed by using LUESP (Land use Ecology Security Patterns) model. This study calculates some index and landscape metrics with the help of which secured ecology patterns have been developed.

Hepinstall-Cymerman et al. (2013) presented a study to determine the LULC change and urban growth using landscape metrics, such as shape index, Shannon's entropy etc. The land use change and urban sprawl have been compared region wise with population growth and economic growth. Also, urban sprawl outside the urban boundaries has been determined for the sustainable and smart growth of regions.

Sankhala and Singh (2014) assessed urban sprawl and LULC change by classifying different years of satellite imagery. The urban area of different years was extracted and overlaid to analyze urban growth. The study reveals that urban sprawl has been taking place in an uncontrolled manner in the south and west directions. The impact of uncontrolled urban sprawl would be on slums and associated health hazards, traffic congestion, pollution and health hazards, reduced social interactions due to low-density sub-urban development.

Alkimim et al. (2015) developed an alternative scenario of pastures land potential areas to be converted into sugarcane crops to meet the demand of Brazil's national commodity. The sugarcane crops have been reduced in a large amount in last few decades in Brazil. The study utilizes a multi-criteria evaluation method to find out the suitable potential areas for sugarcane crops. Land suitability factors were taken into account for making multi-criteria

decision making (MCDM), these include soil suitability, climate, topography, biome, land use and socio-economic (education, age, employed people in farming, the value of agricultural production) and infrastructure variables. To support planning and decision making the analytical hierarchy process was used to incorporate MCE. Also, the GIS model builder has been used to compute MCE.

Sar et al. (2015) assessed water logging hazard vulnerability and risk using a combined approach of GIS and Remote Sensing. The Analytical Hierarchy Process (AHP) has been used along with GIS and remote sensing. The effect of the spatial pattern of green land cover on urban surface temperature has been assessed by linkages between structure, configuration, and composition of grass land cover and urban land surface temperature. Important landscape metrics such as nearest distance, patch area, the parameter to area shape index and core area index were chosen and applied to analyze the potential effects of grass land cover on urban surface temperature. The study reveals that all the metrics were significantly correlated with urban land surface temperature and nearest distance metrics found to be best correlated with urban land surface temperature. A stepwise multiple linear regression (R2) model was developed to explain the relationship between urban land surface temperature and green land cover. The NDVI (Normalized Difference Vegetation Index) and NDWI (Normalized Difference Water Index) were calculated to extract the green land cover and water bodies respectively.

Zeng et al. (2015) determined the spatial pattern of urban sprawl by landscape metrics such as Shannon's entropy, gravity center migration, and spatial autocorrelation index. Spatial autocorrelation of urban land measures the decentralization of urban areas, Shannon's entropy is a well-accepted metric used to measure the degree of spatial concentration and dispersion of built-up land. Potential driving forces behind urban sprawl were determined by using time series data of the area (area affected by urban construction) and area of cultivated land. Two types of spatially explicit regression models were used for spatial modelling. First, a spatial lag model which takes into account spatial autocorrelation as an explanatory variable. Second, a geographically weighted regression model is a locally linear spatial model, the model can embody distances in the form of weights.

Gilani et al. (2015) analyzed LULC change using GIS and Remote Sensing techniques. The object-oriented methods for classification of satellite imagery have been used which improved the accuracy of classification and land use change analysis. This study lacks in

the prediction capability of the method, but we can further integrate the prediction methods to the existing one.

Nolè et al. (2015) analyzed the spatial pattern of urban sprawl using ASTER data of 15-meter resolution and data of 14 bands including the thermal infrared band. Two different methods of image classification were compared i.e. maximum likelihood supervised classification and support vector machine (SVM). GRASS GIS, Q GIS software which was used for database implementation and R software which is basically a statistical software were used for implementing maximum likelihood and supervised algorithms. Different accuracy measures were incorporated in analyzing the accuracy of classified outputs such as the producer's accuracy and consumer's accuracy. In producer's accuracy the ratio of the number of pixels accurately classified for the class/ total number of pixels of that class, whereas, in consumer's accuracy we determine the ratio of the number of pixels accurately classified for the class/ the number of pixels classified for the class.

Magarotto et al. (2016) identified 3-dimensional urban growth using 3 dimensional GIS techniques. The vertical urban growth has been identified by using volumetric index by considering floor heights and number of floors. Also, the prediction of vertical urban growth has been done.

Keshtkar and Voigt (2016) demonstrated the LULC change using an integrated approach of Markov and CA model. Also, weight to the driving factors has been assigned using MCE (multi-criteria evaluation) for creating the land use change suitability maps.

2.8 Concluding Remarks

A variety of approaches and models has been reported which are capable of simulating LULC change and urban growth. Different aspects of LULC change and urban growth modelling and simulation were discussed through representative case studies. A comparative analysis was done about different modelling approaches and urban growth model as presented in Annexure I. Models have been found to be suitable for the different applications, have different input data requirements are suitable for different temporal & spatial scales, have different computational requirements and are based on different modelling approaches. There is no agreement among researchers and users about the most suitable model. An individual model is suitable in a set of conditions and has a different level of limitations also. The SLEUTH model has been found to be a promising LULC

change and urban growth model. To date, SLEUTH has been applied to a variety of international urban regions for various type of applications (Akin et al., 2014, Saxena et al., 2016). The SLEUTH model is a scale-independent, generalized and open source model available with its source code, which has motivated research to further improve and modify it for different applications. Details of reported applications of SLEUTH are presented in ANNEXURE II.

In the Indian context, very few studies have been reported related to urban growth modelling and prediction (KanthaKumar et al. 2011; Sankhala, and Singh 2014: Saxena et al. 2016). Different Authors have used post-classification comparison methods for arriving at LULC changes and trends in urban growth for the different parts of the country (Singh, 1989; Patra and Ghosh, 2008; Kumar and Kaur, 2013). Few authors have tried to study the urban growth form and sprawl using landscape metrics for different parts of the country (Sudhira et. al., 2005; Jat et. al., 2008). However, detailed investigation of urban growth and LULC change modelling using CA-based approaches are lacking from an Indian perspective.

Research issues and challenges have been identified through the literature review which helped in deciding the research question to be addressed in deciding the research objectives. There are many research issues and challenges that still need to be addressed for accurate LULC change and urban growth modelling and prediction. Many approaches and models are available which are based on different assumptions, require different input parameters, have different suitability and are appropriate for a particular spatial & temporal resolutions, consider different change drivers & processes and use different methods to model & predict the LULC change and urban growth. Many models developed and reported in the literature have not been tested for different socio-economic and geographical settings and the sensitivity of their parameters has not been evaluated so far. The following research questions have been formulated based on the research issues discussed above-

- ✓ What are the research issues in LULC change and urban growth assessment approaches and models?
- ✓ What are the important drivers and factors of urban growth?
- ✓ How is the performance of the SLEUTH model in simulating the urban growth of cities/ towns or urban areas having socio-economic conditions of developing countries like India?

- ✓ What is the SLEUTH model sensitivity for different model constants and parameters?
- ✓ What are the important explanatory variables of urban growth and how the performance of the SLEUTH model can be improved by incorporating important explanatory variables of urban growth?
- ✓ How the built-up density/ urban intensity can be simulated?

CHAPTER 3
STUDY AREA AND GIS DATABASE CREATION

3.1 Prologue

Ajmer fringe including Pushkar town has been selected as the study area for the application demonstration of the improved SLEUTH Model. Pushkar municipal area has been used as the study area to develop SLEUTH-Density and SLEUTH-Suitability versions. Their application has been demonstrated for simulation of urban growth and estimation of built-up density for Ajmer fringe. “Smart cities” is the catch line nowadays in India, as the Government of India (GOI) has decided to develop 100 smart cities and Ajmer is one of them. Ajmer is situated in the central part of Rajasthan State in India. Ajmer is one of the important cities having great historical and cultural importance. Its population in the year 2011 was around 551360 and is expected to be 840,000 in the year 2034, as per the present growth rate. The atmospheric conditions of Ajmer fringe are attributed to its arid environment with high temperature and erratic rainfall.

The present study involves LULC change and urban growth modelling which requires historical LULC information as one of the key variables. In early days, LULC information was obtained from aerial maps and ancillary data, after the advancement in the field of geospatial technologies, improved data with better resolution and quality can be captured. Geospatial techniques like Remote Sensing (RS) enable us to capture multi-date and multi-resolution satellite data, which are further processed digitally to extract the LULC information.

In addition to the LULC information, other spatial and non-spatial data are also required for the study like slope, road network, the location of different facilities and land marks, hill shade etc. Spatial data are related to a geographic location such as slope, roads, topographical information etc. On the other side, non-spatial data are free from geometric considerations and contains attributes like population, land cost, distances etc. however, we can relate it with spatial data in a Geographic Information System (GIS). GIS provides a platform for integration of data from diverse sources, available in different formats and resolutions into a uniform and standard format suitable for modelling of LULC change and urban growth. A suitable GIS database with required attributes has been created for the parameterization of models.

The study utilizes a LULC change and urban growth model i.e. SLEUTH which is an acronym for its input layers Slope, Land use, Exclusion, Urban, Transportation and Hillshade for modelling of urban growth. The GIS database, which includes thematic layers of historical urban areas, road, DEM, slope, and hillshade etc. has been utilized for the parameterization of the SLEUTH model and its improved versions.

This chapter presents salient characteristics of the study areas i.e. Ajmer fringe and Pushkar in terms of location & their extent, topography, climate, water resources, transportation, tourism, population, education, urban growth, reserved areas, and land use. It further extends the details of software and data utilized for the processing and analysis of spatial and non-spatial data in the form of the raster, vector data, and text. Subsequently, extraction of LULC information and creation of the GIS database has been discussed in this chapter.

3.2 Location and Extent of Study Area

Ajmer fringe including Pushkar is located between 26°20'N to 26°35'N latitudes and 74°33'E to 74°45'E longitudes (Figure 3.1). Ajmer is the 5th largest city of Rajasthan state and is the center of the eponymous Ajmer District. It is located 135 kilometers southwest of Jaipur, capital of Rajasthan, 190 km from Kota, 274 km from Udaipur, 439 km from Jaisalmer, and 391 km from Delhi. Ajmer is situated between the two valleys, one formed by the Taragarh & Madar Hills and the other by the Madar Hill & Bhutia Dungar. Ajmer is situated along the Aravalli mountain ranges at an average of 486.0 meters above MSL. Pushkar is located around 15 km from the Ajmer city Centre in the west direction.

3.2.1 Population

Ajmer fringe has a population of around 551,360 according to the 2011 census and it is expected to be 0.84 million in 2034, as per the present growth rate. Pushkar town lies in the Ajmer fringe and municipal boundary and its population is around 21,626.

3.2.2 Climate

Ajmer and Pushkar have a hot, semi-arid climate with over 55 centimeters (25.4 in) of average rainfall every year. Usually, rainfall occurs in the Monsoon season, which spread from the month of June to September. Average temperature remains relatively high i.e.,

30 °C throughout the year. The winter months of November to February are mild and average temperature varies from 15 – 18 °C with little or no humidity.

3.2.3 Tourism

Anasagar Lake, Baradari, Dargah of Sufi saint, Moinuddin Chishti and Brahma Ji Temple in Pushkar are eminent tourist centers of the Ajmer fringe which attracts a large number of tourists and a source of income.

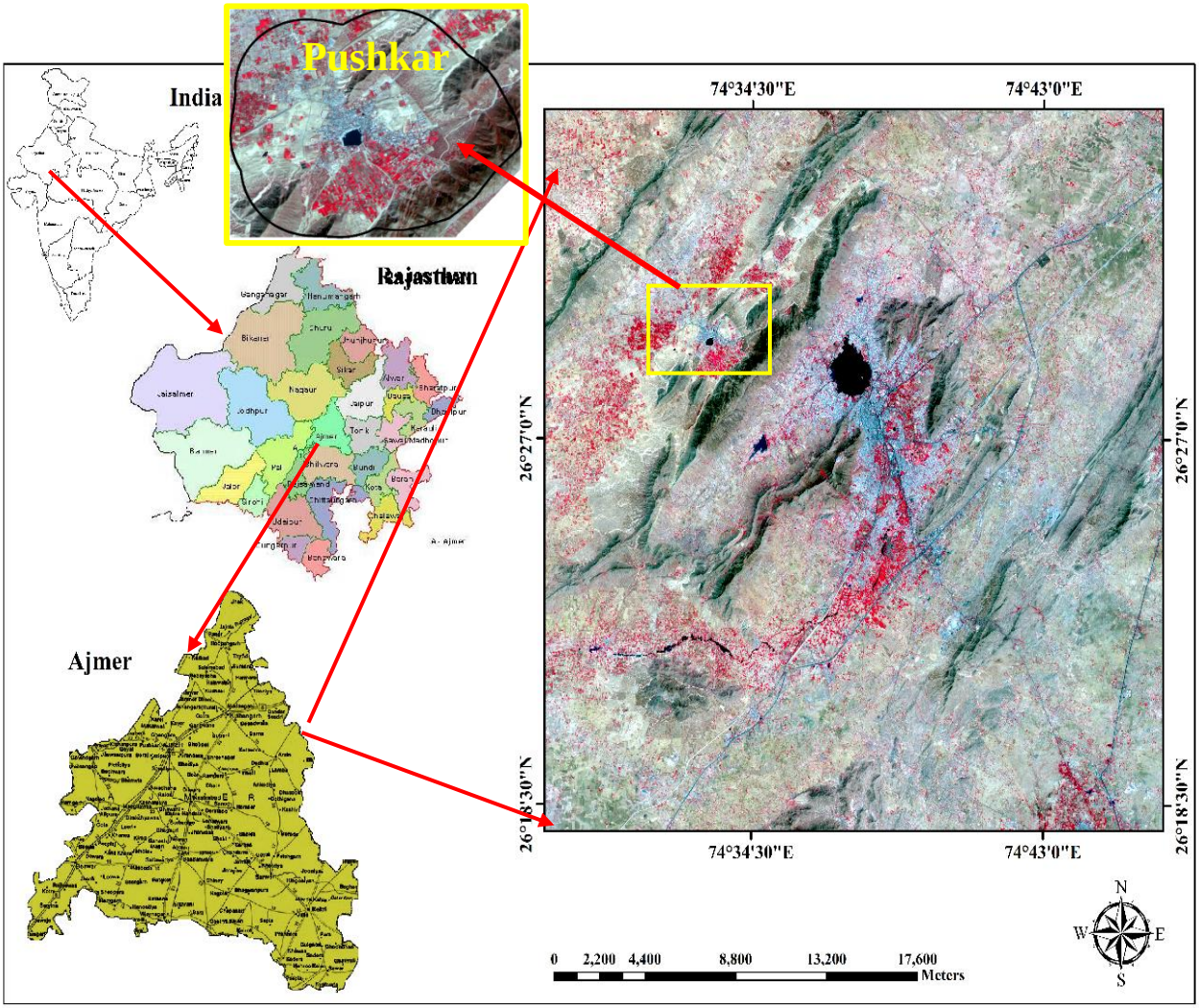

Figure 3.1: Study area

3.2.4 Transportation

Ajmer is well connected by road and railways. The Ajmer Junction is the main railway station situated in the city and was built during colonial times. A good road connectivity via Ajmer-Jaipur expressway i.e. NH-8 has also provided a way for many people to visit Ajmer from nearby locations. Kishangarh airport is situated on NH – 8 around 27 km North-East of Ajmer which connects to New Delhi on a daily basis.

3.2.5 Socio-economic conditions

Apart from having historic importance Ajmer is one of the major centers of higher learning and specialized education in Rajasthan. The official language is Hindi and another language is Marwari. Transportation, animal husbandry and tourism are the major sources of economy.

3.2.6 Land use/ land cover in Ajmer

As per the present master plan, the total urbanized area of Ajmer fringe is 53.8 sq.km of which 45.9 sq.km is the developed area, i.e. 85% of the total urban area. 5% of the total area is government reserved land under CRPF and Defense force. The remaining 10% area comprises open spaces and water bodies. Out of the total developed area, the largest land is under residential use (45%) followed by transport infrastructure (18%) and public & semi-public use (12%). Mixed land use is prominent, in the inner city (Joshi et al., 2011). There are seven (7) major LULC categories in Ajmer fringe including Pushkar like barren, open, rocky terrain, built-up, vegetation, water, and river sand. A number of water bodies exist in Ajmer fringe such as Anasagar, Foy Sagar, and Pushkar Lake, which forms the focal point of the city. The Anasagar zone consisting of Anasagar area, Vaishali Nagar and Chaurasiyawas have the lowest population density of fewer than 2,000 persons/sq.km. While the average population density of the city is 5,750 persons/sq.km.

3.3 Data Used

The present study utilizes seven years of multi-spectral satellite data procured from National Remote Sensing Centre (NRSC), United States Geological Survey (USGS) earth explorer and Global Land Cover Facility (GLCF). The study utilizes DEM (to create a slope map which has been prepared from a 1.0-meter contour map), Ajmer district map, Ajmer & Pushkar Master Plans and Survey of India (SOI) toposheets. Demographic data were obtained from the Census of India for the year 2011 and the land cost data were obtained from the Planning Commission of India and the Department of Revenue, Government of Rajasthan India. Details of the satellite data used in the study are presented in Table 3.1.

Apart from satellite imagery, other data used in the study are an AutoCAD map of Ajmer city, 1.0 m contour map, SOI Toposheets, Ajmer master plan, and Google Earth satellite imagery (for preparing reference point file) as presented in Table 3.2. Few datasets used for the resent work have been presented in Figures 3.2 and 3.3. FCC (False

Color Composite) of the satellite imageries used in the present work has been presented in subsequent sections.

Table 3.1: Salient details for 5 meter resolution satellite imagery

S. no.	Year	Satellite and sensors	Spatial resolution in meter (m)		Spectral resolution
1	1997	IRS 1C PAN + IRS LISS III	PAN	5.8	Single band
			Multispectral	23.5	4 bands
2	2000	IRS 1D PAN + RS 1 LISS III	PAN	5.8	Single band
			Multispectral	23.5	4 bands
3	2004	Resourcesat LISS IV	Reflective	5.8	3 bands
4	2008	IRS 1D PAN + RS 1 LISS III	PAN	5.8	Single band
			Multispectral	23.5	4 bands
5	2013	Resourcesat 2 LISS IV	Multispectral	5.8	3 bands
6	2015	Resourcesat 2 LISS IV	Multispectral	5.8	3 bands
7	2018	Sentinel-2	Multispectral	10	4 bands

3.4 Software Used

The study, processing, and analysis of satellite imagery are very important processes to be followed for extracting LULC information and creation of a GIS database. All these tasks can be done using geospatial techniques, which are available in different image processing and GIS software. There are various image processing software like ERDAS Imagine, ENVI, eCognition, ILWIS etc. In the present study, ERDAS Imagine has been utilized for processing of imagery and ArcGIS has been used for the creation of a GIS database.

Table 3.2: Salient details of other used data

S. no.	Input data	Specifications	Fig no.
1	SOI Toposheet	1:25,000 scale (year1991)	3.2
2	DEM	1.0 m resolution	3.2
3	AutoCAD Map	1.0 m resolution	3.3
4	Ajmer district plan map	1:1000000 scale (year 1991)	3.3

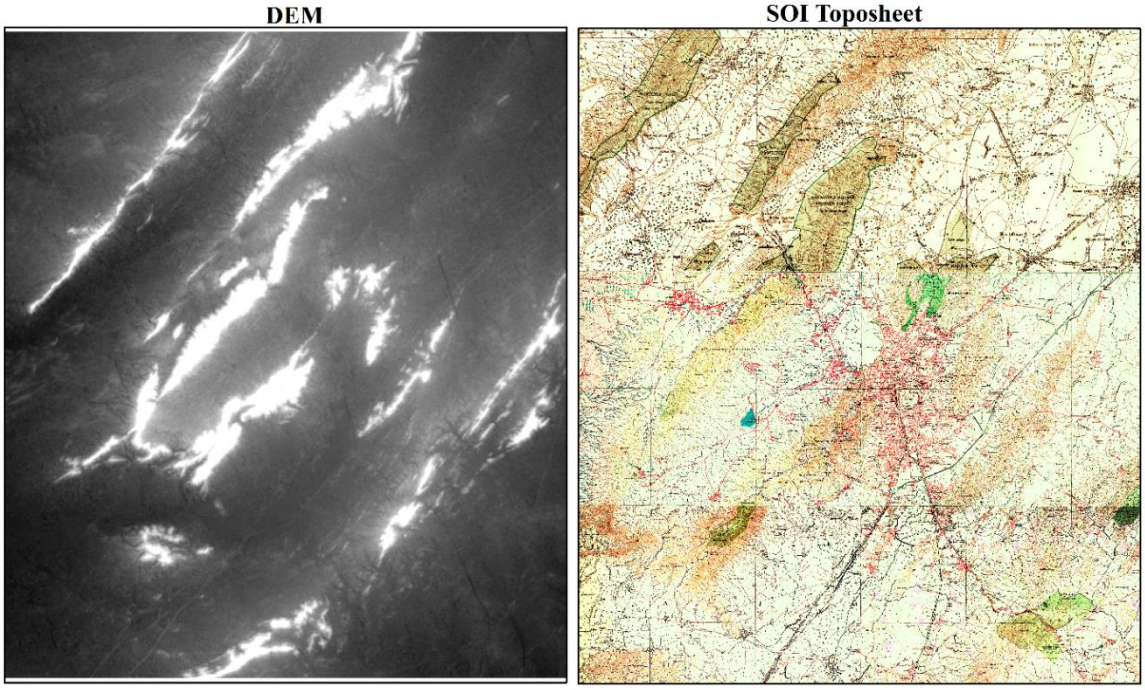

Figure 3.2: DEM and SOI Toposheets

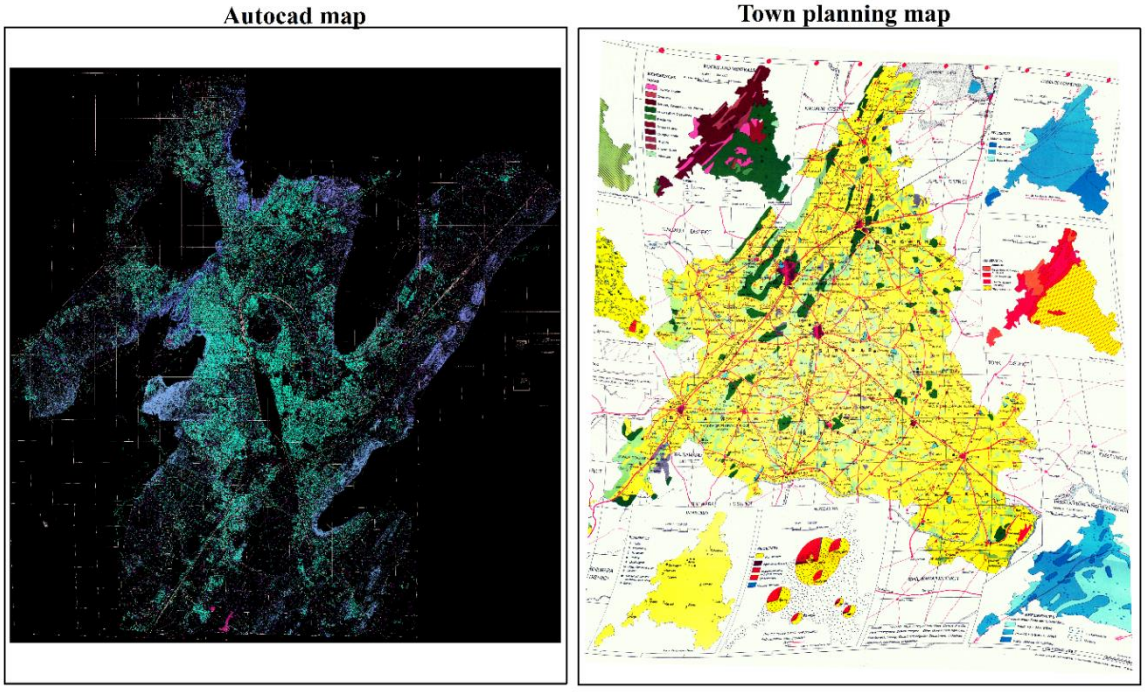

Figure 3.3: AutoCAD map and town planning map

3.4.1 ERDAS Imagine

ERDAS imagine is an image processing software developed by Leica Geosystems (USA). ERDAS Imagine has extensive image processing capabilities like image rectification, radiometric corrections, image enhancement, image classification and processing of stereo images (LPS module) in addition to limited GIS capabilities.

In the present work, ERDAS Imagine version 2013 has been used. ERDAS Imagine includes various modules for the processing and analysis of raster and vector data such as manage module for data management operations like import and export of data etc., raster module for processing of raster data like radiometric correction techniques e.g. haze reduction, noise reduction, LUT stretch, rescaling, histogram matching, topographic normalize resolution merge, image classification etc., vector module for the processing and analysis of vector data like creation of shape file, attribute data handling and analysis, terrain module have tools for the processing of elevation information like preparation of the DEM and its derivatives, multi-spectral module consists of tools to deal with multi-spectral data like layer stacking spectral & spatial profiles, contrast manipulation techniques etc., LPS module for the processing of stereo images and derivation of elevation information, in addition to a few more modules available for different image processing functions.

3.4.2 ArcGIS

ArcGIS is the name of a group of Geographic Information System software developed by Environmental Systems Research Institute (ESRI). In the present study, ArcGIS version 10.5 has been used, which has capabilities for data manipulation, editing, and analysis. ArcGIS is the highest level of licensing in the ArcGIS product line and provides full advanced analysis and data management capabilities including geostatistical and topological analysis tools. It includes and builds on the features of ArcReader, ArcView, and ArcEditor, adding geoprocessing functionality. It is a vector data based software, however, it can be used for raster data analysis also using the Spatial Analyst Module.

ArcGIS comprises three basic modules; ArcMap, ArcCatalog, and ArcToolbox. ArcMap is very simple to use. Its capability of switching on the required module e.g. Spatial Analyst, 3D Analyst etc., at the time of need, made it computationally very efficient. ArcMap is used to display and query maps, create publication-quality hard copies, develop custom map applications, and perform many other map-based tasks. ArcMap provides an easy and natural transition from viewing a map to editing its geography. ArcCatalog is used to explore and manage the spatial data stored in folders on local disks or in relational databases that are available on your network. ArcToolbox provides an environment for performing geo-processing operations, like data conversion, import-export. Also, operations for recoding of data and overlaying of raster layers are

used in ArcMap. ArcMap's layout composer is used to prepare cartographic-quality maps for presentation. ArcGIS has very powerful customization capabilities using Arc Objects and Arc Macro Language (AML), Visual Basics (VB) and Python programming languages.

3.4.3 Cygwin

Cygwin is a software cum emulator used as an interface between two different operating systems like Windows and LINUX/UNIX. Cygwin provides a virtual UNIX environment in Windows to run the SLEUTH model, which is UNIX/ LINUX based.

3.4.4 Other used software

Other software such as Microsoft Word has been used for preparing documents and formatting of reports; Microsoft Excel is used for creating reports in tabular format; Notepad++, ERDAS Imagine produces accuracy reports and error matrices in text format and SLEUTH scenario files are large sized text files which can be best viewed in Notepad++.

3.5 Analysis of Satellite Data

LULC information extraction is the primary objective of satellite data analysis, which includes various crucial steps i.e. pre-processing of satellite data, rectification/ geo-referencing and image classification. Pre-processing of satellite data includes radiometric and atmospheric corrections to be applied before processing the satellite data while rectification/ geo-referencing and classification is the post-processing of satellite data to obtain some meaningful information from the data. Classification of multi-spectral data is the process of sorting out the pixels based on its reflectance values into a finite number of LULC classes. These classes are LULC features available on the Earth surface like water, rocky-terrain, shrubs, forest, built-up, wetland, grassland etc. The pixels satisfying certain criteria are assigned to the respective classes which is known as image classification or segmentation (Jensen, 1996). An algorithm is implemented on a computing system to perform satellite image classification that is called digital image classification. In the present study, ERDAS Imagine software has been used to perform image classification.

The overall methodology of the satellite data analysis and LULC extraction is presented in Figure 3.4.

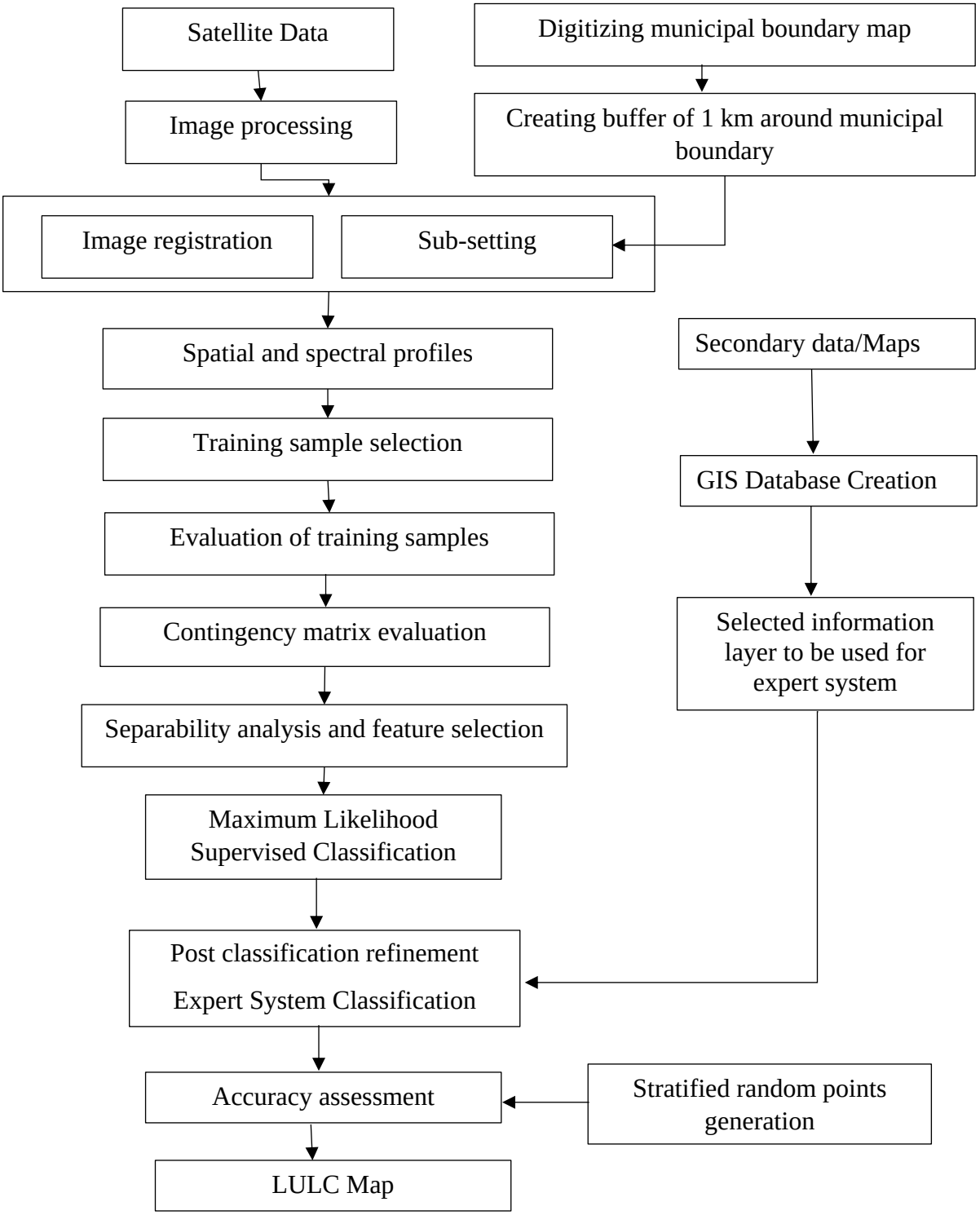

Figure 3.4: Overall methodology for the analysis of satellite data

3.5.1 Pre-processing of satellite data

When satellite data is captured from sensors, it may have some kind of noise/ error like atmospheric and radiometric noise. Such noise can be reduced or removed through atmospheric and radiometric corrections. Satellite data used in the present study is free from such errors except for small cloud cover in an image which has been removed using haze and noise reduction tools available in ERDAS Imagine.

3.5.2 Rectification and projection of satellite data

After performing atmospheric corrections satellite imagery have been rectified and geometrically corrected corresponding to UTM WGS 84 coordinate and projection system (Zone 43). Accurate geometric correction of satellite imagery is an essential part before performing classification. All the images are processed for geometric corrections using ground control points (GCP's) obtained from SOI toposheets. Some of the SOI toposheets are in Polyconic projection system which has first registered to UTM WGS 84 system using nearest neighborhood re-sampling algorithm and third order polynomial geometric model.

The registration error i.e. RMS (Root Mean Square) error was found to be within the acceptable limits i.e. < 1.0 pixel. Further, satellite imagery of different years has been geo-referenced with respect to WGS 84 ellipsoid parameters and UTM projection system (Zone-43). Third order polynomial geometric model was used with 20 GCP's obtained from rectified SOI toposheet. Registration error (RMS error) has been restricted to less than 1.0 pixel. The nearest neighborhood resampling method was used while geo-referencing the images.

3.5.3 Study of satellite images

First of all, rectified satellite imagery was re-sampled for the study area extent, decided as municipal limit plus 1.0 km for Ajmer and Pushkar. Further, FCCs (False Color Composites) were prepared from the stacking of three band data corresponding to three primary colors. The near-infrared, red and green band were stacked corresponding to the red green and blue colors to prepare the color composite. The FCCs prepared for Pushkar town and Ajmer fringe are presented in Figures 3.5 & 3.6, respectively. Since every single satellite image consists of multiple bands, we falsely change the order of bands to get a visually better image. The Green band is falsely assigned to blue, red band is falsely assigned to the green and near-infrared band is assigned to red color. We have chosen this

order to prepare FCCs because more vegetation differences can be clearly identified from the red color for which our eyes are more sensitive. The satellite imagery is explored and studied extensively to ascertain the identifiable LULC classes and their respective ranges of brightness value (i.e. reflectance or digital values). Spectral profiles have been drawn to check the separability and relative differences in brightness values of different LULC class pixels. This method gives an idea about the number of classes present in a landscape in imagery and also the separability of every LULC class in different bands.

Spectral profiles for 5-meter spatial resolution satellite data of different years for different targeted LULC classes have been shown in Figure 3.7. It is evident from Figure 3.7 that the LULC classes like built-up, forest, rocky terrain, water, shrubs, sparse vegetation, paved, river sand and open are almost overlapping in bands 1 & 2 and have some difference in band 3. However, in band 4 almost land use classes can be identified separately with much differences in their brightness values observed. Thus, LULC classes are separable in band 4 for most of the years as shown in Figure 3.7 B & C.

Significant differences in brightness values for different LULC classes in band 3 have been found for the year 2013 and 2015 (LISS-IV sensor data), as shown in Figure 3.7 D & E. Thus, it is clear from the spectral profiles that band 3 and band 4 are the bands in which most of the LULC classes are separable. In addition, the brightness value of pixels related to different LULC classes has been explored through the inquire cursor in ERDAS Imagine to have an idea about the ranges of brightness values in different bands as shown in Table 3.3.

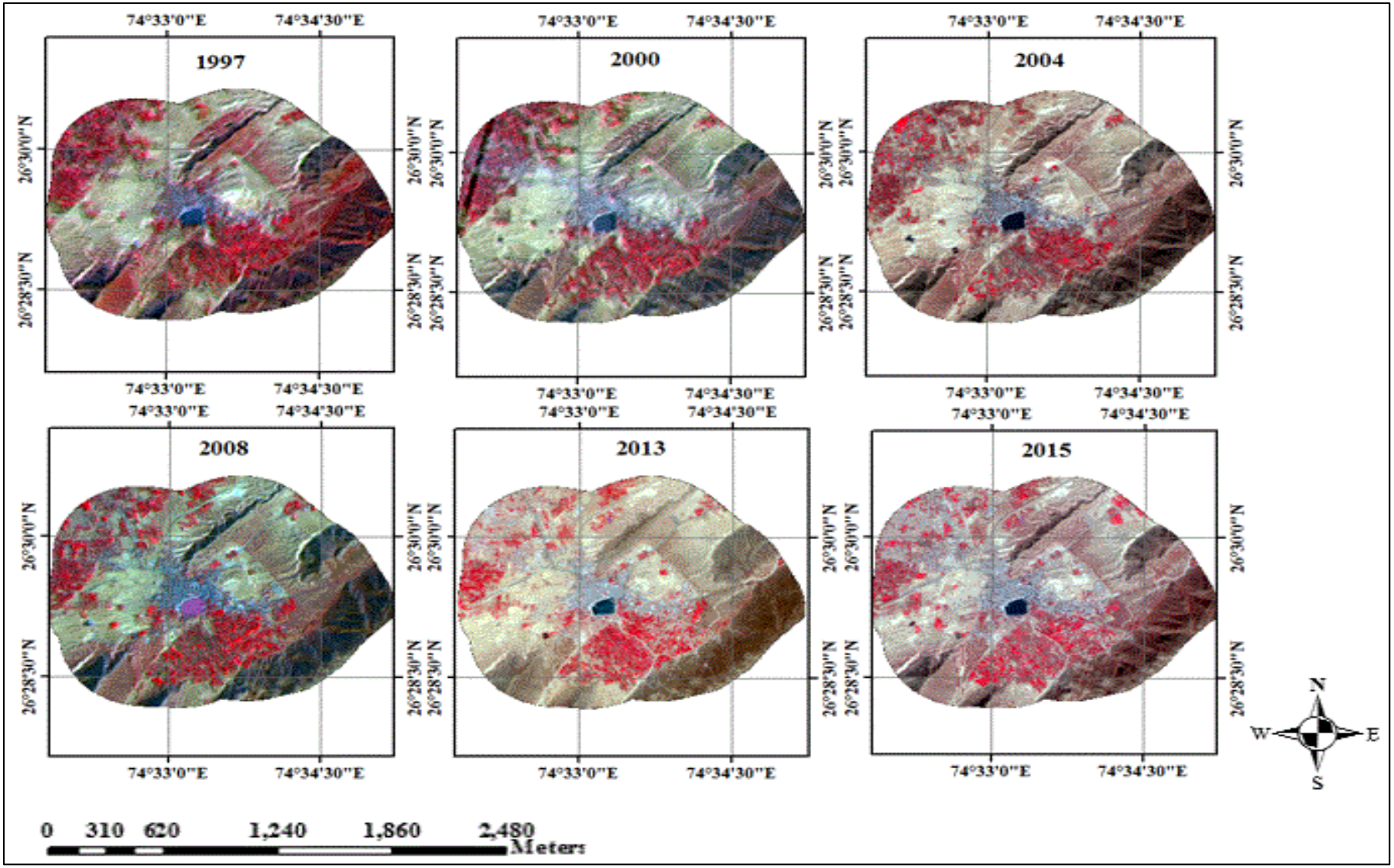

Figure 3.5: False Color Composites (FCCs) for 5 meter spatial resolution satellite imagery of Pushkar town

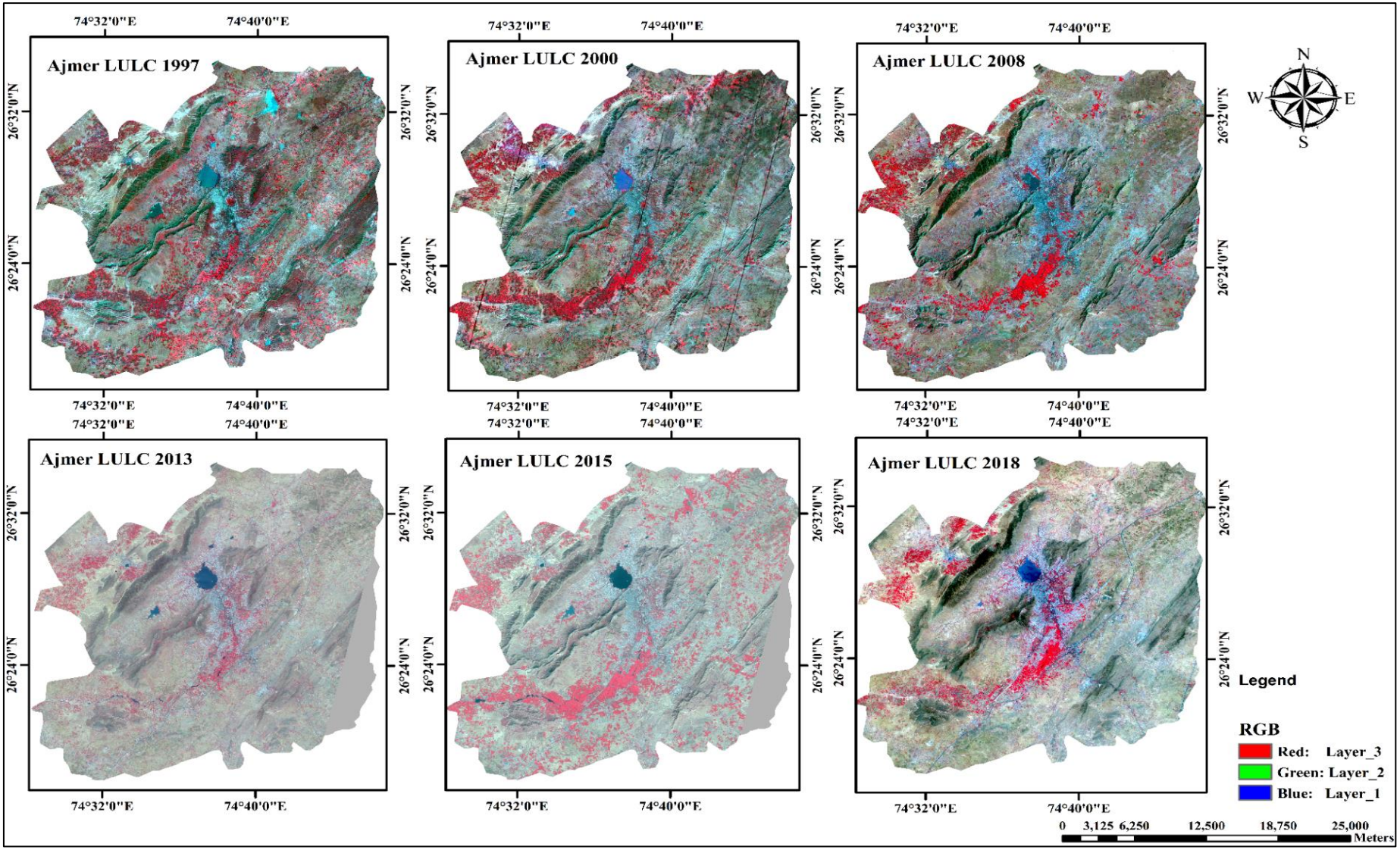

Figure 3.6: False Color Composites (FCCs) for 5 meter spatial resolution satellite imagery of Ajmer fringe

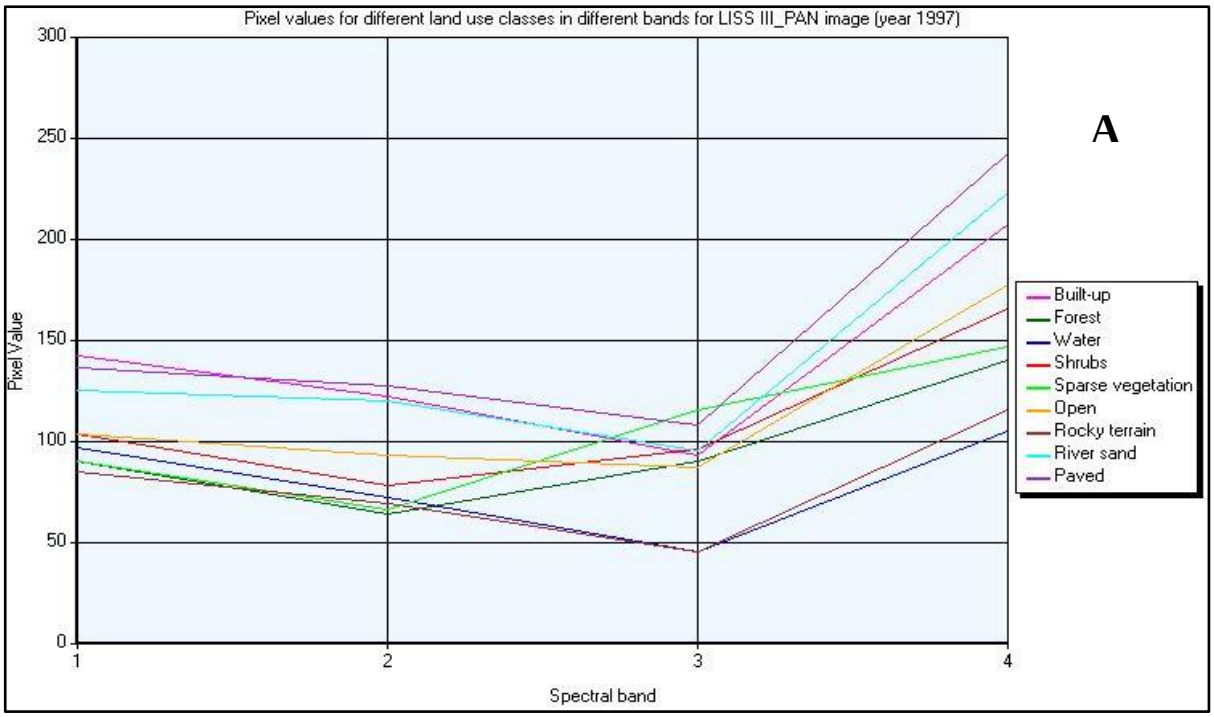
Pixel values for different land use classes in different bands for LISS III_PAN image (year 1997)
A
Pixel Value
Spectral band
Built-up
Forest
Water
Shrubs
Sparse vegetation
Open
Rocky terrain
River sand
Paved

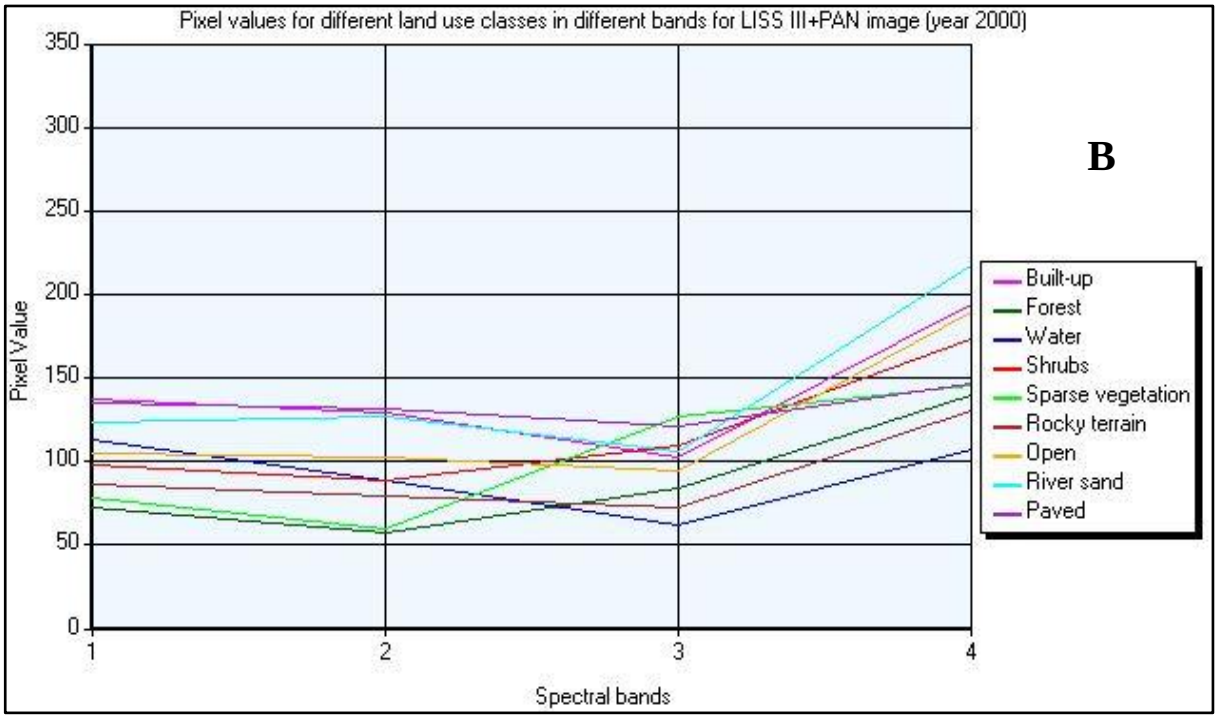
Pixel values for different land use classes in different bands for LISS III+PAN image (year 2000)
B
Pixel Value
Spectral bands
Built-up
Forest
Water
Shrubs
Sparse vegetation
Rocky terrain
Open
River sand
Paved

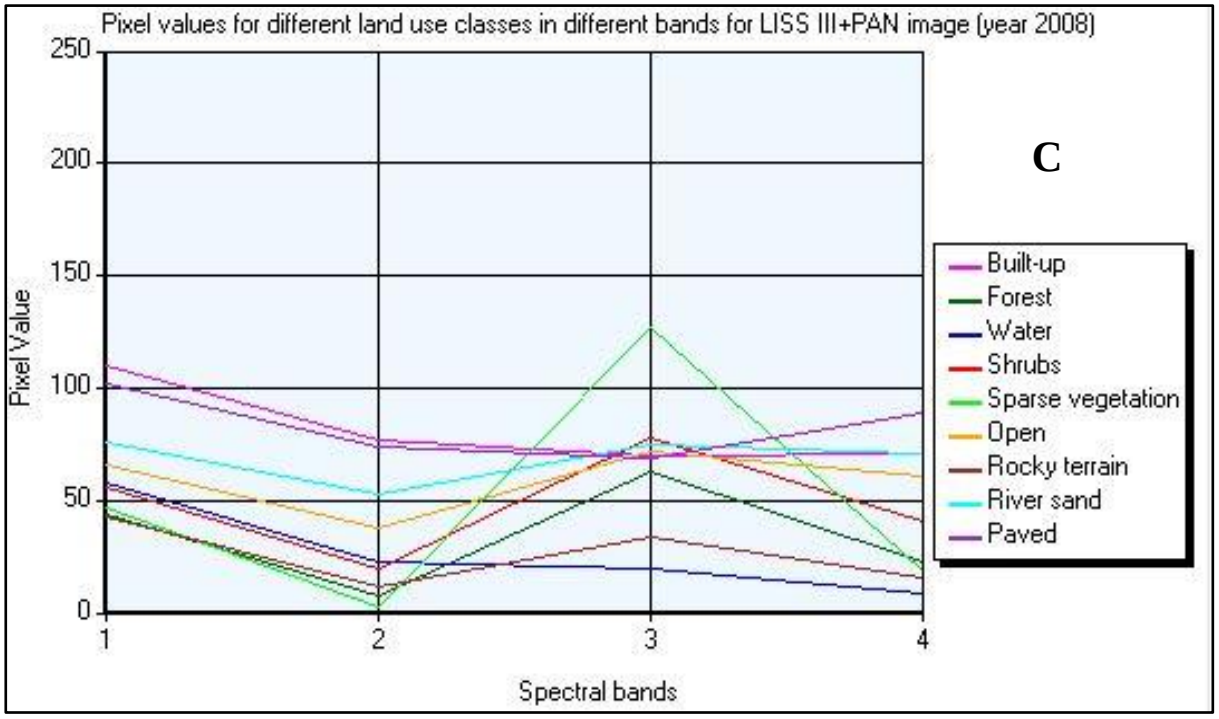
Pixel values for different land use classes in different bands for LISS III+PAN image (year 2008)
C
Pixel Value
250
200
150
100
50
0
1
2
3
4
Spectral bands
Built-up
Forest
Water
Shrubs
Sparse vegetation
Open
Rocky terrain
River sand
Paved

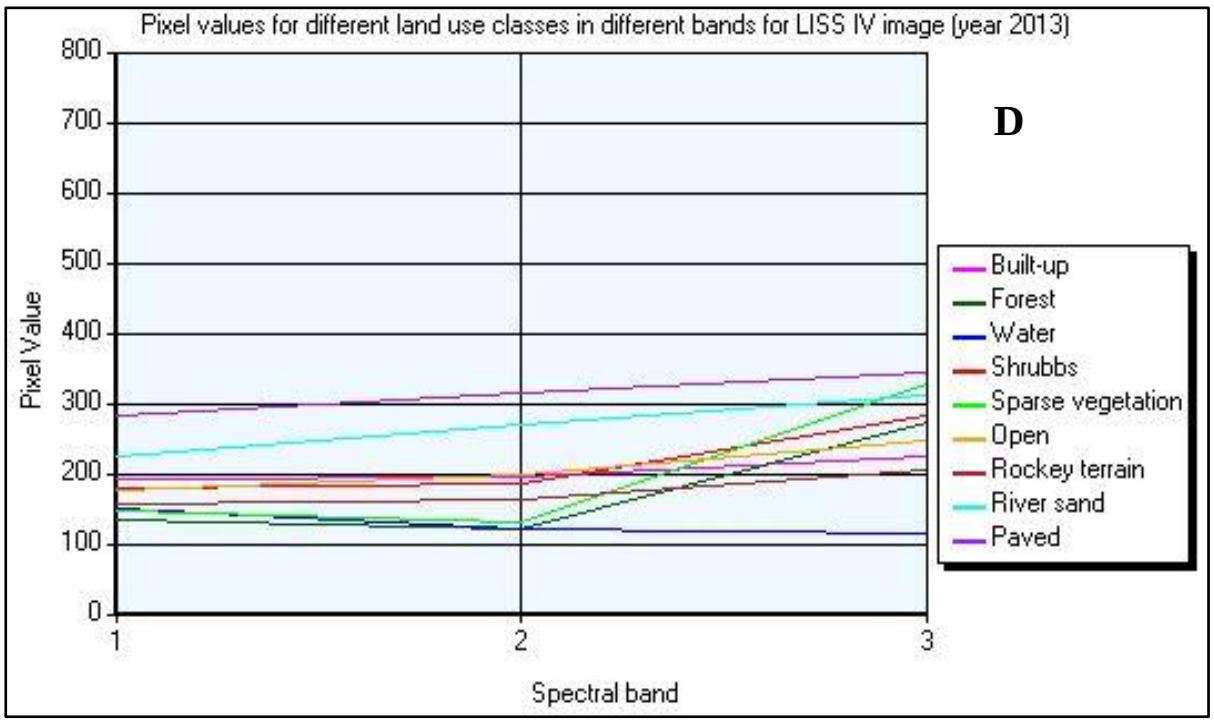
Pixel values for different land use classes in different bands for LISS IV image (year 2013)
D
Pixel Value
800
700
600
500
400
300
200
100
0
1
2
3
Spectral band
Built-up
Forest
Water
Shrubbs
Sparse vegetation
Open
Rockey terrain
River sand
Paved

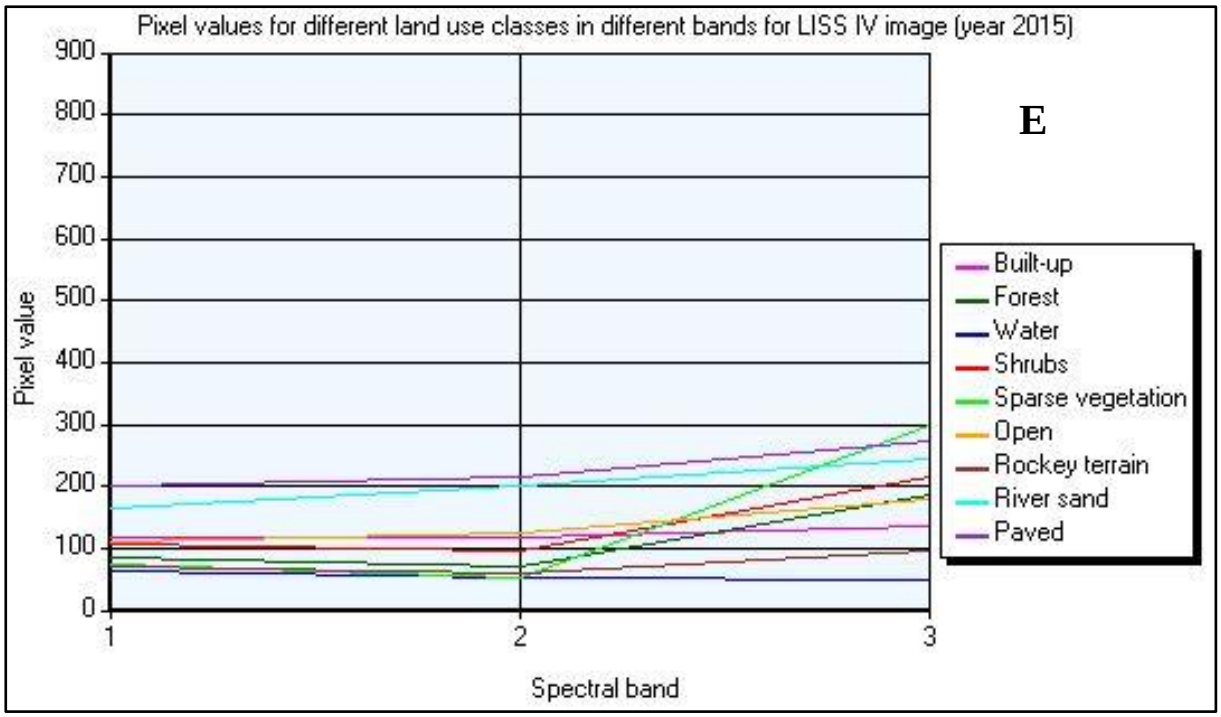

Figure 3.7: Spectral profiles for different targeted LULC classes for different years for LISS-IV sensor data

Table 3.3: Brightness values for multiple temporal satellite imagery

LULC Class	1997	2000	2004	2008	2013	2015
Built-up	50-105	40-120	80-160	35-88	180-210	102-125
Water	40-90	40-70	40-90	15-70	50-140	50-75
Dense forest	50-100	38-88	80-100	20-43	115-300	75-195
Sparse vegetation	50-112	48-101	70-130	10-85	150-301	75-275
Shrubs	80-200	60-151	90-115	40-80	150-325	100-195
Open	75-150	75-125	100-201	60-85	200-300	140-210
River sand	120-180	100-200	135-250	80-125	210-340	150-250
Rocky terrain	45-100	60-75	45-100	20-45	150-190	55-60
Roads	50-110	40-125	80-145	30-50	190-210	100-125

3.6 Preparation of Land use/ Land Cover Maps

The LULC maps are prepared from the classification of imagery using ERDAS Imagine software. There are different classification approaches available which can be categorized on the basis of different criteria. Based on user intervention it can be broadly categorized into two i.e. unsupervised and supervised classification. In unsupervised classification, image pixels are grouped into a user-defined number of classes based on solely reflectance information using a clustering algorithm like ISODATA. There is no user control over

the classification process. Whereas a supervised classification method involves user intervention and it is based on parametric statistics. The user has to train the classification algorithm by providing signature information of respective LULC classes. The supervised classification has been found to be a more accurate and popular method in spite of being more complex and time-consuming. The present study has used the unsupervised classification method to identify the possible no. of LULC classes. Further, supervised classification has been used to classify the multi-spectral satellite imagery of different years. Further, classified outputs have been refined using expert system classification like a knowledge-based classifier. The methodology used for the extraction of LULC information and image classification workflow has been explained in Figures 3.4 and 3.8, respectively.

3.6.1 Unsupervised classification

In the present study, the ISODATA algorithm has been used to perform unsupervised classification to have an idea about separable LULC classes. It is an iterative process of clustering and uses spectral distance as in the sequential method, however, it iteratively classifies the pixels, redefines the criteria for an individual class, and classifies again so that the spectral distance pattern in data gradually emerges. Initially, a large number of targeted LULC classes (i.e. 30) along with a convergence threshold of 0.98 and 24 iterations has been used. The convergence threshold is the maximum proportion of pixels whose cluster assignments can go unchanged between iterations. This threshold prevents the ISODATA utility of ERDAS from running indefinitely. Specifying a convergence threshold of 0.98, means that as soon as 98% or more of the pixels stay in the same cluster from one to the next iteration, the algorithm should stop processing. In other words, as soon as 2% or fewer of the pixels change clusters between iterations, the utility will stop processing. After classification, LULC classes are identified and given meaningful names. The unsupervised classification has been used to identify the targeted LULC classes and for the selection of signatures for the supervised training.

3.6.2 Supervised classification

3.6.2.1 Training of classification algorithm

The supervised classification includes user controlled training of the algorithm for image classification using a Maximum Likelihood Classifier (MLC). It involves the selection of sample pixels for respective targeted LULC classes identified with the help of spectral

profiles and unsupervised classification methods. The process of collecting training sample pixels is called signature selection. Every signature corresponds to an individual LULC class further used to assign a LULC class to each image pixel. Signatures are of two types i.e. parametric and non-parametric. Parametric signatures are based on statistical parameters like mean and the co-variance matrix while non-parametric signatures are based on discrete objects like polygons and rectangles in a feature space image. The supervised training is used to create both types of signatures. The parametric signatures are used to train MLC classifiers which are used in the present study.

3.6.2.1.1 Signature Selection

Nine LULC classes were identified from the study of satellite imagery such as Built-up, Forest, Water, Sparse vegetation, Shrubs, Open, Rocky terrain, River sand and Paved. For each LULC class, a homogeneous group of pixels having similar reflectance has been selected as a training sample for each LULC class. A minimum number of pixels selected for the training of one class is more than n*10, where n is the number of the spectral bands used. This method has been prescribed in various studies for better sample selection and the same has been followed in the present study (Congalton, 1999). The parametric signatures have been collected by on-screen digitization of training pixel polygons from the FCC of the satellite image to be classified using AOI drawing tool in ERDAS Imagine. Region growing tool has also been used to select a larger polygon of pixels having similar reflectance values by considering a spectral Euclidean distance of 5 tolerance limit and a seed pixel. This tool maintains the signature statistics within acceptable limits.

3.6.2.1.2 Signature Evaluation

After selection of training samples for each LULC class, signatures were evaluated using statistical characteristics to ascertain that the signatures are truly representing the classes to be classified. Evaluating selected samples/ signatures is an essential part of LULC map preparation to obtain accurate classified outputs. Signatures are evaluated to test whether the signature data are truly representing the pixels to be classified. Three evaluation criteria have been used to evaluate the collected signatures; (i) histogram plots, to examine various statistical parameters, like standard deviation and unimodality of the histogram, (ii) signature separability using transformed divergence (TD), and (iii) contingency matrix, which contains the number and percentage of pixels which are classified as expected. Signatures are refined, deleted, renamed and merged after evaluation to ensure

the unimodality of their histograms, satisfactory range of statistical parameters, TD and contingency matrix.

3.6.2.1.3 Histogram Analysis

Histograms for all the classes in different bands were plotted separately to check the quality of the training samples selected. A bell-shaped histogram with a single mode indicates good quality of signatures. Signatures having a bi-modal histogram and a large range of reflectance value have to be refined by deleting some training pixels and selecting another training group. Sample histograms plotted for signature evaluation have been shown in Figure 3.9. The same LULC class may have different reflectance range at different locations due to different characteristics e.g. water in different water bodies may have different depth or quality. This is a problem of geographical extension where the same LULC class may have different reflectance values due to change in their characteristics and their reflectance range becomes wide, leading to overlapping in reflectance range of different LULC classes. To deal with such a problem, initially, a number of sub classes of a LULC class can be considered. Their signatures should be collected separately and classified as a separate class. Later such similar classes can be merged into one class. Histograms corresponding to signatures of different LULC classes show a relatively narrow range of pixel values indicating good quality of signatures. Moreover, the reflectance range for the same class varies in different years such as a built-up class in Figure 3.9 ranges from 92 to 104. It may be due to new and old building or change in roof material (such as cement, marble or vegetation on the roof).

3.6.2.1.4 Contingency Matrices

The contingency matrix (error matrix) is another method used in the present study to assess the quality of training samples or signatures. Contingency matrix gives the percentage of misclassification among the signatures of different LULC classes i.e. error matrix which helps in identifying the mistakenly classified LULC classes. It was observed from the contingency matrices that few pixels of some classes like rocky terrain are wrongly classified into built-up classes for which signatures have been further refined and re-evaluated. However, some misclassification of signatures persists even after repeating the sampling process which is due to the similar reflectance of rocky terrain and built-up pixels. Also, some barren or vacant land which is named as open land were wrongly classified into the built-up class due to similar reflectance at some places. For LISS IV

images in different years, misclassification between barren land & rocky terrain, forest & sparse vegetation and built up & rocky terrain has been observed (Table 3.4). Misclassifications of signatures are due to the same reflectance among many classes, heterogeneous surfaces, the combined reflectance is different from the real one. Similarly, for the year 2000, 2004 and 2013 signature quality was assessed using contingency metrics as presented in Tables 3.4 and 3.5.

The maximum misclassification in signatures has been found for the LISS IV image of the year 2015 and LISS III image of the year 2000. The probable reason for a misclassification is high heterogeneity. From the contingency matrices, misclassification has been observed between sparse vegetation & forest, between built-up & rocky terrain and between rocky terrain & barren land LULC class for the year 2015 (LISS-IV image). Similarly, in images of other years, misclassification among different signatures corresponding to the above mentioned LULC classes has been observed as presented in Table 3.5. Separability is slightly poor for the urban settlement as it is mixed with rocky terrain, exposed rocks, and wet alluvium soil land use/cover classes. Misclassification is due to heterogeneous character (different type of construction material and different type of impervious surfaces) of the urban area and surrounding hilly topography (exposed rocks, hills, where reflectance is similar to the built-up areas). Reflectance characteristics of water are overlapping with hill shadow and wet alluvium soil. Rocky terrain comprises of soil found on hilly slopes along with boulders, whose reflectance is similar to barren land in different moisture and vegetation conditions. However, no significant misclassification among signatures of other LULC classes has been observed. Therefore, final signatures have been found to be satisfactory.

3.6.2.1.5 Separability analysis and feature selection

The separability analysis is carried out to determine the optimum band combination which has the highest separability among signatures of different LULC classes. Signature separability is a statistical measure of distance between two signatures and applicable only for the statistical classifiers. It can be calculated for any combination of the spectral bands. If the spectral distance between two samples is not significant for any pair of spectral bands, then they may not be distinct enough to produce an acceptable classification. In the present image analysis, Transformed divergence (TD) has been used to evaluate the signature separability. The formula for computing TD is as below (Swain and Devis, 1978):

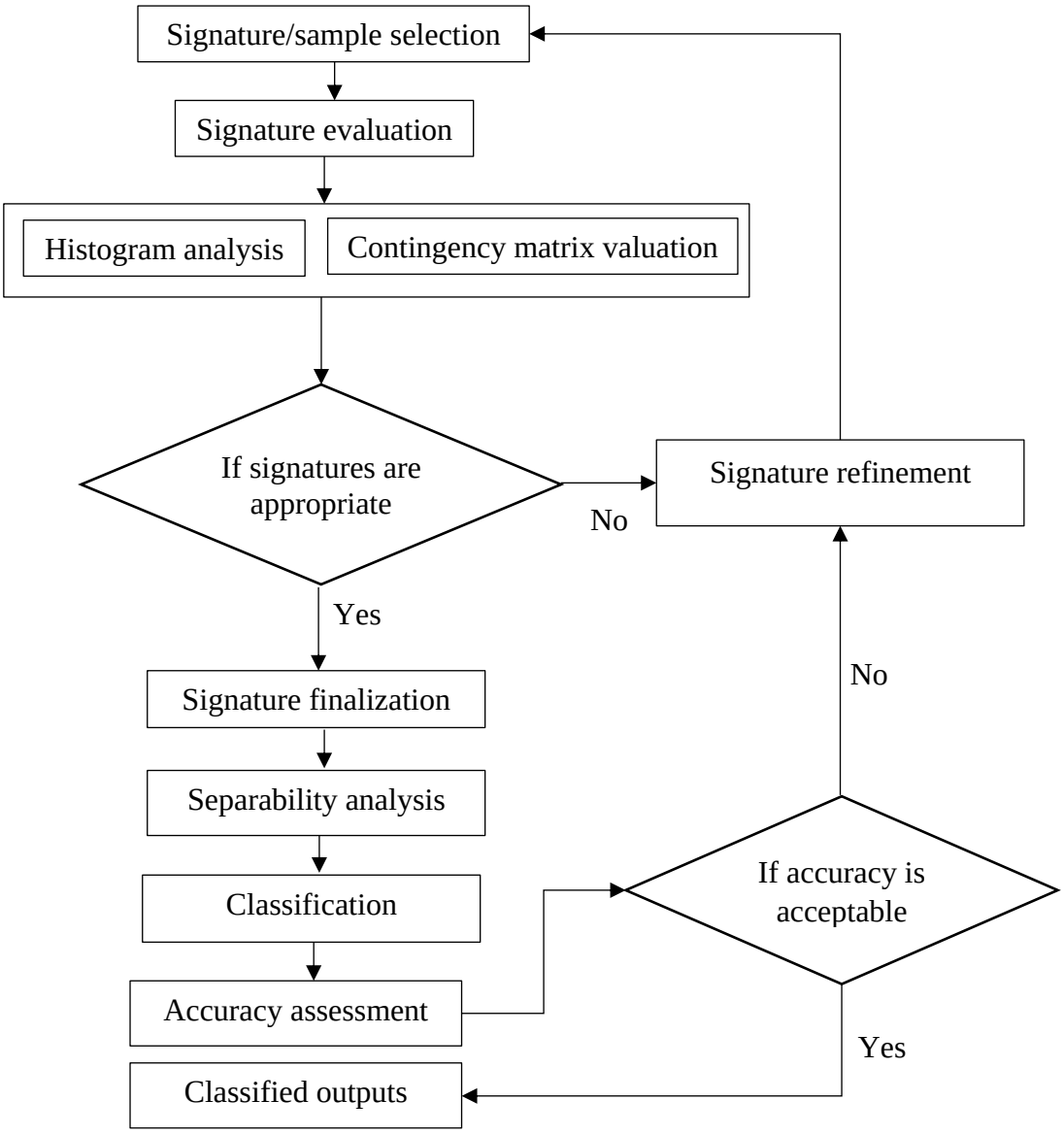

Figure 3.8: Image classification workflow

$$D_{ij} = \frac{1}{2} tr((C_i - C_j)(C_i^{-1} - C_j^{-1})) + \frac{1}{2} tr((C_i^{-1} - C_j^{-1})(\mu_i - \mu_j)(\mu_i - \mu_j)^T)$$
$$TD_{ij} = 2000\left(1 - \exp\left(\frac{-D_{ij}}{8}\right)\right) \quad (3.1)$$

Where, i and j are the two signatures (classes) being compared, Ci is the covariance matrix of signature I, μi is the mean vector of signature I, tr is the truce function, and T is the transposition function. The TD gives an exponentially decreasing weight to increase the distance between the classes. The scale of the divergence values can range from 0 to 2000. As a general rule, if TD values for all land use/cover classes for a pair of spectral bands are greater than 1900, then the classes can be separated.

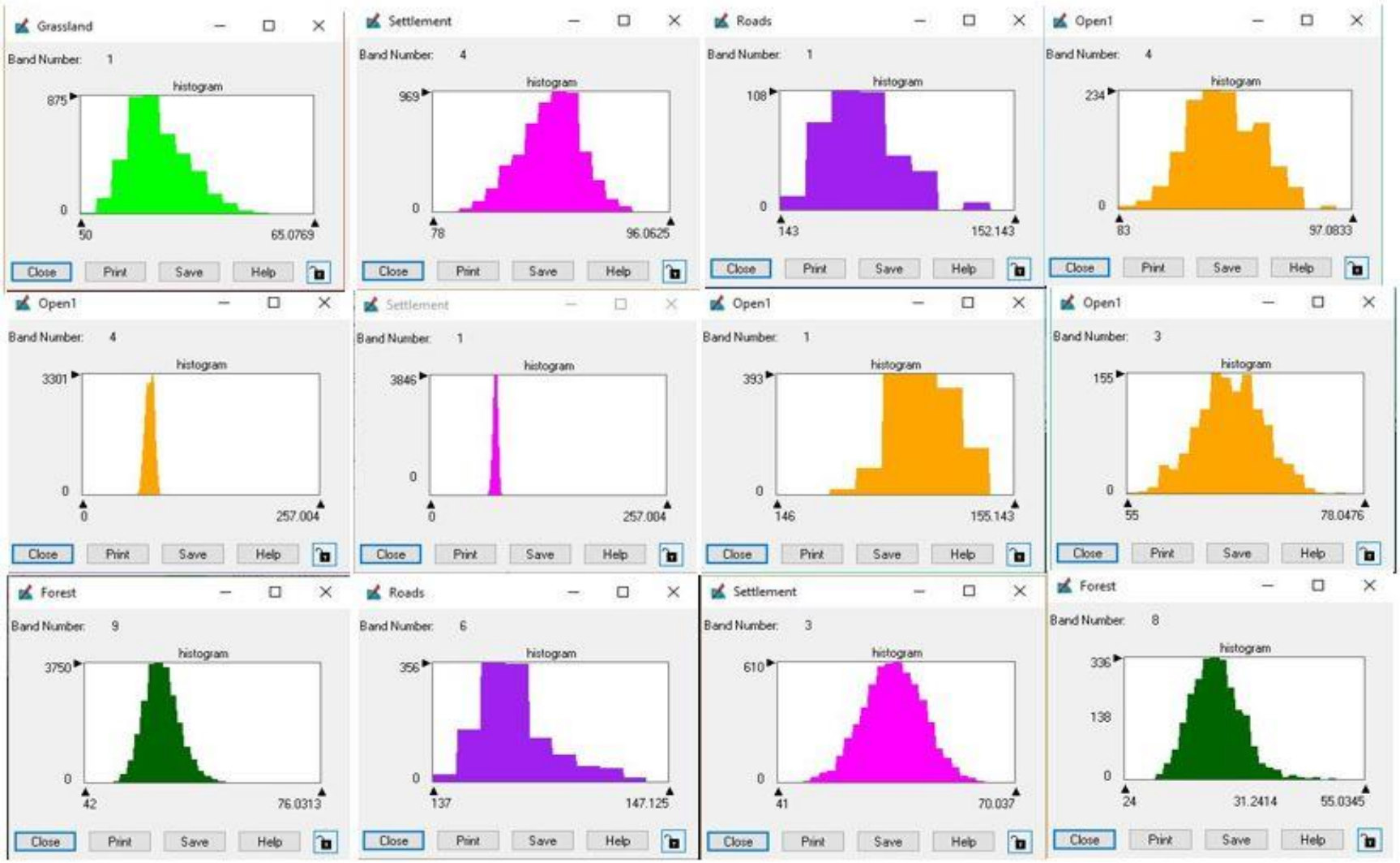

Figure 3.9: Histograms evaluation of training signatures

Table 3.4: Contingency matrix of the year 2015 and 2013

Contingency Matrix of the year 2015 (LISS IV**)**								
Reference Data								
Classified Data	Built -up	Dense forest	Water	Shrubs	Sparse vegetation	Barren land	Rocky terrain	River sand
Built up	99.1	0	0.05	0	0	1.17	10.61	0
Forest	0	97.14	0	0	15.12	0	0	0
Water	0	0	99.46	0	0	0	0	0
Shrubs	0	0	0	100	0	0	0	0
Sparse vegetation	0	2.86	0	0	84.88	0	0	0
Barren land	0.6	0	0.01	0	0	74.76	9.16	1.19
Rocky terrain	0.3	0	0.02	0	0	20.44	80.23	0.4
River sand	0	0	0	0	0	3.63	0	98.41
Contingency Matrix of the year 2013								
Reference Data								
Classified Data	Built -up	Dense forest	Water	Shrubs	Sparse vegetation	Barren land	Rocky terrain	River sand
Built up	100	0	0	0	19.57	0	0	0
Forest	0	99.15	0.57	0	0	0	0	0
Water	0	0	99.34	0	0	0	0	0
Shrubs	0	0	0	100	0	0	0	0
Sparse vegetation	0	0	0	0	80.43	0	0	0
Barren land	0	0	0.07	0	0	82.43	0	0.81
Rocky terrain	0	0	0	0	0	0	100	0
River sand	0	0	0	0	0	17.57	0	99.19

If the value is between 1700 and 1900, the separation is fairly good. If values of TD are below 1700, separation is poor (Jensen, 1996). Thus, it is clear from Table 3.6 that both the TD values i.e. average and minimum are more than 1700 for individual year images which are in acceptable range. From the generated separability matrices the best separable bands for satellite images can also be identified.

Table 3.5: Contingency matrix of the year 2004 and 2000

Contingency Matrix of the year 2004								
Reference Data								
Classified Data	Built -up	Dense forest	Water	Shrubs	Sparse vegetation	Barren land	Rocky terrain	River sand
Built up	100	0	0	0	0	0	0	0
Forest	0	99	0	0	0	0	0	0
Water	0	0	95.49	0	0	0	0	0
Shrubs	0	0	0	100	0	0	0	0
Sparse vegetation	0	0	0	0	99.06	4.98	0	0
Barren land	0	0	0	0	0.94	95.02	0	0
Rocky terrain	0	0	0	0	0	0	100	0
River sand	0	0	4.51	0	0	0	0	100
Contingency Matrix of the year 2000								
Reference Data								
Classified Data	Built -up	Dense forest	Water	Shrubs	Sparse vegetation	Barren land	Rocky terrain	River sand
Built up	100	0	0	0	0	3.69	0	0
Forest	0	93.42	0	0	0	0	31.69	0
Water	0	0	100	0.27	0	0	0	0
Shrubs	0	0	0	97.54	0	0	0	0
Sparse vegetation	0	0.27	0	0	100	0	0.13	0
Barren land	0	0	0	0.13	0	96.31	0	0
Rocky terrain	0	6.3	0	0	0	0	67.8	0.56
River sand	0	0	0	0	0	0	0.38	99.44

The optimum band combination for the year 2015 (LISS 3) and 2013 have been found to be 1, 3 and 4. For the year 2004 and 2000, optimum band combination corresponding to the highest separability has been found to be 2, 3 and 4. Optimum band

combination for the year 2015 (LISS 4) has been found to be 1, 2 and 3. Optimal band combination for all other images has been presented in Table 3.6.

Table 3.6: Transformed Divergence for supervised classification for various years

Image year	No. Of bands	Optimum band combination	Average TD value	Minimum TD value
2015 (LISS 4)	3	1 2 3	1972	1911
2015	4	1 3 4	1991	1879
2013	4	1 3 4	2000	1998
2008	4	2 3 4	1997	1990
2004	4	2 3 4	1998	1879
2000	4	2 3 4	1994	1761

3.6.2.2 Maximum likelihood supervised classification

Supervised classification is a closely user controlled process. After the finalization of signatures, pixels of the image are sorted into classes using a mathematical algorithm, which is also called the decision rule. Decision rules used in the supervised classification can be divided into two categories; (i) parametric decision rule, which is trained by the parametric signature, and (ii) non-parametric decision rule, which is trained by the non-parametric signatures. Parametric rules are based on the properties of the data and every pixel is assigned to a class since it is a continuous decision space (ERDAS, 1994). The non-parametric decision rule is not based on the statistical properties of the data. This rule determines whether or not a pixel is located inside of the non-parametric signature boundary. After the finalization of sample signatures, each pixel of the image is classified into a class using Maximum Likelihood Classifier (MLC). The MLC is a statistics-based parametric method and includes the probability of a pixel of being in a particular class. The algorithm assumes that all classes have an equal probability of a pixel assignment and the pixel values are normally distributed in all the spectral bands. The MLC equation is as follows;

$$D = \ln(a_c) - [0.5\ln(|Cov_c|)] - [0.5(X - M_c)T(Cov_c^{-1})(X - M_c)] \quad (3.2)$$

Where D is the weighted distance (likelihood), c is a particular class, X is the measurement vector of the candidate pixel, Mc is the mean vector of the sample of class c, ac is the percent probability that any candidate pixel is a member of class c, Cov_c is the covariance matrix of the pixels in the sample of class c, $|Cov_c|$ is determinant of Cov_c (matrix algebra), Cov_c^{-1} is the inverse of the covariance matrix, ln is natural logarithm function, and T is

the transpose function. The MLC based classification involves the assignment of a class to the individual pixel based on the lowest weighted distance i.e. likelihood. Initially, nine LULC classes and their sub classes were considered separate LULC classes to address the geographic extension problem however finally they have been merged into nine classes i.e. Built-up, Forest, Water, Shrubs, Sparse vegetation, Open, Rocky terrain, River sand and Paved. Later, one more class was added i.e. Road. Thus, the images have been classified into 10 LULC classes. Classification accuracy of MLC was found low in spite of good separability of the training samples (signature). This is because of the heterogeneity of land use classes and overlapping of the range of spectral reflectance (DN values) in different spectral bands. Significant misclassification has been observed in rocky areas, exposed rocks, and urban settlement. This misclassification occurs due to similar statistical characteristics (mean, covariance) of reflectance values of the surfaces, like built-up areas and rocks, water and hill shadows, urban settlement and wet alluvium soil. Similarly, shallow water bodies and wet alluvium soil have similar spectral statistics, resulting in misclassification.

3.6.2.3 Classification using an expert system

In spite of good signature quality at the training stage of the classification algorithm misclassification was observed in classified outputs of the MLC based method. To improve the classification accuracy rule-based expert classification has been performed using ERDAS Imagine software. The expert system is a hierarchy of no. of rules or decision tree that constitutes constituent information defined by the user from which each pixel of the classified image has to pass and the adjacent decision is taken. The expert classification includes some hypotheses, rules, and variables defined by the user in the form of the raster, vector, spatial models etc. A rule is a sequence of conditional statements formed by user-defined variables. A hypothesis is a decision which has to be taken after passing through the rules for each pixel of a classified image. The expert classification may comprise a no. of variables, rules, and hypothesis which can be linked together to make the final decision or terminal hypothesis. Generally, these rules do not provide a definite decision for the class, therefore, binary values (0 & 1) are attached with each rule indicating how strongly it confirms or disconfirms a particular class or a set of classes in a classification scheme.

In the present investigation, ERDAS Imagine software's Expert Classifier has been used to implement the rule-based approach. This module has two components; (i)

Knowledge Engineer, which facilitates identification of variables, rules, output classes of interest and creates the hierarchical decision tree, (ii) Knowledge Classifier, which classifies the image using the knowledge base developed in Knowledge Engineer. The knowledge-based classification has been used in two ways; (i) classification using only spectral information, and (ii) post classification refinement with the integration of ancillary information. In the first case, spectral variation of the different land use classes in different spectral channels has been used as a criterion for the formulation of the knowledge base. The range of digital values for the different target land use classes in different spectral bands has been determined. A rule base was then built to exploit the spectral information available in different bands corresponding to different land use classes. In the second case, the rule-based approach was used for the post classification refinement i.e. an initially classified output was derived from the imagery by a standard algorithm (e.g. MLC) and then rule-based system applied in an attempt to modify and improve the classification. Ancillary information from the various sources has been integrated with spectral data for the preparation of the knowledge base. Spectral information alone has not been found adequate for the classification of some of the land use/cover classes e.g. urban settlement & exposed rocks, water & hill shadows, urban settlement & wet sand, exposed rocks & sand. While formulating the rule base, both image context and geographic context rules have been used. The former was concerned with enforcing spatial simplicity and spatial consistency in the image using local neighborhood information. The latter was concerned with exploiting background geographic knowledge to correct likely class errors i.e. where the geographical situation of a particular pixel was inconsistent with the class label initially assigned to it. A rule base was used to exploit these data layers in the post-classification process. For all the pixels more than one rule was used with equal class support value (i.e. 1).

In the present study, the rules were formulated by using the DEM layer mainly to refine the misclassification between rocky terrain and built-up classes. The urban settlement is located at a relatively lower elevation as compared to exposed rocky areas. Using such hierarchical rules these two land use classes can be separated, which has not been separated using supervised classification (MLC). Finally, classification has been performed using the knowledge classifier module of the ERDAS Imagine software. It evaluates all the hypotheses at each location (calculating variable values if required) and assigns the hypothesis with the highest confidence value. Further, details of this approach can be found in Willcinson and Megier (1990). A synoptic view of knowledgebase

formulated in Knowledge Engineer has been shown in Figures 3.10 & 3.11. Misclassification has been reduced by using the expert classification. A total of nine to ten LULC classes as discussed earlier, have been identified for all the images.

3.6.3 Accuracy assessment

Accuracy assessment is an important step in the classification of satellite imagery which includes a comparison of classified outputs with referenced geographical data which are assumed accurate in order to assess accuracy. There are various methods to assess the accuracy of classified imagery (Congalton and Green 1999; Foody 2002). The present study utilizes geographically referenced data collected from high-resolution satellite data and other ancillary data for comparing classified outputs. A set of sample pixels (110) distributed over the classified output were selected using stratified random sampling to check the accuracy of classified maps. It was ensured during the selection of sample data that each class has more than 10 sample pixels. The collected reference data was imported into the accuracy assessment module of ERDAS Imagine. The classified image was provided to the module which enables corresponding class values of the referenced pixel. Finally, accuracy assessment of sample pixels of classified output against referenced geographical data was performed. The accuracy assessment report comprises statistics of the accuracy percentage based on the error matrix and kappa statistics which express the proportionate reduction in the error produced by the classification method compared with the error of random classification (ERDAS Field Guide, 2016). Kappa statistics and accuracy percentage are the measures of accuracy. The accuracy assessment reports for different classified maps are given in Tables 3.7 & 3.8.

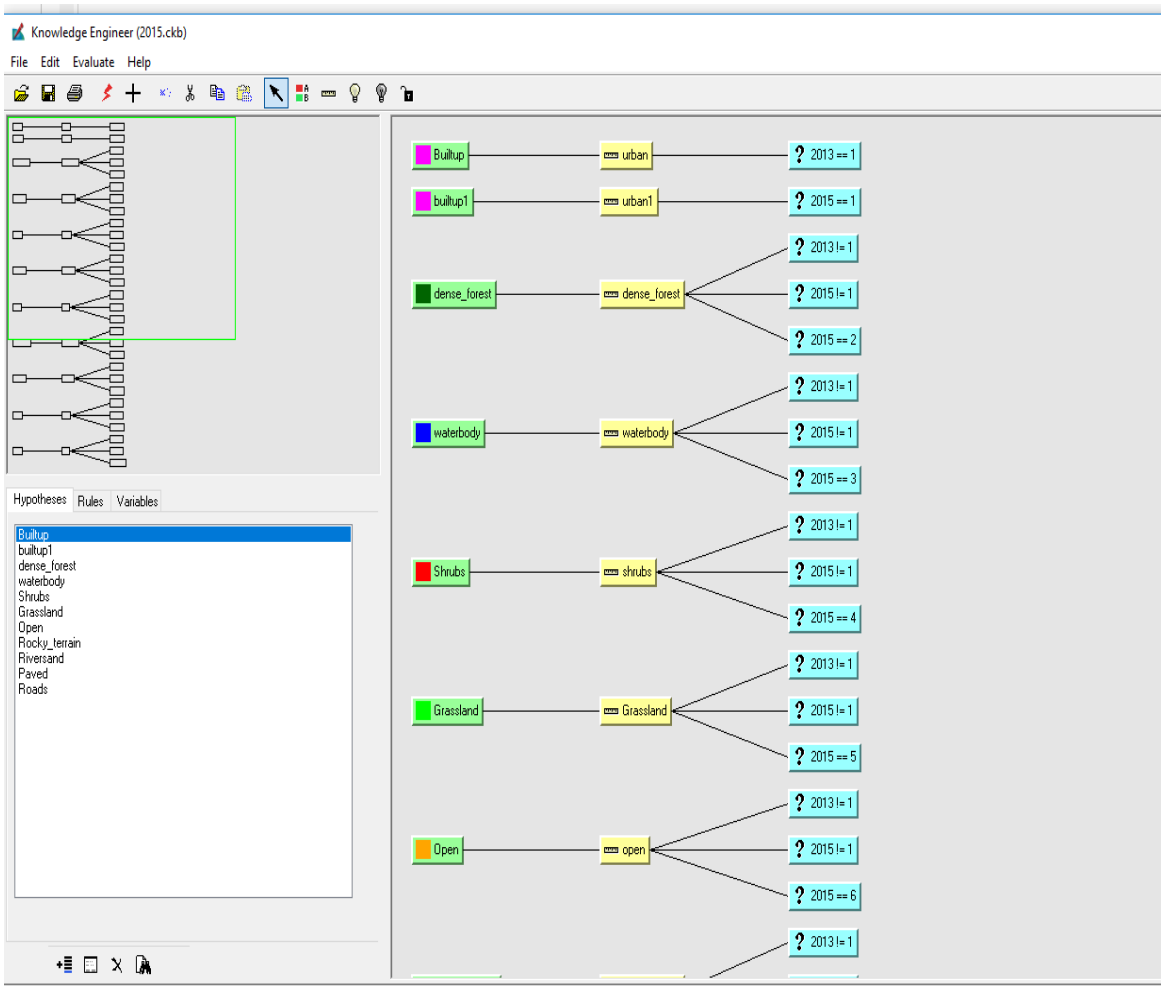

Figure 3.10: Synoptic view of expert classification (a)

The rule-based post-classification refinement approach has been found to be most satisfactory for the classification of spectrally overlapping land use classes. Users and producers accuracy are almost the same for the rule-based approach, which indicates the consistency of classification. The overall accuracy of the rule-based post-classification refinement is highest and more than 80% for all the images irrespective of spatial resolutions. Classification accuracy for all the images of different years has been found to be satisfactory. Accuracy percentage for all the images has been found to be between. 80 % to 94% for different years. The kappa statistics have been found to be 0.73 to 0.92 for all the images. A value of 0.92 as the kappa statistics implies that the classification method is avoiding 92% of the error that a completely random classification generates (Congalton, 1991).

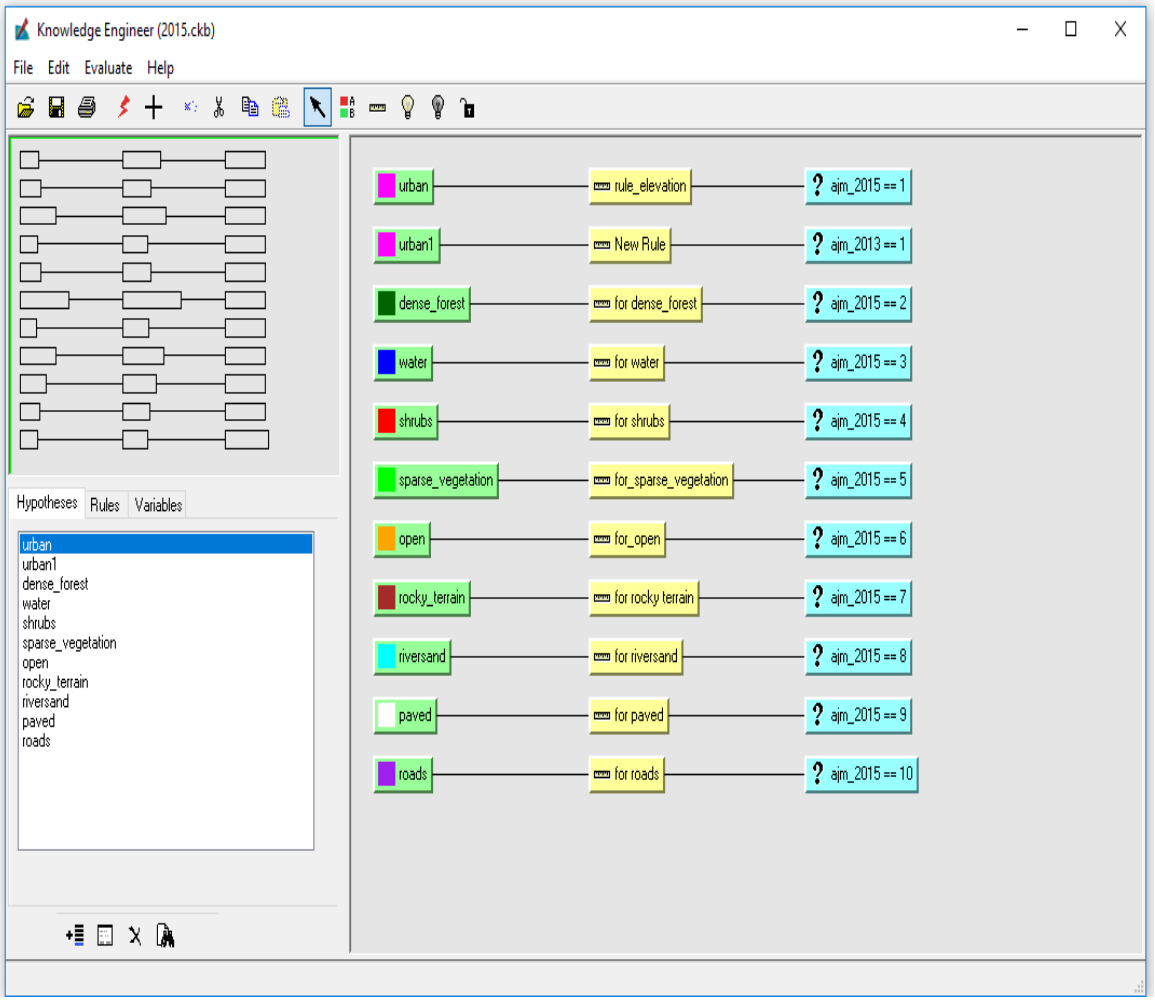

Figure 3.11: Synoptic view of expert classification (b)

3.6.4 Preparation of land use/land cover maps

The land use land cover maps obtained from the classification of satellite imagery of different years for Ajmer fringe including Pushkar are presented in Figures 3.12 & 3.13, respectively. Different LULC classes identified in Ajmer fringe and Pushkar are-

Builtup

This is one of the important land use information used in the present study for parameterization of SLEUTH model.

Table 3.7: Accuracy assessment report for 5-meter resolution satellite data

	1997		2000		2004		2008		2013		2015	
Land use Classes	PA (%)	UA (%)	PA (%)	UA (%)	PA (%)	UA (%)	PA (%)	UA (%)	PA (%)	UA (%)	PA (%)	UA (%)
Built-up	60.00	100.00	60.00	100.00	87.50	77.78	85.71	94.74	100.00	91.30	85.00	89.47
Forest	80.00	75.00	80.00	75.00	100.00	72.73	100.00	84.62	100.00	100.00	90.48	95.00
Water	84.62	91.67	84.62	91.67	92.31	100.00	100.00	100.00	100.00	100.00	92.86	100.00
Shrubs	40.00	66.67	40.00	66.67	66.67	88.89	66.67	100.00	80.00	100.00	37.50	100.00
Sparse vegetation	81.25	92.86	81.25	92.86	90.00	90.00	50.00	63.33	50.00	100.00	100.00	100.00
Open	90.91	64.52	90.91	64.52	84.44	74.51	87.10	81.82	93.94	83.78	92.86	74.29
Rocky terrain	100.00	94.44	100.00	94.44	100.00	100.00	100.00	100.00	88.24	100.00	100.00	100.00
Sand	100.00	83.33	100.00	83.33	-	-	100.00	50.00	-	-	100.00	100.00
Roads	-	-	-	-	-	-	50.00	100.00	33.33	100.00	100.00	80.00

Table 3.8: Accuracy assessment report for 5-meter resolution satellite data

Year	Accuracy percentage	Kappa statistics
1997	82%	0.78
2000	82%	0.78
2004	80%	0.73
2008	89%	0.86
2013	93%	0.91
2015	88%	0.85
2018	94%	0.92

All types of constructions used for human habitation as well as working infrastructure such as buildings, industries, houses, concrete paved etc. comes under the built-up category. Housing construction, buildings, and industries have been classified as settlement and we have separated the paved and roads classes as discussed below. The settlement class is identifiable on the classified imagery by its magenta color.

Forest

The area with dense vegetation has been considered as forest in the present study. It includes forest areas as well as areas with thick vegetation in residential areas or along the roads. In FCC, it appears dark red in color due to its FCC. However, we have signified forest as dark green in classified imagery.

Water

Natural and artificial water bodies have been classified as the water body class which includes lakes, ponds etc. Water can absorb much sunlight but negligible reflectance is there so, it looks black in satellite imagery. Water body class has been signified with a dark blue color.

Shrubs

The areas with higher topography like uplands or high grounds, having shrubs or bushes are classified as Shrubs. A shrub or bush is a horticultural rather than strictly botanical category of woody plant, distinguished from a tree by its multiple stems and lower height, usually less than 6 m tall. A large number of plants can be either shrubs or trees, depending on the growing conditions they experience.

Tonal contrast of the shrubs depends on foliage cover. The areal spread varied in size with irregular and discontinuous shapes. These appeared pink to pink bluish in tone, intermixed with a coarse texture. The coarse to mottled texture has been observed which was due to thin vegetation cover and exposure of terrain underneath. The shrubs are confined mainly on hill slopes and barren land. Some of these areas are part of a reserved forest area.

Sparse vegetation

The thin vegetative areas have been classified as sparse vegetation. It has smooth red texture in FCC of satellite images. Though, it has been assigned a chartreuse green color in the classified output.

Open land

The vacant land or land not in use and barren land have been classified as open land. It may have peculiar texture in FCC of satellite imagery like light green, yellow, dusky yellow, brown and many more. Although, it is orange in color in the classified images.

Rocky terrain

This is also a category of barren land. Areas with brownish red murram (soil in hilly slopes) with boulders with little vegetation are classified as rocky terrain. This appeared in dull greenish to yellow tone and medium to coarse in texture. This land cover category was found in hilly areas along with barren land and shrub land cover classes. This land cover class is extracted carefully as it mixes spectrally with the barren land, settlement, and exposed rocky terrain categories.

River sand

Areas, which have a substantial accumulation of sand, gravels etc. near the streams/ drains, are classified as River sand. This category is available dominantly along with the drain/Nala. These appeared in bright white to yellow with bluish to reddish tone, due to a varied amount of moisture. These were contiguous and linear in pattern. These areas were carefully classified, as their signatures were spectrally mixing with that of exposed rocky terrain.

Paved

A hard surface area generally used for footpaths has been considered as a paved class. It is made up of paving material that's why somewhat similar reflectance has been observed as of settlement land use class. Sometimes, it is covered with a perforated hard surface so reflectance is very high and looks white in FCC. Paved is identifiable in classified images by a white color.

Roads

Roads can be identified as a long impervious strip in a satellite image. Its texture is much similar to paved areas for concrete roads. It can be identified as violet color in classified imagery.

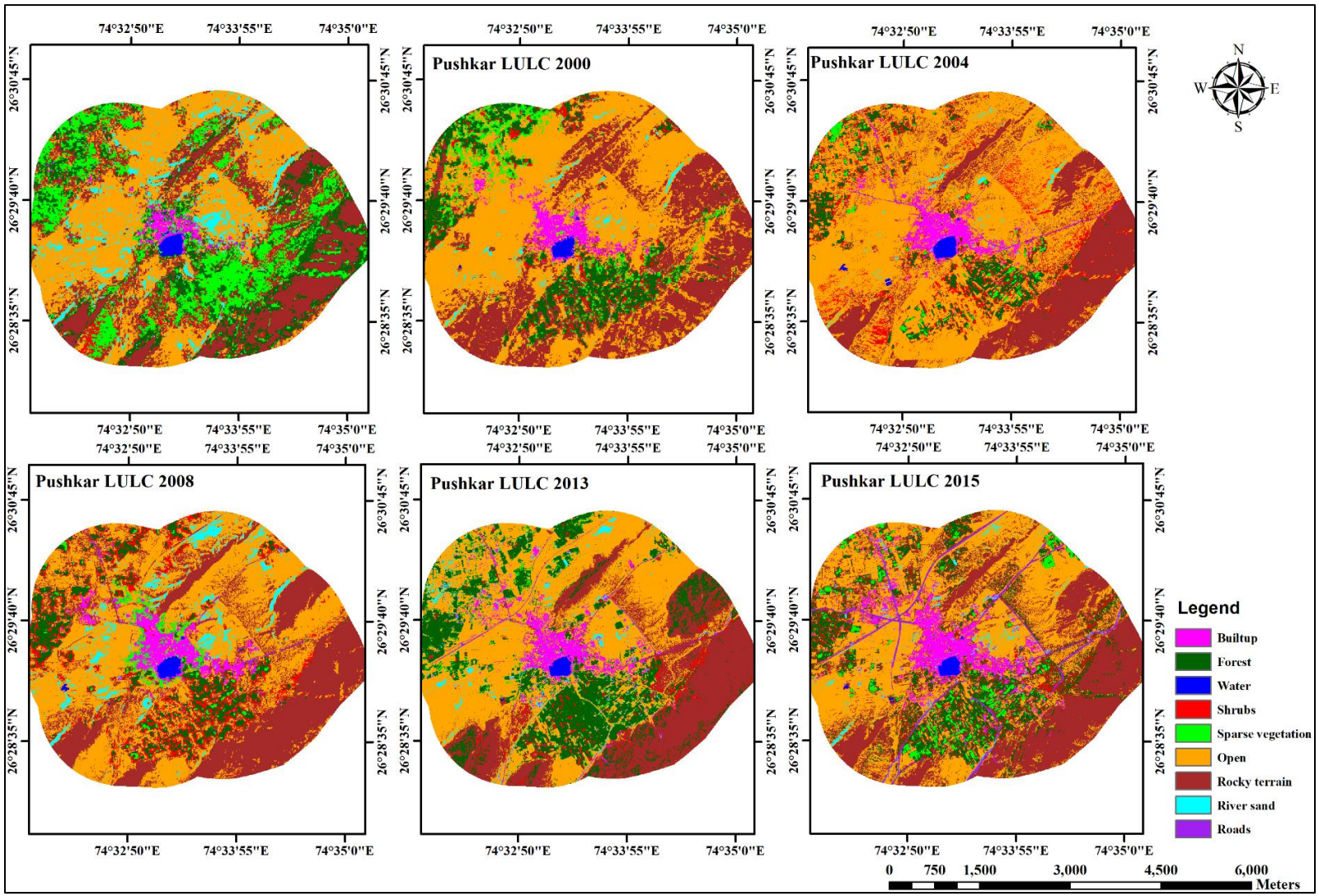

Figure 3.2: Land use/ land cover maps for Pushkar town

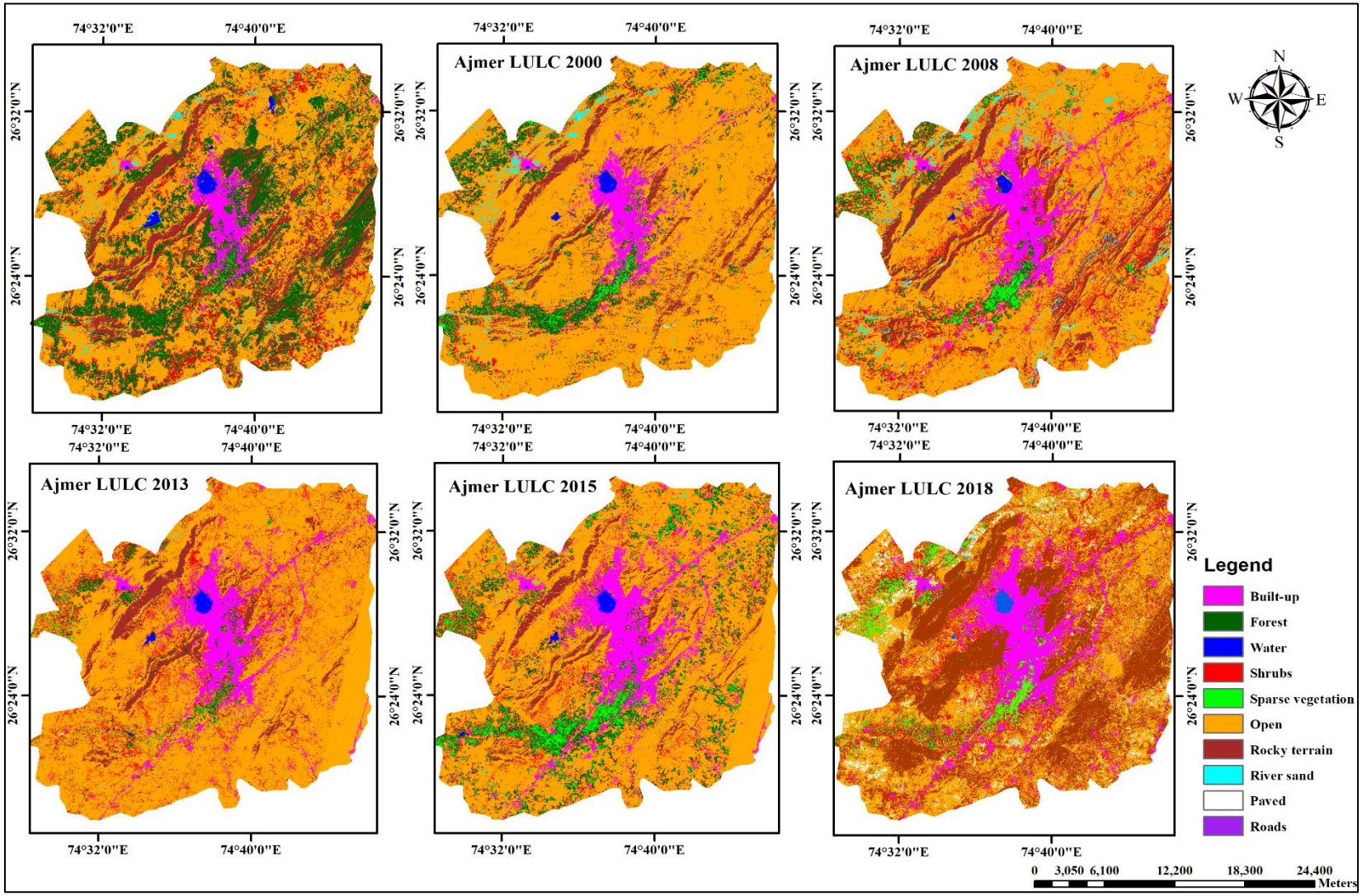

Figure 3.3: Land use/ land cover maps for Ajmer fringe

3.7 Geographic Database Creation in GIS

A geographic database can be classified into two categories i.e. spatial and non-spatial databases. The spatial database stores the data and information related to the geographical objects and features and surfaces while data not containing the information related to the location on the earth surfaces are stated as non-spatial databases. Depending upon the application the geographic database need to be properly designed. A database should be consistent with its terminology, totality, and linkages between its various elements.

3.7.1 Stages of geographic database design

To design a geographic database there are three basic stages i.e. conceptual, logical and physical design (Rao and Jayaraman, 1995). Conceptual design deals with the needs of the user and end goal of the geographic database which is free from the use of hardware and software. The logical design deals with the logical structure of the database which includes specifications of the elements and procedure used in the database creation. Physical design includes the use of hardware and software to deal with file structure & management, system memory, disc space etc.

3.7.2 Level of the geographic database

A geographic database follows a level of aggregation to include scale or details of the contents. A macro-level database requires more details and it should be implicit in the statement of end objective and are characterized by the data used.

In the present study, a geographic database for Ajmer fringe including Pushkar has been created at different scales. For individual thematic layers, the scale has been chosen based on the scale of data available. Most of the thematic layers have been generated at a scale of 1:2,500 to 1:25,000.

3.7.2.1 Spatial elements of the geographic database

The spatial elements of a geographic database are application specific and depend upon the end objectives. It comprises maps obtained from different sources and define the spatial database forming a part of the geographic database. The various spatial elements of the geographic database considered in the present study are:

Land use/cover maps: showing land use/cover classes extracted for the different years using the satellite images of various sensors.

Urban map: prepared from on-screen digitization using high-resolution satellite image i.e. Google Earth (GeoEye sensor) for the year 2017 and 2018. The urban maps of the year 1997, 2000, 2004, 2008, 2013 and 2015 have been extracted from respective years land use land cover maps.

*Road ma*p: showing the road network connectivity of important roads in Ajmer fringe including Pushkar. The road maps have been prepared for the year 1997, 2000, 2004, 2008, 2013 and 2015 from on-screen digitization from the Google Earth high-resolution image of respective years.

Recreational places: showing the places which are used for some recreational purposes like a park, garden etc. in Ajmer fringe including Pushkar. The map is prepared by performing on screen digitization of the locations of recreational places using Google Earth.

Hospitals: important hospitals in Ajmer fringe including Pushkar has been digitized by performing on screen digitization using Google Earth.

Railway stations and bus stand map: important railway stations and bus stands in Ajmer and Pushkar with their locations have been digitized by again performing on screen digitization using Google Earth.

Land cost map: important locations in Ajmer and Pushkar have been digitized by again performing on screen digitization using Google Earth and corresponding land cost value is assigned.

Contour map: showing the topographic elevation in the form of contours, at 1.0 m contour interval. This map has been prepared through onscreen digitization in ArcGIS using Ajmer city map and SOI topographical maps (1:25000 scale).

DEM map: showing the digital elevation values of a topographical surface and has been prepared from the contour map.

Slope map: showing topographical slope in percent of the area. It has been prepared from the DEM (Digital Elevation Model).

Municipal boundary map: showing spatial extent of municipal boundary of Ajmer. This map has been prepared from the Municipal boundary map obtained from internet sources.

Ward map: showing spatial extent of different city wards (administrative zones) of Ajmer. This map has been prepared from the Municipal boundary map and ward boundary map

obtained from internet sources.

3.7.2.2 Non-Spatial elements of the geographic database

Similar to the spatial database, an actual number of non-spatial elements are also application specific and depends upon the end objectives. For example, a non-spatial database for LULC change and urban growth modelling may have data on population, land cost etc. The non-spatial data may be available at different levels like ward, cells, etc., but it is always desirable to collect the data at the lowest spatial unit of the area. The cell or pixel being the smallest spatial unit has been used as a basic unit in the present study for land use land cover change and urban growth analysis. Details of the non-spatial data used in the study have been presented in Chapter 7.

3.7.3 Spatial database creation in GIS

The various thematic information for the study area i.e. layers (shapefiles and geodatabase layers) are created using the ArcGIS package. The methodology of database creation has been shown in Figure 3.14.

3.7.3.1 Digitization of features

Separate layers have been prepared for each theme. The various features of different themes are digitized through onscreen digitization in the ArcMap module of the ArcGIS package and Google Earth. Snapping has been used while digitizing the features to ensure interconnectivity. Details of all the shapefiles/geodatabase layers prepared for the study area along with their spatial features have been presented in Table 3.9.

Table 3.9: Details of GIS layers prepared for the study area

S. no.	GIS layer	Feature type
1	Municipal boundary	Polygon
2	Ward map	Polygon
3	Contour	Polyline
4	Land use/cover maps	Polygon
5	Road maps	Polyline
6	Urban maps	Polygon
7	Hospital map	Point
8	Recreational Places map	Point
9	Bus stand and railway station map	Point
10	Land cost map	Point
11	Exclusion map	Polygon

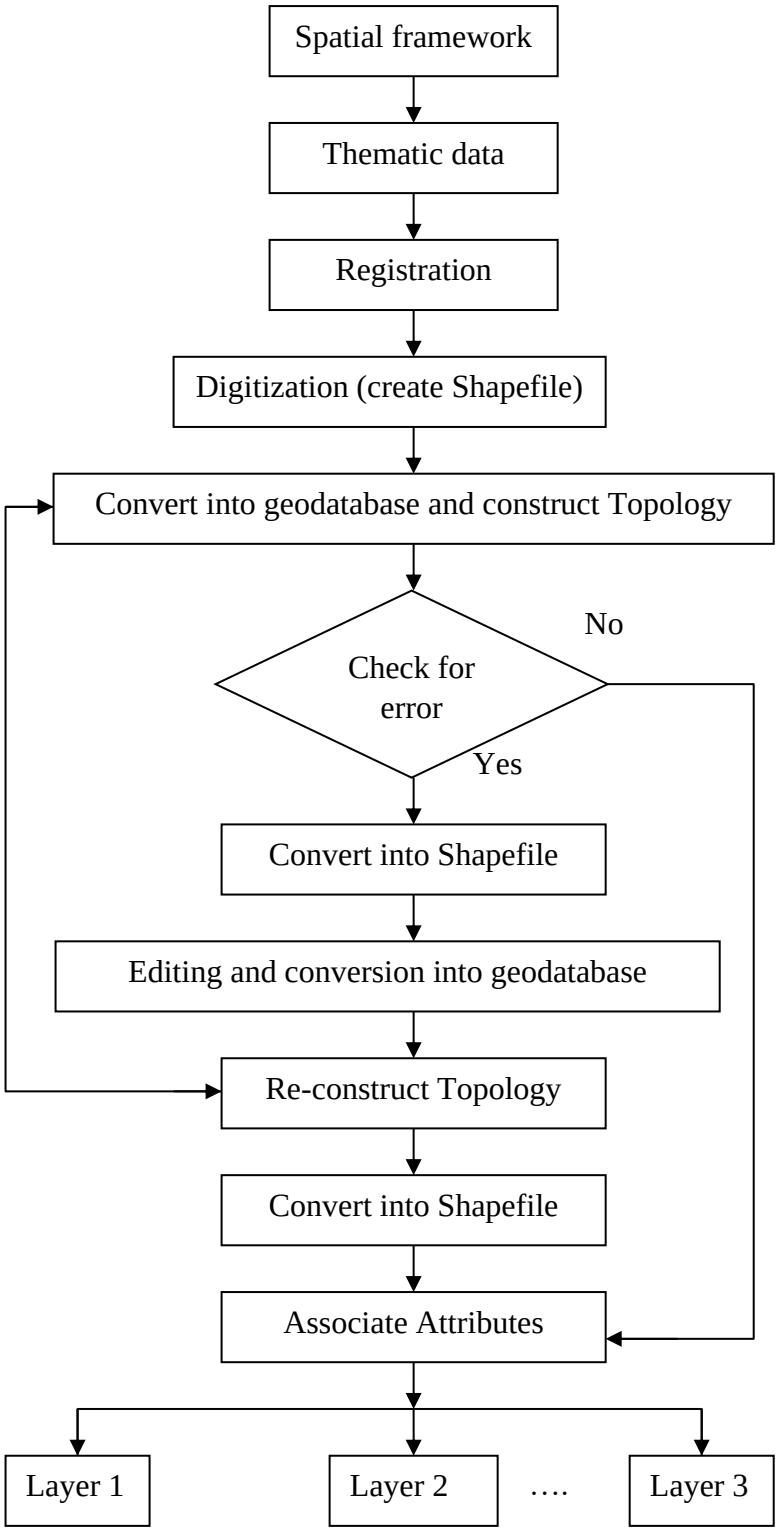

Figure 3.4: Procedure used for the creation of geographical database

3.8 Geographic Database

The present study broadly deals with the land use/ land cover change and urban growth modelling which require a variety of data/information related to the earth surface i. e.

topography or geography of earth, which includes information related to land use/cover and urban growth, topographical slope, road, important places and infrastructure hubs and hillshade etc. Geographical database created in the present study includes various thematic layers related to topographic surface representations (DEM, slope, and hillshade), physical boundaries (municipal boundary and ward map) and land use/cover, socio-economic parameters (population, density, land cost, location of hospital, recreations places, bus stand and railway station etc. Created databases are discussed in subsequent sections.

3.8.1 Contour map

The contour is a line joining the points of equal elevation. Generation of a contour map is a very important aspect of any study related to geographical earth surfaces. The contour map forms a base map for generating a number of GIS layers, such as DEM, slope and hillshade maps. The SOI topographic maps (45 N J/11/1, 3, 4, 5 and 45 N J/10/3, 6 at 1:25,000 scale with contour interval of 10 m) and Ajmer city map (prepared from aerial survey with 1:2,500 scale and 1.0 m contour interval) have been used as the base map for the digitization of contours. The contours within municipal boundary were digitized in a newly created shape file having polyline spatial feature. This shapefile was assigned the same geo-referencing and coordinates as the registered SOI topographic maps. The minimum elevation of contour was found to be 450 m, while the maximum elevation of the contour is 882 m. The digitized shapefile has been exported to coverage to construct the topology. The coverage then converted again to shapefile, which was ready to use for further analysis i.e. generation of DEM, slope and hillside map. The contour map is shown in Figure. 3.15.

3.8.2 Slope map

The DEM was used to generate a slope map (in percent) in raster format. Slope identifies the steepest slope for a location on a surface. In the present study, the slope map has been prepared by using two DEMs, first created from above using digitized contour map (1-meter contour interval) and other obtained from USGS earth explorer (30 m resolution) as digitized contours do not cover the entire fringe of Ajmer. The DEM of 30 m resolution has been resampled and merged with the above prepared fine resolution DEM to form a complete study area (Figure 3.15).

The output slope raster can be calculated as percent slope or degree of slope.

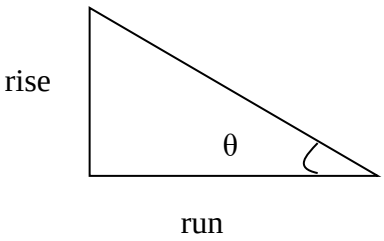

Slope in degrees $\theta = \tan^{-1}(\text{rise/run})$

Slope in percentage = rise * 100/run

When the slope angle equals 45 degrees, the rise is equal to the run and when it is expressed as a percentage, the slope of this angle is 100%. The slope has been generated in the 3D Analyst module of ArcGIS. Classified slope map of the study area (in percentage) has been shown in Fig. 4.15. Topographic slope varies from flat (0%) to very steep (236.8%). Results reveal that about 25% of the area has more than 20% topographic slope which indicates hilly topography of the area.

3.8.3 Municipal boundary and ward map

The municipal boundary of Ajmer city is the geographical area notified by the Competent Authority (Municipal Corporation Ajmer and Town Planning Department) for the urban development. This area is revised from time to time depending upon the development needs. A municipal boundary map has been prepared as a polygon feature layer in GIS through manual onscreen digitization. Ajmer municipal boundary map obtained from Ajmer Town Planning Department has been used as the base map (Figure 3.16).

Wards are the smallest administrative and planning zones formed by the Authority for each city/urban center. These are zones with limited extent decided based on population and other physical features like an important road or any other physical boundary. Wards are used as the basic planning unit while planning the overall development of the city. The ward map has been prepared as a polygon feature layer through manual onscreen digitization using the ward map as the base map. Presently, there are 60 wards in Ajmer (the year 2018) (Figure 3.16).

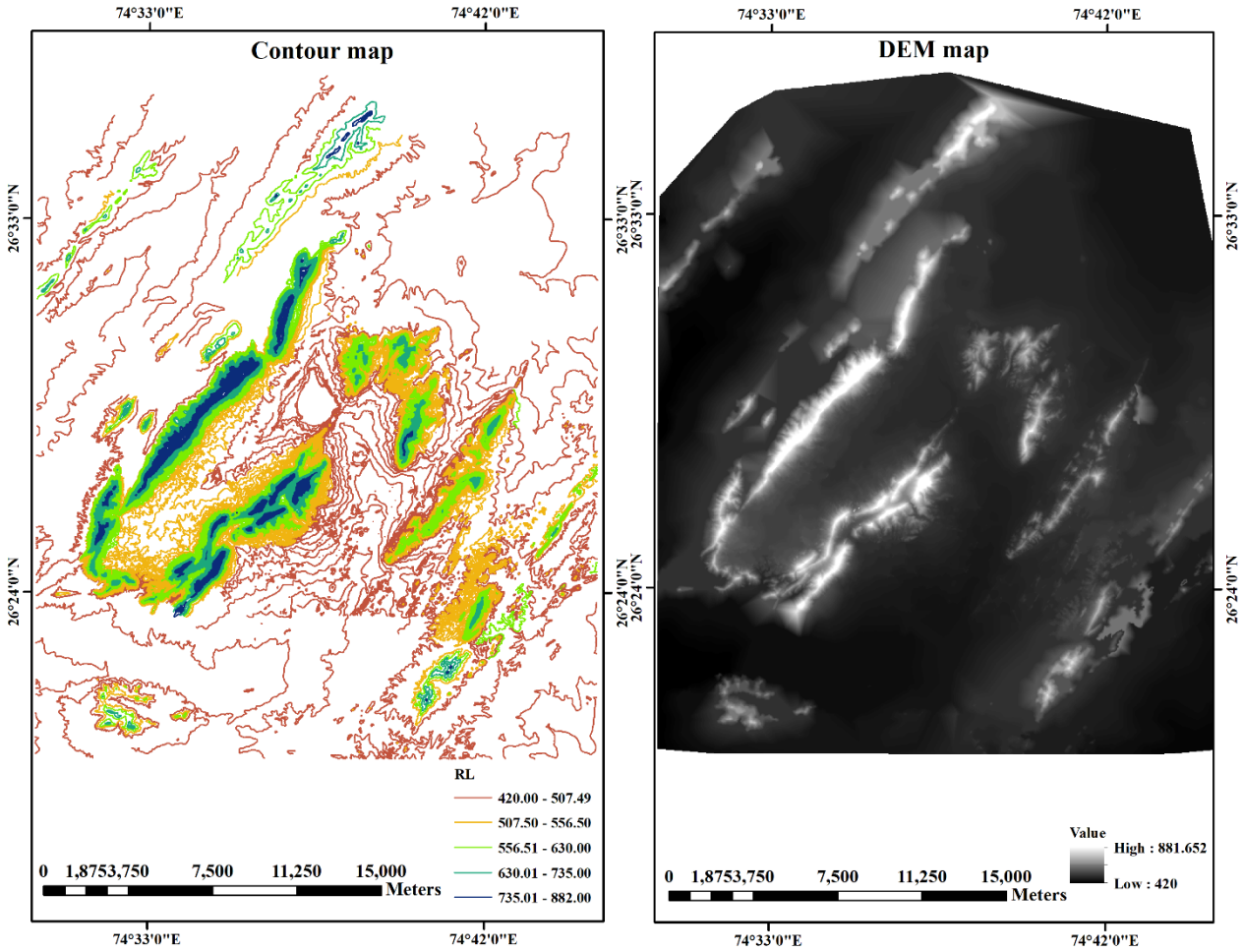

Figure 3.5: Contour map and DEM of the study area

3.8.4 Road layers

Road maps have been prepared by performing on-screen digitization of important roads in Ajmer for the year 1997, 2000, 2008, 2013 and 2015 (the additional year 2004 in case of Pushkar) and the maps are presented in Figure 3.17.

3.8.5 Exclusion Layer

The SLEUTH model incorporates an exclusion layer as one of the important input parameters which restricts land from becoming urbanized. Exclusion layer may include lands which would be restricted from urbanization in present and future as well like, reserved forests, water bodies, historical monuments, and land prohibited to construction. These features were digitized using SOI toposheet and town plan map and are presented in Figures 3.18 & 3.19 for Pushkar and Ajmer fringe, respectively.

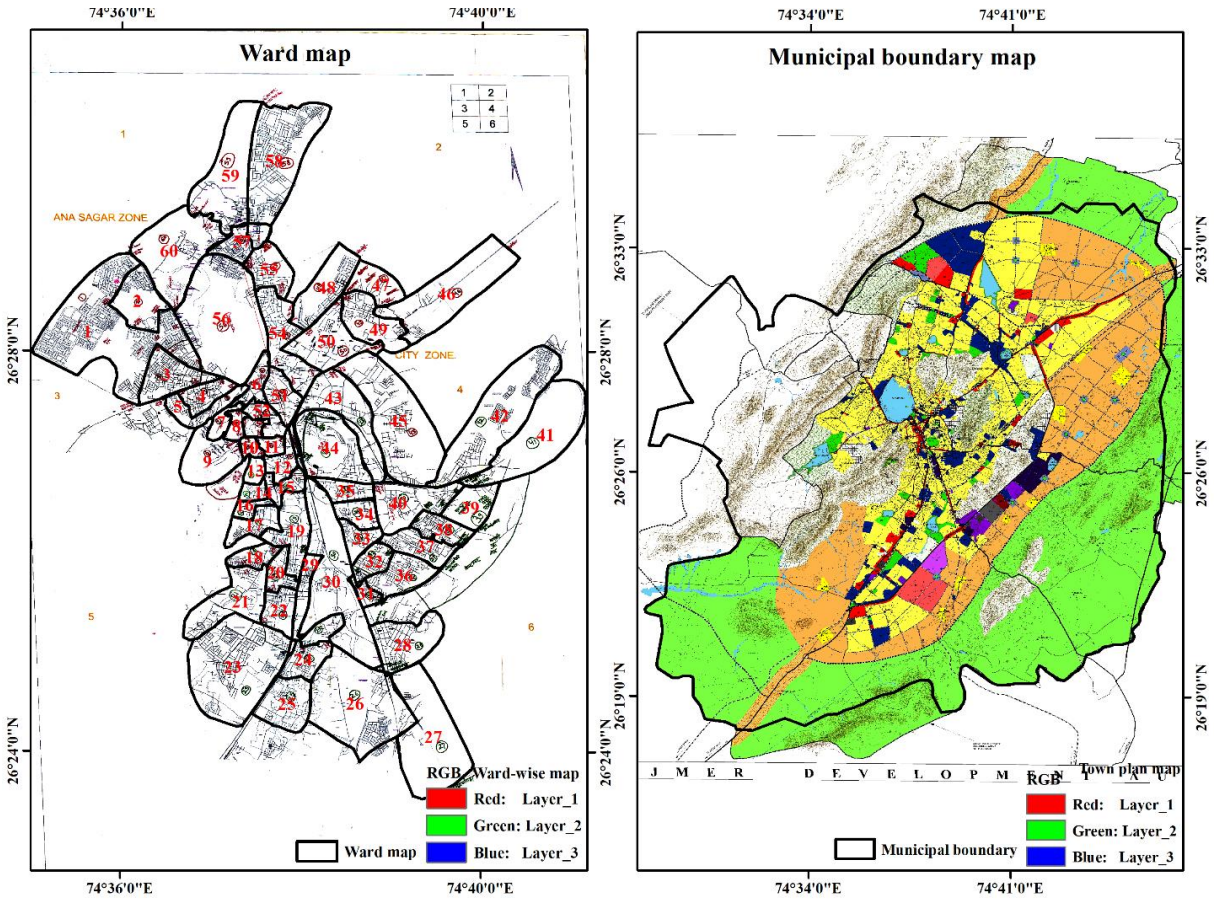

Figure 3.6: Ward map and municipal boundary of the study area

3.8.6 Urban growth map

Urban growth has been found to be increasing over a time period. In the present study, five classified satellite images of different years from 1997 to 2015 (six in the case of Puskar, the additional year 2004) have been used to extract the urban area in respective year (Figures 3.18 & 3.19). These urban maps from the years 1997 to 2015 will be used as input dataset for urban growth modelling. In addition to these, built-up of the year 2017 (Figure 3.21) has been obtained from on-screen digitization using Google Earth for Pushkar and built-up of the year 2018 has been extracted from the classified image of Ajmer fringe including Pushkar. The urban maps of the year 2017 and 2018 of Pushkar and Ajmer fringe respectively have been used for the validation of modelling outcomes. Urban area statistics for Ajmer fringe are presented in Table 3.10. Impervious area (built-up area) has increased from 1059.63 km2 in the year 1997 to 3093.72 km^2 in the year 2015 in Ajmer fringe including Pushkar, however, Pushkar alone has been developed from 116.15 km2 in the year 1997 to 480.17 km2 in the year 2015 in terms of urban growth. Urban growth for Ajmer fringe including Pushkar has been found to be 3411.53 km2 in

the year 2018. This implies that the land is being used for urbanization at a faster rate which refers to the utilization of all land for development initiatives, like commercial, industrial, educational, recreational and residential establishments. The urban growth in different years has been presented in Figures 3.18 & 3.19 for Pushkar and Ajmer fringe, respectively. Built-up area obtained from the classification may have some error due to mixed class pixels. The classification algorithm designates a particular pixel to a particular land use class, depending upon its reflectance characteristics (standard deviation and co-variance) and spatial resolution. The supervised classification used in this study does not deal with sub-pixel classification. However, results are further refined using knowledge-based approach by reducing the problem of mixed pixels.

Table 3.10: Built-up area of Ajmer fringe and Pushkar in different years

Year	Built-up area (km^2) for Ajmer	Built-up area (km^2) for Pushkar
1997	1059.63	116.15
2000	1358.38	221.20
2004	-	278.49
2008	2328.68	320.97
2013	2589.73	353.14
2015	3093.72	480.14
2017	-	539.29
2018	3411.53	-

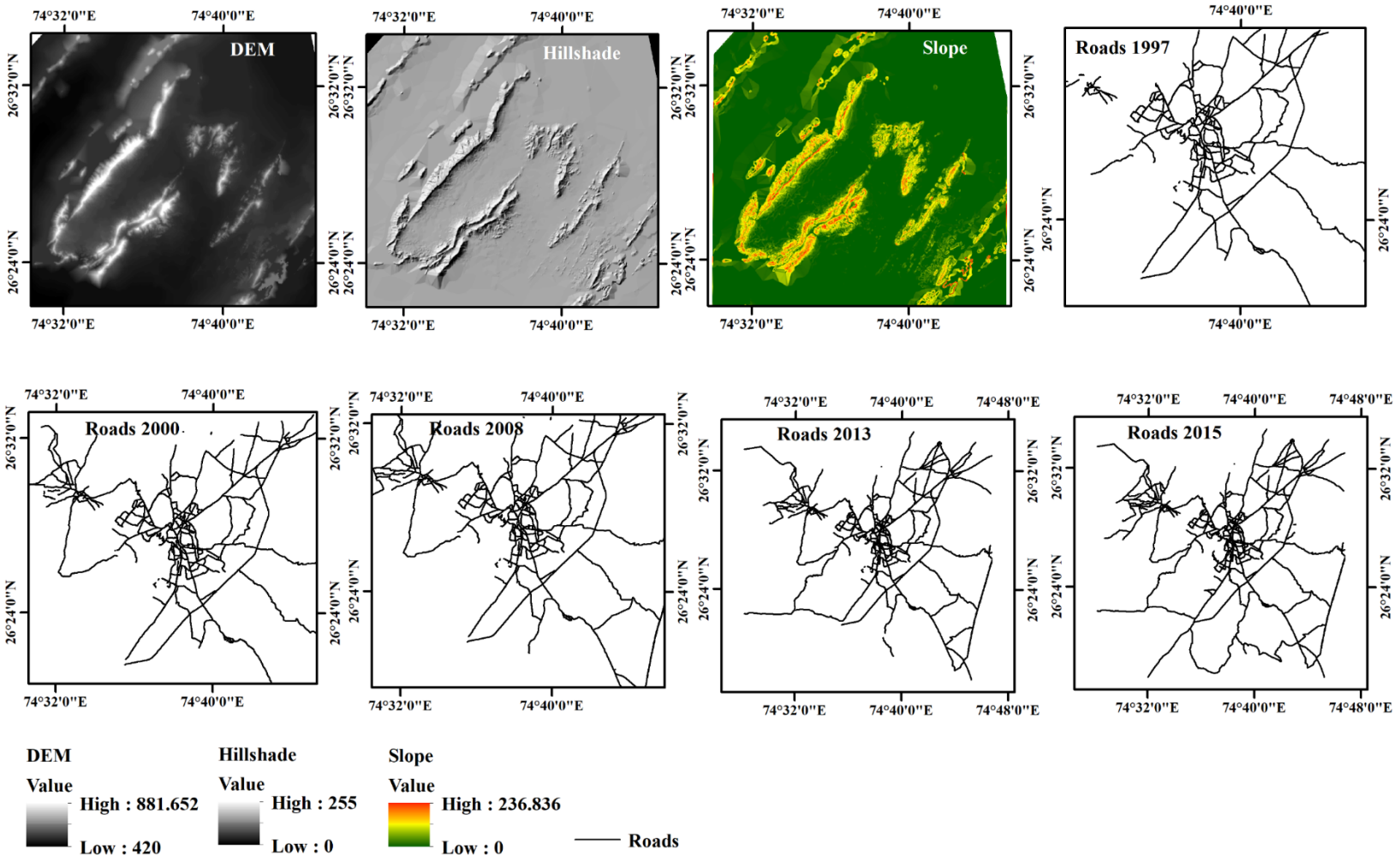

Figure 3.7: GIS database layers for different years

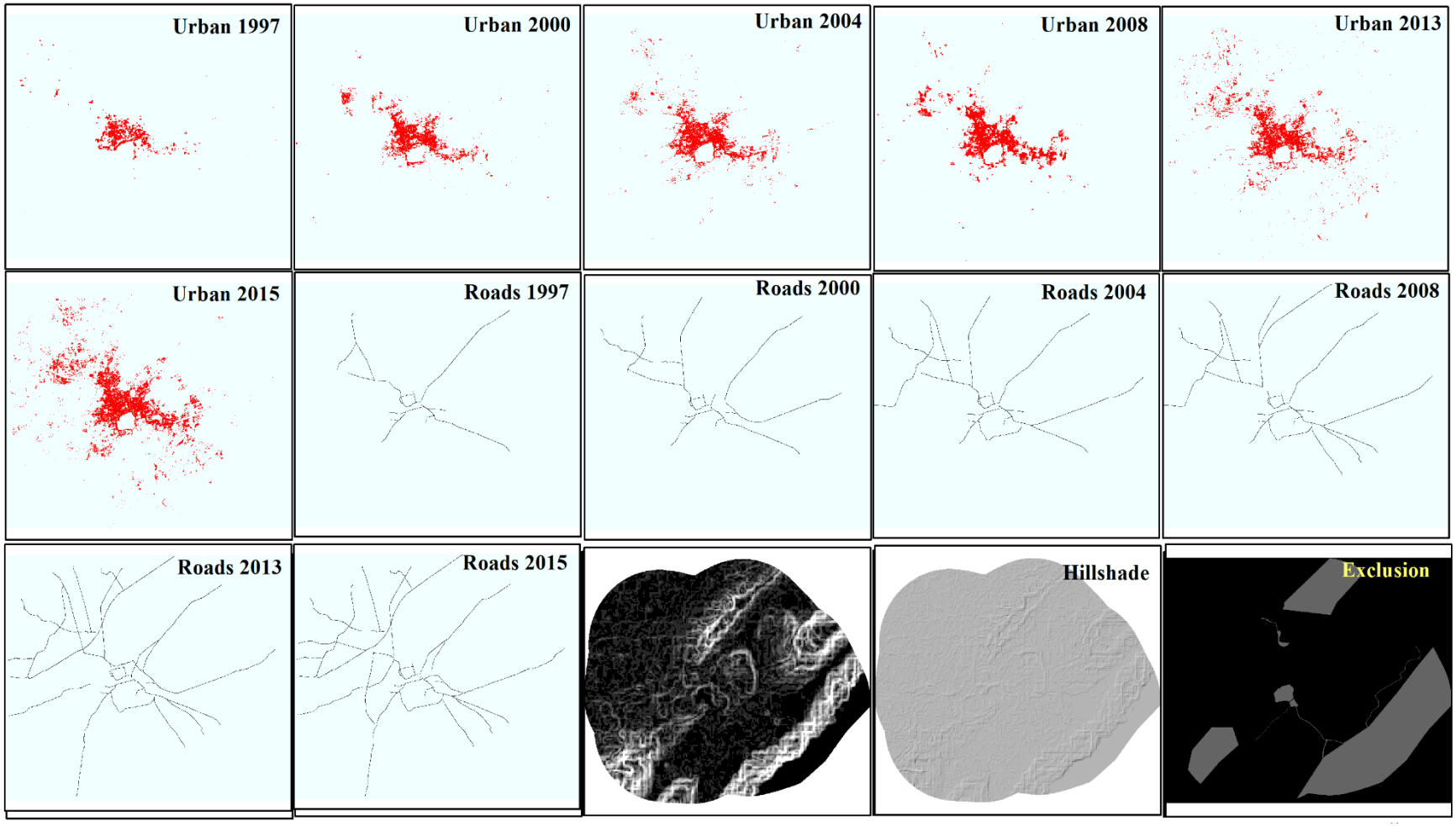

Figure 3.8: Input dataset prepared for Pushkar town

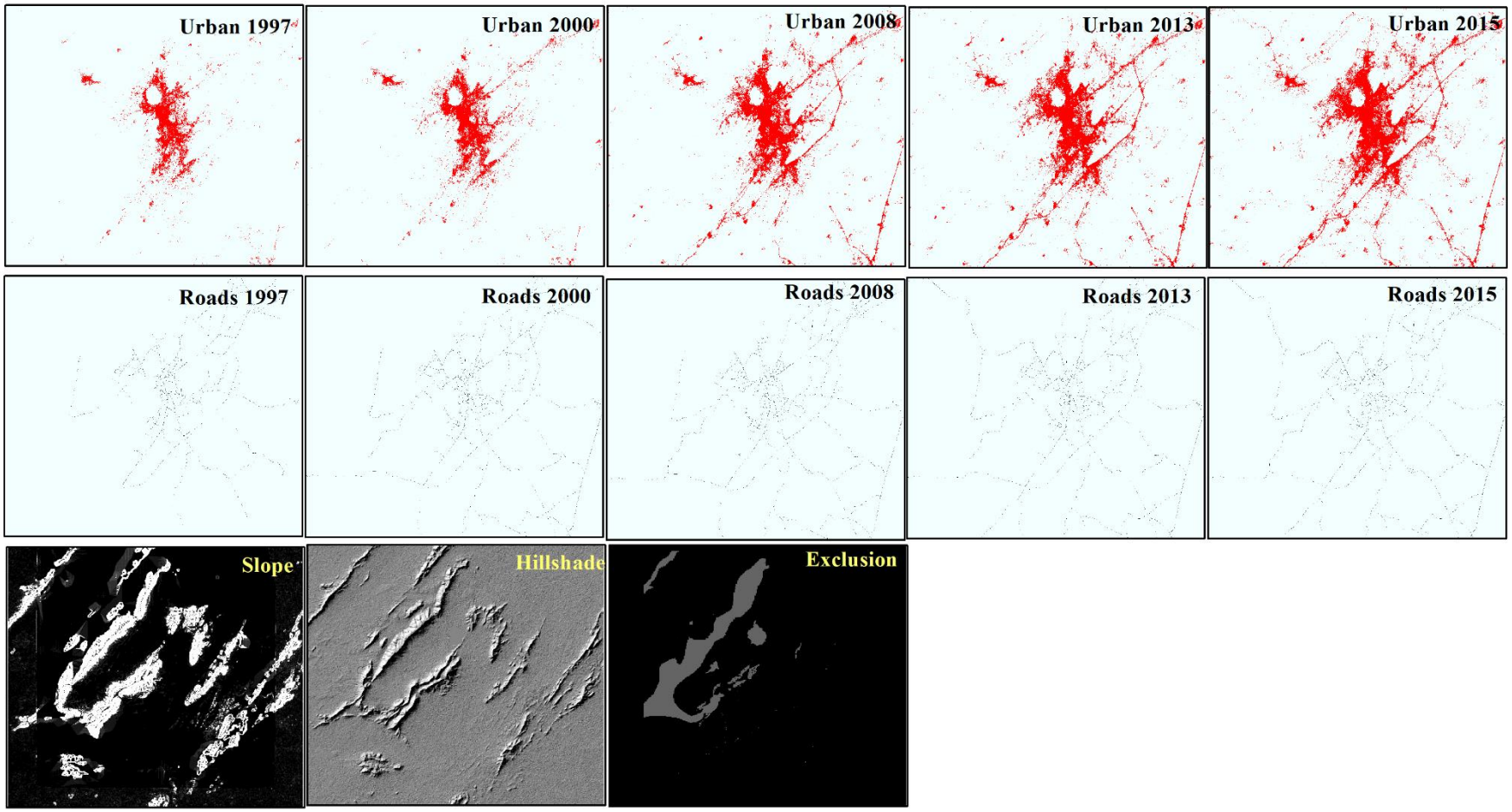

Figure 3.9: Input dataset prepared for Ajmer fringe

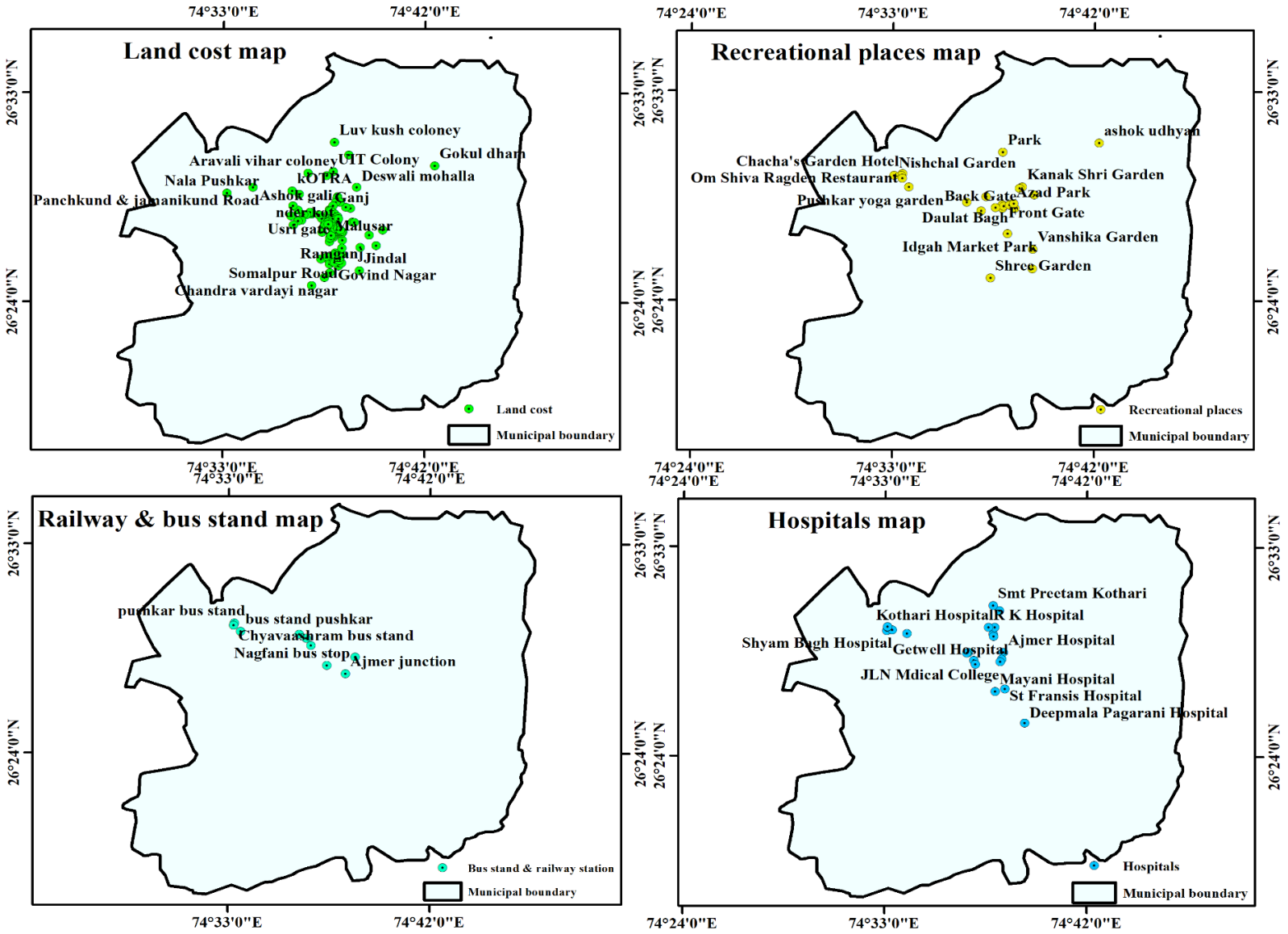

Figure 3.20: Location of different services/ facilities in Ajmer fringe

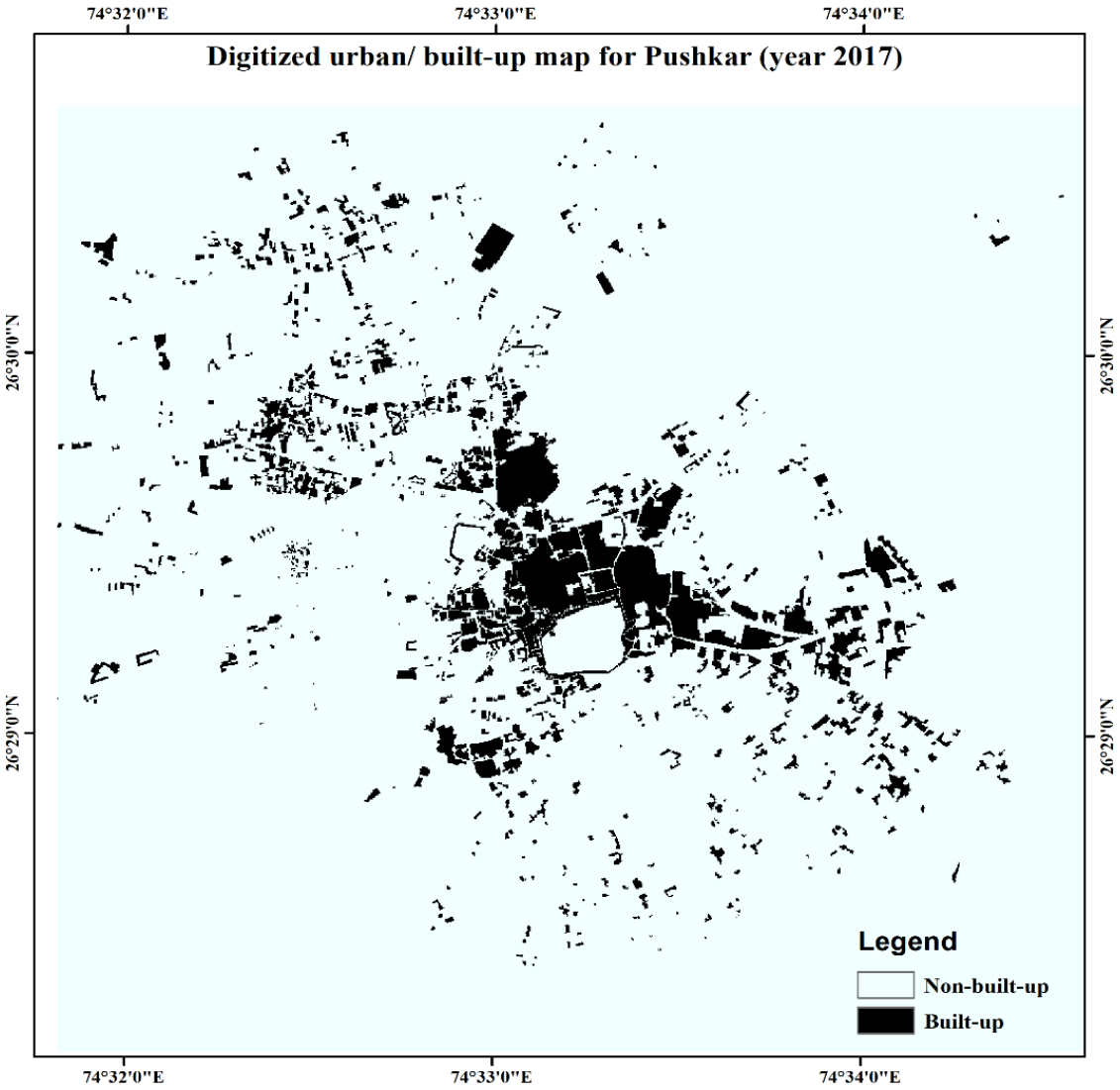

Figure 3.21: Digitized urban map of Pushkar (year 2017)

3.8.7 Locations of services and facilities

Important locations related to recreational places, bus stand & railway station and hospitals in Ajmer fringe including Pushkar has been digitized and prepared thematic layers as given in Figure 3.20. These data layers have been used for estimation of distance maps and further used for the preparation of land suitability decision layer which is discussed in Chapter 7.

3.9 Input Dataset Preparation

SLEUTH is an acronym for its input layers viz. Slope, Landuse (In case of LCD module), Exclusion, Urban, Transportation, and Hillshade maps. For the parameterization of the SLEUTH model, all these layers are used as input datasets. Prepared thematic layers are

converted into a required data and file format so they can be processed by the model. The model accepts the GIF file format thus, all the required input images have been converted into GIF file format and the complete dataset prepared for Pushkar and Ajmer fringe is presented in Figures 3.18 and 3.19, respectively.

3.10 Concluding Remarks

The database forms an essential component of any study-related earth surface like LULC transformation and urban growth. The spatial and non-spatial data both are required for LULC change and urban growth modelling. The spatial database given in this Chapter are prepared for the parameterization of different versions of the SLEUTH model. The methodology for the creation of the geographic databases is discussed in the chapter. Software used for the creation of a database in GIS has been briefly discussed. Basic thematic layers generated have been described in detail.

CHAPTER 4
METHODOLOGY

4.1 Prologue

The present study is aimed to develop improved versions of SLEUTH model which are capable of simulating urban growth more accurately, able to capture different forms of urban growth and capable of estimating the urban density/ intensity. The overall methodology used in the present research is discussed in this chapter. Methodology includes identification of research gaps and formulation of solution hypotheses to answer research questions formulated from an extensive literature review, base urban growth model development, calibration, growth prediction and accuracy assessment, sensitivity analysis for selected model constants and parameters, development of improved versions of SLEUTH i.e., SLEUTH-Density and SLEUTH-Suitability, demonstration of the application of different versions of SLEUTH for simulating the urban growth of Ajmer fringe and comparison of performance of different versions of SLEUTH.

In the present study SLEUTH, a Cellular Automata model has been used and new versions are developed for the simulation of urban growth. Therefore, first of all salient features of the SLEUTH model and its working are discussed. Methodology followed to achieve the research objectives is further discussed in the subsequent sections.

4.2 An Overview of SLEUTH Model

The SLEUTH model is a cellular automata (CA) based LULC change and urban growth model which has been in use for more than 20 years (Clarke et al., 1996; Clarke and Gaydos, 1998). The model has been used to simulate LULC change and urban growth of different cities throughout the world. The SLEUTH model is an integration of two tightly coupled models i.e. Land Cover Deltatron Model (LCDM) and Urban Growth Model (UGM) and together they are known as the SLEUTH model. UGM runs independently, while LCD is dependent on the UGM model. The former is a classic CA based urban growth model, using a Moore neighborhood and simple sequential growth rules (Figure 4.1). It uses weights for deciding probabilities, Monte Carlo (MC) simulation and growth feedback into the parameters through self-modification rules. The latter takes input of the quantity of land use transformation from the Urban Growth model and applies CA in

change space rather than geographic space. In doing so, it relaxes the single time-step rule and allows persistence and aging of cells for longer than one time step.

SLEUTH is an acronym for its input raster layers i.e. slope, land use, exclusion, urbanization, transportation and hillshade. The model is Unix / Linux based however, it can be implemented on windows using a Unix emulator such as Cygwin. The model utilizes land use/land cover maps of two different time periods to give class to class transition matrix among multiple LULC classes. At least four urban layers to represent historical urban growth are required during the calibration phase of the model. The exclusion layer is used to control the urbanization where it is restricted due to local and regional land use policies. Digital Elevation Models of the study area are used to create slope and hillshade maps while the role of the slope layer is to incorporate terrain information into the model and hillshade is for giving topographical background of the study area. Lastly, it requires transportation network information in terms of road layers of different time period to include influence of transportation facilities on urbanization.

In the SLEUTH model, urban growth behaves like a living organism that is trained by its transition rules applied on a cellular basis in a form of nested loops. The outer loop executes Monte Carlo runs while the inner loop executes transition rules. The model utilizes input historical data and provides parametric values to compute how well model runs imitate land use transitions in between input years. The SLEUTH model is framed in a sequence of growth rules and modified Cellular Automata (CA). The SLEUTH includes five growth coefficients as controlling factors; (1) Diffusion coefficient, (2) Breed coefficient, (3) Spread coefficient, (4) Road gravity coefficient, and (5) Slope resistant coefficient. These growth coefficients constitutes four growth rules i.e. (1) Spontaneous Growth (2) New spreading center Growth, (3) Organic Growth, and (4) Road Influenced Growth. Growth coefficients and rules are discussed below in detail:

4.2.1 Growth Coefficients

1. **Diffusion coefficient:** Diffusion coefficient is responsible for overall outward expansion of urban growth.
2. **Breed coefficient:** Breed coefficient determines the probability of newly urbanized pixels, urbanized in previous steps will further leads to urban growth.
3. **Spread coefficient:** Spread coefficient is responsible for edge and infill urban growth.
4. **Road gravity coefficient:** Road gravity coefficient is responsible for road influenced urban growth.

5. **Slope resistance coefficient:** Slope resistance coefficient is a slope based suitability criteria for each type of growth.

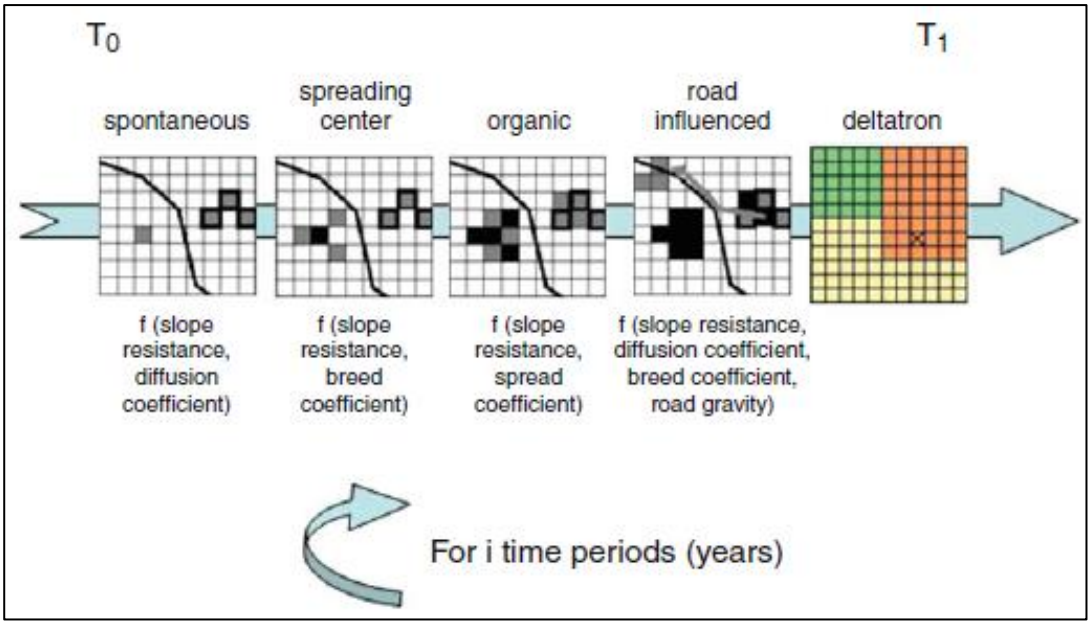

Figure 4.1: At each cycle in the CA model, five sets of behavior rules are enforced. These are controlled by the factors and parameters shown and are applied in sequence for each one "year" iteration of the model (Source: Clarke, 2014)

4.2.2 Self-modification rules

There are four self-modifying parameters i.e. *boom, bust, critical low* and *critical high*. The *boom* state occurs if the growth rate exceeds the *critical high* value. The *bust* state occurs if growth rate falls short of the *critical low* value.

4.2.3 Structure of SLEUTH model

4.2.3.1 Working of growth rules

SLEUTH simulates urban growth by executing four growth rules sequentially. Growth rules of SLEUTH are –

1. **Spontaneous growth** models the development of urban settlements in undeveloped areas.
2. **Diffusive growth** permits the urbanization of isolated cells, which are flat enough to be desirable locations for new urban spreading centers.
3. **Organic growth** promotes the expansion of established urban cells to their surroundings.
4. **Road influenced** growth promotes the urbanization along the transportation network because of increased accessibility.

The growth rules of the SLEUTH model are fixed but vary for its behavioral influence for individual parameter at each time step from zero to highest value. There are five growth controlling coefficients in SLEUTH model (as discussed above), each having an integer value within a range of 0 to 100. SLEUTH simulates urban growth satisfactorily at optimal value of these five constants. To reach out to the optimal set of five growth coefficients, the model employs four growth rules in sequence and the controlling year's simulated urban growth is compared with reference LULC information. The calibration process of the SLEUTH model is automated and processes to finally obtain the optimal set of growth coefficient values.

The optimal growth coefficient values were chosen after extensive trial and error testing. It includes parameters controlling random likelihood of being transformed from non-urban to urban (diffusion coefficient) pixel, the probability of pixels initiating their own growth trajectory independently (breed coefficient), the outward expansion of existing growth areas and infill (spread coefficient), the degree of resistance of being urbanized to growing up steeper slopes (slope resistance coefficient) and an attraction to urban development along the roads (road gravity coefficient). However, growth controlling coefficients are interrelated and controlled by the self-modifying rules, as the entire system grows faster or slower than *critical high* or *low* values, respectively. The effect of *self-modifying parameters* are to amplify rapid urban growth or retard which are termed as *boom* and *bust* stages, respectively. The working of growth rules is presented in Figure 4.2.

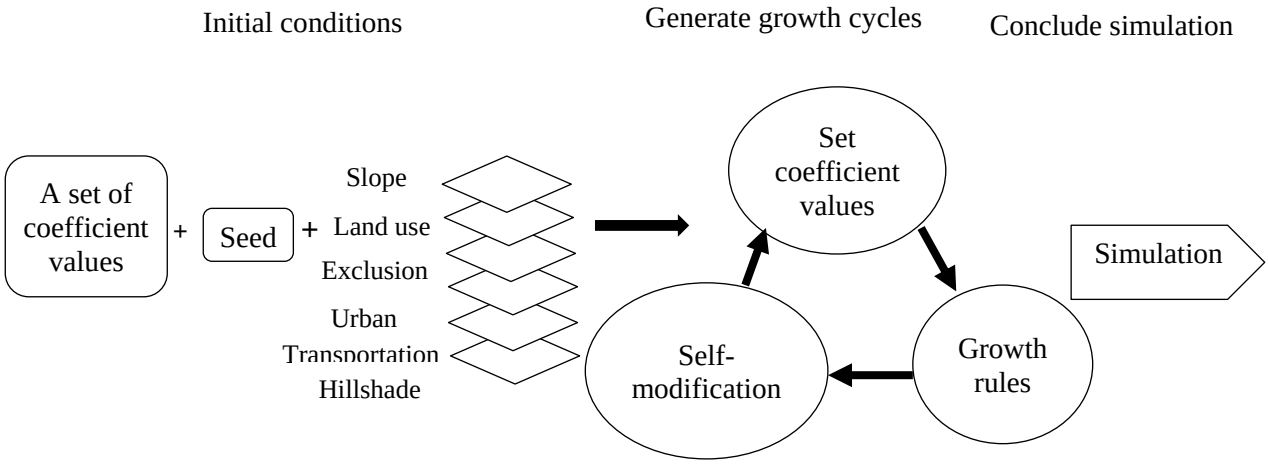

Figure 4.2: Working of growth rules

The growth rules are implemented in the SLEUTH model in a sequential manner and named as phase 1to3 (includes two growth rules itself), phase 4 and phase 5 as discussed below. The output of one phase is utilized in to the second phase and similarly it goes on executing further phases to generate urban growth patterns using historical urban area in different years as input or seed.

- Phase 1-3 growth (Spontaneous and New Spreading Centre Growth)
- Phase 4 growth (Edge Growth)
- Phase 5 growth (Road Influenced Growth)
- Self-modification Rules

4.2.3.1.1 Phase 1-3 Growth (spontaneous and new spreading center growth)

Phase 1-3 is composed of two sequential growth rules i.e. spontaneous and new spreading center growth rules. A chain of conditional loops are performed to execute this phase. Spontaneous growth utilizes diffusion and slope resistance coefficients to perform the rule in such a way as discussed below in a form of pseudo code;

Spontaneous growth (diffusion coefficient, slope resistance coefficient)

{

A loop over total diffusion coefficient values has been executed to randomly select a pixel for urbanization subject to the suitability conditions and growth rules.

Then a new spreading center growth rule is applied on randomly urbanized pixels in the spontaneous growth rule. The new spreading center growth rule utilizes the breed and slope resistance coefficients to carry out new spreading center growth as discussed below;

New spreading center growth (breed coefficient, slope resistance coefficient)

{

If the pixel gets urbanized it tries to urbanize neighboring pixels by selecting some randomly to test the random breed coefficient test

}

}/* end of phase1-3 growth */

Here, the phase 1-3 growth ends.

4.2.3.1.2 Phase 4 growth (edge growth)

Phase 4 is basically an edge growth which incorporates spread and slope resistant coefficient to perform phase 4 growth as discussed below;

Edge growth (Spread coefficient, slope coefficient)

{

A loop over all pixels of a grid selected sequentially to check whether it is urban and does it pass the random spread test. If both the conditions are met then total urban neighboring pixels are counted. Then game of life rule is applied to randomly select neighboring non-urban pixels to urbanize.

}/* end of phase 4 growth */

Here, the phase 4 growth ends.

4.2.3.1.3 Phase 5 Growth (Road Influenced Growth)

Phase 5 growth rule is composed of the utilization of diffusion, breed, spread, road gravity and slope resistant coefficients and perform in such a way as discussed below;

Road influenced growth (diffusion coefficient, breed coefficient, spread coefficient, slope resistance coefficient, road gravity coefficient)

{

If there is a new growth, begin processing the road trips. Determine the maximum search index and then select the newly growth pixel randomly to start a search for a road.

If there is a road found then walk along a random distance.

If the end pixel of road found -

{

Try to urbanize its neighboring pixel.

If urbanized

{

For maximum three tries try to urbanize neighboring pixel of the neighboring pixel randomly.

}

}

}/* end of phase 5 growth */

Here, the phase 5 growth rule ends.

After performing primary growth rules i.e. spontaneous, new spreading center, edge and road influenced growth rule, secondary growth rules, self-modification is performed to incorporate dynamism into the SLEUTH modeling.

4.2.3.1.4 Self-modification rules

The SLEUTH model also includes an another set of rules i.e. *self-modification rules* which are responsible for controlling rapid and depressed growth rates by using multiplying factors for growth coefficients.

4.2.3.2 SLEUTH programming modules and operation

The growth coefficients space is set into the scenario file, each coefficient value after the specified step value is called and setup by the coeff_obj.c program (Figure 4.3). The initialization of the model includes initialization of input grids, printing a banner statement, set up of flat memory, initialization of color tables, computation of base statistics, counting the total number of processing runs, initialization of p grids (processing grids) and reading of input data files. After setting up of the initialization it is checked whether the processing type is prediction or not. If processing type is prediction, the model is run in prediction mode (there are three modes in SLEUTH; test, calibrate and predict) in which it will set the stop year to the year up to which the urban growth prediction is to be done (Figure 4.3). The current growth coefficients values are also set and then the main simulation driving function starts working, which is denoted as 'A' in Figure 4.3. The part 'A' has been explained in Figure 4.4. After completion of simulation runs the output 'gif' images and statistics are generated. If processing type is not a prediction mode a spiral chain of loops start to access each coefficient values one by one. For each individual coefficient settings the model simulation runs take place by calling the main simulation drive function represented as 'A'.

4.2.3.2.1 Simulation driver function – 'A'

Inside the simulation driver function first the total number of pixels in each image is calculated. The driver function is mainly developed for dealing with the number of MC runs. The total number of MC runs decided by the user is invoked and for each run the model starts performing growth rules sequentially and this process gets repeated until the MC runs complete. After completion of each MC run the model produces a gif output which is temporarily stored in the working grids. When all the MC iterations are performed the cumulative form of all produced images into a single layer for every year gets generated. Along with gif outputs some predefined statistical measures are also generated with the gif images outcomes. The MC simulation itself is an important activity

into the model which is represented in Figure 4.5 as ‘B’. The details of MC iteration are given in preceding sections.

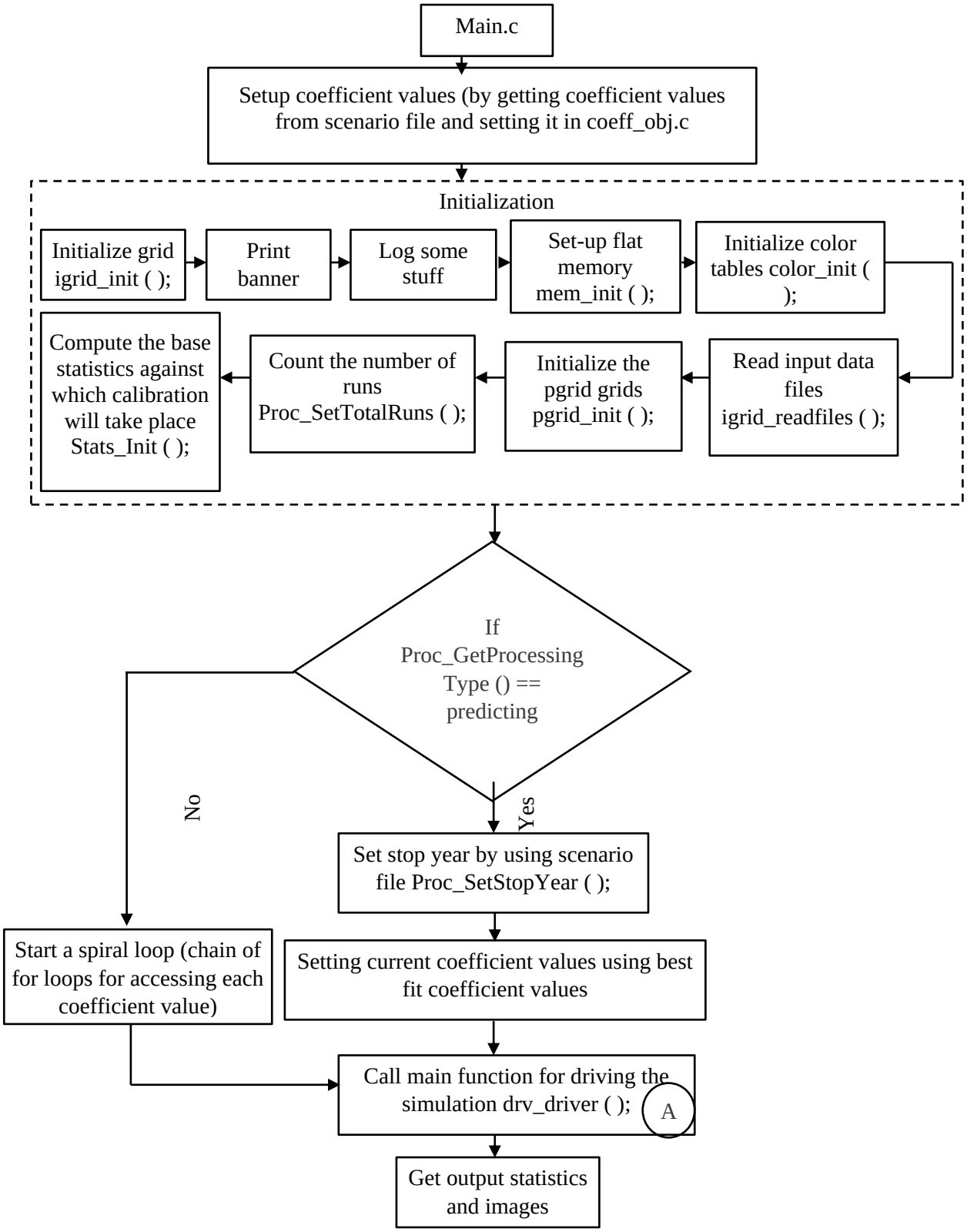

Figure 4.3: Working of SLEUTH program

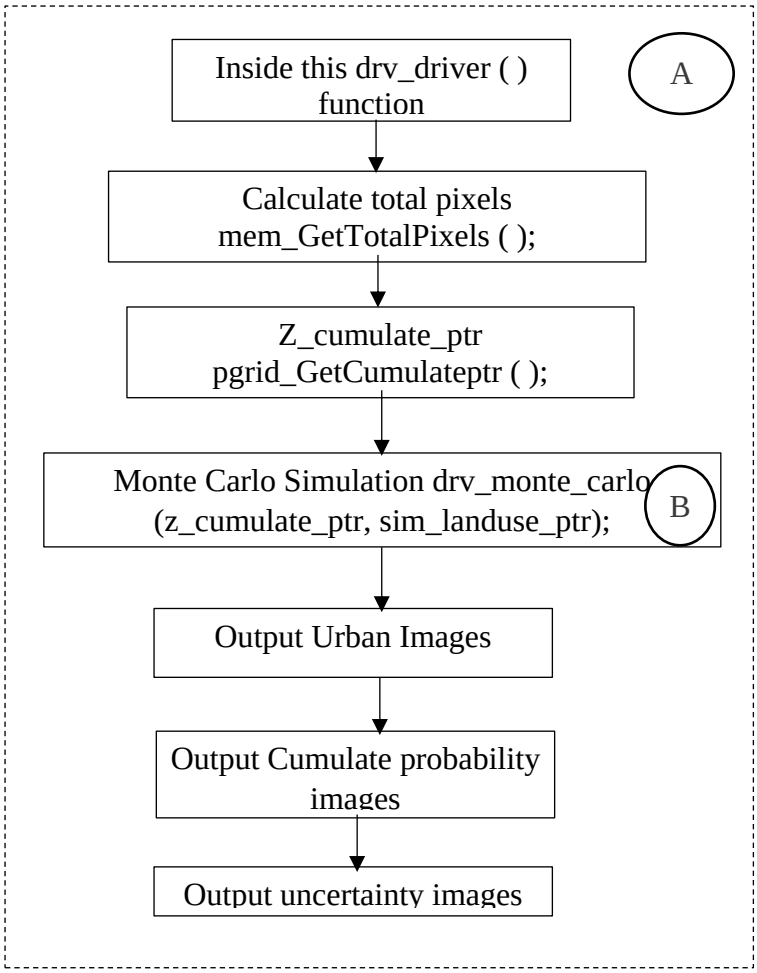

Figure 4.4: Working of Simulation driver function – 'A'

4.2.3.2.2 Monte Carlo simulations – 'B'

Monte Carlo simulations are a part of driver function and runs under the driver function. First, a function in called to get the total number of MC runs decided by the user and for this number a loop is formed so the simulations can be performed for each MC run. A loop starts and the current MC number is called. For this current MC number current growth coefficient values (i.e. diffusion, breed, spread, slope resistant and road gravity) are also set by calling the respective functions as given in Figure 4.5. For these current MC run and growth coefficients settings urban growth simulation is performed by calling grw_grow function which is a growth function. Inside this function, step by step rules are performed to simulate urban growth. The details of this growth function has been given in the preceding sections which also include another main function of performing growth rules i.e. spread. The growth function has been presented in Figure 4.6. The grw_grow function is presented as 'C'.

4.2.3.2.3 Growth function (grw_growth) – 'C'

Inside growth function two pgrids (processing grids) i.e. z_ptr for storing urban growth information, land1_ptr for storing land use change and D_ptr for built-up density related information are given as parameters of a function. Since the SLEUTH model is an integration of urban growth model (UGM) and land cover deltatron model (LCDM) as discussed previously. Therefore, these two parameters are passes into the grw_growth function. However, the primary focus of present research is urban growth simulation therefore, we would be more focusing on UGM rather LCDM model of SLEUTH.

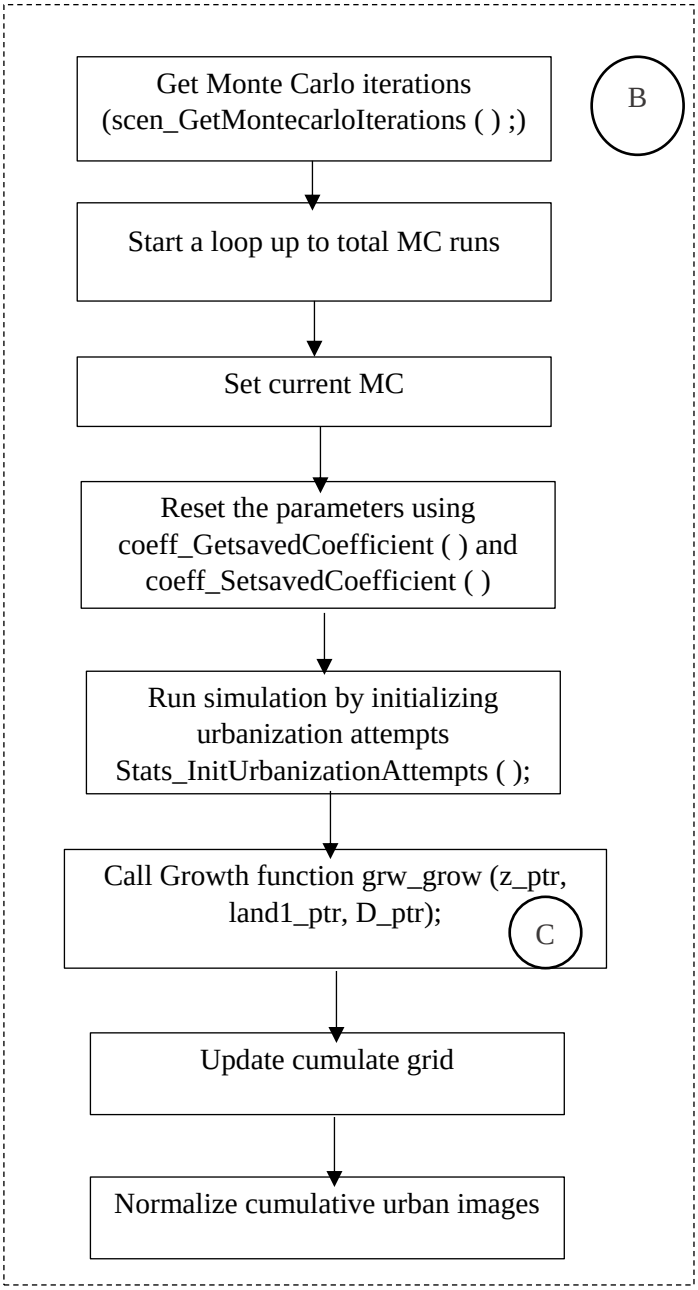

Figure 4.5: Working of Monte Carlo simulations – 'B'

The prediction dates which are given in the model scenario file are invoked to set the prediction start and stop year which indicates the duration for which simulation is to be performed. The z_ptr and D_ptr grids are initialized with '0'. The cellular automata rules for this current year as given above starts computing by calling a main function (i.e. spread) of these CA rules. This spr_spread function is named here as 'D' and is separately discussed in further sections. The methodology for spr_spread function has been presented in Figure 4.7.

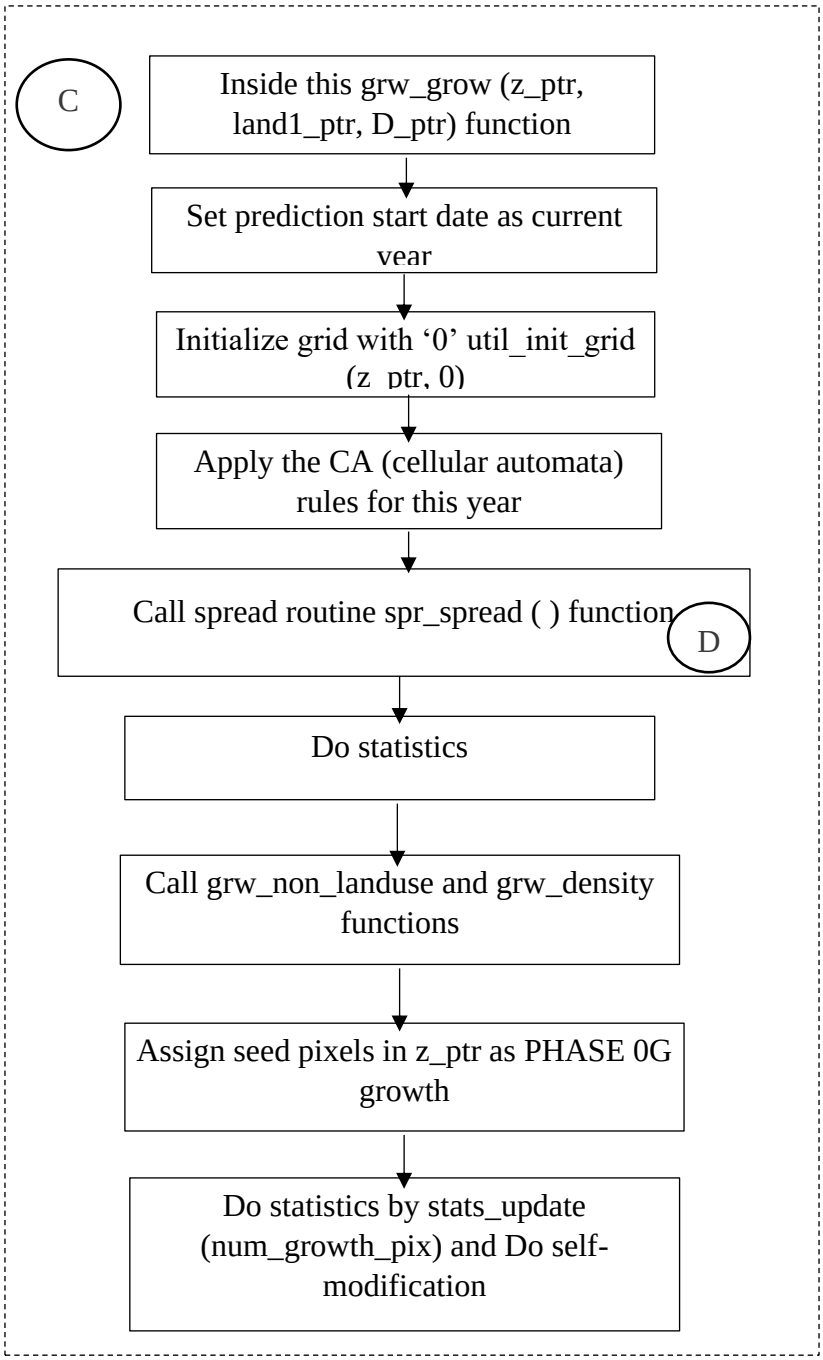

Figure 4.6: Growth function (grw_growth) - 'C'

4.2.3.2.4 Spread function (spr_spread) – 'D'

The spread function is the major function to perform cellular automata based game of life rules to simulate urban growth. The CA growth rules are performed sequentially for each growth cycle. There are in total four growth rules to be performed sequentially which are interdependent as well and named as phase 1-3 which included two growth rules i.e. diffusive or spontaneous growth and new spreading center growth rules respectively. The phase 4 includes spread growth and phase five includes road influenced growth rules, as given in Figure 4.7.

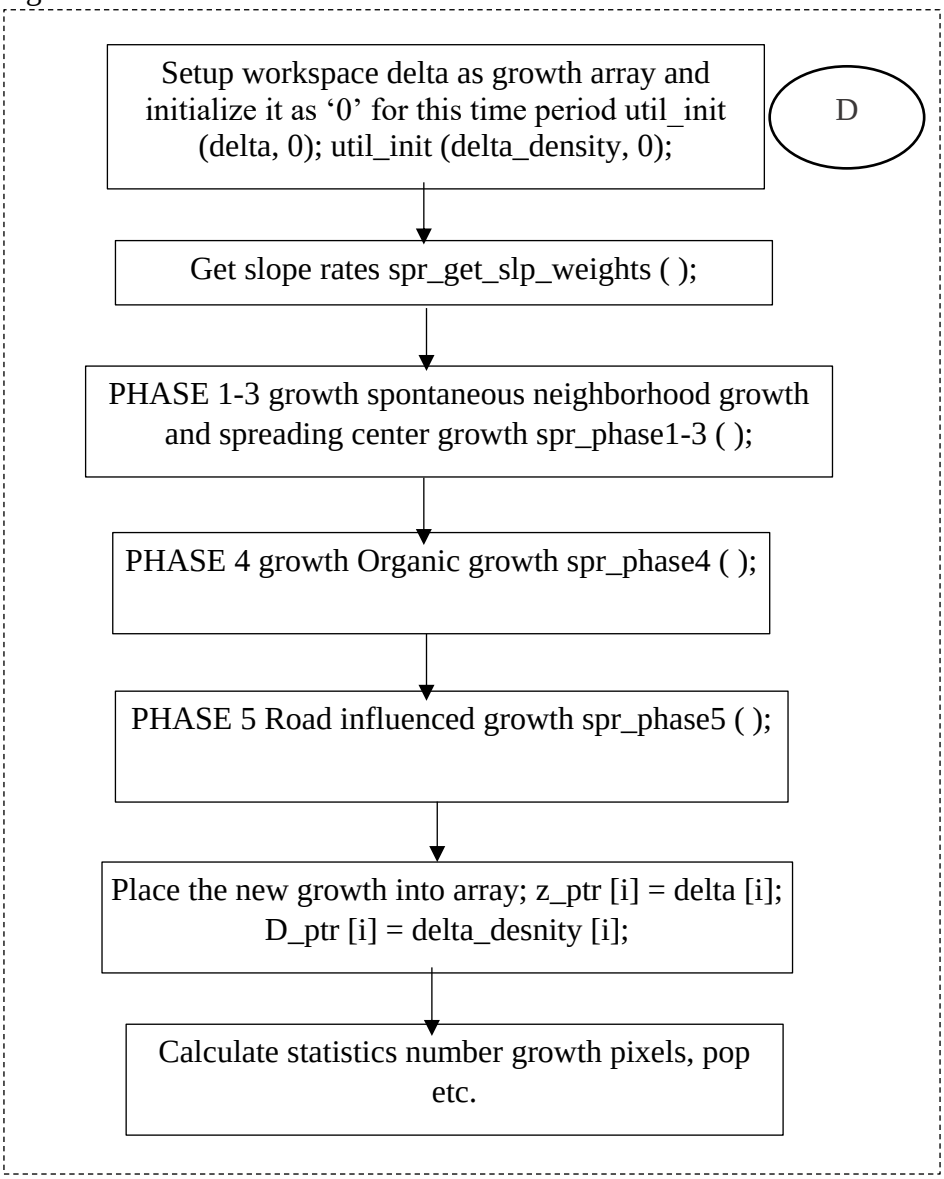

Figure 4.7: Spread function (spr_spread) – 'D'

4.2.4 Operations of SLEUTH model

A Cellular Automata (CA) is a mathematical framework that allows computational experiments in a complex spatial system over time. The main components of a CA

framework are; a cell based structure usually raster cells or pixels covering a landscape, state of cells like urban and non-urban or in detail LULC classes (i.e. forest, urban, water, wetland etc.), transition rules that control the states of cells change over time, a system clock in which rules are applied to a state for a specific time period and base condition of the framework. The SLEUTH model is parameterized from historical urban area in different years in the form of a raster dataset. All the layers are set to a fixed spatial extent and resolution. A successive application of transition rules with system synchronous updates of each cell is considered as a year.

The SLEUTH model calibration begins by first preparing model input information for the hind casting. The input data layers should be first geographically registered which include urban area maps for a minimum of four controlling years, transportation layers for two or more years, one exclusion layer, slope and hillshade map in raster format.

Urban area layers are supplied to the model in the form of binary maps, representing urban and non-urban pixels. Similarly, road layers are also supplied in the form of binary or weights. One single run is equivalent to the sequential implementation of all growth rules, including all five growth parameters or coefficients. For an individual run, model behavior and performance is tested with the help of 13 measures of goodness of fit between the modelled and actual urban area. A composite measure of these measures of fit averaged over several Monte Carlo runs is further used to decide the coefficient set.

The SLEUTH model simulates urban growth in three phases; test, calibration and the prediction phase. In the test phase, input data and model control parameters are tested for their appropriateness and readiness of the model for the calibration phase. The calibration phase uses brute force or GA based methods for the model the calibration. After completion of each years growth cycle, self-modification rules are applied which slightly alters the coefficient values to simulate accelerated or depressed urban growth. The *Boom* state occurs if the growth rate exceeds the critical high value. The *Bust* state occurs if the growth rate decreased to the critical low value. The growth rate is determined by Eq. 4.1;

$$Growth\ rate = \frac{\text{number of growth pixel}}{\text{total number of urban pixels}} * 100 \qquad (4.1)$$

The operations of the SLEUTH model is explained in Figure 4.8.

4.3 Methodology

The proposed research is aimed to understand and study the urbanization processes, drivers & mechanism of urban growth, different modelling approaches & models to develop an appropriate model which is suitable for simulating realistic urban growth and its prediction, considering selected drivers & variables using CA and geo-spatial techniques.

An effort has been made to improve and enhance the performance & capabilities of the CA based SLEUTH model by examining its sensitivity to different model parameters & constants, which have not been examined so far, by estimating the urban density and by adding another decision rule i.e., the land suitability which explains a few important urbanization explanatory variables. Further, model performance and application will be demonstrated through modelling and prediction of urban growth for a selected urban area. The methodology followed to achieve the stated research objectives is explained in Figure 4.8 and briefly summarized below.

i. Literature review to understand the present state of knowledge related to LULC change, urban growth modelling and research challenges,
ii. Collection of spatial and non-spatial data from different sources required for parameterization of SLEUTH,
iii. Preparation of land use/ land cover maps for different years through processing of satellite images,
iv. Creation of GIS database for required explanatory variables of urban growth,
v. Conceptualizations and parameterization of CA based SLEUTH model,
vi. Calibration of model for base case with existing SLEUTH model and default constant values for the test case study area,
vii. Sensitivity analysis of model for selected model input parameters and constants like spatial resolution of input variables, critical slope coefficient and self-modification constants etc.,
viii. Development of new version of SLEUTH model capable of estimating the built-up density/intensity,
ix. Development of new version of the SLEUTH model by incorporating another decision rule which explains influence of selected important explanatory variables of urbanization to improve the performance of model in realistic urban growth simulation, modelling and prediction,

x. Comparison of model performance before and after improvements in simulating the urban growth of the selected area,

xi. Demonstration of application of improved SLEUTH model for simulating the urban growth of a real urban area.

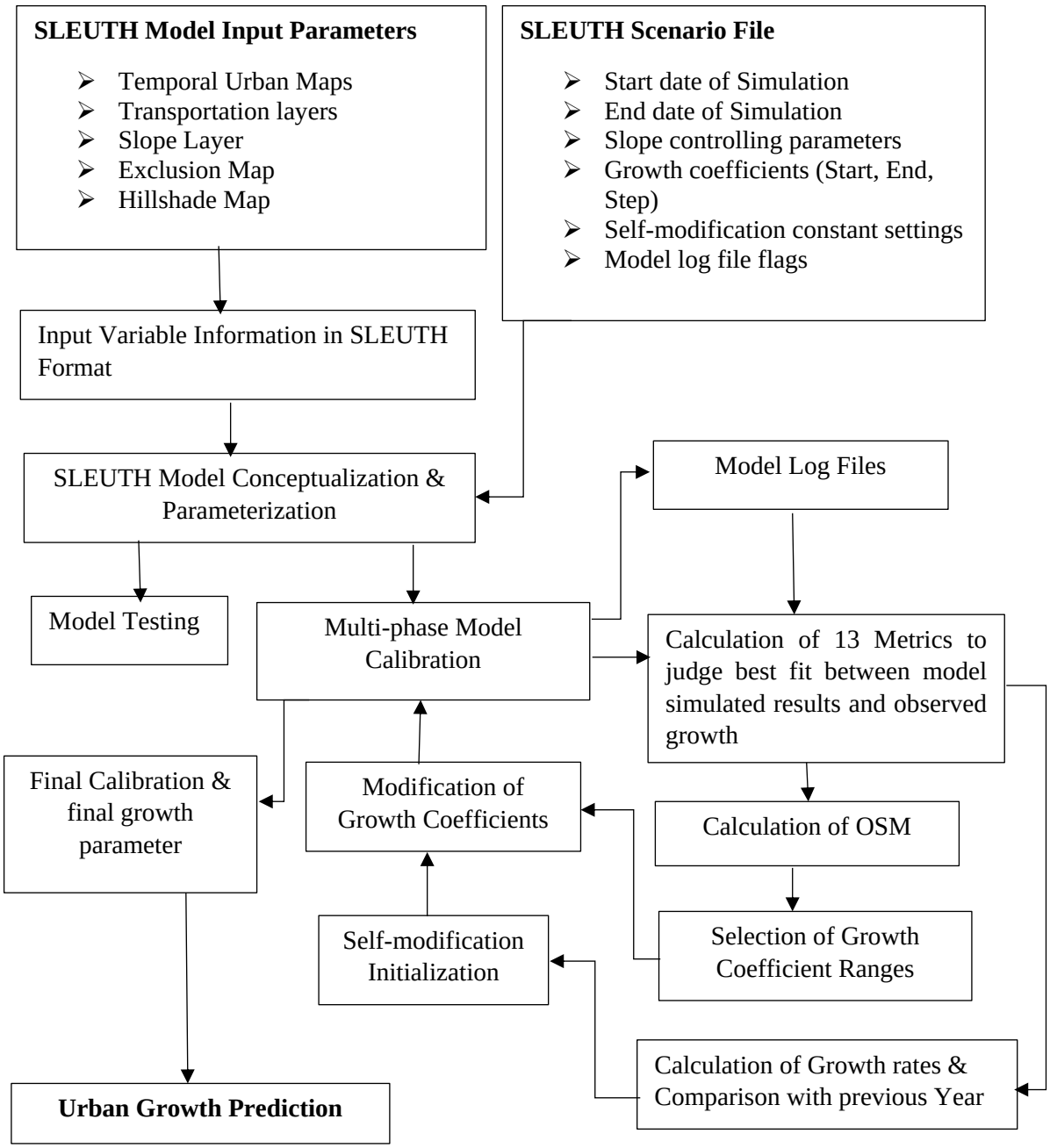

Figure 4.8: Working of SLEUTH model

Briefly, research work includes collection of spatial and non-spatial data required for the study, as discussed in Chapter 3. The required GIS database was created using appropriate methodology as discussed in Chapter 3 in detail and various thematic layers like LULC maps for different years, road layer, slope, hillshade etc. have been generated. Historical LULC information has been extracted from the satellite imagery using standard digital

image processing methods like image registration, rectification, training or classification algorithm and accuracy assessment. The other bio-physical, socio-economic and demographic data utilized as the attributes for the respective thematic layers are used as input datasets for parameterization, calibration or in development and testing of improved versions of the SLEUTH model.

The SLEUTH model has been conceptualized for Pushkar and Ajmer areas in a base case scenario using the default model constants/ parameters. Base case model has been calibrated successfully and urban growth is predicted. Further, base model performance has been tested in predicting the urban growth of Ajmer and Pushkar through accuracy assessment with respect to reference data. Performance of the base model has been found to be fair and model limitations and their probable causes were identified. The model is not able to capture the fragmented urban growth and different form of urbanization well. It was observed that model performance can be enhanced by determining the optimal value of some of model constants through sensitivity testing. Model performance can further be enhanced by incorporating a few other important explanatory variables of urbanization in the urban growth simulations like land suitability as an additional growth rule which can be defined by land cost, distance from important roads, and distance from important places like railway station, bus stand, recreational places and city center.

Rigorous sensitivity analysis has been carried out to judge the behavior of the model with respect to changes in a few selected model constants using the Pushkar data. Model sensitivity has been tested for some of the crucial parameters of the SLEUTH model such as self-modifying parameters (i.e. boom, bust, critical low and critical high), critical slope, Monte Carlo iterations, cellular neighborhood, game of life rules and diffusive value parameter using an iterative procedure. Details of the sensitivity analysis are discussed in Chapter 5 in detail and in subsequent sections of this chapter. Further, performance of SLEUTH with optimal model constants has been determined through accuracy assessment. Further, to improve the SLEUTH performance, efforts have been made to develop a new improved version of the SLEUTH model i.e., SLEUTH-Suitability which can simulate urban growth using an additional growth decision rule i.e., land suitability. A suitable algorithm is developed, required code was written and integrated with SLEUTH code. Land suitability decision variables includes influence of selected urbanization explaining variables. The SLEUTH-Suitability was developed and tested using the Pushkar datasets.

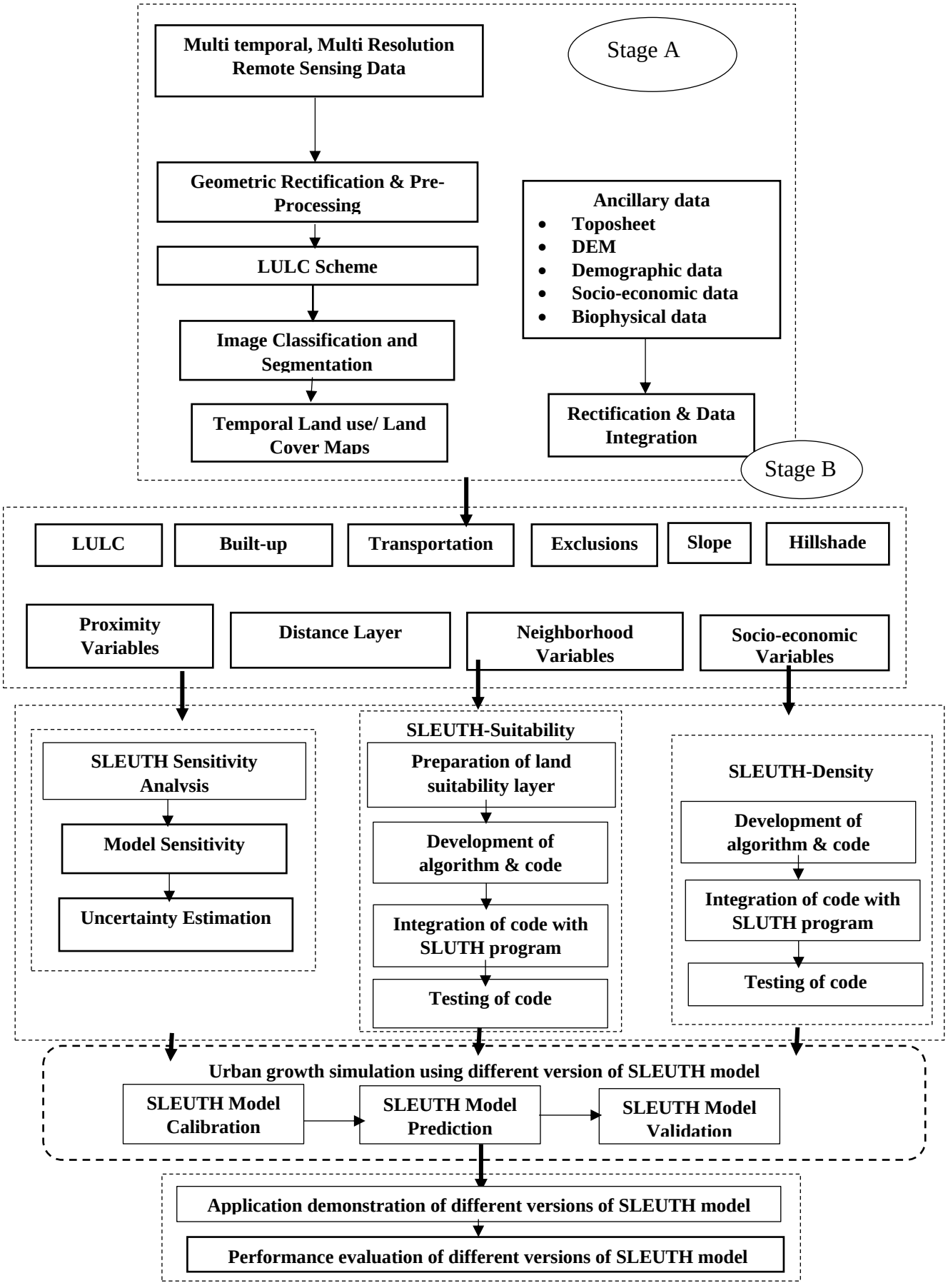

Figure 4.9: Overall methodology of research work

The performance of SLEUTH-Suitability was tested again through accuracy assessment with respect to two reference data sources (urban area obtained from classified satellite image of year 2018) and ground truth information collected from the field survey for both Pushkar and Ajmer fringes. Development, testing and application demonstration of SLEUTH-Suitability is discussed in the Chapter 7 in detail.

A new version of the SLEUTH i.e., SLEUTH-Density has been developed by adding additional capability to the existing model to estimate and predict built-up density/ urban intensity. The new module has been developed by developing a density estimating algorithm, developing programming code and integrating with code of the existing SLEUTH model. Details of the SLEUTH-Density development, testing and application demonstration are presented in Chapter 6.

Further, performance of different versions of SLEUTH i.e., base version with default constants, SLEUTH with optimal model constants and SLEUTH-Suitability has been examined by comparing urban growth simulations for the Ajmer fringe. Performance has been judged in the form of different statistical metrics, visual urban growth matching and accuracy assessment with respect to ground truthing. Comparative performance evaluation of different versions of SLEUTH is presented in Chapter 8. Methodology has been explained in detail in subsequent sections.

4.3.1 SLEUTH parameterization

To parameterize and conceptualize different versions of the SLEUTH, input data has been extracted in the required format (raster grid) at selected resolution from the GIS database. Input data includes urban & transportation maps of different years (five years, 1997, 2000, 2008, 2013 and 2015) in binary format like urban as 1 and non-urban as 0, percentage slope, exclusion map and hillshade map (Figure 4.9) for both the study areas i.e., Ajmer fringe and Pushkar. Creation of the GIS database and preparation of different thematic layers from where input data was extracted has been discussed in Chapter 3 in detail. Input data required for other versions like SLEUTH-Suitability and SLEUTH-Density was extracted from the GIS database. Additional input data prepared for SLEUTH-Suitability includes the data layers related to proximity, distances and land cost explanatory variables which are used to prepare an additional decision rule i.e., land suitability. These datasets have also been extracted from the GIS database in raster format and used during model calibration and urban growth prediction. Database related to years 2016, 2017 and 2018

have been prepared for evaluation of model performance for both Ajmer and Pushkar study areas. SLEUTH parameterization has been explained in *Stage A & B* in Figure 4.9.

4.3.2 Model calibration and urban growth prediction

The SLEUTH model simulates the urban growth in three phases i.e. test, calibration and prediction. In the test phase all the input variables including input data layers are checked whether they are in the required format or not. After the test phase the model transfers the control to the calibration phase which is the crux of the model. Model calibration includes various tools and techniques which attempt to determine the model growth coefficient values at which model best replicates historical growth. The model utilizes different constants like diffusivity constant, self-modifying parameters, etc. which remain internal to the model and can be chosen in some specific conditions. It is the first stage of calibration to determine growth coefficients, as a part of model design. The model calibration also depends on growth coefficients (as discussed above) which are selected by the user based on the model fitness criterial and metrics in each phase. SLEUTH model calibration can be either performed by Brute Force or Genetic Algorithm (GA) based methods and it involves Moore Neighborhood (8-cell). SLEUTH-GA is the new version of the model which optimizes time complexity and has been released recently.

The traditional method of calibration in SLEUTH is by brute force which is a sequential multi-stage optimization process. Every possible permutation and combination of growth coefficients for decided ranges is tested to reach an optimal solution (Silva and Clarke, 2002). Through the Brute Force method, the controlling growth coefficients are refined in different phases sequentially i.e. coarse, fine and final and the best fit coefficient values are determined on the basis of Optimal SLEUTH Metric (OSM), a composite model fitness metric. A number of possible combinations within a large growth coefficients' space i.e. 0 - 100 is refined over a number of Monte Carlo iterations (i.e. 10). Initially, the model is calibrated for the coarse phase to refine the coefficient values, thereafter fine phase calibration is performed using refined coefficient values in the earlier calibration phase. In the fine phase refined coefficient values are further used for final phase calibration. The motive of the calibration phase is to refine the growth coefficient values for further growth prediction. Calibration process in Brute force method is user monitored through selecting the growth coefficient values manually for each calibration phase based on sorted model best fit statistics and subsequently selected growth coefficients are used for the next phase of calibration.

The Genetic algorithms (GA) is heuristic approach which can be used to simulate natural evolution to obtain an optimal result. GA has an advantage as it avoids human intervention completely from the calibration process. SLEUTH-GA iteratively explores the entire coefficient space in one go with no need to pass through multiple calibration phases (as in case of conventional SLEUTH). In SLEUTH-GA, coefficient and parameter values related to GA like crossover, mutation, fitness, evaluation and survival selection based constants (such as population size, generation, number of offspring, mutation rate and number replaced) are needed to be selected during calibration. In GA, the chromosome is a string of growth coefficients in a predefined order i.e. diffusion, breed, spread, slope resistant and road gravity where individual values represent a gene. A set of genes is called as a chromosome which is evaluated one gene at a time. The initial population used to start the calibration process which is termed the seed population and further successive population forms a generation. The SLEUTH-GA has been set for its default parameter values which are extracted from a rigorous evaluation of best performing parameter values. In the present work, population size as 55, generations as 100, mutation rate as 0.13, number of offspring as 55 and number replaced have been adopted as 50. Each generation replaced the weakest gene in the old population with the strongest gene in the new population (Clarke, 2017, 2018) corresponding to the best fitness measure (i.e. OSM).[2]

The SLEUTH model generates 13 goodness of fit metrics regressed between actual and simulated urban area (Table 4.1) for its individual calibration phase. For every possible set of growth coefficient values a corresponding 13 metrics values are generated. However, the highest fit value of a metric may often lead to the disagreement among other metrics. Therefore, Lee Sallee metrics which is an urban pattern index and OSM metrics (a product of 'compare', 'population', 'edges', 'clusters', 'slope', 'X-mean', and 'Y-mean') are the most preferred metrics for selecting optimum growth coefficient values. Deciding the number of Monte Carlo (MC) runs is also a crucial step in model calibration. In various studies, (Rafiee et al., 2009; Wu et al., 2009) 10 MC runs are set as model calibration to optimize the time and performance of model calibration and in present study also the same number of MC runs have been used in calibration. On final completion of calibration the best fit coefficient values averaged over a number of Monte Carlo runs are obtained and urban growth prediction (i.e. third phase of SLEUTH simulation) is

[2] http://www.ncgia.ucsb.edu/projects/gig/

performed. The prediction phase produces simulated urban growth for the desired year in the forms of raster maps presenting historic and future trends of urbanizations and statistics like urban area, growth rate etc. The flow of SLEUTH model run has been explained in Figure 4.10 which is considered as Stage-C in methodology.

Present study has utilized both the calibration methods as SLEUTH-GA is recently developed and launched and it has been used in present study as well.

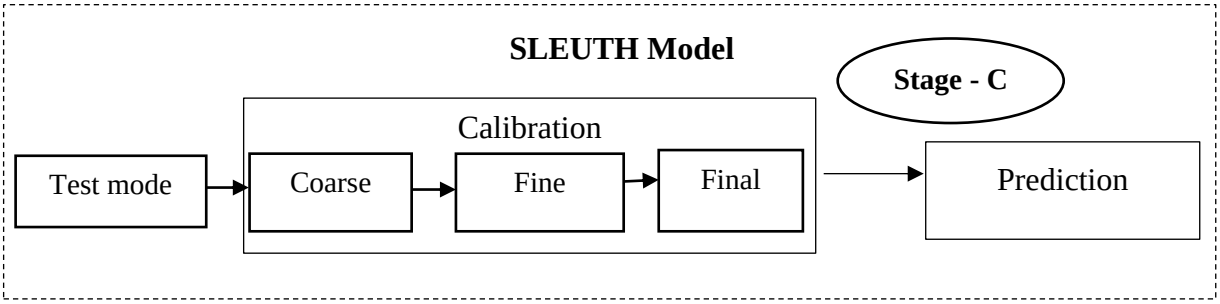

Figure 4.10: Work SLEUTH calibration and growth prediction process

Table 4.1: Model fitness metrics

S.no.	Metrics	Description
1	Compare	Modeled population for final year/actual population
2	Pop	Least squares regression score for modeled urbanization compared to actual urbanization for the control years
3	Edges	Least squares regression score for modeled urban edge count compared to actual urban edge count for the control years
4	Clusters	Least squares regression score for modeled urban clustering compared to known urban clustering for the control years
5	LeeSallee	A shape index, a measurement of spatial fit between the model's growth and the known urban extent for the control years
6	Xmean	Least squares regression of average x_values for modeled urbanized cells compared to average x_values of known urban cells for the control years
7	Ymean	Least squares regression of average y_values for modeled urbanized cells compared to average y_values of known urban cells for the control years
8	Radius	Least squares regression of standard radius of the urban distribution, i.e. normalized standard deviation in x and y
9	OSM	a product of 'compare', 'population', 'edges', 'clusters', 'slope', 'X-mean', and 'Y-mean'
10	Mean cluster size	least squares regression score for modeled average urban cluster size compared with known mean urban cluster size for the control years
11	Average slope	Least squares regression of average slope for modeled urbanized cells compared with average slope of known urban cells for the control years
12	Urban (%)	Least squares regression of percent of available pixels urbanized compared with the urbanized pixels for the control years
13	F match	A proportion of goodness of fit across land use classes.

4.3.3 Sensitivity analysis

The sensitivity analysis of selected SLEUTH model parameters/constants has been carried out using iterative process as explained in Figure 4.11.

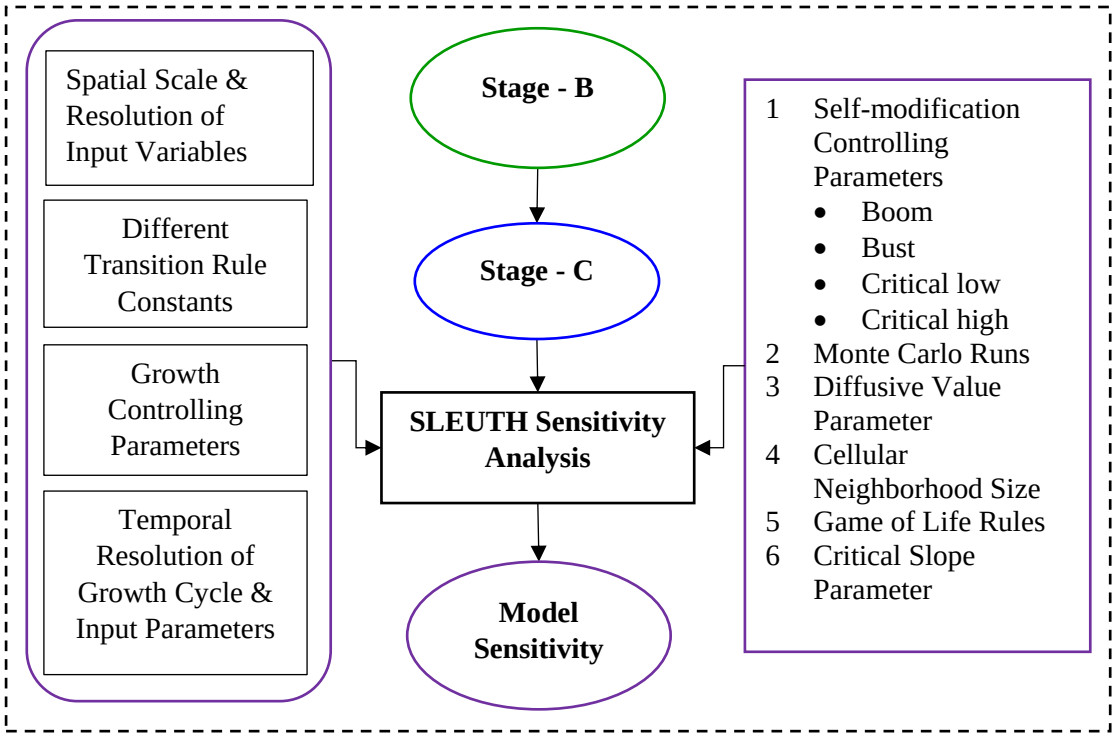

Figure 4.11: Process of sensitivity analysis

Few crucial model constants/ parameters for which SLEUTH sensitivity has not been tested so far (Silva and Clarke, 2002; Jantz and Goetz, 2005; Kantakumar et al., 2011; Clarke, 2014; Houet et. al., 2016) are selected for the present sensitivity analysis. Sensitivity analysis has been carried out using an iterative procedure (Figure 4.11). The model has been parameterized, calibrated and urban growth was predicted for a range of selected model constants. Relative change in model response in term of change in simulated urban area and other statistical best fit metrics with respect to change in each constant value has been determined by running the model number of times for a range of values of each constant at a time, keeping other model constants at same level. Six model constants have been selected for their sensitivity testing in the present study. These constants include; self-modifying parameters i.e. *boom*, *bust*, *critical low* and *critical high*, critical slope, diffusive value parameter, cellular neighborhood size, game of life rules and number of Monte Carlo runs. Methodology of sensitivity analysis has been presented in Figure 4.12.

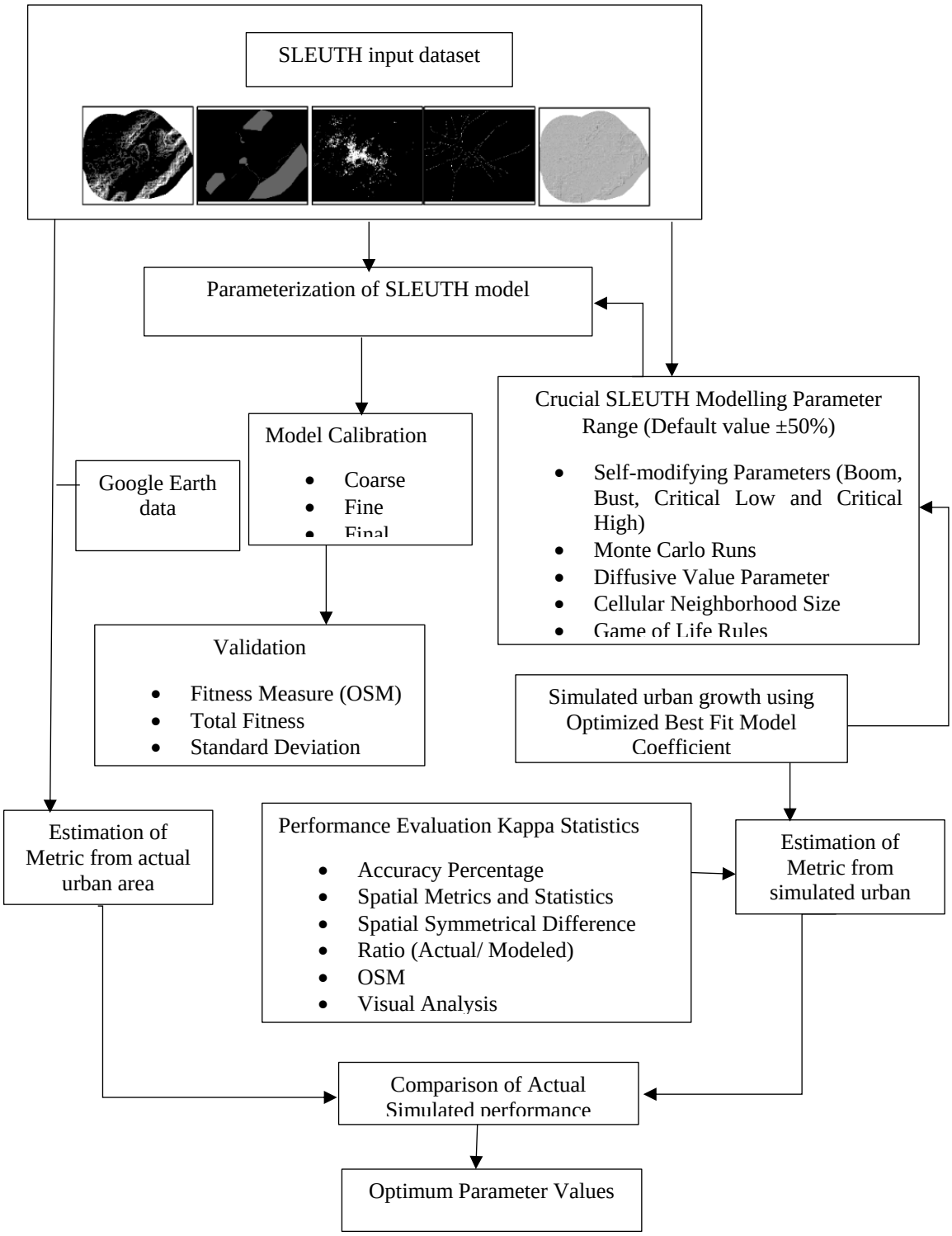

Figure 4.13: Methodology for sensitivity analysis

Model sensitivity analysis includes model parameterization for a range of values of individual constant decided as the default value ±50% prescribed for that constant independently. Furthermore, calibration has been performed to obtain an optimal set of growth coefficient values on the basis of model fitness measure i.e. OSM and final urban growth was predicted up to year 2040 for each and individual constant range,

independently. Finally, accuracy of the predicted urban growth has been assessed to determine the optimum parameter values for which model is more accurate in imitating the real urban growth, able to capture different form of urban growth and patterns. The accuracy has been assessed on the basis of accuracy percentage, kappa statistics, goodness of fit metrics, spatial and statistical measures, OSM and visual analysis with reference to Google Earth image and input dataset based actual data for the respective years. Sensitivity analysis has been presented in detail in Chapter 5.

4.3.3.1 Self-modifying parameters

The SLEUTH model has four self-modifying parameters i.e. *boom, bust critical low* and *critical high*. The default value of *boom* constant is 1.01. For testing the model sensitivity to the boom constant, model has been run iteratively for a range of boom values from 0.5 to 1.5 and relative change in model response (urban growth) has been determined for each value using the methodology explained above. Relative change in model response has been determined in terms of spatial and statistical metrics and accuracy assessment with respect to reference data. Optimum value of boom constant is the value at which model simulated growth has been found to be most satisfactory in term of criteria as explained above.

Similarly, model sensitivity to other self-modifying parameters like *bust*, critical high and critical low was determined by simulating the urban growth iteratively for a range of these parameters individually and comparing simulated urban growth with the actual growth corresponding to default value of that particular parameter. Model sensitivity has been checked for *bust* constant for a range of 0.05 to 1.35 (default value is 0.09), for *critical high* for a range of 0.65 to 1.95 (default value is 1.3) and for *critical low* constant for a range of value from 0.5 to 1.5 (default value is 0.97).

For each self-modifying parameter model sensitivity and optimum value have been obtained by comparing simulated urban growth for each value of individual constant with the urban growth corresponding to the default value and actual urban growth obtained from the reference data for year 2016 and 2017. This rigorous sensitivity analysis has been done to improve existing knowledge of the model behavior as a function of these constants. The total 39 sets of different values of self-modifying parameters have been tested for sensitivity. The 39 sets leads to (39 * 3) 117 calibration and growth prediction runs.

4.3.3.2 Monte Carlo runs

The SLEUTH urban growth model is a stochastic model therefore, to include randomization into the modelling, Monte Carlo simulation has been adopted. It provide an estimate of variances in outputs. For a single set of coefficients multiple simulation runs are generated to have an idea about the quantitative and qualitative variances in outcomes. Deciding the number of Monte Carlo runs for model calibration is always a complex decision and a set of model results are generated for different sets of parameter combination in order to determine the best fit coefficient set. In a few studies, it has been reported that 10 ~ 100 number of MC runs are used in practice, however the higher number of MC runs the more the requirement of computational resources (Goldstein et al., 2005(. To investigate the influences of different MC runs on model performance during calibration, model sensitvity to the number of MC iterations has been tested by running the model with the same input dataset and model constants for a range of MC runs i.e., 10 to 300 and determining the relative chnage in model response with respect to calibration performance and in resulting urban growth prediction. This is discussed in detail in Chapter 5.

4.3.3.3 Cellular neighborhood

The cellular automata based SLEUTH model has the capability to effectively include the neighborhood influences on urbanization while simulating the urban growth. The size of cellular neighborhood plays an important role to quantify the extent of neighborhood influences on urban growth. Presently, the SLEUTH model is utilizing 8 cell Moore neighborhood extent. There may be some other sizes of cellular neighborhood which can incorporate the neighborhood extent influence correctly in the urban growth simulation. Thus, to identify the effect of extent of neighborhood on model response (urban growth) urban growth for an area (with same input data and model constants) was simulated considering different sizes of cellular neighborhood in SLEUTH i.e. Von Neumann 4 cell neighborhood, 8 cell Moore Neighborhood and 12 cell extended Moore neighborhood. For all the three neighborhood sizes, the SLEUTH model code was modified separately and the model redeveloped. Optimum value of neighborhood extent size was determined by comparing the model outcomes and model fitness metrics with the actual urban area extracted from reference datasets and their respective metrics. A particular extent size for which spatial and statistical metrics calculated from reference data and simulated growth are comparable with minimum difference will be the optimum neighborhood size.

4.3.3.4 Game of life rules

There is another crucial parameter of the CA based SLEUTH model i.e. game of life rule which play a crucial role in modelling of urban growth. CA has the ability to easily incorporate complexity and dynamism of urbanization influencing phenomenon where human behavior is involved. The SLEUTH model incorporates game of life rules for simulating urban growth. The game of life rules helps in determining the state of a cell/ pixel based on the neighborhood conditions in the form of birth, survival and death. The birth state implies a non-urban pixel becomes urban, survive state infers an urban pixel remains urban and death state is when an urban pixel becomes non-urban. The threshold value in game of life rules plays an important role in imitating the urban growth of a study area. Urbanization is a function of many socio-economic, cultural and topographical characteristics of an area. Game of life rule which is capable in simulating the urban growth of a particular country with a particular socio-economic characteristics may not be suitable for other countries having different socio-economic characteristics like developed countries and developing countries. Therefore, model sensitivity to the game of life rule has been tested by running the model iteratively for three type of game of life rules i.e., Type I, Type II and Type III. Suitable game of life rules for correctly simulating the urban growth in socio-economic conditions like India has been determined by comparing the spatial and statistical metrics computed from simulated growth corresponding to different rules and metrics calculated from reference data sets. Detailed discussion and results of sensitivity analysis are discussed in Chapter 5.

4.3.3.5 Critical slope

The critical slope parameter in the SLEUTH model is responsible to include the effect of less chances of urbanization on locations with steeper slope into urban growth simulation. It is used for deciding slope weights in a look up table with the help of the slope resistant coefficient which takes part in decision making of urban growth in terms of growth rules. Currently, the SLEUTH model uses 15 as the default critical slope value. The model sensitivity to the critical slope parameter has been determined using the methodology discussed above by calculating the change in model response (change in urban growth) for different critical slope values i.e., 1 to 29. The optimum value of the critical slope parameter will be that particular value at which spatial and statistical metrics calculated from the simulated urban growth is nearest to the metrics calculated from the reference data. The details are presented in Chapter 5.

4.3.3.6 Diffusive value parameter

The SLEUTH model uses four growth rules for simulation of urban growth i.e. diffusive, new spreading center, spread or edge and road influenced growth. These four types of growth rules are constituted by five growth coefficients i.e. diffusion, breed, spread, slope resistant and road gravity coefficients as discussed above. The first growth rule i.e. diffusive growth is responsible for spontaneous urban growth and it is enforced by the diffusion coefficient as given in Eq. 4.2.

$$diffusion\ value = \left((\text{diffusion coefficient} \times 0.005) \times \sqrt{nrows^2 + ncols^2}\right) \quad (4.2)$$

The diffusive growth rule attempts to urbanize non-urban cells or pixels and how many times this attempt will be made for a single run is calculated in terms of diffusive value to be calculated using Eq. 4.2. For calculating diffusive value the current diffusion coefficient is multiplied with 0.005 times the image diagonal (i.e. square root of the sum of squares of number of rows and columns). The numeric value of '0.005' which is called the diffusive parameter value remains constant throughout the urban growth simulation. For different geographical locations urban growth forms and patterns may vary. The diffusive growth parameter value may also be different for urban areas of different socio-economic and topographical settings. Therefore, SLEUTH sensitivity to diffusive growth parameter has been studied using methodology discussed above by determining the relative change model response corresponding to a range of values (0.0025 to 0, 0.0075) of this parameter.

4.3.4 Development of SLEUTH-Suitability

To incorporate the influence of other LULC change and urban growth explanatory variables in urban growth simulations, a newer version of SLEUTH i.e. SLEUTH-Suitability has been developed using the methodology presented in Figure 4.13. The input data layers prepared in stage B (Figure 4.4) were used for preparing different layers of explanatory variables like land cost, proximity from main roads, railways, recreational places, bus stand and hospitals and topographical variables like slope, which were further used to prepare another decision input dataset i.e., land suitability. A land suitability layer has been prepared using AHP based Multi-criteria Evaluation (MCE) technique. The AHP weights were decided based on the available literature. Preparation of the land suitability layer has been discussed in detail in Chapter 7. The SLEUTH model algorithm has been improved to include one additional growth rule based on land suitability for urbanization.

Suitable code has been developed and integrated with the base SLEUTH code to develop SLEUTH-Suitability version. The details describing the methodology of suitability module in to the SLEUTH model is explained in Chapter 7. In addition preparation of MCE and AHP based suitability layers for different years has also been explained in Chapter 7.

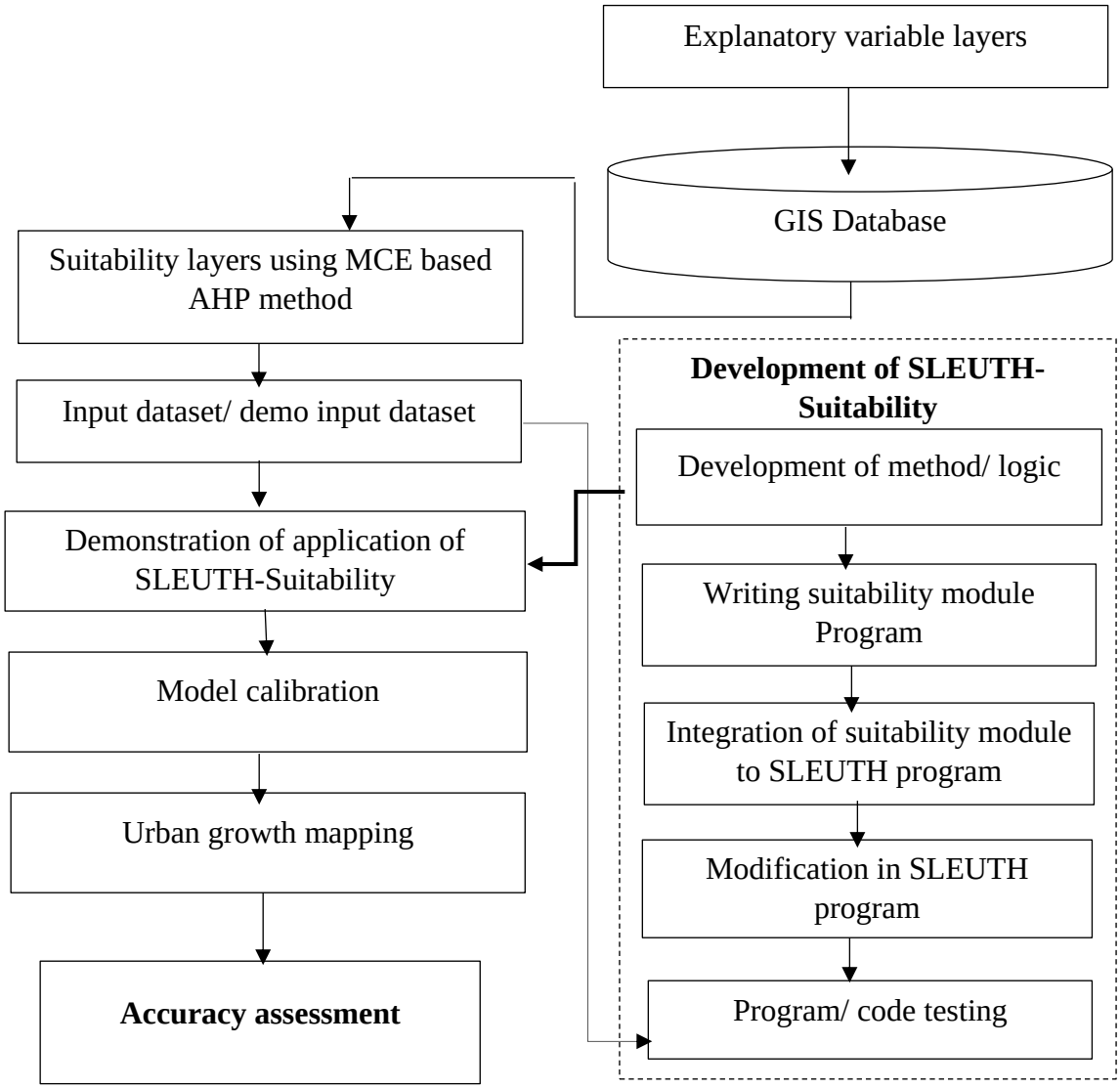

Figure 4.14: Methodology used for development of SLEUTH-Suitability

The code/ program of SLEUTH-Suitability has been tested for a small size demo input dataset to check the consistency of the SLEUTH-Suitability model. Initially, the model is calibrated and the urban growth has been simulated for a demo input dataset and the output maps are printed at each stage to check the influence of land suitability on urban growth. After successful implementation of SLEUTH-Suitability for a demo input dataset the land suitability layers as a function of different urbanization explanatory variables have been

prepared using AHP based MCE technique. Moreover, the application of SLEUTH-Suitability has been demonstrated for a larger study area i.e. Ajmer fringe using prepared input data layers. The SLEUTH-Suitability has been calibrated to obtain the optimal growth coefficient values and further urban growth was predicted for year 2040. Model results have been checked through accuracy assessment as discussed in subsequent sections.

4.3.5 Accuracy assessment

Accuracy assessment is an important step in modeling. Accuracy of simulated urban growth has been assessed by using different methods like percentage of accuracy & kappa statistics for a set of random test pixels, model best fit statistics i.e., OSM and Lee Sallee goodness of fit metrics, spatial & statistical measures, hit-miss-false alarm method and visual analysis (Figure 4.14).

- The accuracy assessment has been performed for the simulated outcomes using several methods that validate the success of the model. The model has utilized the input data of year 1998, 2000, 2008, 2013 and 2015 for the conceptualization and calibration of the and based on that urban growth has been predicted or simulated up to year 2040. The simulated urban growth of year 2018 (current year) has been used for the accuracy assessment. The accuracy percentage and kappa statistics are determined by comparing the simulated land use of more than 100 stratified random test points with reference urban area obtained from high resolution Geo-eye (GE) satellite image of year 2018.
- The test pixels were overlaid on the GE image and the actual land use information in terms of binary numbers has been collected. The classification is done for urban and non-urban pixels/ points as ‘1’ and ‘0’ respectively. The confusion matrix is prepared for observed and simulated urban area for year 2018 to calculate the users and producers accuracies. The kappa statistics and accuracy percentage has been computed.
- Furthermore, model performance was checked through ground truthing also. Land use information of randomly selected locations was collected from the field and compared with the land use obtained from simulated results. Ground truth obtained from 78 locations as shown in Figure 4.15. Further accuracy assessment has been discussed in Chapter 8

- The accuracy assessment on the basis of field observations has also been performed for year 2018 in two ways i.e. for only newly constructed locations in year 2017-18 and for overall urban features construction to know whether the model simulated the urban growth well. During a field visit it was planned to capture only those sites which seem to be under construction or newly constructed in year 2017 - 18 so that accuracy of urban growth happened in 2017-18 can be determined.
- Model performance has also been validated using Hit-Miss-False alarm method in term of seven metrics, hit (H), miss (M), false alarms (F), HOC, MOC, FOC and FOM.
- Hit, miss, false alarms and null successes are the components of correctness and errors which are statistically computed and visually analyzed. The quantitative comparison between the simulated urban areas for a given year and reference data has been done. Further, identifying how much of the simulated urban growth is correct i.e. hit (H), how much urban growth has been missed by the model which actually exist i.e. miss (M), how much urban growth is falsely simulated by the model i.e. false alarms (F) and the null successes (observed persistence simulated as persistence). Moreover, three metrics i.e. HOC (hits to observed change (eq 4.3), MOC (misses to observed change, (eq 4.4) and FOC (false alarms to observed change (eq 4.5) which represent hits to observed change, misses to observed change and false alarms to observed change have been computed. Another metric i.e. FOM (Figure of Merit (eq 4.6) which assesses the agreement of urban growth has been calculated. The above-discussed metrics were computed using the following formulae;
    - $HOC = \frac{H}{H+M} \ldots\ldots\ldots\ldots\ldots\ldots$ (4.3)
    - $MOC = \frac{M}{H+M} \ldots\ldots\ldots\ldots\ldots\ldots$ (4.4)
    - $FOC = \frac{F}{H+M} \ldots\ldots\ldots\ldots\ldots\ldots$ (4.5)
    - $FOM = \frac{H}{H+M+F} \ldots\ldots\ldots\ldots\ldots$ (4.6)

In modelling the visual comparison between modeled and actual maps is an important step. It is helpful to analyze the efficiency of the model in capturing the roadside development, fragmented, scattered and other urban growth forms.

4.3.6 Comparison of performance of different SLEUTH versions

Performance of the three versions of the SLEUTH model i.e., SLEUTH with default model parameters, with optimum parameters obtained from sensitivity analysis and SLEUTH-Suitability has been tested by comparing the urban growth simulations for the Ajmer and Pushkar towns in term of accuracy achieved which is estimated using different methods as discussed in previous section. All three versions of the model were parameterized using the same input data of the Ajmer fringe, calibrated and urban growth was predicted for year 2040 using the methods presented in Figure 4.14. Further, accuracy assessment has been done for the urban growth simulated from the three versions and the performance was compared in term of percentage accuracy, kappa statistics, spatial & statistical metrics, hit, miss & false estimated for the simulated growth and reference urban areas obtained from reference data (urban maps obtained from LULC maps, urban area digitized from high resolution satellite data). Accuracy assessment has also been done with respect to ground truth collected from the field survey held in the month of June-July, 2018 for a number of randomly selected pixels (Figure 4.15). Performance evaluation of three versions of model is discussed in detail in Chapter 8.

Accuracy Assessment

- **Hit-Miss-False Alarm Method**
  - ✓ Identifying how much of the simulated built-up growth is correct i.e. hit (H),
  - ✓ how much built-up growth has been missed by the model which actually exist i.e. miss (M),
  - ✓ how much urban growth is falsely simulated by the model i.e. false alarms (F)
  - ✓ HOC (hits to observed change),
  - ✓ MOC (misses to observed change)
  - ✓ FOC (false alarms to observed change)
  - ✓ FOM (figure of merit)

- Accuracy percentage and kappa statistics using remote sensing data (Google Earth) as referenced data
- Field validation of overall modelled built-up growth in year 2018
- Field Validation of newly constructed locations in year 2018

Figure 4.15: Accuracy assessment methods

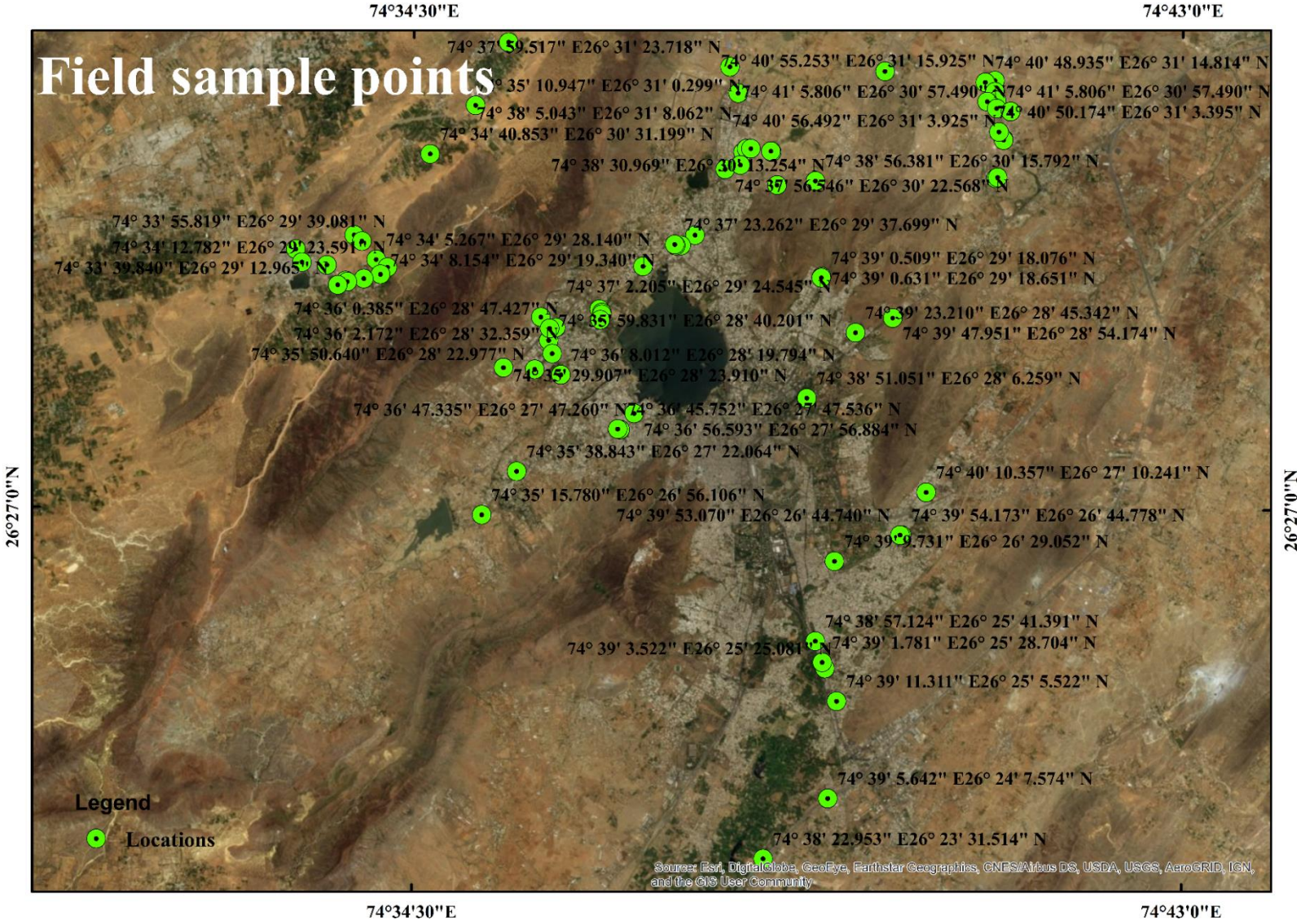

Figure 4.16: Field observation points

4.3.7 Development of SLEUTH-Density and estimation of built-up density

Methodology adopted for development of new version of SLEUTH-Density and estimation of built-up density/ intensity has been explained in Figure 4.16. Required algorithm has been developed for estimation of built-up density/intensity. Suitable code was developed in the C++ programming language and integrated with the existing SLEUTH code. Further, code has been tested for a demo data set and each stage of model outcome was verified manually. The model was developed and tested using the small size input demo dataset. After satisfactory performance of SLEUTH-Density version, its application was demonstrated for the estimating the built-up density for different years up to year 2040 for the Ajmer fringe including Pushkar.

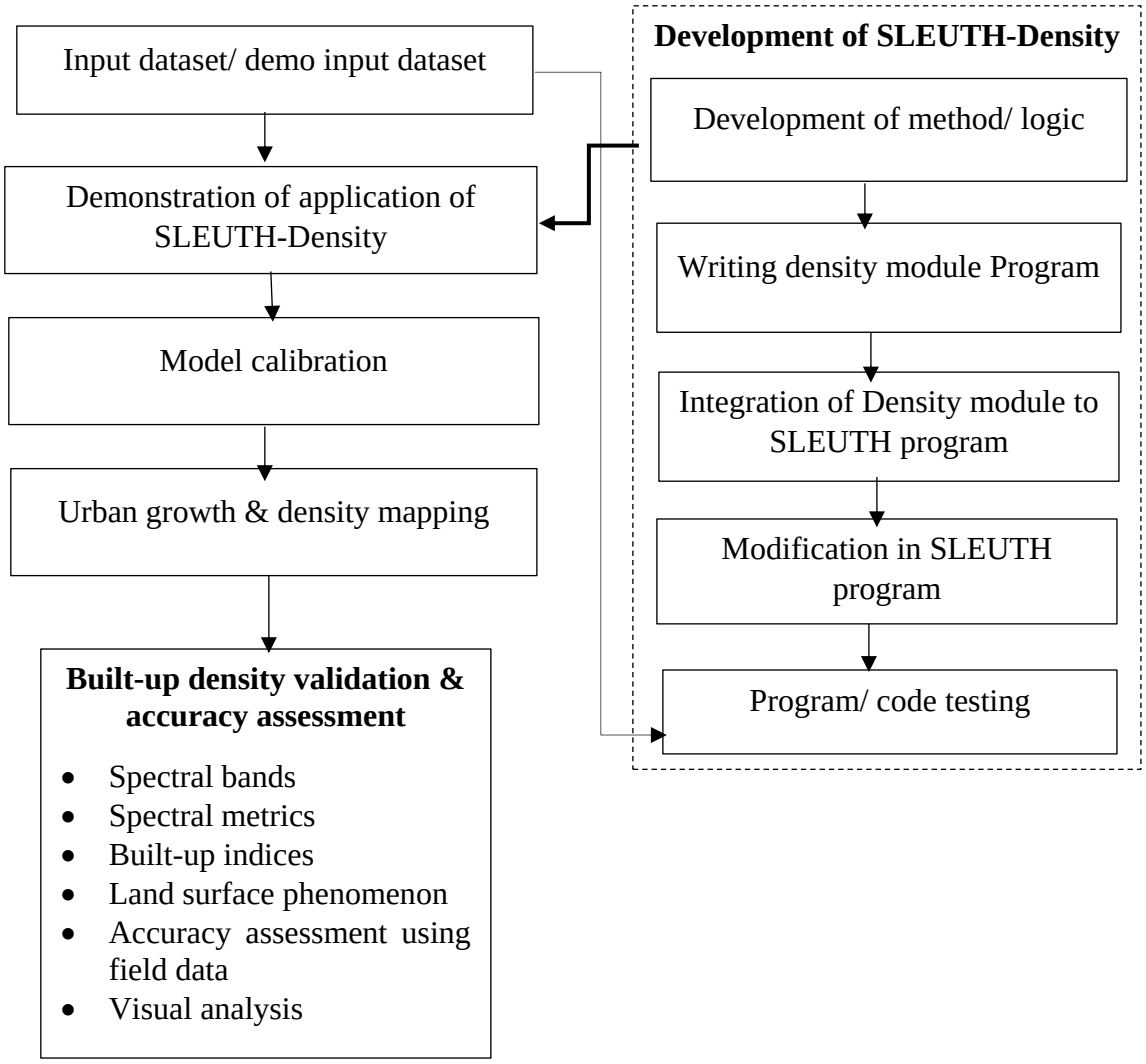

Figure 4.17: Methodology used for development of SLEUTH-Density

Further, simulated built-up density/ intensity has been validated using different methods like Spectral bands, Spectral metrics, Built-up indices, Land surface temperature and accuracy assessment from ground truthing as explained in Figure 4.16. Development of SLEUTH-Density and demonstration of its application is discussed in detail in Chapter 6.

4.4 Concluding Remark

The present chapter includes the complete methodology aimed to achieve the objectives of the present research. The objective wise methodology has been discussed in respective sections. Further details can be find in respective chapters.

CHAPTER 5
SENSITIVITY ANALYSIS

5.1 Prologue

The SLEUTH model is a cellular automata based computer simulation model that utilizes historical land use/ land cover (LULC), slope, road, and hillshade information to calibrate and simulate the land use/land cover change and urban growth. The SLEUTH model has been widely used throughout the world in the recent past. In addition to historical LULC information the model also utilizes parameters to derive the behavioral (model urban growth) coefficient values that best capture the landscape structure and dynamics of the LULC change history.

Over the years several modifications and improvements have been made to the SLEUTH model by analyzing the sensitivity of scale, temporal scale in terms of length, frequency, irregularity of the spacing of time-slices used both in input data & output and level of aggregation of LULC classification (Candau, 2002; Goldstein et al., 2005; Dietzel and Clarke, 2006; Clarke et al., 2007; Clarke, 2008b). Apart from these other important model parameters like *self-modifying parameters, number of Monte Carlo runs, cellular neighborhood size, diffusive value parameter, game of life rule* and *critical slope value* are key model parameters/constants which affects SLEUTH model behavior critically and their sensitivity has not been tested so far. Sensitivity testing is helpful in determining the influence of these crucial parameters on modelling outcomes for different parametric settings. Sensitivity analysis also helps in determining the relative contribution of uncertainties of model input parameters into the model results. Such information helps decision makers in knowing about the consequences of possible errors in the model results so that informed decisions about land use policies can be made.

In the present study, model sensitivity to the self-modifying parameters like *critical low, critical high, boom* and *bust* has been tested for a range of values and relative change in model response in comparison to the default parameter values. The model sensitivity to the *diffusive value* has been tested by simulating the urban growth of selected study area for a range of value i.e., default value ± 50% and comparing model response with urban growth obtained from the default value of 0.005. Such an investigation also helps in determining the model capability to capture different types of urban growth like

fragmented, clustered, road influenced and new spreading center growth and to determine the best *diffusive value* for a developing country scenario. The *critical slope* also varied for a range to capture the significant influence of rocky terrain to model the actual urban growth scenario. The number of *Monte Carlo simulations* plays a crucial role in modelling. To determine the model sensitivity to MC runs, the urban growth of the selected area has been simulated considering a different number of MC run settings.

The *cellular neighborhood* has a significant influence on urban growth simulation using SLEUTH and currently it works on an 8 cell Moore neighborhood. In what way does *cellular neighborhood* affect the model performance? To find out the answer, the model was developed with 4 cell von Neumann and 12 cell extended Moore neighborhood and urban growth is simulated for the selected study area and the model response has also been compared with actual growth to determine the model sensitivity to the size of the *cellular neighborhood*. Model sensitivity to the *game of life rules* has also been investigated by simulating urban growth corresponding to different rules and comparing model outcomes.

In the present study, a univariate sensitivity approach has been used for the sensitivity analysis in which model outcomes were analyzed with respect to the variation of one parameter/constant at a time while other modelling parameters remain constant. The changes in modelling outcomes relative to different parametric settings have been measured and model performance was evaluated by computing landscape metrics for both the actual and modelling outcomes for respective years. Also, accuracy assessment has been done using % accuracy and kappa statistics to determine the change in the model performance with a different value of model constants. A particular set of values model parameters when model performance is best, have been selected as the optimum parameter values.

The chapter includes discussion on the parameterization of the base SLEUTH model corresponding to default parametric settings for the study area. Afterwards, urban growth of the selected area was simulated corresponding to a range of above mentioned parameter values and model constants to test the sensitivity of the model by comparing model output with actual urban area in term of spatial and statistical measures (i.e. urban area, no. of clusters, co. of edges, mean cluster size and radius), goodness of fit metrics (Lee Sallee, OSM, pop, cluster, edge, radius, mean cluster size), kappa statistics, accuracy percentage and visual matching of urban patterns.

5.2 The significance of Modelling Parameters Selected for Sensitivity Analysis

5.2.1 Self-modifying parameters

The SLEUTH model has a self-modification capability, which is intended to more realistically simulate urban growth rates over different time periods. Three model growth coefficients i.e., diffusion, breed, and spread are multiplied by a multiplier coefficient when the growth rate exceeds or reduces as compared to an already specified critical threshold of the growth rate (Clarke et al., 1997). When the growth rates exceed the *critical high*, the three model growth coefficients are multiplied by a factor greater than one, simulating a '*boom*' cycle. This increase imitates the tendency of an expanding system to grow even more rapidly. Likewise, when the growth rate falls below an already specified critical threshold (*critical low*), the growth coefficients are multiplied by a factor less than one, simulating a '*bust*' cycle, causing growth to taper off as it does in a depressed and saturated system. Without this capability of self-modification, SLEUTH may not be able to produce non-linear growth rates and it would be producing linear growth rate till the availability of land belittles. As urbanization takes place the availability of land decreases and the growth rate also. Due to the self-modification rule, new values for the growth coefficients become active from the beginning of next annual growth cycle, effectively lowering down these values and retarding growth during a *bust* cycle. Likewise, when SLEUTH enters the *boom* cycle, it signifies that more land is available for urbanization and a multiplier greater than one is applied to the growth coefficients. *Critical low* and *critical high* are the thresholds which are utilized in the *bust* and *boom* cycle of self-modification in the SLEUTH model. To understand the sensitivity of the model with respect to self-modification rules and its critical parameters, the model has been run for a range of *self-modifying parameter* values sequentially by changing one parameter at a time and determining the relative change in model response as compared to growth corresponding to default values of these parameters.

5.2.2 Number of Monte Carlo runs

The SLEUTH model is stochastic in nature and utilizes the Monte Carlo method to produce multiple urban growth simulated outcomes for each unique set of growth coefficients. Model best-fit statistics are averaged over the Monte Carlo trials (Goldstein et al., 2005). To obtain spatial variability and computational efficiency, while maintaining the rigorous calibration procedure, it is essential to perform sensitivity of the *number of*

Monte Carlo (MC) iterations by simulating urban growth for a selected area corresponding to different MC runs and then comparing the model outcomes.

5.2.3 Diffusive value parameter

While simulating urban growth using the SLEUTH model, diffusive/ spontaneous and edge / organic growth dominates the system and both are dependent on the number of pixels randomly selected for potential spontaneous urban development at a particular time step. Such spontaneous urbanization attempts are controlled by the *diffusive value*, a constant multiplier of the image diagonal embedded in the SLEUTH program (Clarke et al., 1997; Clarke and Gaydos, 1998). How *diffusive value* is affecting the random selection of spontaneous urban growth pixels is discussed in later sections. The *diffusive value* constant reflects the unique spatial characteristics of the study area. For different sub-regions, the default *diffusive value parameter* (0.005) may not efficiently capture urban growth and overestimate or underestimate the number of urban pixels. When the *diffusive value* parameter is increased or decreased, the spontaneous urbanization attempts may vary accordingly. To analyze such a significant influence of *diffusive value* on SLEUTH performance, it is very crucial to understand the spatial interaction through sensitivity analysis.

5.2.4 Critical slope value

The *critical slope* in the SLEUTH model has the ability to include topographical influence in simulating the urban growth. The critical slope is a threshold value above which no urban development should take place. By modifying this value, the model allows developing different planning scenarios as it directly influences the decision making of urban development. Appropriate *critical slope value* can be best identified by rigorous sensitivity analysis. While the SLEUTH model presently has a default *critical slope value* as 15 which may not be suitable in different socio-economic and geographical settings. Model sensitivity to this parameter needs to be understood. Therefore, urban growth has been simulated for a range of *critical slope values* and relative change in urban growth is determined to understand the relative impact of this parameter on urban growth simulations.

5.2.5 Size of cellular neighborhood

In cellular automata modelling, the size of the *cellular neighborhood* plays an important role in simulating the behavior of a phenomenon considered. The size should be uniform

throughout the modelling space and it must be the closest set of cells. In urban growth modelling systems, the *cellular neighborhood* must be extended as per the regional and local considerations. When the *cellular neighborhood size* is extended, the distance decay effect is incorporated in the simulation and the influence of neighboring cells minimizes (Li and Liu, 2006; Li et al., 2014; Liao et al., 2014). Likewise, when *cellular neighborhood size* is reduced the distance decay effect reduces and the distant cells become a part of less consideration as compared to neighboring cells or pixels. While the SLEUTH model utilizes 8 cell Moore neighborhood and therefore, it is of interest to check the model sensitivity to *cellular neighborhood size* in simulating the urban growth. The default *cellular neighborhood size* i.e. 8 cell Moore neighborhood may or may not be suitable for all type of development in different socio-economic settings and capturing different urban forms. Therefore, the SLEUTH model has been developed for two different sizes of a *cellular neighborhood* in addition to the default and urban growth is simulated for the individual. The relative change in urban growth is determined to understand the relative impact of the different size of *the cellular neighborhood* on urban growth simulations.

5.2.6 Game of life rules

The urban growth simulations in a CA-based model depend on the current state of cells, their neighbors and the transition rules. The *game of life rules* allows a cell to urbanize or de-urbanize by implying a set of transition rules. The *game of life rules* supports the urban growth system to behave like a living organism. Any living entity grows where surroundings persist and it demolishes due to overcrowding of that place. Likewise, urban growth phenomenon can be understood as urban development takes place where surroundings are already urbanized. As in CA, cells represent the state of land use class in the form of urban/ non-urban and a non-urban cell becomes urbanized only after passing through the game of life rules. The SLEUTH model urbanizes a non-urban pixel as per the game of life rules if it has at least 3 neighboring urban cells/ pixels. However, the numeric value of 3 may or may not be suitable in all conditions of urban development in different socio-economic settings. To understand the influence of this parameter it is essential to determine the model sensitivity with respect to the different critical threshold values in a *game of life rules*. Model sensitivity has been tested by modifying the SLEUTH code and running model corresponding to the different *game of life* critical threshold values. The relative difference in model performance in capturing urban growth for

different critical threshold values of the *game of life rule* has been determined to quantify the sensitivity.

5.3 Development of Base SLEUTH Model

As discussed in methodology presented in Chapter 4, the SLEUTH model simulated urban growth by applying 04 growth rules (i.e. spontaneous/ diffusive, new spreading center, edge, and road influenced growth) sequentially. Growth rules are controlled by five growth coefficients (i.e. diffusion, breed spread, slope resistance, and road gravity). Further, non-linearity of the growth is ensured by performing secondary rules i.e., self-modifying parameters (i.e. *boom, bust, critical high* and *critical low*). The model calibration is performed to determine the optimal value of growth coefficients by running the model for a range of growth coefficients and comparing the simulated growth with the historical actual growth for different years. Secondary *self-modifying* parameters once set in the model scenario file remains constant throughout the simulation runs. The default values of constants and parameters of the model i.e. *self-modifying* (*critical low, critical high*, *boom* and *bust*), *diffusive value*, *critical slope*, a *game of life* critical threshold, *cellular neighborhood size* and *Monte Carlo runs* have been given in Table 5.1.

Table 5.1: Default values for model constants / parameters

S.no.	Parameter/ constant		Default value
1	Self-modifying	Boom	1.01
		Bust	0.09
		Critical low	0.97
		Critical high	1.3
2	Diffusive value		0.005
3	Critical slope		15
4	Game of life critical threshold		3 cells
5	Cellular neighborhood size		8 cell Moore neighborhood
6	Monte Carlo runs		5-100

5.3.1 Model calibration

Present version (Base) of the SLEUTH model was parameterized using required input datasets for the Pushkar town as discussed in the methodology section of Chapter 4. SLEUTH model calibration was performed using GA based algorithm by utilizing input dataset of 5.0-meter spatial resolution and 10 MC runs. The constants/ parameters were set as default values, as presented in Table 5.1. The calibration was completed in 6 hours 53 minutes on a 64 bit windows 7 operating system with Intel (R) Xeon (R) CPU E5- 2699

v3 @ 2.30 GHz processor. The time elapsed in calibration was significantly reduced in SLEUTH-GA as compared to brute force method in SLEUTH. Computational efficiency of GA based SLEUTH model motivated us to perform repeated calibration (in three phases) by keeping all GA parameters as constant to achieve better calibration with better model fitness. Three phases of calibration phases were named as coarse, fine and final.

The optimal values of growth coefficients are determined with respect to the composite fitness criteria i.e. OSM, total fitness (overall model fitness) and standard deviation. In the coarse phase, the optimal value of the diffusion coefficient has been found to be low which indicates reduced spontaneous growth. However, breed and slope resistance coefficient are high and indicates new spreading center growth and maximize the chances of urban development at a steeper slope. The OSM fitness measure has been found to be 0.258 corresponding to optimal growth coefficients and having a low standard deviation i.e. 0.06. The overall model fitness attained was 10.711. The fitness criteria show a good fit, though we repeated the calibration further in the fine and final phase to see in what way it influences the model performance. The investigation was found to be helpful.

The model fitness improved from 0.258 to 0.263 and standard deviation (i.e. from 0.06 to 0.055) value was also reduced. However, total fitness was somehow reduced from 10.711 to 9.748. Again the model was calibrated in final phase with same GA constants and input dataset. The results were exciting as model fitness improved further from 0.263 to 0.276 with an even better standard deviation which has reduced further from 0.055 to 0.053. Also, the total fitness increased slightly in the final and third phase of calibration from 9.748 to 10.279. Among three phases of calibration, we observed that OSM has given better fitness value in the final phase as compared to the other two phases and the standard deviation was found to be 0.053 in the final phase.

Therefore, final phase calibration has been accepted. The diffusion and breed coefficients were found to be 49 and 45, respectively indicating moderate spontaneous and new spreading center urban growth. Also, these values lie in between other coefficients values obtained from two calibration phases with a better model fitness. While slope resistance value was significantly reduced in the final phase as compared to other two calibration phases i.e. from 95 in fine phase to 68 in the final phase. It was evident from multi-phase calibration that optimized growth coefficient set in the final phase is optimal one with improved model fitness (Table 5.2).

The model simulated urban growth was compared with the actual urban growth captured from satellite images of respective years to validate the modelling outcomes. In

addition, a ratio based metric was also computed for the respective years to have an idea about the closeness of simulated and actual urban growth. Variation between actual and simulated urban growth has been presented in Figure 5.1(a). The simulated urban growth has been found to be under captured for almost years i.e. the year 2000, 2004, 2008 and 2015, while it is over captured for the year 2013.

The ratio between actual and simulated urban area with default model constants has given an idea about the accuracy of simulated outcomes for respective years and it was found to be slightly better for the year 1997, 2013 and 2015 as compared to the year 2000, 2004 and 2008 as presented in Figure 5.1 (b). Simulated and actual growth comparison has been presented in Figure 5.1 (a) and (b).

Table 5.2: Base model calibration with the default parameter setting

Coefficient values	Diffusion	Breed	Spread	Slope resistance	Road gravity	Best OSM	Total fitness	Standard deviation
Coarse phase calibration						0.258	10.711	0.06
Best fit value	6	87	30	82	45			
Fine phase calibration						0.263	9.748	0.055
Best fit value	69	51	14	95	85			
Final phase calibration						0.276	10.279	0.053
Best fit value	49	45	25	68	46			

Accuracy has been found to be reduced for years 1997-2000 and 2000-2004. However, accuracy has been found to be better for the year 2005-2008, 2008-2013 and 2013-2015 (Figure 5.2). With the increased time between input datasets, model accuracy has been found to be reduced, whereas accuracy has been found to be improved with a lesser time gap between input datasets.

The investigation indicates that the temporal gap of the seed (input) data affects the simulation accuracy, as revealed by the model fitness metrics and through the visual examination of simulated and actual urban area. Significant differences between simulated and actual urban area have been observed at specific locations during different years, as presented in Figure 5.1 (a) and (b). It was evident that fragmented urban growth and small size built-up area, as well as different forms of the urban growth, were not captured well by the model.

Figure 5.1(a): Comparison between actual and modeled urban area

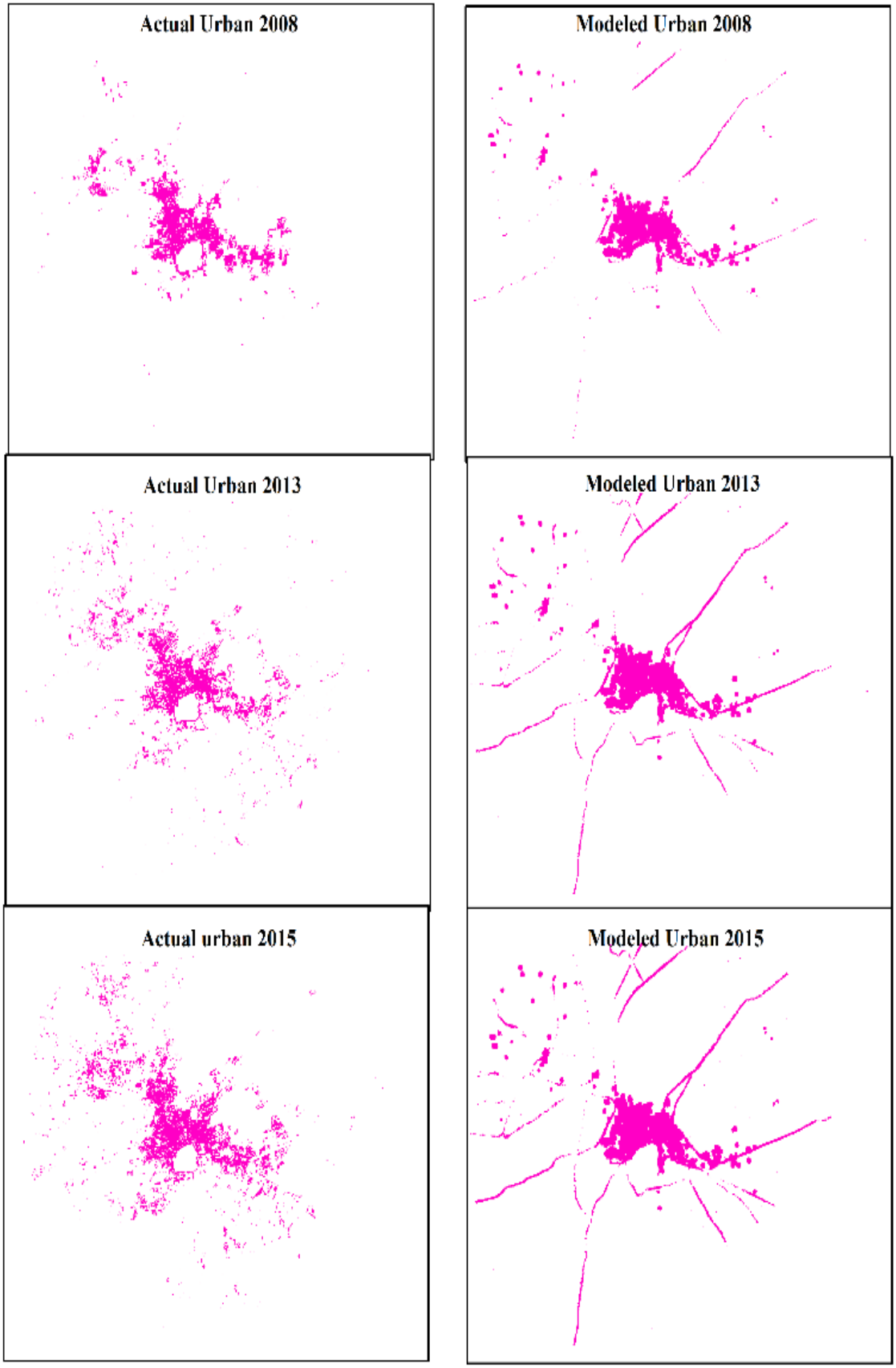

Figure 5. 1(b): Spatial differences between actual and simulated urban growth for different years

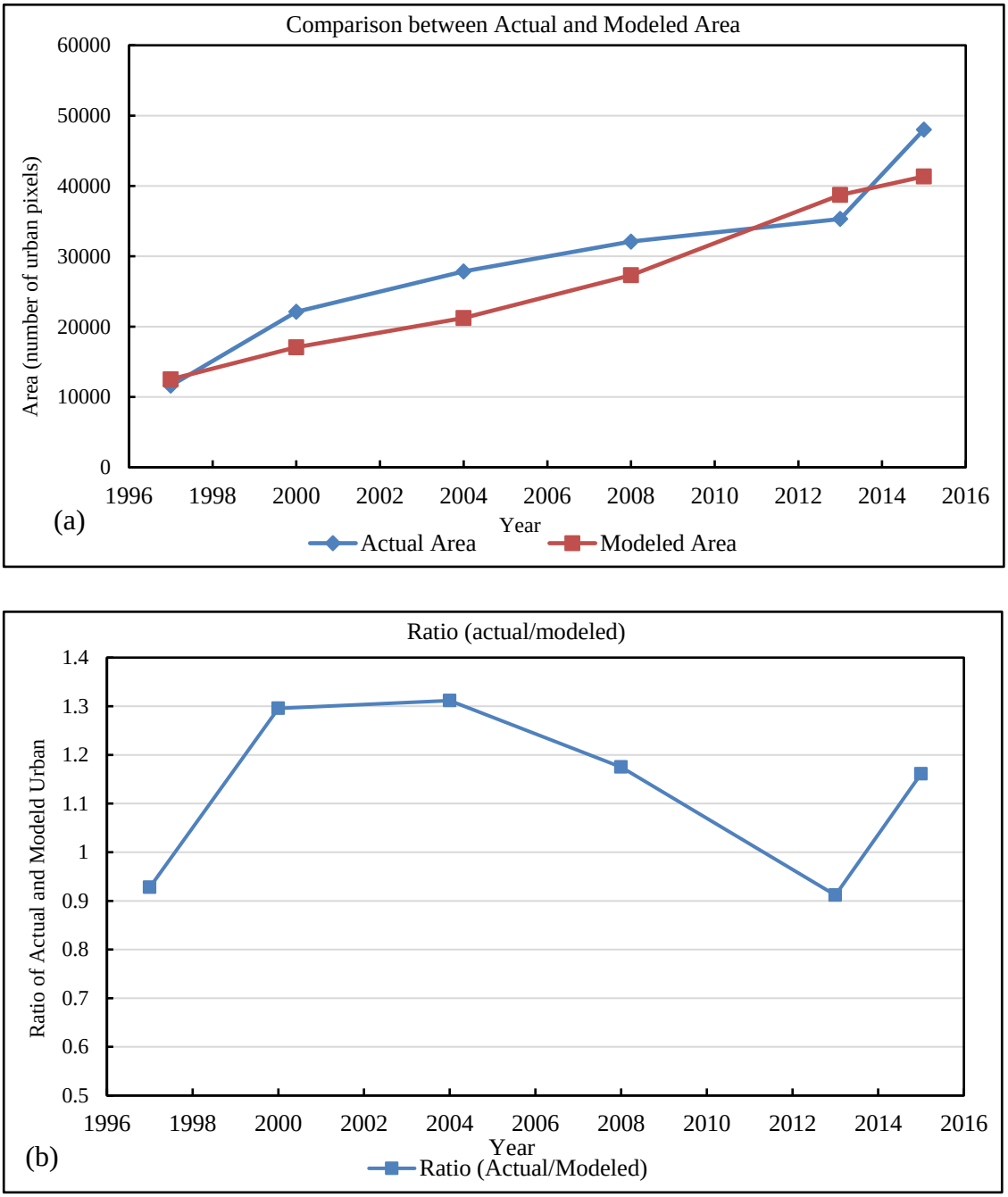

Figure 5.2: Comparison and ratio between actual and simulated urban area

The urban growth simulation might be improved by the suitable values of model constants/parameters which can be determined through model sensitivity testing for other important parameters as discussed earlier.

It can be concluded from the above discussion that multi-phase GA calibration may enhance the model performance by optimizing growth coefficients more efficiently as compared to single phase calibration. Final phase calibration outcomes have been accepted to simulate urban growth for the future i.e. up to the year 2040.

Model sensitivity has been tested using the dataset of Pushkar study area for the selected model constants/ parameters using the methodology as discussed in Chapter 4 and in subsequent sections using the base model with default model parameters/constants.

5.4 The methodology of Sensitivity Analysis

Sensitivity analysis of important selected SLEUTH parameters is required to assess relative change in model outcome with respect to change in the value of constants/ parameters (in both positive and negative side of default value). The methodology adopted for the sensitivity analysis has been presented in Figure 5.3. The model calibration is assessed based on the goodness of fit metrics and model simulation/ prediction capability has been analyzed by the comparing spatial and statistical measures obtained from simulated results and same statistics calculated from original/ actual data. It measures the sensitivity of chosen model constant and model accuracy & performance can be improved by determining the optimal value of constant at which difference between spatial and statistical measures calculated from simulated urban growth and actual urban area (obtained from reference data) is minimum and the value of goodness of fit metrics are closer to '1.0'. In addition, accuracy percentage, kappa statistics, and visual analysis have also been involved in deciding the optimal values of constant/ parameters while performing sensitivity testing.

The study includes preparation of the input dataset (slope, exclusion, urbanization, transportation, and hillshade) for Pushkar study area for SLEUTH parameterization. These input layers were resampled to 5.0 m spatial resolution and utilized for model calibration. First, the base SLEUTH model was run while the base term represents the SLEUTH model with default parametric settings. The model calibration was done in three phases as discussed earlier. The calibration results were validated by using OSM, standard deviation, and total fitness. The optimized growth coefficient values were used for urban growth prediction. The results were assessed by using spatial and statistical measures, spatial symmetrical differences and ratio of actual and modeled urban growth. Afterward, the SLEUTH model sensitivity for the selected parameters has been tested. Model sensitivity to the selected parameters was examined for a range of values of each parameter, decided as default constant value ± 50%. The model was calibrated in three subsequent phases i.e. coarse, fine and final, further urban growth has been simulated for a range of values of each parameter, changing one parameter at a time iteratively.

Each model calibration outcome determined on the basis of OSM, total fitness, and standard deviation.

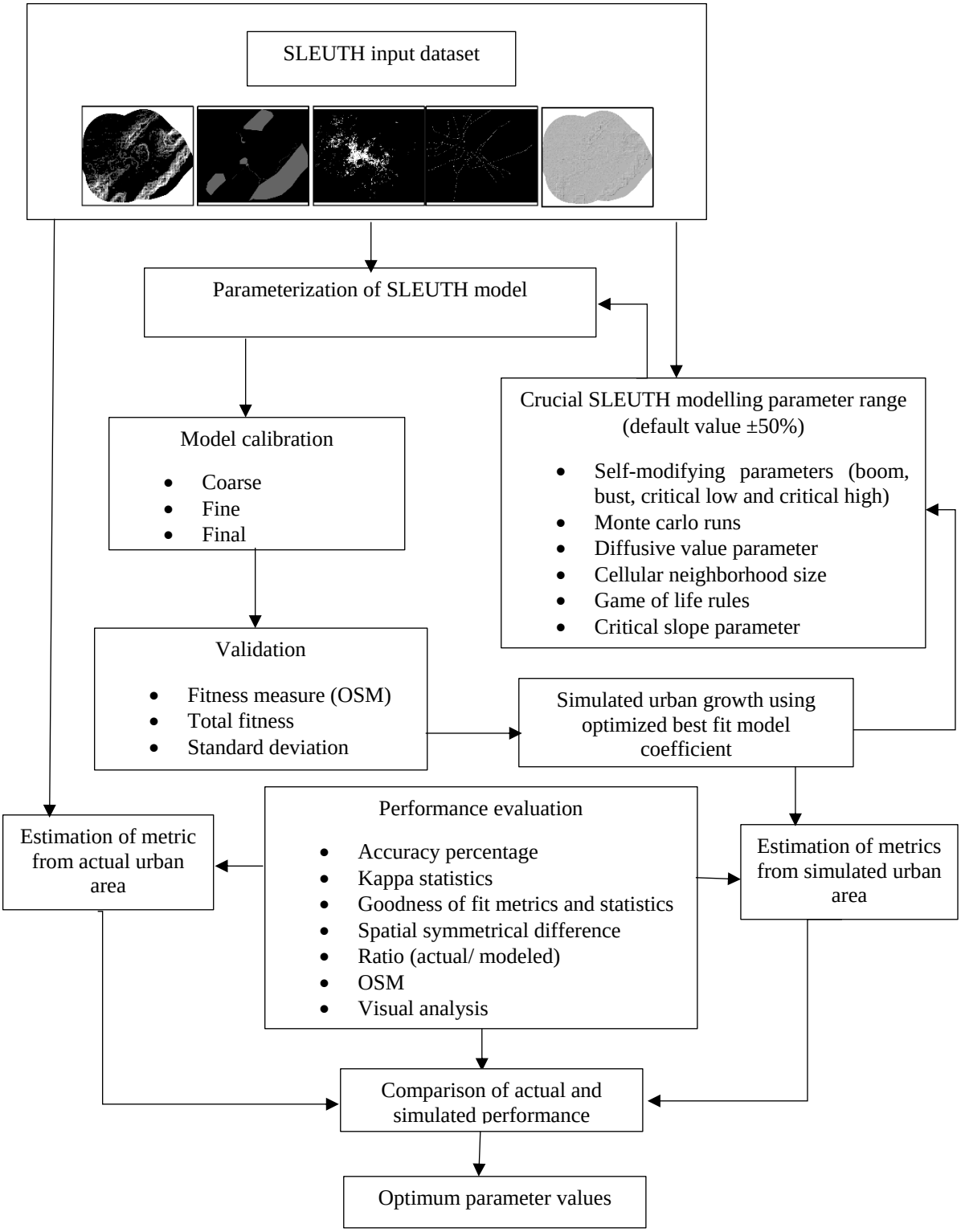

Figure 5.3 Methodology for sensitivity analysis

The best performing calibration phase produced optimized growth coefficients which were utilized for the final simulation of urban growth. Nearness of simulated results

for each parameter value in different model runs was determined by comparing accuracy and statistically based criteria calculated from simulated results with the same measures calculated from the actual urban area from reference datasets (seed urban area of the year 2015 and urban area digitized from high-resolution image for the year 2017). Each individual simulated outcomes produced from different parametric settings was also evaluated with the actual urban area in different years by means of kappa statistics, accuracy percentage, spatial and statistical measures, the goodness of fit metrics, spatial symmetrical difference, the ratio (actual/ modeled), OSM and visual analysis.

Sensitivity analysis has been carried out using the above mentioned methodology for following parameters and discussed separately in subsequent sections.

1. Self-modifying Parameters
2. Monte Carlo Runs
3. Diffusive Value Parameter
4. Cellular Neighborhood Size
5. Game of Life Rules
6. Critical Slope Parameter

5.4.1 Quantifying sensitivity in terms of spatial and statistical measures

The closeness of simulated urban growth corresponding to a particular set of model constants with the actual urban growth has to be determined to ascertain the value of model constant for which model is simulating urban growth most near to the actual urban growth. Statistical and spatial measures like actual urban area, urban edges, urban clusters, mean cluster size, and cluster radius were estimated from the model simulated urban growth corresponding to each set of model constants and compared with the values of these measures calculated from the actual urban area in respective years to determine the value of model constants for which simulated urban growth that is most near to the actual growth. Measures corresponding to the actual urban growth were estimated from two reference datasets; one obtained from the digitization of the urban area from high-resolution Geo-eye satellite image of the year 2017 and the second obtained from classified satellite image of the year 2015 which was used as input urban maps to the model. For analyzing different urban forms, urban area, urban clusters, urban edges, cluster radius and mean cluster size statistics were computed against different parameter values. The area is calculated as a total number of urban pixels, urban clusters are representing a group of two or more urban pixels which indicates clustered or spread

growth. Urban edges are calculated as the number of pixels which are neighbors of an urban pixel representing the fragments of urban growth. Cluster radius is basically a representation of infill growth of an urban cluster. Mean cluster size is an indication of an average size of the compact urban form.

5.4.2 Quantifying sensitivity in terms of accuracy percentage and kappa statistics

Accuracy assessment is a general term used to compare the simulation results with the reference geographical data, which is assumed to be true in order to determine the accuracy of simulated outcomes. Various methods are available for the accuracy assessment of simulated outcomes and have been discussed in detail in many studies (Congalton and Green, 1999; Foody, 2002). For each set of model constants, accuracy assessment has been carried out by determining the percentage of randomly selected urban pixels correctly captured by the model. Reference ground truth data was obtained from high-resolution GeoEye satellite data for the years 2016 & 2017. Agreement and disagreement between actual and simulated outcomes in term of percentage accuracy and kappa statistics were calculated. To evaluate the accuracy, a set of random sample points (more than 100) has been used. Reference pixels have been selected using a stratified random sampling technique to avoid any biases. In this type of sampling, the number of points selected are stratified to the distribution of the simulated output. Then an accuracy assessment cell array was created to compare urban simulated map with reference data. The cell array is a simple list of class values (in terms of urban (1) and non-urban (0)) for the pixels in the simulated map and the class values corresponding to the reference pixels. Class values of the simulated pixels have been set manually after examining each simulated pixel against to the reference data. Further, the Kappa statistic has been calculated which expresses the proportionate reduction in the error generated by the simulation outcomes compared with the error of a random simulation.

In addition, the visual analysis was also carried out to establish the closeness between simulated and actual urban growth. First of all base statistics (*bs*) (for above discussed spatial and statistical measures) have been calculated from the actual urban area obtained from two reference datasets as mentioned above. Subsequently, selected spatial statistical measures were calculated from the simulated urban growth corresponding to different set of model constants values. Comparison of above mentioned spatial and statistical measures will reveal how closely the model is able to simulate the urban growth or is able to imitate the historical urban growth in different years and corresponding to

which value of model constant, indirectly giving the optimal parameter value. Such an exercise also gives model sensitivity with respect to different model parameters/constant.

5.5 Sensitivity Analysis of Self-Modifying Parameters

Self-modifying parameters in SLEUTH like *critical low* and *critical high* are set as boundary conditions for the growth rate that if modelling outcomes violate these conditions it will take some requisite actions to get a required trend of urban growth by avoiding linear or exponential growth. In logical terms it can be understood, as if the growth rate falls below the *critical low* value it should be tapered off and if it increases above the *critical high* then it should be *boom*, even more, to gain an increased urban growth rate as described in pseudo code below;

If (growth rate < critical low)

{

Code to implement - Multiply growth coefficients with a *bust* parameter to taper off the growth rate

}

Else if (growth rate > critical high)

{

Code to implement - Multiply growth coefficients with *boom* parameter to increase growth rate even more

}

Else

{

No change

}

The self-modification invokes by increasing growth coefficients (diffusive, breed and spread) by a multiplier greater than one in case of *boom* phase and growth coefficients (diffusive, breed and spread) are decreased by a multiplier less than one in case of the *bust* cycle. The detailed methodology of sensitivity analysis of self-modifying parameters has been presented in Figure 5.4. To test the sensitivity a range of default value ± 50% was decided as presented in Table 5.3. With varying step values for individual

coefficients range was decided and to have a number of possible combinations to calibrate separately. SLEUTH was run to simulate with all possible values of the individual parameter for the whole range iteratively, keeping other model constants/ parameters same. For *boom*, 0.5, 0.7, 0.9, 1.1, 1.3 and 1.5; for *bus*t, 0.05, 0.06, 0.08, 0.10, 0.12, 0.35, 0.65, 0.95, 1.25 and 1.35; for *critical low*, 0.50, 0.70, 0.75, 0.80, 0.90, 1.0, 1.25 and 1.50; and for *critical high*, 0.65, 0.90, 0.95, 1.05, 1.20, 1.25, 1.35, 1.50, 1.55, 1.75 and 1.95 have been tested. Thirty-five (35) combinations were decided to calibrate independently and individual calibration itself was passed through the three phases, so, in total 105 calibration runs were performed to arrive at optimal self-modifying parameter settings corresponding to the improved performance of the model.

Table 5.3: Sensitivity analysis parameters and selective ranges

Self-modifying parameters	Default values	Decided ranges
Boom	1.01	0.5- 1.5
Bust	0.09	0.05- 1.35
Critical Low	0.97	0.5- 1.5
Critical High	1.3	0.65- 1.95

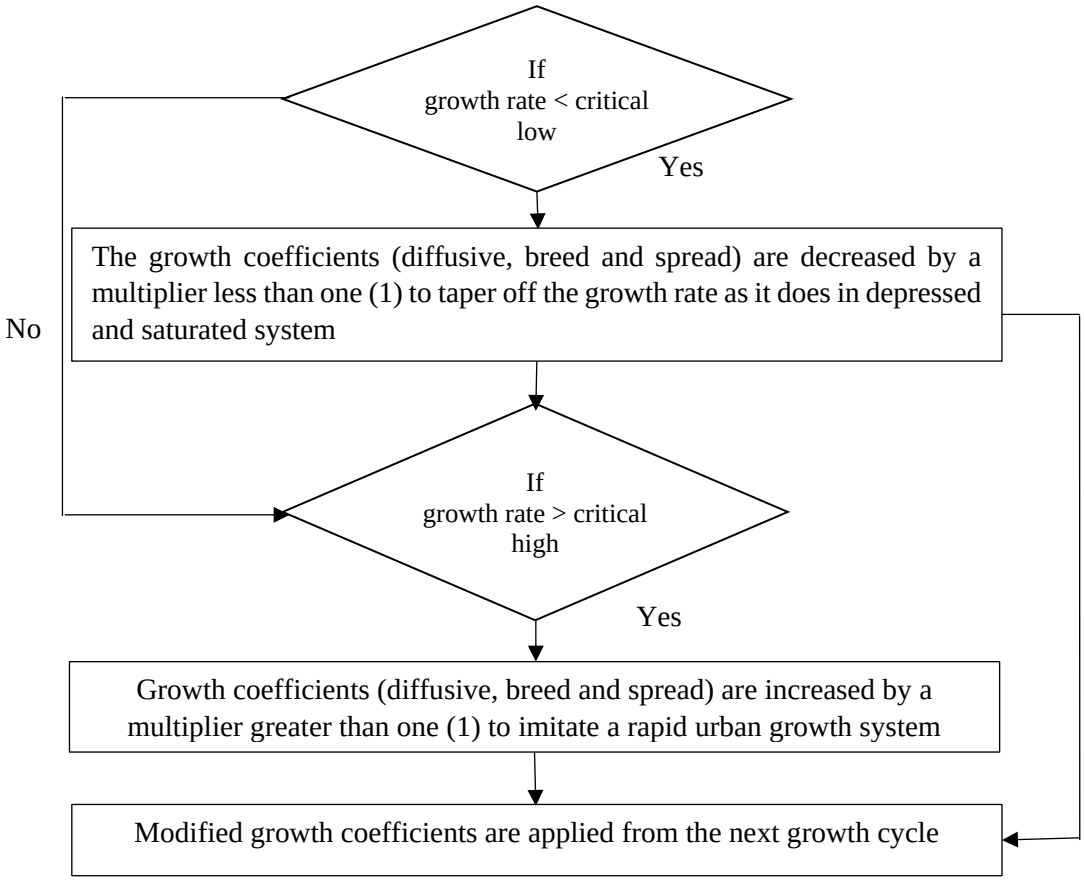

Figure 5.4: Methodology for sensitivity analysis of self-modifying parameters

The decided range for each coefficient was used for calibrating the SLEUTH-GA one at a time by keeping other as the default value. In this way, a large number of calibrations has been performed for carrying out robust sensitivity testing.

Table 5.4: Sensitivity analysis of self-modifying constants and best-fit values

Self-modifying parameters	Diffusion coefficient	Breed coefficient	Spread coefficient	Road gravity coefficient	Slope resistant coefficient	Best OSM
Boom 0.50	100	28	32	62	17	0.26
Boom 0.70	35	90	23	87	38	0.08
Boom 0.90	64	89	93	54	37	0.18
Boom 1.01	49	45	25	68	46	0.28
Boom 1.10	6	11	60	92	55	0.28
Boom 1.30	12	1	12	12	12	0.32
Boom 1.50	16	60	2	88	54	0.25
Bust 0.05	2	53	96	83	37	0.28
Bust 0.06	60	74	18	97	45	0.27
Bust 0.08	2	71	88	90	5	0.28
Bust 0.09	49	45	25	68	46	0.28
Bust 0.10	69	22	39	51	31	0.29
Bust 0.12	34	12	66	0	28	0.29
Bust 0.35	16	19	79	82	50	0.27
Bust 0.65	56	48	32	98	32	0.28
Bust 0.95	34	66	34	58	18	0.27
Bust 1.25	28	35	54	91	5	0.26
Bust 1.35	30	71	36	78	24	0.27
Critical Low 0.50	72	10	49	1	73	0.33
Critical Low 0.70	79	9	59	3	51	0.31
Critical Low 0.75	57	37	37	85	30	0.28
Critical Low 0.80	2	97	90	93	1	0.30
Critical Low 0.90	73	8	51	2	0	0.34
Critical Low 0.97	49	45	25	68	46	0.28
Critical Low 1.0	80	18	39	83	87	0.27
Critical Low 1.25	60	36	30	2	16	0.30
Critical Low 1.50	48	19	48	40	39	0.27
Critical High 0.65	39	40	39	71	40	0.26
Critical High 0.90	48	58	29	48	1	0.29
Critical High 0.95	64	41	30	53	45	0.28
Critical High 1.05	1	50	90	82	35	0.28
Critical High 1.20	45	70	28	78	25	0.26
Critical High 1.25	58	53	28	98	70	0.28
Critical High 1.30	49	45	25	68	46	0.28
Critical High 1.35	76	79	15	95	37	0.28
Critical High 1.50	45	26	47	85	57	0.28
Critical High 1.55	3	27	91	85	58	0.27
Critical High 1.75	5	61	79	99	9	0.25
Critical High 1.95	68	28	36	64	36	0.28

Since SLEUTH-GA has better computation efficiency so it would be easier for one to evaluate as many numbers of calibrations for reaching out to the best parameter settings which will eventually lead to the improved model accuracy. All sets of parameters selected for sensitivity were applied iteratively to derive the best fit coefficients for urban growth prediction. The prediction was done up to the year 2040 for each parametric setting. It would be a tedious task to quote and discuss 105 calibration results so as to optimize this only best-attained coefficient set against best OSM have been discussed and presented in Table 5.4.

The rigorous calibration was performed and the best fit coefficient values were obtained as presented in Table 5.4. Model fitness was observed in between 0.08 to 0.32 for different values of *boom* constant. For different values of the *bust, critical low* and *critical high* OSM value was found to be between 0.26 to 0.29, 0.27 to 0.34 and 0.26 to 0.29 respectively. Since the SLEUTH model is a stochastic model and randomization is involved in its functionality to represent human behavioral aspects, no clear trend was observed for its growth coefficients by increasing or decreasing the self-modifying parameters. However, it has given an idea of best performing parameter values at which the model imitate urban growth more accurately as compared to default constant values.

Value of *boom* constant as 1.30 was found more suitable as compared to default value i.e. 1.01 which signifies that growth rate will be increasing due to the availability of land to get urbanized. A difference was observed in model fitness values as OSM achieved corresponding to boom value of 1.30 was 0.32 which is better than the value obtained corresponding to the default (OSM achieved as 0.28 for boom 1.01) value (Table 5.4). The optimal value of *bust* constant has been found to be 0.10 to 0.20 corresponding to the best value of OSM i.e., 0.29. Higher *bust* values i.e. 0.10 and 0.12 were found appropriate for the modeling which are more capable of imitating the current urban development scenario as compared to default i.e. 0.09 for developing Pushkar town. However, other *bust* settings lead to poor model fitness for the study (Table 5.4).

Pushkar town has just started developing in the recent past and it is more likely to get urbanized in the near future due to the availability of suitable land and increased tourism activities. The high *boom* value clearly indicates that the urban growth rate will be increasing in upcoming years until the availability of land suitable for urbanization is reduced. However, the growth rate may be tapered off after a few decades when all suitable land will get occupied. While there may be chances of vertical growth in Pushkar after significantly expanding horizontally. Better model fitness against high *bust* values

supports the conclusions drawn from best *boom* values as discussed above. A significant difference was observed in the case of different *critical low* constant values. The optimal value of *critical low* has been found to be as 0.90 in place of 0.97 (default value) with an improved fitness value (OSM) from 0.28 to 0.34. When growth rate is less than 0.90 then growth coefficients should be decreased to taper off the urban growth to imitate the urbanization process accurately. As discussed earlier that Pushkar town is a small and newly developing town and there may be the situation of declining growth rate in the future after less availability of urban suitable land. The analysis reveals that the growth rate may be less than 0.90. In such a case model should be able to incorporate such changes to accurately imitate the urban growth. The best model fitness (OSM) has been found to be 0.29 corresponding to the optimal value of the *critical high* (1.25). This indicates that if the growth rate increases beyond the *critical high* i.e. 1.25 then growth coefficients of the model should be increased even more for accurately imitating the urban growth. The above discussion was based on model fitness in term of OSM metric, however, to validate these findings closeness of simulated results with the actual phenomenon (urban growth) in terms of spatial & statistical measures and visual analysis is also necessary which has been discussed in next section.

5.5.1 Comparison between spatial and statistical measures computed from input dataset and simulated outcomes

To determine the model sensitivity with different parameter/constants and to obtain best constant value from a range selected for sensitivity testing, spatial and statistical measures calculated from simulated urban growth corresponding to a different set of model constants have been compared with the measures calculated from two reference data sets as discussed in the previous section. Spatial statistics calculated from simulated urban growth results against different parameter values are very much different from the base statistics *bs* (calculated from actual data (i.e. classified maps of remote sensing image of the year 2015) and it is indicated from the yellow color in the graphs). In addition, it was identified that default parametric/ constant settings may not be so appropriate for simulating the urban growth of cities and towns in developing countries with different socio-economic conditions. The fitness measure i.e., OSM may give an idea of overall model fitness but it may not correctly imitate the different forms of urban growth. Therefore, to ascertain model capability to capture different forms of urban growth spatial and statistical measures can be helpful.

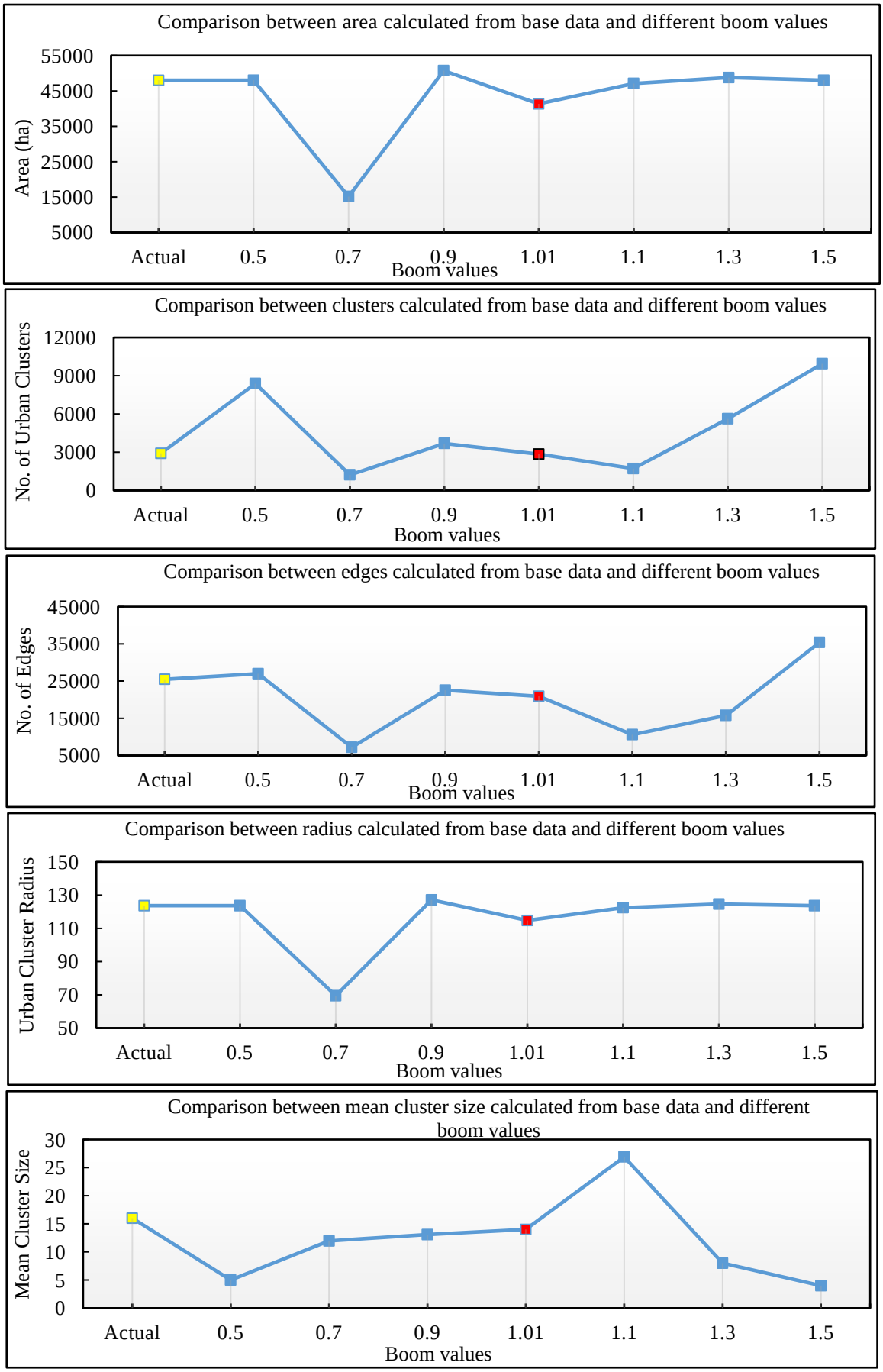

Figure 5.5: Comparison between actual (bs) and modeled urban cluster radius for different boom values

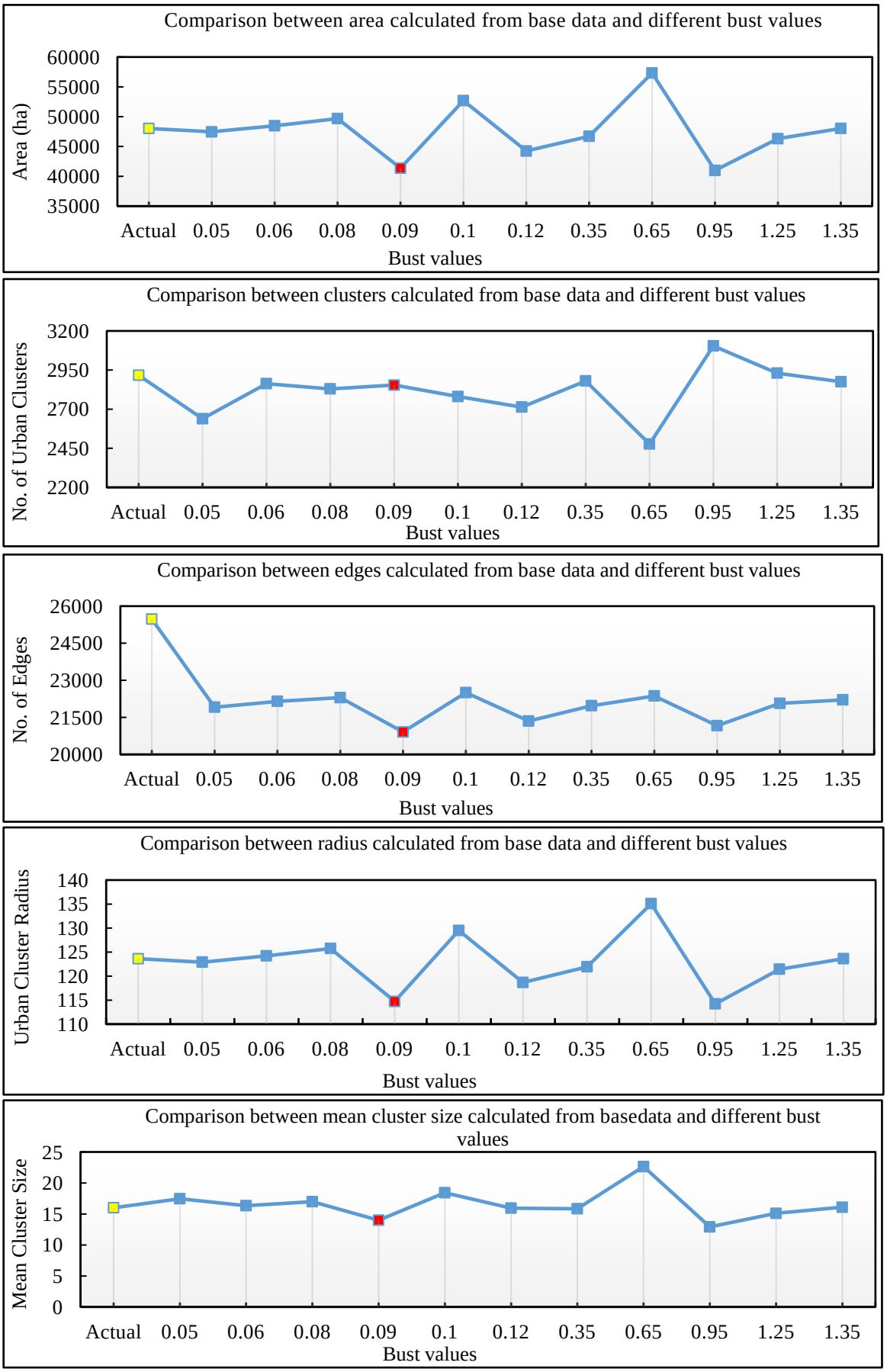

Figure 5.6: Comparison between actual (bs) and modeled urban cluster radius for different bust values

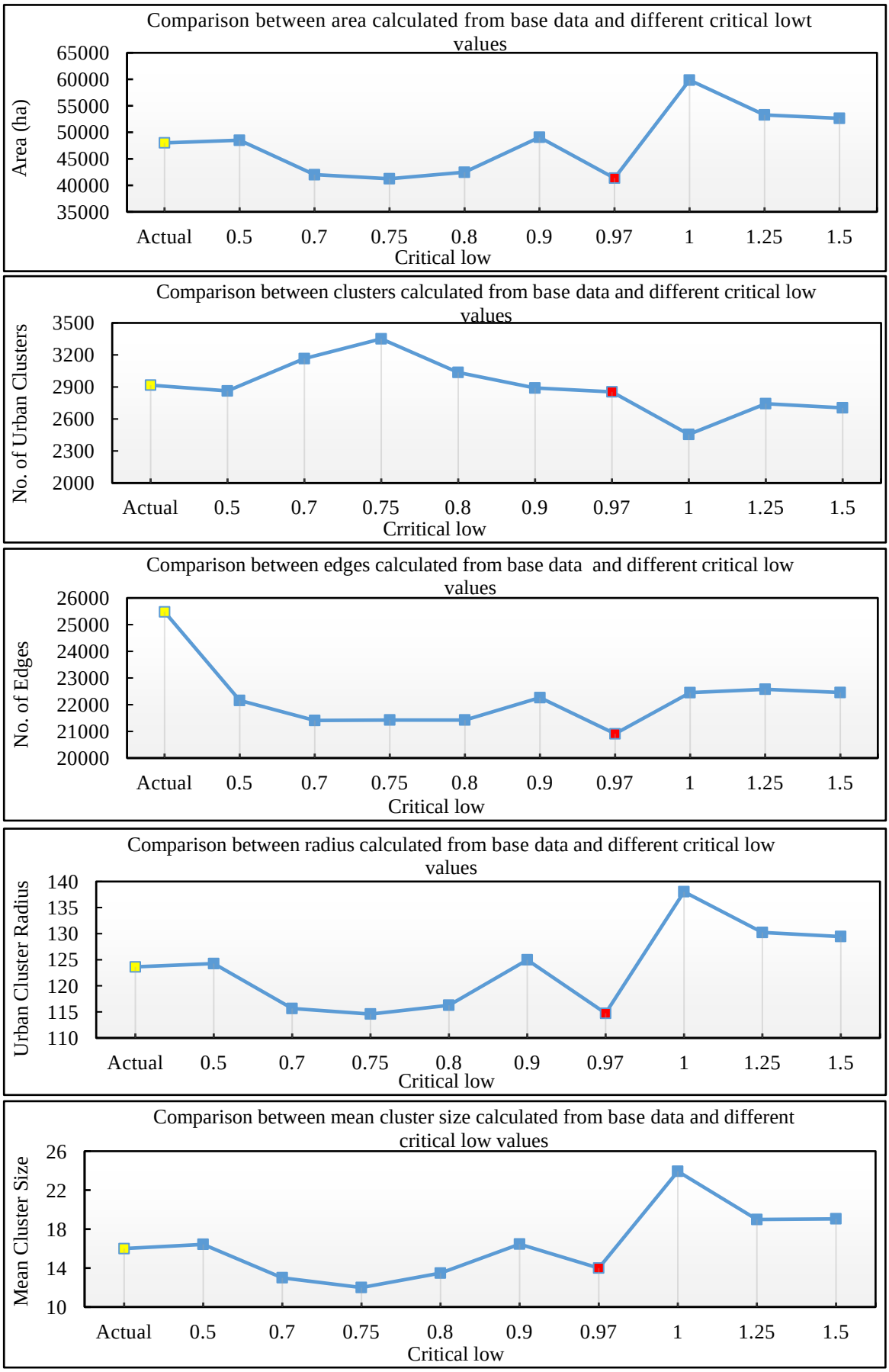

Figure 5.7: Comparison between actual (bs) and modeled urban cluster radius for different critical low values

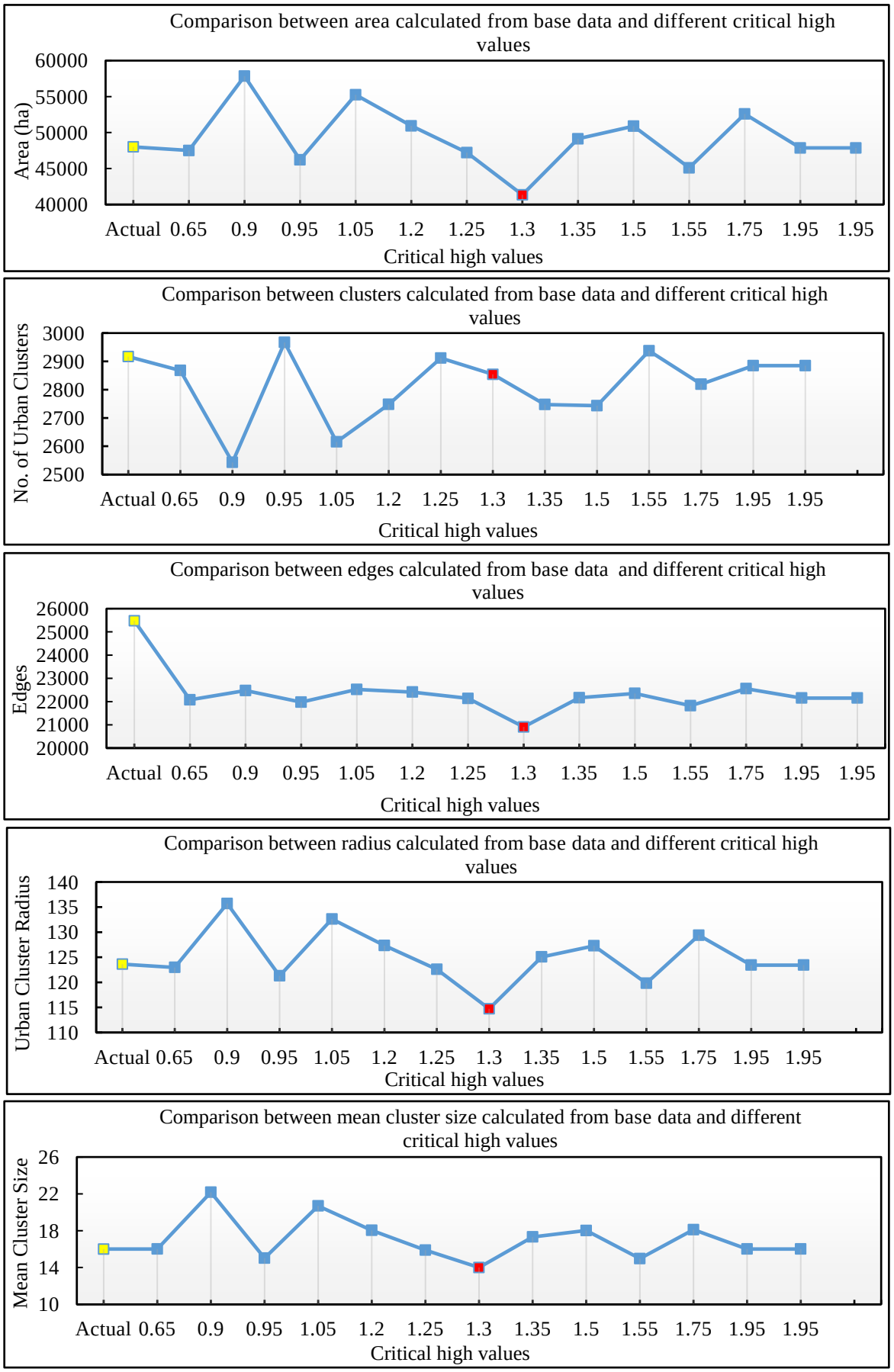

Figure 5.8: Comparison between actual (bs) and modeled urban cluster radius for different critical high values

The yellow color in the graph is indicating statistical measure corresponding to the reference data i.e., *bs* while red color indicates statistics measured against default parameter values. The blue color is for statistics measured against selected constant values (Figure 5.5- 5.8).

A significant difference has been observed between urban area calculated corresponding to different *boom* values and base area. The urban area for default *boom* value i.e. 1.01 was able to imitate only 41470.92 ha which is significantly less than the actual area i.e. 48014 ha (Figure 5.5). The default *boom* value is not capable of simulating the urban growth correctly. However, the model is able to capture urban area more accurately corresponding to the value of 0.5 and 1.3 (Figure 5.5). The best model fitness i.e., OSM was achieved at *boom* value of 1.3 i.e. 0.32. The number of urban clusters i.e. clustered growth and an urban cluster radius, indicating infill growth, are better captured at *boom* values of 1.1 and 1.3, respectively. While the number of urban edges which represents fragmented urban growth are better captured at a *boom* value of 0.5 as compared to 1.3. The analysis suggests that the overall model fitness may be helpful in giving an idea about urban growth. However, to analyze and quantify different urban forms, it is important to closely identify each urban form against different *boom* values.

The default *bust* value i.e. 0.09 is not able to capture urban area well. However, the *bust value* of 0.05 and 0.06 are able to capture urban area more accurately. Clustered, fragmented infill and compact growth are more accurately captured for *bust value* at 0.35, 0.1, 0.05, and 0.12 respectively. It was identified through model calibration that the model was the best fit against the *bust* value of 0.10 and 0.12, corresponding to higher (OSM) model fitness i.e. 0.29 for both the values. The optimal *bust* value was decided based on the higher OSM model fitness along with the ability to capture different urban forms accurately. Thus, corresponding to higher model fitness (i.e. OSM 0.29) the *bust* values i.e. 0.10 and 0.12 were analyzed more closely for capturing different forms of urban growth. The urban area was more satisfactorily captured at the *bust* value of 0.12 as compared to *bust* 0.10 (Figure 5.6). However, the *bust* value of 0.10 is able to closely capture a number of urban edges representing fragmented growth and urban clusters with a better model fitness (Figure 5.6).

It is evident from the analysis that different *bust* values can capture different urban forms well, however, a single value may not be able to accurately capture all the forms of urban growth together. Thus, it's difficult to suggest a single bust value that would be fitted best and able to capture different urban forms. However, the sensitivity analysis

gives an idea of an optimal value of the constant for which the model may imitate overall urban growth well and be able to capture some of the urban forms. Here, we may say that the *bust* value of 0.10 is the optimal value simulating urban growth satisfactorily and also can capture fragmented and clustered urban growth well.

The study reveals that urban area is captured well against best fitted *critical low* value i.e. 0.90 as compared to other *critical low* values. However, we found some closer combinations capturing urban growth well but the overall model fitness for those are not as good as at *critical low* value of 0.90. In addition, the *critical low* value of 0.90 is also able to capture fragmented, urban clustered, compact and infill growth well (Figure 5.7).

In the case of *critical high,* the best model fitness was achieved as 0.29 corresponding to the default value of 1.3. However, targeting different urban forms a *critical high* value of 1.25 has been found to be more suitable (Figure 5.8). The urban edges i.e. fragmented urban growth, urban clusters, urban cluster radius and mean cluster size are satisfactorily captured at a *critical high* value of 1.25 as compared to other values (Figure 5.8) along with a higher model fitness.

The overall sensitivity analysis of self-modifying parameters gives an idea about the values for which the model would be simulating urban growth well and satisfactorily in agreement with actual urban growth. The *boom* value of 1.3, the *bust* value of 0.10, the *critical low* value of 0.90 and *critical high* value of 1.25 have been found to be optimal in capturing the urban growth, and different forms of the growth in a better way as compared to other constant values.

However, the choice of parameter selection may be done according to urban development practices. All types of urban forms may not be of interest for one as in a developing country scenario, fragmented growth is of most common interest. So, by targeting specific urban forms one may change self-modifying parameters accordingly. Moreover, the best obtained individual self-modifying coefficient value may produce better urban form capturing results.

5.5.2 Comparison between spatial and statistical measures computed from Geo-eye data and simulated outcomes

To investigate the accuracy of the above-discussed outcomes, sensitivity results have been validated and compared in terms of spatial and statistical measures estimated from the reference urban area obtained through manual digitization from the Geo-Eye satellite data obtained from Google Earth for the year 2017. Spatial and statistical measures were

computed from the urban area captured from reference data and compared with the simulated outcome based statistics. Such an investigation has led to a better clarity of the optimal self-modifying constants values. With finer resolution data very small size built-up areas and edges of urban growth have been well captured as compared to the input dataset prepared from the classified satellite imagery. Also, urban cluster numbers may not be correctly captured from the manual onscreen digitization of urban patches. Thus, it is genuine to find the differences in computed spatial and statistical measures from the two i.e. actual urban area (Geo-Eye, 0.5 m resolution data) and simulated urban area (5.0m resolution).

However, a relative comparison of spatial and statistical measures between actual and simulated outcomes may be found useful to decide the optimal values of the self-modifying constant. The default *boom* i.e. 1.01 has been found to be poorly capturing the urban growth area than different values of *boom* except for *boom* value of 0.7. The boom value of 0.5, 0.9, 1.1 and 1.3 has been found to be more closely capturing urban growth area however, boom value of 1.3 is found to be more accurate with better model fitness (i.e. OSM 0.32) value (Figure 5.9). The number of urban edges, clusters and mean cluster size have been better captured for boom values of 0.9, 0.7 and 1.1, respectively with poor model fitness value. However, at 1.3 *boom value* satisfactory spatial and statistical measures have been found with a better model fitness value. While urban cluster radius has found to be accurately captured at 1.3 *boom value*. (Figure 5.9). The similar outcomes were obtained from input dataset based comparisons which validate the current findings also. The best model fitness was achieved for the *bust value* of 0.1 and 0.12 as discussed above. Among different *bust* values, only two were able to give best model fitness i.e. 0.10 and 0.12. However, spatial and statistical measures computed against input datasets revealed that *bust* value of 0.10 is more suitable to capture different urban forms in a different socio-economic condition like scenarios. The Geo-Eye (GE) data based statistics also reveal the same findings as area computed against GE data and urban area captured corresponding to the *bust* value of 0.10 are quite closer with better model fitness (Figure 5.10). The number of urban edges and mean cluster radius are also better captured at the *bust* value of 0.1 (Figure 5.10). The simulated number of urban clusters and mean cluster size seem to be mismatched with the actual no. of urban clusters and mean cluster size computed from the GE data due to on-screen digitization (Figure 5.10).

The default *critical low* value i.e. 0.97 has not been able to capture urban area as well as compared to other *critical low* values (Figure 5.11).

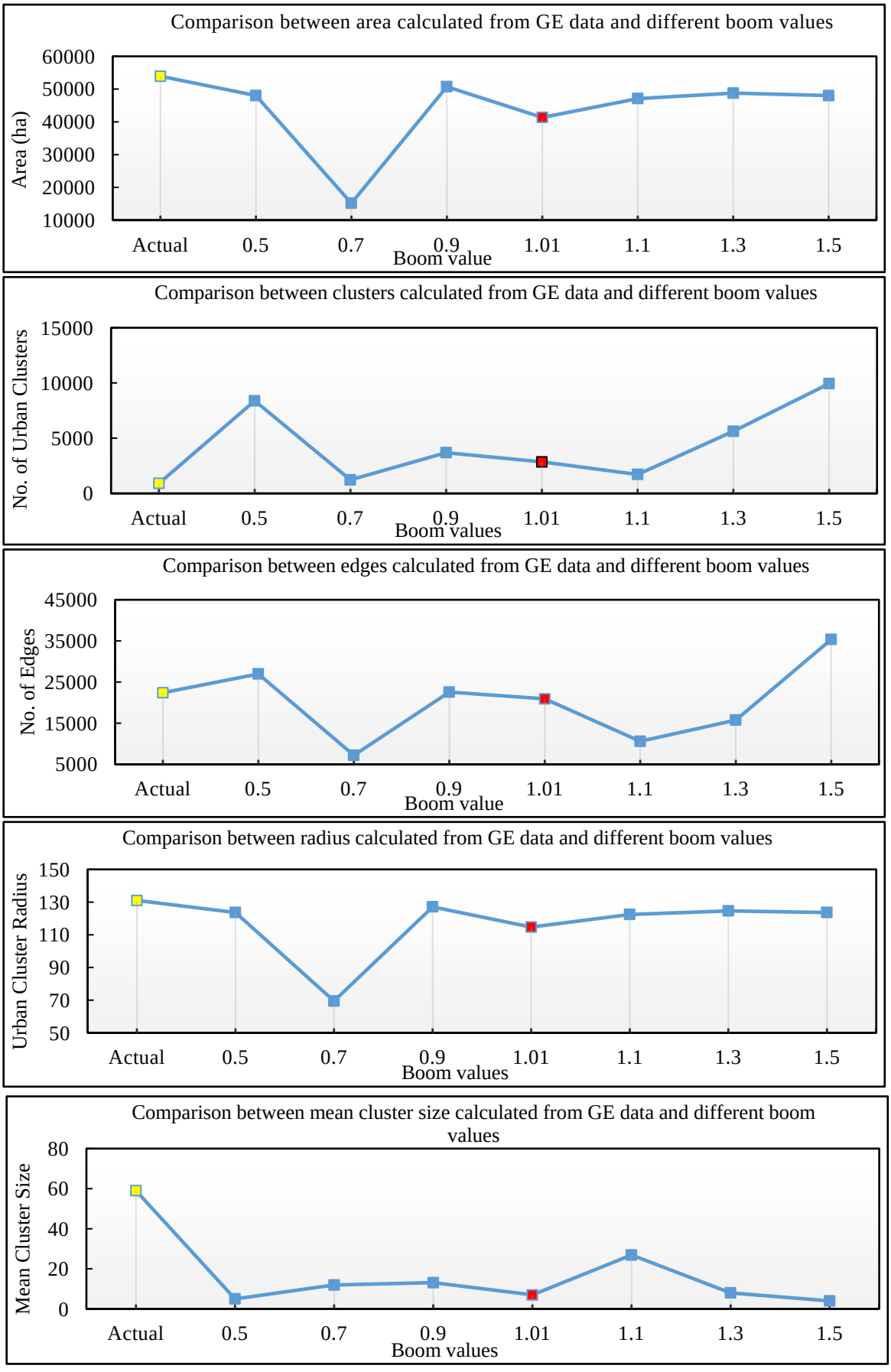

Figure 5.9: Comparison between actual (bs) and modeled urban cluster radius for different boom values

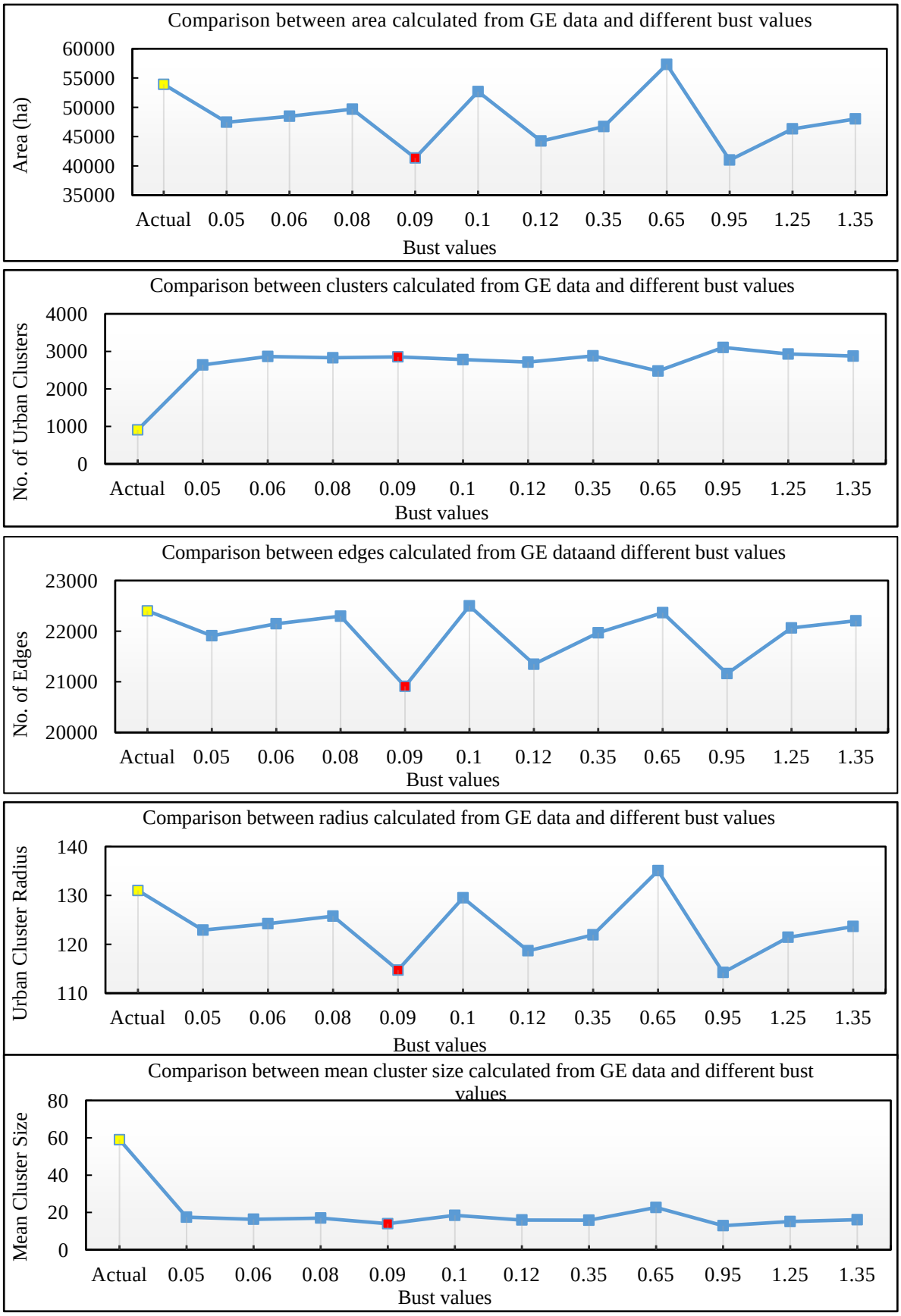

Figure 5.10: Comparison between actual (bs) and modeled urban cluster radius for different bust values

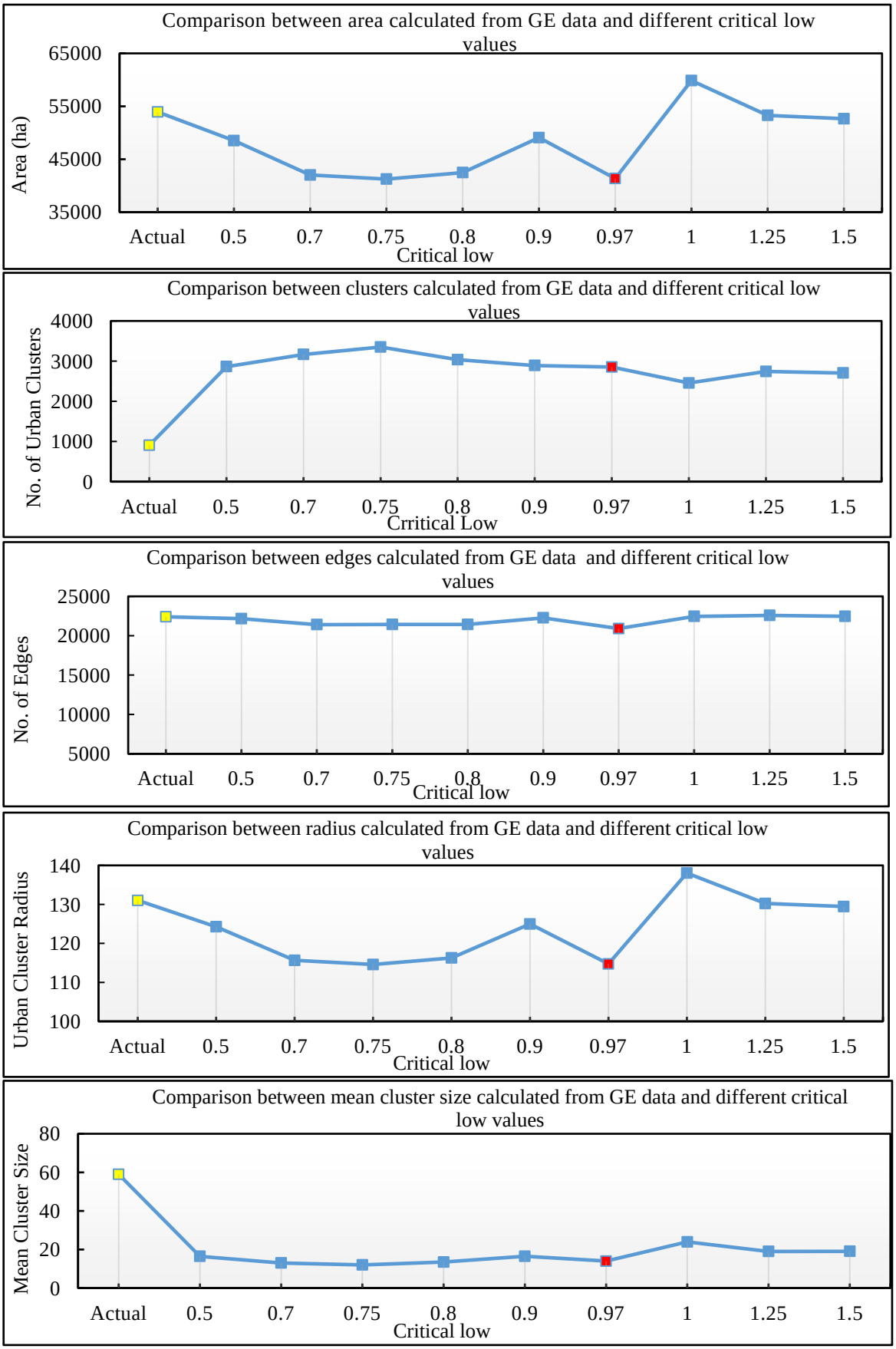

Figure 5.11: Comparison between actual (bs) and modeled urban cluster radius for different critical low values

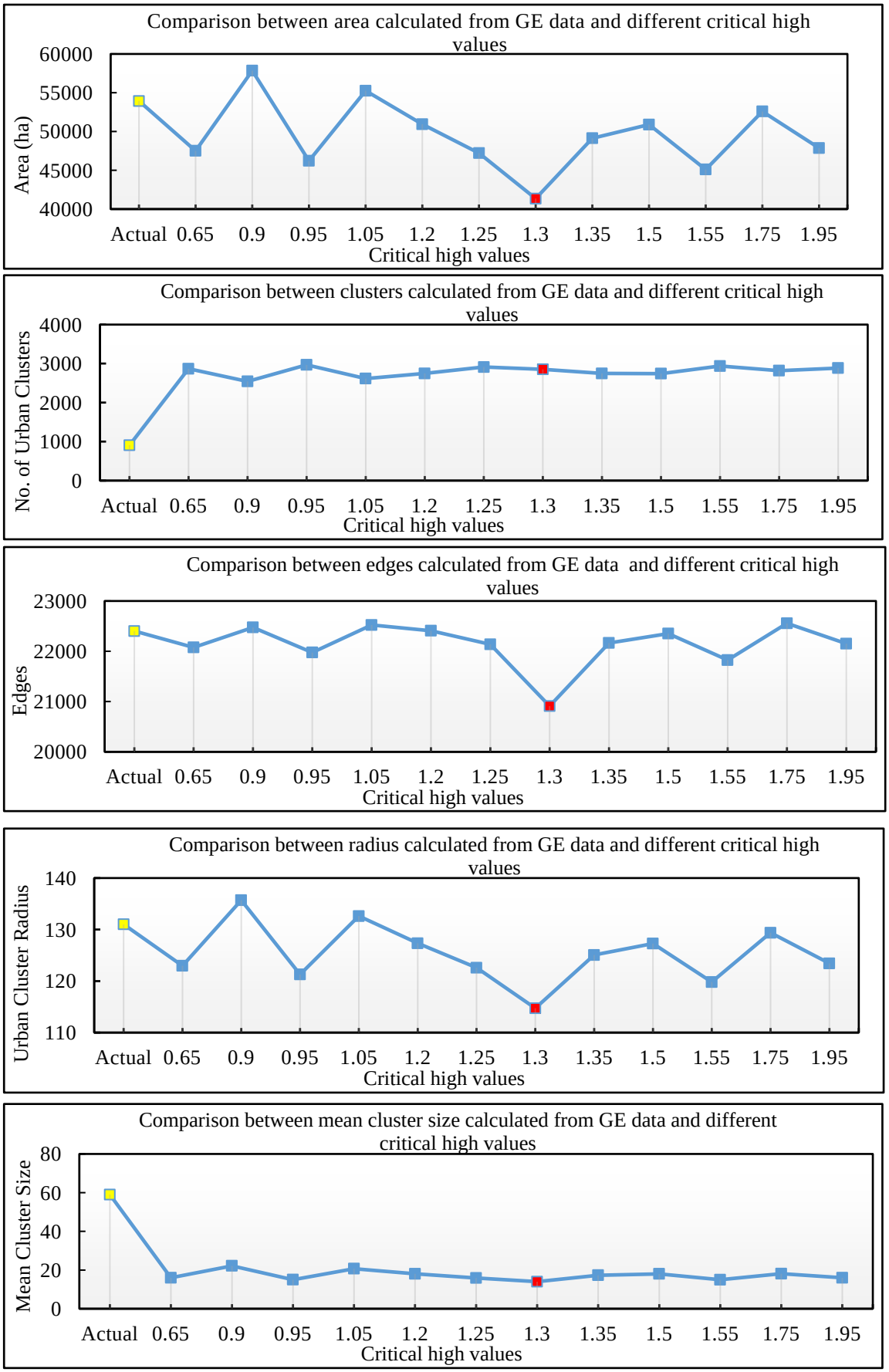

Figure 5.12: Comparison between actual (bs) and modeled urban cluster radius for different critical high values

The urban area has been found to be satisfactorily captured at 0.9, 1.25 and 1.3 critical low values, however, higher model fitness values were achieved at 0.9 *critical low* value. The number of edges representing fragmented growth has been captured well at 0.90 *critical low* value with better model fitness value. However, simulated mean cluster size and number of urban clusters have shown many differences with the actual statistics computed from GE data against all the critical low values. The cluster radius representing infill growth has been more accurately captured with 0.97 *critical low* value (Figure 5.11).

The urban growth simulated with default *critical high* value i.e. 1.3 has not been found to be satisfactory as compared to other *critical high* values. The urban area has been better captured at 1.25 *critical high* value with a better model fitness (Figure 5.12). The no. of urban edges indicating fragmented growth has been found to be accurately captured for a *critical high* of 1.25. However, other urban forms like clustered, compact and infill growth have shown differences between statistics calculated from actual and simulated urban area (Figure 5.12).

5.5.3 Accuracy Assessment

The optimum value of the constant/ parameter is one corresponding to which the accuracy of the model is highest and better than accuracy obtained from model outcome with the default parameter value. Accuracy assessment has been performed by testing the urban growth of a number of test pixels selected through a stratified random sampling technique. Simulated LULC of test pixels was compared with LULC of the same pixels in the reference datasets i.e., high-resolution images obtained from Google Earth for the year 2016 & 2017. The lowest accuracy has been achieved at 1.01 default *boom* value in both the years i.e. 2016 & 2017 i.e., 73 % and 77%, respectively. The simulated urban growth has been found to be more accurate with at 1.3 *boom* value with 81% and 83% percent accuracy for the year 2016 and 2017, respectively. The accuracy percent for simulated urban growth at 0.09 default *bust* value has found to be low in both the years i.e. 2016 & 2017 i.e., 73% and 77%, respectively. The best percentage accuracy has been achieved at 0.10 *bust* value for both years i.e. 2016 & 2017 as 81% and 86%, respectively. The accuracy percentage has been improved from default value of *critical low* at 0.97 in year 2016 & 2017 i.e. 73% & 77% to 80% & 85% in year 2016 & 2017, respectively with a *critical low* value of 0.10.

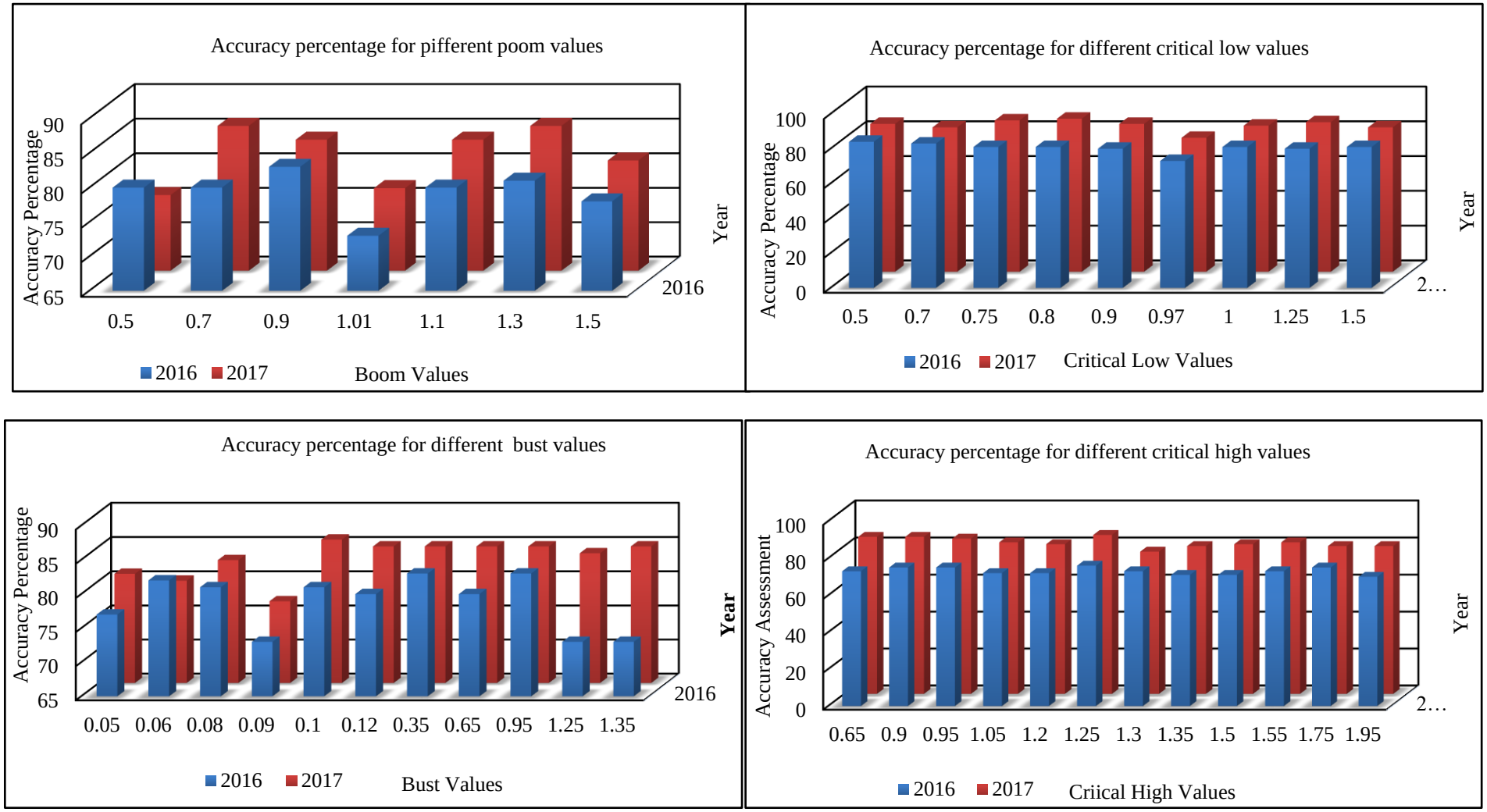

Figure 5.13: Percentage accuracy for different values of self-modifying parameters

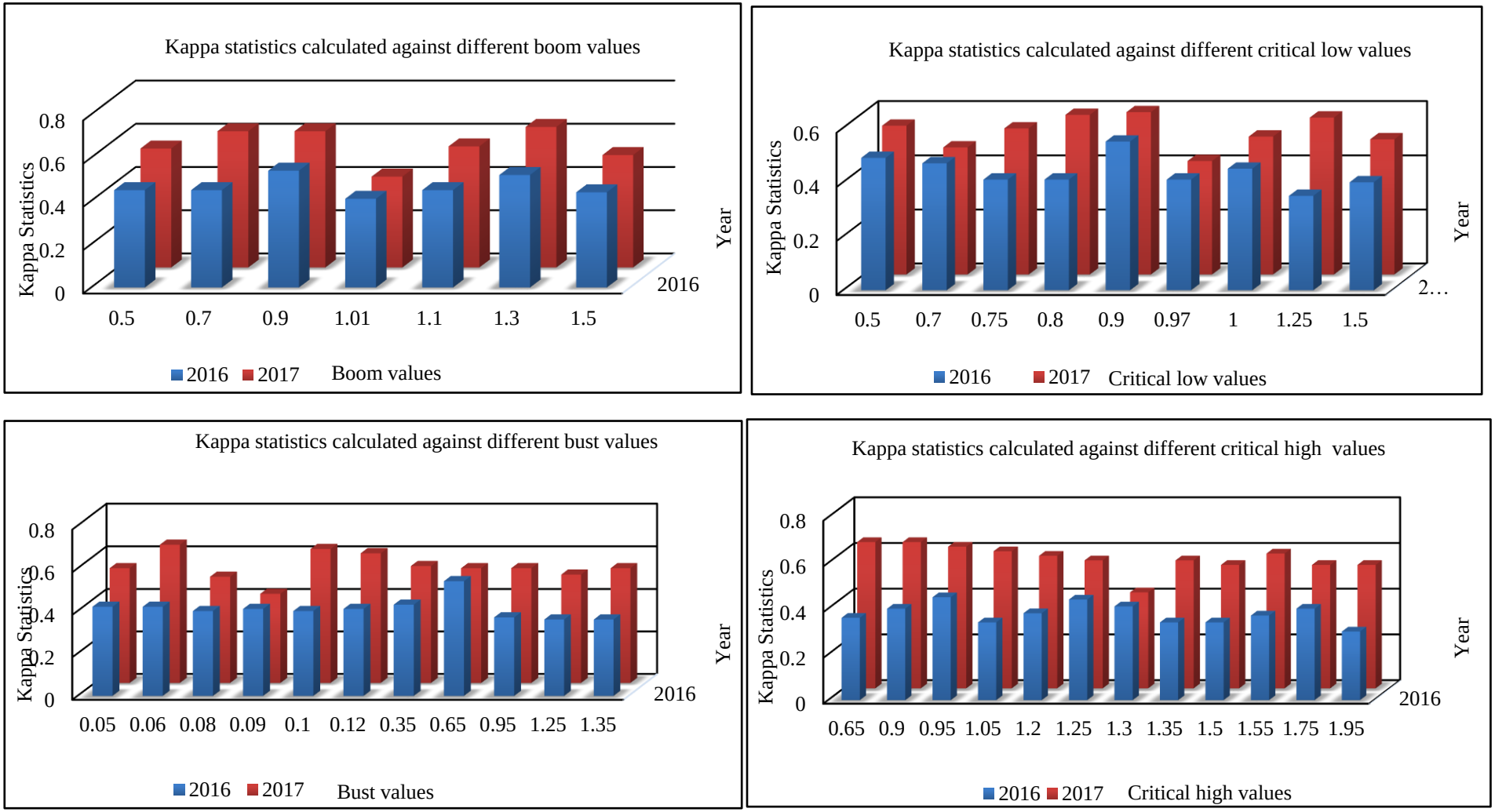

Figure 5.14: Kappa statistics for different values of self-modifying parameters for year 2016 and 2017

Finally, better accuracy, 76% & 86% for the year 2016 & 2017 respectively have been obtained from a *critical high* value of 1.25 as compared to the accuracy achieved with default *critical high* value of 1.3. Details are presented in Figure 5.13.

The kappa statistics representing the proportionate reduction in the error generated by simulated urban growth compared with respect to the error of a random simulation have also been computed for different sets of self-modifying constant values. The kappa statistics have been found to be better with a *boom* value of 1.30 (0.52 and 0.62 for the year 2016 and 2017 respectively) as compared to kappa statistics obtained for the urban growth simulated corresponding to the default *boom* value of 1.01 (0.41 and 0.42 for the year 2016 and 2017 respectively). Best kappa statistics (0.40 and 0.60 for the year 2016 & 2017 respectively) have been obtained for the urban growth corresponding to 0.10 *bust* value as compared to 0.41 and 0.42 obtained with the default value of 0.09 for the year 2016 and 2017 respectively. Details are presented in Figure 5.14.

Likewise, better kappa statistics (0.55 and 0.60) have been obtained corresponding to the 0.90 *critical low* value as compared to the kappa statistics obtained with 0.97 default *critical low* value (0.41 and 0.42) for the year 2016 and 2017, respectively. Similarly, better kappa statistics (0.44 and 0.45) have been obtained corresponding to the 1.25 *critical high* value as compared to the kappa statistics obtained with 1.3 default *critical high* value (0.41 and 0.42) for the year 2016 and 2017, respectively (Figure 5.14).

5.5.4 Visual analysis

The visual analysis of simulated urban maps at optimal parameter values for the year 2015 was compared with the actual urban growth obtained from remote sensing data of the year 2015. The simulated urban growth at default parameters has shown many differences with the actual urban growth in the year 2015 (please refer to the Figure 5.15). However, simulated urban maps against individual best self-modifying parameter values reveal very realistic urban patterns for the optimal self-modifying parameters obtained from sensitivity analysis. However, at a few places some urban edges and small size clusters were inaccurately formed which may be due to the limitation of the stochastic nature of the modelling approach and the misclassification present in classified LULC maps as it was evident from the satellite images that some vegetation shadows fall over built-up land which was not identified as urban by remote sensing but was observed in simulated maps. Since, CA rules are applied over a 3*3 neighborhood at a time, therefore, due to a higher probability of neighboring pixels getting urbanized it automatically simulated those non-

urban pixels as urban which was not visible as urban but in reality persists. This is the beauty of CA at best replicating a complex urban system that even can forecast urban future as well. The present study investigated the influences of different self-modifying parametric/ constant values on urban growth simulation outcomes. Optimal values of different constants/ parameters have been determined on the basis of best model fitness, comparison of spatial and statistical measures computed from actual (two reference datasets) and simulated outcomes, accuracy percentage and kappa statistics. The model is able to simulate urban growth more realistically and is able to capture different forms of urban growth with optimum self-modifying parameters determined through sensitivity analysis.

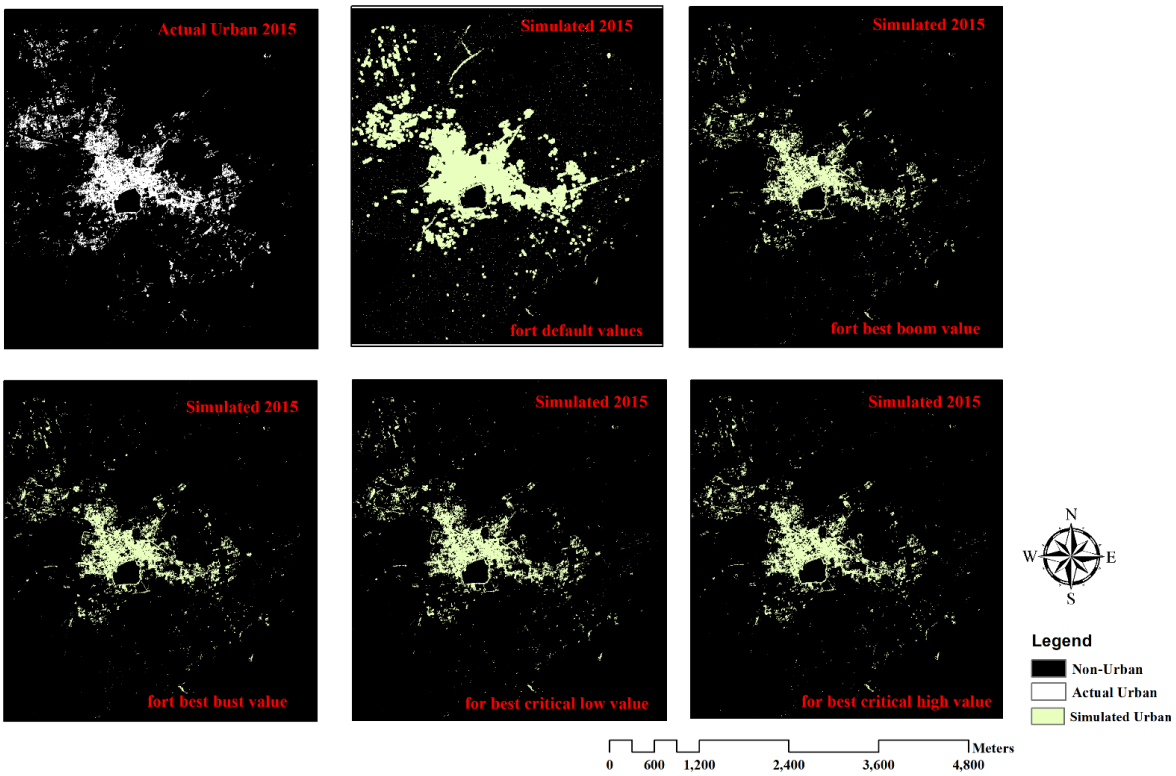

Figure 5.15: Comparison between actual & simulated urban growth for year 2015

5.6 Sensitivity Analysis of Diffusive Value Parameter

The SLEUTH model uses four growth rules sequentially to simulate LULC change and urban growth. The first rule simulated diffusive growth which affects the behavior of the remaining three growth rules. Therefore, any uncertainty in diffusive growth may lead to incorrect overall growth simulated by the model. Diffusive growth is responsible for determining the overall dispersion of urban growth, spontaneously taking place at a suitable landscape and it is the first growth rule to be performed in SLEUTH modelling.

In CA, a landscape is considered as a cellular structure, the smallest unit is a cell represented by a pixel and it has a state in terms of urban or non-urban. Transition rules are applied on a pixel or cell basis selected randomly or sometimes sequentially based on the growth rules to be performed. The diffusive growth takes place in such manner as explained below;

For (k = 0; k < 1 + (int) diffusive value; k++)

{

A pixel will be randomly selected from overall raster grid and will be attempted to get urbanized by passing through suitability conditions like slope and exclusion.

}

Diffusive or spontaneous growth is controlled by a parameter i.e., a Diffusive value which is estimated using equation 5.1 as mentioned below. Here, the diffusion coefficient is the value sequentially selected from the coefficient space i.e. 0 - 100, for the first run it would be '0'.

$$diffusive\ value = \left((\text{diffusion coefficient} \times 0.005) \times \sqrt{rows^2 + cols^2}\right) \ldots\ldots 5.1$$

When the diffusion coefficient is maximum i.e. 100, the diffusive value will be maximum and would be equal to 50% of the image diagonal. However, the diffusive value is a function of 0.005, a multiplying parameter/constant which may be called as the *diffusive value parameter*. The model sensitivity with respect to the *diffusive value parameter* has not been tested and its optimum value may be different for different geographical and socio-economic settings. By default, the value of this parameter has been adopted as 0.005 in equation 5.1. Therefore, an effort has been made to investigate the model sensitivity in term of change in model response as a function of *the diffusive value parameter*. An iterative procedure has been used to test the sensitivity of *diffusive value parameter* by simulating urban growth of Pushkar town for a range of *diffusive value parameter* and quantifying the relative change with respect to the growth simulated corresponding to its default value. *The* detailed methodology for performing a sensitivity analysis of diffusive value parameters has been discussed in detail in a subsequent section. The methodology adopted for the sensitivity analysis of the model with respect to the *diffusive value parameter* is presented in Figure 5.16. The diffusion coefficient is responsible for spontaneous growth, new spreading center growth and road influenced growth.

The growth rules are performed in a sequential manner and each is dependent on the previously captured urban growth. In present study, a range of *diffusive value parameter* i.e., default value (0.005) ± 50% (0.0025, 0.0030, 0.0035, 0.0040, 0.0045, 0.0050 (default), 0.0055, 0.0060, 0.0065, 0.0070 and 0.0075) has been selected for performing sensitivity testing. For the individual parametric setting, the SLEUTH program has been modified and calibrated independently. Further, calibration was judged based on the goodness of fit metrics and optimal growth coefficient values are determined and urban growth has been predicted for up to the year 2040 for the individual setting.

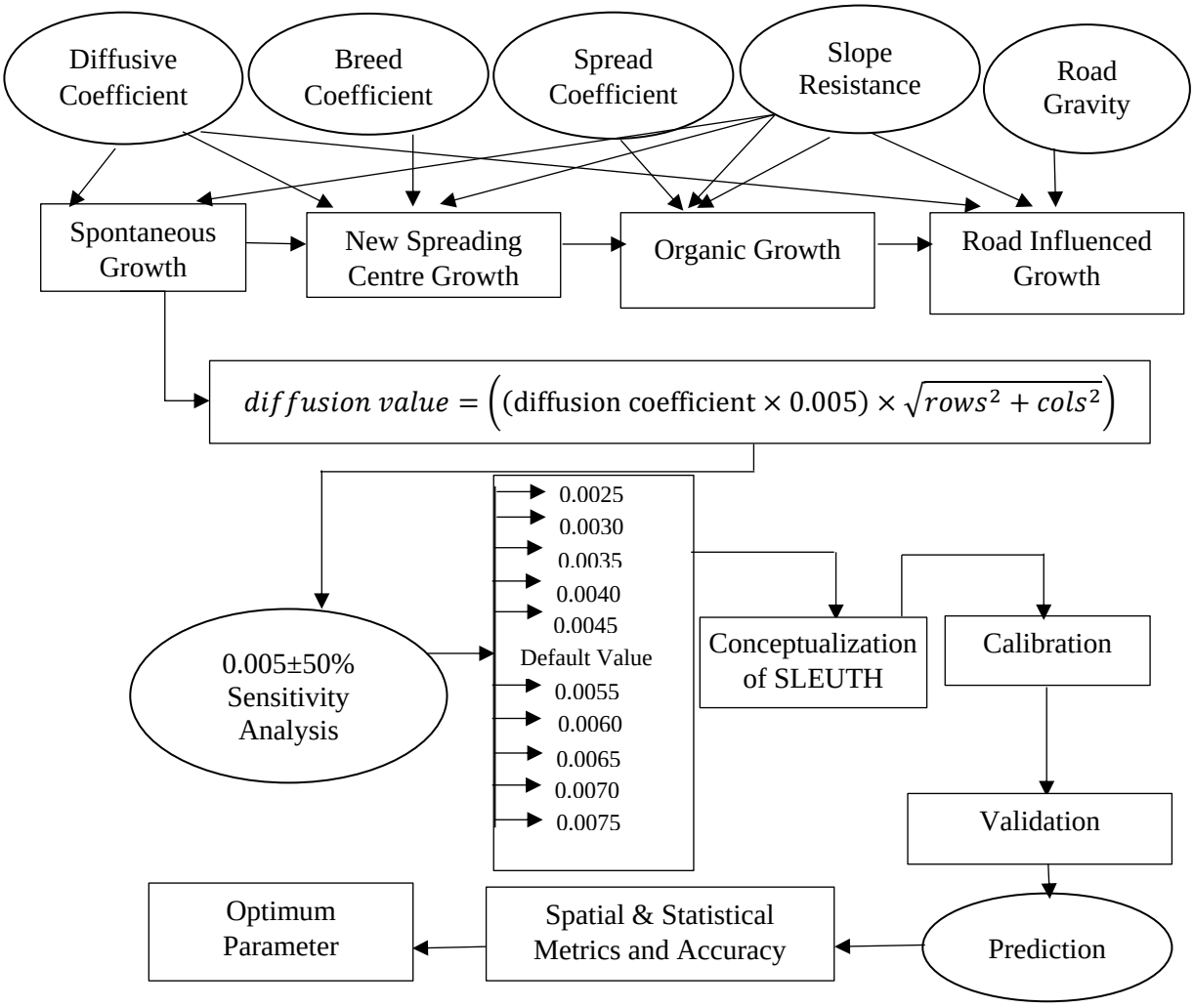

Figure 5.16: Methodology of sensitivity analysis of diffusive value parameter

To determine the optimal value of *diffusive value parameter* the simulated outcomes have been compared with the actual urban area obtained from two reference data on the basis of spatial and statistical measures calculated from both simulated growth and actual urban area, as discussed earlier. Optimum parameter values have also been determined by comparing the accuracy of urban growth for different parameter values with the

percentage accuracy obtained for the default parameter. Optimum *diffusive value parameter* value will be that at which percentage accuracy of simulated growth is highest. Calibrated value of growth coefficients for a range of *diffusive value parameter* has been presented in Table 5.5. Due to the stochasticity in the modeling, no significantly increasing or decreasing trend was observed in best-fit growth coefficient values. Although, the study is able to give the optimal value of *diffusive value parameter*.

Table 5.5: Best fit growth coefficient values for individual diffusive growth parameters

Diffusive Growth Parameter	Best fit Diffusion Coefficient	Best fit Breed Coefficient	Best fit Spread Coefficient	Best fit Slope Resistant Coefficient	Best fit Road Gravity Coefficient	Best OSM
0.0025	54	54	43	54	54	0.28
0.0030	1	93	13	98	90	0.27
0.0035	44	24	60	89	87	0.26
0.0040	77	37	34	76	38	0.28
0.0045	73	34	32	45	23	0.27
0.0050	49	45	25	68	46	0.28
0.0055	53	19	47	10	30	0.37
0.0060	57	22	49	3	27	0.28
0.0065	32	10	66	2	7	0.25
0.0070	55	39	29	79	45	0.28
0.0075	45	51	24	42	1	0.27

The highest model fitness i.e. OSM, 0.37 has been achieved for *diffusive value parameter* at 0.0055 which is far better than remaining other values of *diffusive value parameter* including the default. The optimal growth coefficient value has been achieved at *diffusive value parameter* 0.0055 as 53, 19, 47, 1 and 3 for diffusion, breed, spread, slope resistance, and road gravity coefficients, respectively. The diffusion coefficient based spontaneous/ diffusive growth and spread coefficient based organic/ spread growth have been found to be dominating the urban growth. The model sensitivity to the *diffusive value parameter* has been determined by calculating the relative change in urban growth simulated for its different values keeping other constants the same. Further, spatial and statistical measures have been calculated for all values of the *diffusive value parameter*. Percentage accuracy and kappa statistics were also estimated corresponding to the different values of the *diffusive value parameter*.

5.6.1 Comparison between spatial and statistical measures computed from input datasets and simulated outcomes

The present section discusses the comparison between actual and simulated urban area for different years in term of spatial and statistical measures to determine the optimal set of the *diffusive value parameter*. The simulated urban growth for default *diffusive value parameter* i.e. 0.005 has been found to be 41354 ha as compared to 48014 ha urban area obtained from reference data for the year 2015, however at 0.0045 value urban area has been found to be better. The urban growth has been more accurately captured at 0.0055 of *diffusive value parameter* with improved model fitness i.e. OSM of 0.37. The urban growth at 0.0055 value of *diffusive value parameter* has been found to be more realistic as indicated by a more accurate no. of urban clusters, edges, urban cluster radius and mean cluster size statistical measures with a better Optimal SLEUTH Metric (OSM), model fitness i.e., 0.37 as compared to 0.27 value obtained from default value (0.005) (Figure 5.17). The urban cluster radius has been found to be better captured at 0.0055 with better model fitness value. The difference between actual and simulated mean cluster size has been found lesser at 0.0035 however with lesser model fitness, therefore, diffusive value parameter at 0.0055 with higher model fitness value i.e. 0.37 is found to be more reliable and optimum for capturing the urban growth.

5.6.2 Comparison between spatial and statistical measures computed from Geo-eye data and simulated outcomes

To determine the optimum value of *diffusive value parameter*, spatial and statistical measures have been estimated for the simulated urban area corresponding to different values of *diffusive value parameter* and compared with measures calculated from the urban area extracted from high-resolution image of Geo-eye satellite for the year 2017 (actual urban area). At 0.0055 value of diffusive value parameter, an urban growth area, edges and mean cluster radius have found to be satisfactorily in agreement with measures calculated from reference urban area with an improved model fitness i.e. 0.37.

The difference between the actual and simulated number of urban clusters and mean cluster size has been observed because clusters may be lost while digitizing the urban areas from high-resolution GE data (Figure 5.18).

The present investigation revealed that different values of the diffusive value parameter may affect the model performance in capturing the different type of urban growth or form.

The *diffusive value parameter* i.e., 0.0055 has been found to be optimum and the model is able to capture different forms of urban growth corresponding to different socio-economic conditions of developing countries. The optimum value of *diffusive value parameter* as 0.0055 has been arrived at based on the closeness of the spatial and statistical measures calculated from the simulated urban growth and reference datasets corresponding to the year 2015 and 2017.

5.7 Sensitivity Analysis for Monte Carlo Runs

In the modern world of the computer, geo-simulation has become possible by a powerful tool like Monte Carlo simulations. Generally, the stochastic model assumes Gaussian behavior and runs multiple times to produce a distribution of outputs that describe the randomness and variability into the modeling outcomes against model goodness of fitness metrics. However, in geostatistics, there is no standard heuristics to identify the appropriate or best number of Monte Carlo iterations a model should run. A greater number of MC runs will have good model diversity however at the expense of model computational resources. On the other side, very few numbers of Monte Carlo simulation runs may steal the opportunity of reaching out to the best model calibration. Also, how it affects the model calibration performance and simulated growth eventually has not been evaluated well so far.

Evaluation of model calibration behavior against the number of Monte Carlo runs on the basis of model goodness of fit and different spatial metrics or statistical measures may be helpful in deciding an appropriate number of MC runs for a modelling exercise.

The CA-based SLEUTH model utilized less Monte Carlo runs (i.e. 6-10) for its calibration phases due to higher computational overhead. Many efforts have been made to improve the computational efficiency of the SLEUTH model recently. The SLEUTH sensitivity to MC iterations has been tested by running the model for a range of MC runs i.e., 10 to 300; 10 – 100 with an equal interval of 10 and three simulations with 150, 200 and 300 MC iterations. The SLEUTH model has been calibrated for 13 different sets of MC runs independently and urban growth was predicted with the same input dataset. The model has been calibrated for each Monte Carlo set independently and change in model performance was analyzed on the basis of goodness of fit metrics such as compare, urban population (pop), edges, clusters, mean cluster size, Lee Sallee and cluster radius, model fitness measure (i.e. OSM), kappa statistics, accuracy percentage and visual analysis.

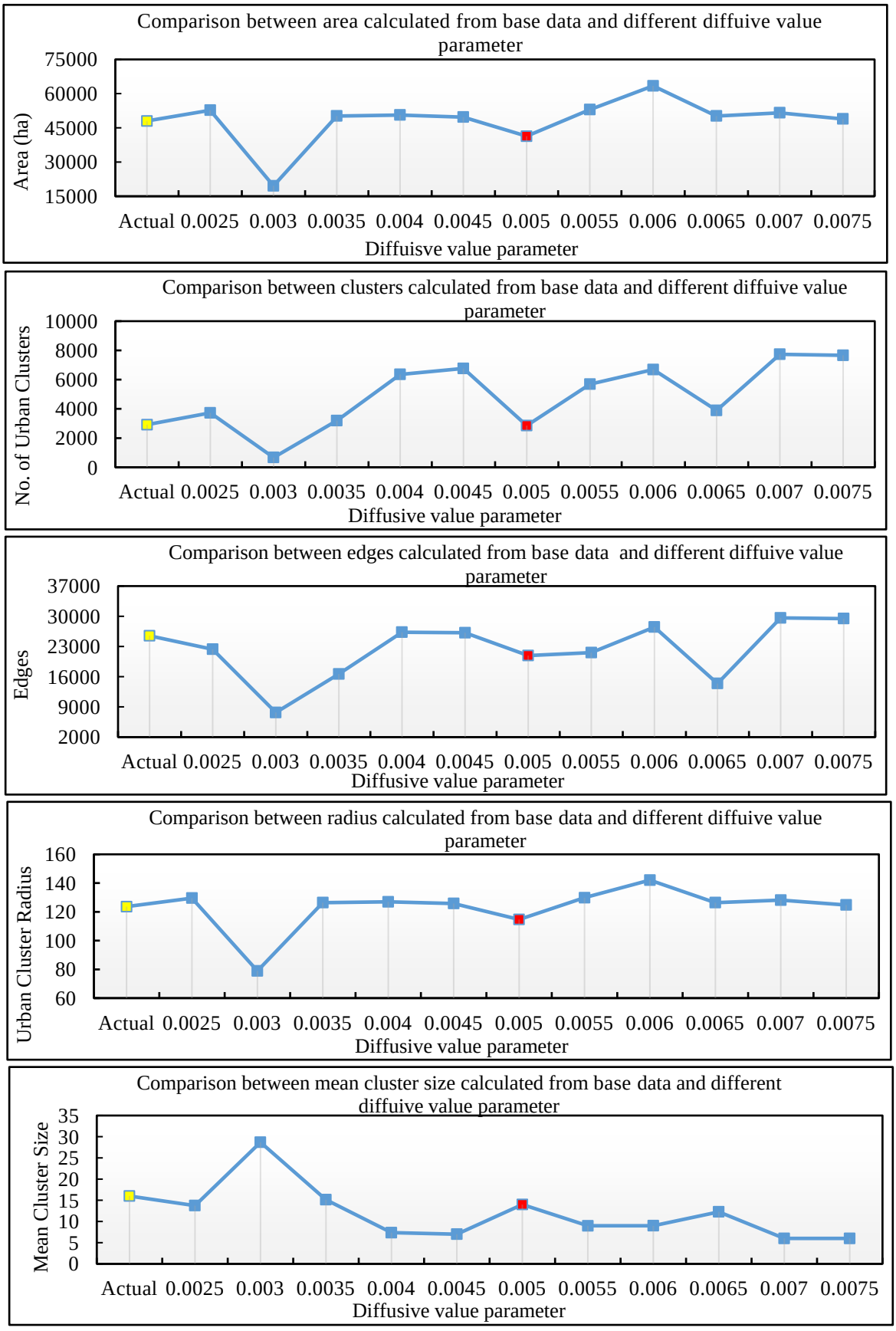

Figure 5.17: Comparison of spatial and statistical measure estimated for urban growth w.r.t. different values of diffusive value parameter and actual urban growth (bs)

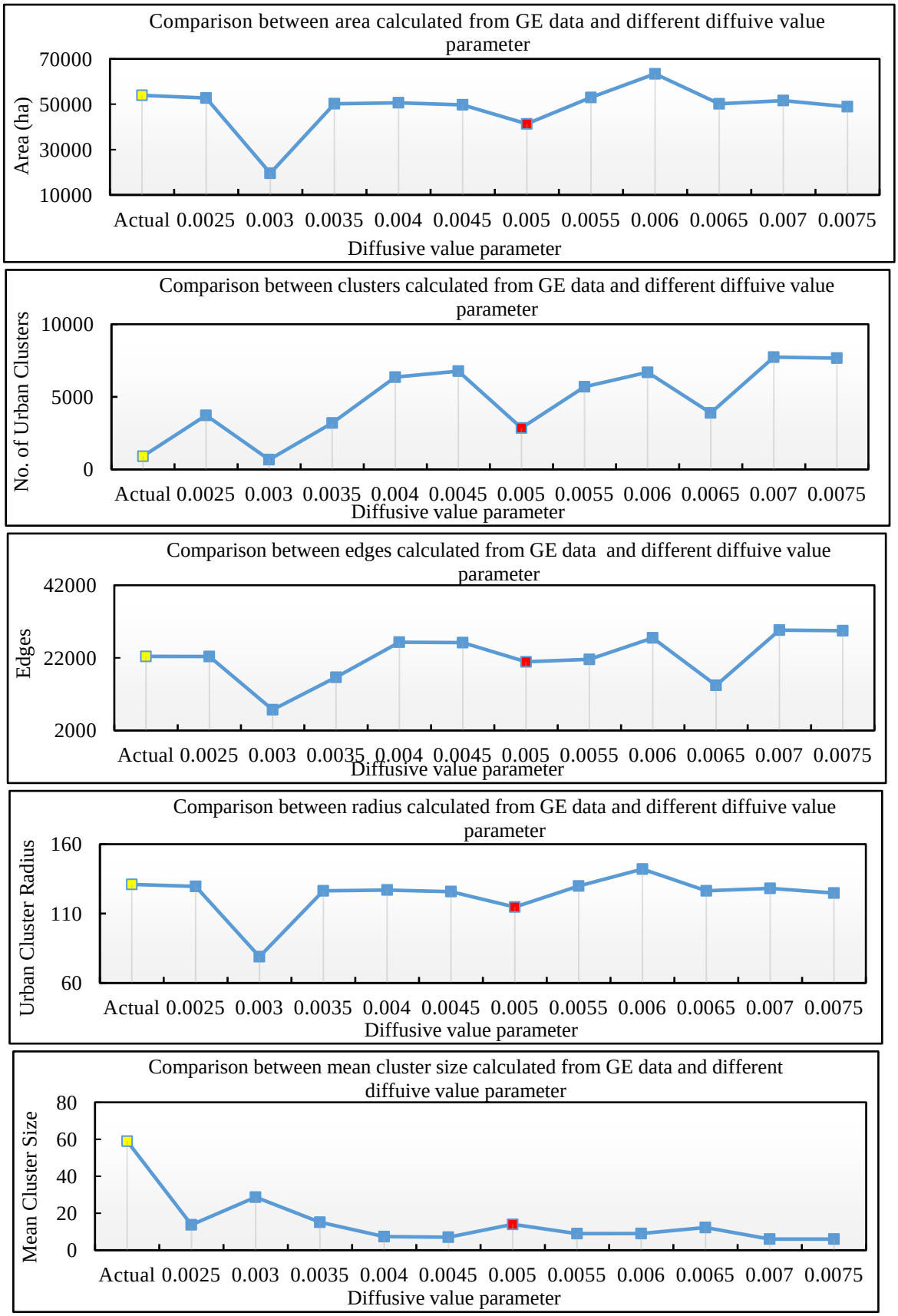

Figure 5.18: Comparison of spatial and statistical measure estimated for urban growth w.r.t. different values of diffusive value parameter and GE based actual urban growth (bs)

An optimal number of MC iterations is that number where simulated urban growth is in close agreement with reference urban area of the respective years in term of above-mentioned goodness of fit metrics and OSM value. The detailed methodology for the sensitivity analysis with respect to MC iterations has been presented in Figure 5.19.

The model fitness measure i.e. OSM has been evaluated for an individual set of different MC iterations and it has been observed that model calibration is not affected significantly by the number of MC iterations. Highest model fitness measure i.e., 0.30 has been achieved for 60 number of MC iterations and 10, 20, 70, 80, 100 and 300 MC number of iterations it was found to be 0.27 or less, as presented in (Figure 5.20). It can be concluded that the model is able to capture better diversity at 60 MC iterations. In addition to OSM value, several goodness of fit metrics are computed to determine the SLEUTH sensitivity to the MC iterations as discussed above and details of each can be found in Chapter 4.

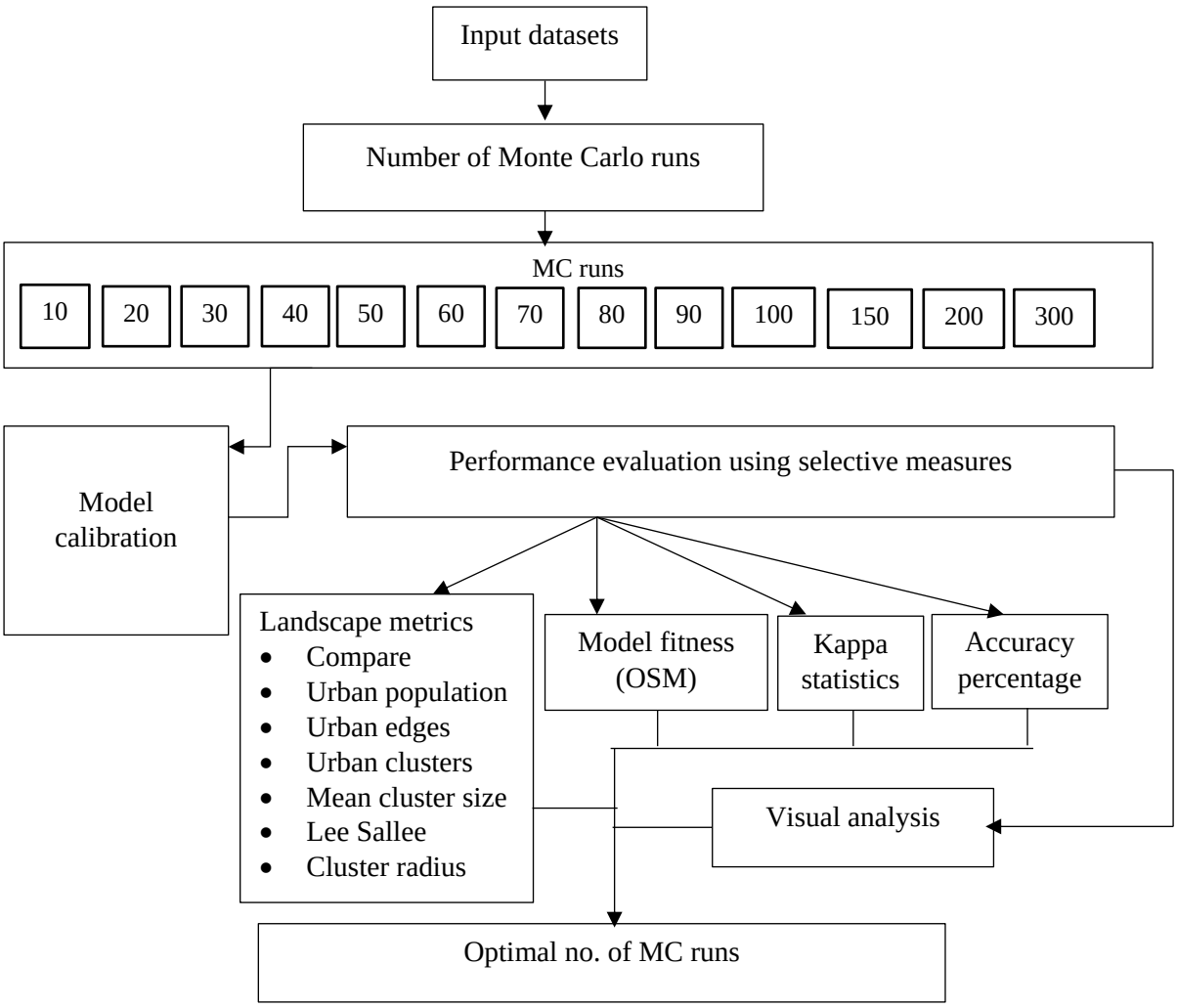

Figure 5.19: Methodology of sensitivity analysis of Monte Carlo analysis

The compare metric compares the simulated and actual urban extent of control years and it achieved the best in the case of 60 MC runs i.e. 0.99. The lowest urban extent comparison is achieved in the case of MC 80 and 200, i.e. 0.76 (Figure 5.20). Due to the stochastic nature of the model, no specific trend for the goodness of fit metrics has been observed as a function of MC iterations and the urban extent comparison metric lies in the range of 0.76 to 0.99. The pop (urban population/ no. of urban pixels) metric gives the regression score of comparison between actual and simulated urban pixels. In the present study, a pop metric calculated for an individual set of MC runs has been found in between 0.87 and 0.88 with respect to the model outcome for different MC iterations. Again, no significant effect has been observed on pop metric for a different number of MC iterations. However, at MC 60 iterations urban pop metric has been found to be closer to the same computed from reference data. The Lee Sallee shape index represents spatial fit between simulated urban growth patterns and actual urban growth pattern. In the present investigation, the highest Lee Sallee value achieved as 0.33 which is a good shape measure value for such a heterogeneous landscape (Rafiee et al., 2009; Hui-Hui et al., 2012; Akın et al., 2014; Dezhkam et al., 2014). However, not many differences in Lee Sallee shape index have been noticed during model calibration performed with different MC runs (Figure 5.20).

The edge metric measures the least square regression fit between actual and simulated urban edge count which has been observed lying in between 0.11 and 0.92. The highest edge metric value achieved in the case of 200 MC iterations and the lowest edge metric was achieved at 50 MC iterations. Significant variation in values of the urban edge metric has been observed for different MC iterations. However, the highest value of urban edge metric i.e., 0.90 has been found at 60 MC iterations, which is closer to the best value achieved (i.e. 0.92) (Figure 5.20).

The urban cluster radius which compares the average radius of the simulated and actual urban pixels enclosed circle has been found to be highest i.e. 0.9 for the calibration performed at 60 MC iteration and the lowest radius metric is achieved as 0.8 for calibration performed at 30 MC iteration. The calibration performed at other MC runs resulted into the similar value of radius metric i.e. 0.89 (Figure 5.20).

The investigation reveals that calibration performed at different MC iterations has not been given any significant trend in term of different goodness of fit metrics computed during the model calibration with respect to an individual set of MC iterations. However, calibration performed at 60 MC iteration has been found to be more consistent and

goodness of fitness landscape metrics calculated from the simulated urban growth are closer to the metrics calculated from the reference urban area for the reference year i.e., 2015.

In addition to the goodness of fit metrics and model fitness measure i.e. OSM the effect of different sets of MC runs on model calibration has been analyzed through visual analysis. The visual comparison of simulated urban growth map using different sets of MC runs with the actual urban map for reference year i.e., 2015 is presented in Figure 5.21. It is evident from Figure 5.21 that the model has been able to capture urban growth nearest to the actual growth at 60 MC iterations. Calibration performed at MC runs 70, 80, 90, 100, 150, 200 and 200 has over captured the urban growth despite obtaining good goodness of fit metrics (Figure 5.21). Beyond the optimum number of MC, iterations model starts repeating the previously obtained growth coefficient values and similar urban patterns which gets superimposed over the number of MC runs.

The sensitivity of MC runs might be useful for deciding the suitable number of runs for a specific modelling application. Knowing the optimum number MC iterations required for model calibration may lead to better model simulation and prediction accuracy. It was observed that MC 60 is the most appropriate value for performing model calibration and therefore, obtained refined parameter set from the calibration is used for predicting urban growth for up to the year 2040.

Further, accuracy assessment has been done for the simulated outcomes at MC runs 60 with respect to the GE data as reference dataset by using random sample points as discussed earlier. The accuracy in percent and kappa statistics have been computed for the year 2016 and 2017. The accuracy percent for an urban simulated map of the year 2016 & 2017 has been obtained as 82 % and 87% respectively which is quite good for a model application. The computed kappa statistic achieved as 0.63 and 0.71 for the year 2016 and 2017 respectively (Table 3.7) which is stating that simulated outcomes are able to avoid 63% and 71% chances of error that may incur by a complete random modelling process. Obtaining such good kappa statistics and overall accuracy percentage is very crucial in modelling. The urban growth predicted maps have been presented in Figure 5.22.It is evident from the predicted urban growth for the year 2040 (Figure 5.23) that urban growth of Pushkar will spread horizontally outward, especially in the north-west direction with a very high probability i.e. above 90%.

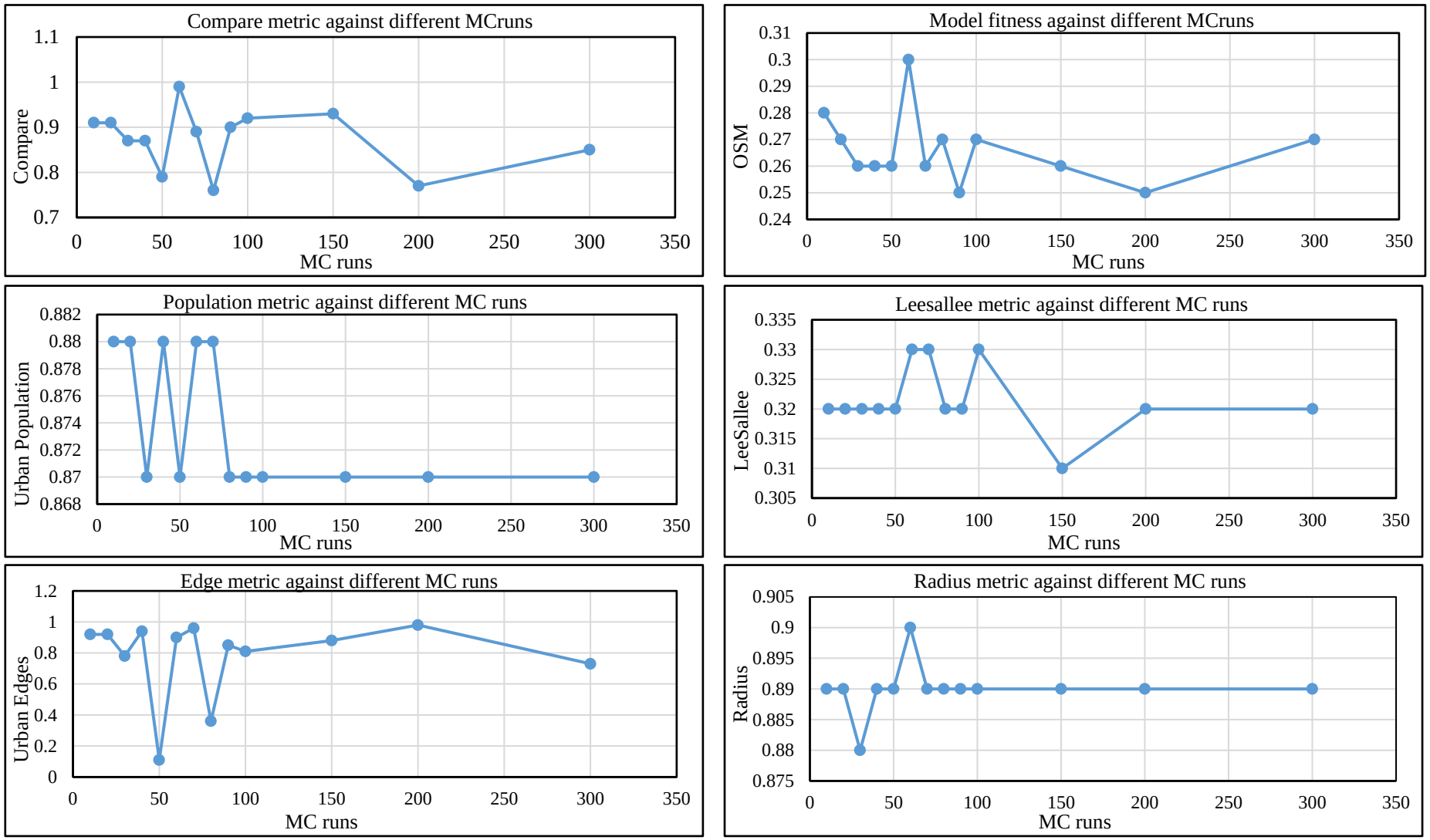

Figure 5.20: SLEUTH sensitivity to number of Monte Carlo iterations in term of goodness of fit metrics

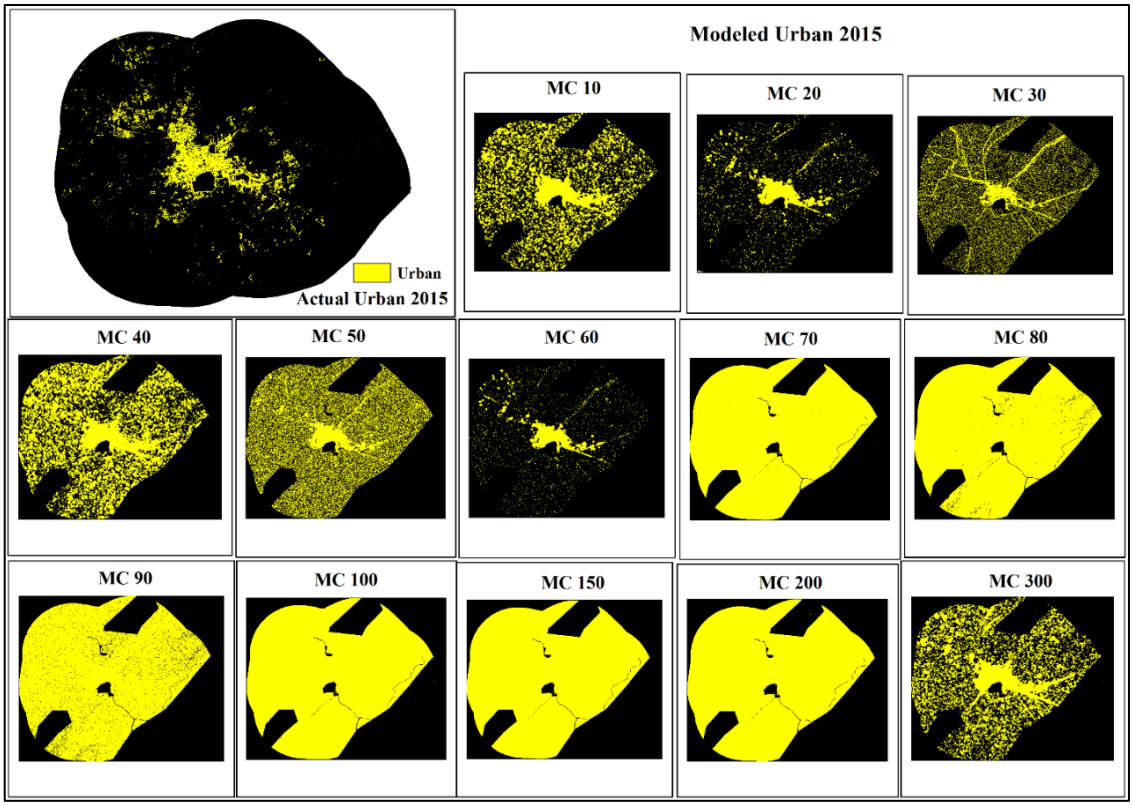

Figure 5.21: Simulated urban growth for year 2015 for different Monte Carlo Iterations

The area along Sardarshahar – Ajmer road and Ajmer- Nagpur road may be developed with a probability of 61 -70%. Area along the Brahma Temple road may be developed rapidly due to the tourist inflow being a religiously important area. In general, Pushkar will develop rapidly along the important road where suitable land is available for development and provide better transportation connectivity as revealed in Figure 5.23. Urban growth prediction indicates an ongoing trend of development of Pushkar town. The Pushkar is developing at a fast pace due to migration from nearby areas in the aspiration of a better livelihood, increased tourist activities being a religious importance because of Brahma temple at Pushkar Ghat. Though, there is not a significant difference it has been observed in the calibration performance of the model as a function of a number of MC iterations. However, model sensitivity to MC iterations gives an optimum number of MC iterations at which the model is satisfactorily able to capture the diversity of the urban development and helps in reducing the uncertainties in selecting the MC iterations.

Table 5.6: Accuracy assessment report for modelling outputs using mc 60 suite

Monte Carlo iterations	Accuracy percentage (%)		Kappa statistics	
	2016	2017	2016	2017
60	82	87	0.63	0.71

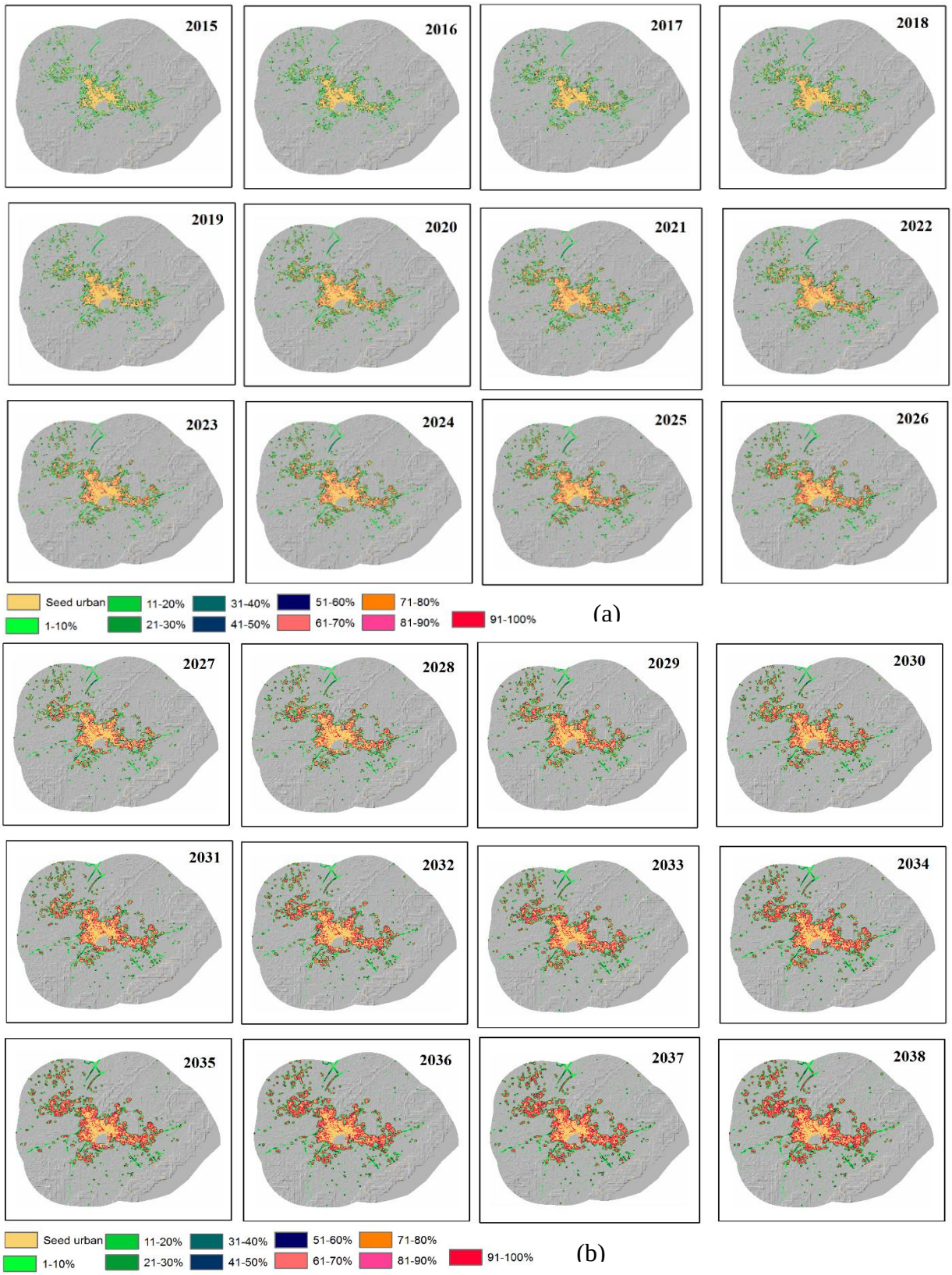

Figure 5.22: Model simulation outcomes for year 2015 to 2040 for different Monte Carlo iterations

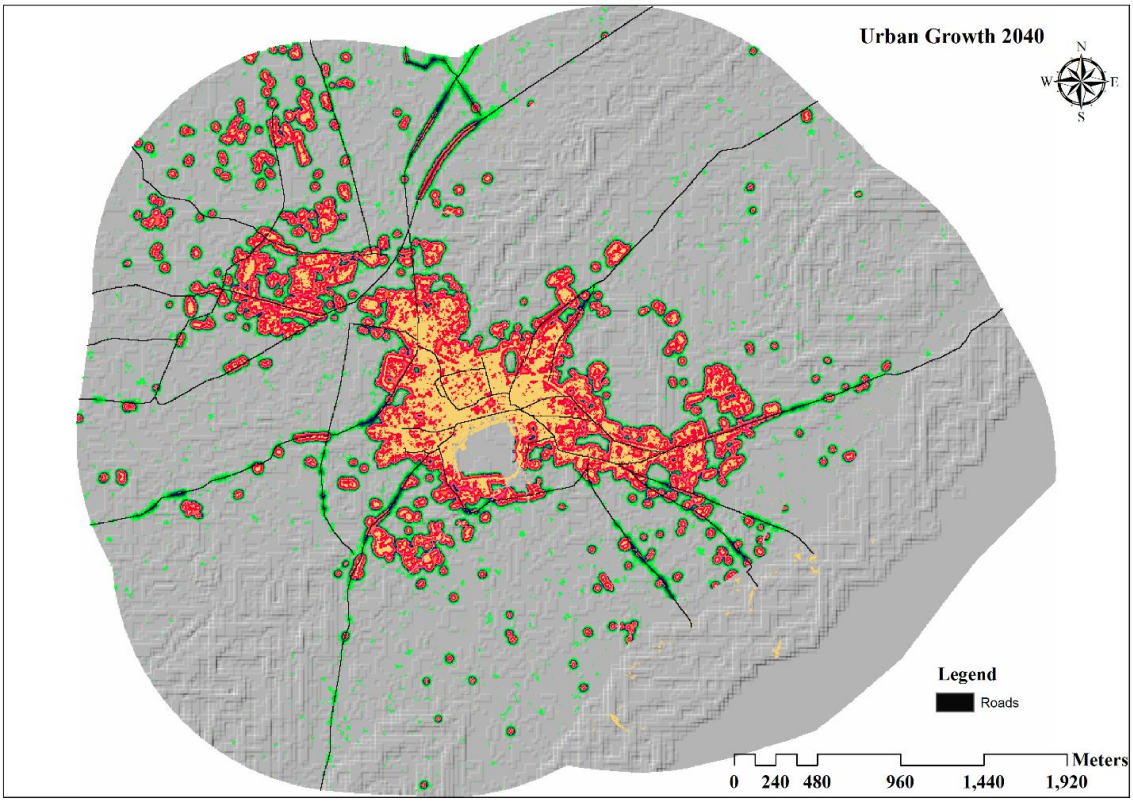

Figure 5.23: Urban growth prediction for year 2040 with 60 MC iterations

5.8 SLEUTH Sensitivity with Respect to Game of Life Rules

Cellular Automata (CA) has evolved as an important tool for LULC change and urban growth modelling techniques owing to its simplicity, ease of implementation and ability to incorporate dynamism and complexity of the urban growth phenomenon. The CA based SLEUTH model uses *game of life rules* as a core process in urban growth simulation. As discussed previously, SLEUTH uses five growth coefficients i.e. diffusion, breed, spread, slope resistance and road gravity coefficient and four growth rules i.e. diffusive, new spreading center, edge or spread and road influenced growth while simulating the urban growth. The *game of life rules* helps in determining the state of a cell/ pixel based on the neighborhood conditions in the form of birth, survival and death of a living organism i.e., urbanization. The birth state implies a non-urban pixel becomes urban, survive state infer an urban pixel remains urban and death state is when an urban pixel becomes non-urban. The threshold value in *game of life rules* plays an important role in imitating the urban growth of an area. Currently SLEUTH implements the *game of life rules* for determining spreading growth in such a manner that a non- urban pixel or cell will get urbanized if it is surrounded by at least two urban neighboring pixels this state is known as the active state. SLEUTH has been used to simulate the urban growth of different cities, most of it

in developed countries using such a *game of life rule* with threshold value of 2 urbanized pixels to urbanize a non-urban pixel. This threshold value of 2 pixels may not be suitable to simulate the urbanization of other cities having different socio-economic conditions. Therefore, to simulate the urban growth of cities having diverse socio-economic conditions, a suitable *game of life rule* with appropriate threshold value for active state needs to be determined or the sensitivity of the model with respect to different threshold values of the active state threshold need to be determined. Model sensitivity with respect to *game of life rule* has been tested in the present research work by determining the relative change in simulated outcome corresponding to different *game of life rules*. Sensitivity analysis also helped in determining the optimum *game of life rule* at which model simulates urban growth more realistically.

The methodology followed for testing the SLEUTH model sensitivity for a *game of life rule* has been discussed in subsequent sections.

5.8.1 Methodology for sensitivity analysis for game of life rules

As discussed earlier that SLEUTH is a CA-based model and a landscape is represented in a form of cellular structure in which each cell represent the state of land use class. While the present study incorporates urban growth modeling only, therefore, we have considered a landscape in a form of urban and non-urban. The flexibility in CA allows simulating urban growth more realistically by modifying transition rules in the SLEUTH model. To facilitate model sensitivity to a *game of life*, model code has been modified for three different *game of life rules* i.e., type I, type II and type III. The model is calibrated for the individual set and the urban growth has been simulated up to the year 2040. The method to perform sensitivity analysis has been implemented as discussed below.

5.8.1.1 Type-I game of life rule

Type-I rules state that the state of each cell is a function of its current state and its neighbor's state. It can be implemented exclusively by counting the number of urban cells in a specified cellular neighborhood. In the type-I rule, a non- urban pixel will get urbanized if it is surrounded by at least one urban pixel. This rule has been successfully added into the SLEUTH source code and pseudo code is as follows;

```
If ((urban count >= 1) && (urban count <= 8))
{
Try to urbanize
```

}

From a cellular grid which represents a landscape, a pixel is tested for performing a *game of life* transition rules. First, the pixel or cell is selected to check whether it is urban or not. If this state gives true i.e. yes the pixel is urban then it further checks the state of other neighboring pixels in an 8 cell neighborhood (default cellular neighborhood size). For implying type-I rule it is considered that in a developing country housing may be of very small size and only a single urban pixel will be capable enough to start spreading at its edges. If in the 8 cell size neighborhood the total urban pixels are in between 1 and 8 (both inclusive) then a randomly selected non-urban pixel will be urbanized if found suitable to the set of conditions (Figure 5.24). Otherwise, it will not be urbanized and this process will remain to continue till all the cells of the grid are traversed.

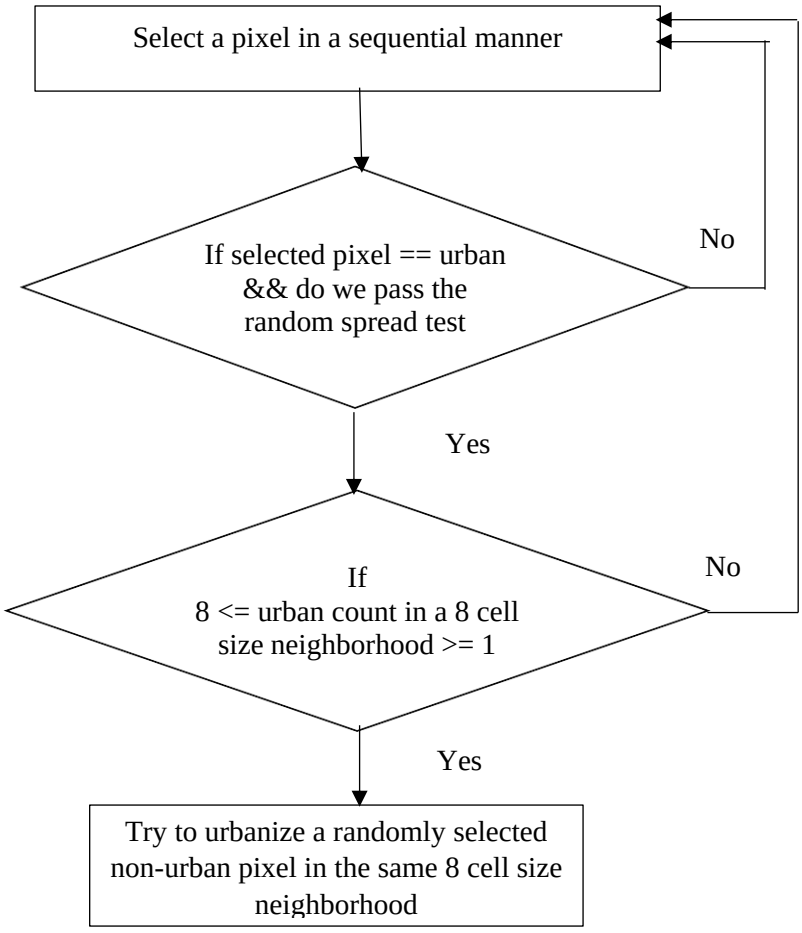

Figure 5.24: SLEUTH code for sensitivity testing for type-I game of life rule

5.8.1.2 Type-II game of life rules

Type-II *game of life rule* is implemented in the original SLEUTH source code in such a way that a non-urban pixel will get urbanized if it is surrounded by at least two urban pixels in an 8 cell neighborhood. In place of 1 urbanized pixel in the type-I rule, the

minimum threshold for the active state has increased to 2 pixels, while simulating the urban growth. The rest of the steps remain same as discussed in a type-I *game of life rule* (Figure 5.25) sensitivity testing explained above.

```
If ((urban count >= 2) && (urban count <= 8))
{
Try to urbanize
}
```

Default case

5.8.1.3 Type-III game of life rules

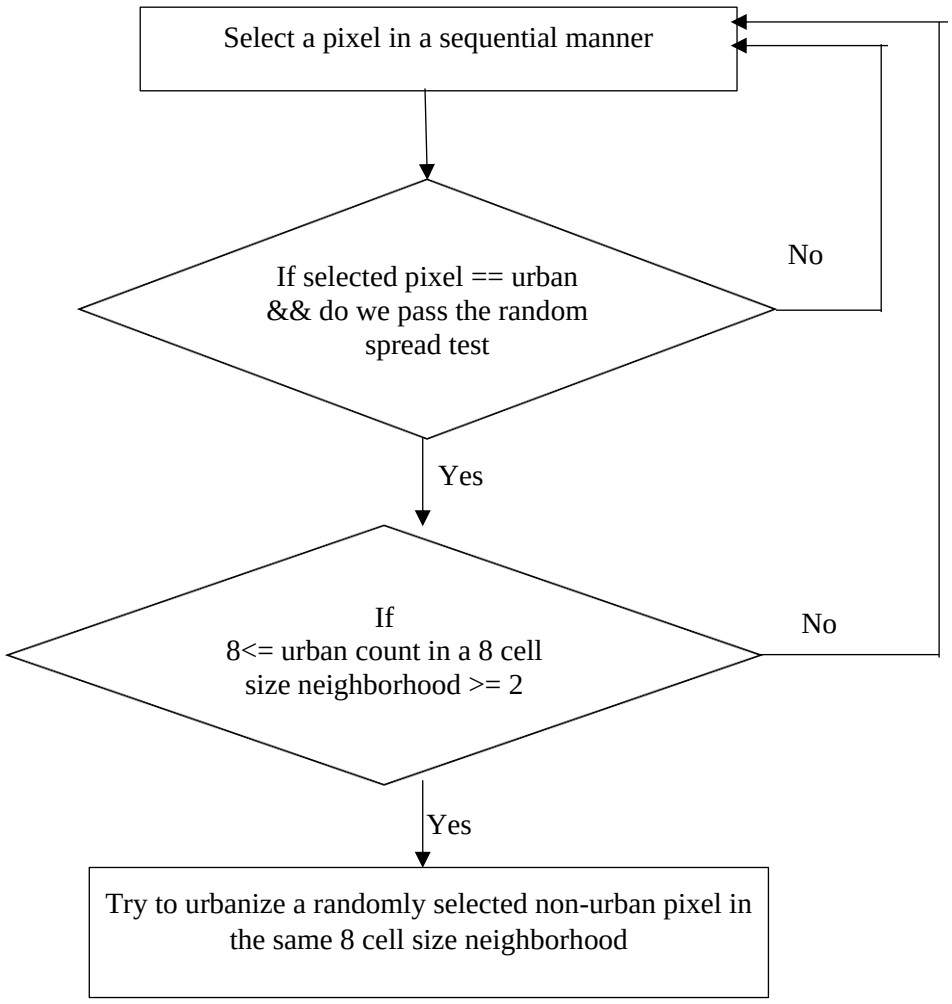

Figure 5.25: SLEUTH code for sensitivity testing for type-II game of life rule

Type-III *game of life rule* is implemented in the original SLEUTH source code in such a way that a non-urban pixel will get urbanized if it is surrounded by at least three urban pixels in an 8 cell neighborhood. In place of 2 urbanized pixels in the type-II rule, the

minimum threshold for the active state has increased to 3 pixels, while simulating the urban growth. The rest of the steps remain same as discussed in a type-II *game of life rule* (Figure 5.26) sensitivity testing explained above.

If ((urban count >= 3) && (urban count <= 8))

{

Try to urbanize

}

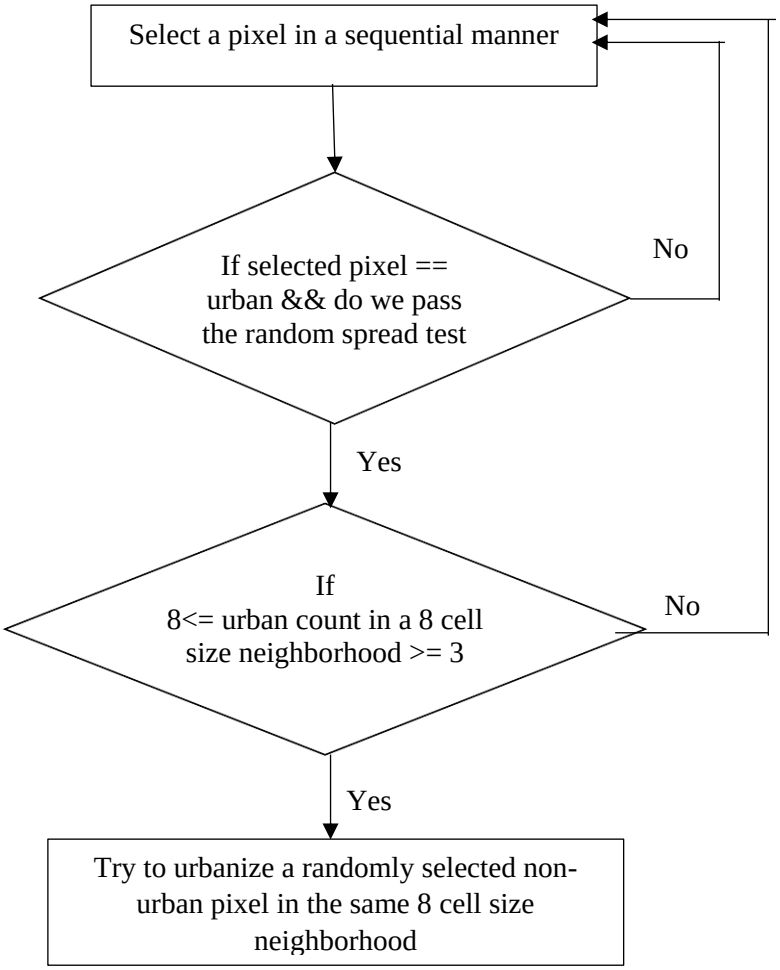

Figure 5.26: SLEUTH code for sensitivity testing for type-III game of life rule

The type-III *game of life rules* was implemented in similar ways as explained in section 5.8.1.1 and 5.8.1.2 only the minimum threshold values were modified to analyze the influence of different game of life rules on simulated urban growth and effect of models ability to capture a different type of urban forms (Figure 5.26).

5.8.2 The sensitivity of game of life rule

For the individual type of *game of life rules* i.e. type-I, type-II & type-III the program code of SLEUTH–GA model has been modified as discussed in the previous section. The model has been calibrated in three subsequent phases to refine the growth coefficient space and to obtain optimal growth coefficient values against best model fitness value i.e. OSM for each *game of life rule*. Among three phases of calibration, one best-fitted calibration phase is selected for an individual *game of life rule*. The study reveals that high diffusion coefficient value i.e. 52 was achieved in case of type-III *game of life rule*, it reduced slightly to 45 in case of a type-II *game of life rule* and further found to be reduced significantly up to 7 for a type-I *game of life rule*. It is evident from the study that diffusive growth will be increasing when an increase in the threshold value for the active state which means it increases the possibility of spontaneous/ diffusive urbanization attempts. In a developing country scenario fragmented urban growth and smaller size built-ups are very common. Thus increasing the lower threshold value will eventually shift the possibility of spread growth towards diffusive growth therefore, higher diffusion coefficient value is observed in the case of type-III game of life rule. The value of breed coefficient has been found to be very much less in a type-I *game of life rule* (3) as compared to type-II (65) and type-III *game of life rule* (97). Spontaneous diffusive urban growth starts developing new urban centers to form isolated clusters i.e. breed growth. Type-III *game of life rule* consequently increased the diffusive growth coefficient which showed the possibility for newly spontaneous urbanization to become a new spreading center. Therefore, a higher value of the diffusion coefficient led to the increased possibility of new urban center growth i.e. higher breed in type-III *game of life rule*. In the type-I *game of life rule,* the diffusive urbanization attempts are found to be decreasing which however did not lead to an increase in the spread of urbanization due to some spatial suitability constraints. According, to type-I rule, the lower threshold value has been reduced to 1 urbanized pixel that means at least one urban pixel should be in the neighborhood to spread urban growth and form large urban clusters. However, it is evident that spread growth has been reduced as a consequence of lower threshold value for the active state in the *game of life rule* (Figure 5.27). For developing spread growth it is not necessary only to get surrounded by a few urban pixels while there may be some important land suitability factors involved. Likewise, the slope resistance coefficient has also observed a lower value of 4 in the case of a type-I *game of life rule* as compared to type-II (11) and type-III (94). Reverse

implications were observed on the road gravity coefficient except for type-I. The road gravity coefficient was found highest for a type-II *game of life rule* i.e. 71, for type-I and type-III it was found to be 5 and 9, respectively. For type-I, spread coefficient was found highest among all the growth coefficients as the chances of spread growth increased by lowering the threshold value of the *game of life rule*. For type-II and type-III *game of life rule*, breed coefficient was found the highest. For high slope resistant value low road gravity coefficient has been observed and vice versa for type-II and type-III *game of life rules*.

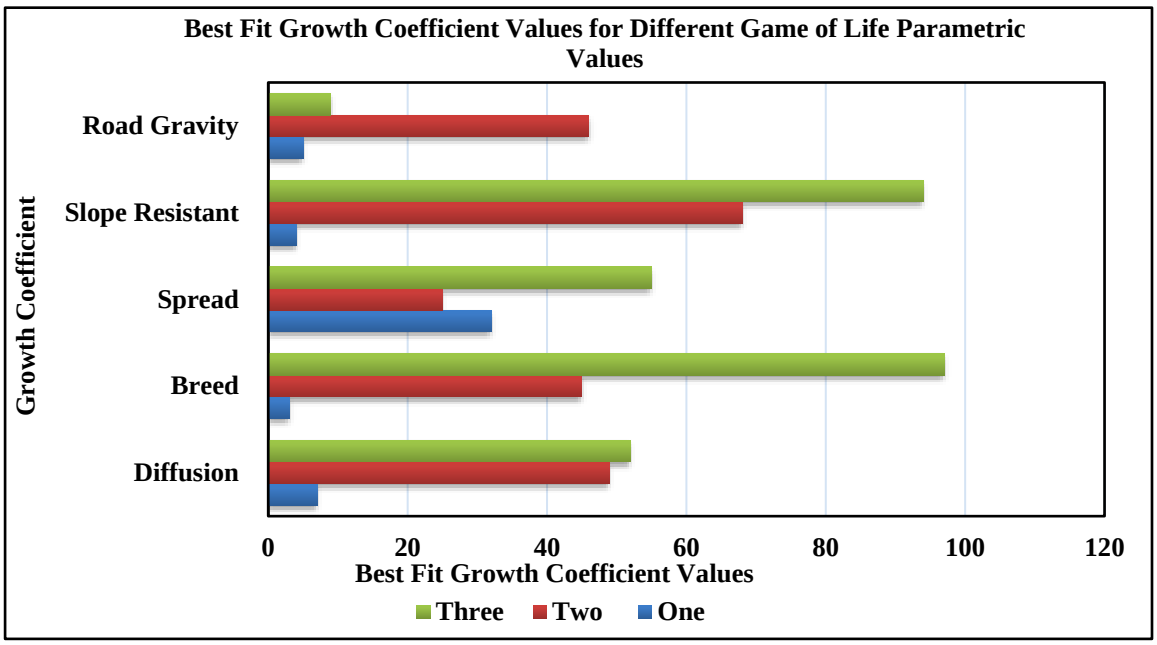

Figure 5.27: Best fit growth coefficient values for different game of life parametric values

The highest model fitness i.e., OSM has been found for the type-I *game of life rule* (0.34) and lowest OSM has been found for the type-III *game of life rule* (0.25) (Figure 5.28). The type-I *game of life rules* have been found to be optimal for simulating more accurate urban growth patterns in different socio-economic conditions. The type-II *game of life rule* (default in original SLEUTH source code) may not be appropriately imitating the different forms of urban growth for scenarios that persists in developing countries.

To further support the *game of life* sensitivity results, as discussed above, the accuracy of simulated growth corresponding to the different *game of life rules* have been estimated and compared. The accuracy of simulated urban growth has been determined in term of percentage accuracy and kappa statistics with respect to a reference dataset captured from the high-resolution Geo-eye satellite through manual onscreen digitization, as discussed below-.

The modelling outcomes obtained from the individual *game of life rules* have been assessed for accuracy with respect to urban area captured from a high-resolution Geo-eye image obtained from Google earth images years 2016 and 2017. The stratified random sampling method was used to select the test pixels for both the years and their urbanization status was checked from reference data. The statistics of agreement and disagreement between actual and simulated urban area was calculated and an overall agreement in the form of kappa statistics has been computed for different *game of life rules* as presented in Table 5.7. Also, accuracy percentage has been calculated for the year 2016 and 2017 for

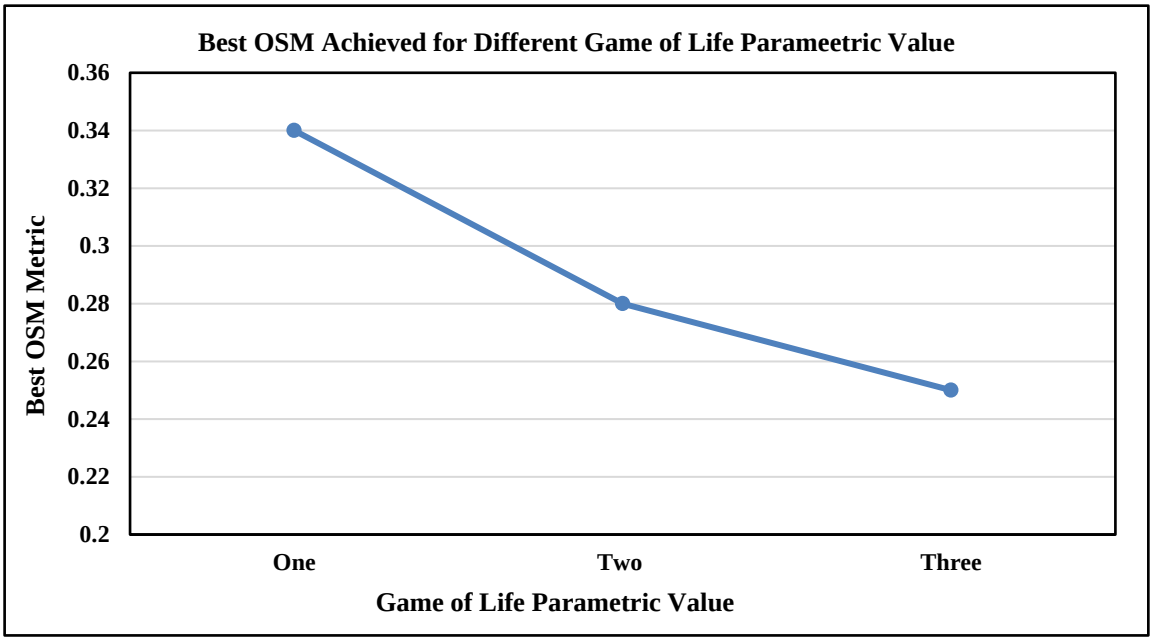

Figure 5.28: Best OSM metric value achieved against different game of life parametric value

individual setting of the game of life rules. The accuracy assessment results strongly support the type-I *game of life rule* as we got the highest accuracy percentage and kappa statistics for both the years as compared to other *game of life rules*.

Table 5.7: Accuracy assessment for a different game of life parametric settings

Game of life rules	Accuracy percentage (%)		Kappa statistics	
	2016	2017	2016	2017
Type I	82	80	0.54	0.48
Type II	73	77	0.41	0.42
Type III	79	78	0.3	0.4

5.9 Model Sensitivity with Respect to Size of Cellular Neighborhood

As discussed in Chapter 4, the extent of the *cellular neighborhood* used while implementing the different growth rules in SLEUTH model for simulation of LULC

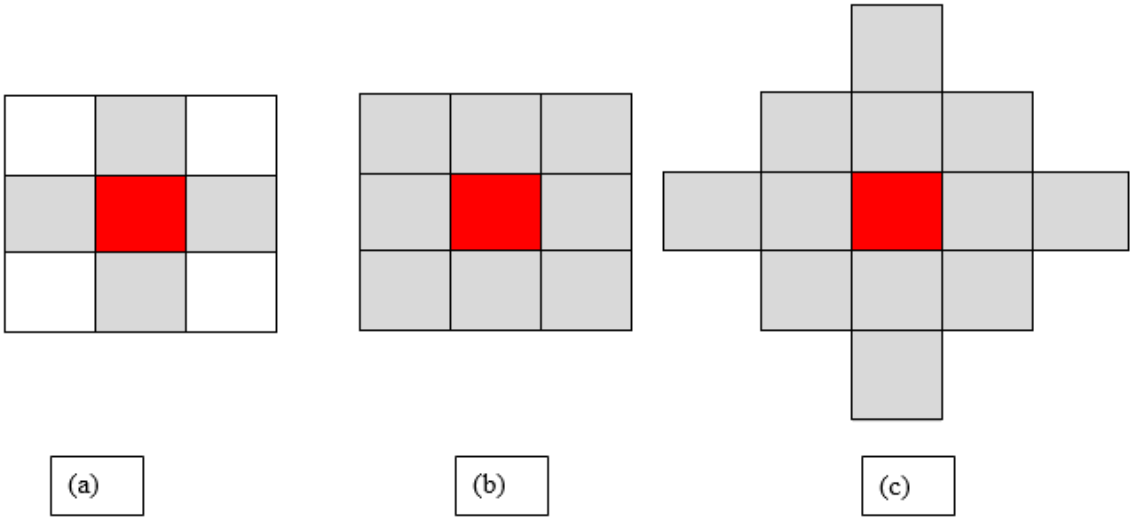

Figure 5.29: different Cellular Neighborhood (a) 4 cell Von Neumann Neighborhood, (b) 8 cell Moore Neighborhood and (c) 12 cell Extended Moore Neighborhood

change and urban growth has been a very important parameter and affects the ability of the model to simulate urbanization. The *size of the cellular neighborhood* remains a static and geometrically closest set of cells throughout the modelling. To capture different forms of growth correctly in areas with different socio-economic conditions optimal extent of affecting neighborhood may be different than the default 8 cell size neighborhood available in SLEUTH. Increasing the *size of the cellular neighborhood* will reduce neighborhood effect of urbanization on non-urbanized pixels. However, it is difficult to determine what should be an appropriate *size of a cellular neighborhood* in urban land use change modelling. Sensitivity analysis for different *size of the cellular neighborhood* may provide an opportunity to determine the optimum value of the extent of the neighborhood.

CA-based SLEUTH model is a widely used model, however, its sensitivity with respect to the *size of the cellular neighborhood* has not been tested so far. Therefore, model sensitivity to the *size of the cellular neighborhood* has been determined by determining the change in the ability of the model to correctly simulate the urban growth with different *sizes of the cellular neighborhood*. The urban growth was simulated for three *cellular neighborhood* sizes i.e.,4 cell neighborhood (Von Neumann neighborhood), 8 cell neighborhood (Moore neighborhood) and 12 cell neighborhood (Extended Moore neighborhood) (Figure 5.29) and growth was compared with the reference urban area

(actual urban area) extracted from a high-resolution Geo-eye image of the year 2017 through manual digitization.

5.9.1 Methodology for sensitivity analysis of the size of the cellular neighborhood

The SLEUTH model has been developed for three different *cellular neighborhood* i.e. 4 cell neighborhood (Von Neumann neighborhood), 8 cell neighborhood (Moore neighborhood) and 12 cell neighborhood (Extended Moore neighborhood) (Figure 5.29). The SLEUTH model code was modified to simulate urban growth for three different *sizes of the cellular neighborhood*. The details have been discussed in the form of pseudo code in the respective sections.

5.9.1.1 Von Neumann (4 cell-based) cellular neighborhood

The transition rules are influenced by the *size of the cellular neighborhood* directly and indirectly both. Some of the transition rules in SLEUTH like breed coefficient responsible for new spreading center growth and spread coefficient responsible for organic or edge or spread growth are directly influenced by the *size of the cellular neighborhood*. However, some of the transition rules are dependent on these rules i.e. diffusion and road gravity coefficient responsible for spontaneous or diffusive and road influenced growth respectively are indirectly influenced by the *size of the cellular neighborhood*. For 4 cell Von Neumann neighborhood pseudo code used in the present work has been given below,

```
Breed coefficient
{
For (max_tries =0; max_tries <4; max_tries++)
{
Try to urbanize neighboring pixels of the selected urban pixel
}
}
Spread coefficient
{
If ((urban count >= 2) && (urban count < 4))
{
```

Try to urbanize

}

}

5.9.1.2 Moore Neighborhood (8 cell-based) cellular neighborhood

Similarly, for 8 cell it implies in a manner that transition rules can be implemented in an 8 cell Moore neighborhood.

Breed coefficient

{

For (max_tries =0; max_tries <8; max_tries++)

{

Try to urbanize neighboring pixels of selected urban pixel

}

}

Spread coefficient

{

If ((urban count >= 2) && (urban count < 8))

{

Try to urbanize

}

}

5.9.1.3 Extended Moore Neighborhood (12 cell based) cellular neighborhood

Likewise, for 12 cell size Extended Moore neighborhood transition rules are implemented.

Breed coefficient

{

For (max_tries =0; max_tries <12; max_tries++)

{

Try to urbanize neighboring pixels of the selected urban pixel

}

}

Spread coefficient

{

If ((urban count >= 2) && (urban count < 12))

{

Try to urbanize

}

}

These individual *cellular neighborhoods* have been implemented into the SLEUTH-GA to perform the sensitivity analysis. The model has been calibrated in three consecutive phases to obtain the optimal growth coefficient values against the optimal model fitness measure i.e. OSM and from among three phases, one best set of growth coefficient values have been selected for urban growth simulation for individual *cellular neighborhood* independently. Model sensitivity has been determined by estimating the change in simulated urban growth and calibrated growth coefficients corresponding to three *cellular neighborhood sizes*.

5.9.2 Model Sensitivity to the size of the cellular neighborhood

It was observed that the diffusion coefficient was highest in the case of 12 cell neighborhood (i.e. 60) due to its increased possibility of spontaneous urbanization because of the increased number of random selection of pixels for urbanization attempt during the implementation of different growth rules. A higher *cellular neighborhood* increases the possibility and lower *cellular neighborhood* reduces the possibility of spontaneous urbanization. Also, it is clearly evident from the study that spontaneous urbanization will eventually reduce when we move from higher to lower *cellular neighborhood* size i.e. from 60 in 12 cell to 45 in 8 cell to 33 in 4 *cellular size neighborhood*. The breed coefficient is responsible for new spreading center growth which takes place around newly spontaneously urbanized cells. However, increasing the *cellular size of the neighborhood* may not be able to introduce neighborhood decay effect for new spreading center growth

to take place. Therefore, a lower value of breed coefficient was noticed for the 12 cell neighborhood. The growth coefficients are influenced by neighborhood and distance decay in neighborhood effect.

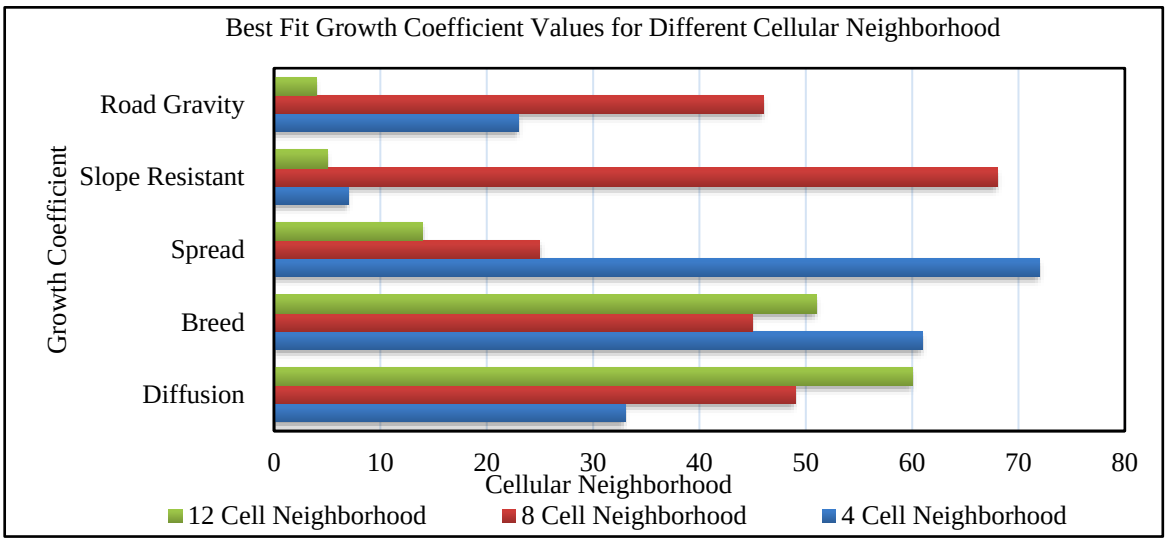

Figure 5.30: Best fit growth coefficient values against different size cellular neighborhood

The effect of distance decay can be best reflected in case of the diffusion coefficient as it is responsible for spontaneous urbanization. Therefore, in cases of higher *cellular neighborhood* i.e. 12 cell breed and spread coefficients have been found to be reducing as compared to other *cellular neighborhoods*. Similarly, due to the distance decay effect slope resistant and road gravity coefficient have also been found to be the lowest in the case of 12 cell Extended Moore neighborhood (Figure 5.30). While the highest spread coefficient is achieved in case of 4 cell neighborhood i.e. 72. Currently, the SLEUTH model utilizes an 8 cell neighborhood to perform its transition rules. However, we have identified that some of the growth rules are dependent on the distance decay effect and some are influenced by the neighborhood decay effect. To incorporate a distance decay effect into the modelling it is important to implement transition rules on a 12 cell neighborhood, however, for introducing a neighborhood decay effect a 4 cell neighborhood size would be appropriate. If the modeler is well aware from the socio-economic & geographical conditions and urban practices of the study area he/ she can suggest the *size of cell neighborhood* to better simulate the urban growth patterns. In developing countries, the size of urban development is relatively less and diffusive growth takes place at large. So, for socio-economic simulations like developing countries, a 12 cell neighborhood would be an optimal size to simulate urban growth more appropriately using the SLEUTH model.

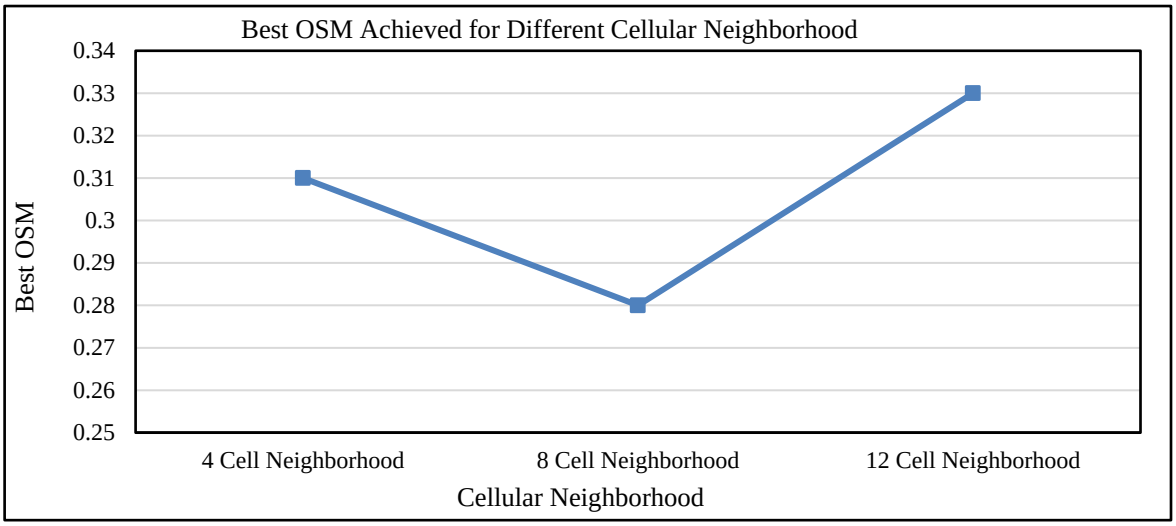

Figure 5.31: Best OSM metric value achieved against different game of life parametric value

The model fitness has an important role in establishing that which *size of the cellular neighborhood* is responsible for simulating urban growth and its different forms more accurately. The study can be well supported by comparing the model fitness measure calculated from individual *cellular neighborhood size* i.e. Von Neumann, Moore, and Extended Moore cell neighborhood. Among the three the best model finesses has been observed in the case of the Extended Moore neighborhood (12 cell) i.e. 0.33 (Figure 5.31).

Further, accuracy has been assessed for simulated urban growth obtained from individual settings of *cellular neighborhood* i.e. 4 cell, 8 cell and 12 cell with respect to reference data of the year 2016 and 2017.

5.9.3 Sensitivity through accuracy assessment

The modelling outcomes obtained from individual *cell neighborhood* method have been assessed by comparing percentage accuracy and kappa statistics for the simulated growth corresponding to the different *size of the cellular neighborhood*. Reference urban area has been obtained from the high-resolution Geo-eye satellite images obtained from Google earth for the year 2016 and 2017. The stratified random sampling method is used for spreading random test pixels for these two years and reference information in terms of urban and non-urban was recorded from reference data. The statistics of agreement and disagreement between actual and modeled urban were calculated and an overall agreement in the form of kappa statistics was computed for different *cell neighborhood* as presented in Table 5.8. The 12 cell neighborhood has been found to be more accurate as compared to other two *cell neighborhood* as the accuracy percentage achieved was 82% and 83%

and the kappa statistics as 0.43 and 0.66 for the year 2016 and 2017, respectively (Table 5.8).

Table 5.8: Accuracy assessment for a different game of life parametric settings

Cellular neighborhood values	Accuracy percentage (%)		Kappa statistics	
	2016	2017	2016	2017
4 cell	80	78	0.28	0.28
8 cell	73	77	0.41	0.42
12 cell	82	83	0.43	0.66

5.10 Sensitivity Analysis of Critical Slope

There is one another important parameter in the SLEUTH model i.e. *critical slope* which takes care of the effect of topographic slope in the simulation of urbanization through deciding the slope weights in the look-up table with the help of slope coefficient values. The urban development takes place at lower slopes rather than steeper slopes (Figure 5.32). When percent slope will be at that level where urban development is near impossible is known as *critical slope*. The relative pressure to build upon steeper slopes is dynamic and related to the proportion of flatland available and the steeper area's proximity to an already established settlement. When a location is being tested for suitability of urbanization, the slope at that location is considered. Instead of enforcing a simple linear relationship between the percent of slope and urban development, the slope coefficient acts as a multiplier.

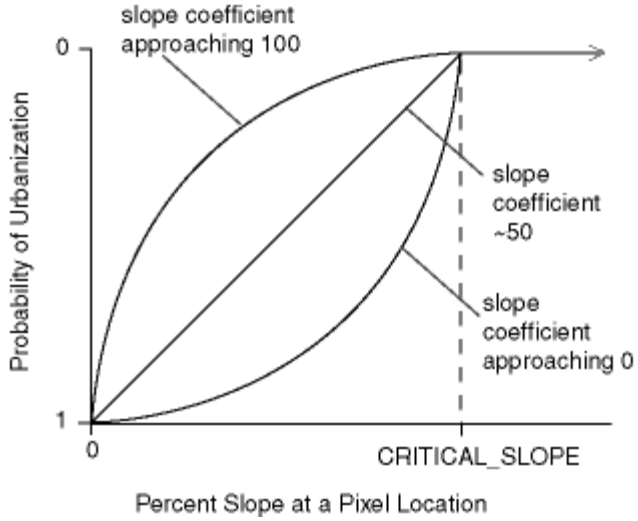

Figure 5.32: Relation between critical slope and probability of urbanization (Hui-Hui et al., 2012)

However, a *critical slope* with a default value of 15 remains constant throughout the simulation. The modification in its *critical slope* value may influence the possibility of

urbanization at locations having different slopes. The influence of different values of *critical slope* on modelling outcomes can be determined by performing sensitivity analysis and an optimal *critical slope* value can also be determined. For a range of value of *critical slope* SLEUTH model was developed, calibrated, validated and urban growth was predicted. The performance of simulation outcomes has been analyzed in terms of model fitness measure, accuracy percentage and kappa statistics.

5.10.1 Methodology for sensitivity analysis of critical slope parameter

The detailed methodology for carrying out a sensitivity analysis of different *critical slope values* in SLEUTH modelling has been discussed in Figure 5.33.

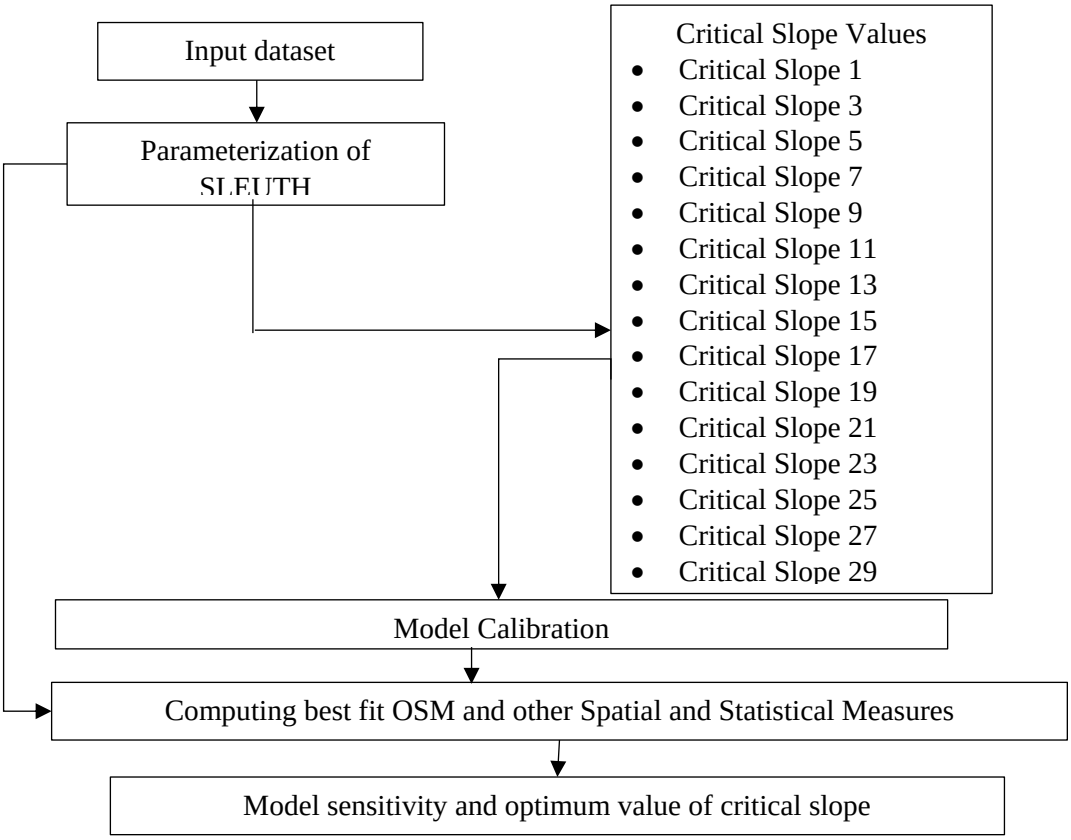

Figure 5.33: Methodology adopted for sensitivity analysis for critical slope value

The same input dataset used for sensitivity analysis of other model parameters has been used for *critical slope* also. The sensitivity analysis has been performed for a range of *critical slope values* i.e. from 1 to 29 with a step value of 2 is used. The model response was simulated for a total of 15 different values of *critical slope* and relative change in model-simulated growth in term of model fitness measure i.e. OSM and other goodness of fit metrices has been determined.

The way of selecting best fit coefficient values remain same throughout the sensitivity process of *critical slope value* as well. Afterward, the influence of *critical slope values* on

model performance has been analyzed by determining the relative change in urban growth simulated in term of the goodness of fit metrics. Finally, sensitivity in term of change in urban growth prediction accuracy for different *critical slope values* has been determined by estimating percentage accuracy and kappa statistics.

5.10.2 Model sensitivity in term of the goodness of fit metrics with respect to critical slope

The crucial findings of the present study are that the *critical slope values* influence modelling performance and its optimum value may be different for an area having different socio-economic, construction practices and topographical characteristics. The model calibration with different sets of *critical slope values* resulted in different best fit growth coefficient values against optimal model fitness measure i.e. OSM. The lowest OSM value has been obtained at *critical slope* 1 which signifies poor model fitness. Pushkar town is surrounded by rocky terrain and development at steeper slopes cannot take place. For introducing the intricacy of the topographical characteristics into the model, the critical slope should not be 1 but above this value.

The highest OSM is achieved at the *critical slope* of 19 i.e. 0.35 (Figure 5.34). At *critical slope value* of 19, the value of slope resistance coefficient is obtained as 17 which allowed urban development at topographical suitable locations only. The diffusion coefficient was achieved as 30. The breed and spread coefficients have been observed as 69 and 83, respectively. For the *critical slope* of 19 spread coefficient is higher as compared to other coefficient values which suggest higher spread or edge growth in the study area.

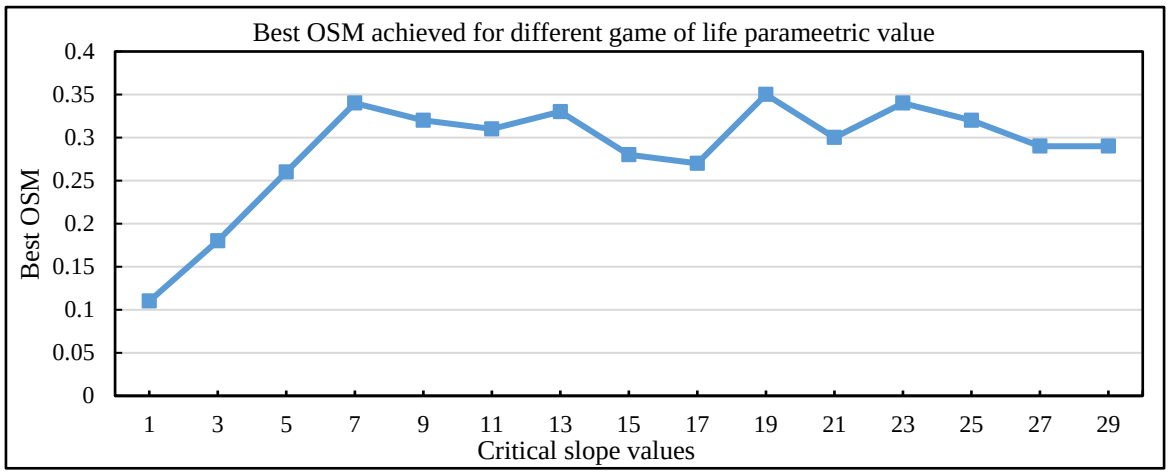

Figure 5.34: Best OSM metric value achieved against different critical slope value

However, there are some other values which give average model fitness e.g. default *critical slope value* (i.e. 15) i.e. 0.28. How well a model captures different urban forms cannot be answered on the basis of the optimal fitness of model i.e. OSM. No specific trend has been observed with different values of *critical slope*, as the urbanization process is stochastic and governed by the behavior of many random variables.

Further, different spatial and statistical measures computed from the simulated outcomes and the actual urban area obtained from two reference sources have been compared for different sets of *critical slope value*. The optimal value of the *critical slope* is that value at which the difference in statistical measures calculated from simulated urban growth and reference urban area for a given year is minimum. Here, the statistics computed from actual data is called as base statistics (bs) indicated by the yellow color in graphs and the statistics calculated against default *critical slope value* is called as default indicated by the red color in the graph. It is evident from Figure 5.36 that urban growth has been simulated more accurately at the default *critical slope value* i.e. 15 as compared to other *critical slope values*. In spite of higher model fitness for *critical slope value* of 19, it is not able to capture urban area as accurately as at *critical slope value* of 15. Urban edges which basically represents fragmented urban growth have been captured more accurately at *critical slope value* of 15 as compared to any other *critical slope value* (Figure 5.36). Significant differences in statistical measures lead to the conclusion that optimal model fitness may be helpful in determining average fitness for urban growth pattern but may not be adequate to establish appropriateness for different forms of urban growth. Urban clusters which represent clustered growth have been captured satisfactorily at the default value of the *critical slope*. However, *critical slope values* of 1 and 17 also seem closer to the base statistics of the urban cluster but for other spatial measures, it is not appropriate. The mean cluster size indicates compact urban growth which is also captured satisfactorily at default *critical slope value* as evident from Figure 5.36.

The urban cluster radius indicates the infill growth that is captured well at the default *critical slope value* i.e. 15 (Figure 5.36). So, the sensitivity analysis of *critical slope values* is not a mere exercise but gives some crucial findings which would help modelers to work on it. The study suggests that before projecting urban growth through modeling it is utmost important to verify the suitability of the *critical slope value*.

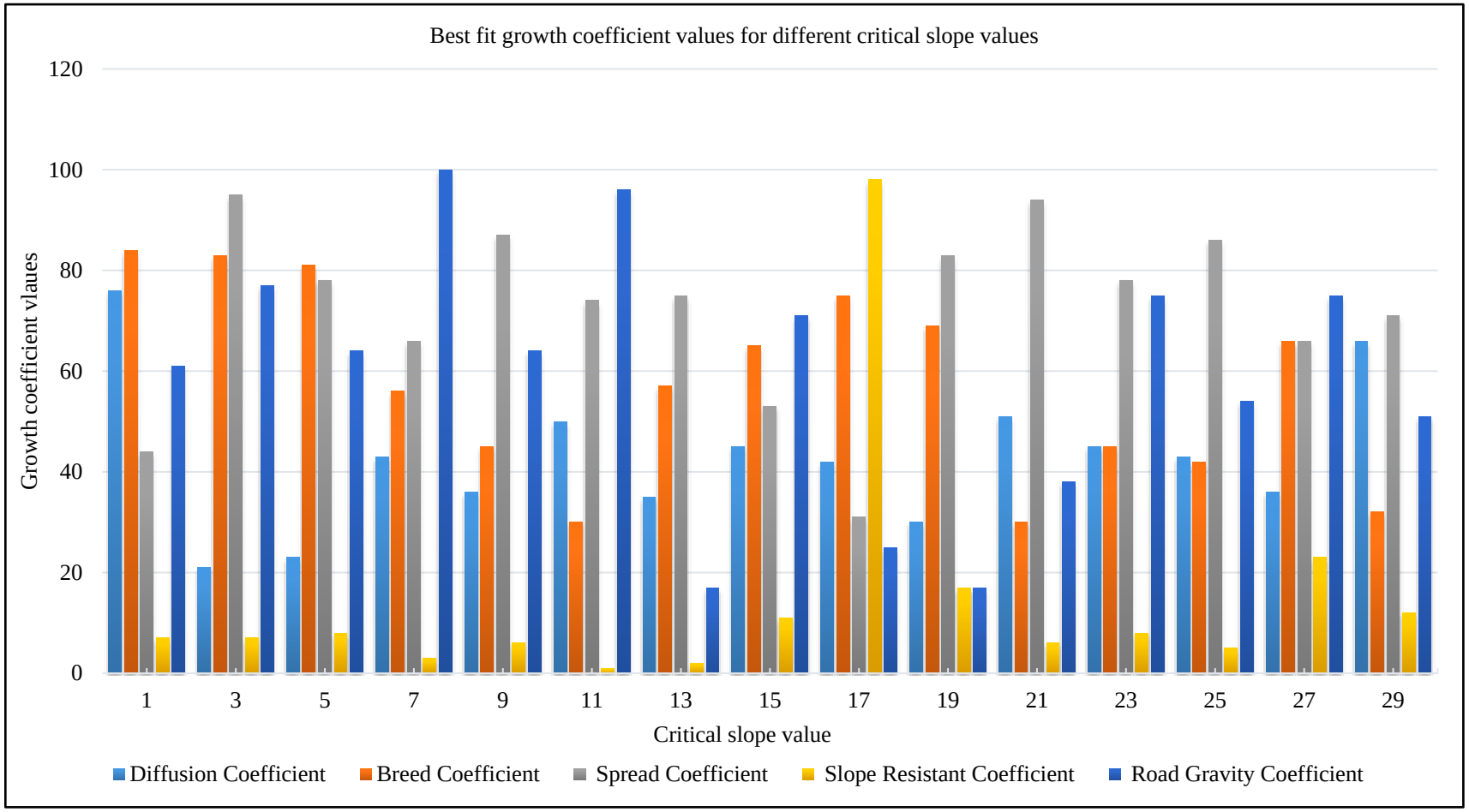

Figure 5.35: Optimal growth coefficient value achieved against different critical slope value

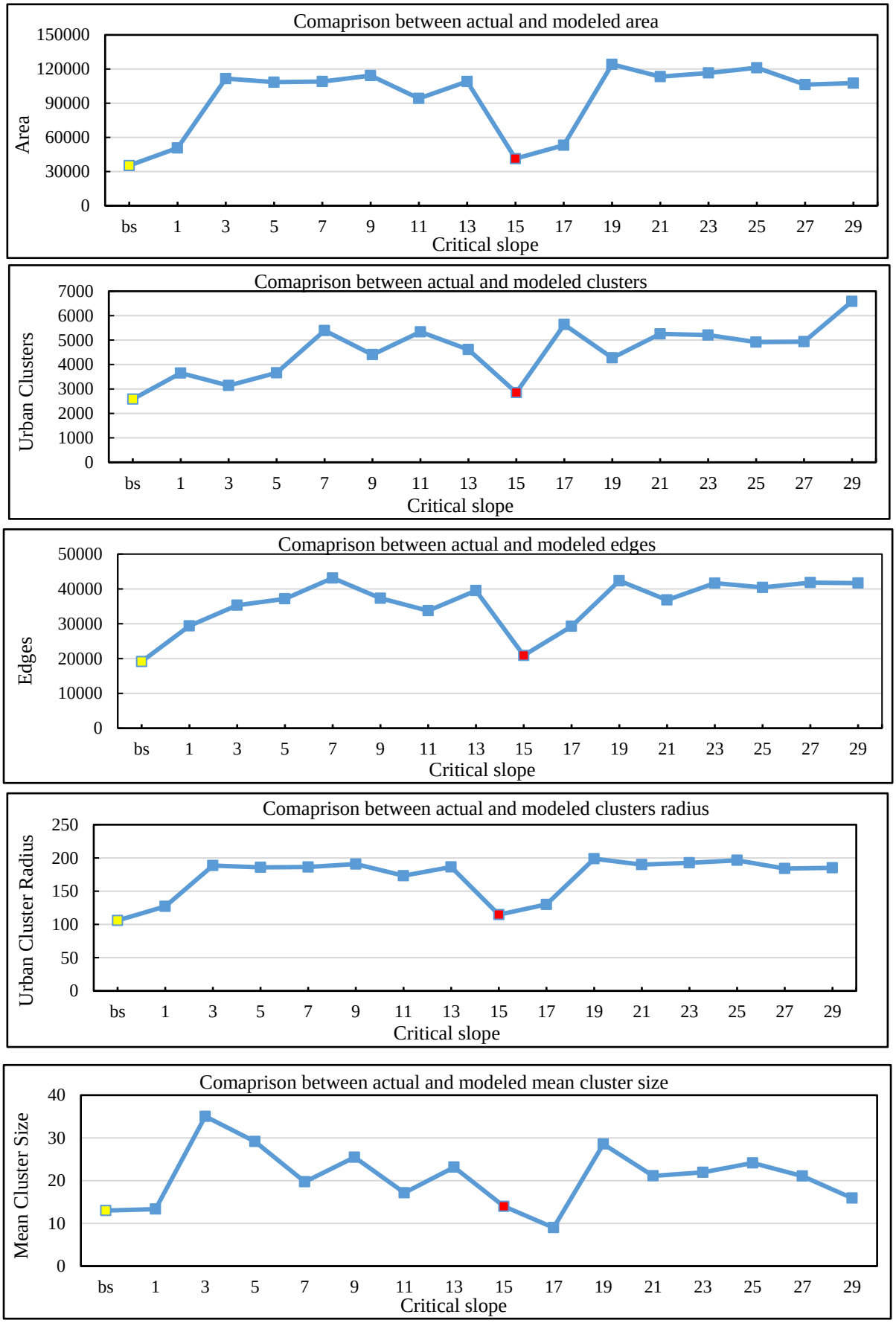

Figure 5.36: Model sensitivity in term of landscape metrics for critical slope value

The default *critical slope value* used in the model may not be suitable for other geographical conditions. Thus, to perform a sensitivity analysis of *critical slope* to find out the suitable value at which model is able to produce not only accurate urban growth pattern but would be helpful in determining different urban forms. From the present investigation default value of *critical slope* has been found to be an optimum value.

5.10.3 Model sensitivity in terms of accuracy for different critical slope values

The accuracy has been assessed with respect to the referenced data obtained from GE satellite. The accuracy percentage and kappa statistics for simulated growth corresponding

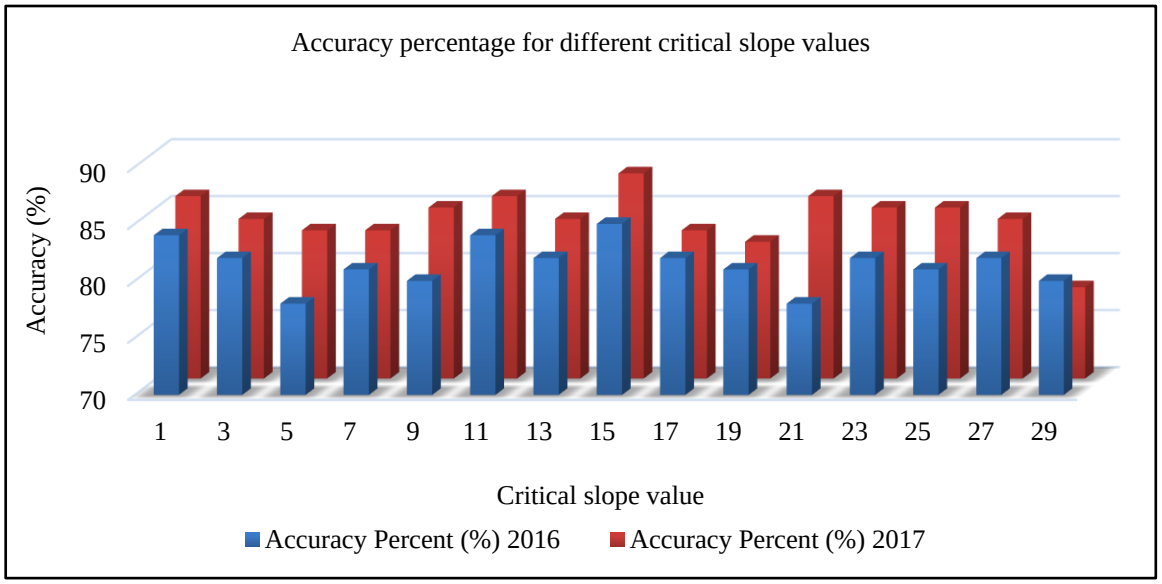

Figure 5.37: Accuracy percentage achieved against different critical slope value

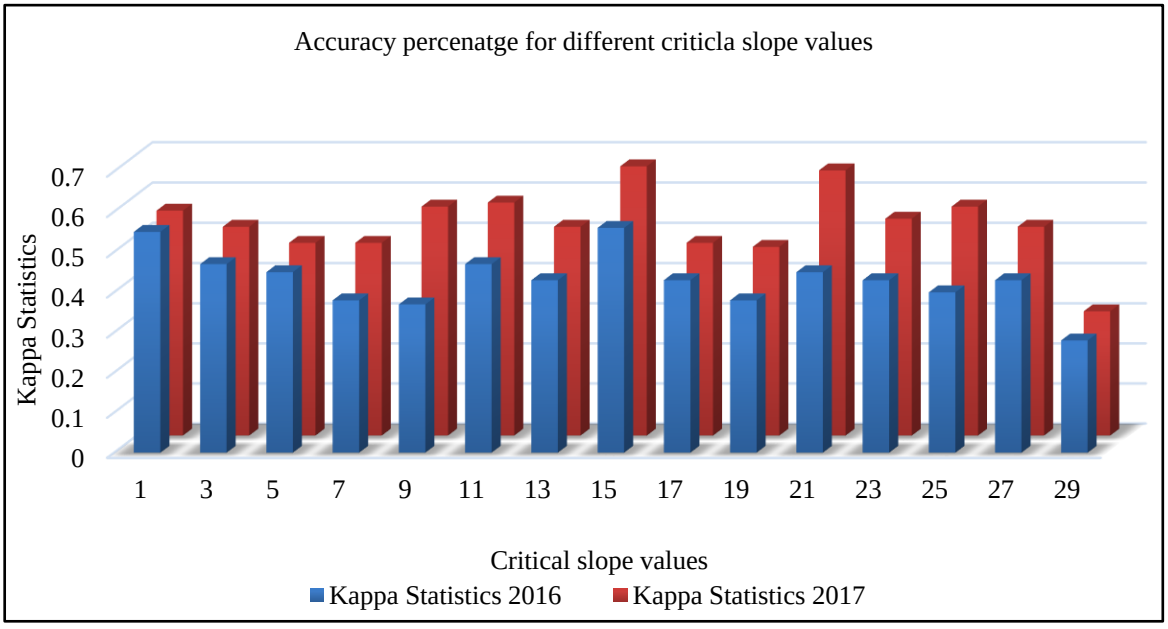

Figure 5.38: Kappa statistics value achieved against different critical slope values

to different *critical slope values* have been determined for two reference years 2016 & 2017 as presented Figure 5.37 & 5.38. The optimal values of different model constants/ parameters have been determined by performing sensitivity testing which is able to simulate urban growth and different urban forms more accurately (Table 5.9).

Table 5.9 Default values for model constants / parameters

S.no.	Parameter/ constant		Default value	Optimal values
1	Self-modifying	Boom	1.01	1.3
		Bust	0.09	0.10
		Critical low	0.97	0.90
		Critical high	1.3	1.25
2	Diffusive value		0.005	0.0055
3	Critical slope		15	15
4	Game of life critical threshold		3 cells	1 cell
5	Cellular neighborhood size		8 cell Moore neighborhood	12cell Extended Moore neighborhood
6	Monte Carlo runs		5-100	60

5.11 Concluding Remarks

SLEUTH sensitivity to some of the important model parameters/constants like *self-modification* (i.e. *boom, bust, critical low* and *critical high*), *diffusive value parameter, number of MC iterations, a game of life rule, size of the cellular neighborhood* and *critical slope* has been studied in the present work. Model sensitivity to such parameters has not been reported so far. An iterative process has been used to determine the model sensitivity to a range of parameters decided as the default value ± 50% at a suitable step. The model was rigorously calibrated for each value of every parameter independently keeping other parameters constant and model sensitivity was determined in term of relative change in model performance indicating goodness of fit metrics like (area, urban edges, urban clusters, mean cluster size and urban cluster radius). Furthermore, a comparison between statistical measures calculated from the reference urban area and simulated urban growth for the year 2017 & 2015 respectively have been made to determine the model sensitivity. Reference urban area for the year 2017 was captured from high-resolution Geo-eye satellite data obtained from Google Earth through manual digitization. Urban clusters and cluster size may have not been correctly captured in the digitized datasets. Further, model sensitivity to the model parameters was also determined in term of relative change in

accuracy and kappa statistics for simulated urban growth corresponding to a range of values of model parameters selected for sensitivity testing.

The overall study took a lot of CPU hours (around 5-6 hours per model calibration on a 64-bit windows 10 operating system with Intel(R) Core (TM)i5 CPU, 650 @3.20GHz 3.19 GHz) to calibrate the model multiple times for performing exhaustive sensitivity analysis. The optimum value of different model parameters has been determined at which model is able to capture the urban area as well as different forms of the urban growth more satisfactorily as compared to the same obtained from default values of those parameters. The study revealed that there is a significant influence of different model parameters on model performances. There is no definite trend in model performance found during sensitivity analysis because of the possible stochastic process involved in urbanization and urban growth simulation.

The optimal values of this constant/ parameter (Table 5.9) have been further tested and used to demonstrate the application of SLEUTH model for a larger study area i.e. Ajmer fringe including Pushkar town of similar socio-economic conditions and have been discussed in Chapter 8.

CHAPTER 6
ESTIMATION OF BUILT-UP DENSITY

6.1 Prologue

Urban growth is a complex spatiotemporal phenomenon that includes built-up activities horizontally, and vertically in different forms and patterns. The density of the built-up activities may be different at a different location as a function of desirability and suitability of location in term of quality of public services available, availability of good infrastructure, neighborhood, the vibrancy of socio-economic & cultural characteristics, connectivity with other areas and other important factors.

In many cities in India and worldwide, it has been seen that few localities were planned & developed for specific land use and density, however, in due course of time low built-up density areas are converted into high then to very high dense built-up areas because of increased demand of that area on account of change in desirability of that locality in term of the factors mentioned above. Different public & infrastructure facilities like water supply, sewerage system and space for parking & recreational activities which were designed to support a particular population and built-up densities become inadequate leading to a variety of problems. Such conditions may lead to an increase in pollution, traffic congestion, low level of public services and many climate implications like urban heat islands (UHI). Upgrade of facilities may further require huge funds and lead to lots of landscape disturbances, conflicts, and problems (Mills and Tan 1980; Cohen 2004; Kantakumar et al., 2011).

Increase in built-up densities in different parts of cities is one of the serious issues in developing countries like India, China, Nepal, Sri Lanka etc.as it overpowers the meager natural resources & public facilities and leads to unsustainable situations. Such a problem can be avoided by considering land suitability/desirability and resulting built-up densities in due course of time into land use planning decisions. Moreover, land use planning, planning & provisioning of public services, budget estimation, and estimation of natural resources requirements like water, ascertaining land use related adaptation measures to deal with the increase in temperature or UHI on account of climate change etc. are also function of population and built-up densities.

Therefore, estimation of built-up density/urban intensity for upcoming years, in advance, as a function of land suitability/ desirability which may be obtained in term of

different urbanization drivers, is very necessary and may help planners, and land use policy decision makers in making optimum and sustainable land use policy decisions while making appropriate provisions for the services as per the probable increase in built-up or population densities. Thus, it is important to develop such a tool/technique for the estimation and prediction of built-up densities or urban intensity for sustainable land use planning and development of smart cities. LULC change and urban growth modelling may help in dealing with such problems. Various LULC change and urban growth models have been developed which simulate LULC change processes or urban growth, primarily in terms of land use of a particular place or cell and how it changes over time. Models are not available or have not been reported which are capable of simulating the built-up density or urban intensity or density including vertical development. The CA-based SLEUTH model is widely known and popular model for LULC change and urban growth modeling. However, in its present form, it is not able to simulate urban/built-up density (Dovey and Pafka 2014).

Therefore, an effort has been made in the present research to improve the capability of the SLEUTH model to estimate and simulate the built-up density as a function of a few selected geo-spatial urbanization drivers. A new version of SLEUTH i.e., SLEUTH-Density has been developed, tested and demonstrated in its application for simulating the urban growth and built-up-density for a fast developing city in India i.e., Ajmer. Development of SLEUTH-Density, which includes the development of a density algorithm, writing the appropriate programming code and integration with the existing SLEUTH code, testing of algorithms and code is discussed in this Chapter in subsequent sections. Further, demonstration of the application of SLEUTH-Density is also discussed.

6.2 Understanding Built-up Density

Built-up density is one of the serious issues and challenges in developing countries where urbanization is taking place rapidly (Mills and Tan 1980; Cohen 2004; Kantakumar et al., 2011). In those urban centers which experienced huge demand for development and wish to further grow or develop, vertical growth or increase in built-up density/ urban intensity are the only option with limited land availability. Also, the built-up density can relate with the population or household of the respective areas. How much the area is densely urbanized is also proportional to the population i.e. population density, In addition, built-up development on a unit area i.e. urban intensity can also be a built-up density (Dovey and Pafka 2014). In more general terms, further development of a location/ region due to its

higher suitability may lead to increased built-up activities within available land either horizontally or vertically can be called built-up density. Further development may be in terms of urban intensity or density or vertical growth, all commutatively can be defined as built-up density.

Cellular automata is a cell-based structure on which a few rules are implemented to simulate the transition of cells from one land use to another to simulate the LULC change and urban growth (White and Engelen 1997; Batty 2007). Since urbanization is a probabilistic phenomenon, thus, randomization is involved in the selection of non-urban pixels for transition into urban pixels based on some growth rules. However, in this random process, a pixel can be selected for urbanization multiple times due to its higher suitability for development in terms of better public services, infrastructure facilities, neighborhood etc. The number of times a pixel/ cell is selected for urbanization out of the total number of attempts made for urbanization for all the pixels/ cells in CA-based LULC change and urban growth simulation can be related to or called built-up density in relative terms. So, the idea is to calculate the no. of attempts in which a cell has been selected for urbanization out of the total attempts made for urbanization may give a relative idea of desirability or suitability of that particular cell or location which in turn can be related to the possible built-up density at that location.

6.2.1 Defining urban or built-up density

Urban/built-up density has been defined in many ways by researchers belonging to different disciplines or specializations (Godefroid and Koedam 2007; Dovey and Pafka 2014). In physics, density can be defined as mass per unit volume. As applied to urban studies, built-up density can be understood as a certain quantity of built-up activity in term of land use per unit land area (Mills, 1970; Harrison and Kain, 1974). The built-up quantity can be anything related to urbanization like dwellings, building volume or floor area, impervious areas of any form as a part of urbanization. In architecture and planning, FAR (floor area ratio) which is the ratio between total floor area and site area is commonly used (Pan et al., 2008) as the measure of built-up density or urban intensity. In planning and social sciences, dwelling density i.e. residential unity per hectare is used for built-up density or urban intensity. These densities may be either net or gross. The density calculated at a development site is called net density while density calculated at a wider scale incorporating public space is termed as gross density (Yu et al., 2010). The two other terms related to density are internal and external density which depends on persons per room or

floor area and neighborhood, respectively. These density concepts are quantifiable and referred to as measured density which is different from perceived density mainly used in perception based environmental studies. A number of floors of a building may also be referred to as built-up or urban density which is synonymous to vertical growth (Li et al., 2014; Perini and Magliocco, 2014).

Thus, quantification of the probability of a land piece being converted into urban is a function of land suitability is termed as urban or built-up density (Palme and Ramírez, 2013). In the present study, estimation of built-up density cumulatively is gives the prospectus or probability of a particular area being of higher developmental potential which may be in terms of more people residing or more built-up or even possible vertical growth. So far, numerous significant research studies has been made in the area of LULC change and urban growth modelling where land use change of one particular location was targeted. However, the estimation of urban density/ intensity/ vertical urban growth is still lacking in urban growth modelling (Salvati et al., 2013; Li et al., 2014).

6.2.2 Approaches and methods to estimate urban intensity or built-up density

Estimation of built-up density is commonly done by the methods of built-up extraction (land coverage) from remote sensing data which involves major concern of the accuracy of the classification method used (Han-qiu, 2005; Xu, 2007, 2008). The built-up extraction is possibly a very challenging task since numerous urban structures may exhibit similar spectral and textural characteristics like roads, built-up etc. In addition, the viewing angle of the remote sensor is often incapable of capturing the real built-up footprints (Zhang et al., 2002). Generally, most of the built-up areas are best captured in visible bands and the vegetation is responsive in NIR (Near Infrared) bands. Moreover, multi-spectral bands and spectral differences have much potential to identify built-up and non-built-up features which can be utilized in built-up density estimation (Sudhira et al., 2012).

In numerous studies, remote sensing data has been actively utilized for built-up density estimation. A remote sensing based technology i.e. LiDAR (Light detection and ranging) is capable of providing surface elevation estimation accurately which can produce accurate building footprints helpful in precisely calculating built-up density. However, it incurs the extraordinary cost of data collection and processing (Rottensteiner and Briese, 2002, 2003; Hu et al., 2004; Vu et al., 2009). Another remote sensing type of data obtained from synthetic aperture radar may also be used to calculate built-up density by taking textural and polarization information into consideration (Quartulli and Datcu, 2004).

However, the scattering phenomenon in urbanization may reduce the accuracy of SAR for built-up density estimation. By the advancement in remote sensing technology and availability of VHR (optical very high resolution) images providing rich geospatial data and also has opened the various possibilities of accurate built-up density estimation. Thus far, most of the previous research has emphasized built-up area extraction and built-up detection without quantitative detailing of built-up density information (Franceschetti et al., 2007).

Mathematical morphology related to set theory is helpful in dealing with numerous remote sensing problems of land use classification and segmentation. Since built-ups areas are bright structures which cast shadows and produce high local contrast, geographical and structural characteristics of built-ups are easily captured as they are morphological features (Weidner and Förstner, 1995; Sohn and Dowman, 2007). The differential morphological profiles are used to establish the co-occurrence relationship between built-up areas and their shadows as they are capable of highlighting the dark and bright built-up features. Textural information of geographical features is also helpful in identifying built-ups and so for built-up density estimation. The tonal variation signifies the relative built-up density and an important technique of image processing and their interpretation (Chao et al., 2016). GIS-based cellular automata models were used to explore the vertical growth by taking into account a number of important urbanization drivers including accessibility, population density, and building density & height (Lin et al., 2014). Using regression analysis, descriptive statistics and a PCA (Principal Component Analysis) method, the change in vertical profiles of the building was observed by different researchers (Salvati et al., 2013). In another study, the Floor Area Ratio (FAR) and Building Coverage Ratio (BCR) were extracted from satellite images of high resolution to have an idea about built-up intensity (Pan et al., 2008).

In the present study, we have attempted to develop an algorithm for built-up or urban density estimation by using geospatial technologies and the cellular automata based SLEUTH model. Therefore, an effort has been made to develop a new version of SLEUTH, i.e., SLEUTH-Density which is capable of simulating the urban growth and urban density or built-up density. The model algorithm was developed, tested and its programming code was integrated with the code of the original SLEUTH. It was discussed earlier that visible and near infra-red bands have the capability to capture the built-up signatures well and can be used to identify the built-up area or built-up density relatively, therefore, different spectral difference based metrics have been utilized to validate the simulated built-up

density/ urban intensity using newly developed SLEUTH-Density (Zha et al., 2003; Xu, 2008). Another method which shows a strong relationship between built-up intensity is the LST (Land Surface Temperature), LST is proportional to the built-up density or impervious hard surface (Morabito et al., 2016). Therefore, LST has been compared with the urban density or built-up density to further validate the model results.

6.3 Methodology

The overall methodology for the development of SLEUTH-Density includes the development of method/ logic, programming implementation, integration of program with the SLEUTH model, program/ code testing, demonstration of SLEUTH-Density for the study area and finally validation of obtained simulated maps of built-up density with the traditional approaches of density estimation. Each step of the methodology is discussed in detail in subsequent sections and presented in Figure 6.1.

6.3.1 Development of algorithm

The SLEUTH program has been modified to develop SLEUTH-Density model which is an improvised version of SLEUTH model. The basic structure of the SLEUTH model has been discussed in detail in Chapter 4.

6.3.1.1 Workflow of SLEUTH-Density

The overall methodology adopted for the development of SLEUTH-Density and estimation of built-up density has been presented in Figure 6.1. The built-up density algorithm has been developed and SLEUTH code was modified to integrate the built-up density estimation program into the SLEUTH model (Figure 6.1).

The growth rules are implemented in the SLEUTH model in a sequential manner and named as phase 1-3 (includes two growth rules itself), phase 4 and phase 5 as discussed in Chapter 4 in detail. The output of one phase is utilized into the second phase and similarly, it goes on executing further phases to generate simulated urban growth and built-up density using historical urban area in different years as input or seed. The working of growth rules and a complete structure of SLEUTH has been discussed in detail in Chapter 4. Following growth, rules are implemented in SLEUTH-Density.

- Phase 1 - 3 growth (Spontaneous and New Spreading Centre Growth)
- Phase 4 growth (Edge Growth)
- Phase 5 growth (Road Influenced Growth)

- Self-modification Rules

Here, z_ptr and D_ptr are the parameters of an urban density estimation function used for storing urban growth information and for built-up density related information respectively (Figure 6.1). Functioning of the SLEUTH model along with execution of different growth rules, initiation of the model, the setting of parameters in scenario file and details about different program function have been explained in detail in section 4.2.4 in Chapter 4.

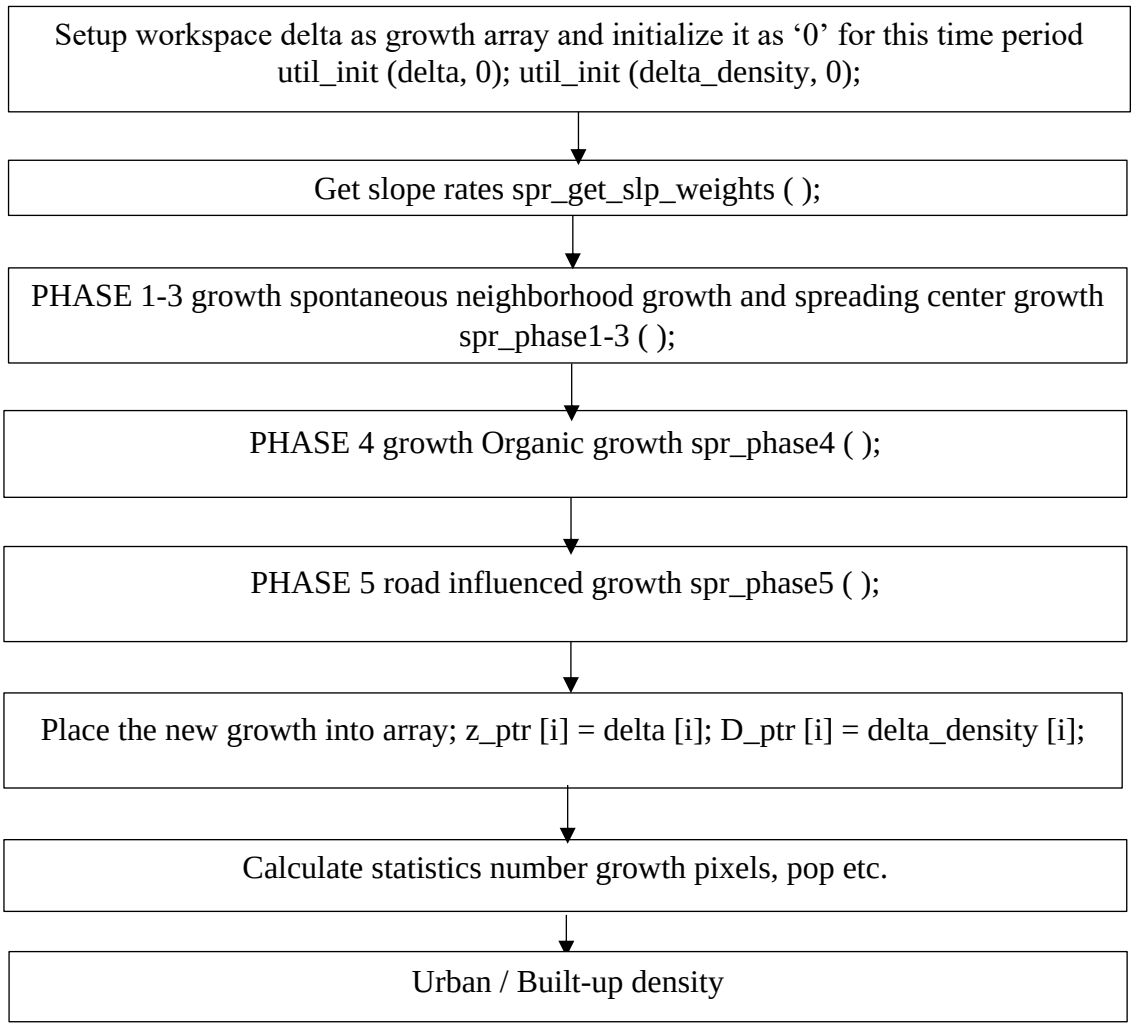

Figure 6.1: Methodology for built-up density estimation module

6.3.1.2 Programming implementation

A number of successful urbanization attempts for a location/ pixel out of the total number of attempts as a function of higher suitability/desirability or demand can be referred to as built-up/urban density. Development in the form of either urban intensity or density or vertical growth commutatively has been referred to as built-up/urban density.

The number of times a pixel/ cell is selected for urbanization out of the total number of attempts made for urbanization has been defined as built-up density in relative terms. So, the suitable logic/algorithm has been developed based on the hypothesis i.e., a number of attempts found suitable for urbanization of each pixel out of total number of attempt in all Monte Carlo iterations will be the possible built-up density. A pixel selected number of times for possible urbanization randomly and further checked for its suitability, indicating the potential of that pixel/ location being in higher demand for possible urbanization, means more no. of people are interested in that place which can be represented in term of the probability of development or urbanization or urban growth. The probability of higher chances of development of an area or a pixel for the development is the number of times a pixel is randomly selected for possible urbanization out of a total number of Monte Carlo iterations. So this probability can be considered as a relative measure of built-up density.

The main module of SLEUTH-Density is composed of sub-modules of different functionality and are essential for the integration and execution of the built-up density module. The model utilizes processing grids (p grids) to process the simulation runs and working grids (w grids) are used as a memory buffer to store intermediate stage outcomes. The number of p grids and w grids are utilized as per the requirement of the application and is initialized with "0". After initialization of p grid and w grid, a driver module is invoked by the system to perform a number of simulations runs i.e. MC runs identified by the system by calling drv_monte_carlo (function). The growth rules are performed for the decided number of MC runs for a number of desired years. For individual MC runs all the growth rules are performed in a sequential manner as explained in Chapter 4. The two p grids were used to storing and processing of urban growth and built-up density named as z_ptr and D_ptr respectively. Inside MC loop, z_ptr and D_ptr are initialized with "0" as shown in Figure 6.2.

Main function ()

Initialization of all p grids (processing grids) w grids (working grids) memory maps and input grids.

Then calling drv_drive function

Call **drv_drive function ()**

{

Start Monte Carlo iterations by calling **drv_monte_carlo** function

drv_monte_carlo (z_cumulate_ptr, sim_landuse_ptr)

{

Inside this

Call z p grid and D p grid in z_ptr and D_ptr p grid respectively;

z_ptr = pgrid_GetZptr ();

D_ptr= pgrid_GetDptr ();

Now, start Monte Carlo iteration loop;

For (imc=0; imc< scen_Getmontecarlo (); imc++)

{

Reset the coefficient values;

Run Simulation;

Call **grw_grow** function;

grw_grow (z_ptr, land1_ptr, D_ptr)

{

Inside this

Initialize the p grids with ‘0’;

Z_ptr

0	0	0
0	0	0
0	0	0

D_ptr

0	0	0
0	0	0
0	0	0

Figure 6.2: Initialization of Z_ptr and D_ptr with “0”

util_init_grid (z_ptr, 0);

util_init_grid (D_ptr, 0);

After initializing grids with ‘0’;

Now, call **spr_spread** function for applying growth rules in five phases which will run in a sequence as, phase 1n3, phase 4 and phase 5. These growths will be assigned with respective numbers as given below;

PHASE 1G - 4

PHASE 2G - 5

PHASE 3G - 6

PHASE 4G - 7

PHASE 5G - 8

spr_spread (&average_slope, &num_grow_pix, &sng, &sdc, &og, &rt, &pop, z_ptr, D_ptr);

{

Inside this

Setup workspace;

delta = workspace1;

delta_density = workspace2;

urban_seed_layer = igrid_GetUrbanGridPtr (__FILE__, func, __LINE__, 0);

urban_seed_test = urban_seed_layer;

urban_seed_layer is the base urban layer and suppose, urban seed layer is as in Figure 6.3. Here, '1' is showing urban pixel and '0' is showing non-urban pixel.

For running the spread module two working grids are taken and named as delta and delta density for storing temporary working files of urban growth and urban density module respectively. Initially, it has been set to "0" as given in Figure 6.4.

urban_seed_layer

1	0	1
0	1	0
0	1	0

Figure 6.3: Example of the urban seed layer

init_grid (delta, 0);

init_grid (delta_density, 0);

delta

0	0	0
0	0	0
0	0	0

delta_density

0	0	0
0	0	0
0	0	0

Figure 6.4: Working Grids of delta and delta_density

Now, initialize delta_density grid with seed urban pixels by calling util_condition_gif function as it is urbanized once in the base year so, it would be initialized in delta_density

grid also util_condition_gif (total_pixels, urban_seed_test, GT, 0, delta_density, 1) (Figure 6.5);

delta_density

1	0	1
0	1	0
0	1	0

Figure 6.5: Initialized seed urban in delta_density

Now, apply phase1n3 growth rules by calling **spr_phase 1n3 ()**;

spr_phase 1n3 (diffusion_coefficient, breed_coefficient, Z_ptr, D_ptr, delta, delta_density, slp, excld, swght, sng, sdc);

{ Get current diffusion value (calculation of diffusive value has been explained further)

For (k=0; k<1+diffusion_value; k++)

{

Randomly selects a pixel (i, j) as shown in Figure 6.6;

delta

0	(i, j)	0
0	0	0
0	0	0

Figure 6.6: Randomly selected pixel to get urbanized in delta grid

Now, it tries to urbanize a pixel (i, j) by calling **spr_urbanize** function for PHASE 1G growth

spr_urbanize (i, j, z, D_ptr, delta, delta_density, slp, excld, swght, PHASE 1G, sng) …eq (1)

{

Inside this it checks a set of conditions for the randomly selected pixel (i, j)

```
if (z[OFFSET ((row), (col))] == 0)
  {
    if (delta[OFFSET ((row), (col))] == 0)
```

```
{
 if (RANDOM_FLOAT > swght[slp[OFFSET ((row), (col))]])
 {
  if (excld[OFFSET ((row), (col))] < RANDOM_INT (100))
  {
   delta [OFFSET (row, col)] = pixel_value;
   (*stat)++;
```

At this stage, if all conditions are true then delta grid becomes (Figure 6.7),

delta

0	4	0
0	0	0
0	0	0

Figure 6.7: Decision of randomly selected pixel to get urbanized in delta grid

```
if (delta[OFFSET (row, col)] > 0)
        {
            delta_density [OFFSET (row, col)] ++;
        } /* end of delta [OFFSET (row, col)] */
```

And at this stage delta_density grid becomes (Figure 6.8);

delta_density

1	1	1
0	1	0
0	1	0

Figure 6.8: After making a decision of pixel to get urbanized in delta_density grid

```
stats_IncrementUrbanSuccess ();
    } /* end of excld [OFFSET ((row), (col))] */
    else
    {
     stats_IncrementExcludedFailure ();
    }
  } /* end of RANDOM_FLOAT */
```

```
    else
    {
      stats_IncrementSlopeFailure ();
    }
  } /*end of delta [OFFSET ((row), (col))] == 0 */
  else
  {
     stats_IncrementDeltaFailure ();
     delta_density [OFFSET (row, col)] ++;
   }
 } /*end of z [OFFSET ((row), (col))] == 0 */
 else
 {
     stats_IncrementZFailure ();
    delta_density [OFFSET (row, col)] ++;
  }
 }/* end of spr_urbanize function */
if (RANDOM_INT (101) < (int) breed_coefficient)
{
max_tries =8;
for (tries=0 ; tries < max_tries; tries++)
{
Urbanized = FALSE;
Urbanized = spr_urbanize_neighbor ();
```

Inside **spr_urbanize_neighbour** function, it selects a neighboring pixel randomly by calling **spr_get_neighbor ()** function then it tries to urbanize that neighboring pixel with PHASE 3G growth by calling **spr_urbanize ()** function

Suppose, in above step it randomly selected pixel (2) to get urbanized by calling the spr_urbanize function as discussed above. But this pixel is already urbanized in the delta grid so according to the conditions specified above, only a non-urban pixel can get urbanized. So, it fails the if (delta [OFFSET (row, col)] > 0) test and automatically goes to execute else statement which is;

```
else
```

```
{
    stats_IncrementDeltaFailure ();
    delta_density [OFFSET (row, col)] ++;
}
```

This else statement defines that those pixels which are already urban can be counted for built-up density and register themselves in delta_density grid. Here, the idea is if an already urbanized pixel is being attempted for urbanization again it would be suitable for further development/ urbanization. However, it cannot be urbanized in delta grid. So, that pixel (2) increases its counter in delta_density grid, however delta grid remains unchanged (Figure 6.9).

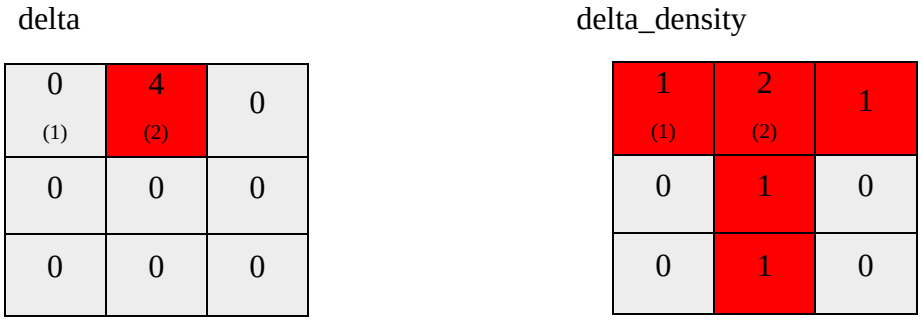

Figure 6.9: After making a decision of a pixel to get urbanized in delta and delta_density grid

Now, in the second attempt of max_tries loop suppose, it selected pixel (1) in delta grid to get urbanized by calling spr_urbanize (eq 1) function and it passes all the conditions specified in the spr_urbanize function. So, it becomes urban (by PHASE 3G i.e. '6') now in delta grid and in delta_density counter increases by '1' and both grids become (Figure 6.10);

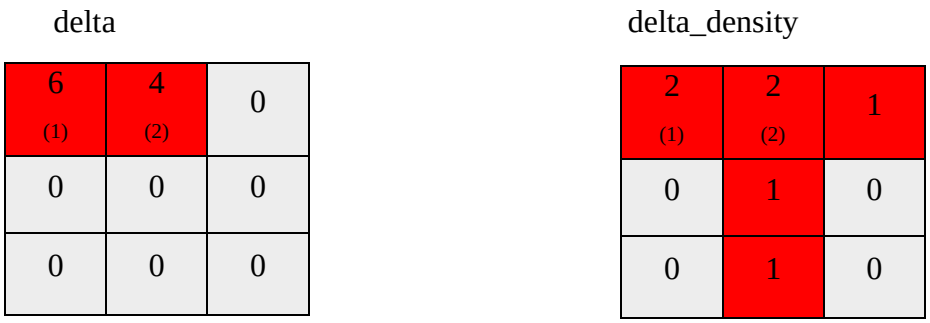

Figure 6.10: making decision of pixel to get urbanized in delta and delta_density grid

```
} /* end of max_tries loop */
} /* end of for loop for diffusion value */
```

}/* end of spr_phase1n3 function */

Suppose, at the end of spr_phase 1n3 function applying the same rules throughout the whole process we get the following delta and delta_density grids (Figure 6.11);

delta

6	4	0
0	6	0
0	0	0

delta_density

3	2	1
0	2	0
0	1	0

Figure 6.11: delta and delta_density grid after completing phase1n3 growth rule

Now, apply phase4 growth rules by calling **spr_phase 4 ()**;

spr_phase4 (spread_coefficient, z, D_ptr, excld, delta, delta_density, slp, swght, og);

{

Inside this

Loop over the interior pixels looking for urban from which to perform organic growth;

For (row=1; row < nrows; rows++)

{

For (col=1; col< ncols; col++)

{

Sequentially selects pixels and checks if it is an urban pixel and does it pass the random spread test

If ((z [OFFSET (row, col)] > 0 && (RANDOM_INT (101) < spread_coefficient))

{

Now, examine the eight cell neighbors spread at random if at least two are urban pixel must be urban (3)

urb_count = util_count_neighbors (z, row, col, GT, 0);

if (urb_count >= 2) && (urb_count < 8)

{

Randomly selects a pixel and try to urbanize that pixel by calling **spr_urbanize ( )** with PHASE 4G

} /* end of urb_count statement */

} /* end of z [OFFSET (row, col)] > 0 && (RANDOM_INT (101) < spread_coefficient */

} /*end of for loop for col */

} /*end of for loop for row */

} /* end of spr_phase 4 growth */

Suppose, at the end of spr_phase 4 function applying same rules throughout the whole process we get the following delta and delta_density grids (Figure 6.12);

delta

6	4	0
7	6	0
7	0	0

delta_density

3	2	1
1	3	0
1	1	0

Figure 6.12: delta and delta_density grid after completing phase4 growth rule

Now, apply phase5 growth rules by calling **spr_phase 5 ()**;

spr_phase5 (road_gravity, diffusion_coefficient, breed_coefficient, z, D_ptr, excld, delta, delta_density, slp, swght, rt, scratch_gif3);

{

Inside this

Now, determine the total growth count and save the row and col location of the new growth pixels;

If there is new growth, begin processing road trips;

If (growth_count > 0)

{

For (iii=0; iii < breed_coefficient; iii++)

{

Determine the maximum search index;

Randomly select a growth pixel to start search for road;

Search for road about this growth point;

If there is a road found then walk along it;

If the end of road pixel found,

{

Try to urbanize the neighboring pixel of road with PHASE 5G growth;

If urbanized;

{

Max_tries = 3;

For (tries=0; tries < max_tries; tries++)

{

Urbanized = spr_urbanize_neighbor (with PHASE 5G growth);

} /* end of max_tries loop */

} /* end of urbanized statement */

} /* end of end road pixel found */

} /* end of road pixel found */

} /* end of breed_coefficient loop */

} /* end of growth_count statement */

} /* end of spr_phase 5 growth */

Suppose, at the end of spr_phase 5 function applying same rules throughout the whole process we get following delta and delta_density grids (Figure 6.13);

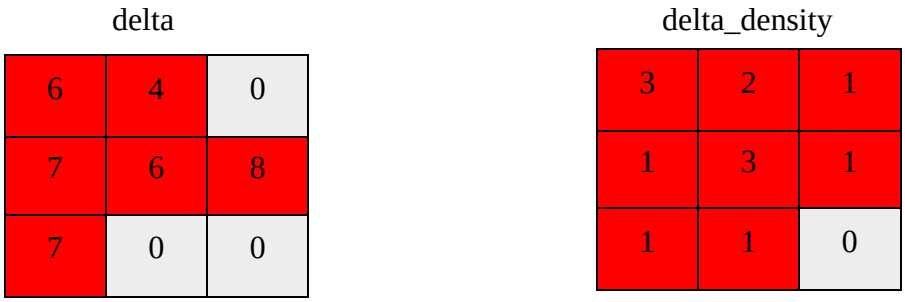

Figure 6.13: delta and delta_density grid after completing phase5 growth rule

Now, place the growth (delta) array into the current array (z) (Figure 6.14);

For (i=0; i< total_pixels; i++)

{

If ((z[i] ==0) && (delta[i] > 0))

{

z[i] = delta[i];

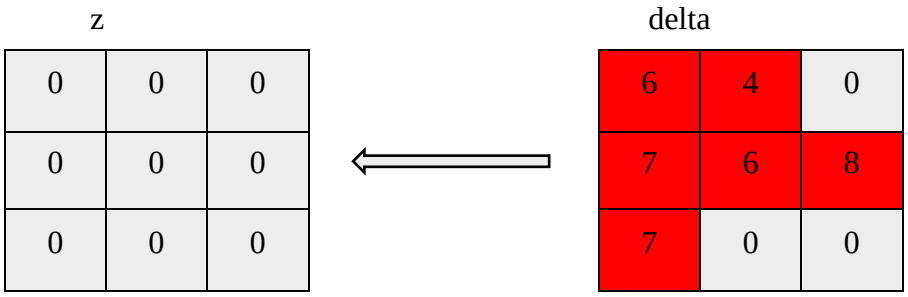

z

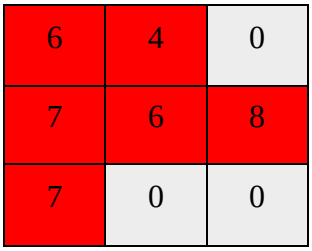

Figure 6.14: z Grid after completing all the phases of growth rules

} /* end of if statement */

if (delta_density[i] > 0)

{

D_ptr[i] = delta_density[i];

Now, place the delta_density array into current density (D_ptr) array (Figure 6.15);

} /* end of if statement */

} /* end of for loop */

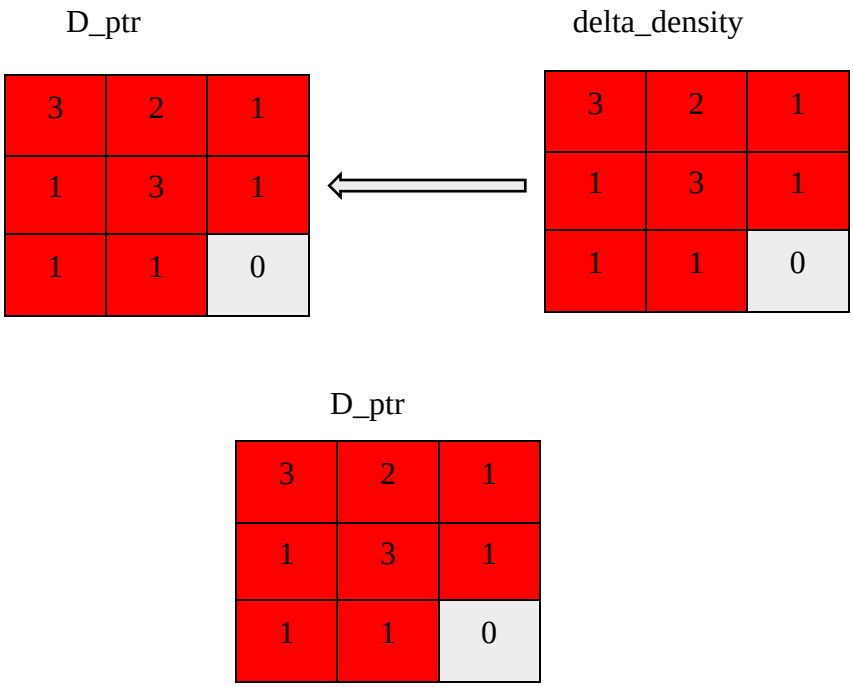

Figure 6.15: D_ptr grid after completing all the phases of growth rules

} /* end of spr_spread function */

Now, perform **grw_non_landuse ( )** function;

grw_non_landuse (z_ptr);

{

Inside this

cumulate_monte_carlo = workspace1;

Now, check for first Monte Carlo iteration;

if (proc_GetCurrentMonteCarlo ( ) == 0)

{

Zero out the accumulation grid (Figure 6.16);

util_init_grid (cumulate_monte_carlo, 0);

cumulate_monte_carlo

0	0	0
0	0	0
0	0	0

Figure 6.16: Initialization of cumulate_monte_carlo grid with “0”

} /* end of (proc_GetCurrentMonteCarlo () == 0) statement */

else

{

Read in the accumulation grid;

Sprintf (gif_filename, "%scumulate_monte_carlo.year_%u", scen_GetOutputDir (), proc_GetCurrentYear ());

inp_slurp (gif_filename, cumulate_monte_carlo, memGetBytesPerGridRound ());

} /* end of else statement */

Now, accumulate z over Monte Carlos;

```
for (i = 0; i < mem_GetTotalPixels (); i++)
   {
    if (z_ptr[i] > 0)
    {
      cumulate_monte_carlo[i] ++;
    } /* end of if statement */
   } /* end of for loop */
```

After completing first Monte Carlo iteration cumulate_monte_carlo becomes (Figure 6.17);

cumulate_monte_carlo

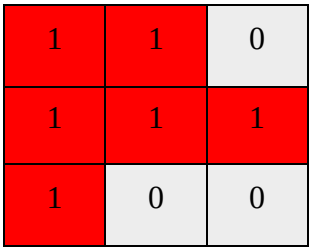

Figure 6.17: After completing first Monte Carlo iteration cumulate_monte_carlo grid

When Monte Carlo iterations get completed;

```
if (proc_GetCurrentMonteCarlo () == num_monte_carlo - 1)
{
```

Suppose, after completing total Monte Carlo (Let 5) iterations cumulate_monte_carlo grid is as (Figure 6.18);

cumulate_monte_carlo

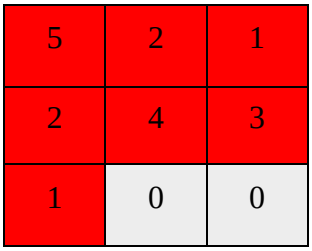

Figure 6.18: After completing all Monte Carlo iterations cumulate_monte_carlo grid

Print urban image using util_WriteZProbGrid ();

```
util_WriteZProbGrid (cumulate_monte_carlo, name);
if (proc_GetCurrentMonteCarlo () != 0)
    {
      Sprintf (command, "rm %s", gif_filename);
      System (command);
    } /* end of if statement */
} /* end of proc_GetCurrentMonteCarlo () == num_monte_carlo – 1 statement */
Else
{
```

Dump accumulation grid to disk;

```
Sprintf (gif_filename, "%scumulate_monte_carlo.year_%u", scen_GetOutputDir (),
proc_GetCurrentYear ());
out_dump (gif_filename, cumulate_monte_carlo, memGetBytesPerGridRound ());
} /* end of else statement */
```

} /* end of grw_non_landuse */

Now, perform **grw_density ()** function;

grw_density (D_ptr);

{

Inside this

cumulate_density_monte_carlo = workspace3;

Now, check for first Monte Carlo iteration;

if (proc_GetCurrentMonteCarlo ( ) == 0)

{

Zero out the accumulation grid (Figure 6.19);

util_init_grid (cumulate_density_monte_carlo, 0);

cumulate_density_monte_carlo

0	0	0
0	0	0
0	0	0

Figure 6.19: Initialization of cumulate_density_monte_carlo grid with “0”

} /* end of (proc_GetCurrentMonteCarlo () == 0) statement */

else

{

Read in the accumulation grid;

Sprintf (gif_filename, "% cumulate_density_monte_carlo.year_%u", scen_GetOutputDir (), proc_GetCurrentYear ());

inp_slurp (gif_filename, cumulate_density_monte_carlo, memGetBytesPerGridRound ());

} /* end of else statement */

Now, accumulate D_ptr over Monte Carlos (Figure 6.20);

for (i = 0; i < mem_GetTotalPixels (); i++)

{

cumulate_density_monte_carlo[i] = D_ptr[i] + cumulate_density_monte_carlo[i];

} /* end of if statement */

} /* end of for loop */

Same as, when Monte Carlo iterations get completed;

if (proc_GetCurrentMonteCarlo () == num_monte_carlo - 1)

{

Suppose, after completing total Monte Carlo (Let 5) iterations cumulate_density_monte_carlo grid is as (Figure 6.21);

Print density image using util_WriteDProbGrid ();

util_WriteDProbGrid (cumulate_density_monte_carlo, name);

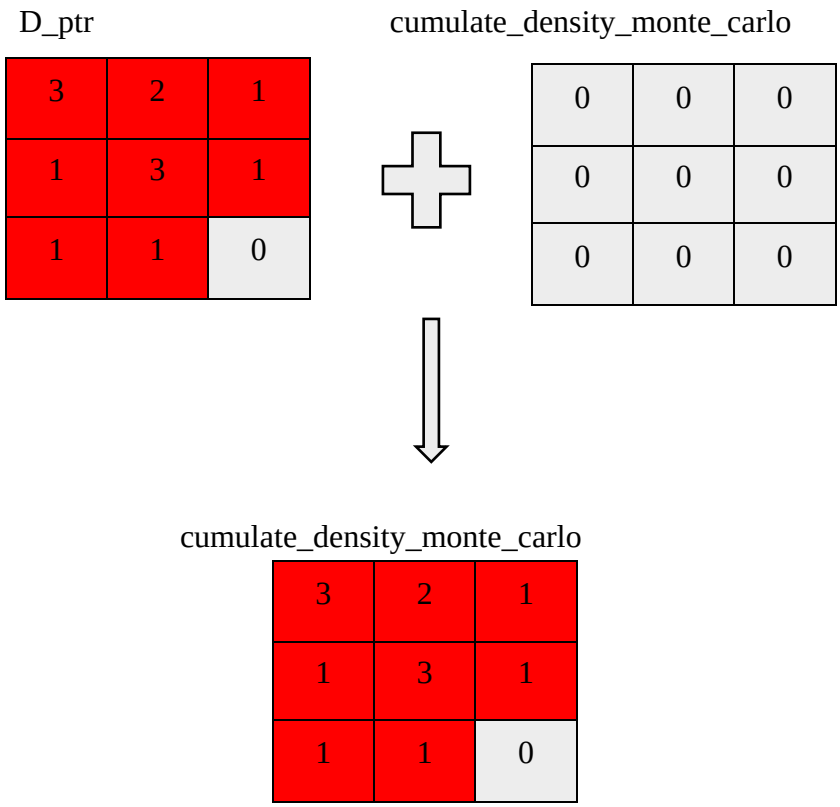

Figure 6.20: cumulate_density_monte_carlo Grid

cumulate_density_monte_carlo

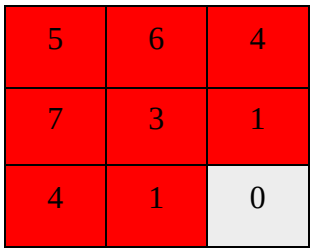

Figure 6.21: Final cumulate_density_monte_carlo grid

```
if (proc_GetCurrentMonteCarlo () != 0)
    {
      Sprintf (command, "rm %s", gif_filename);
```

```
        System (command);
      } /* end of if statement */
} /* end of proc_GetCurrentMonteCarlo () == num_monte_carlo – 1 statement */
Else

{

Dump accumulation grid to disk;
Sprintf (gif_filename, "%s cumulate_density_monte_carlo.year_%u", scen_GetOutputDir
(), proc_GetCurrentYear ());
out_dump (gif_filename, cumulate_density_monte_carlo, memGetBytesPerGridRound
());
} /* end of else statement */
} /* end of grw_density function */
}/ * end of grw_grow function */
}/* end of for loop for Monte Carlo iterations */
} /* end of drv_monte_carlo function */
}/* end of drv_drive function */
```

6.3.1.3 Built-up density algorithm/ program testing

Model algorithm/ program testing is equally important in model development to verify or validate the outcomes of the model for which it is developed. The algorithm and programing code was tested to verify whether it is giving the outcomes for which it is developed. In the present study, to test the algorithm programming code a small size demo input dataset of 16*11 grid size was prepared with input layers such as urban (for year 1997, 2000, 2004, 2008, 2013 and 2015), transportation (for year 1997, 2000, 2004, 2008, 2013 and 2015), exclusion, slope and hillshade at 5 meter spatial resolution (Figure 6.22). The demo input dataset has been used for the parameterization of the SLEUTH-Density. It passed through the four growth rules driven by five growth coefficients (as discussed in Chapter 4), which sequentially executes in a loop for a total number of Monte Carlo iterations and at each stage the simulated outcomes were printed to check the progression of the density estimation algorithm. This process gives an insight about the internal working of the density estimation method. In addition, to validate the method, the cumulate of all the intermediate grids generated, must be equal to the single output grid which gives urban growth for the respective year.

For the demo input dataset, randomly selected best-fit growth coefficient values suitable for the growth prediction have been adopted for testing the algorithm. Best fit values for diffusion, breed, spread, slope resistance and road gravity dummy values used are 15, 24, 20, 60 and 70, respectively.

The decision of a pixel being urbanized passes through a set of conditions/rules at all five stages in SLEUTH-Density program similar to the original SLEUTH model. Five empty grids have been taken for storing each decision at every single stage of growth rules and named as one, two, three, four and five. In addition, for intermediate attempts of urbanization in the individual grid, it is numbered starting from 0 as a suffix (e.g. One0, One1, Two0, Two1 and so on).

First, the model passes through phase 1-3 rules, which itself includes diffusive growth and new spreading center growth, therefore, grid One and Two will be produced to store intermediate stages of density estimation. The diffusive value was first calculated using equation 6.1 to perform diffusive growth.

$$diffusive\ value = \left((\text{diffusion coefficient} \times 0.005) \times \sqrt{rows^2 + cols^2}\right) \ldots\ldots \quad 6.1$$

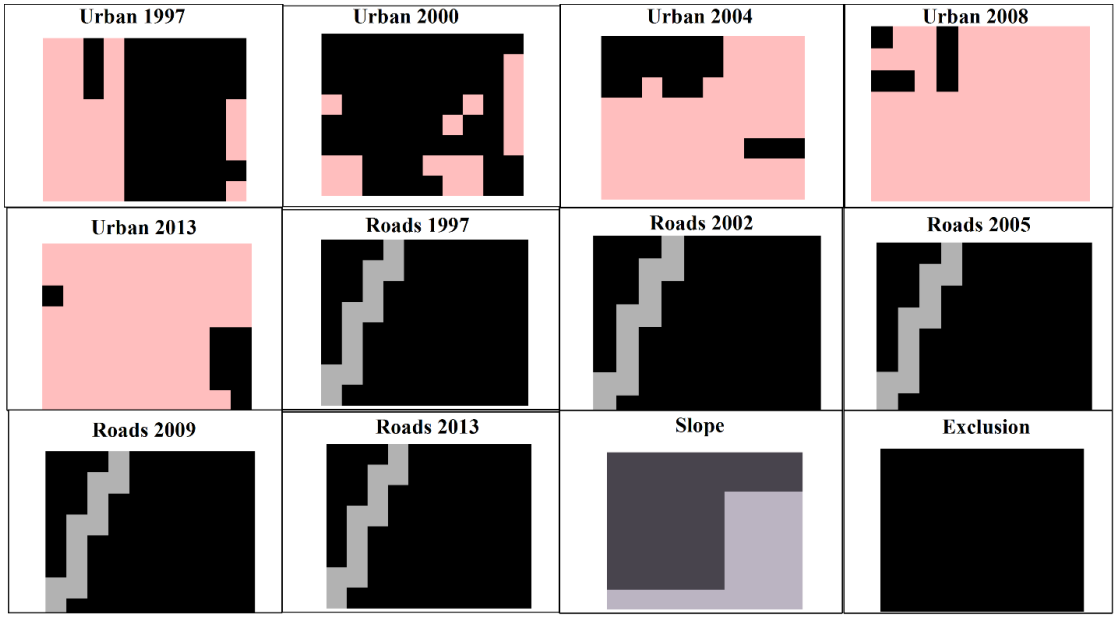

Figure 6.22: Demo input dataset used for model cost testing

Here, the best-fit diffusion coefficient, and number of rows and columns are 15, 11 and 16, respectively. So, a calculated diffusion value would be 1.45. Diffusive growth can take place till the diffusion value does not reach this value as;

for (k = 0; k < 1 + (int) diffusion_value; k++)

(Here, diffusion value is 1 and the loop will continue up to 2 diffusion value)

{

For the first diffusion value, a random pixel from the grid is attempted to get urbanized.

}

If this random pixel is already an urban pixel, it is added to the density grid. The number of times the same pixel is attempted to get urbanized, it increments its density which shows the probability of that pixel to get urbanized even vertically also due to some suitable conditions. In the case of first diffusion value, the attempted pixel was already an urban so it incremented to 2 (One0) (Figure 6.23 (a)). Since the attempted pixel was already urban pixel so, it will not be evaluated for spreading center growth further and will pass the counter to the next diffusion value i.e. 2. Again, it randomly selected the pixel to get urbanized and this time also, the selected pixel was already urban so, the density of that pixel incremented to 2 (One1). Phase 1-3 will be terminated here, as no new pixel got urbanized and the control will pass to phase 4. In phase 4, the whole grid is checked one pixel at a time to pass the random spread test for becoming a spreading center. It checks whether the first pixel is urban and it passes the random spread test, if this condition is true it further checks for the game of life rules i.e. whether it has at least 2 urban neighbors but not more than 8. After, positively passing through these phases, in its 8-bit neighborhood it randomly attempted a pixel to get urbanized. In a given grid, first two urban pixels are not urbanized and it may possibly have not found the suitable pixel to get urbanized in the first row of the grid. In the second row, the fourth column of the grid, it found a suitable pixel to get further urbanized and this phase 4 program remained to continue till every pixel gets checked for random spread test and the game of life rules (Figure 6.23(a)). In between, it successfully encountered 11 in total pixels to get urbanized. The Three_0, Three_1 and Three_2 grids captured the already urban pixel to get further urbanized one at a time and its density incremented to 2. In grid Three_3, a new non-urban pixel got urbanized while, in Three_4, an already urbanized pixel got urbanized and the density of that pixel incremented to 2. In grid Three_5, that pixel has incremented its density to 3 as well. In grid three_6, a new pixel got urbanized, in grid three_7, an already urbanized pixel got urbanized and its density incremented to 2. In grid Three_8, a new pixel got urbanized and in grid Three_9 and Three_10, the already urbanized pixels incremented its density to 2 by

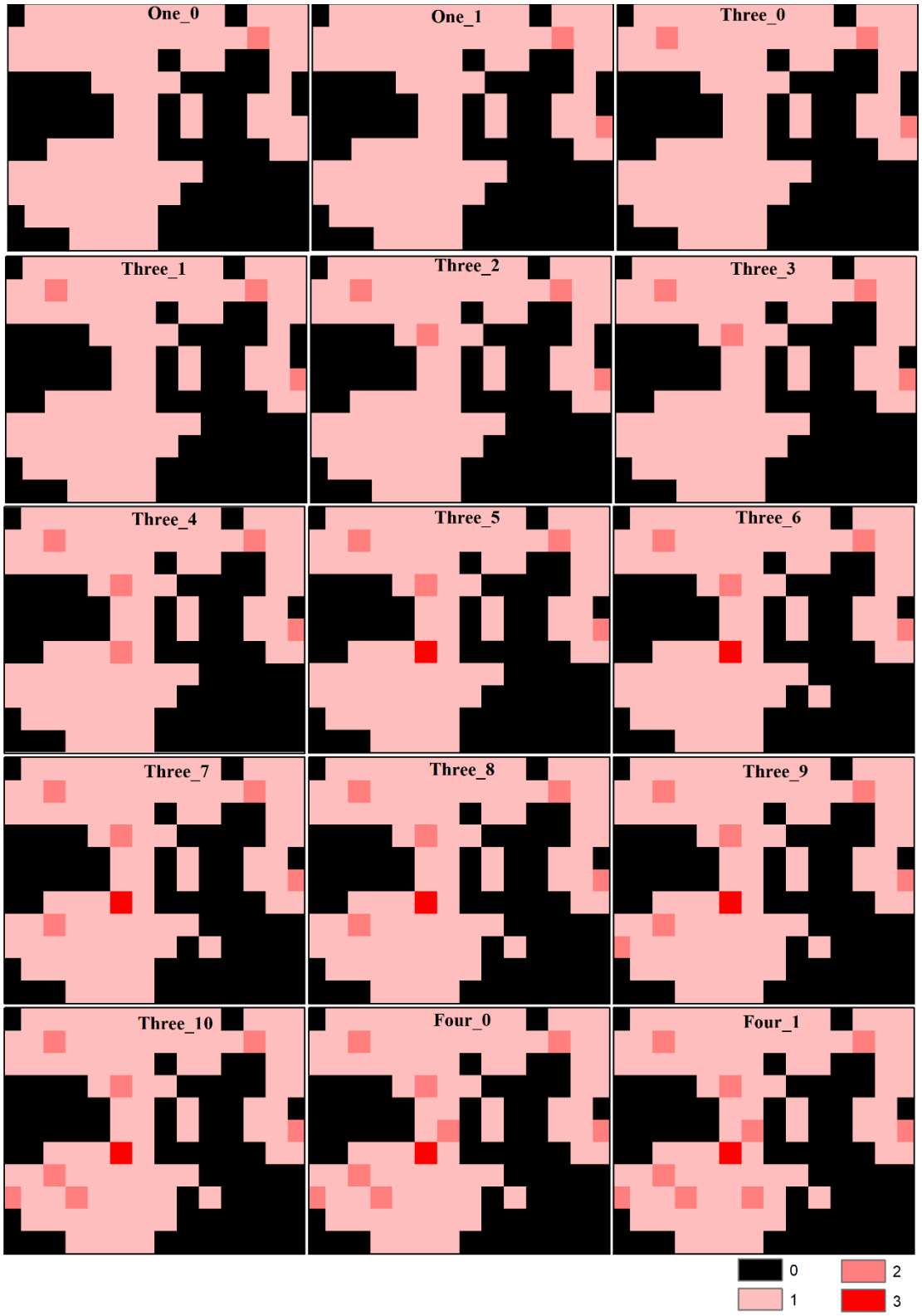

Figure 6.23(a): Model outcome produced at each stage

an attempt made for these to get further urbanized. After terminating phase 4, phase 5 is evoked in which at two places a pixel is checked to get urbanized. In phase 5 first of all, the total number of growth pixels were calculated and if no new growth has been taken

place in the last phase then phase 5 terminates here. But, currently, the new growth pixels were observed in previously performed growth rules as shown in Figure 6.23(b).

The breed coefficient would be used to calculate the road influenced growth here in phase 5. The breed coefficient is 24, so, it will be passing through 25 times to randomly attempt a pixel to get urbanized. Using the road gravity value which is calculated by eq 6.2, the maximum road search index was determined using eq no. 6.2, 6.3, 6.4, 6.5 and 6.6). The road pixel would be searched for this maximum search index.

$$rg\_value = (rg\_coeff/MAX\_ROAD\_VALUE\ ) * ((row + col)/16.0) \ldots\ldots\ldots\ldots \quad (6.2)$$

$$int\_road\_gravity = spr\_GetRoadGravValue(road\_gravity) \ldots\ldots\ldots\ldots\ldots\ldots\ldots \quad (6.3)$$

$$\max\_search\_index = 4 * (int\_road\_gravity * (1 + int\_road\_gravity)) \ldots\ldots \quad (6.4)$$

$$\max\_search\_index = MAX(\max\_search\_index, nrows) \ldots\ldots\ldots\ldots\ldots\ldots\ldots\ldots\ldots \quad (6.5)$$

$$\max\_search\_index = MAX(\max\_search\_index, ncols) \ldots\ldots\ldots\ldots\ldots\ldots\ldots\ldots\ldots \quad (6.6)$$

If the road pixel is found then it will check its neighboring pixels to get urbanized. If it becomes true, it further checks its surrounding pixels for a maximum three times to urbanize. Here, in current case grid Four_0, Four_1, Four_2, Four_3, and Four_4 have incremented density to 2 of a pixel, one at a time. Since no growth took place in each of the intermediate stages, it will not go to the fifth rule further. In grid Four_5, a new pixel was urbanized and the control was transferred to the fifth rule in which surrounding pixels were tested to become urbanized for a maximum three times.

Grid Five_0 has observed a new urbanized pixel, grid Five_1 and Five_2 observed an already urbanized pixel one at a time and incremented its density to 2. Now, the control is transferred back to rule four. Grid Four_6 has observed an already urbanized pixel and incremented its built-up density to 2, however, in grid Four_7 density has incremented to 3 (Figure 6.23 b). Further urbanization has been attempted in grid Four_0. Similarly, in grid Four_8, Four_9 and Four_10 urban density has been incremented but no new growth was taken place. So, it was not checked for rule five further. In grid Four_11, a new pixel was urbanized, so its density becomes 1 and the control was transferred to rule five. Its neighboring pixels have been tried to urbanize for maximum three times to get urbanized. In Grid Five_3, Five_4 and Five_5 urban density have been incremented by one as presented in Figure 6.23(b)).

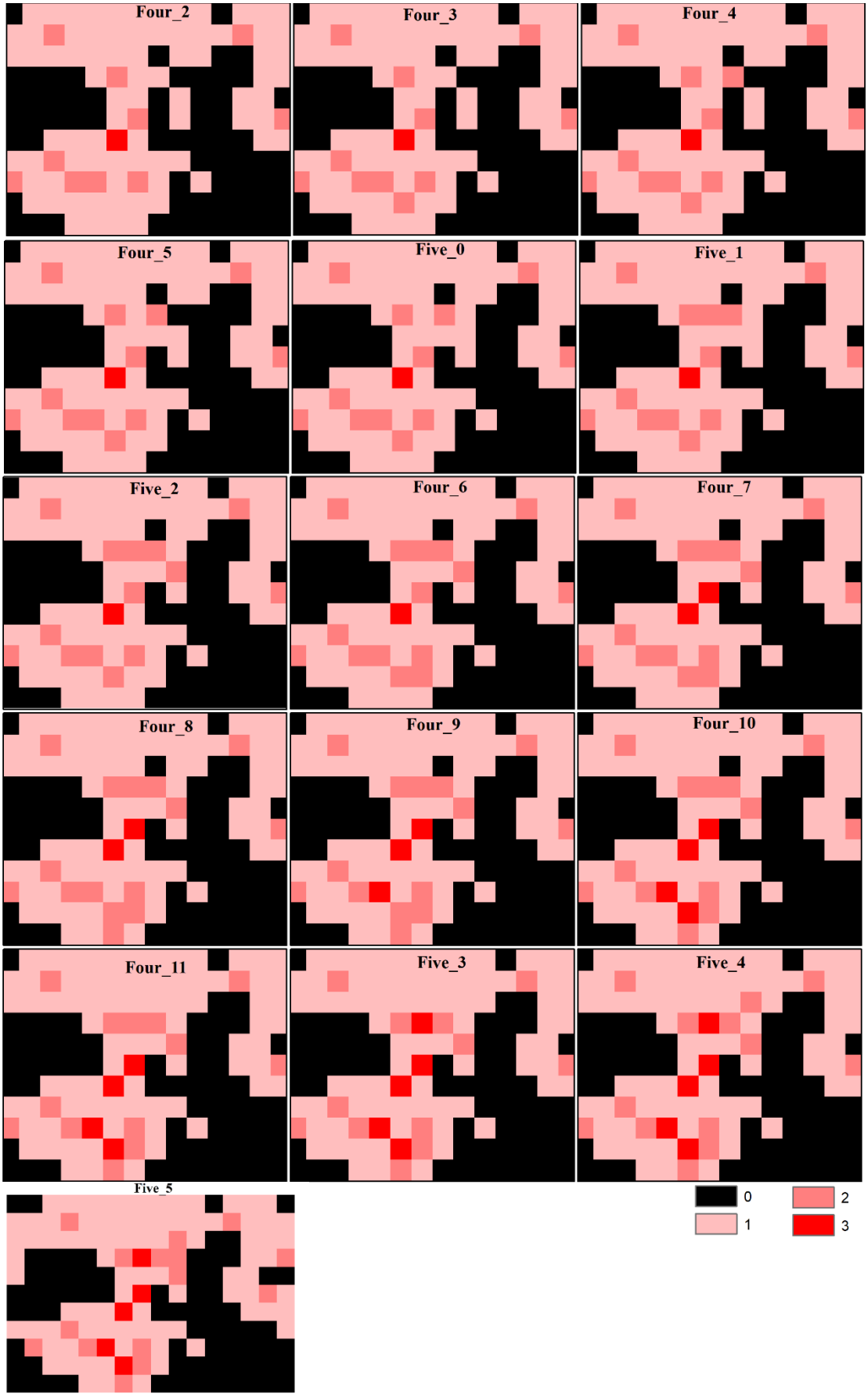

Figure 6.23(b): Model outcome produced at each stage

6.4 Built-up Density Estimation using SLEUTH-Density

After successful testing of the developed SLEUTH-Density model, it has been parameterized for the input dataset prepared for Ajmer fringe including Pushkar town and required model parameters including self-modifying parameters obtained from the rigorous sensitivity analysis as discussed in Chapter 5. The model has been calibrated in three consecutive phases to refine the growth coefficient values and finally, a set of optimal coefficient values has been obtained. The more details of model parameterization can be found in Chapter 4.

6.4.1 Calibration

For reducing the subjectivity in making choices of the growth coefficients, the Genetic Algorithm (GA) method calibration method has been used in the SLEUTH-Density in place of the brute force calibration method. The GA calibration populates a chromosome with five coefficient combinations i.e. genes. These coefficient combinations are utilized for model calibration runs and the optimal combination is selected for mutation while the worst performing combination is replaced with randomly selected values. The optimal value of the growth coefficient i.e., diffusion, breed, spread, slope resistance and road gravity for the Ajmer fringe has been found to be as 87, 100, 100, 60 and 44, respectively while their values for Pushkar has been found to be 26, 7, 9, 41 and 26, respectively. Growth coefficient values for Ajmer fringe has been found to be higher as compared to Pushkar which indicates relatively higher urban growth in Ajmer.

The goodness of fit landscape metrics has been used to judge the performance of the model calibration and to obtain the optimum growth coefficients. Compare metric has been found to be 0.57 for Ajmer and 0.99 for the Pushkar. The compare and Pop metrics refer to the similarity between seed urban area referred to as actual and simulated urban area which has been found to be satisfactory for both Ajmer fringe and Pushkar except the value of Compare (i.e. 0.57) in the case of Ajmer fringe. The modeled no. of urban clusters regressed against the known no. of urban clusters estimated from seed urban area has been found to be 0.96 and 0.69 for Ajmer fringe and Pushkar, respectively. The Edge metric which indicates a correlation between modeled and actual no. of urban edges for the control years has been found to be 0.97 and 0.88 for Ajmer fringe and Pushkar, respectively. The LeeSallee metric indicating the degree of shape (pattern) match between seed urban area and modeled urban growth was found to be 0.52 and 0.25 for Ajmer fringe and Pushkar, respectively. Landscape metrics obtained from the calibration were found in line with other

studies reported (Rafiee et al., 2009; Wu et al., 2009; Akin et al., 2014). The OSM composite metric includes the multiplication of compare, population, edges, clusters, slope, X-mean, and Y-mean metrics (Dietzel and Clarke, 2007) is found to be 0.08 for Ajmer fringe and 0.26 for Pushkar, respectively. Lower OSM value for Ajmer fringe can possibly the indicator of heterogeneous urban growth (Clarke, 2017). The landscape metrics indicating the goodness of fit measure like LeeSallee, Pop, Edges, Clusters, Mean cluster size, Xmean and Radius are found to be better for Ajmer fringe as compared to Pushkar which indicates the success of SLEUTH calibration for a larger study area. However, OSM, compare, slope and Ymean are found to be a little less in the case of Ajmer fringe (Table 6.1) indicating more heterogeneous growth. The initial control parameters and goodness of fit metrics show that the general growth characteristics of both the study areas are distinct as Ajmer fringe dominates the new spreading center and organic/spread growth while Pushkar has experienced majorly diffusive or dispersive growth in the controlling years.

6.4.2 Urban growth prediction

The developed model i.e., SLEUTH-Density was first implemented to estimate built-up density for a smaller town i.e. Pushkar which is also a part of Ajmer fringes. Built-up density for Pushkar town has been estimated using 100 Monte Carlo simulations and input dataset with 5m spatial resolution. Urban /Built-up density for Ajmer fringe has been simulated using input data of 15 m spatial resolution to reduce the computational time during model calibration. After performing rigorous calibration, urban growth and built-up/ urban density were simulated up to the year 2040 for both the areas.

The predicted change should be identical to the observed change to judge the modelling accuracy. With respect to the difference between spatial and statistical measures like an urban area, no. of edges & clusters, radius and mean cluster size estimated from simulated growth and from reference urban area including the year 2018, the performance of the SLEUTH-Density model has been found to be consistent and satisfactory. Urban area for the year 2018 was not used as input data for the model calibration therefore, to check how well model is capable of predicting urban growth, predicted urban growth for the year 2018 is compared with the actual urban growth in the year 2018 which is obtained from the LULC map obtained from classification of satellite image of the year 2018 (Figure 6.24). The SLEUTH model predicted 3037.45 km^2 of the total urban area for Ajmer fringe in the year 2018, which is less compared to the observed urban area of 3411.53 km^2. The number of Edges representing fragmented growth is predicted to be 1872 for the year 2018

as compared 1496 Edges obtained from the referenced urban area of the year 2018. The no. of urban clusters were found to be 266 in the year 2018 from simulated growth as compared to 257 obtained from a referenced urban area. The cluster radius representing infill growth has been found to be 311 as compared to 330 obtained from referenced or actual urban year in the year 2018. Modeled urban area, edges, clusters, and cluster radius have been found to be satisfactory and model performance is consistent. Cluster size for the year 2018 has been predicted as 11 while actually, it is 13 in the year 2018 (Figure 6.24). The reasonable error may be due to the misclassification in classified outputs. Thus, the SLEUTH model has shown strong and consistent performance.

The rapid and rampant urbanization in developing countries is posing severe stresses on resources and environment which often outpaces the planning processes (Pathiranage et al., 2018). The study shows that rapid urban growth is taking place in Ajmer along the Jaipur road (NH8), the area near the highway has grown more rapidly through the years (Figure 6.25). The area around Ana Sagar Lake has urbanized at a faster rate in the past few years as the population density of that area has grown rapidly. The area nearby Foy Sagar depicted very high urban growth which may be due to the development of new colonies in relatively flat areas. Pushkar bypass Road is showing road influenced growth as new development has taken place recently and is likely to further grow in the near future. Madar area which is in a North-East direction to Ana Sagar Lake is also showing growth in huge amounts as new railway colonies have been developed and is more likely to get developed in the future. Beawar Road, which is in south direction is also showing road influenced growth. Many educational institutes are developing along highway due to which nearby development is also taking place. So, the study area will be developing at a faster rate in upcoming years. Nasirabad Road is in the east direction also shows urban growth at a faster rate in the past few years. The area around Bisal Sagar has grown rapidly as a huge amount of population is shifting to earn their livelihood. Areas nearby Khanpura Pond is also likely to get developed at a smaller pace as many industrial activities are taking place at this region. The Pushkar region is one of the most important places in Ajmer fringe which is depicting higher growth in upcoming years. Pushkar region is a religious and popular place, commercialization is being increased and also the urban density is getting higher at this place. In upcoming years it will be growing rapidly (Figure 6.25 & 6.26).

Table 6.1 Model calibration parameterization

Best fit Coefficient Values	Diff	Brd	Sprd	Slp	RG	LeeSallee	OSM	Compare	Pop	Edges	Clusters	X_mean	Y_mean	Rad
Ajmer	87	100	100	60	44	0.51	0.08	0.57	0.98	0.97	0.93	0.95	0.52	0.98
Pushkar	26	7	9	41	26	0.25	0.26	0.99	0.89	0.88	0.69	0.95	0.88	0.9

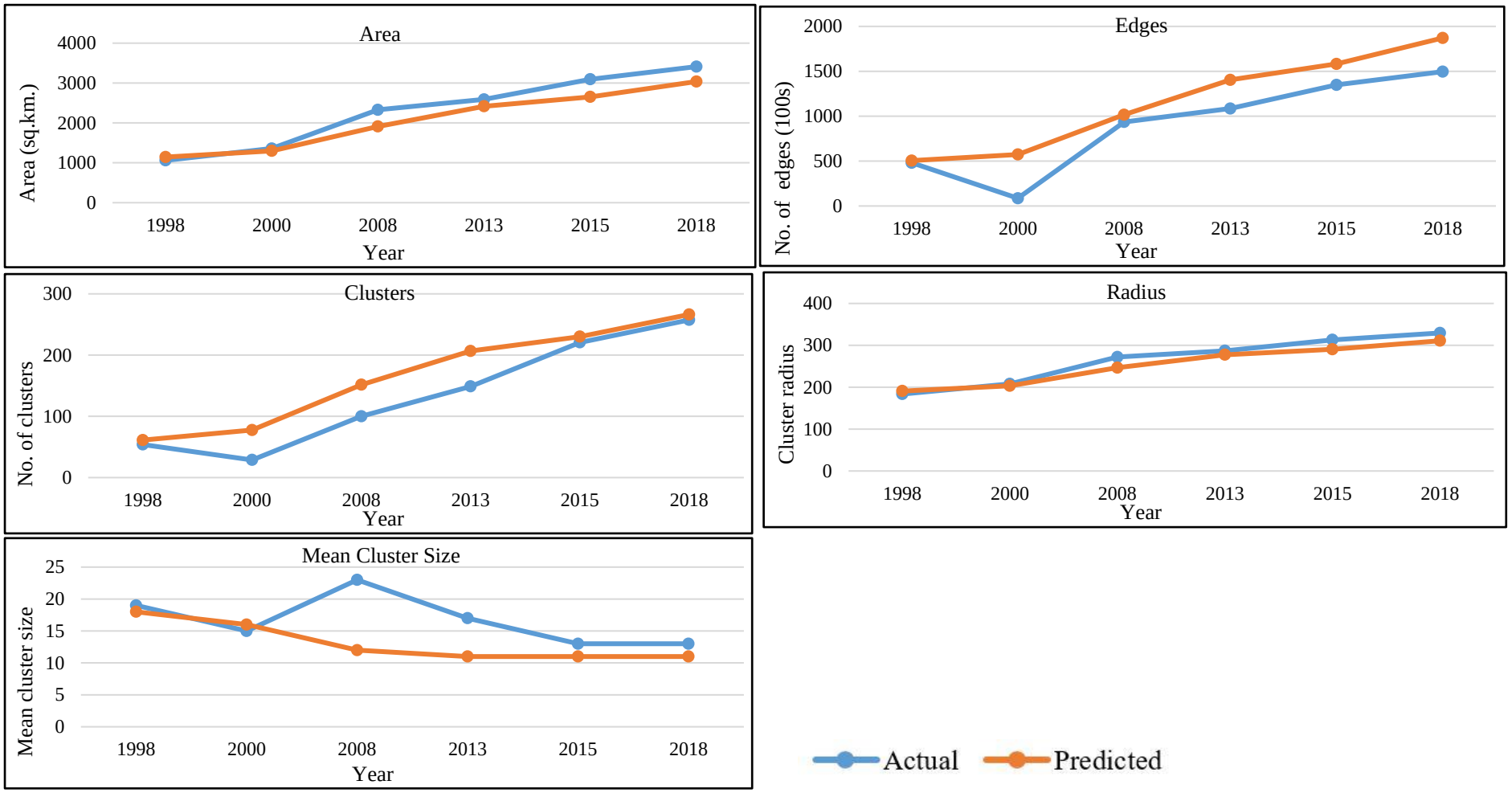

Figure 6.24: Comparison between actual and predicted statistics for different years

6.4.3 Urban density estimation for Ajmer

In the previous section, the prominent locations which became urbanized rapidly in the past few years have been identified. Urban growth analysis is useful to have an idea about horizontal urban growth or sprawl but a vertical expansion, urban intensity and built-up density at different locations which are essential for land use and urban planning have not been simulated through various modelling approaches. The newly developed SLEUTH-Density is capable in estimating the built-up/urban density of a landscape for the present as well as for future. Built-up density has been simulated for Ajmer fringe and results are presented in Figure 6.25 & 6.26.

Built-up density for the year 2018 has been shown in Figure 6.25. It is very exciting to see the built-up density results as it is well validated with the traditional built-up density retrieval approaches and higher density values are achieved where rapid urban growth has been observed in past few years. It surprisingly achieved higher built-up density values at edges rather than a central part of Ajmer. The reason is quite certain as we have observed urban sprawl approaching outskirts of Ajmer and the central Ajmer has not grown further significantly in past few years due to the unavailability of suitable land. So, the outer Ajmer has the major possibility of urban development in the future. Built-up density is higher at edges, along with major roads, important colonies, and newly centered clusters.

Built-up density was simulated up to the year 2040 and it was evident that the density of a location has been increased over the years. In the year 2018, Ajmer fringe is having a maximum of 113 as relative density which has increased to 131 in the year 2040. Here, the density value is relatively explaining the probability of having a chance of density in the future (Figure 6.25 & 6.26).

Further, built-up density simulated from the SLEUTH-Density for the year 2017 has been compared and relationships were established with the urban densities estimated from other conventional approaches using reference data of the year 2017. Simulated built-up density has also been compared and related with few reflectances in particular wave length based indices, spectral indices, built-up indices and land surface phenomenon like land surface temperature (LST) to validate the model results indirectly. Different type of indices used to validate the built-up density results has been presented in Figure 6.27. SLEUTH-Density validation has been discussed in subsequent sections.

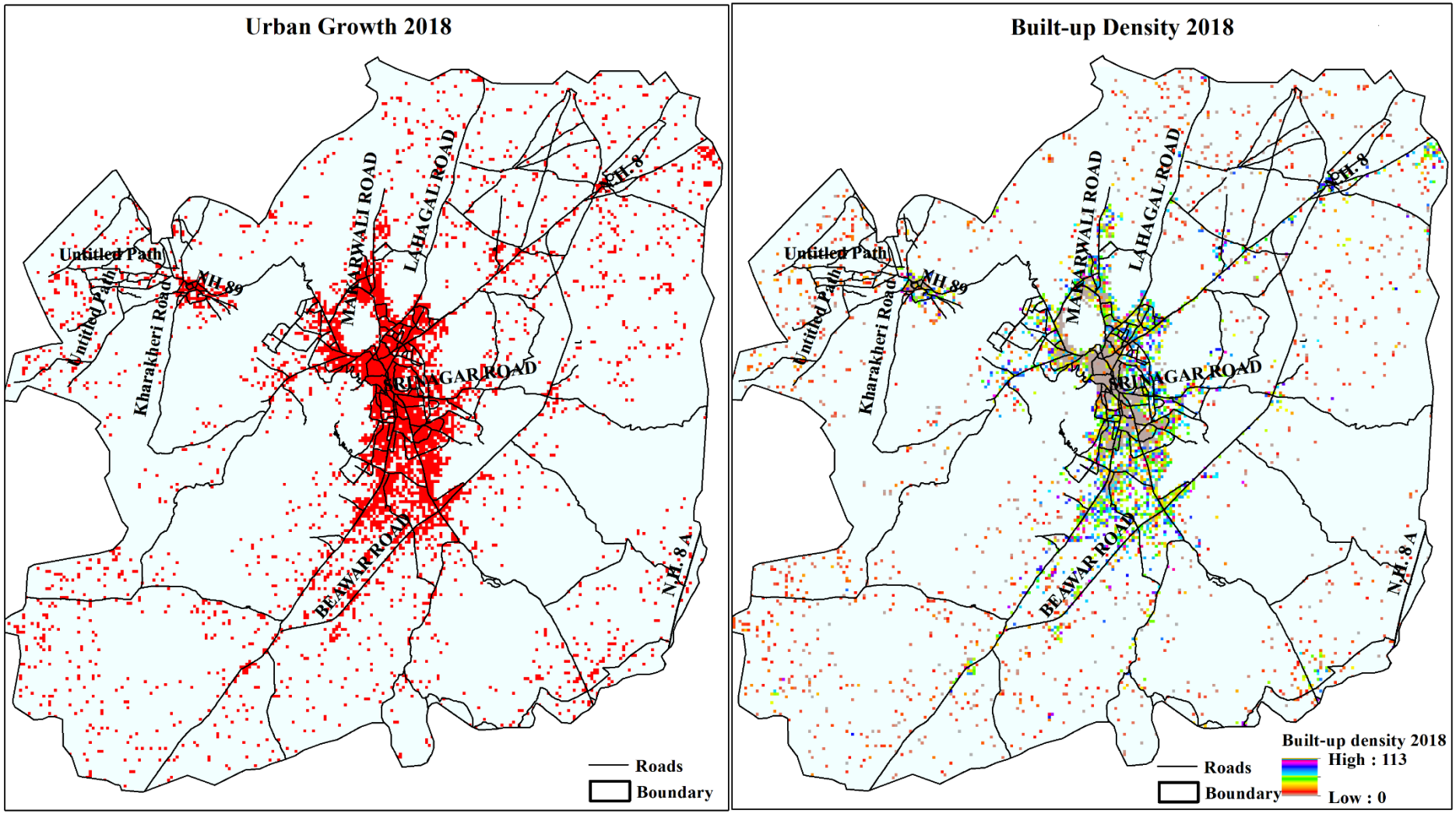

Figure 6.25: Urban growth and density for year 2018

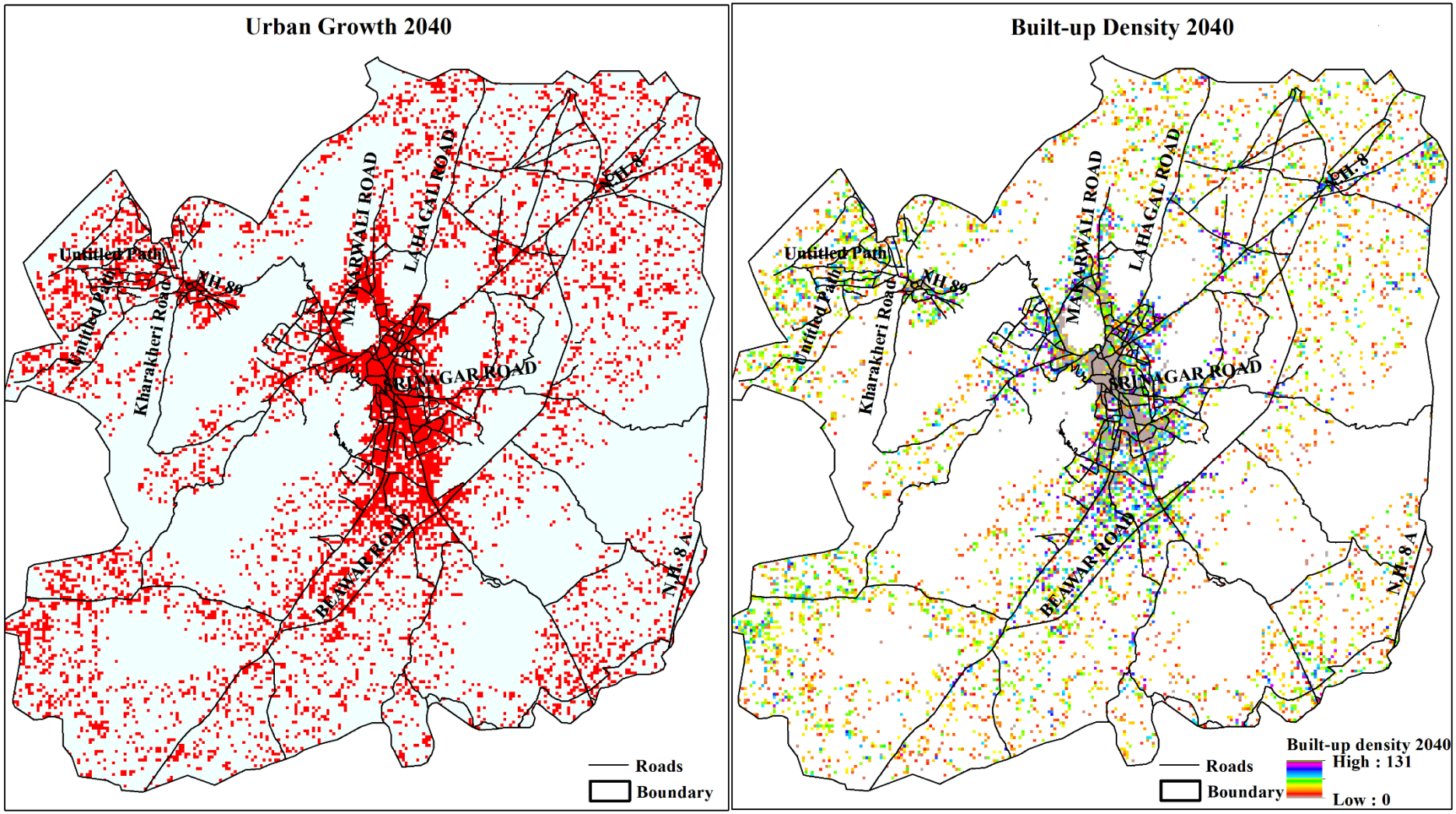

Figure 6.26: Urban growth and density for year 2040

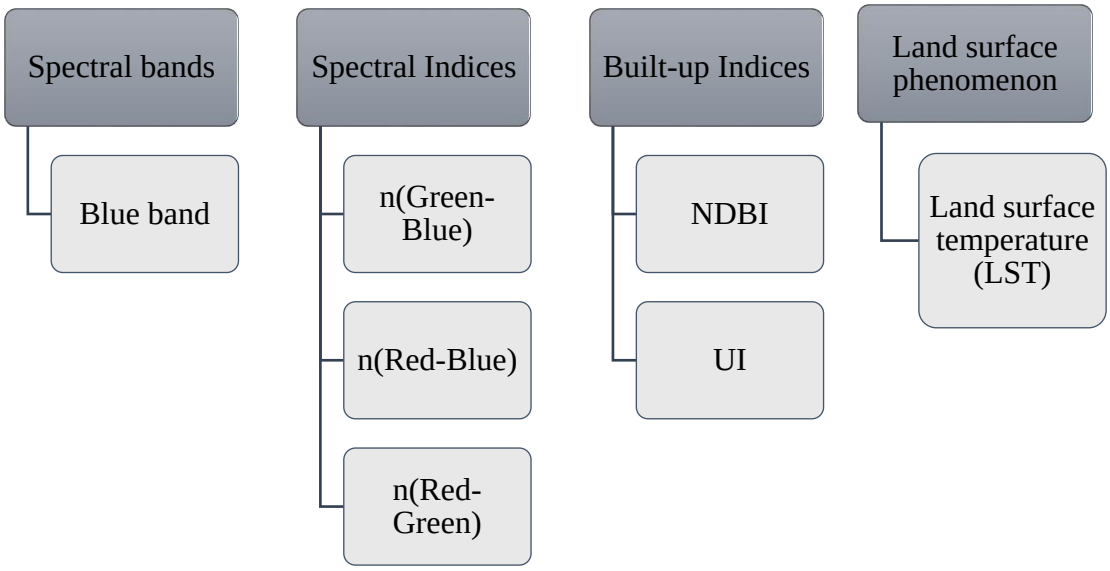

Figure 6.27: Built-up density indices used for SLEUTH-Density validation

6.4.4 Validation of simulated built-up density from SLEUTH-Density

Model result validation is an exercise carried out to determine how well a model simulates the inherent characteristics of a real system in means of model integrity, replicability and prediction. Built-up density is a complex phenomenon to determine and there are very few approaches which can give an idea of built-up density. For validating the built-up density results obtained from SLEUTH-Density various methods as presented in Figure 6.27 have been utilized and discussed in subsequent sections. Results of the built-up density have been validated by comparing the relative built-up density at more than 100 randomly generated points with the value of respective indices at those points for the year 2017. More than 100 points have been selected using stratified random sampling throughout the study area. Further, built-up density values have been recorded from these points and one by one compared with the values of different indices estimated from the reference image of the year 2017 to judge the quality of model simulation.

6.4.4.1 Validation of built-up density results using spectral bands

Remote sensing has the capability to capture reflectance of spatial features in multiple wavelength bands. The built-up area appears brighter because of higher reflectance in the visible bands while non-built-up area appears darker (Rottensteiner and Briese, 2002, 2003; Hu et al., 2004; Vu et al., 2009). Therefore, we have considered the band in which reflectance from built-up areas is the highest. It is understood that the higher the brightness

value of the built-up feature will be proportional to the built-up density. It can be seen in Figure 6.28, that locations having higher reflectance also have the higher built-up density for the year 2017, which indicates that the model is able to capture the built-up density satisfactorily.

6.4.4.2 Validation of built-up density results using spectral indices

Built-up density results have also been validated in term of different spectral indices which can differentiate the built-up and non-built-up areas. Model results of built-up density can be correlated with the results of the spectral indices in term of their relative values for the year 2017 at different locations like locations with a higher value of built-up density have a higher value of spectral indices. Spectral indices are the band ratio images obtained using Eq. 6.7 to Eq. 6.9 for the reference year 2017. A higher value of indices indicates more the built-up. The higher the value of indices may indicate higher built-up density for different locations (Figure 6.28).

$$n(Green - Blue) = \frac{(Green - Blue)}{(Green + Blue)} \quad \ldots\ldots (6.7)$$

$$n(Red - Blue) = \frac{(Red - Blue)}{(Red + Blue)} \quad \ldots\ldots (6.8)$$

$$n(Red - Green) = \frac{(Red - Green)}{(Red + Green)} \quad \ldots\ldots (6.9)$$

It can be seen from Figure 6.30 that the trend of simulated built-up density for the year 2017 matches quite satisfactorily with the trend of spectral indices estimated from the satellite image of the same year. Matching trend indicates locations having higher built-up density values also have higher built-ups estimated from the indices.

6.4.4.3 Built-up indices

Few built-up indices were developed to extract built-up information from a satellite image such as NDBI (Normalized Difference Built-up Index), UI (Urban Index), IBI (Index based Built-up Index) etc. (eq. 6.10 to 6.11). These indices have been used to extract information about the built-up density (Godefroid and Koedam, 2007**)**. In the present study, NDBI and UI indices have been used to extract built-up areas from a satellite imagery of the year 2017 (Figure 6.29). Model built-up density results can be assumed to be satisfactory if built-up density values at a number of test points are following the trend

of values of built-up indices. Results presented in Figures 6.35 &36 indicate a good matching trend in values of simulated built-up density and built-up indices for a number of test points (Figure 6.35 & 36).

$$NDBI = \frac{(SWIR1 - NIR)}{(SWIR1 + NIR)} \dots\dots\dots\dots\dots\dots\dots\dots\dots\dots\dots\dots\dots\dots\dots\dots\dots\dots\dots\dots\dots\dots\dots\dots.. (6.10)$$

$$UI = \frac{(SWIR2 - NIR)}{(SWIR2 + NIR)} \dots\dots\dots\dots\dots\dots\dots\dots\dots\dots\dots\dots\dots\dots\dots\dots\dots\dots\dots\dots\dots\dots\dots\dots\dots (6.11)$$

The matching trend revealed that model performance in simulating built-up density for the year 2017 is satisfactory and acceptable.

6.4.4.4 Land surface phenomenon

LULC changes have a significant influence on land surface temperature and also temperature varies from one land use class to another. The urban or built-up surfaces are made of concrete or stones or bricks which are impervious in nature and absorbs more radiations during daytime and re-radiate longwave radiation in the night causing an increase in nighttime temperature, It has been reported in a few studies that the built-up density can be correlated with the land surface temperature (Weng et al., 2004; Couttset et al., 2007). Built-up density values at different points can be correlated with the land surface temperature values (during daytime or night time). The simulated value of urban density should be proportional to the Land Surface Temperature (LST) at same locations. Higher the LST value will be the representation of densely built-up areas. While correlating the simulated built-up density of more than randomly selected points for the year 2017 with LST values, the performance of SLEUTH-Density has been found to be consistent. There are various methods available for estimation of LST from thermal band images like a single window, split window method etc. The thermal band image of remote sensing data was utilized to estimate the LST. However, there is a limitation of coarse spatial resolution in the thermal band data available from different satellites like band 10 and 11 (Thermal Infrared 1 and Thermal Infrared 2 respectively) of Landsat 8 have a spatial resolution of 100 m, however it has been resampled to 30 m spatial resolution to match the Operational Land Imager (OLI) bands. The Landsat collects data around 5:30 am in the morning from India therefore, reverse behavior of LST has been obtained from the Landsat thermal band.

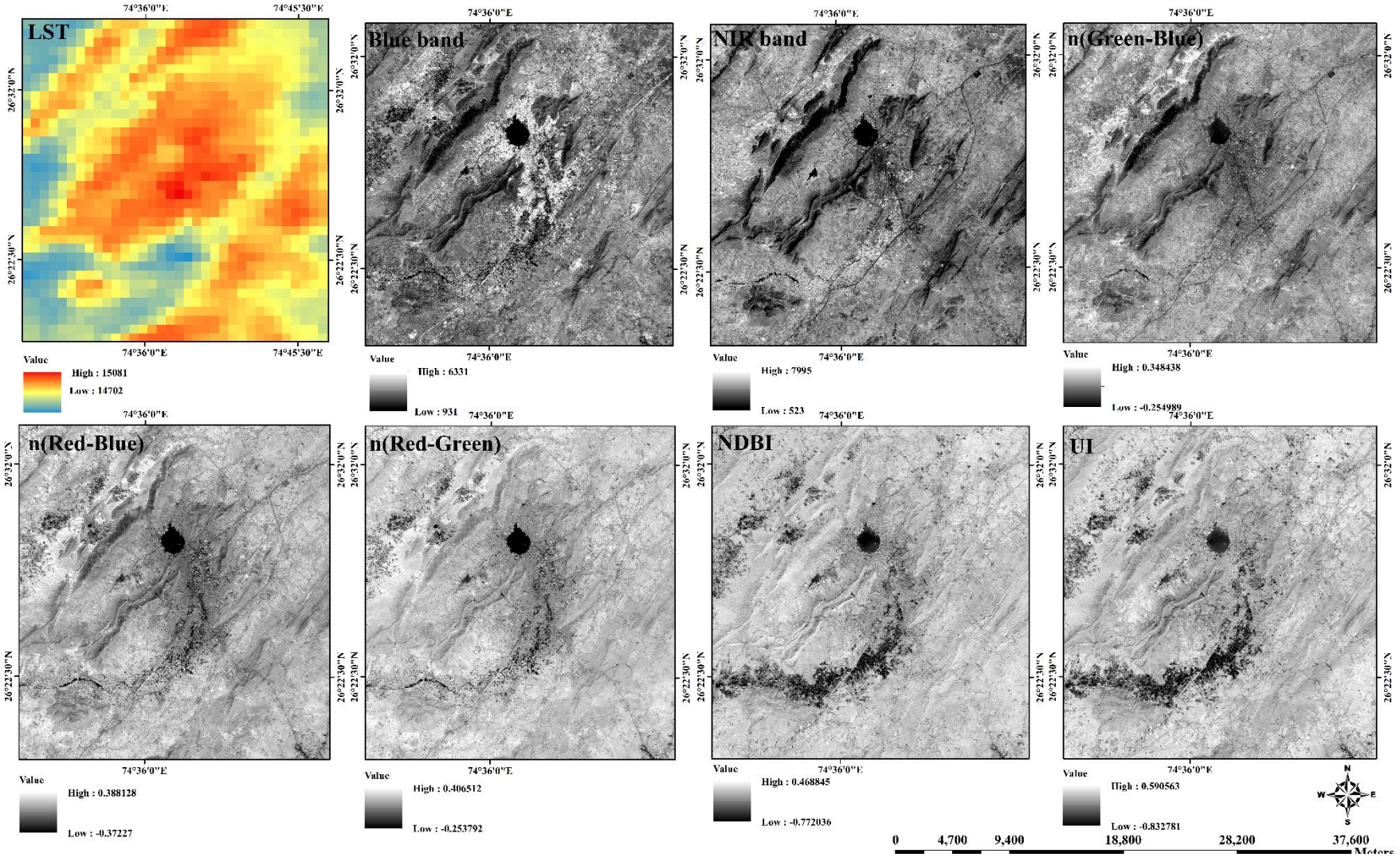

Figure 6.28: Built-up density indices maps

Since the Landsat satellite passes over the Indian region in the early morning and at that time impervious surfaces are cooler as compared to other surfaces it results in lower LST values from the built-up areas. Further LST was estimated from the Aster satellite data (90m spatial resolution) for daytime and compared with the simulated built-up density results. Further day time as well as night time LST has been estimated for the year 2017 using MODIS (Moderate Imaging Spectroradiometer) satellite data (250m, 500m 1km spatial resolution). Since MODIS is capable of providing moderate spatial resolution data therefore, the LST data products were resampled equal to the spatial resolution of the other input datasets of the model. Simulated built-up density at 100 randomly selected points has been correlated with the values of LST at the same points, as presented in Figure 6.29 & 30. It is evident from the comparison of the trend of simulated built-up density and LST for number points that built-up density is proportional with the LST and trends are matching satisfactorily.

6.4.4.5 The relationship between simulated built-up density and traditional approaches of built-up density retrieval used for model validation

To establish the relationship between the simulated built-up density obtained from SLEUTH-Density model and density indicative indices estimated from the traditional approaches (which may not be technically upgraded), their values at more than 100 sample points selected through stratified random sampling method were compared. The comparison of modeled built-up density and values of density indicative indices calculated using traditional approaches is useful to validate the efficiency of the SLEUTH-Density.

The range of absolute value of built-up density estimated from the SLEUTH-Density and different other indices are quite different. Therefore, they cannot be compared in terms of their absolute value. Thus, to determine the relative relationship in their trend, values have been normalized and then they have been compared to find out the relationship between estimated built-up density and calculated from other methods for model result validation. The LST values of 100 random sample points for both day and night time in the year 2017 were compared with the corresponding estimated built-up density values from the SLEUTH-Density model. The established relationship between day and night time LST and estimated built-up density was found to be quite similar to the trend for both, matched quite well. For higher LST values the estimated density was also found to be higher and vice-versa (Figure 6.29 & 30).

For the same random sample points the values of spectral metrics i.e. n(Red-Green), n(Red-Blue) and n(Green-Blue) were extracted and compared with the estimated built-up density by SLEUTH-Density model. A consistent relationship between individual spectral metrics and estimated or simulated built-up density by the model was found as evidence in the Figures 6.31, 6.32 and Figure 6.33. The trend was found to be matching quite well which states that the estimated built-up density by the SLEUTH-Density model is well capable in representing the actual built-up density. It can be found from Figure 6.31, 6.32 and 6.33 that for values of individual spectral indices are following the trend of normalized values of simulated built-up density. The matching trend is justifying the success of the SLEUTH-Density model in simulating the actual built-up density. Furthermore, for the same random test sample points the values of spectral band i.e. blue band which is considered as a good representation of built-up density in conventional approaches has also been compared with the estimated/ simulated built-up density for the same points. The relationship between the spectral band and the estimated density through the SLEUTH-Density model was found to be matching quite well. A consistent relationship for the same was found as clear from Figure 6.34.

Additionally, the built-up indices i.e. UI and NDBI which are used for analyzing built-up density in conventional ways have also been compared with the estimated/ simulated built-up density obtained from SLEUTH-Density model for the same more than 100 random sample test points. A well-matching trend was found for both the built-up indices which indicates that the estimated built-up density values from the SLEUTH-Density model are representing actual built-up density relatively (Figure 6.35 & 6.36). The study indicates that SLEUTH-Density model with its prolific skills enabled to determine the relative built-up/urban density which means relatively higher built-up density indicates the possibility of a location of being relatively highly dense is populated or developed because of locations suitability in term of different characteristics discussed previously like topographical, socio-economic, neighborhood related and biophysical variables. Similarly, moderate and lower density values would be indicating relatively moderate and lower suitability of that location respectively. The exact density value may neither refer to the vertical growth in terms of no. of floors nor built-up intensity (change in built-up per unit area) nor urban density (no. of household living per unit area). However, the estimated built-up density by the SLEUTH-Density model would have the

capability of giving a combined relative information of all the three indicators of density i.e. vertical growth, urban intensity and urban density in the name of built-up density.

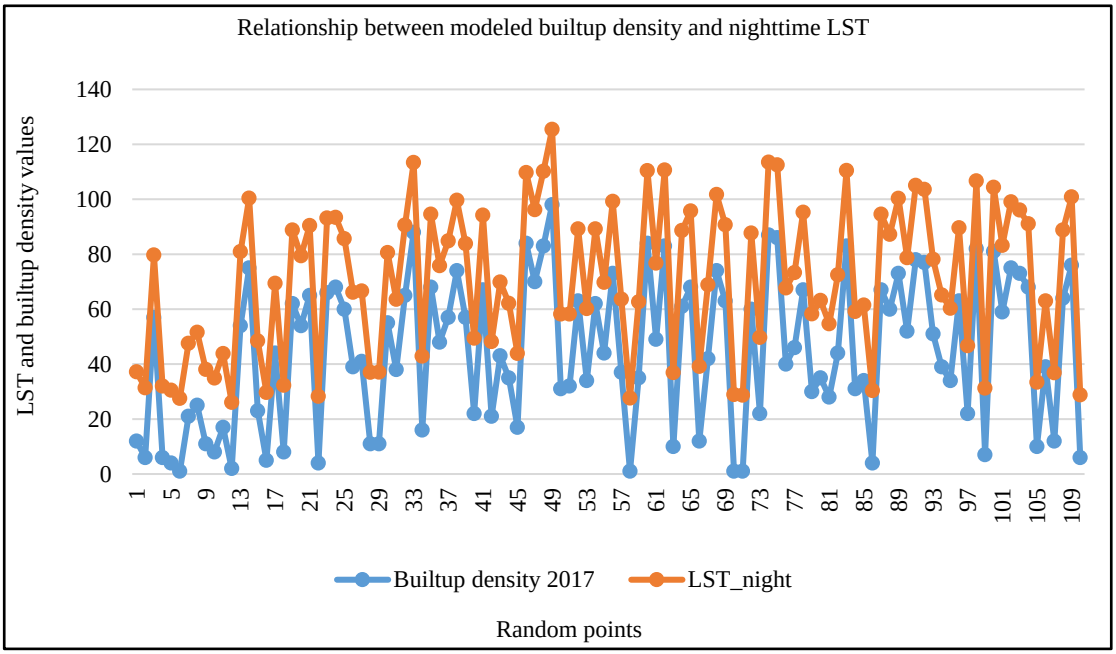

Figure 6.29: Relationship between modeled built-up density and daytime LST

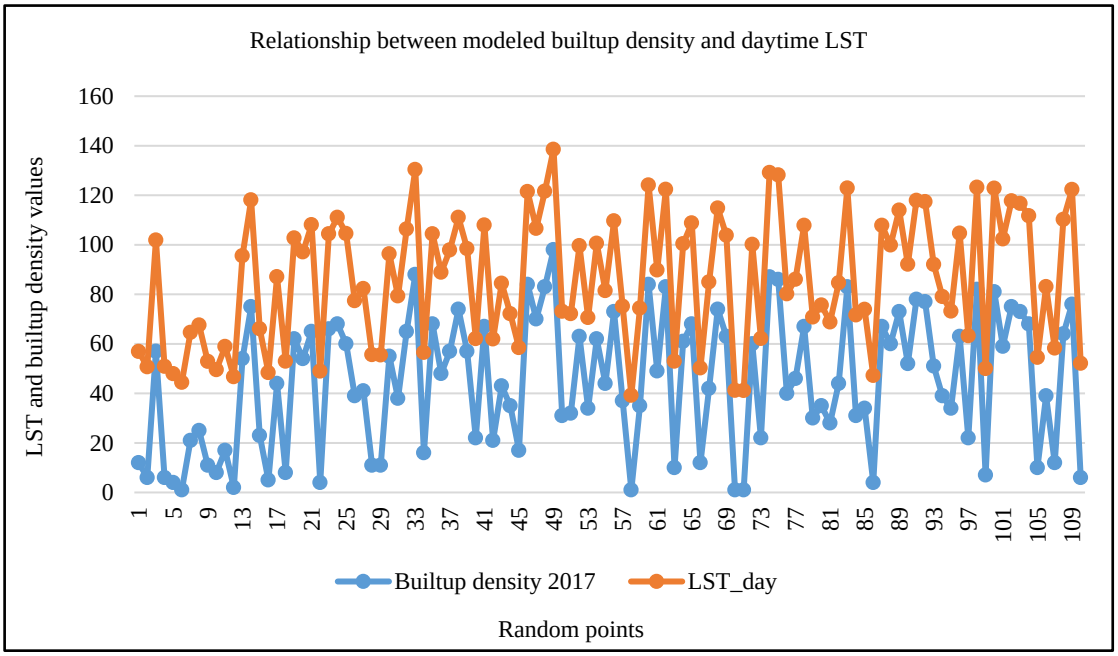

Figure 6.30: Relationship between modeled built-up density and daytime LST

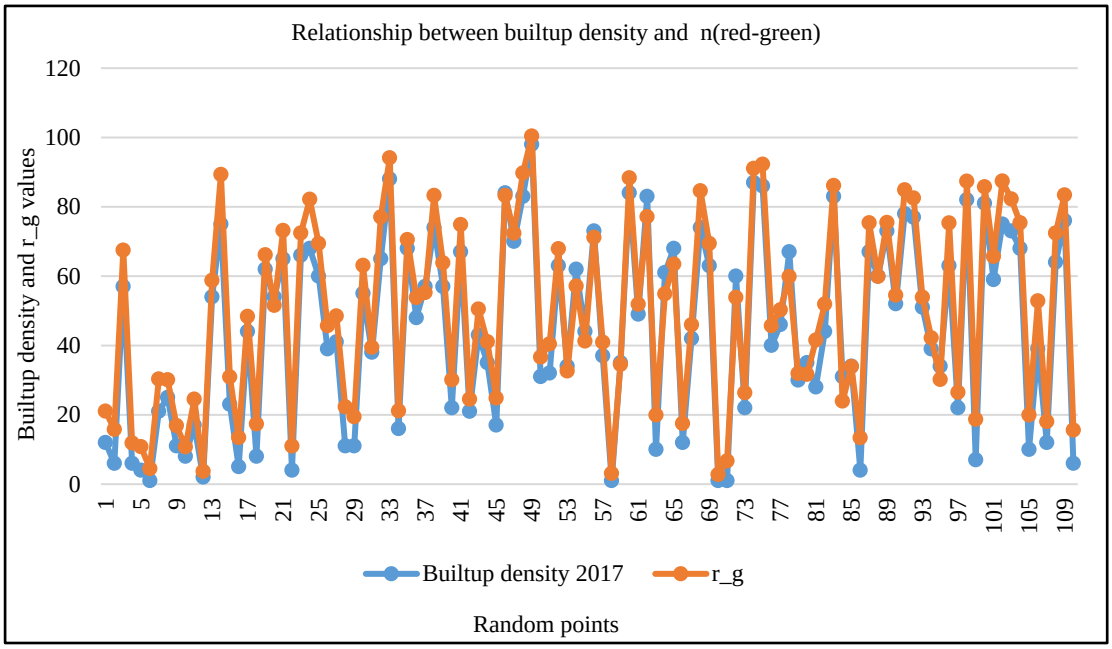

Figure 6.31: Relationship between modeled built-up density and n(red-green)

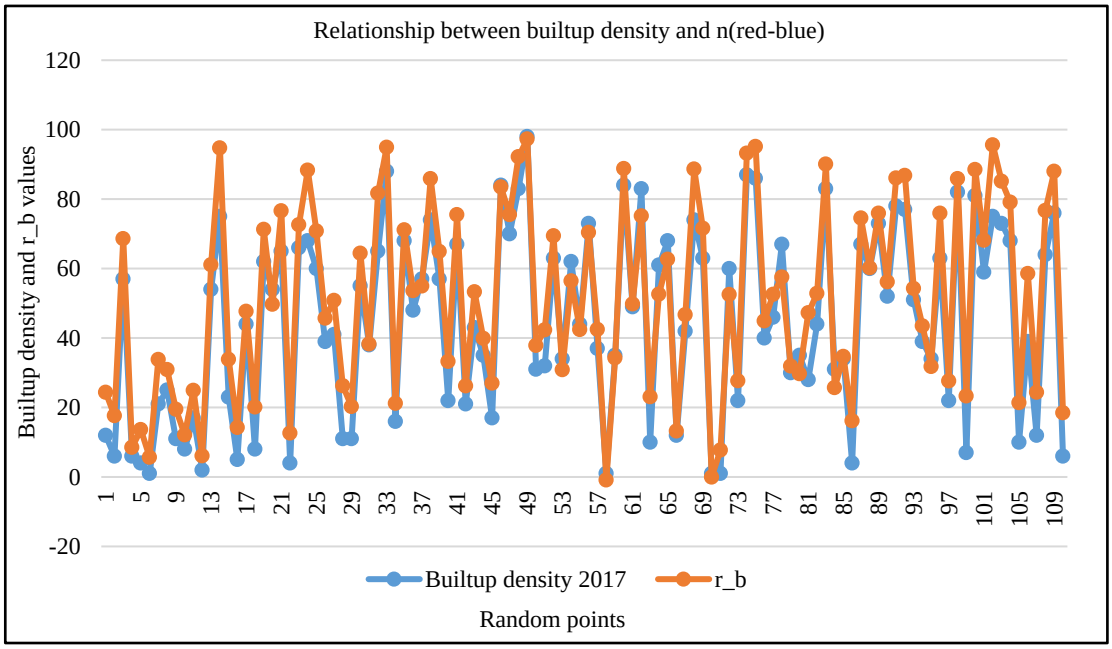

Figure 6.32: Relationship between modeled built-up density and spectral index n(Red-Blue)

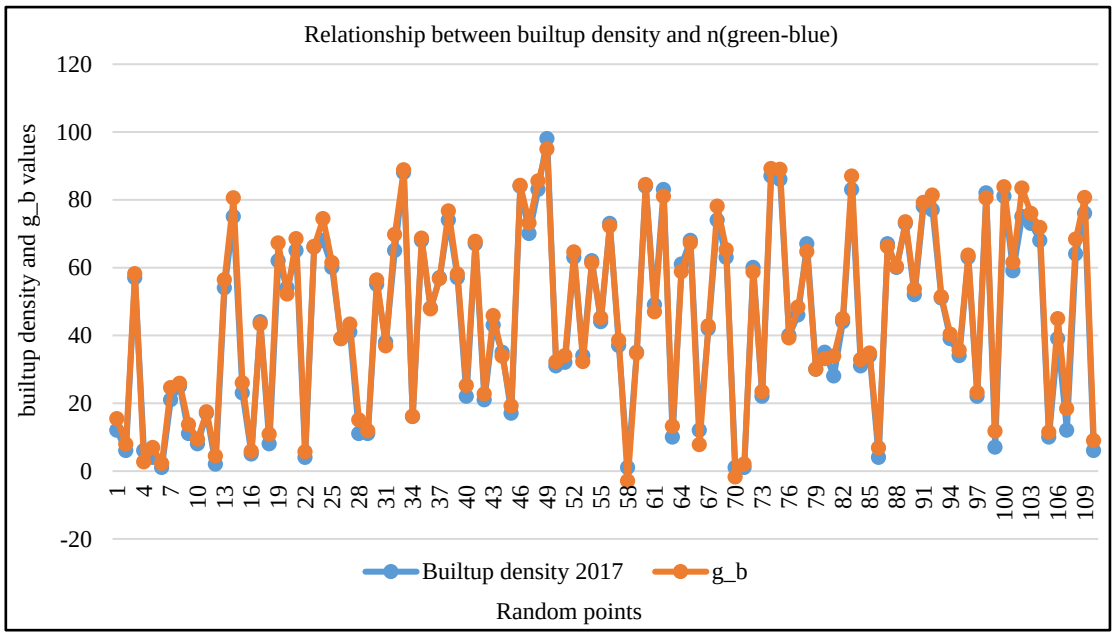

Figure 6.33: Relationship between modeled built-up density and spectral index n(Green-Blue)

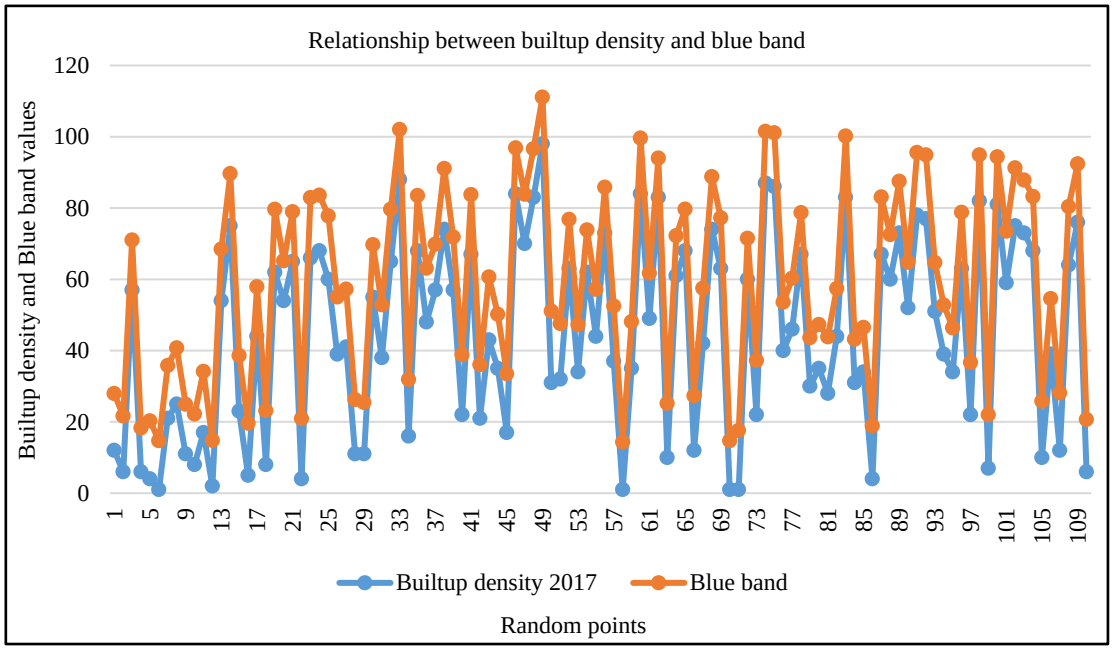

Figure 6.34: Relationship between modeled built-up density and spectral blue band

The conventional approaches of built-up retrieval methods were used to retrieve built-up density in different ways. However, the present study has come up with the prolific skills of the SLEUTH model to estimate/ simulate built-up density in the name of SLEUTH-Density that is an enhanced capability of the existing widely applied and popular model

in the area of urban growth modelling. The study found a consistent relationship between simulated built-up density obtained from SLEUTH-Density and retrieved density from other conventional approaches. Thus, the SLEUTH-Density may be utilized to simulate the built-up density for different regions and for future as well.

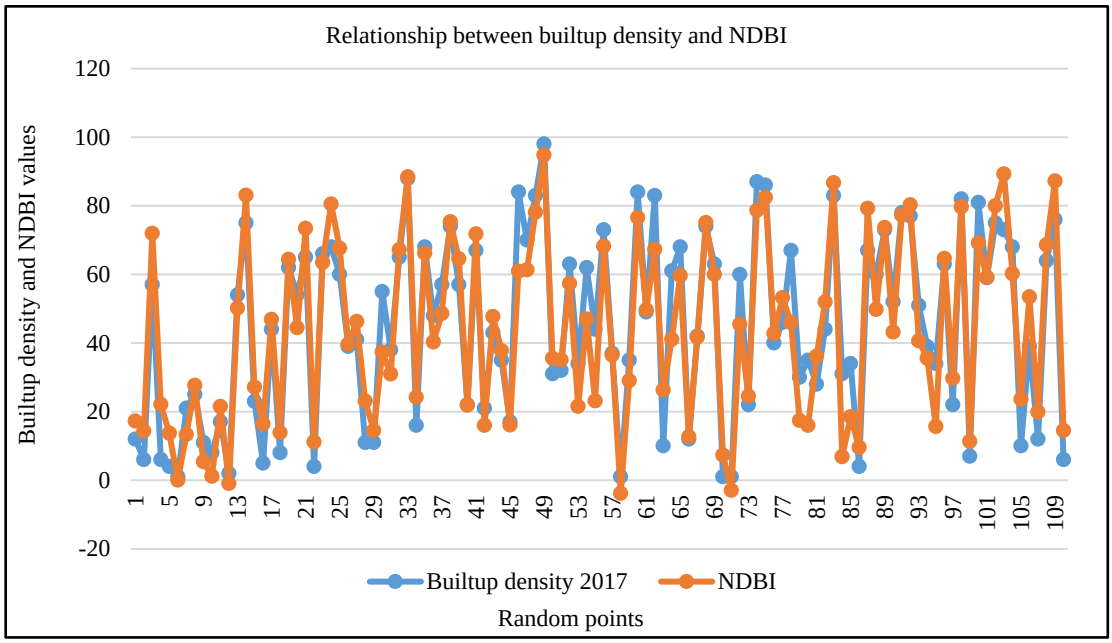

Figure 6.35: Relationship between modeled built-up density and NDBI index

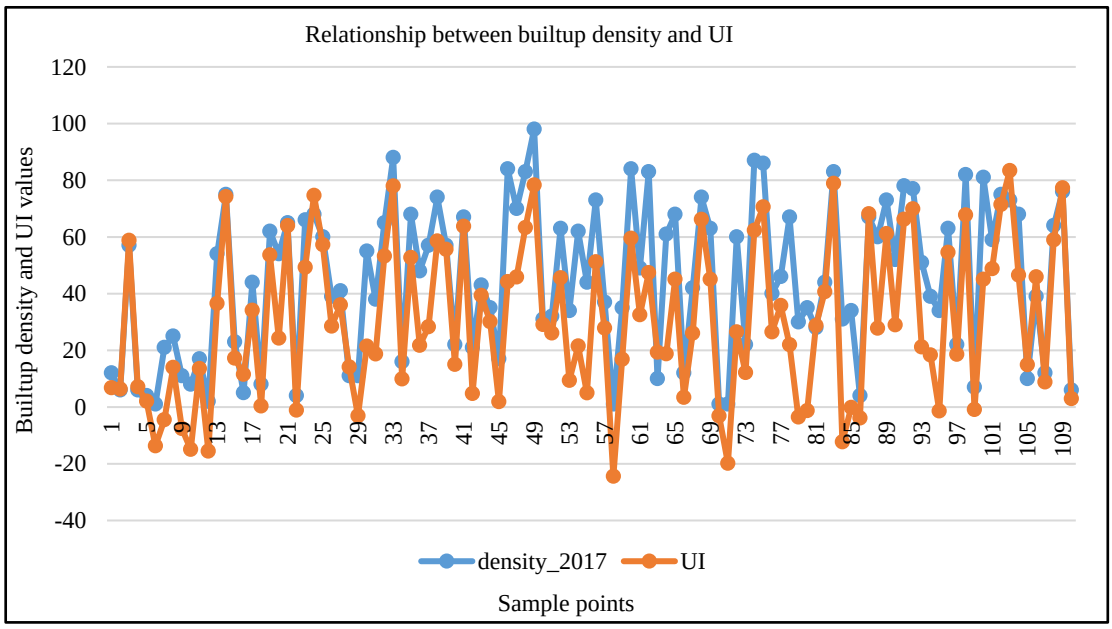

Figure 6.36: Relationship between modeled built-up density and UI index

Furthermore, the estimated built-up density has been validated with the field observed data as well to set assure the outcomes of improvised SLEUTH-Density model. The next

section includes the more detailed discussion of field validation of estimated built-up density.

Similarly, urban growth and built-up density were also estimated for Pushkar up to the year 2040. Simulated urban growth and built-up density maps for different years for Pushkar have been presented in Figure 6.37 and 6.38.

Built-up density results obtained from the model were also validated for the Pushkar town as well. The same methodology has been used as discussed for the validation of results for the Ajmer. A number of random test locations (100) have been selected using stratified random sampling and simulated built-up density values at these locations for the year 2017 were compared with the values of individual built-up density representative indices presented in Figure 6.37. The trend in simulating density for different test points have been plotted and compared with the trends of the results of different representative indices, as shown in Figure 6.39 to Figure 6.46. The relationship between simulated built-up density from SLEUTH-Density and the conventional method were found to be consistent and satisfactory for the Pushkar town as well.

Therefore, it can be concluded that SLEUTH-Density results are satisfactory and considered as validated, as results have been validated for two cities of different size.

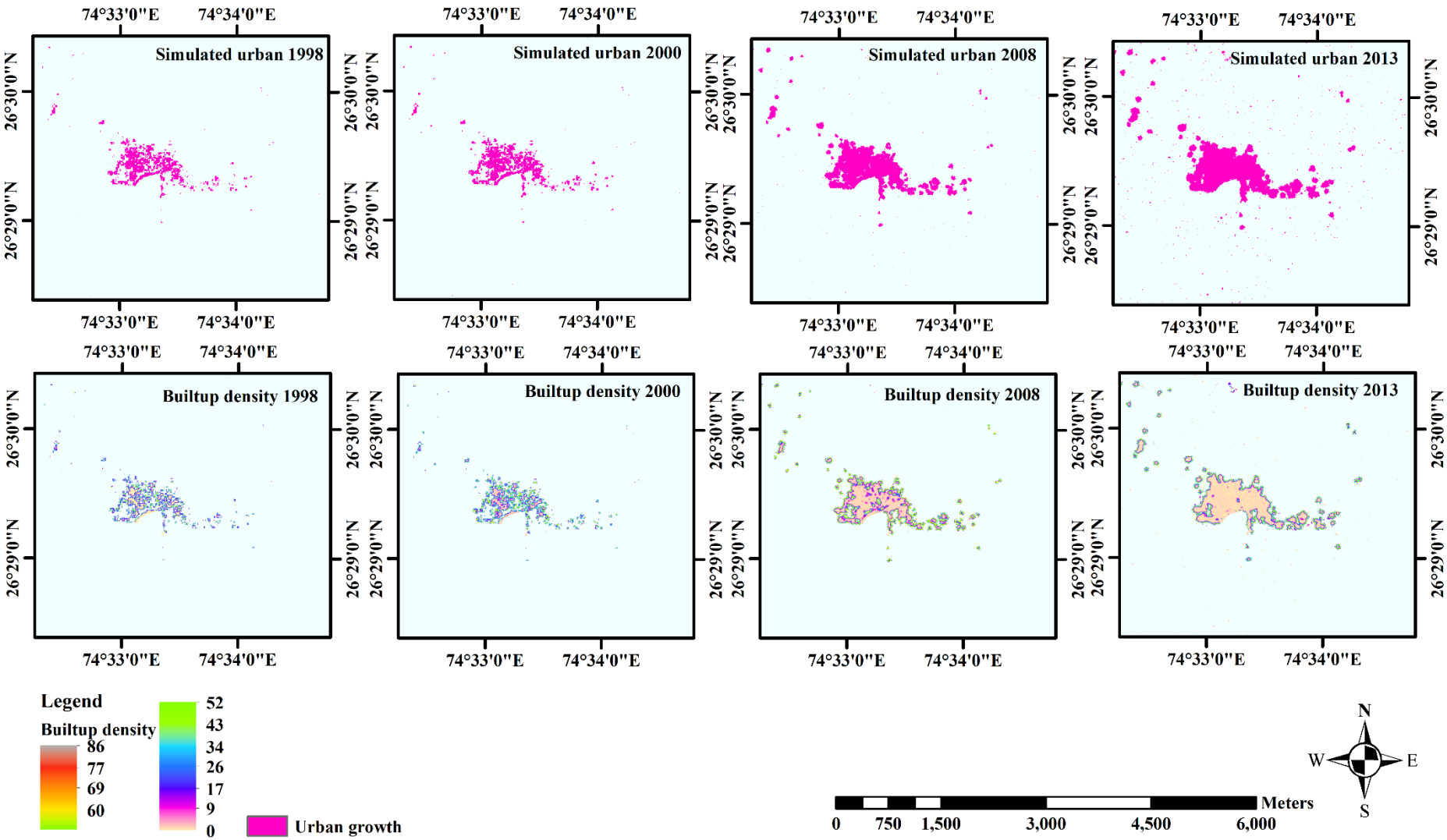

Figure 6.37: Urban growth and built-up density for Pushkar for year 1998, 2000, 2008 and 2013

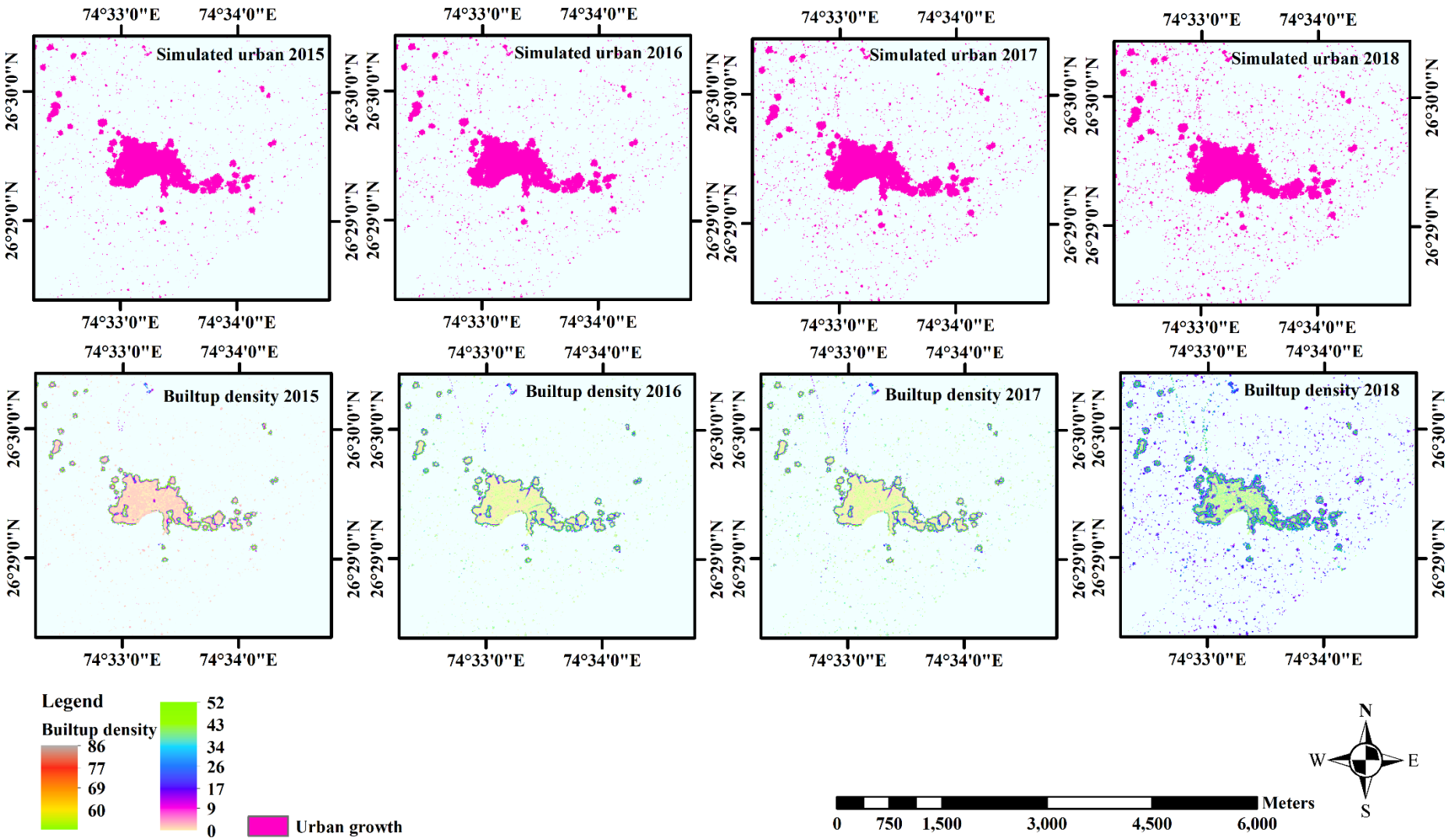

Figure 6.38: Urban growth ad built-up density for Pushkar for year 2015, 2016, 2017 and 2018

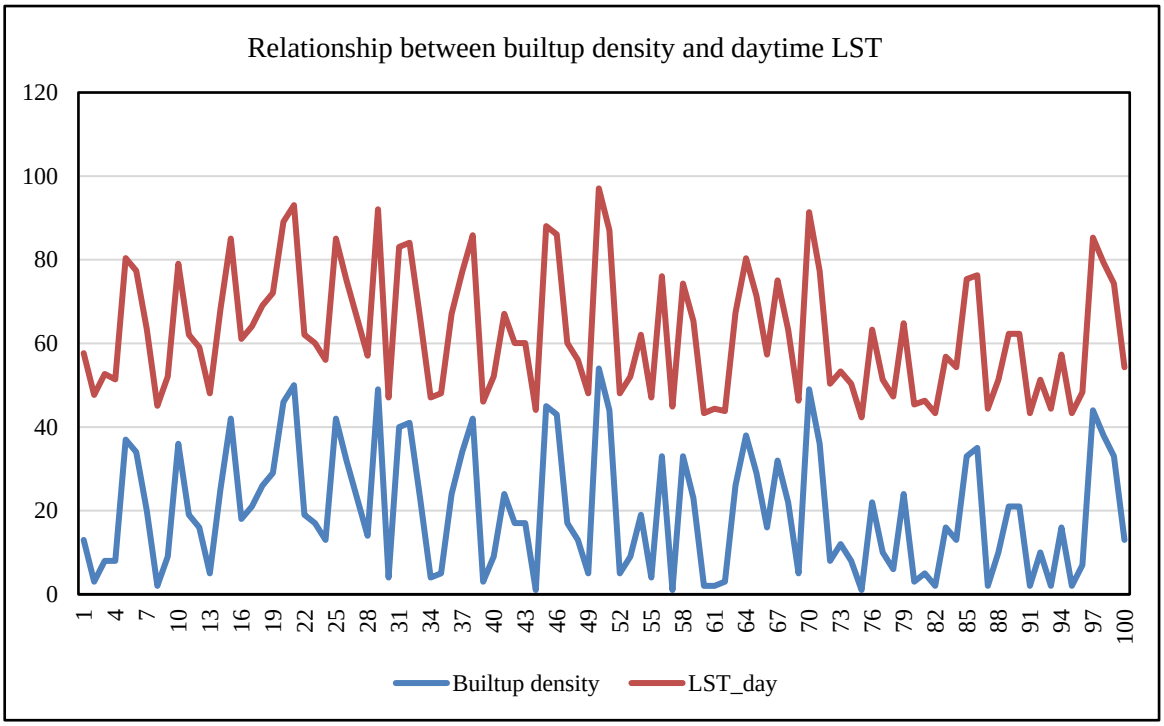

Figure 6. 39: Relationship between modeled built-up density and daytime LST

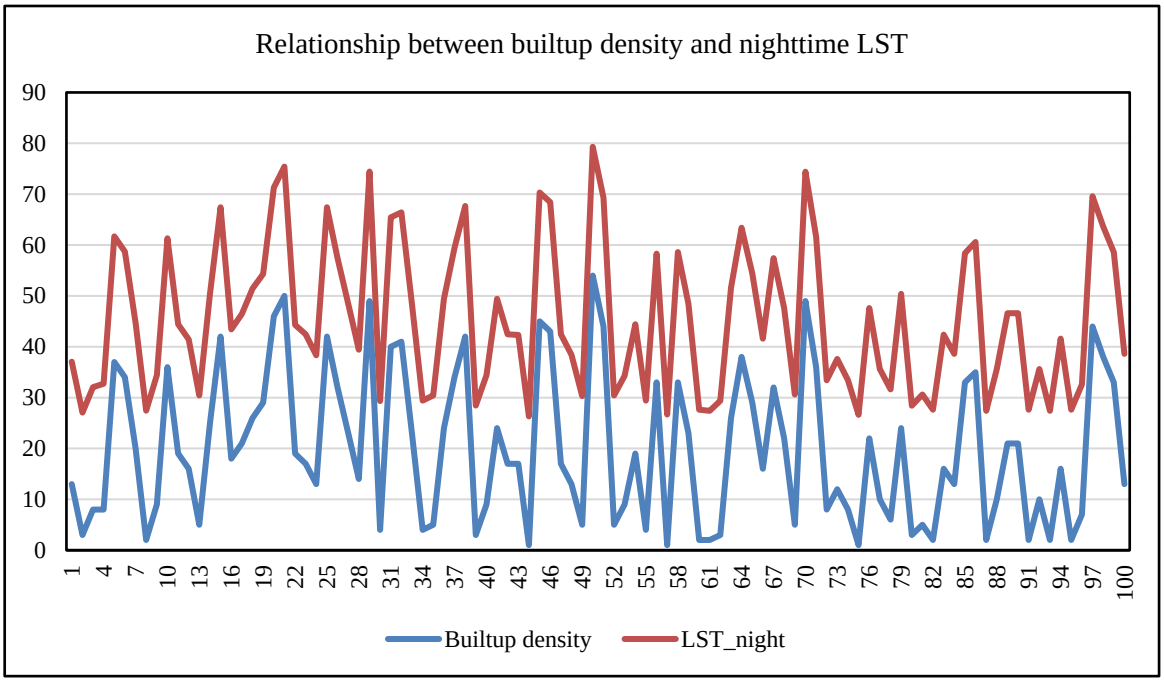

Figure 6. 40: Relationship between modeled built-up density and nighttime LST

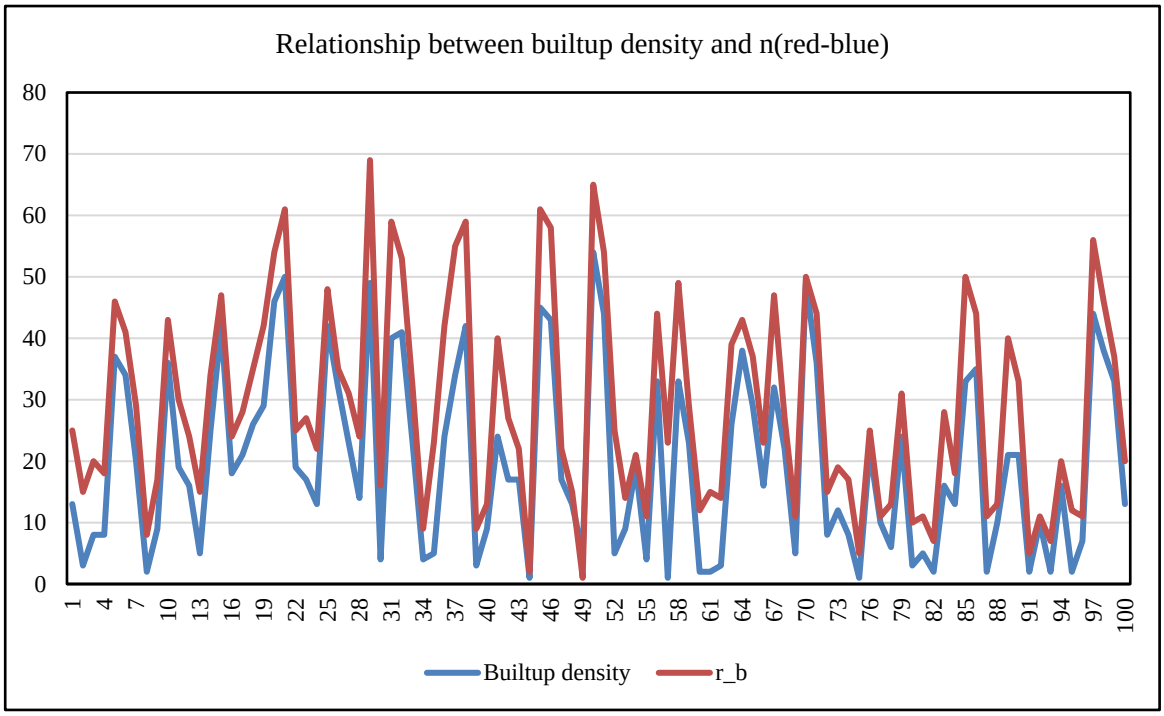

Figure 6.41: Relationship between modeled built-up density and spectral index n(Red-Blue) for Pushkar

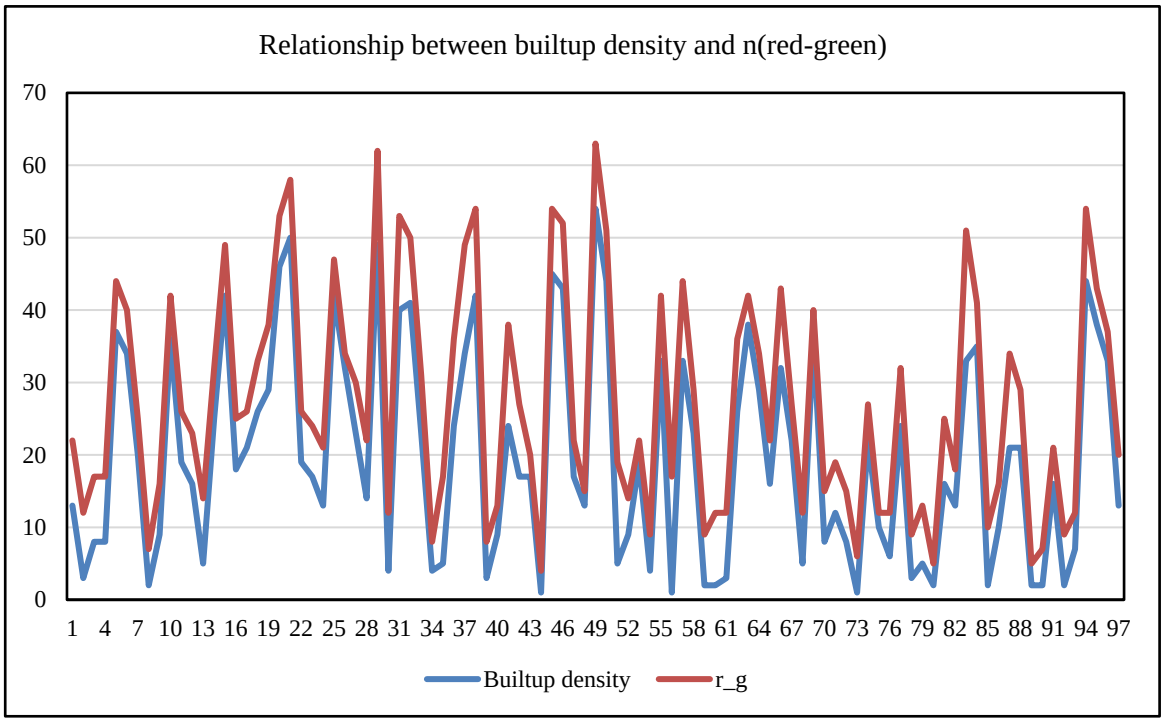

Figure 6.42: Relationship between modeled built-up density and spectral index n(Red-Green) for Pushkar

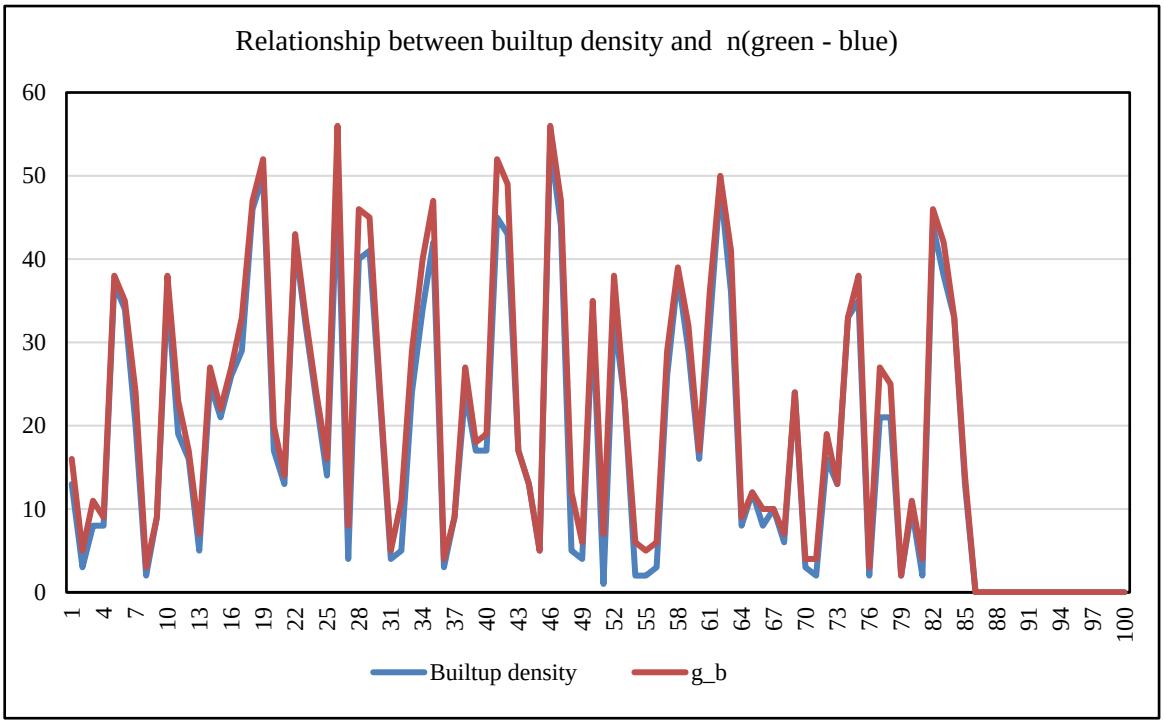

Figure 6.43: Relationship between modeled built-up density and spectral index n(Green-Blue) for Pushkar

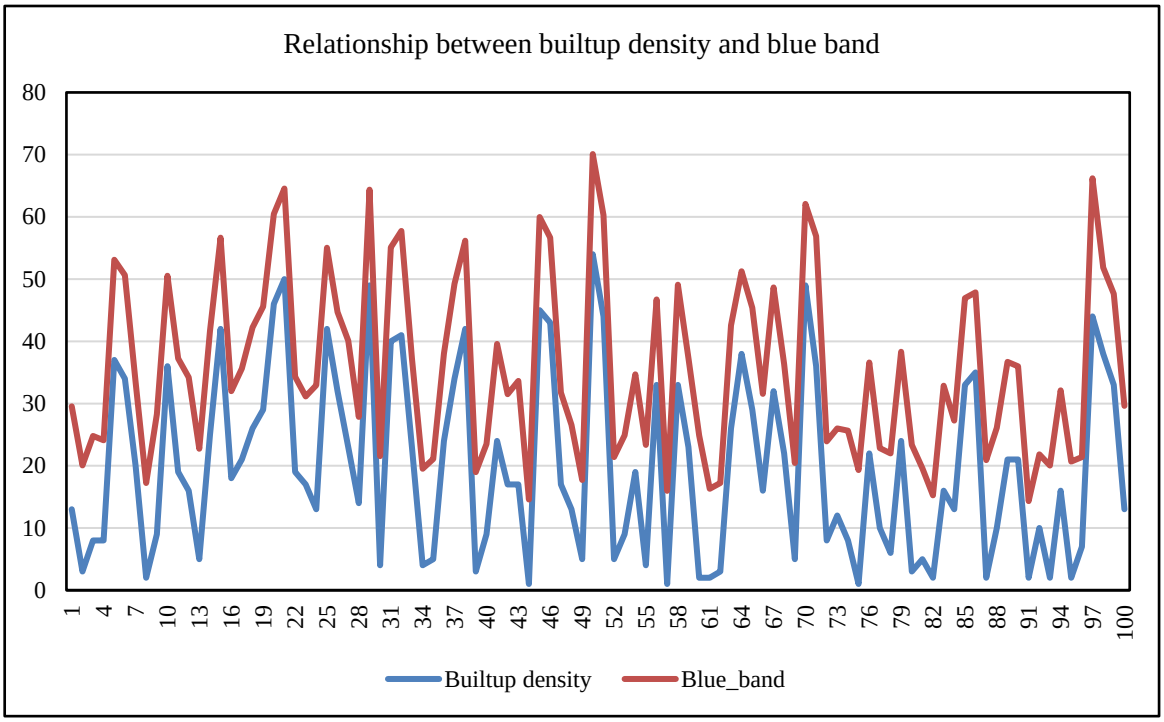

Figure 6.44: Relationship between modeled built-up density and spectral blue band for Pushkar

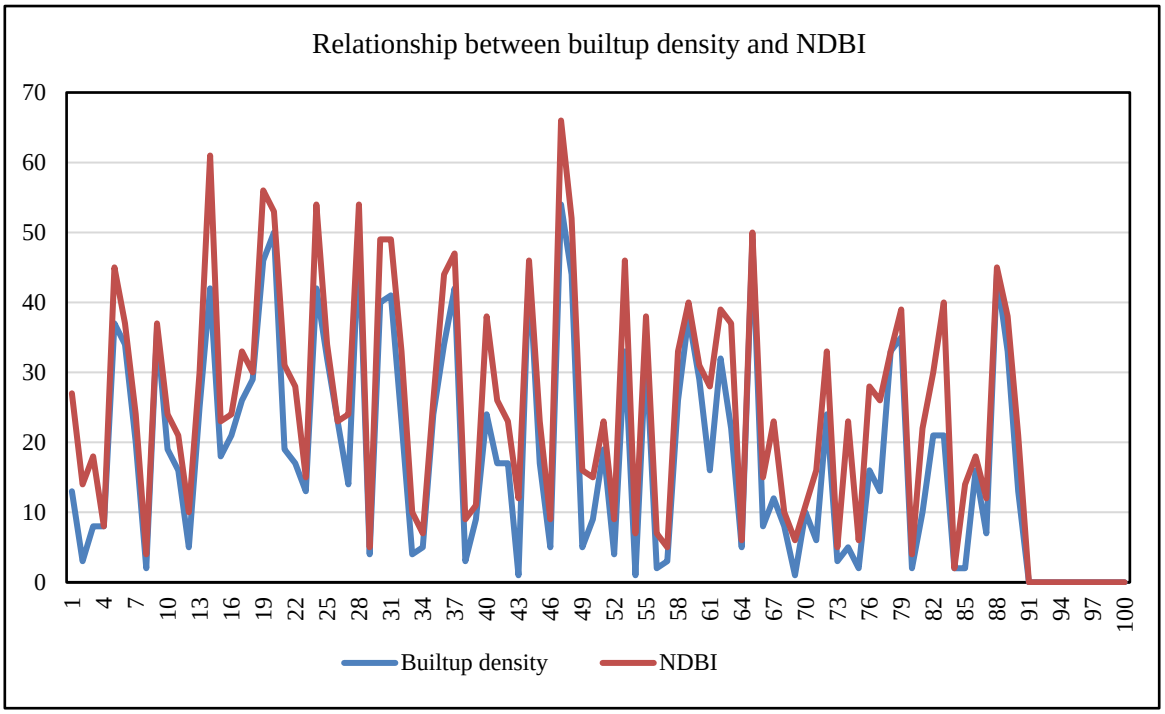

Figure 6.45: Relationship between modeled built-up density and NDBI index for Pushkar

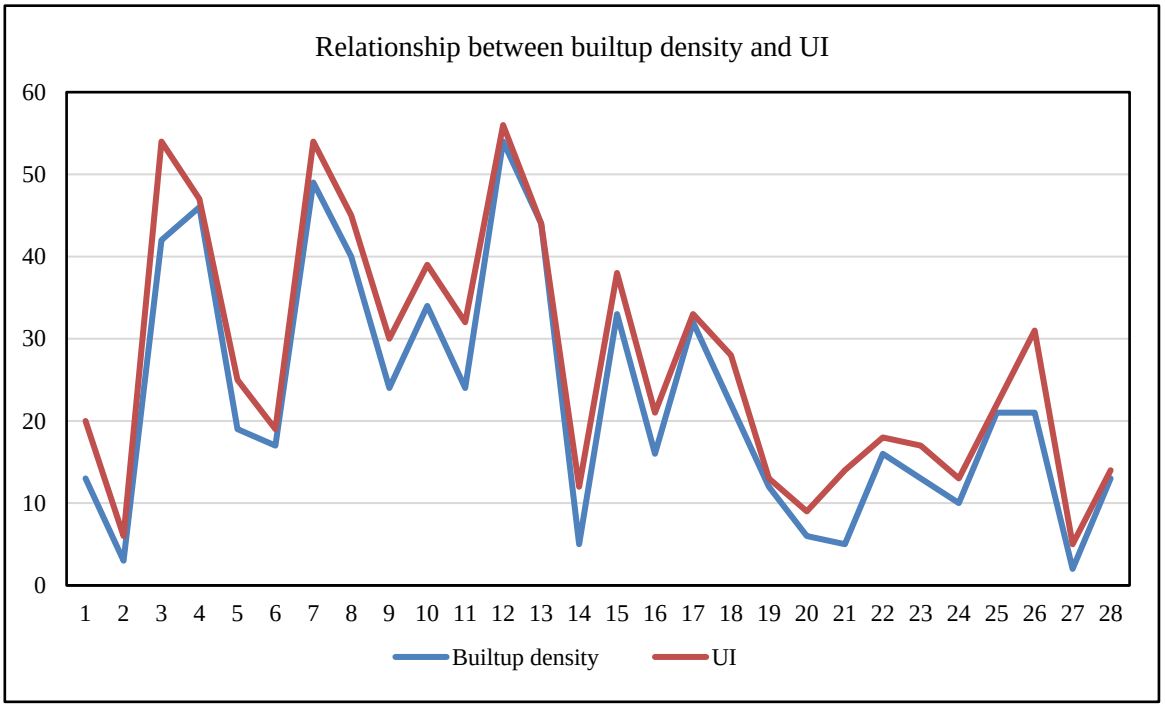

Figure 6.46: Relationship between modeled built-up density and UI index for Pushkar

6.4.4.6 Built-up density validation with field observed data

The hypothesis for the field validation of simulated built-up density includes establishing a correlation between a number of floors of built-up features at different locations randomly selected with the simulated built-up density at those points in relative terms. In field validation, a count of no. of floors in a building at a location has been determined and correlated with estimated/ simulated built-up density values. Since the exact no. of built-up density has nothing to do with the no. of floors (as discussed earlier). Only the normalized relative built-up density information can be correlated with the field observations. Thus, both the no. of floor count and the estimated built-up density were classified into 10 classes with an equal interval to normalize them and the consistency in the relationship was examined.

A total of 78 locations (ground control points - GCP) in Ajmer fringe were randomly visited and the no. of floor counted in the built-up feature for the respective locations was recorded using a handheld GPS tool. The GCPs taken for the density validation are presented in Table 6.2 which is shows the GCP coordinates and the no. of observed built-up storeys and corresponding class values based on the no. of floors. To validate the built-up density the simulated built-up density map of the year 2018 was taken and again it was normalized into 10 classes of equal interval. Furthermore, the correlation between the simulated/ estimated built-up density values and the field observed number of floors of the built-up locations was established.

The analysis reveals that there is a quite good relationship between observed and simulated built-up density class values. The trend of observed no. of floors class values are matching with the trend of simulated/estimated built-up density class values, as shown in Figure 6.47. The lower no. of floors, class values are also found to be matching with the low estimated built-up density class value. The results as discussed above indicate the satisfactory performance of the SLEUTH-Density model in simulating the built-up density and results are well validated with the field observed built-up density values. The study is giving us an idea of built-up density which can well relate with the no. of floors well. For validating this fact statistically, regression analysis has been carried out between observed and simulated built-up density class values. The statistical relationship was found to be satisfactory with an R^2 value of 0.74, which is satisfactory and acceptable (Figure 6.48). In addition, the accuracy for simulated/estimated built-up density with field validated data

was assessed and found to be 75% that is quite acceptable for such applications (Table 6.3).

Moreover, some sample pictures have been presented that are also showing built-up features (multi-storey buildings) which were also simulated successfully by the SLEUTH-Density model and simulated density class values are also matching with a number of floors class value (Figure 6.49, 6.50, 6.51). Figure 6.51 is representing the view of a multi-storey building at Pancheel Nagar location which is successfully captured by the SLEUTH-Density model with a higher density class value of 10. It is clear from the Figure 6.49 that the same coordinate i.e. 74° 38' 13.51" E 26° 30' 34.96" N was observed in Google Earth image as well as for the same GCPs and simulated density has a higher class value of 10. Figure 6.50 is showing a multi-storey building on Pushkar road that is successfully captured by the SLEUTH-Density with higher density class value i.e. 10. The same coordinate i.e. 74° 33' 32.64" E 26° 29' 24.82" N was observed on Google Earth map, GCPs and modeled density map with higher built-up density class value.

In another Figure 6.51, a multi-storey in Panchsheel Nagar block 2 was successfully captured with higher density class value by the SLEUTH-Density model and the GCPs i.e. 74° 38' 10.64" E 26° 30' 34.95" N are also validated with the Google Earth imagery. In Vaishali Nagar, a multi-storey named as Castle Royal was also successfully captured by the SLEUTH model with higher built-up density values i.e. 10. The coordinates of the location i.e. 74° 37' 36.70" E 26° 29' 43.29" N were also validated with Google Earth image (Figure 6.52).

Table 6.2: Ground control points for built-up density validation

X-coordinate	Y-coordinate	Comment	Storeys	No of floors
74° 35' 32.667" E	26° 31' 38.006" N	Kanas village near push needevdl	new multi-storey	10
74° 39' 42.319" E	26° 31' 21.255" N	Multistorey pushar road	three storey	3
74° 40' 55.347" E	26° 31' 9.256" N	Sai jyoti nagarnew const	three storey new	3
74° 38' 5.043" E	26° 31' 8.062" N	Rajgharana residency	two storey	2
74° 40' 56.492" E	26° 31' 3.925" N	New development green colony	three storey	3
74° 35' 10.947" E	26° 31' 0.299" N	Boodhapushakar	single storey new	1
74° 41' 1.139" E	26° 30' 41.002" N	Nee construction near jaipur road	two storey new	2
74° 41' 1.206" E	26° 30' 40.447" N	Multi storey construction jaipur	two storey	2
74° 40' 58.048" E	26° 30' 45.221" N	Kesr kripa vihr coloney consruti	three storey	3
74° 38' 8.354" E	26° 30' 32.858" N	Panchsheel ngar	two storey	2
74° 38' 10.646" E	26° 30' 34.951" N	Panchsheel nagar2	multi storey	10
74° 38' 13.514" E	26° 30' 34.969" N	Panchsheel nagare	multi-storey	10
74° 38' 27.431" E	26° 30' 32.907" N	Panchsheel nagar5	new construction multi-storey	10
74° 38' 26.856" E	26° 30' 33.419" N	Panchsheel naar6	multi-storey	10
74° 38' 56.381" E	26° 30' 15.792" N	Near globl public school	new three storey	3
74° 40' 56.064" E	26° 30' 17.588" N	Mds university jipur road	three storey	3
74° 40' 57.210" E	26° 30' 18.183" N	New consgfunctuon mds road	new multi-storey	10
74° 37' 36.705" E	26° 29' 43.290" N	Castle royal vaishli ngr	new multi-storey	10
74° 37' 27.513" E	26° 29' 37.083" N	Vaisali nagar 1	new three storey	3
74° 37' 23.923" E	26° 29' 37.119" N	Vaishli nagar 2	new two storey	2
74° 37' 23.262" E	26° 29' 37.699" N	Vaishali nagar3	new two storey	2
74° 33' 11.970" E	26° 29' 34.237" N	Newconstru tionpush	new two storey	2
74° 33' 32.643" E	26° 29' 24.822" N	Multistoreupushroad	four storey	4
74° 33' 16.069" E	26° 29' 26.439" N	Muktistryconspushar	multi storey	10
74° 39' 0.631" E	26° 29' 18.651" N	Vishwamitra bhavan lohagarh road	five storey	5
74° 39' 0.509" E	26° 29' 18.076" N	Shastri nagar 2	five storey	5
74° 34' 8.154" E	26° 29' 19.340" N	Pushkar road newmulti	three storey	3

74° 33' 57.067" E	26° 29' 16.788" N	Pushlar roadmuktistry tajgardn	two storey	2
74° 33' 45.076" E	26° 29' 15.569" N	Pushkarzbaktideephsptl	five storey	5
74° 33' 46.207" E	26° 29' 14.894" N	Multistrypushfoad	five storey	5
74° 33' 39.840" E	26° 29' 12.965" N	Muktistriespushrdbithside	five storey	5
74° 36' 35.049" E	26° 28' 56.878" N	Haribhau nagar new construction	three storey	4
74° 36' 35.020" E	26° 28' 55.881" N	Haribhahu multi2	five storey	5
74° 36' 33.938" E	26° 28' 52.651" N	Haribhau multi3	six storey	6
74° 36' 4.501" E	26° 28' 47.956" N	Haribhau multistorey houses	three storey	4
74° 36' 0.385" E	26° 28' 47.427" N	Haribhahu upadhyay nagar multi	three storey	4
74° 36' 2.172" E	26° 28' 32.359" N	Azad ngr multi redidential	multistoreys	10
74° 35' 50.640" E	26° 28' 22.977" N	Pragati nagar multiresidential	multistoreys	10
74° 35' 29.907" E	26° 28' 23.910" N	Pragati nagar multistprey constr	multistoreys	10
74° 36' 8.012" E	26° 28' 19.794" N	Azad ngr multi	multistoreys	10
74° 38' 51.051" E	26° 28' 6.259" N	Rilwaycoloneymultistories	mmultistoreys	10
74° 36' 56.593" E	26° 27' 56.884" N	Krishna coloney ramnagar	three storey	4
74° 36' 47.335" E	26° 27' 47.260" N	Foysagar road multi,storey	new four storey	4
74° 36' 45.752" E	26° 27' 47.536" N	Foy sagar road multistorey	three storey	3
74° 35' 38.843" E	26° 27' 22.064" N	Foy sagar rawat nagar hotel grand	multistorey _6-7floor	6
74° 40' 10.357" E	26° 27' 10.241" N	Madarroad twostories	three storey	3
74° 35' 15.780" E	26° 26' 56.106" N	Near foy sagar ddvelopmnt	twos storey	1
74° 39' 53.070" E	26° 26' 44.740" N	Singlestoriess	two storey	3
74° 39' 9.731" E	26° 26' 29.052" N	Mehu road underconstruction	two storeys	2
74° 38' 57.124" E	26° 25' 41.391" N	Bihari gnjmultistorey	three storeys	4
74° 39' 3.522" E	26° 25' 25.081" N	Adarshnaar multistorey	two storeys	3
74° 39' 1.781" E	26° 25' 28.704" N	Adarshngr construction multistory	new three storey	4
74° 39' 11.311" E	26° 25' 5.522" N	Adarsh nagar new,construction	new three storey	5
74° 39' 5.642" E	26° 24' 7.574" N	Single stories bewar road	single storey	2
74° 38' 22.953" E	26° 23' 31.514" N	Bewar road	new four storey	5

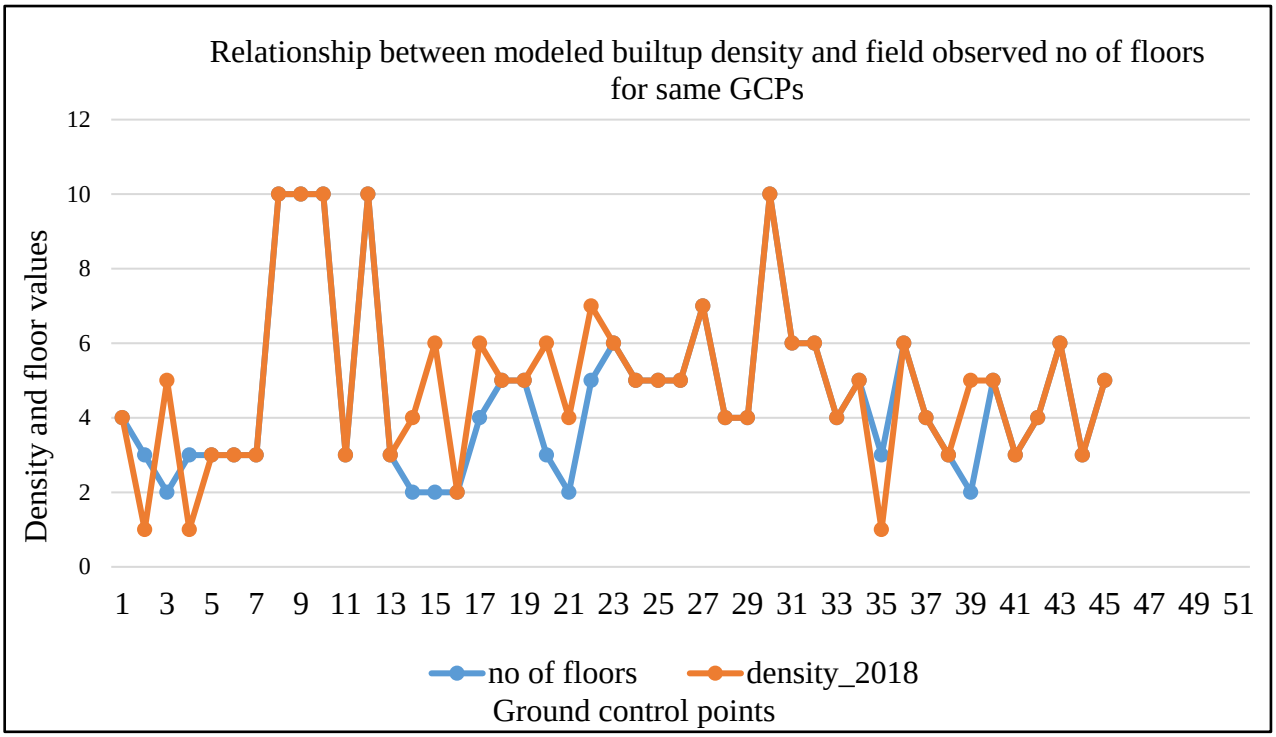

Figure 6.47: Relationship between field observed no. of floors and modeled built up density for the same GCP's

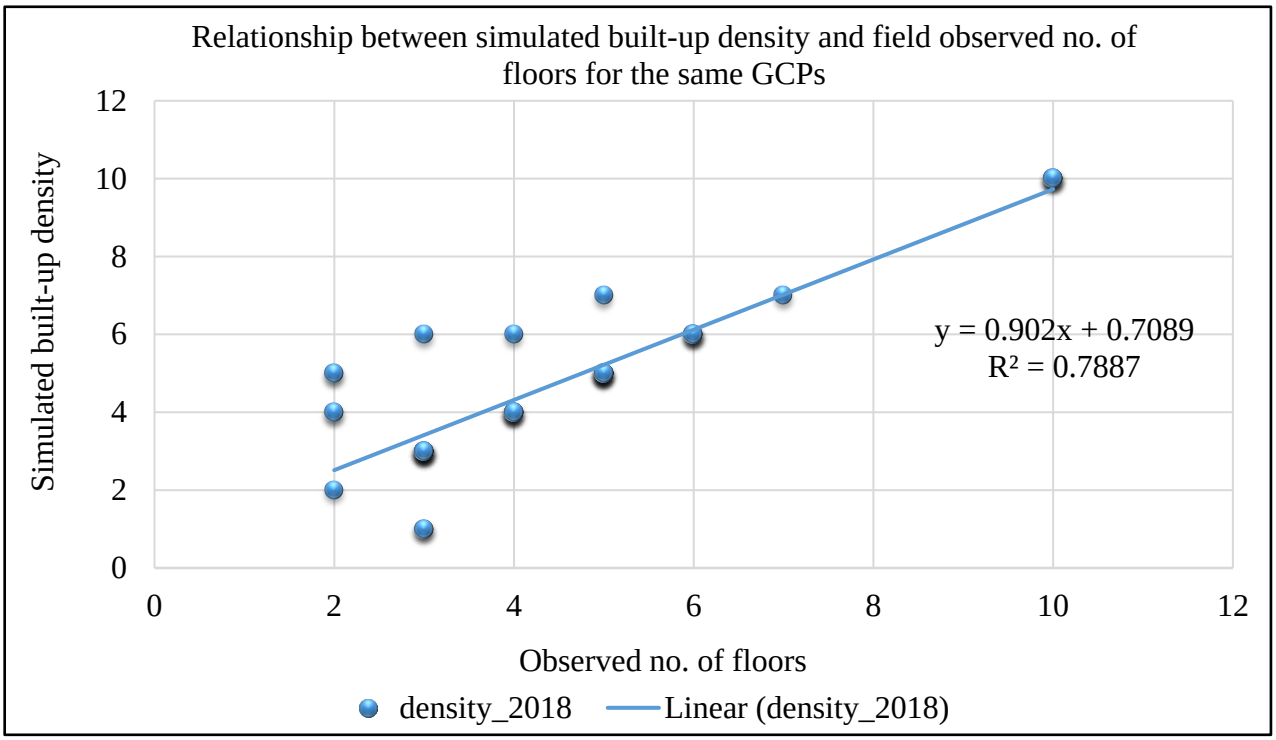

Figure 6. 48: Relationship between field observed no. of floors and modeled built up density for the same GCP's on a scatter plot

The above discussion leads to the successful field validation of simulated built-up density results obtained from SLEUTH-Density. The results are quite good and satisfactory in simulating the built-up density. At a few places, some differences between the no. of floors and built-up density class value have been noticed. However, these differences were not so significant as to misinterpret the density values.

Table 6.3: Accuracy assessment of estimated built-up density with field validation

Accuracy assessment (%)	
SLEUTH-Density	75%

Figure 6. 49: A picture showing multi-storey at Pushkar road

Further research is required to validate the SLEUTH-Density results for different study areas in different socio-economic conditions. Also, the land use change and urban growth modelling are regional application-based study and having a closer idea or approximation of built-up density for a location by the modelling would be a good approach in giving solutions to many urban planning issues.

Figure 6. 50: A picture showing multi-storey at Panchsheel Nagar

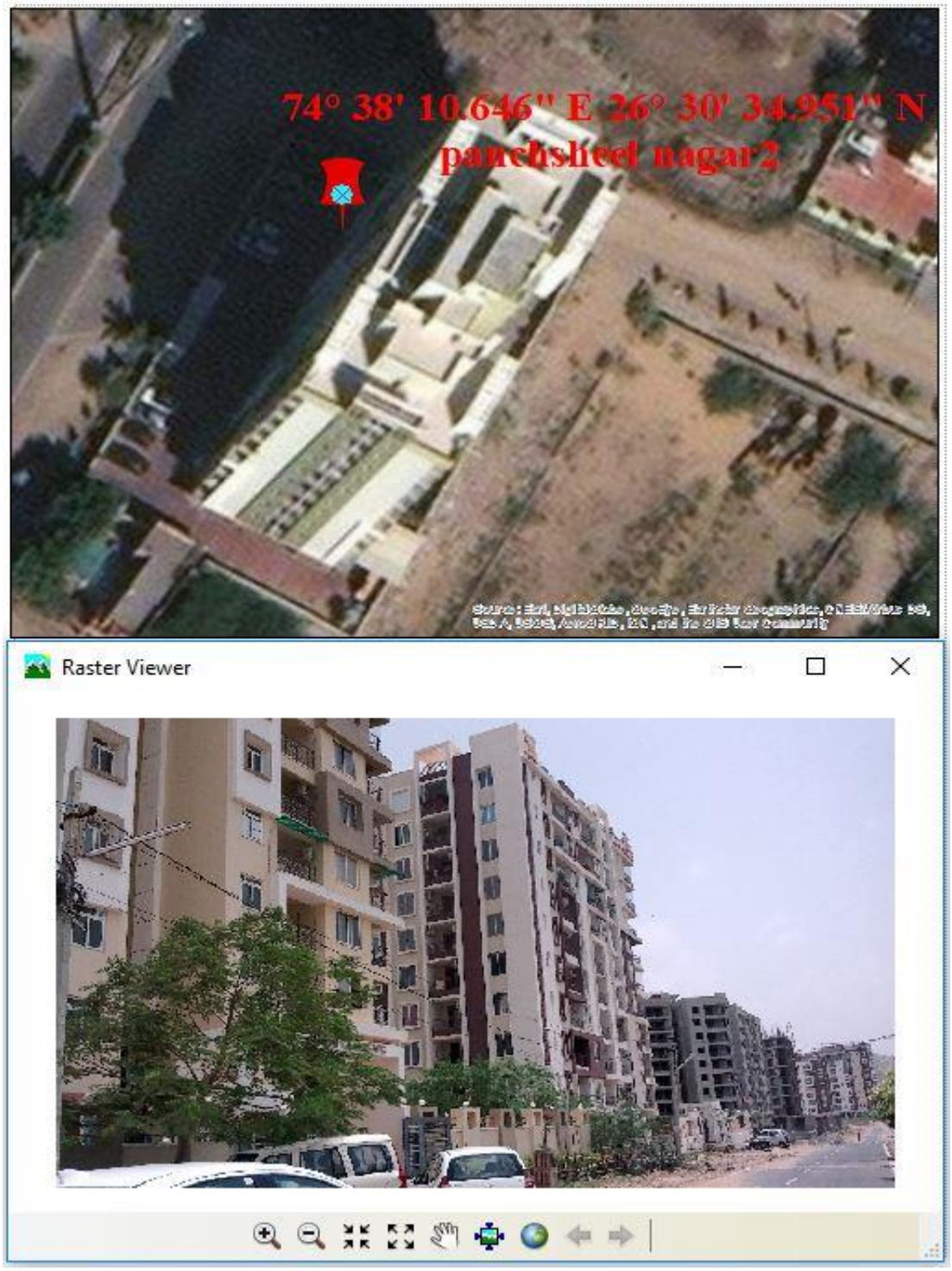

Figure 6. 51: A picture showing multi-storey at Panchsheel Nagar 2

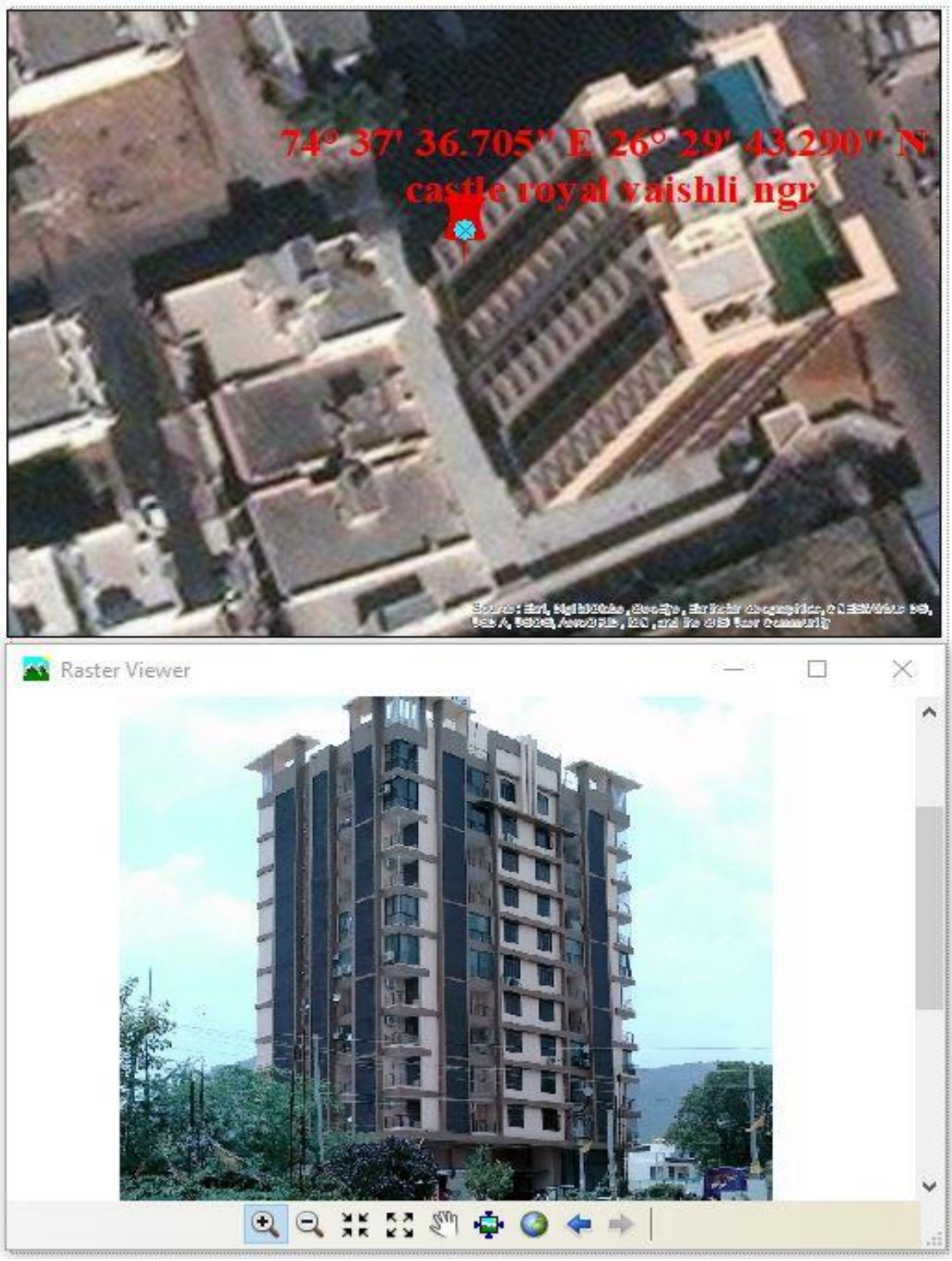

Figure 6. 52: Picture showing multi-storey 'Castle Royal' at Vaishali Nagar

6.4.5 Demonstration of application of SLEUTH-Density Model

The application of SLEUTH-Density has been demonstrated for Ajmer fringe. The built-up density was simulated for up to the year 2040 after successful model parameterization and calibration. The study is successful in identifying the probable locations which are prone to get denser built-up activities in upcoming years.

Ajmer fringes are quite large spatially and therefore, to better interpret the estimated built-up density results were classified ward-wise and related with the demographic characteristics. The present study has used an updated municipal corporation ward map of Ajmer obtained from the official website. The map was first geo-referenced in ArcGIS software using municipal boundary map as a reference map. The UTM WGS 84 zone 43°N was used as projection and coordinate system. The ward map was digitized then and respective ward numbers were assigned to each ward. In addition, ward population was also stored against respective wards of Ajmer. The current ward map includes 60 wards and the newly added 6 wards of Ajmer lacks various details like population, literacy rate, male and female population etc.

In the present study, built-up density has been related to the three identifiers of density i.e. urban intensity, urban density, and vertical growth. Here, the cumulative term i.e. built-up density is representing all the three indicators of density. To establish the relationship of simulated built-up density with urban density, intensity, and vertical growth ward wise interpretation has been done.

6.4.5.1 Ward wise built-up density

Present section discusses built-up density in different wards. The study reveals that ward numbers 1, 2, 3, 60, 59, 58, 46, 45, 42, 41, 21, 23, 26 and 27 have observed increased built-up density over the years as compared to other wards. The built-up density was found to be higher over the years for outer wards than inner wards. This analysis suggests that built-up density would be higher in outer wards which lies on edges rather than in the central part of Ajmer. Such a result has also been in agreement with the validation of model results using other indices. The central part of Ajmer includes ward no. 50, 51, 54, 55, 56, 57, 43, 44, 33, 34, 35 and 19 which are showing very low built-up density and supports the model results. Here, lower built-up density does not suggest that these areas are vacant and no built-ups are there.

However, these areas have developed fully and growth has not been observed in the past few years, therefore, there is the least possibility of further development or vertical growth of the central part of Ajmer (Figure 6.53). The study signifies that outer areas of Ajmer along the main roads are developing rapidly as compared to the central part and have a higher probability to have higher built-up densities in the near future.

Since output maps are raster data and each cell represents different density values. To normalize the density number for an individual ward the mean built-up density for each ward was calculated which enhanced the understanding of ward-wise built-up density.

6.4.5.2 Ward wise mean built-up density

The ward-wise means built-up density was estimated for each ward which supported the inferences and helped in identifying the highly built-up wards. The mean built-up density for individual wards indicates the probability of getting denser in terms of horizontal as well as vertical urban growth and no. of people residing in relative terms. In the year 2018, mean built-up density for outer wards was found to be higher as compared to the inner wards. For ward no. 2, 5 and 53 the mean built-up density was found to be 50, 53 and 54 respectively which are the highest mean built-up density values in the year 2018. These wards have experienced rapid urbanization in the last few years due to the availability of residential and occupational suitable conditions.

The Pragati road in ward no. 2 connects to NH 89 which further connects to Ajmer-Pushkar road and based on historical data as well more urban growth has been experienced in these areas. Higher mean density values also validate the rapid urbanization in ward no. 2. The Kirti Nagar road in ward no. 5 connects to Foy Sagar road which has experienced a lot of urban development in recent years, therefore, a simulated density map has also shown relatively higher mean built-up density in ward no. 5. Ward no. 53 is connected to Dargah bypass road and dargah bazar road which is relatively high in mean built-up density. Ward no. 3, 8, 11, 20, 21, 22, 23, 25, 26, 27, 34, 39, 41, 42, 45, 46, 49 and 59 have experienced mean density values as 43, 42, 47, 45, 45, 50, 44, 40, 50, 44, 40, 50, 40, 47, 44, 46 and 40, respectively which are also representing relatively higher mean built-up density in these wards but not as high as ward no. 2, 5 and 53. These wards have also been found to be relatively more urbanized than the remaining wards, however, few among them have not experienced much change in built-up density due to the unavailability of suitable conditions for urbanization. Ward nos. 22, 23, 25, 26, 34, 39, 41, 45, 46, 49 and 59 have experienced a very small change in mean built-up density, as these are inner wards and have already densely urbanized years before thus, not much scope for further urban expansion horizontally as well as vertically. Therefore, built-up density simulation has also shown a higher density for these areas. The mean built-up density values for different wards is presented in Figure 6.54.

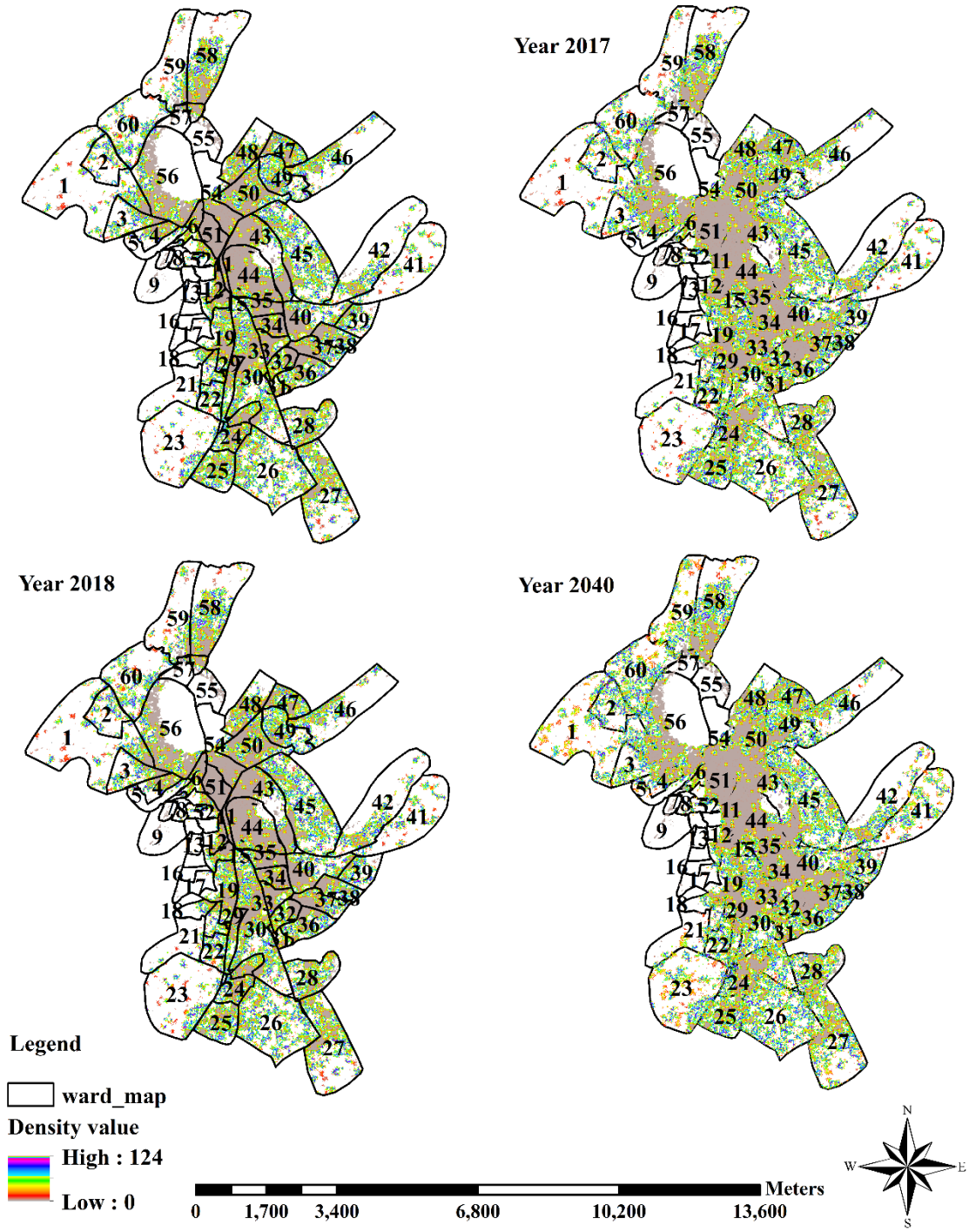

Figure 6. 53: Urban density in different wards in the year 2016, 2017, 2018 and 2040

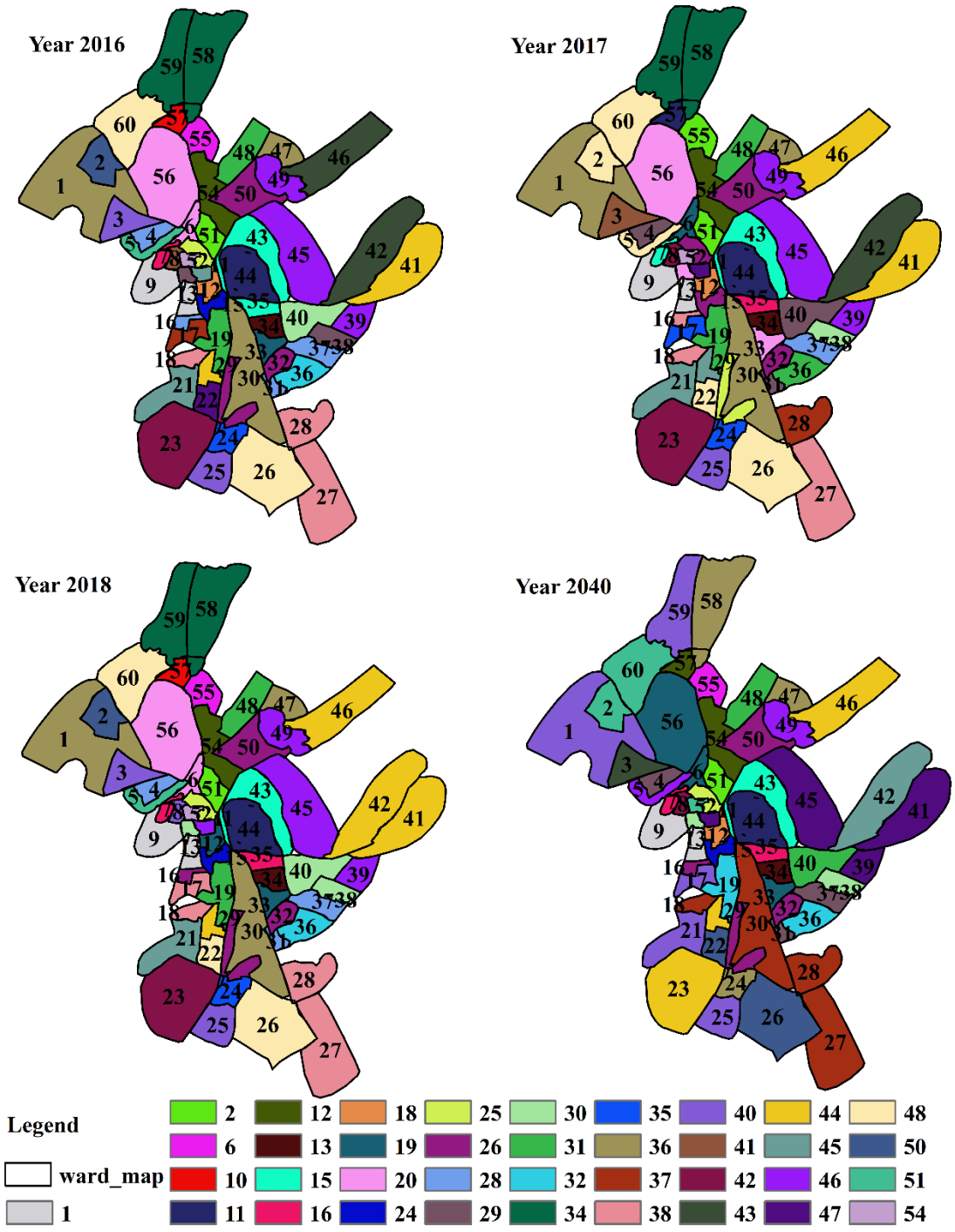

Figure 6.54: Mean urban density in different wards in the year 2016, 2017, 2018 and 2040

6.4.5.3 Wards with higher built-up density

For identifying wards which have a higher probability of high built-up density, ward-wise classification of built-up density was performed. The built-up density was classified into five classes i.e. very low, low, medium, high and very high based on the change in density from the year 2017 to 2018. The present study identifies the wards which have become

denser in the year 2018 than others. The study revealed that ward 45 and 60 have become denser than any other wards in the year 2017 which lie in the outer part of Ajmer city. Although, the inner or central wards have experienced a very low change in built-up density which includes ward no. 1, 2, 7, 9, 13, 14, 19, 22, 23, 25, 26, 28, 29, 30, 32, 33, 34, 35, 37, 38, 39, 40, 41, 43, 44, 45, 46, 47, 48, 49, 50, 51, 52, 53, 54, 55, 56, 57, 58, 59 and 60. Wards 4 and 15 have medium built-up density class. Built-up density has been found to change in wards 10 and 12 significantly. Highest change in built-up density from the year 2017 to 2018 has been observed for ward number 16 (Figure 6.55). The overall analysis clearly indicates that as moving from a very core part of Ajmer to slightly outer, significant increase in built-up density has been observed from the year 2017 to the year 2018. The outer wards are denser than inner wards and more likely to become denser in upcoming years. The obvious reason for getting built-up density higher at outer wards is the development of the transportation system, industries, educational institutions and colonies in these wards. The inner wards include older architecture and highly populated areas and further growth of those areas is near to impossible. Therefore, the only possibility of further development lies in the outer wards of Ajmer due to the higher suitability like open spaces, transportation facilities, and public services in these wards.
Furthermore, how the built-up density in different wards has been increased from the year 2017 to 2018 and most likely to be in the year 2040 also has been presented in Figure 6.56 and 6.57.

6.4.5.4 The relationship between built-up density and population (i.e. urban density)

To understand the estimated built-up density by the SLEUTH-Density model in terms of urban density (no. of household residing on per unit area) correlation has been established between built-up density and population for different wards. Figure 6.58 is showing that for high population built-up density is higher and vice-versa. However, it has been seen that few highly populated wards have shown lower built-up density. The possible reason is that the wards lie in the core part of Ajmer which is highly populated but in past few years, no further built-up development has been noticed in those wards i.e., 54 and 55. The SLEUTH-Density based built-up density module estimates density on the basis of urban growth taken place in the past few years. However, the outer wards are correctly matching the built-up density with the population density which further validates the model results (Figure 6.58 & 6.59).

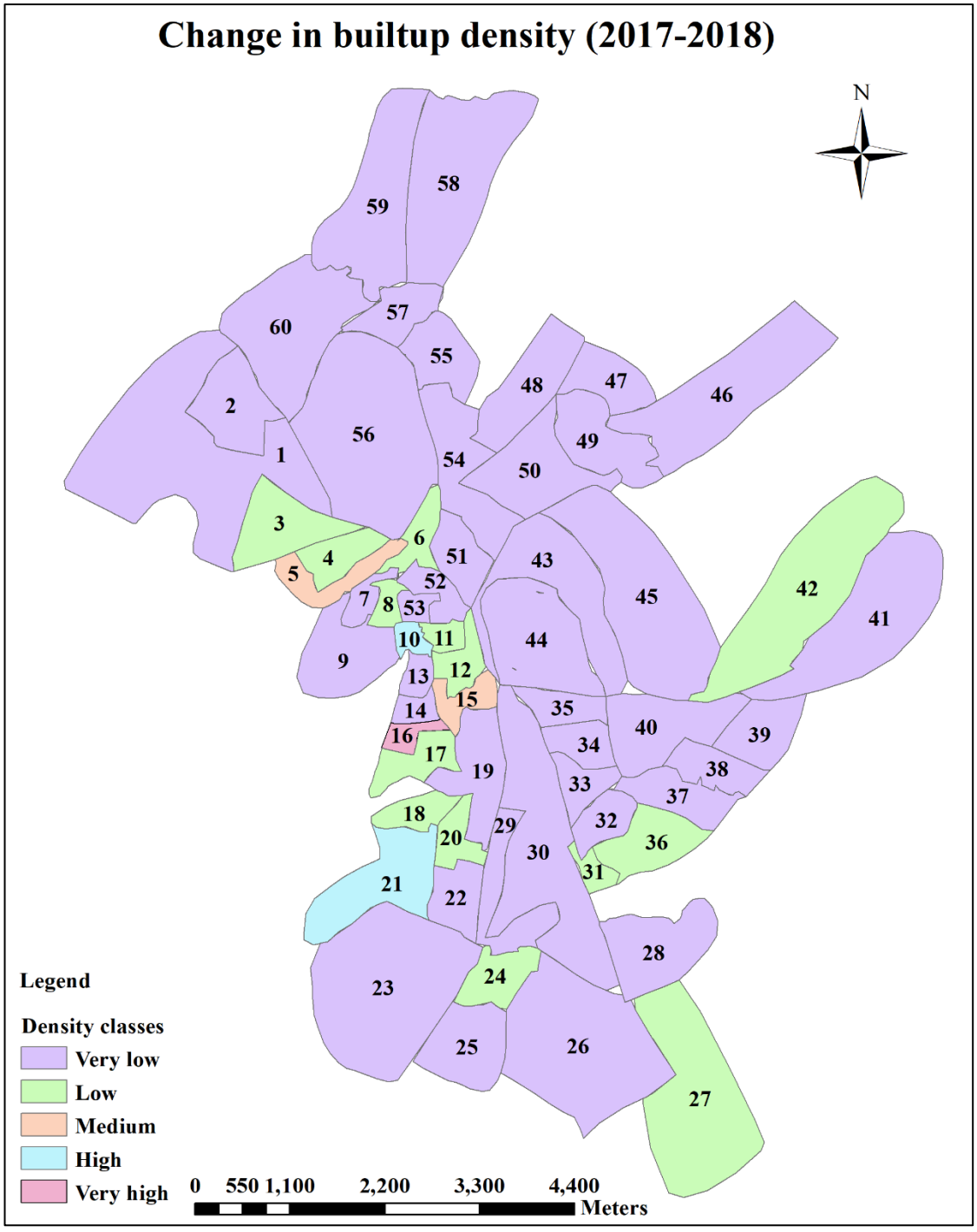

Figure 6.55: Change in built-up density from the year 2017-2018

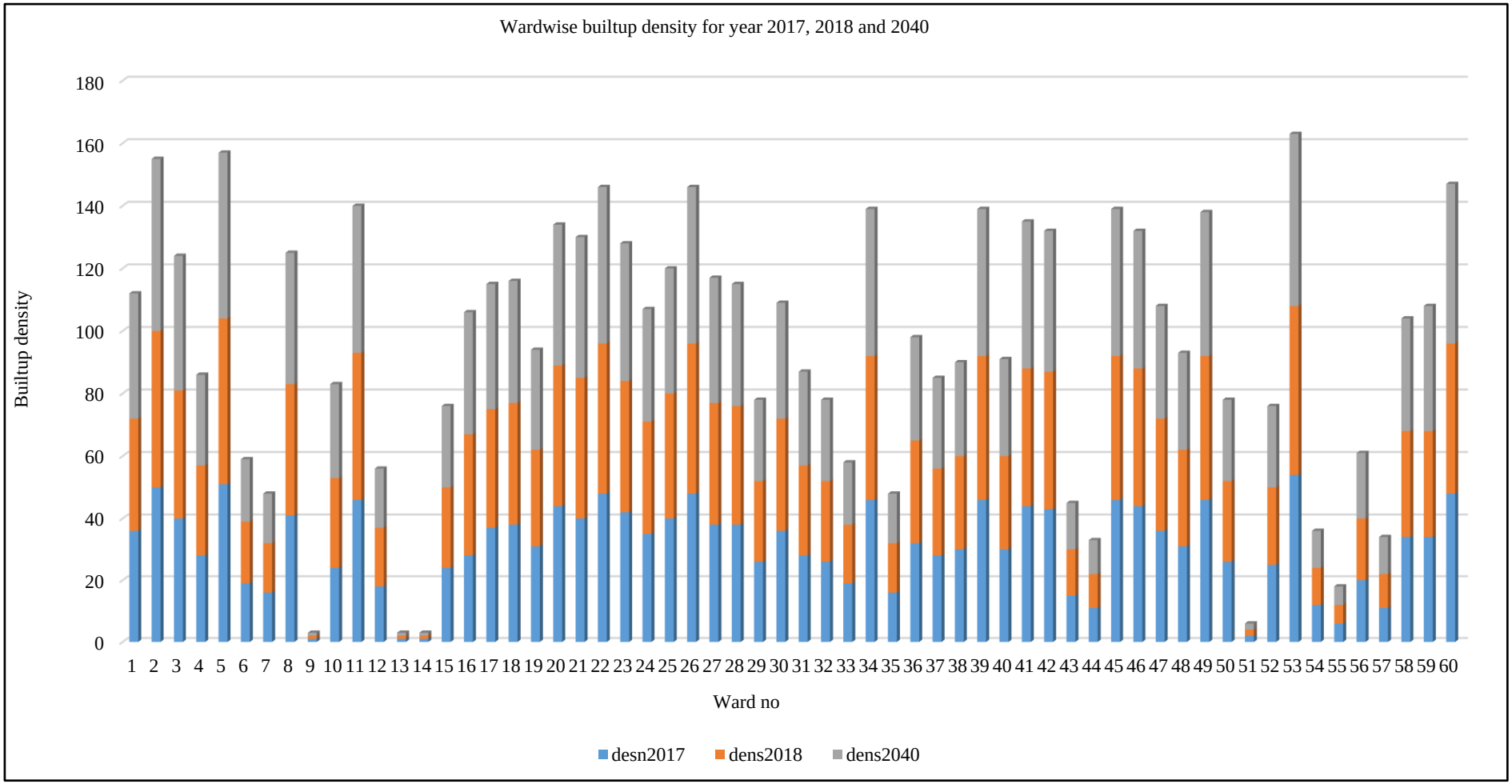

Figure 6. 56: Urban density in different years

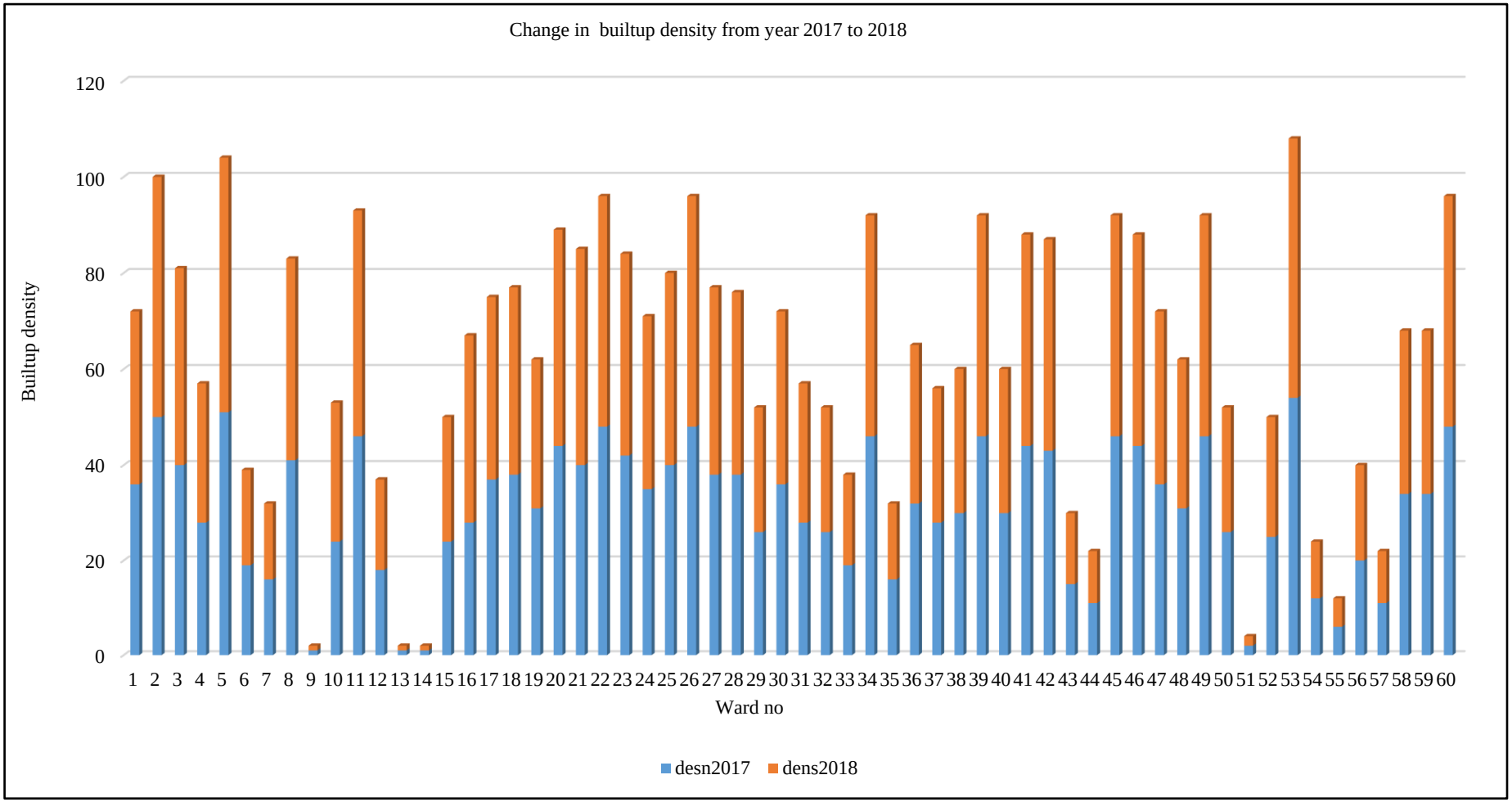

Figure 6. 57: Ward wise built-up density in the year 2017 and 2018

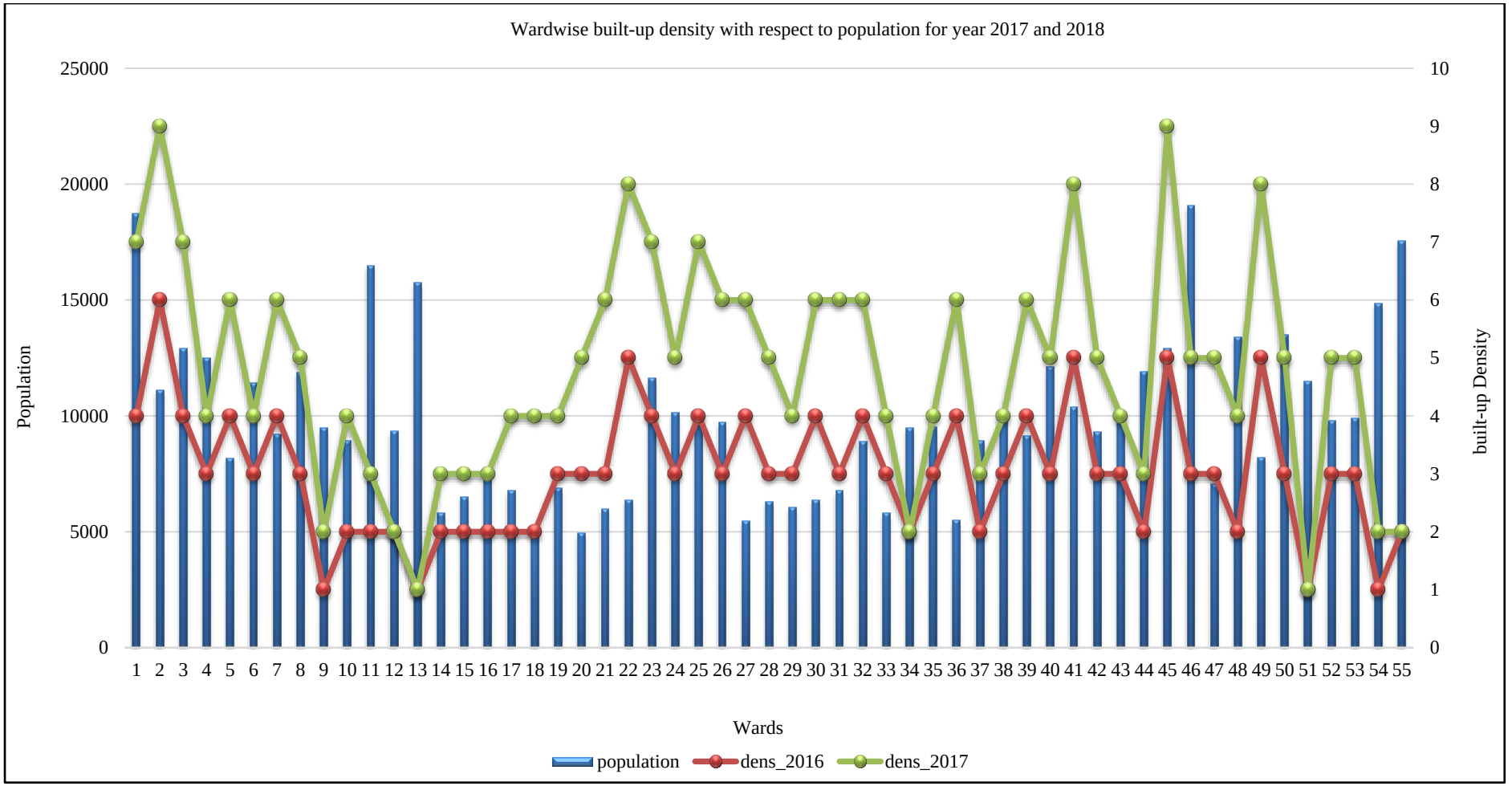

Figure 6.58: Relation between population and built-up density in different wards in the year 2017 and 2018

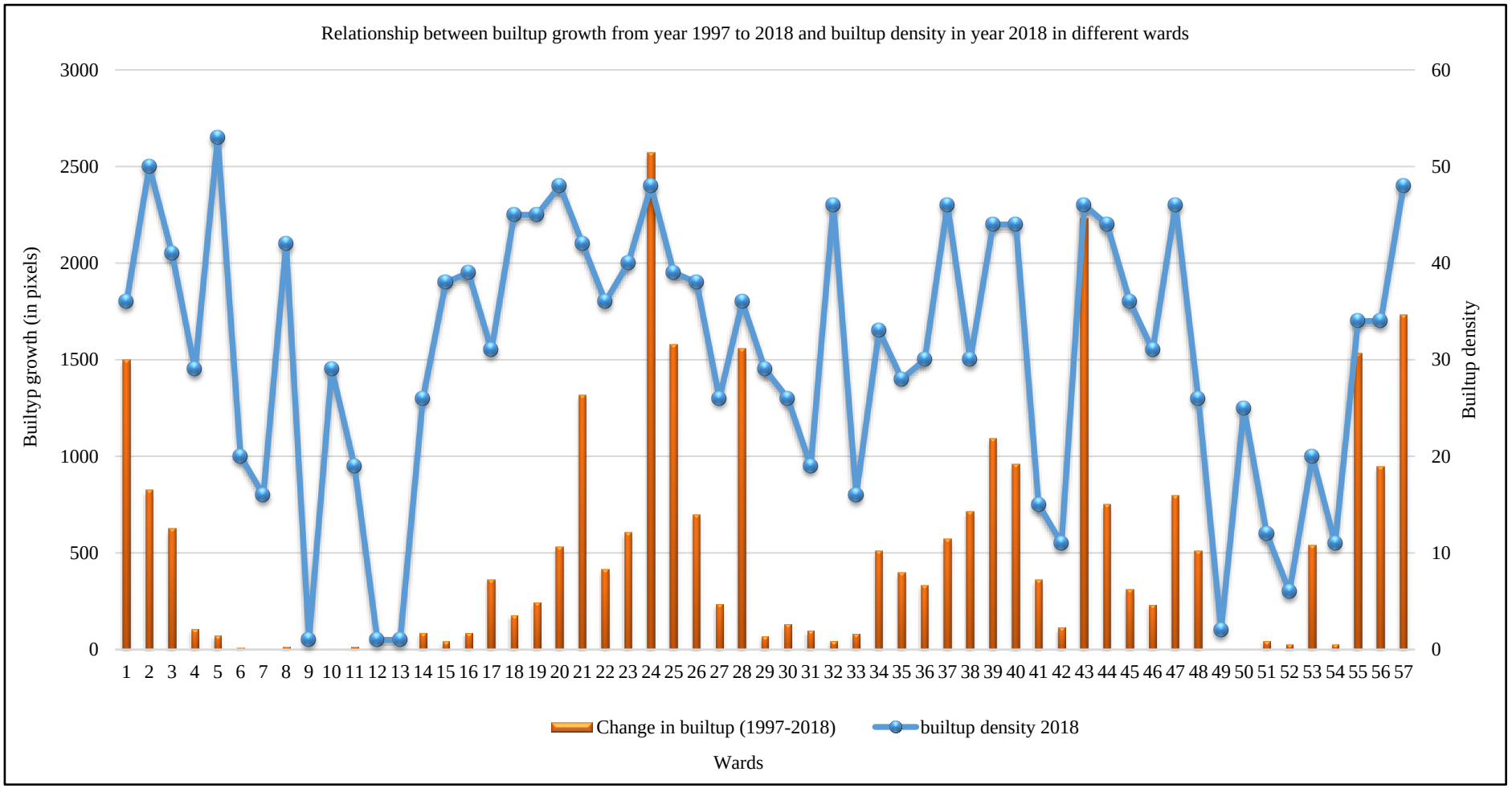

Figure 6. 59: Relation between change in urban growth (1997-2018) and built-up density in the year 2018 i.e. urban intensity

6.4.5.5 The relationship between built-up density and change in urban growth (i.e. urban intensity)

The relationship has also been established between change in urban growth from the year 1997 to 2018 and built-up density estimated using SLEUTH-Density. It can be seen from Figure 6.59 that the wards which have experienced low urban growth also have lower built-up density. On the other side, the wards which have experienced higher urban growth also have a higher built-up density (Figure 6.59). Results indicate that urban growth trend from the year 1997 to 2018 is satisfactorily matching with the built-up density in the year 2018. Such a relationship improves the understanding that as the urban growth takes place the built-up density will also increases, which suggests vertical growth. Here, built-up density can also be correlated with vertical growth or urban intensity. However, urban intensity and vertical growth are two different terms and it can be used with different urban planning perspectives. Built-up density is related to urban change which is higher for higher urban growth change wards which may directly relate with the term intensity. On the other side, for different years built-up density values have changed (mostly increased) for an individual ward without expanding into areal terms (Figure 6.57). Thus, the built-up density may possibly represent vertical growth which took place due to the higher suitability of those locations to further get urbanized. The suitability factors of SLEUTH-Density are roads, slope and new spreading centered clusters which help in selecting only those pixels repeatedly which fell into these suitability conditions. If a number of pixels are getting selected again and again for urbanization even after it has already urbanized, it indicates the potential of vertical growth. As we have observed from the ward-wise built-up density results that urban growth has not been taken places horizontally in the area, but have higher built-up density. Thus it indicates the possibility of vertical growth which can now easily be simulated using SLEUTH-Density model.

6.4.5.6 Visual analysis

The estimated built-up density was also validated visually by overlying built-up density map of the year 2018 over Google Earth image and the density values were compared with the ground condition. It was evident from Figure 6.60 that the area near Srinagar road has experienced urban growth of relatively higher built-up density (i.e. 50-90 density values) as compared to the rocky terrain side development i.e. built-up density (i.e. 1-10 density values). As revealed from the Figure 6.60, that near Chungi road higher built-up density

values were found to the corresponding high rise buildings. The area near Foy sagar has found to be of lower density as compared to the outer part of Foy Sagar area (Figure 6.60).

Figure 6. 60: Visual analysis of simulated/estimated built-up density

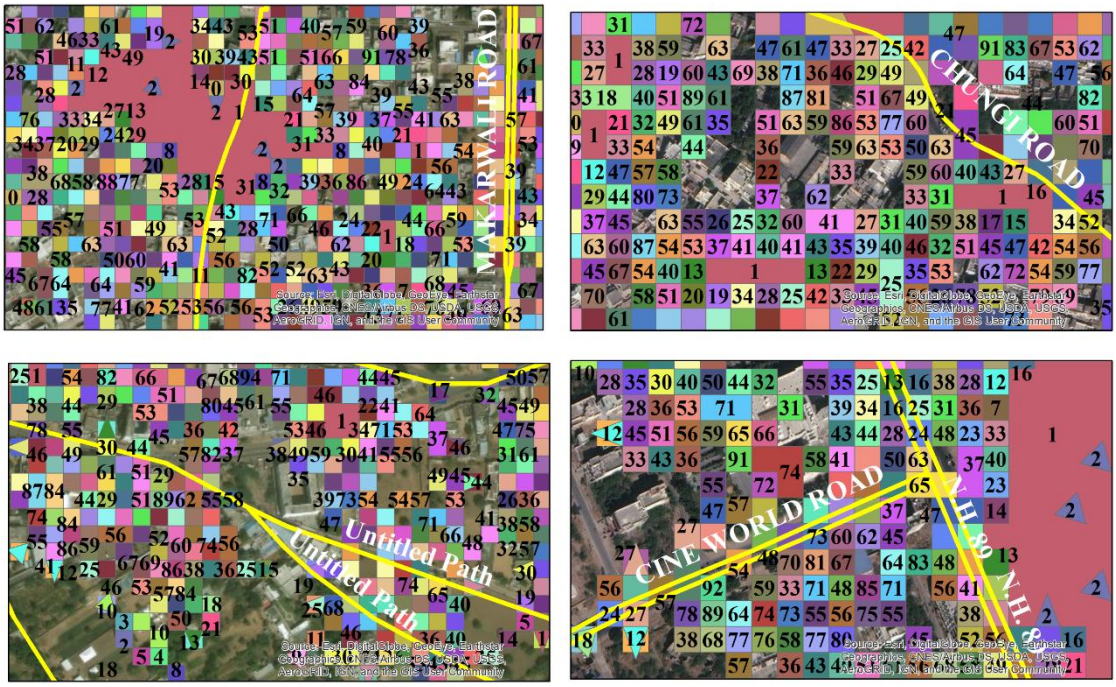

Figure 6. 61: Visual analysis of simulated/estimated built-up density

From a closer view of different locations (Figure 6.61) it can be seen that higher built-up densities have been found at the locations where multi-storey buildings are visible. The low rise buildings are having relatively lower density values as seen Figure 6.61.

6.5 Concluding Remarks

The SLEUTH model has been improved and a new version named SLEUTH-Density has been developed, which is capable of simulating the built-up/ urban density in addition to simulating the urban growth. A suitable algorithm has been developed to estimate built-up density, required programming code be written and integrated with the base SLEUTH code. SLEUTH-Density code was further tested for a demo dataset and found to be satisfactory and acceptable. The SLEUTH-Density model was successfully parameterized and calibrated using the methodology as discussed in Chapter 4. Further, built-up density was simulated up to the year 2040 for Ajmer fringes. Results indicate urban growth with higher built-up densities in outer areas of Ajmer along the main roads as compared to the central part of Ajmer. Since the central part of Ajmer has developed long before and it does not have suitable land and infrastructure facilities like good roads. Built-up density results have been validated with respect to a number of spectral and built-up indices which are representative of built-up density including LST. Normalized built-up density values at more than 100 randomly selected locations have been correlated with the values of different indices including LST. Trends of simulated built-up density are satisfactorily matching with the trends of the different indices including LST, which indicates the satisfactory and acceptable performance of SLEUTH-Density. Model results were also validated through the ground truthing and found to be satisfactory. The further model application was demonstrated by simulating the built-up density for Ajmer fringe. Built-up density was also analyzed at the ward scale. Results indicate that outer wards may have a higher built-up density as compared to the central part because of availability of suitable land, better infrastructure facilities, and road connectivity.

CHAPTER 7
DEVELOPMENT OF SLEUTH-SUITABILITY

7.1 Prologue

While simulating urban growth using the original SLEUTH model with its default model parameters, it was observed that performance of the model can be further improved by addressing two possible limitations. First, suitable values of model parameters need to be identified and second, the influence of a few important LULC change and urban growth explanatory variables (identified from the literature) should be included in the simulation process like land cost, distance from main roads, distance from facilities like bus stand, railway station, recreational sites etc. as discussed in Chapter 2. The present version of SLEUTH simulates urban growth by considering four growth rules which operate upon few input variables i.e., slope, land use, urban, road network and exclusions. However, there are many important variables, as mentioned above, which affect the urbanization process significantly and urban growth can be better modelled by their inclusion in the simulation process. Considering all such variables in terms of land suitability growth decision rules, the present version of model can be improved so that it can capture different forms of urban growth like fragmented, scattered, road influenced, small size urban growth etc. more realistically. A land suitability variable represents the relative desirability of a particular piece of land for development for different uses. The first limitation of the model was addressed by determining optimal values of different model parameters and by testing their sensitivity, as discussed in Chapter 5. To address the second limitation of the model, an effort has been made to develop a newer version of the SLEUTH i.e., SLEUTH-Suitability by developing a suitable algorithm to include a new growth rule in terms of land suitability into the simulation process. The effect of few important urbanization explanatory variables like land cost, important proximity variables like distance from main roads, distance from facilities like bus stands, railway stations, recreational sites etc. have been integrated into a land suitability decision variable using AHP based on the MCE technique. Appropriate code has been written to implement the land suitability growth rule and integrate it with the existing SLEUTH code. Development of the SLEUTH-Suitability model which includes development of the algorithm, writing of code, integration of the code with the existing model and model testing is discussed in this chapter. Further, development of a land suitability decision layer using AHP based on MCE technique, sensitivity testing of AHP

weights and model accuracy assessment is also discussed in this chapter in subsequent sections.

7.2 Introducing Land Suitability into SLEUTH Decision Making

SLEUTH, despite being a popular model for LULC change and urban growth modelling, can further be improved by incorporating the influence of important urbanization explanatory variables/ drivers like land cost, proximity to important roads, hospitals, recreational places, bus stands and railway stations into the simulation process. In a study, Wu and Webster (1998) proposed an integrated approach of MCE (Multi-criteria Evaluation) and Cellular Automata (CA) to employ transition rules for urban growth simulation. Li et al. (2008) integrated MCE with CA to simulate urban growth for the Pearl River Delta. Li and Liu (2008) applied agent-based modelling in conjunction with CA to develop alternative growth patterns for the Pearl River Delta. However, very few studies have been reported in which major growth influencing variables were included into urban growth modelling using the SLEUTH model. Mahiny and Clarke (2012) proposed an integrated approach of MCE and SLEUTH which combined the land suitability layer with the exclusion layer to simulate urban growth. Yin et al. (2015) applied different ecological sustainable scenarios through the exclusion layer in SLEUTH to incorporate the ecological sustainable policies in urban growth simulations. Mahiny and Clarke (2013) came up with an idea of incorporating hydrological influence on urban growth with the help of MCE in SLEUTH modelling. Mahiny and Gholamalifard (2011) also integrated MCE with the SLEUTH model for the dynamic allocation of sites. Although, inclusion of some important explanatory variables into the SLEUTH model actually can improve the urban growth modelling in consideration with sustainable policies still needs to be studied in detail. In most of the previous studies, urban growth was simulated by considering land suitability and other variables as a part of exclusion layer to reflect the effect of land use policies on urban growth. There were no studies found which can employ urban suitability considering various explanatory variables into the urban growth modelling process. Inclusion of land suitability as a decision rule will eventually enhance the reliability of the model by enforcing modelling outcomes towards more realistic growth predictions. Multi-criteria Evaluation (MCE) is specifically used for integrating multiple raster layers to arrive at a single land suitability layer. The inclusion of the urban suitability layer prepared from MCE considering various socio-economic, proximity, topographic and ecological variables into

the SLEUTH modelling may entail more desirable modelling outcomes. The SLEUTH model derives growth rules in calibration phases followed by self-modifying rules. Since the model requires less user intervention to devise the growth rules therefore, studies only modified or combined the exclusion layer with the suitability layer to reflect suitability in to modelling outcomes. However, to combine the exclusion layer with suitability may not give impressive results as transition rules will perform randomly and suitability factor cannot be treated as a random phenomenon but deterministic. Therefore, a new version of the model i.e., SLEUTH-Suitability has been developed to include one more growth rule i.e., land suitability into simulation process at each stage of urban growth rules decision making during model calibration as well as prediction phases. In doing so, the suitable code was written in the C programming language to include the land suitability algorithm into the existing code of SLEUTH successfully and named as SLEUTH-Suitability. Further SLEUTH-Suitability code was tested and validated at each stage of the growth rule implementation during calibration to arrive at whether it is giving outcomes for what it is developed.

7.3 Materials and methods used for development of SLEUTH-Suitability

Ajmer fringe has been selected as the study area for the demonstration of the application of SLEUTH-Suitability and to investigate the land suitability decision rules sensitivity to the AHP weights for individual urbanization explanatory variables. Required model input layers for the preparation of the land suitability decision layer and model parameterization have been extracted from the GIS database, as discussed in Chapter 3. Input data used in the present work includes the slope layer in percent, hill shade for depicting background, historical urban maps of year 1997, 2000, 2008, 2013 and 2015, road network layers of year 1997, 2000, 2008, 2013 and 2015, the exclusion layer which prohibit important natural reserves from being urbanized and land suitability layers of year 1997, 2000, 2008, 2013 and 2015 which includes LULC change and urban growth explanatory variables with relative desirability or potential of land for development.

7.3.1 LULC change and urban growth drivers and factors

LULC change and urban growth is a function of different drivers/explanatory variables such as neighborhood, proximity, demographic, socio-economic, institutional, suitability, biophysical drivers and restrictive variables (Park et al., 2011; Romano et al., 2005; Li et al., 2018; Wentz et al., 2018)

- **Neighborhood** variables include human choices and preferences for building houses, for example, a person would be more interested in constructing his/her house on the basis of neighboring conditions like proximity to residential areas, city center cleanliness etc.
- **Proximity** variable includes distance to market, distance to road, distance to hospitals, distance to railways, distance to highways, and distance to schools etc. which influences the urbanization process.
- **Demographic** variables like population density, literacy and other variables related to population represent demand for development and also affects urbanization process and urban growth.
- **Socio-economic variables** and drivers like land cost, time to travel, opportunity cost, tradition, status, education etc. affect the development decisions and choices of individuals about the development
- **Institutional variable** affects the decision taken by managerial authorities relating to the construction, nearby already established industries and institutions.
- **Suitability of land for different purposes also affects the developmental choices.**
- **Economic variables** like land tenure, farm size, income may be important factors to be considered while making choices of development.
- **Climatic drivers** like climatic variability, life zones are the factors which individual consider while building their houses.
- **Bio-Physical drivers** like topography, elevation, slopes, soil types, altitude also affect the decision making of development and construction and
- **Restriction variables** which comprise a prohibited area for development such as reserved forest, green belt, historical places, airport side area etc. The detailed list of explanatory variables and driving factors of LULC change and urban growth is presented in Table 7.1.

A LULC changes and urban growth drivers are important and may be applicable in general for all locations and urban areas like topographical slope, land cost, proximity to public services and transportation network, neighborhood variables and demographic factors like population growth. Population growth has been one of the major growth influential parameters which increases the demand for development and also affects the land and infrastructure. Proximity to important roads has been another growth influential parameter and applicable to every city and town. With development and improvement in road

transportation, networking terms of increased road/railway connectivity with important places and suburbs promoted the urbanization at fringes and outskirt. Thus, proximity to main roads influences urbanization extensively.

Table 7.1 Explanatory variable of land use change and urban growth (Park et al., 2011; Romano et al., 2005; Li et al., 2018; Wentz et al., 2018)

S.no.	Class of Explanatory Variables	Variables
1	Neighborhood	proximity to residential areas, city center cleanliness etc.
2	Proximity	distance to market, distance to road, distance to hospitals, distance to railways, distance to highways, and distance to schools etc.
3	Demographic	population density, literacy and other variables related to population
4	Socio-economic variables	land cost, time to travel, opportunity cost, tradition, status, education etc.
5	Institutional variable	Industries and institutions.
6	Suitability	land suitability factor for building houses, agriculture etc.
7	Economic variables	land tenure, farm size, income
8	Climatic drivers	climatic variability, life zones
9	Bio-Physical drivers	topography, elevation, slopes, soil types, altitude
10	Restriction variables	reserved forest, green belt, historical places, airport side area etc.

Other important facilities like educational, recreational market and job potential also promote migration of people into cities and thus affects the process of urbanization and demand for development.

Some other parameters like proximity to hospitals, recreational places and bus stand & railway stations also affect the demand for the development of any place and play a crucial role in decision making for urbanization. Therefore, in the present work few important urbanization explanatory variables like topographic slope, land cost, proximity in term of distance from road network, distance from facilities like railway station, bus stand and recreational places and hospitals have been selected to develop the land suitability decision layer which will make the basis of land suitability growth rule in SLEUTH-Suitability.

7.4 Development of Urban Suitability Module

The SLEUTH-Suitability model development consists of the development of an algorithm to include one more urban growth decision variable i.e., land suitability in the simulation process, development of the computer program and integration with the existing SLEUTH code. SLEUTH-Suitability uses six raster input data layers i.e. land suitability, slope, urban area, exclusion, transportation layers and hillshade for different control years. The land suitability growth decision variable explain the influence of different selected urbanization explanatory variables as discussed in previous sections. The SLEUTH code has been modified to include another land suitability urban growth decision rule in the growth simulation process. The model is a scale-independent CA, the growth rules are uniformly employed throughout a gridded structure of a geographical space and applied on a cellular basis. One iteration of the CA corresponds to a single time span and all changes are applied at the end of each time period synchronously. The initial conditions and the set of growth rules are integral to the data set being used since they are defined in terms of the natural and physical characteristics of the area under study. The calibration process evokes the model adapting its local environment with the help of explanatory variables and rules. The urban seed layer is the initial condition to start the process, the growth occurs one pixel or cell at a time with the independent role of each cell. The urban patterns emerge during growth cycles as the urban organism learns more about its surroundings and neighborhood.

The initial year layer is the seed urban information and the extent is decided based on historical maps. The rules are applied on a cell at a time and the complete cellular grid is updated at the completion of an annual iteration. The modified array forms the basis for further urban expansion in every succeeding year. The potential of cells or pixels for urbanization is checked by selecting pixels randomly. The growth rules check the potential of cells and their neighbors like whether they are already urban or not, what their topographical slope is, how near they are to a road, whether it is a part of the exclusion layer and what their land suitability weight is. The decision of a pixel to become urban is based on a set of weighted probabilities along with mechanistic growth rules that inhibit or encourage growth.

Five growth coefficients i.e. diffusion, breed, spread, slope resistance, and road gravity control the system behavior as explained in Chapter 4 in detail. The diffusion coefficient determines the overall dispersion of the urban distribution outwardly; breed coefficient specifies how likely a newly detached urban cell is to begin its own growth

cycle; spread coefficient controls how much organic expansion occurs from the existing urban; slope resistance coefficient influences the likelihood of urban growth extending up steeper slopes and road gravity coefficient attracts new urbanization towards and along roads.

There are four growth rules constituted by the model i.e. spontaneous, new spreading center, organic and road influenced. The spontaneous growth occurs when a randomly drawn pixel falls in a suitable location for urbanization and simulates the fragmented urban forms with the influence of existing urban on their surroundings. The new spreading center growth allows these newly spontaneous urban pixels to start their own growth cycle on land which is flat enough and suitable for the desirable location of urban development.

The phase 1 n 3 comprises these two growth rules i.e. spontaneous and new spreading center growth. The organic or spread growth promotes outward expansion from the existing urban cores which reflects the nature of all urban areas to expand. Phase 4 includes organic or spread growth. The road influenced growth encourages road side urban development which reflects increased accessibility and it falls under phase 5 as given in Figure 7.1.

Each rule passes through a set of conditions which include, whether the pixel or cell is already urban or not, whether the slope of that pixel is suitable for urbanization, whether it is a part of prohibition or exclusion and whether the pixel lies in the desirable range of a weighted land suitability decision variable. Land suitability decision variable participates in urbanization decision of pixels after each growth rule through 1 to 5. The decision of urbanization of each pixel by any rule has to pass the land suitability decision rule. In the present study, initially, the decision of the slope variable is executed separately. Further, the slope variable was integrated with the land suitability decision variable as one of the urban growth explanatory variables. After successfully passing through each urban growth decision the pixel becomes urbanized which ensures more realistic urbanization due to an added decision of land suitability variable into the simulation process.

SLEUTH-Suitability version also uses the same calibration process as SLEUTH. Calibration performance and selection of optimum growth coefficients have been measured in a similar way with the help of a model fitness metric i.e., OSM. The visual analysis is one of the most important parts in the initial phases of calibration to establish growth coefficient ranges and to have a rough idea about the parameter settings. It is also important

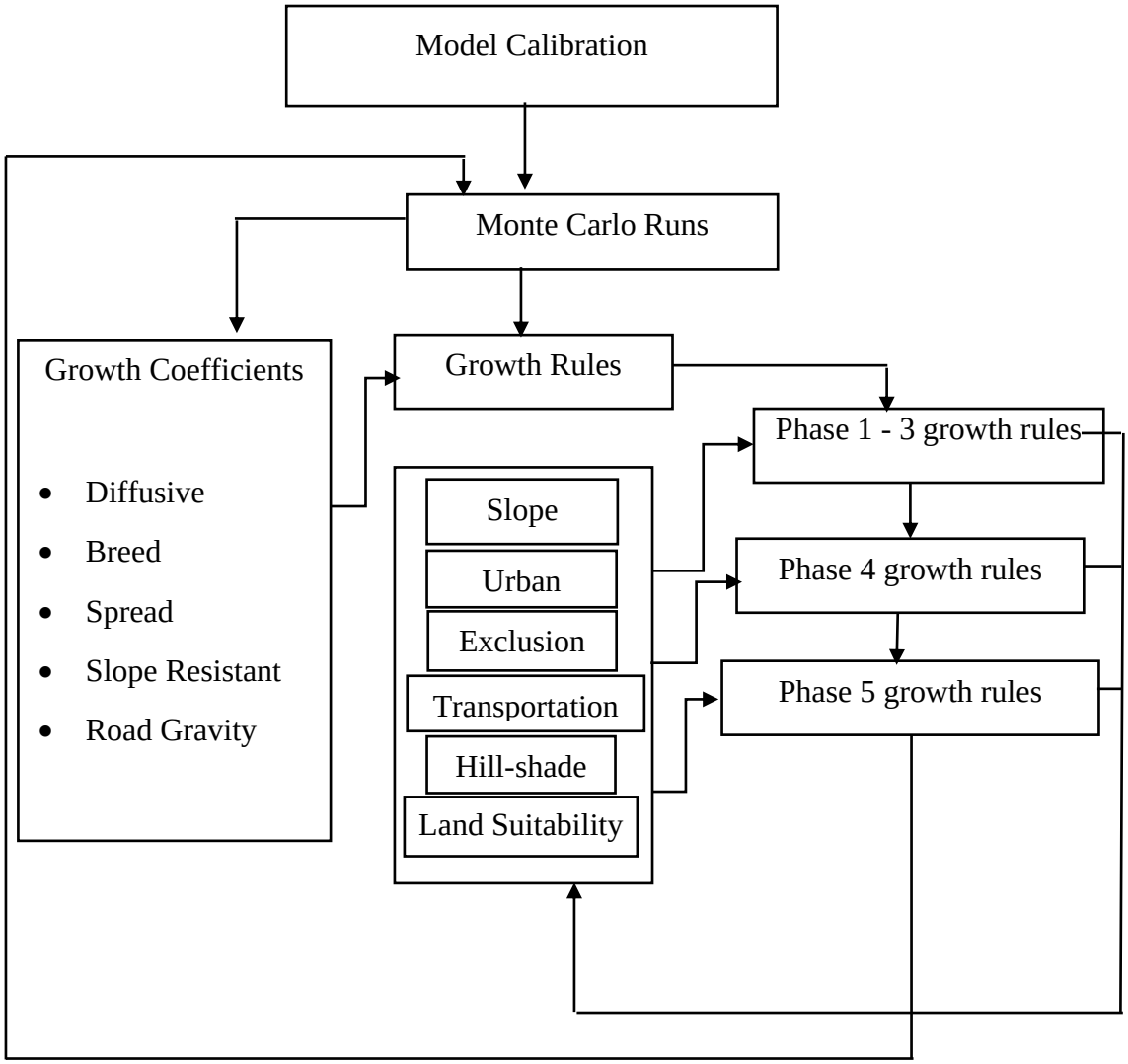

Figure 7.1: Methodology for the development of SLEUTH-Suitability

to verify the fact that the model is actually replicating the urban spatial pattern and extent of historical growth which couldn't be determined by statistical measures alone. Once several initial parametric settings passed the visual maps, the model was again passed through the goodness of fit comparisons of various spatial and statistical measures & metrics. The comparison of visual maps played an important role during initial phases of calibration. Statistical metrics consisted of computing Pearson's correlation coefficient (r^2) for several parameters e.g. area, edges, clusters, cluster size, radius, slope, xmean, ymean, %urban etc. for the modeled and actual urban area in the controlling years. Methodology of model calibration and development of SLEUTH-Suitability has been explained in Chapter 4.

The programming code has been written for the inclusion of land suitability growth decision variable and was tested at each stage to check the consistency with the model outcomes.

7.5 Testing of SLEUTH-Suitability Program

After the development of the land suitability version of SLEUTH, it was tested using a demo input dataset to ascertain its correct functioning. The land suitability growth decision variable has been incorporated in the algorithm for making urbanization decisions of unorganized pixels along with each urban growth rule. The land suitability decision rule is directly involved in all the growth rules of the model during all the calibration phases. The algorithm validation has been performed roughly for a demo dataset of small extent. The dataset was prepared which included four years of historical urban maps (i.e. 2000, 2008, 2013 and 2015), two years of roads layers (i.e. 2013 and 2015), one slope, one exclusion, and one land suitability layer. Here, we have prepared a dummy suitability layer of a grid size of 14*12 and cell size of 16 meters by assigning land suitability weights by some random numbers in between 1-12 to each cell (Figure 7.2).

Model testing includes generating urban growth output maps at each step of the implementation of each growth rule after parameterization of the model with the required data (demo data). This process gives an insight about the internal working of the SLEUTH-Suitability algorithm. In addition, cumulative growth from each stage of growth rule implementation was also compared with a single output grid which was generated after completing the prediction of growth for the respective year. The urban growth model consists of four growth rules driven by five growth coefficients, which sequentially executes in a loop for a total number of Monte Carlo iterations. For the input dataset, we assumed prediction best fit coefficient values for testing of the SLEUTH-Suitability algorithm.

Best fit values for diffusion, breed, spread, slope resistant and road gravity growth coefficients were adopted as 15, 24, 20, 60 and 70, respectively. The decision of a pixel being urbanized passes through a set of conditions including land suitability also at five stages of urban growth simulation. The idea is to check whether the newly inserted land suitability decision grid works well with all the growth rules. For just evaluating we put up a condition in programming that an attempted pixel should be urbanized if it lies in between 5 and 10 value of land suitability weights. We took empty grids for storing each decision taken at every single stage of growth rules and named it as, one, two, three, four and five. In addition, for intermediate attempts of urbanization in the individual grid is numbered starting from 0 (i.e. One_0, One_1 and so on).

First, the SLEUTH-Suitability passes through growth phase 1 n 3 rules which itself includes diffusive growth and new spreading center growth, therefore, grid One and Two will be produced to store intermediate stages of employing growth rules with suitability. The diffusive value was first calculated to perform diffusive growth using Eq. 7.1.

diffusive_value = ((diffusion_coeff * 0.005) * sqrt (rows_sq + cols_sq)) … 7.1

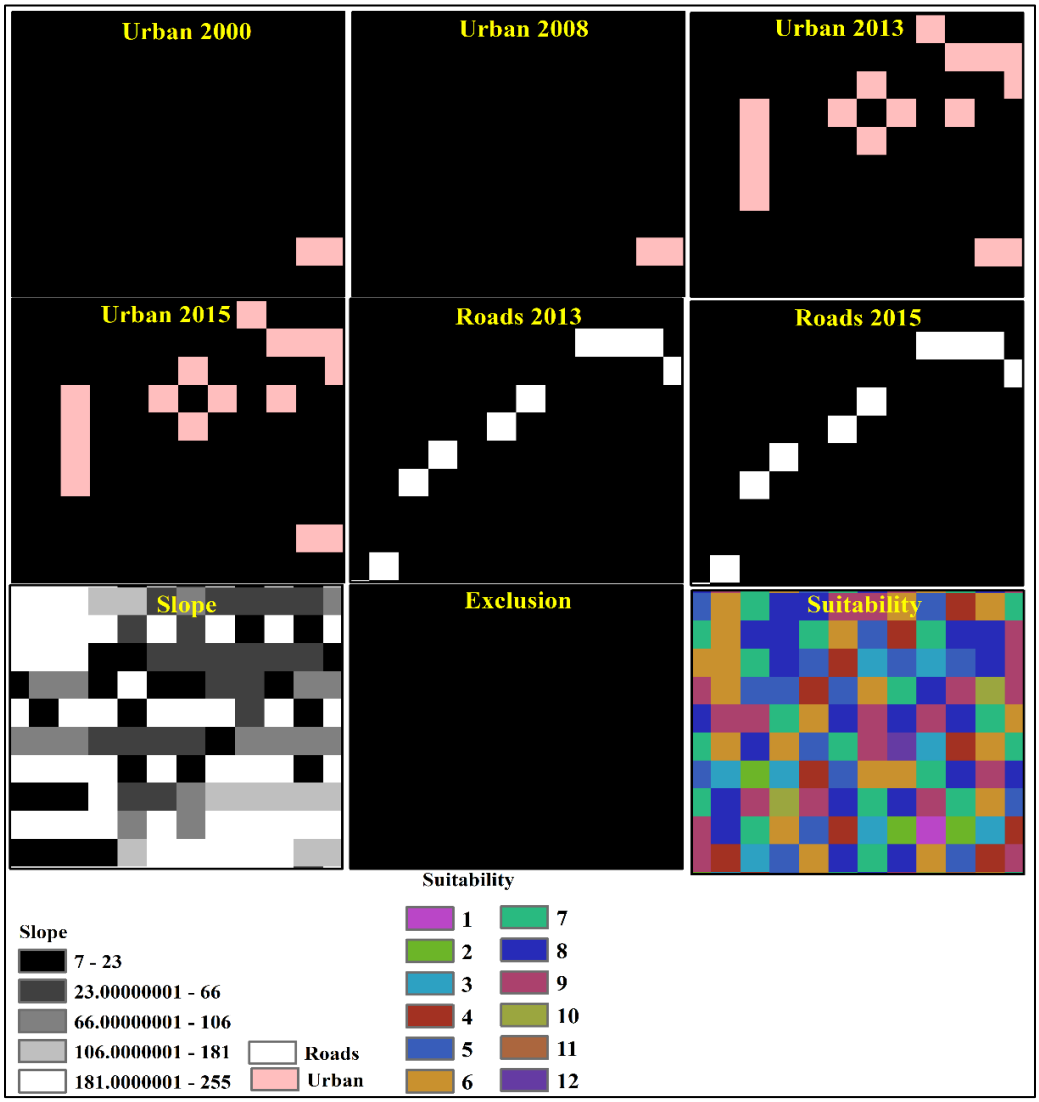

Figure 7.2: Demo input dataset for SLEUTH-Suitability program testing

Here, the best-fit diffusion coefficient, number of rows and number of columns are 15, 12 and 14, respectively for the demo data. So, the calculated diffusive value would be 1.45. Diffusive growth can take place until the diffusive value does not reach as;

for (k = 0; k < 1 + (int) diffusive_value; k++)

(Here, the diffusive value is 1 and the loop will continue up to 2 tries)

{

For first diffusive value, a random pixel from the grid is attempted to get urbanized.

}

This randomly selected pixel will pass through a set of conditions if it finds all true then only it may get urbanized. The set of conditions are as,

```
if (selected pixel is not already an urban pixel in input grids)
 {
   if (it is not urbanized in previously  performed growth rules)
   {
     if (it passes through a slope weights conditions)
     {
       if (it is not a pixel from the exclusion layer)
       {
          if ( the land suitability weight lies between 5 and 10)
            {
                        Pixel will get urbanized;
                }}}}}
```

The first pixel attempted to get urbanize in a grid One_0 was rejected and could not be urbanized due to the land suitability value for the pixel does not lie between 5 and 10. In the second attempt i.e. One_1, a pixel found suitable with the suitability of 8 and became urbanized. After becoming urbanized the counter passed through the random test for new spreading center growth rule (i.e. if (RANDOM_INT (101) < (int) breed_coefficient)) in which a randomly generated number is found greater than the breed coefficient value, therefore, it could not pass the breed test. Again, for the next diffusive value, a pixel was attempted to get urbanized and it successfully became urbanized with the land suitability value of 9 (i.e. > 5). Now, the diffusive value completes and the counter will go to the next phase of growth rule i.e. random spread coefficient test. The first pixel of the grid was attempted and passed through the random spread test as if ((pixel is already an urban pixel) && (RANDOM_INT (101) < spread coefficient)). Since the first pixel of the grid is not an urban so it could not pass this ‘if’ condition and also couldn’t proceed for the urban land

suitability decision rule. Similarly, the process will go on for each pixel of the grid and whenever it passes an 'if' statement successfully as discussed above it will again check for a set of conditions. In our case, only a single time was a pixel attempted to finally urbanize but rejected due to some conditions but not because of land suitability (see the grid Three_0 in Figure 7.3). After completing phase 1 n 3 and phase 4 rules the counter pass to the phase 5 rules.

The breed coefficient would be used to calculate the road influenced growth here in phase 5 as given below;

For (iii = 0; iii < 1 + (int) (breed_coefficient); iii++)

{

Determine the max index into the glb_rd_search_indices array using Eq. 7.2-7.6 and for this search radius start making the search for road pixel. If road found then try to urbanize neighboring pixels.

}

The breed coefficient is 24, so, it will be passing through 25 times to randomly attempt a pixel to get urbanized. Using the road gravity value which is calculated by Eq. 7.2, maximum road search index was determined (using Eq. 7.2 to 7.6). The road pixel would be searched for this maximum search index.

$$rg\_value = (rg\_coeff/MAX\_ROAD\_VALUE\ ) * ((row + col)/16.0) \ldots\ldots\ldots\ldots (7.2)$$

$$int\_road\_gravity = spr\_GetRoadGravValue(road\_gravity)\ \ldots\ldots\ldots\ldots\ldots\ldots (7.3)$$

$$\max\_search\_index = 4 * (int\_road\_gravity * (1 + int\_road\_gravity))\ \ldots\ldots (7.4)$$

$$\max\_search\_index = MAX(\max\_search\_index, nrows)\ \ldots\ldots\ldots\ldots\ldots\ldots\ldots\ldots\ldots (7.5)$$

$$\max\_search\_index = MAX(\max\_search\_index, ncols)\ \ldots\ldots\ldots\ldots\ldots\ldots\ldots\ldots\ldots (7.6)$$

If the road pixel is found, then it will check its neighboring pixels to get urbanized. If it becomes true, it further checks its surrounding pixels for a maximum three times to get urbanized.

In the first attempt of phase 5 rules a pixel couldn't pass the set of urbanization tests and is rejected for becoming an urbanized pixel but not because of suitability conditions (see grid Four_0 in Figure 7.3). In the next attempt of phase 5 rules, a pixel was attempted to get urbanized but rejected because of suitability failure (see grid Four_1 in Figure 7.3). In

another attempt, again a pixel couldn't be urbanized due to lesser suitability i.e. 5 as in grid Four_2 in Figure 7.3. Again, a pixel was not successfully urbanized due to the failure in the set of conditions of urbanization but not because of the suitability in next few attempts as in grid Four_3 and Four_4. In the next attempt, a pixel was successfully urbanized with the suitability of 6 i.e. grid Four_5. In grid Four_5, a new pixel was urbanized, therefore, the control now will be transferred to another rule of phase 5 in which surrounding pixels were tested to become urbanized for a maximum three times.

In the first attempt, a pixel was urbanized as its suitability is 8 (see grid Five_0 in Figure 7.4) and the second attempt rejected the pixel from becoming urbanized as land suitability is 4 (see grid Five_1). In the third attempt of this rule, a pixel couldn't be urbanized due to the failure of a set of conditions of urbanization but not because of the land suitability decision rule (see grid Five_2). After completing the second phase of phase 5 rules the control was transferred to the first phase of phase 5 rules. In an attempt, a pixel was rejected due to the suitability failure (see grid Four_7). In another attempt pixels were rejected from becoming urbanized due to the failure of urbanization conditions (see grid Four_8 and Four_9). However, in the next attempt a pixel got urbanized as the suitability of the pixel was 7 (see grid Four_10; Figure 7.5). Whenever a pixel successfully gets urbanized in the first phase of growth rule 5, it is intended to pass through the second phase of phase 5 rules which are performed in three consecutive steps. In the first attempt, a pixel was rejected from being urbanized due to land suitability failure (see grid Five_6). In the next attempt a pixel was urbanized as land suitability of that pixel was 6 and the third attempt did not succeed in making a pixel urbanized due to the failure of sets of conditions of urbanization excluding the land suitability decision rule (see grid Five_7 and Five_8). After completing this second phase of phase 5, again control was transferred to the first phase of phase 5.

The next three attempts resulted into the unsuccessful attempts to urbanize due to the failure in the set of conditions of urbanization but not because of the land suitability decision rule (see grid Four_11, Four_12 and Four_13 in Figure 7.6 & 7.7). In the next

attempt also an unsuccessful attempt for urbanization was made however, this time it failed because of the land suitability decision rule (see grid Four_14).

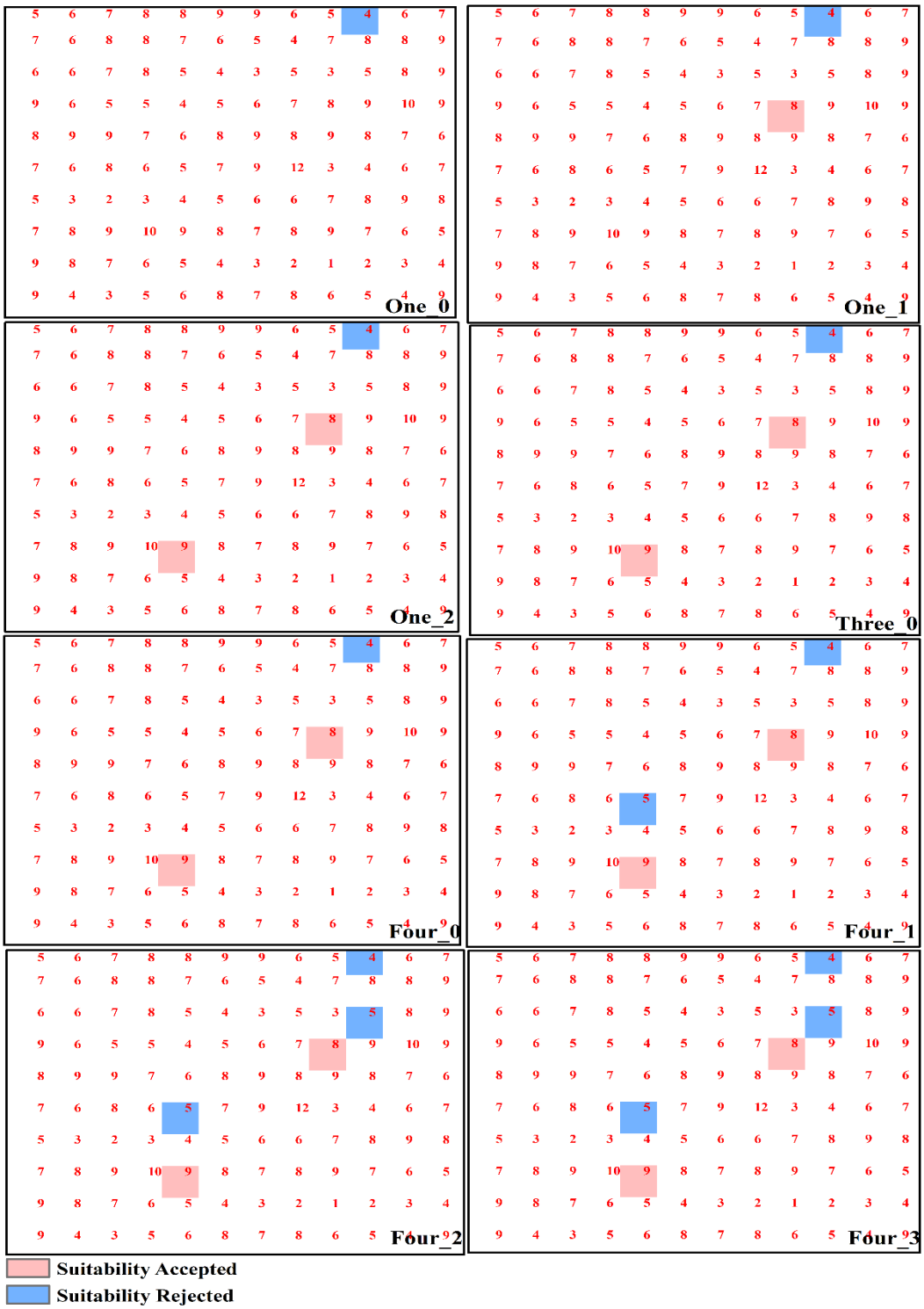

Figure 7.3: SLEUTH-Suitability program testing outcomes (a)

In the next two attempts also, the pixels didn't get urbanized due to the failure of urbanization conditions excluding land suitability decision (see grid Four_15 and Four_16).

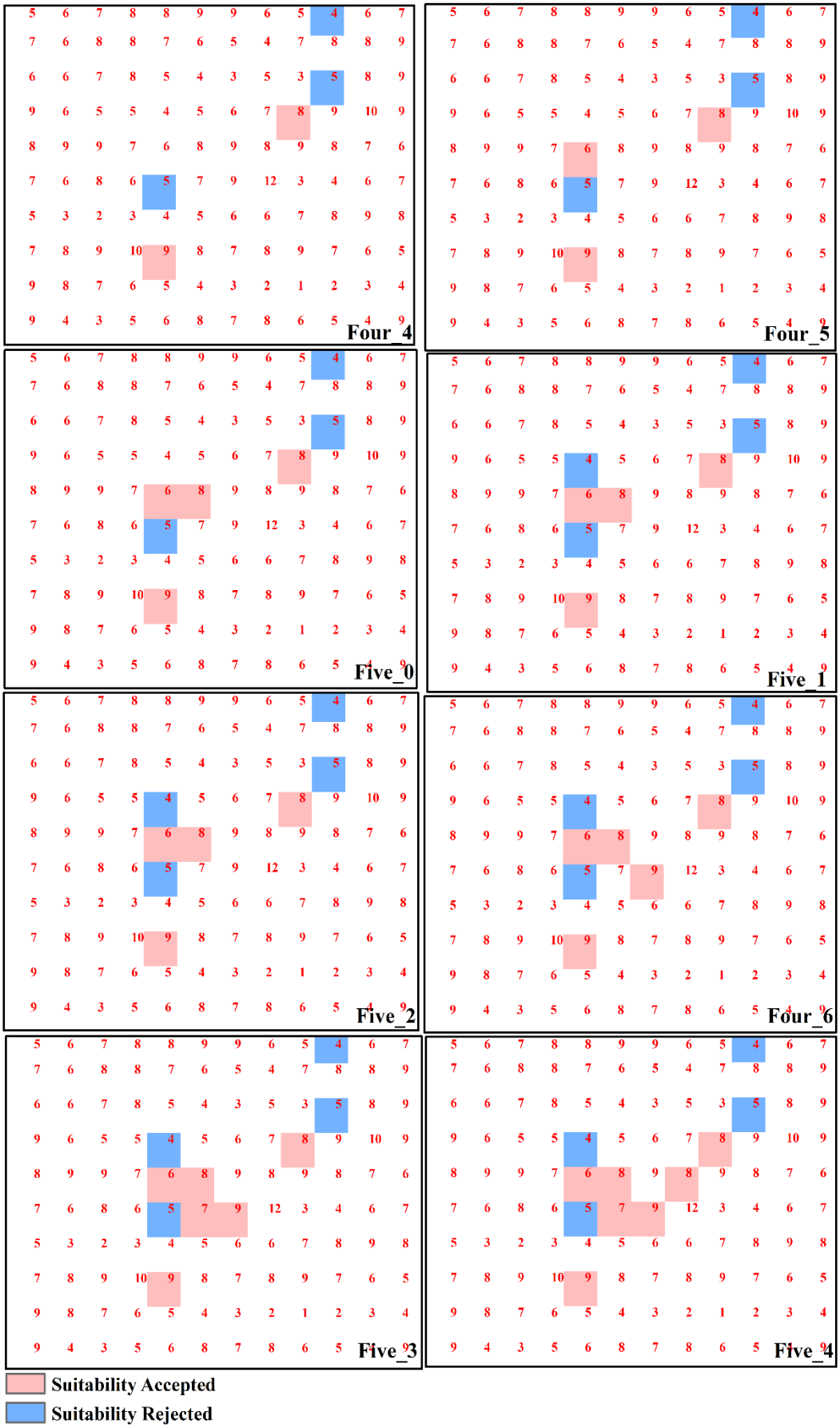

Figure 7.4: SLEUTH-Suitability program testing outcomes (b)

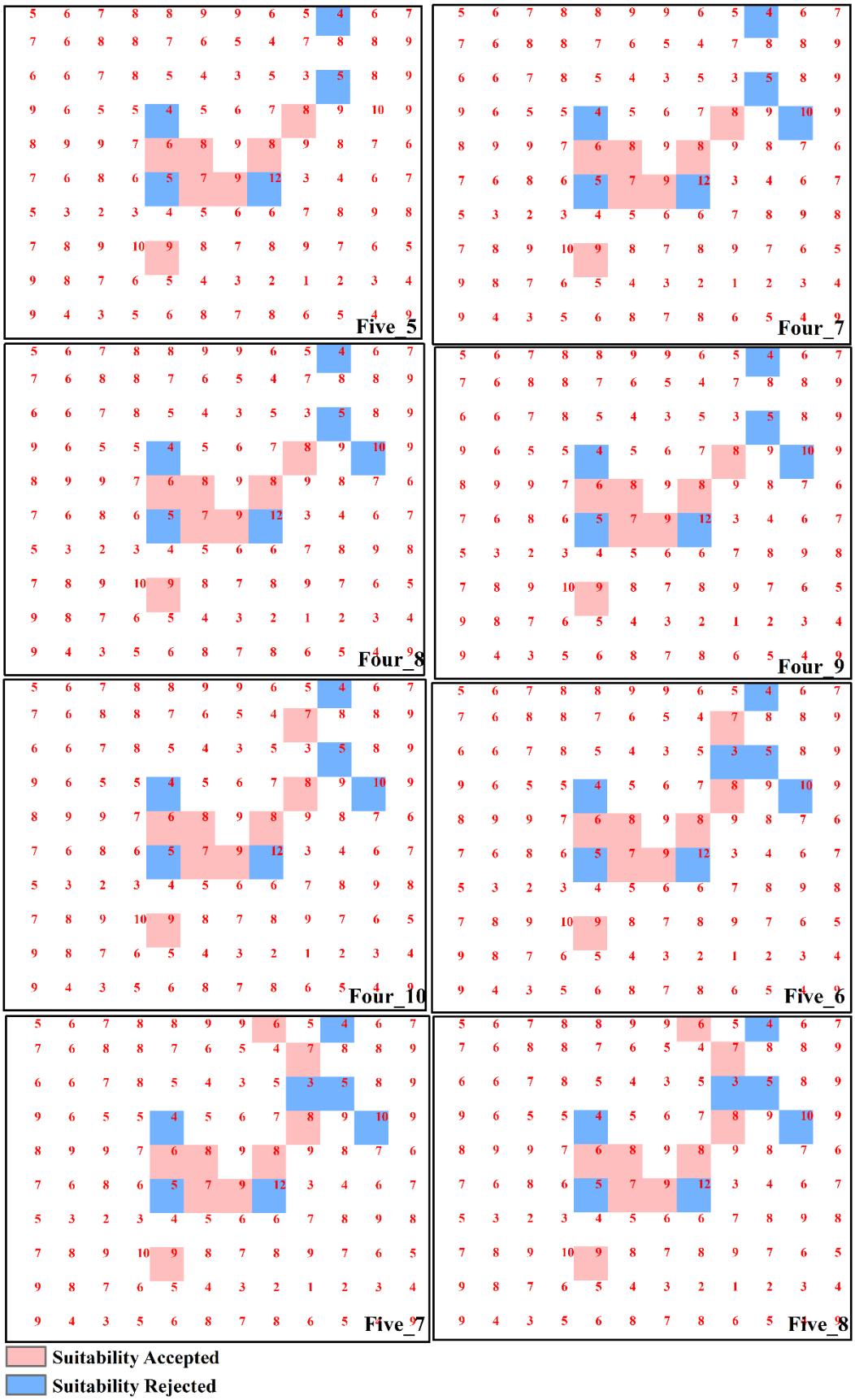

Figure 7.5: SLEUTH-Suitability program testing outcomes (c)

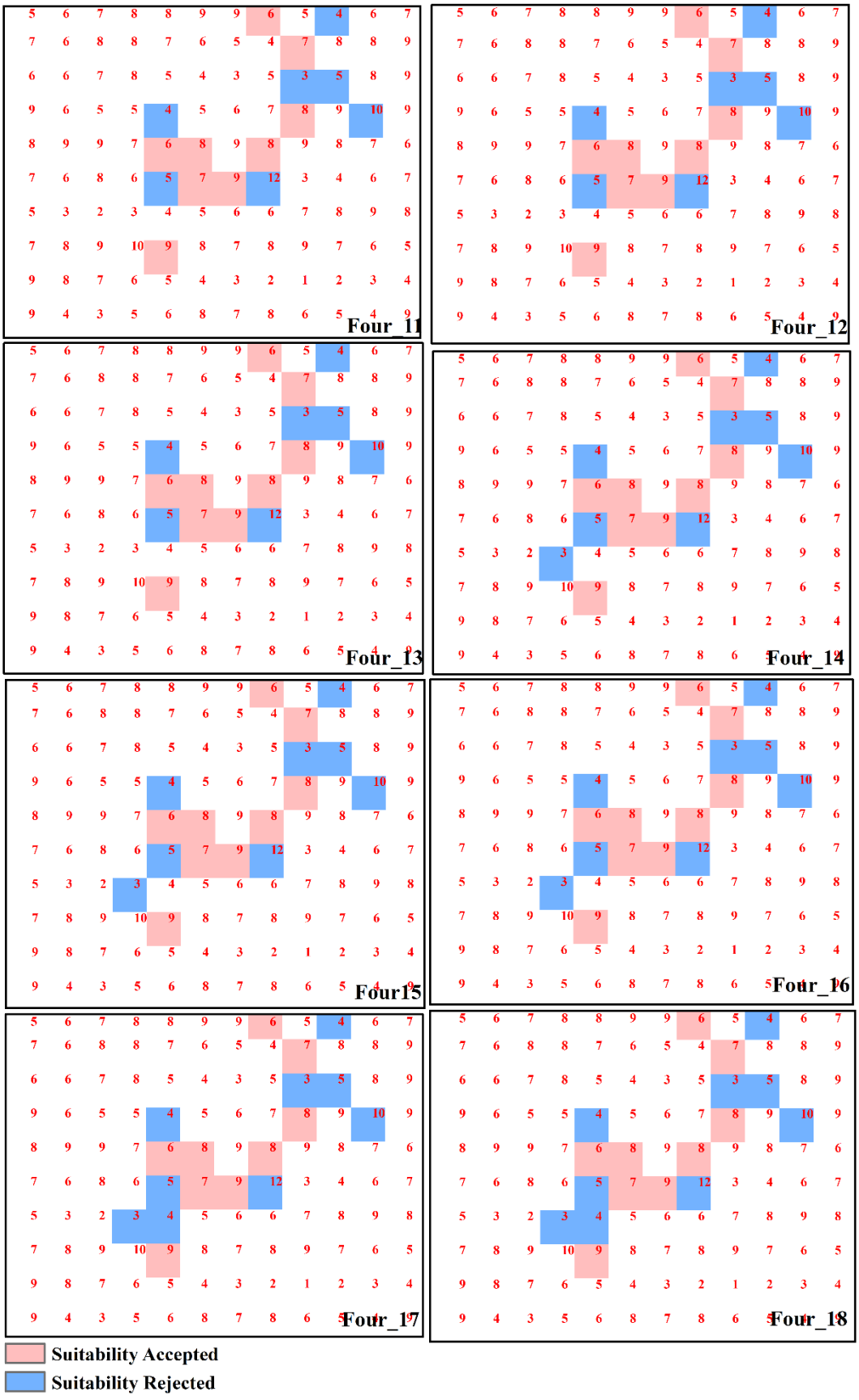

Figure 7.6: SLEUTH-Suitability program testing outcomes (d)

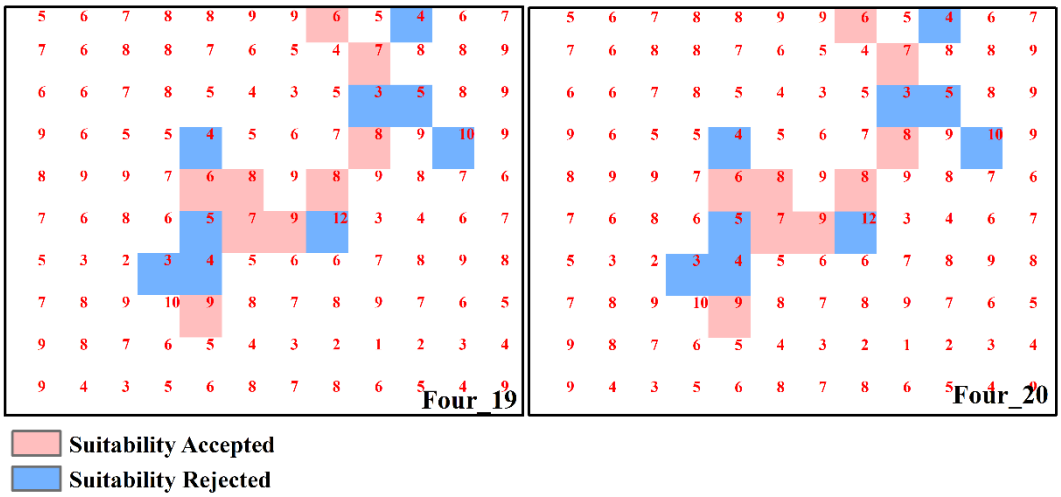

Figure 7.7: SLEUTH-Suitability program testing outcomes (e)

In the next attempt also pixel was unsuccessful to get urbanized due to land suitability decision failure (see grid Four_17). In addition, the next three attempts were failed to urbanize the pixels due to the failure of urbanization conditions (see grid Four_18, Four_19 and Four_20).

The above discussion leads to the successful examination of the SLEUTH-Suitability model. Testing of the model revealed that SLEUTH-Suitability is functioning well and all the growth rules, MC iterations and goodness of fitness metrics are implemented as desired and consistently producing desired model outcomes at each stage. SLEUTH-Suitability has been found to be working well and its application can be demonstrated for simulating the urban growth of any city or town. SLEUTH-Suitability requires six input data layers i.e., slope, urban, transportation, exclusion, land suitability, and hillshade.

SLEUTH-Suitability requires a land suitability decision variable which needs to be prepared to account for the aggregate influence of (land cost, distance from road network, and distance from important facilities like railway station, bus stand, hospital, and recreational places) selected urbanization explanatory variables. The land suitability decision layer has been developed using the AHP method based on MCE technique and information of selected urbanization explanatory variables.

The GIS-based multi-criteria evaluation (MCE) method is a process enables to integrate and transform geographic map criteria and judgment values in terms of preferences of decision makers and uncertainties to obtain an overall analysis for choosing among a number of alternatives or locations.

There are various MCE based methods for the preparation of suitability map e.g. Boolean overlay, weighted linear combination, ordered weighted averaging and analytical

hierarchy process (AHP). Development of land suitability decision variable has been discussed in the subsequent section.

7.5.1 Preparation of land suitability layers

Land suitability for urbanization can be defined as a set of information items required to make informed choices of urban development. Urban suitability analysis helps in identifying suitable sites for urban development that meet the prerequisite conditions by considering different urban growth explanatory variables. This exercise greatly reduces the time and efforts to be put otherwise manually. As discussed above that numerous explanatory variables play an important role in urbanization can be classified into five categories; natural, demographic, infrastructure services, social and land use. However, all the variables may not be contributing to urbanization equally therefore, equal weight should not be given while deciding the overall land suitability. For deciding the weights of every individual variable considered to derive land suitability like slope, distance from main roads (DMR), bus stands & railway station (DBR), recreational places (DRP), distance from hospitals (DH) and land cost variables has been evaluated for assigning weights using MCE method in the present study.

7.5.1.1 Multi-Criteria Evaluation (MCE)

MCE is basically a raster-based technique employed on multiple geospatial variables (input maps) intended to affect the suitability of a location for urbanization. Using MCE, raster layers of different explanatory variables are prepared. MCE has the ability to facilitate decision making for a complex set of numerous choices. In various studies, integration of MCE and GIS has been proposed which utilizes geo-referenced data for developing and structuring the platform for analysis with the aim of supporting urban planning. Identifying urban suitable land and incorporating this suitability factor in urban growth modelling and simulation help in the better simulation of urban growth. Through land suitability, urban growth corresponding to different land use policy scenarios can be investigated and arrive at optimum developmental decisions. Preparation of a land suitability layer using GIS and AHP based on the MCE technique has been discussed in subsequent sections. Methodology adopted to derive the land suitability has been presented in Figure 7.8.

Boolean overlay, which implies that all the factors and constraints be combined by some logical operators like union (OR) and intersection (AND) to produce discrete Boolean maps. Weighted linear combination is an aggregation approach that allows the variability

of discrete and continuous factors to be retained which requires all the factors standardized to a common numeric range and then combined by weighted averaging. Ordered weighted averaging allows for the continuous adjustment between intake level of risk and tradeoff between the criteria which gives a complete control along risk and tradeoff to make out the decisions. The Analytical Hierarchy Process (AHP) is crucial in determining the weights for a large no. of variables and is used to calculate the weight factors in association with criterion layers with the help of a preference matrix, where all the relevant criteria are compared with all others using a pairwise comparison method. Various MCE based approaches are available to deal with such problems. In the present study the AHP method of MCE has been used for determining land suitability considering selected urbanization explanatory variables, as discussed above. Land suitability preparation is discussed in detail in subsequent sections.

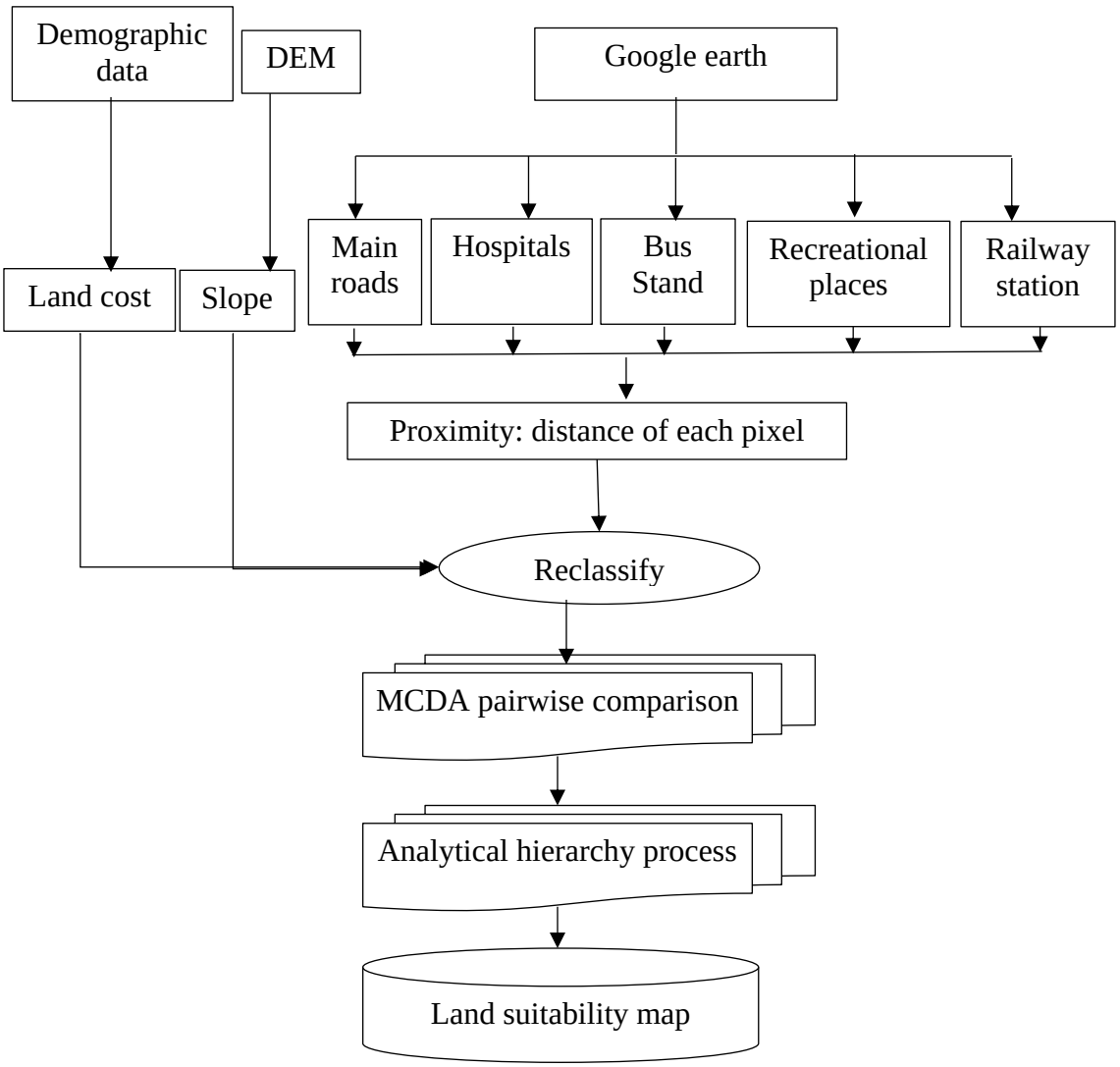

Figure 7.8: Urban suitability analysis using MCE

7.5.1.2 Analytical Hierarchy Process (AHP)

The Analytical Hierarchy Process (AHP) is a technique which can be used to determine MCE weights. It can be implemented in a GIS environment in two ways i.e. factor weights are calculated for an individual parameter with the help of a preference matrix which is prepared by computing pairwise comparison matrix and the AHP can aggregate the priority at each hierarchy level representing alternatives. The principal steps include (Figure 7.9) identifying and defining the goal or objective of the problem and decomposing an objective into hierarchical order. After decomposition, identifying and specifying the relative importance of various urban growth explanatory variables in terms of their contribution to the achievement of the overall objective.

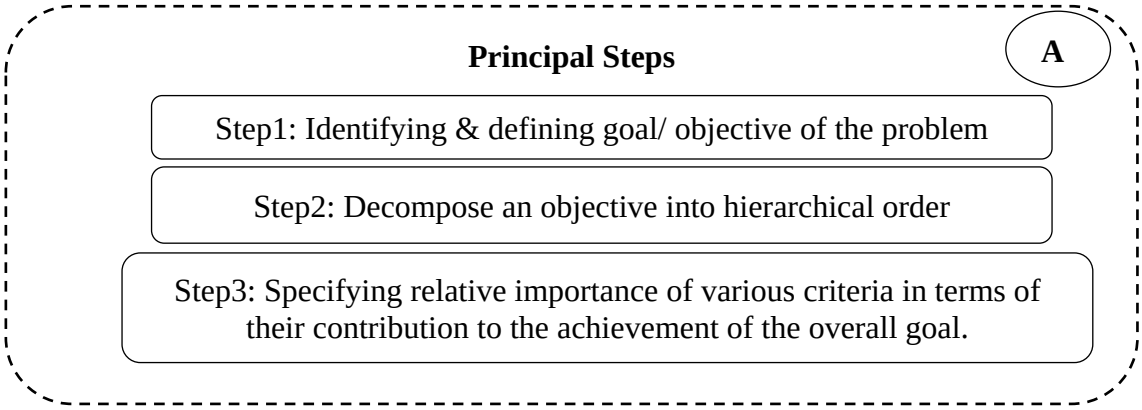

Figure 7.9: Principal steps of AHP

7.5.1.2.1 Synthesis

The synthesis of values as performed in four steps, as presented in Figure 7.10; first, the summation of all the values present in each column was done and then the pairwise comparison of the matrix was completed. Second, each variable in the matrix was divided by its column total which gives the normalized pairwise comparison matrix. Third, computation of the average of the variables present in each row of the normalized matrix. This exercise gave an estimate of the relative priorities of the variables being compared. In the fourth step, the consistency check of the pairwise comparison matrix is needed which is elaborated in subsequent sections. The detailed procedure for individual synthesis steps is described in respective sections below;

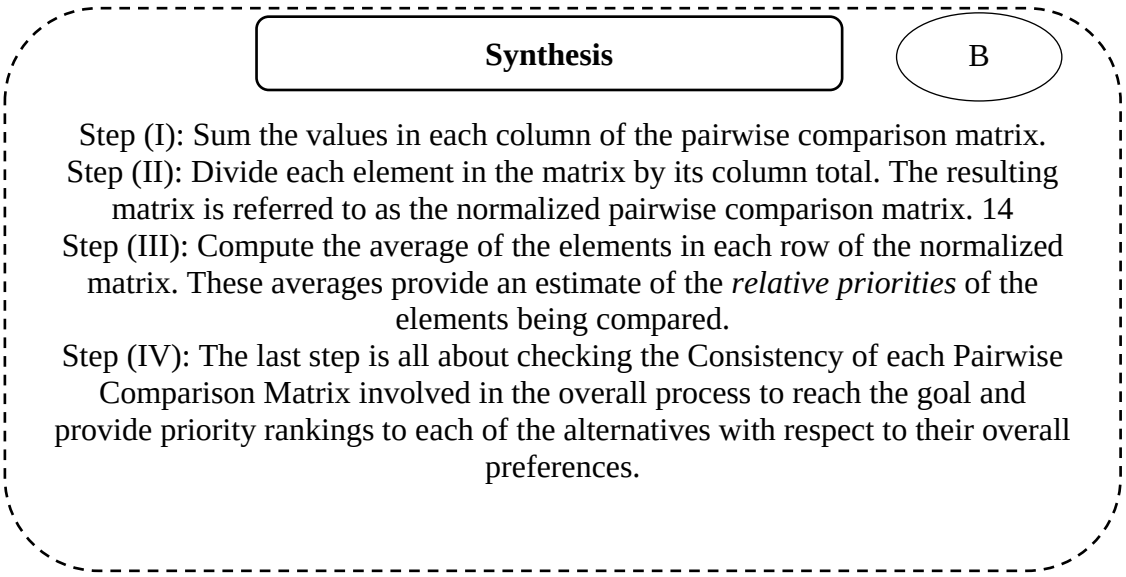

Figure 7.10: Synthesis process of AHP

7.5.1.2.2 Pairwise comparison matrix

Pairwise comparison of the matrix has also been performed in five steps (Figure 7.11). The first step includes analyzing the preferences for individual explanatory variables and preparation of a matrix constituting all variables like element *Cij* of the matrix shows the measure of preference of the item in row *i* when compared to the item in column *j*. In the second step, a value of 1 is assigned to all the diagonal elements of the matrix because of the fact that if we compare any item with itself, the judgments should be equally preferable. In the third step, preference value of element Cji is assigned as the reciprocal of element Cij. The preference value of 2 indicates that alternative i is twice as important as alternative *j*. Thus, the alternative *j* must be one-half as important as alternative *i*. In the fourth step, according to the above rules, the number of entries actually filled in by decision makers is ***(n2 – n)/2***, where ***n*** is the number of elements to be compared. In the final step, preference ratings to various items are given according to the scale suggested by Saaty, 1986, as presented in Table 7.2.

7.5.1.2.3 Consistency ratio

The consistency ratio needs to be checked to ascertain the consistency of the weights assigned to an individual variable. To compute the consistency ratio is determined in a few steps as presented in Figure 7.12, first, by multiplying each value in the first column of the pairwise comparison matrix by the relative priority of the first item considered. Similarly, it can be calculated for other items

Table 7.2: Saaty's degree preference table

Degree of Preference	Equal	Mode-rate	Strong	Very Strong	Extremely Strong	Intermediate	Less Important
Relative Importance	1	3	5	7	9	2,4,6,8	Reciprocals

Less ← Importance → More

Sum the values across the rows to obtain a vector of values labeled "weighted sum." Second, divide the elements of the vector of weighted sums obtained in Step 1 by the corresponding priority value. Third, Compute the average of the values computed in step 2. This average is denoted as $\lambda_{max.}$ Fourth, compute the consistency index (CI) using eq.7.7.

$$CI = ((\lambda max - n))/((n-1)) \quad \text{(7.7)}$$

Where n is the number of items being compared. In the final step, consistency ratio (CR) can be computed using Eq. 7.8.

$$CR = CI/RI \quad \text{(7.8)}$$

7.5.1.2.4 Consistency check and development of priority ranking

The consistency of weights assigned to the different variables have been checked using CR and found to be acceptable, as it is less than 0.12. Further, the priority ranking map was developed. In the present research work, the land suitability layer was prepared by aggregating the effect of land cost, slope, and distance from recreational places (DRP), distance from main roads (DMR), distance from hospitals (DH), distance from bus station and railway station (DBR) in deciding the desirability of land for development.

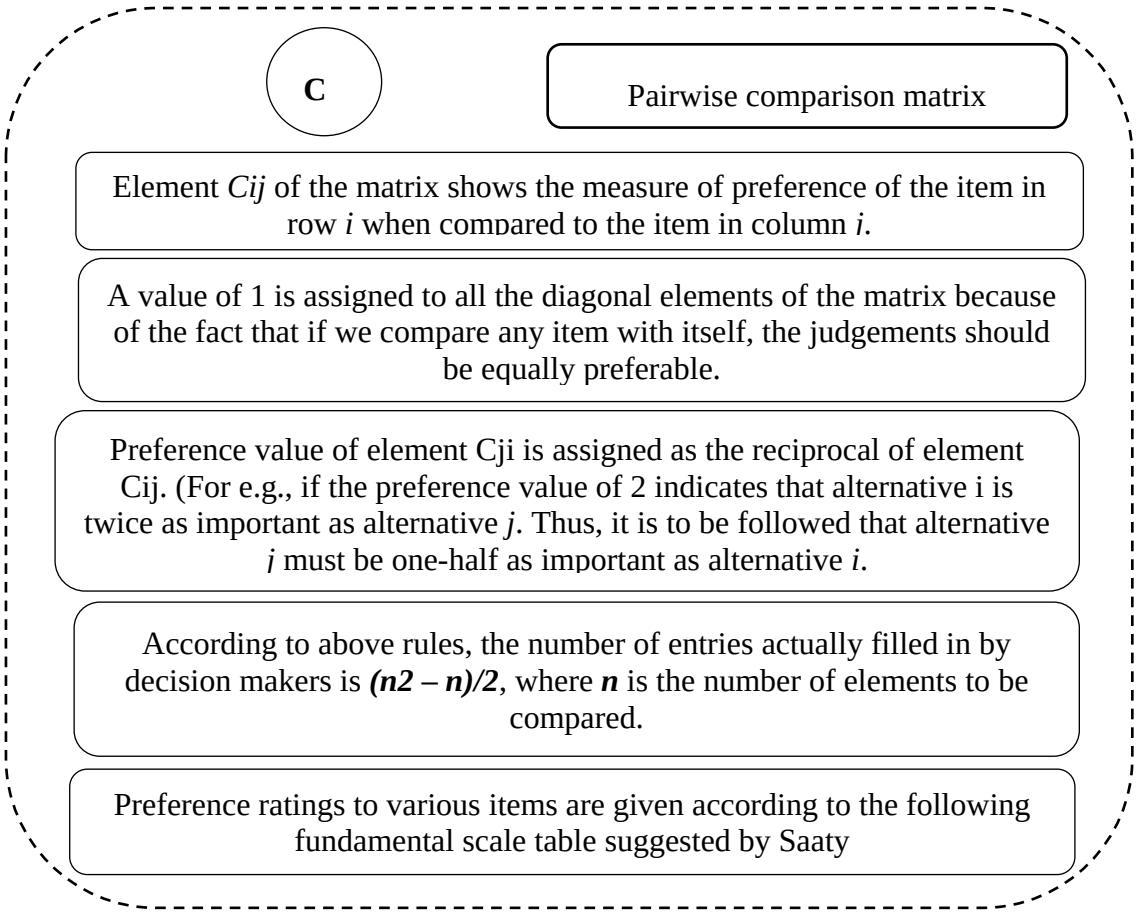

Figure 7.11 Pairwise comparison matrix

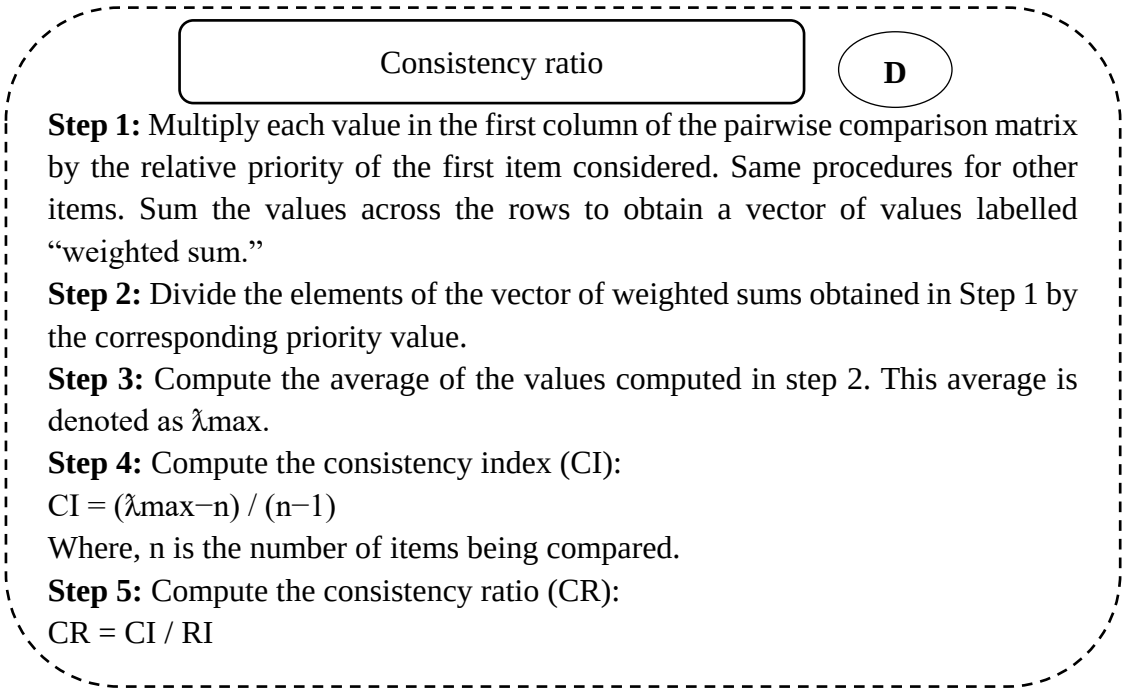

Figure 7.12: Consistency ratio

Slope

The slope map is prepared from DEM which ranges from 0 - 810 %. However, urbanization generally cannot take place on land where the slope is more than 20%. Thus, more than 20% was given lower class values.

The slope map has been classified into 10 classes at an interval of 5% as given in Table 7.3. The classification has been done in such a way that lower slope values are assigned higher class values representing higher suitability for urbanization e.g. class value '10' represents the highest suitability for urbanization.

Table 7.3: Slope class values

S.no	Slope class range (%)	Class value	S.no	Slope class range (%)	Class value
1	0-5	10	6	25-30	5
2	5-10	9	7	30-35	4
3	10-15	8	8	35-40	3
4	15-20	7	9	40-45	2
5	20-25	6	10	> 45	1

Land cost

Land cost for different years i.e. 1997, 2000, 2008, 2013 and 2015 was obtained from official website of Registration and Stamps, Department of Revenue, Govt. of Rajasthan, India and NITI Aayog (Govt. of India) for various places in Ajmer. A GIS point layer was prepared for the cost data. Further, point cost data were interpolated using IDW (Inverse Distance Weighted) interpolation technique in ArcGIS.

The land cost (DLC rates) per sqm ranges from Rs. 7.48 - 2901.42 for year 1997, 9.22 - 3576.62 for year 2000, 14.07 - 5458.64 for year 2008, 54.09 - 8413.69 for year 2013 and Rs. 60.88 to 9468.80 for the year 2015. Further, the land cost layer was reclassified into 10 classes to assign class values for the suitability. The number 10 was assigned to the lowest class of land cost and so on, where 10 represents the highest suitability (Table 7.4).

Distance from Main roads

The road transportation layer has been prepared by onscreen digitization using satellite data of respective year i.e., 1997, 2000, 2008, 2013 and 2015 obtained from Google Earth. Further, a distance of each pixel from the nearest road was determined using Euclidian distance algorithm in ArcGIS and a distance raster layer was generated for each year.

Table 7.4: Land cost (per sq. m) class values

S.no	Land cost (Rs)					Class value
	1997	2000	2008	2013	2015	
1	7.48-296.87	9.22 - 365.96	14.07 - 558.53	54.09 - 890.05	60.88 - 1001.67	10
2	296.87 - 586.27	365.96 - 722.70	558.53 - 1102.98	890.05 - 1726.01	1001.67 - 1942.46	9
3	586.27 - 875.66	722.70 - 1079.44	1102.98- 1647.44	1726.01 - 2561.97	1942.46 - 2883.25	8
4	875.66 - 1165.05	1079.44 - 1436.18	1647.44- 2191.90	2561.97 - 3397.93	2883.25 - 3824.05	7
5	1165.064 - 1454.45	1436.18 - 1792.92	2191.90- 2736.35	3397.93 - 4233.89	3824.05 - 4764.84	6
6	1454.45 - 1743.84	1792.92- 2149.66	2736.35 - 3280.81	4233.89 - 5069.85	4764.84 - 5705.63	5
7	1743.84- 2033.24	2149.66 - 2506.40	3280.81 - 3825.27	5069.85 - 5905.81	5705.63 - 6646.43	4
8	2033.24- 2322.63	2506.40 - 2863.14	3825.27 - 4369.72	5905.81 - 6741.77	6646.43 - 7587.22	3
9	2322.63 - 2612.03	2863.14 - 3219.88	4369.72 - 4914.18	6741.77 - 7577.73	7587.22 - 8528.01	2
10	2612.03 - 2901.42	3219.88- 3576.62	4914.18- 5458.64	7577.73 - 8413.69	8528.01 - 9468.80	1

The obtained distance maps were again classified into the ten number of classes with 10 as highest suitability assigned to the nearest distance class (Table 7.5).

Distance from recreational places (DRP)

A point thematic layer of various recreational places in Ajmer was prepared from the manual digitization in ArcGIS using Google Earth data as a reference map. Further, a distance raster map was generated by determining the Euclidian distance of each pixel from recreational places in ArcGIS. Further, recreational distance maps were reclassified into 10 classes, and class values are assigned as inversely proportional to the distance from the recreational place. (Table 7.6).

Distance from Bus and Railway Station (DBR)

Similarly, distance raster maps were prepared for the distance from bus and railway stations. A Euclidian distance algorithm was used to prepare raster distance map in ArcGIS. Further, distance maps were reclassified into 10 classes, and class values are assigned as inversely proportional to the distance from the bus and railway station (Table 7.7).

Table 7.5: Distance to main roads class values

S.no	Distance to Main Roads (DMR) Range (m)					Class value
	1997	2000	2008	2013	2015	
1	0 -395.61	0 - 1395.61	0 - 1395.61	0 - 834.70	0 - 652.93	10
2	1395.61 - 2791.22	1395.61- 2791.22	1395.61- 2791.22	834.70 - 1669.41	652.93 - 1305.86	9
3	2791.22 - 4186.83	2791.22- 4186.83	2791.22- 4186.83	1669.41 - 2504.12	1305.86 - 1958.79	8
4	4186.83 - 5582.44	4186.83- 5582.44	4186.83- 5582.44	2504.12 - 3338.82	1958.79 - 2611.72	7
5	5582.44 - 6978.05	5582.44- 6978.05	5582.44- 6978.05	3338.82 - 4173.53	2611.72 - 264.65	6
6	6978.05 - 8373.66	6978.05- 8373.66	6978.05- 8373.66	4173.53 - 5008.24	3264.65- 3917.59	5
7	8373.66 - 9769.27	8373.66- 9769.27	8373.66- 9769.27	5008.24 - 5842.94	3917.59 - 4570.52	4
8	9769.271- 11164.88	9769.27- 11164.88	9769.27- 11164.88	5842.94 - 6677.65	4570.52 - 5223.45	3
9	11164.88- 12560.49	11164.88- 12560.49	11164.88- 12560.49	6677.651 - 7512.36	5223.45 - 5876.38	2
10	12560.49- 13956.1	12560.49- 13956.1	12560.49- 13956.1	7512.36 - 8347.07	5876.38 - 6529.31	1

Table 7.6: Distance to recreational places class values

S.no	Distance to Recreational Places (DRP) Range (m)	Class value
1	0 - 2031.4	10
2	2031.4 - 3828.5	9
3	3828.5 - 5547.4	8
4	5547.4 - 7188.3	7
5	7188.3 - 8829.1	6
6	8829.1 - 10548.0	5
7	10548.0 - 12266.9	4
8	12266.9 - 14064.0	3
9	14064.0 - 16095.5	2
10	16095.5 - 20002.2	1

Distance from the Hospitals (DH)

A point thematic layer of various health facilities (Hospitals) in Ajmer was prepared from the manual digitization in ArcGIS using Google Earth as a reference map.

Table 7.7: Distance to bus and railway station (DBR) class values

S.no	Distance to Bus and Railway Station Ranges (DBR) (m)	Class value
1	0 - 2661.1	10
2	2661.1 - 4790.1	9
3	4790.1 - 6830.3	8
4	6830.3 - 8693.1	7
5	8693.1 - 10644.6	6
6	10644.6 - 12596.2	5
7	12596.2 - 14547.7	4
8	14547.7 - 16587.9	3
9	16587.9 - 18805.6	2
10	18805.6 - 22708.6	1

Further, distance raster map was generated by determining the Euclidian distance of each pixel from health facilities in ArcGIS. Further, distance maps were reclassified into 10 classes, and class values are assigned as inversely proportional to the distance from the location of hospitals (Table 7.8).

Table 7.8: Distance to hospital (DH) ranges class values

S.no	Distance to Hospitals (DH) (m)	Class value
1	0 - 2392.4	10
2	2392.4 - 4519.0	9
3	4519.0 - 6468.4	8
4	6468.4 - 8417.8	7
5	8417.8 - 10278.6	6
6	10278.6 - 12050.8	5
7	12050.8 - 13911.6	4
8	13911.6 - 15949.6	3
9	15949.6 - 18430.6	2
10	18430.6 - 22683.8	1

The different LULC change and urban growth explanatory variable raster layers have been prepared as discussed above and presented in Figure 7.13. Furthermore, the prepared explanatory variable raster layers are classified into 10 classes as discussed above and suitability class weights were assigned (Figure 7.14).

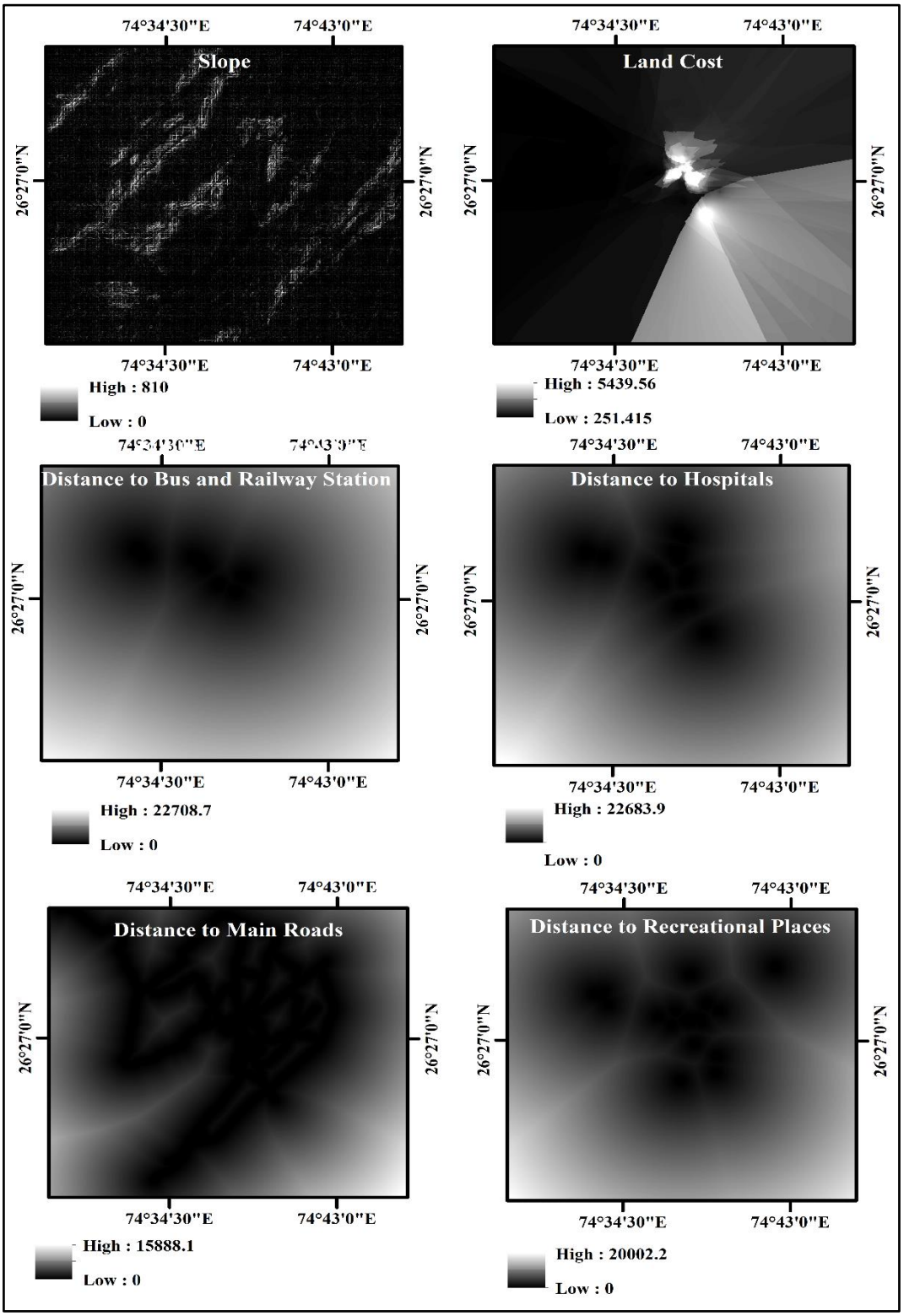

Figure 7.13: Different land use change and urban growth explanatory variables layers

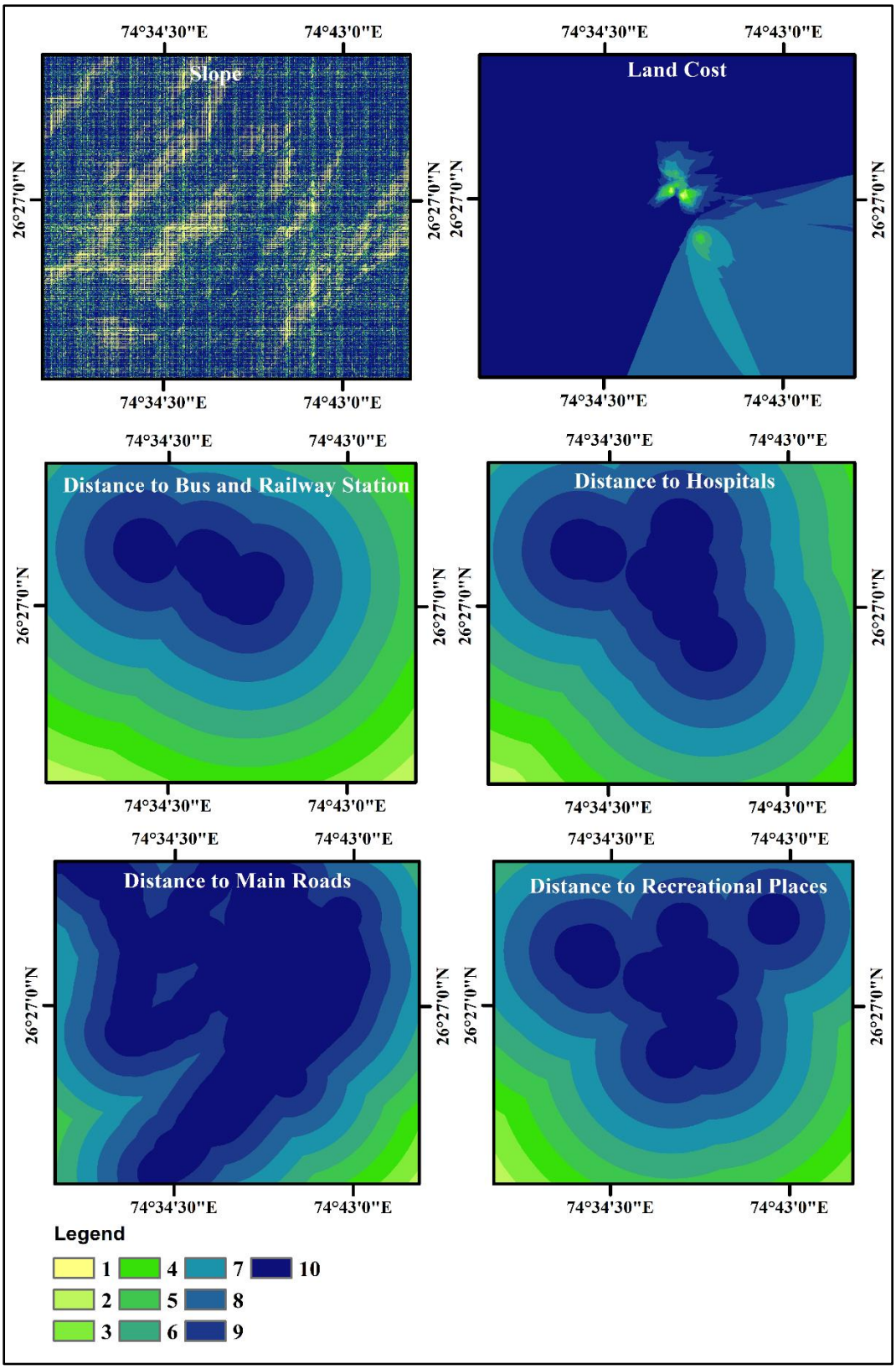

Figure 7.14: Suitability weights for different variables

After preparing each LULC change and urban growth explanatory variables defining land suitability layer and classifying them into ten number of classes the pairwise comparison

matrix was prepared based on the prior understanding of weights given to individual parameters. In the present investigation, two types of land suitability layers have been prepared i.e. suitability layer with a slope as an explanatory variable and land suitability layer without slope as an explanatory variable. It was observed in the literature (Svoray et al., 2005; Kumar et al., 2013; Youssef et al., 2011) that slope is given three times higher preference than main roads, seven times higher than the distance from hospitals, recreational places, bus stands, and railway stations. While distance from main roads was preferred three times more than the distance from hospitals & recreational places and seven times of distance from bus and railway stations. However, the land cost was given 2 times higher priority than the distance from main roads, hospitals, and recreational places. The complete pairwise comparison matrix used in the present study is presented in Table 7.9.

Table 7.9: Pairwise comparison matrix

Urbanization explanatory variables	Slope	DMR	DH	DRP	Land cost	DBR
Slope	1	3	7	7	1	7
DMR	1/3	1	3	3	1/2	7
DH	1/7	1/3	1	1	1/2	1
DRP	1/7	1/3	1	1	1/2	1
Land Cost	1	2	2	2	1	1/2
DBR	1/7	1/3	1	1	2	1

After pairwise comparison, consistency ratio was computed against weights of variables and it was found to be 0.12 that is near optimal solution (i.e., 0.10). Weights to selected variables have been finalized corresponding to a consistency ratio of 0.12. The weight of the topographic slope has been found to be highest as 41.37 which is quite obvious due to hilly surroundings of Ajmer and development is not allowed at the higher slope. The distance from the main roads has the weight of 16.48, distance from hospitals has a weight of 6.54, distance from recreational places has 6.54 weight, land cost has second highest weight at 18.41 and distance from bus and railway station has 10.63 weight. The details of weights are given in Table 7.10.

Table 7.10: Suitability weights for a set of variables including slope

Urbanization explanatory variables	Weights	
Slope	41.37	CR = 0.12
Distance from main roads (DMR)	16.48	
Distance from hospitals (DH)	6.54	
Distance from recreational places (DRP)	6.54	
Distance bus stand & railway station (DBR)	18.41	
Land cost	10.63	

On the basis of assigned weights to the individual urbanization explanatory variable, the land suitability layer was prepared as shown in Figure 7.8. It was clear from the land suitability layer that higher suitable locations were found near the core of Ajmer and its fringes excluding rocky areas.

Table 7.11: Pairwise comparison matrix for without slope layer

Urbanization explanatory variables	DMR	DH	DRP	Land cost	DBR
DMR	1				
DH	2	1			
DRP	1/3	1	1		
Land Cost	1/2	1	1	1	
DBR	1	1	4	2	1

However, in a few other studies distance from the roads was given 3 times more weight than the distance from recreational places, hospital, land cost and distance to bus stand & railway station were preferred 4 times over distance from recreational (Hart, 1997; Georgiadou et al., 2005). Based on these a weighted pairwise comparison metric was prepared (Table 7.11) and finally, weights for an individual variable were obtained as; distance from main roads 22.95, hospitals 22.4, recreational places 9.22, and Bus Stand & Railway Station 26.67 and for land cost 18.74 (Table 7.12).

Table 7.12: Suitability weights for a set of variables excluding slope

Urbanization explanatory variables	Weights	
DMR	22.95	CR = 0.10
DH	22.4	
DRP	9.22	
Land Cost	18.74	
DBR	26.67	

7.6 Land Suitability Mapping for Urban Growth

As discussed above a new urban growth decision variable i.e., land suitability has been developed using AHP based on MCE technique. A land suitability variable layer has been prepared and the suitability algorithm & required programme code are developed and integrated with the original SLEUTH code. While developing the land suitability decision variable and simulating urban growth using SLEUTH-Suitability, topographical slope was considered in two ways i.e., as a part of land suitability variable, without part of land suitability. Also, the sensitivity of SLEUTH-Suitability with respect to the land suitability weights was also investigated to arrive at the optimum weights for different urbanization

explanatory variables included into the land suitability decision rules. Model sensitivity as a function of land suitability weights has been quantified in terms of relative change in the goodness of fit metrics and nearness with the statistical measures calculated from the actual urban areas corresponding to the input data of control years and the urban area obtained from the classified output of the year 2018. Sensitivity analysis has also been tested with respect to the accuracy of urban growth prediction with respect to reference data of the year 2018.

7.6.1 Insertion of suitability layer in different ways

The topographic characteristics significantly influence urbanization. SLEUTH model simulated growth as a function of slope also. To determine the optimal way of considering the effect of slope in urban growth simulation in the SLEUTH-Suitability four experiments were conceptualized and model performance was studied. These are; (1) slope in both land suitability decision variable as well as in decision of urbanization, (2) slope only in land suitability decision but not in decision of urbanization, (3) slope only in decision of urbanization but not in land suitability decision variable and (4) only slope in urbanization decision without land suitability decision variable. For the first three scenarios, the suitability layer was prepared and accordingly the SLEUTH-Suitability model was calibrated for individual scenario independently. In the fourth scenario, the model was calibrated without the land suitability decision variable. The motive of this process was to arrive at an optimal way of using topographical slope in urban growth simulation. These scenarios have been discussed in more detail in the following sections.

7.6.1.1 Scenario 1: Slope in land suitability decision variable as well as in decision of urbanization

This scenario includes the land suitability variable prepared by combining slope with other important explanatory variables into a single land suitability decision variable using AHP based on the MCE method. Along with the land suitability variable, the decision of urbanization also will pass through the slope weight layer, which is an integral part of the SLEUTH model urban simulation. The land suitability decision variable map prepared in both ways is presented in Figure 7.15.

7.6.1.2 Scenario 2: slope only in land suitability decision variable and not in the decision of urbanization

In this scenario, the land suitability variable has been prepared to incorporate slope with other important explanatory variables. However, the slope has been removed from the urbanization decision process of the model. In this scenario, the slope decision variable has been replaced with the land suitability decision variable and a suitable code of SLEUTH-Suitability was modified. The model has been calibrated and urban growth is predicted using the methodology presented in Chapter 4.

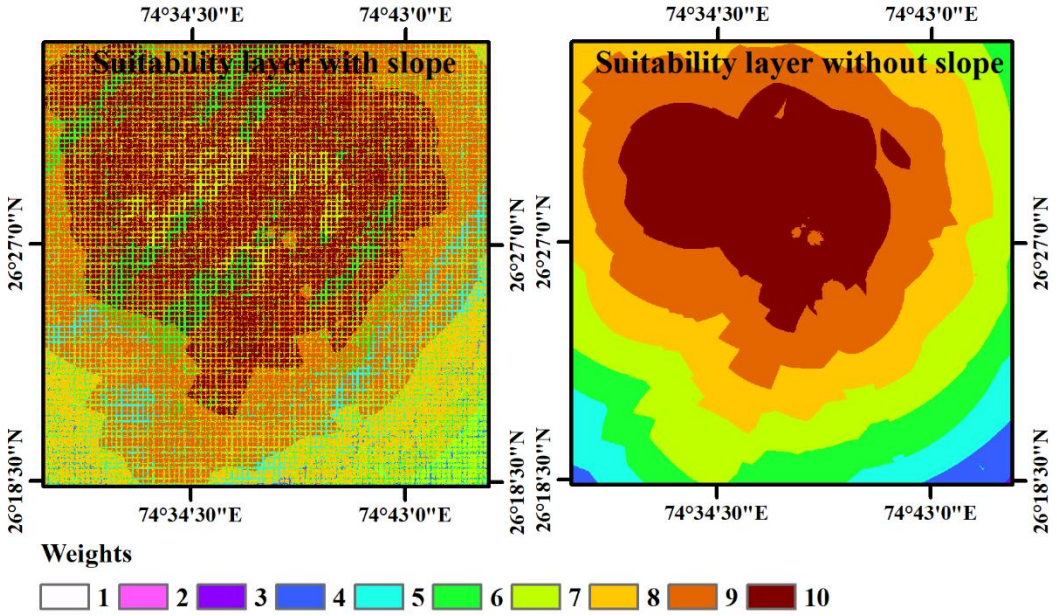

Figure 7.15: Land suitability variable weights with slope and without slope

7.6.1.3 Scenario 3: slope only in the decision of urbanization but not in suitability layer

In this scenario, the slope was not considered in the land suitability decision variable and considered as separate decision rule in urban growth simulation, as it does in the present version of SLEUTH. Model code was modified suitably. Further, the model was calibrated and urban growth was predicted using the methodology presented in Chapter 4.

7.6.1.4 Scenario 4: without suitability layer

This includes the calibration of the SLEUTH model without incorporating land suitability decision variable means using the original SLEUTH version with optimum model parameters obtained from sensitivity analysis. This scenario has been explored to check the

influence of the land suitability decision variable on correctly simulating the urban growth for a case study area using the existing SLEUTH model.

7.6.2 Model performance in different scenarios of slope and land suitability

For each scenario, suitable logic has been developed and accordingly programming code of the SLEUTH-Suitability was modified. For each scenario model calibrated successfully, urban growth was predicted. The accuracy of the modelling outcomes for each scenario was assessed independently. Performance of the model was assessed in terms of relative change in few spatial and statistical measures through the relative change in model accuracy in predicting the urban growth. Accuracy was assessed with respect to the urban area obtained from a classified satellite image of the year 2018. Important spatial and statistical measures like urban area (in km^2), total no. of urban edges (in 100s), total no. of urban clusters (in 100s), urban cluster radius and mean cluster size was estimated from the simulated outcomes for different years i.e. 1997, 2000, 2008, 2013 and 2015 and compared with the same metrics calculated from the input data (urban area) for the respective years to judge the quality of the model calibration. This comparison basically gives an idea of the model's capability of replicating the historical urban growth thus the performance of the model calibration. The scenario for which differences between values of these landscape metric (calculated from simulated urban growth and input datasets) is minimum has been adopted as the final configuration for the SLEUTH-Suitability. The performance of the model in term of comparison of spatial and statistical measures, for different scenarios, is presented in Figure 7.16.

It is evident from Figure 7.16 that urban area captured for the year 2000 in different scenarios is close to the reference (considered as actual) urban area. However, urban growth in succeeding years seems to be varying in case of scenario 1 which includes slope both in land suitability variable and decision of urbanization. It may have excess influence in making urbanization decisions which resulted in lesser urbanization as compared to the actual area. The urban area was optimally captured for scenario 2 which includes slope in suitability layer and replaces the additional slope layer into the SLEUTH model as compared to the other scenarios. Scenario3 which excludes slope in suitability layer but includes in the decision of urbanization as an additional slope layer was not able to capture urban area well as compared to scenario 2. However, it performed better than scenario 1 as the urban area is much closer to actual in the case of scenario 3 than scenario 1. The scenario 4 which doesn't include suitability module has not been able to capture urban area well as

compared to scenario 2 and 3. However, it was better in capturing urban area compared to scenario 1. Comparison of results in different scenarios revealed that SLEUTH-Suitability version is better (scenario 2) in simulating the urban growth as compared to the original version of the model (scenario 4). In Scenario 2, with land suitability decision variable simulated urban edges are closely matching with urban edges computed from the input data indicates that SLEUTH-Suitability is better in capturing fragmented growth. The difference in urban clusters and mean cluster size indicates that pixels are grouped in large clusters in the reference urban area as it is obtained from the LULC maps prepared from the classified satellite images (Figure 7.16). However, scenario 2 gives a much closer no of captured urban clusters as compared to other scenarios. Furthermore, cluster radius was more accurately captured in the case of scenario 2 than other scenarios. The mean cluster size showed many differences between actual mean cluster sizes. The sequence of performances of different scenarios remained the same as in case for the urban area. The inclusion of an additional slope layer in urbanization decision and not including in land suitability decision variable also (scenario 3) has not been found better than scenario 2. In addition, it requires more time in simulating the urban growth as compared to scenario 2 during calibration. Therefore, it can be concluded that model performance is better in scenario two where the slope is considered as an explanatory variable in the land suitability decision variable and slope decision variable in replaced with the land suitability decision rule in the SLEUTH-Suitability. The study gives some important insights about the model performances, these are; (1) the inclusion of land suitability decision rule into the SLEUTH model is helpful in better simulation of urban growth than the existing SLEUTH model, (2) the land suitability decision variable must have slope as one of the urbanization influencing variable and no need of slope as an additional decision rule in the model (i.e. scenario 2), (3) Relatively poor performance of the model in capturing urban clusters and mean cluster size indicates aggregation of pixels in large size clusters in the reference urban area during image classification. Thus it cannot represent the poor model performance.

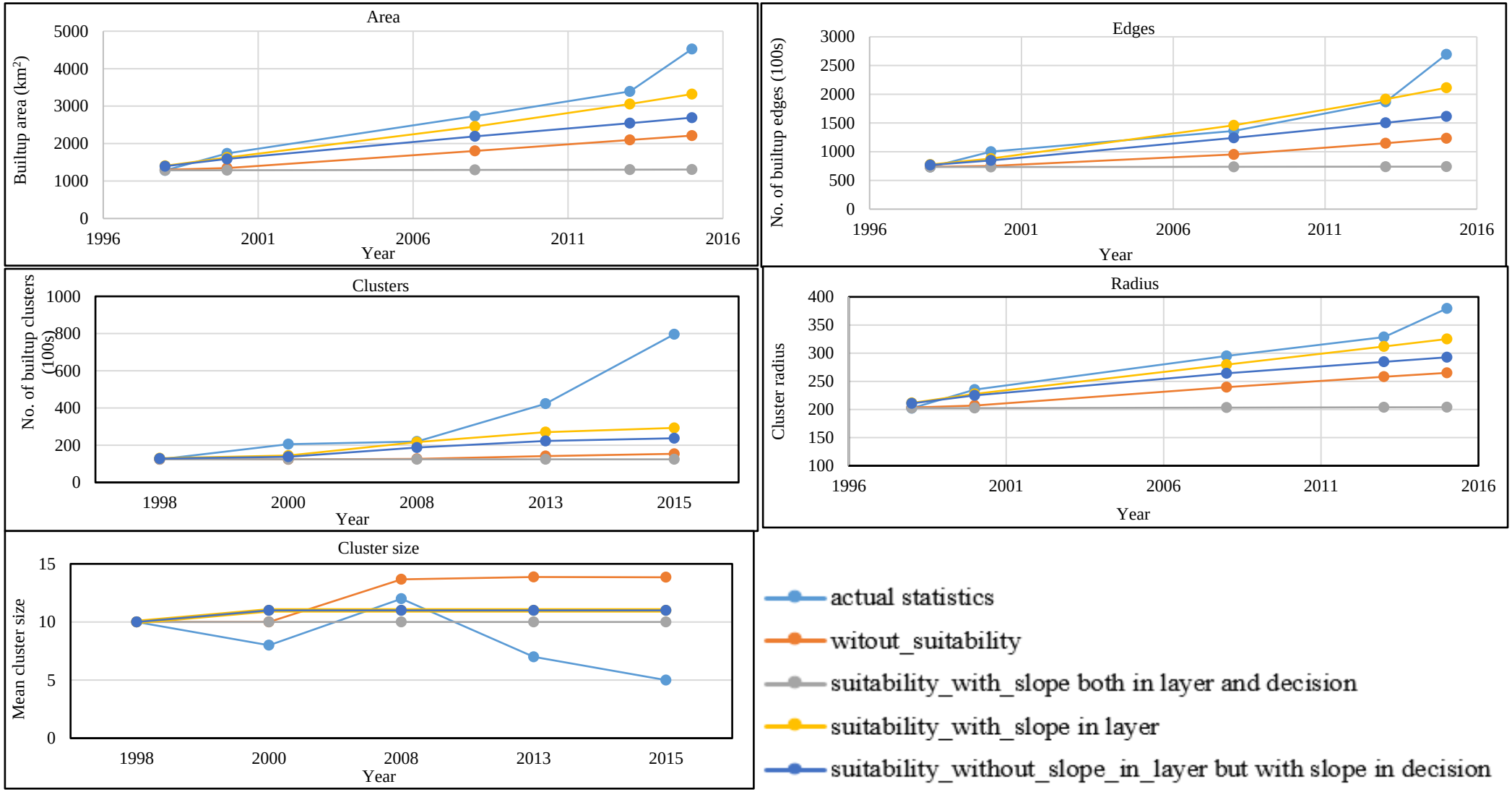

Figure 7.16: Comparison of spatial and statistical measures computed from actual and modeled outcomes for different scenarios

Performance of the SLEUTH-Suitability may be further improved by exploring more explanatory variables in the land suitability decision variable or by identifying better weights for the individual urbanization influencing variables considered in the derivation of land suitability variable through sensitivity testing of the model for AHP weights.

7.6.3 Sensitivity analysis of land suitability variable threshold

Land suitability decision variables participate in the urbanization decision and implementation stage of each growth rule in the model. A pixel will be urbanized if it has land suitability weight more than a particular threshold value i.e., 5 in the present case. The suitable value of this threshold needs to be examined. The SLEUTH-Suitability model was tested with different values of land suitability variable threshold i.e., 4, 5, 6 and 7. For the individual case, the program of SLEUTH-Suitability model is modified and for individual case, the model has been calibrated and urban growth predicted. Change in model performance and ability to capture urban growth correctly during calibration and prediction with respect to different threshold values of land suitability decision rule was compared in term of spatial and statistical measures as discussed in previous sections. In addition, urban growth results with different threshold values have been compared with the actual growth by superimposing simulated growth over a satellite image of respective year in Google Earth. It was observed that at a threshold value of 4 and below, that unsuitable terrain like rocky areas, water bodies etc. were captured as urban areas by the model which is not in line with the actual urban area. Similarly, for threshold values 7 and more, urban area at many locations have not been captured leading to significant underestimation of urban areas. The results revealed that a land suitability threshold of 5 is appropriate and produces satisfactory urban growth as compared to growth with other threshold values. Less than or equal to 4 value has over captured the urban whereas at 6 and 7 threshold suitable locations were left out from the urbanization i.e., poorly captured the fragmented growth.

7.6.4 Sensitivity analysis for urbanization explanatory variable AHP weights

As discussed above, the performance of SLEUTH-Suitability can be further improved by using appropriate weights to each urbanization explanatory variables participating in land suitability variable. Appropriate weights for the variables can be determined through sensitivity analysis. An iterative procedure has been used to perform a sensitivity analysis by simulating urban growth with different land suitability variables derived with different

combinations of weights for different explanatory variables. For each combination of weights land suitability decision variable layers are prepared for every control year i.e. 1997, 2000, 2008, 2013 and 2015. Each set of suitability layers has been utilized for performing model calibration and urban simulations independently. The no. of combinations of weights of different variables are decided in the form of gradually increasing or decreasing weights for an individual variable by keeping remaining variables as constant. In such a way, 16 no of combinations are decided, named as scenario 'a' to 'q' and land suitability decision layer named with prefix 'suitability_' e.g. suitability_a) and for each combination of weights land suitability layers of controlling years were prepared using AHP method in GIS. The suitability weights calculated for individual land suitability decision variable layers are presented in Table 7.13 to 7.29. In scenario suitability_a, the highest priority has been given to the slope over the distance from bus stand & railway station (DBR), hospital (DH), recreational places (DRP), main roads (DMR) and land cost (Table 7.13). Second highest priority has been given to the land cost and then to the distance from the main roads (DMR). The remaining three variables belongs to services and facilities and therefore, kept all three variables with similar preference. In this way, weights calculated for slope, land cost, and distance from main roads are 28.02, 22.13 and 17.48, respectively. For the remaining three variables weight is 10.78 each. These weights were calculated with a good CR i.e. 0.022.

Table 7.13: Pairwise comparison matrix and weights for Suitability_a scenario

Urbanization expl. variables	Slope	DBR	DH	DRP	DMR	Land cost	Final weights
Slope	1						28.02
DBR	0.5	1					10.78
DH	0.5	1	1				10.78
DRP	0.5	1	1	1			10.78
DMR	0.5	2	2	2	1		17.48
Land cost	0.5	2	2	2	2	1	22.13
CR = 0.022							

Suitability_b layer was prepared again with the highest slope weight i.e. 49.77, and assigning the same weight to land cost and main roads as 15.39. The remaining variables were given a weight equal to 6.48. For this scenario, CR has been found to be 0.023. In Suitability_b the slope variable has higher weight as compared to other variables as presented in Table 7.14.

Table 7.14: Pairwise comparison matrix and weights for Suitability_b scenario

Urbanization expl. variables	Slope	DBR	DH	DRP	DMR	Land cost	Final weights
Slope	1						49.77
DBR	0.1	1					6.48
DH	0.1	1	1				6.48
DRP	0.1	1	1	1			6.48
DMR	0.5	2	2	2	1		15.39
Land cost	0.5	2	2	2	1	1	15.39
CR =0.023							

Suitability_c was prepared by giving highest weight to the land cost variable i.e. 28.02 then second highest weight was assigned to slope variable i.e. 22.13 and third highest weight was assigned to the distance from main road (DMR) as 17.48. The remaining three variables were assigned the same weights i.e. 10.78 each (Table 7.15).

Table 7.15: Pairwise comparison matrix and weights for Suitability_c scenario

Urbanization expl. variables	Slope	DBR	DH	DRP	DMR	Land cost	Final weights
Slope	1						22.135
DBR	0.5	1					10.785
DH	0.5	1	1				10.785
DRP	0.5	1	1	1			10.785
DMR	0.5	2	2	2	1		17.483
Land cost	2	2	2	2	1	1	28.027
CR = 0.022							

The suitability_d layer was prepared in such a manner that land cost should have a higher weight as compared to variables. Then the distance from main roads (DMR) and slope variables was given second and third highest weights i.e. 10.43 and 8.24, respectively. The distance from bus railway (DBR), hospital (DH) and recreational variables (DRP) were given low weights equal to 5.08 (Table 7.16).

Table 7.16: Pairwise comparison matrix and weights for Suitability_d scenario

Urbanization expl. variables	Slope	DBR	DH	DRP	DMR	Land cost	Final weights
Slope	1						8.242
DBR	0.5	1					5.085
DH	0.5	1	1				5.085
DRP	0.5	1	1	1			5.085
DMR	2	2	2	2	1		10.436
Land cost	10	10	10	10	10	1	66.067
CR = 0.022							

Suitability_e layer was prepared with the highest land cost suitability i.e. 28.23 then main roads and slope with 19.9 and 15.15 respectively. The weight of the remaining three variables were increased 12.23 each (Table 7.17).

Table 7.17: Pairwise comparison matrix and weights for Suitability_e scenario

Urbanization expl. variables	Slope	DBR	DH	DRP	DMR	Land cost	Final weights
Slope	1						15.154
DBR	0.9	1					12.234
DH	0.9	1	1				12.234
DRP	0.9	1	1	1			12.234
DMR	2	2	2	2	1		19.905
Land cost	2	2	2	2	2	1	28.239
CR = 0.013							

In suitability_f scenario distance from main roads (DMR) were given higher weight i.e. 44.52 then land cost and slope variables were second and third highest weight as 25.25 and 15.71, respectively. The remaining three variables were given very low weights as of 4.83 (Table 7.18).

Table 7.18: Pairwise comparison matrix and weights for Suitability_f scenario

Urbanization expl. variables	Slope	DBR	DH	DRP	DMR	Land cost	Final weights
Slope	1						15.712
DBR	0.2	1					4.835
DH	0.2	1	1				4.835
DRP	0.2	1	1	1			4.835
DMR	6	6	6	6	1		44.523
Land cost	4	4	4	4	0.4	1	25.259
CR = 0.079							

In suitability_g scenario, a higher weight was assigned to the slope as 57.29. The distance from main roads and land cost variables were given equal weights as 13.92 each. The distance from bus railway (DBR), hospital (DH) and recreational places (DRP) were again given lower and equal weights of 4.95 (Table 7.19).

Table 7.19: Pairwise comparison matrix and weights for Suitability_g scenario

Urbanization expl. variables	Slope	DBR	DH	DRP	DMR	Land cost	Final weights
Slope	1						57.279
DBR	0.1	1					4.958
DH	0.1	1	1				4.958
DRP	0.1	1	1	1			4.958
DMR	0.2	3	3	3	1		13.923
Land cost	0.2	3	3	3	1	1	13.923
CR = 0.004							

In suitability_h scenario, distance from main roads (DMR) and land cost were assigned weight of 17.1 and distance from bus railway (DBR), hospital (DH) and recreational places (DRP) were assigned weights of 5.42 each. The highest weight was assigned to the slope as 49.52 (Table 7.20).

Table 7.20: Pairwise comparison matrix and weights for Suitability_h scenario

Urbanization expl. variables	Slope	DBR	DH	DRP	DMR	Land cost	Final weights
Slope	1						49.52
DBR	0.1	1					5.426
DH	0.1	1	1				5.426
DRP	0.1	1	1	1			5.426
DMR	0.4	3	3	3	1		17.101
Land cost	0.4	3	3	3	1	1	17.101
CR = 0.002							

In suitability_i scenario again the order of weights was kept similar to the suitability_h but the weight of the slope layer was slightly reduced to 42.49 and the weights of remaining variables increased. The distance from bus railway (DBR), hospital (DH) and recreational places (DRP) were assigned weights of 5.62 while the distance from main roads and land cost were assigned similar weights of 20.31 (Table 7.21).

Table 7.21: Pairwise comparison matrix and weights for Suitability_i

Urbanization expl. variables	Slope	DBR	DH	DRP	DMR	Land cost	Final weights
Slope	1						42.49
DBR	0.1	1					5.62
DH	0.1	1	1				5.62
DRP	0.1	1	1	1			5.62
DMR	0.8	3	3	3	1		20.31
Land cost	0.8	3	3	3	1	1	20.31
CR = 0.027							

Suitability_j layer distance from bus n railway (DBR), hospital (DH) and recreational places (DRP) were assigned weights of 5. The slope was set to 34.24 with the highest weight. The distance from main roads (DMR) and land cost were given weights of 25.52 (Table 7.22).

In preparing suitability_k land suitability decision layer the distance from main roads was given higher weight i.e. 53.79, slope and land cost variables were given almost equal weight as 13.79 and 12.86, respectively. The remaining three variables were given weights of. 6.51 each (Table 7.23).

Table 7.22: Pairwise comparison matrix and weights for Suitability_j scenario

Urbanization expl. variables	Slope	DBR	DH	DRP	DMR	Land cost	Final weights
Slope	1						34.24
DBR	0.2	1					4.90
DH	0.2	1	1				4.90
DRP	0.2	1	1	1			4.90
DMR	0.5	6	6	6	1		25.52
Land cost	0.5	6	6	6	1	1	25.52
CR = 0.021							

Table 7.23: Pairwise comparison matrix and weights for Suitability_k scenario

Urbanization expl. variables	Slope	DBR	DH	DRP	DMR	Land cost	Final weights
Slope	1						13.793
DBR	0.3	1					6.515
DH	0.3	1	1				6.515
DRP	0.3	1	1	1			6.515
DMR	10	3	3	3	1		53.795
Land cost	1	3	3	3	0.1	1	12.868
CR = 0.169							

Suitability_l was prepared with the highest weight assigned to the distance from main roads (DMR) but slightly smaller to what was assigned in the suitability_k i.e. 43.48. The weights to slope and land cost variables have been kept as 17.89 and 16.77, respectively. The remaining three variables were again kept at the same weight but slightly increased to 7.28 (Table 7.24).

Table 7.24: Pairwise comparison matrix and weights for Suitability_l scenario

Urbanization expl. variables	Slope	DBR	DH	DRP	DMR	Land cost	Final weights
Slope	1						17.894
DBR	0.3	1					7.284
DH	0.3	1	1				7.284
DRP	0.3	1	1	1			7.284
DMR	5	3	3	3	1		43.481
Land cost	1	3	3	3	0.2	1	16.772
CR = 0.08							

In suitability_m the highest weight was again given to distance from main roads (DMR) i.e. 33.37 however, reduced compared to scenario l. The slope and land cost variables were assigned slightly increased weights i.e. 30.9 and 22.14, respectively. The remaining three variables were kept at weight of 4.52 each (Table 7.25).

In suitability_n scenario, the land cost variable was assigned highest weight i.e. 53.76. The slope and distance from main roads (DMR) were assigned weights of 13.11 and the remaining three variables were also set to the weights of 6.67 each (Table 7.26).

Table 7.25: Pairwise comparison matrix and weights for Suitability_m scenario

Urbanization expl. variables	Slope	DBR	DH	DRP	DMR	Land cost	Final weights
Slope	1						30.906
DBR	0.111	1					4.524
DH	0.111	1	1				4.524
DRP	0.111	1	1	1			4.524
DMR	2	5	5	5	1		33.374
Land cost	1	5	5	5	0.5	1	22.148
CR = 0.034							

Table 7.26: Pairwise comparison matrix and weights for Suitability_n scenario

Urbanization expl. variables	Slope	DBR	DH	DRP	DMR	Land cost	Final weights
Slope	1						13.112
DBR	0.333	1					6.674
DH	0.333	1	1				6.674
DRP	0.333	1	1	1			6.674
DMR	1	3	3	3	1		13.106
Land cost	10	3	3	3	10	1	53.76
CR = 0.016							

In suitability_o, the weight to the land cost variable was slightly reduced to 43.51 as compared to scenario n. The weights DMR and slope variables was slightly increased to 17.03. The weight of the remaining three variables was also increased to 7.47 (Table 7.27).

Table 7.27: Pairwise comparison matrix and weights for Suitability_o scenario

Urbanization expl. variables	Slope	DBR	DH	DRP	DMR	Land cost	Final weights
Slope	1						17.038
DBR	0.333	1					7.473
DH	0.333	1	1				7.472
DRP	0.333	1	1	1			7.472
DMR	1	3	3	3	1		17.031
Land cost	5	3	3	3	5	1	43.514
CR = 0.074							

In suitability_p, the land cost was again assigned highest weight but less than scenario o as 31.70. The weights of DMR and slope variables were again given weights of 21.90 but slightly increased as compared to the previous scenario. Slightly increased weight to the remaining three variables was assigned as 8.16 (Table 7.28).

Table 7.28: Pairwise comparison matrix and weights for Suitability_p

Urbanization expl. variables	Slope	DBR	DH	DRP	DMR	Land cost	Final weights
Slope	1						21.906
DBR	0.333	1					8.166
DH	0.333	1	1				8.166
DRP	0.333	1	1	1			8.166
DMR	1	3	3	3	1		21.894
Land cost	2	3	3	3	2	1	31.703
CR = 0.013							

In suitability_q, the distance to main roads was given the highest weight as 42.81 and slope and land cost variables were given similar weights i.e., 20.14. Other variables were assigned weight of 5.41 (Table 7.29).

Table 7.29: Pairwise comparison matrix and weights for Suitability_q

Urbanization expl. variables	Slope	DBR	DH	DRP	DMR	Land cost	Final weights
Slope	1						20.143
DBR	0.2	1					5.414
DH	0.2	1	1				5.414
DRP	0.2	1	1	1			5.414
DMR	5	4	4	4	1		42.813
Land cost	1	5	5	5	0.3	1	20.802
CR = 0.079							

With each combination of the weights assigned to different selected urbanization explanatory variable, the land suitability decision variable layer was prepared for each control year i.e., 1997, 2000, 2008, 2013 and 2015. Therefore testing the SLEUTH-Suitability sensitivity to weights of variables/drivers used in land suitability decision variable, a total of 85 times the model was calibrated and urban growth simulated. Land suitability layers prepared for the year 2015 are presented in Figure 7.17-7.20. Locations with higher weight are suitable for urbanization.

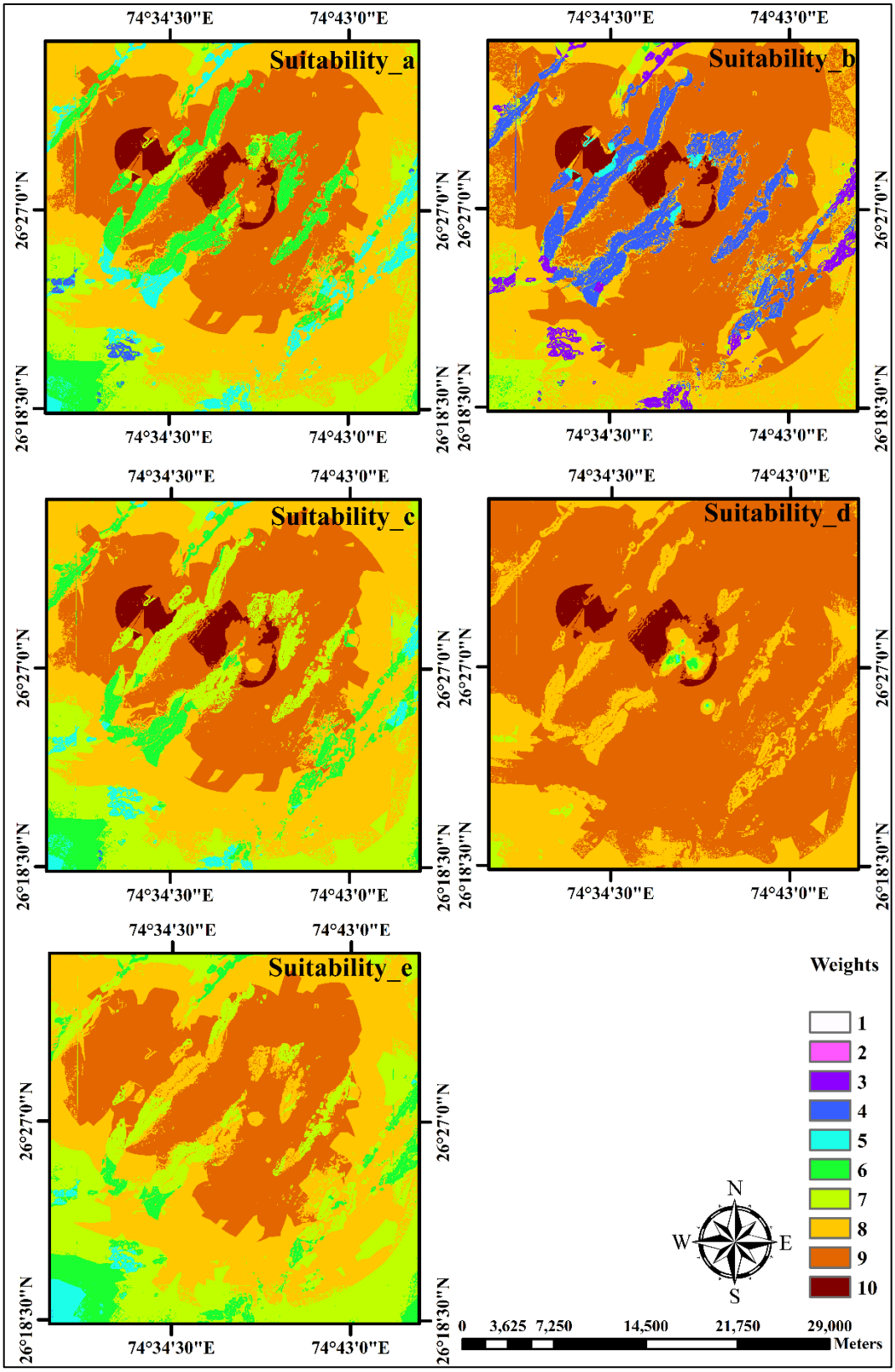

Figure 7.17: Land suitability layers for different weightage scenarios (a-e) for year 2015

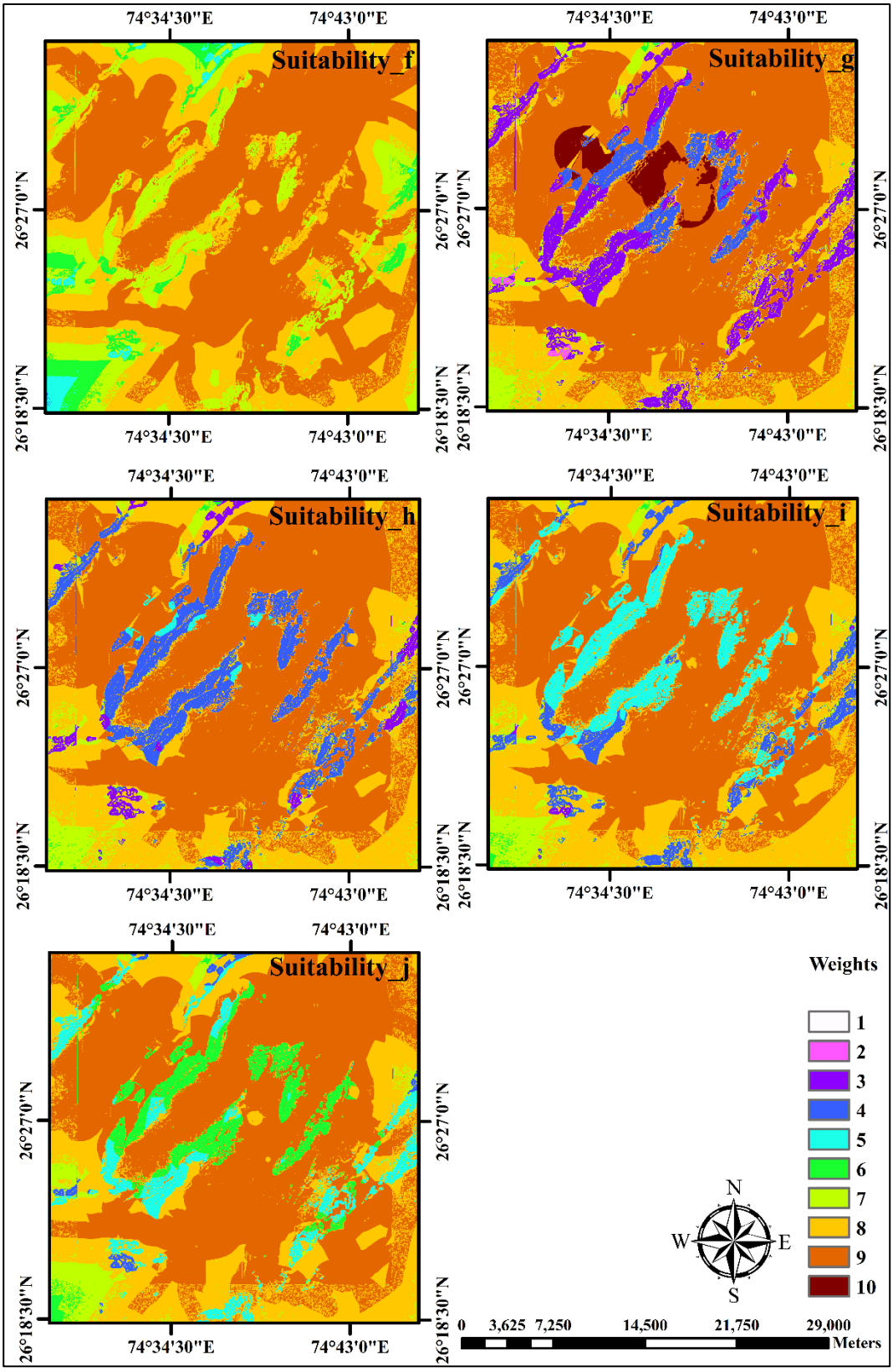

Figure 7.18: Land suitability layers for different weightage scenarios (f-j) for year 2015

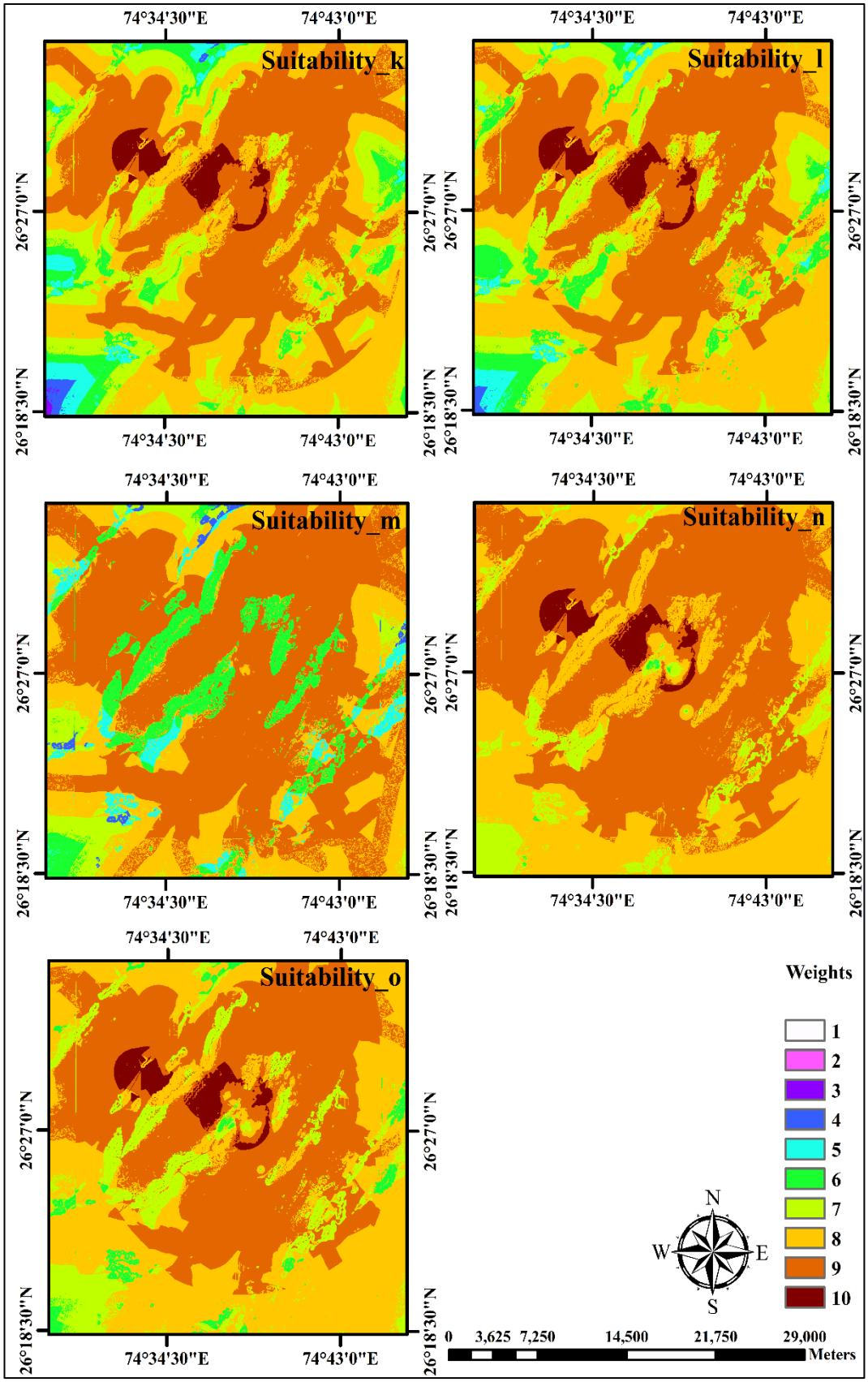

Figure 7.19: Land suitability layers for different weightage scenarios (k-o) for year 2015

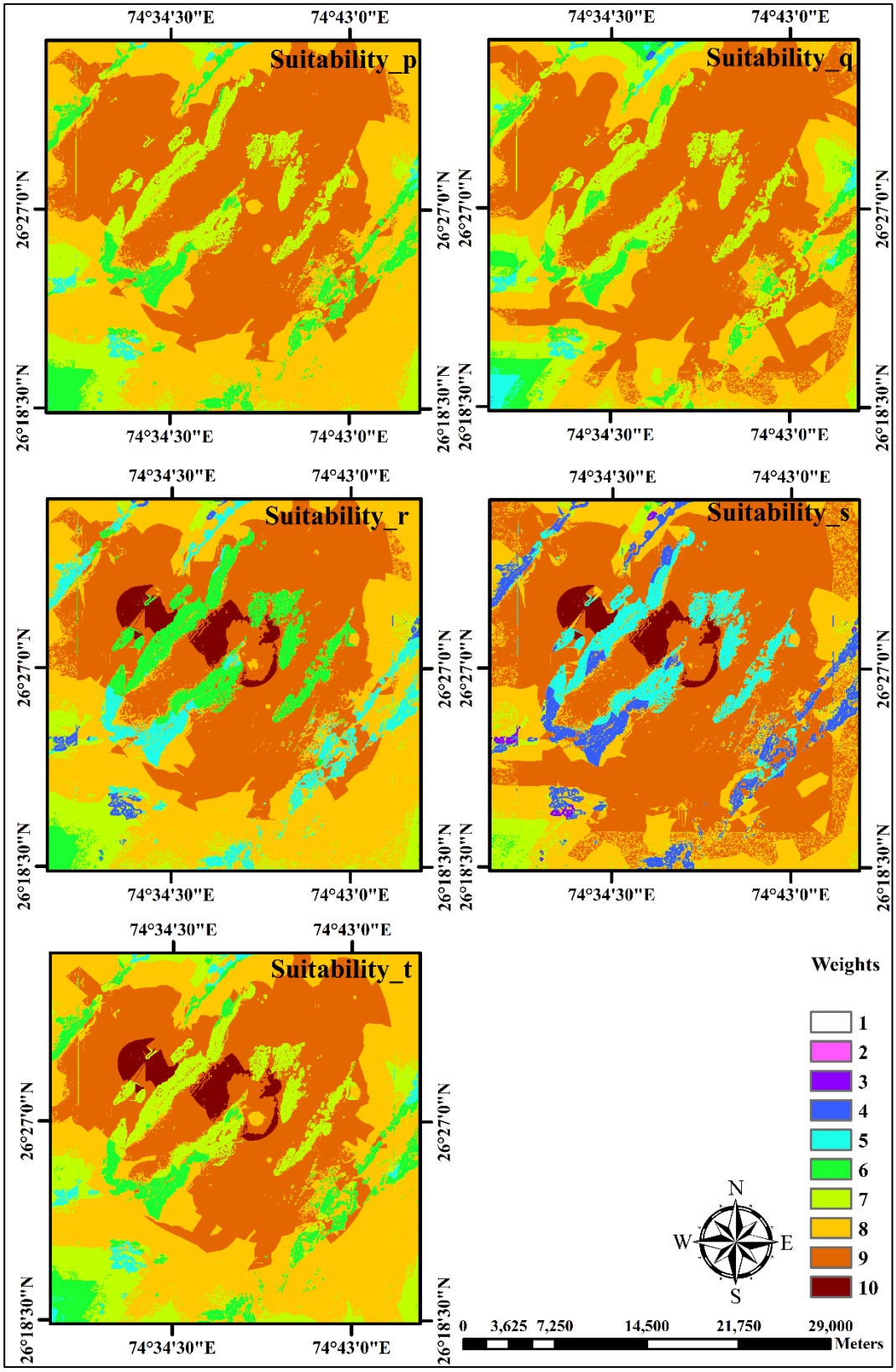

Figure 7.20: Land suitability layers for different weightage scenarios (p-t) for year 2015

7.6.5 SLEUTH-Suitability sensitivity for AHP weights of urbanization drivers

Each land suitability layer was then converted into GIF file format to bring them into the same file format as other input layers to meet the prerequisite conditions of the SLEUTH-Suitability model. The SLEUTH-Suitability was parameterized for each combination of urbanization driver weights using land suitability decision variable layer of a particular scenario at a time and other standard input layers like historical urban maps, road transportation layer, exclusion layer, and hillshade for all control years i.e., 1997, 2000, 2008, 2013 and 2015.

SLEUTH-Suitability uses a GA based calibration method. Optimum model parameters/ constant values (e.g. *self-modifying parameters*) obtained from the sensitivity analysis were used in the model. The model was calibrated for all combinations and optimum growth coefficients values were obtained for each land suitability scenario. According to Dietzel and Clarke (2007) out of the 12 goodness of fit metrics available in original SLEUTH model, OSM is a composite metric obtained from a subset of seven metrics that can be used to judge the calibration performance of the model. However, twelve metrics along with OSM have been used in the present study to evaluate the performance of SLEUTH-Suitability calibration. These 12 metrics are the goodness of fit measure and their value near 1 is indicative of finer model fitness.

Performance of the SLEUTH-Suitability in simulating the urban growth was assessed in term of spatial and statistical measures like urban population, urban edges, urban clusters, cluster mean size and cluster radius etc., as discussed in chapter 4.

The compare metric has found to be highest desirable in case of suitability_c and suitability_i i.e. 0.88 and 0.82, respectively. Pop is mostly above 0.9 for almost all suitability scenarios showing the consistency of the SLEUTH-Suitability model. The edge metrics is found to be greater for suitability_c, suitability_k and suitability_l i.e. 0.96, 0.96 and 0.94, respectively. However, it is high in almost all suitability combinations. The Clusters metrics has found to be the highest i.e. 0.96 in the case of suitability_b, suitability_d and suitability_h and almost in all combinations model fitness is good. Only a few suitability combinations were found to be below 73% in capturing urban clusters i.e. suitability_j, suitability_m, suitability_o and suitability_p with 0.69, 0.58, 0.65 and 0.39, respectively. The comparison of SLEUTH-Suitability model calibration for an

individual set of input layers based goodness of fit metrics i.e. Compare, Pop, Edges and Clusters is presented in Figure 7.21.

Moreover, the Leesallee spatial metric which represents an urban pattern index is found to be above 0.45 for all the suitability scenarios and above 0.5 for suitability_c, suitability_h, suitability_i, suitability_j, suitability_m, suitability_o and suitability_p. It is quite difficult to achieve such a high LeeSallee value, achieving more than 0.45 indicates good model performance (Rafiee et al., 2009; Hui-Hui et al., 2012; Akın et al., 2014; Dezhkam et al., 2014). The Xmean was achieved more than 95% for suitability_a, suitability_b, suitability_c, suitability_e, suitability_h, suitability_i, suitability_k, suitability_l, suitability_o, suitability_p and suitability_q. the Highest Ymean was achieved for suitability_d, suitability_p i.e. 0.82, 0.93 and 0.89 respectively. The Radius was achieved greater than 0.93 for all the suitability scenarios except suitability_d. The goodness of fit metric OSM which is a combination of seven metrics has been found to be satisfactory (0.23) for suitability_b, suitability_h, and suitability_n. However for other scenarios like suitability_g, suitability_i, and suitability_o OSM values have been found to be on the lower side as 0.19, 0.14 and 0.15, respectively. Getting higher composite OSM values is also a crucial factor in SLEUTH modeling. In various studies, lower OSM values were found to be satisfactory for urban growth simulations using the SLEUTH model (Clarke, 2017). Comparison of different metrics like LeeSallee, Xmean, Ymean, Radius and OSM corresponding to different suitability scenarios are presented in Figure 7.21

A higher value of Pop, Edges, Xmean and radius metrics (i.e., > 0.9) and Compare, clusters and Ymean goodness of fit (50%-95%) in almost all suitability combinations indicates a very good calibration performance of the SLEUTH-Suitability which is a good improvement over the original SLEUTH model.

Furthermore, in addition to good calibration performance of the model in term of the goodness of fit metrics, SLEUTH-Suitability model performance in simulating the urban growth (prediction phase outcome) can be judged in term of few spatial and statistical measures like an urban area, no. of edges, clusters, radius and mean cluster size. Further, the sensitivity of SLEUTH-Suitability with respect to AHP weights to the urbanization drivers used in land suitability decision variable can be determined with respect to a relative change in urban growth predictions which can be quantified in term

of relative change in spatial and statistical measures for all suitability scenarios i.e., a to p.

The comparison of spatial & statistical measures has been done with respect to the similar statistics calculated from the urban area of the same year (obtained from classified outputs of remote sensing data) for every individual input dataset prepared from varying combination of suitability weights of different explanatory variables. This comparison has been performed for every control year (i.e., 1997, 2000, 2008, 2013 and 2015) as well as for the year 2018 for predicted urban growth which indicates the performance of the model in urban growth prediction as presented in Figure 7.22 - 7.25. The suitability weight scenario for which difference in spatial and statistical measures calculated from the simulated urban growth and measures calculated from the reference urban area extracted from the LULC map of control years as well as for the year 2018 (assumed as correct one) is minimum, has been adopted as the optimum land suitability decision variable layer and corresponding weights to the participating urbanization drivers as optimum AHP weights.

Different combinations of suitability layers and the calibration & simulation-based statistics have been represented with a series of alphabetical characters (i.e., a-q) as presented in Figure 7.22-7.25. The suitability layer combination a-f are presented in Figure 7.22. The urban area, no. of clusters, cluster radius and mean cluster size captured against scenario suitability_c have been found to be closest to the statistical measures calculated from the actual urban area as compared to other scenarios ’a’, ‘b’, ‘d’, ‘e’ and ‘f’. However, urban edges have found to be more accurately captured in scenario ‘a’ as compared to the ’b’, ‘c’, ‘d’, ‘e’ and ‘f’ (Figure 7.22).

The comparison of results for suitability layer combinations g to j is presented in Figure 7.23. The urban area, no. of urban clusters, mean cluster size and radius are more accurately captured in case of scenario ‘i’ than ‘g’, ‘h’ and ‘j’. However, no. of edges are more accurately captured in case of scenario ‘h’.

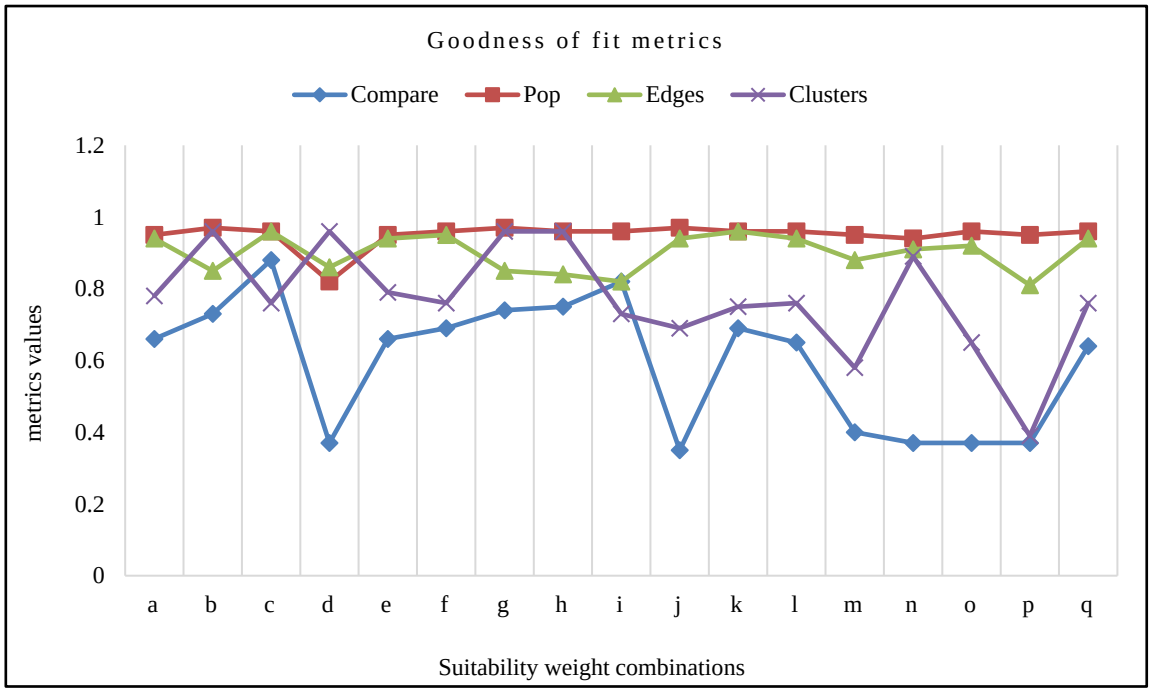

Compare, Pop, Edges and Clusters

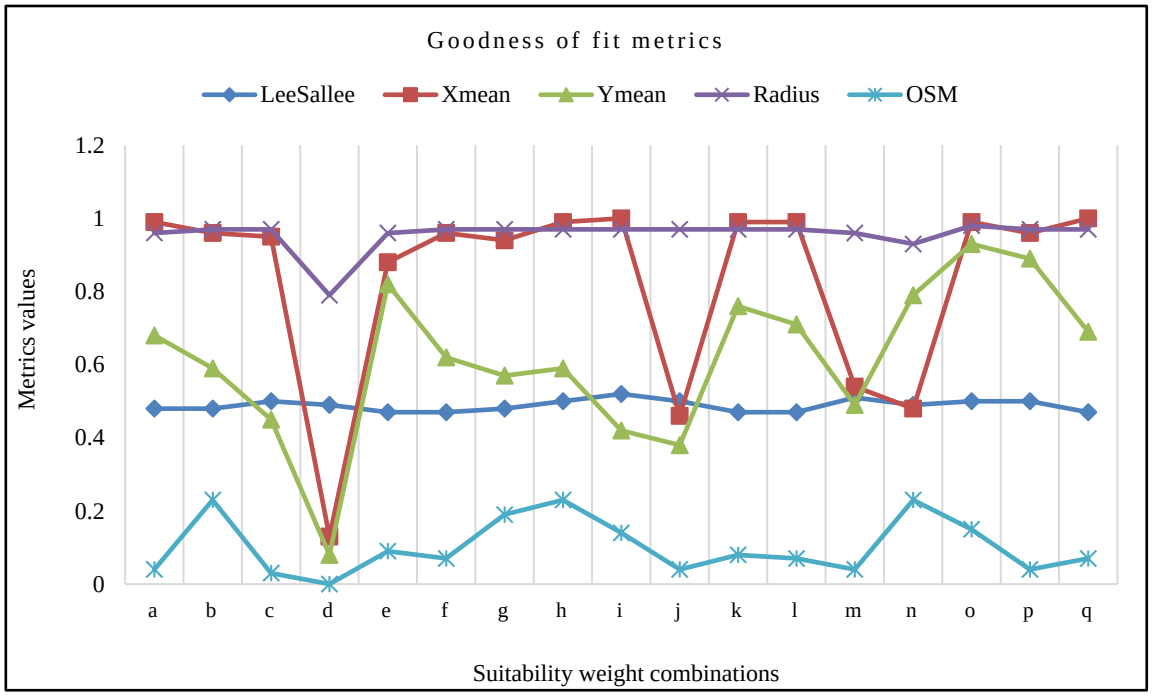

LeeSallee, Xmean, Ymean, Radius and OSM

Figure 7.21: Comparison of different spatial and statistical goodness of fit metrics for different land suitability scenarios

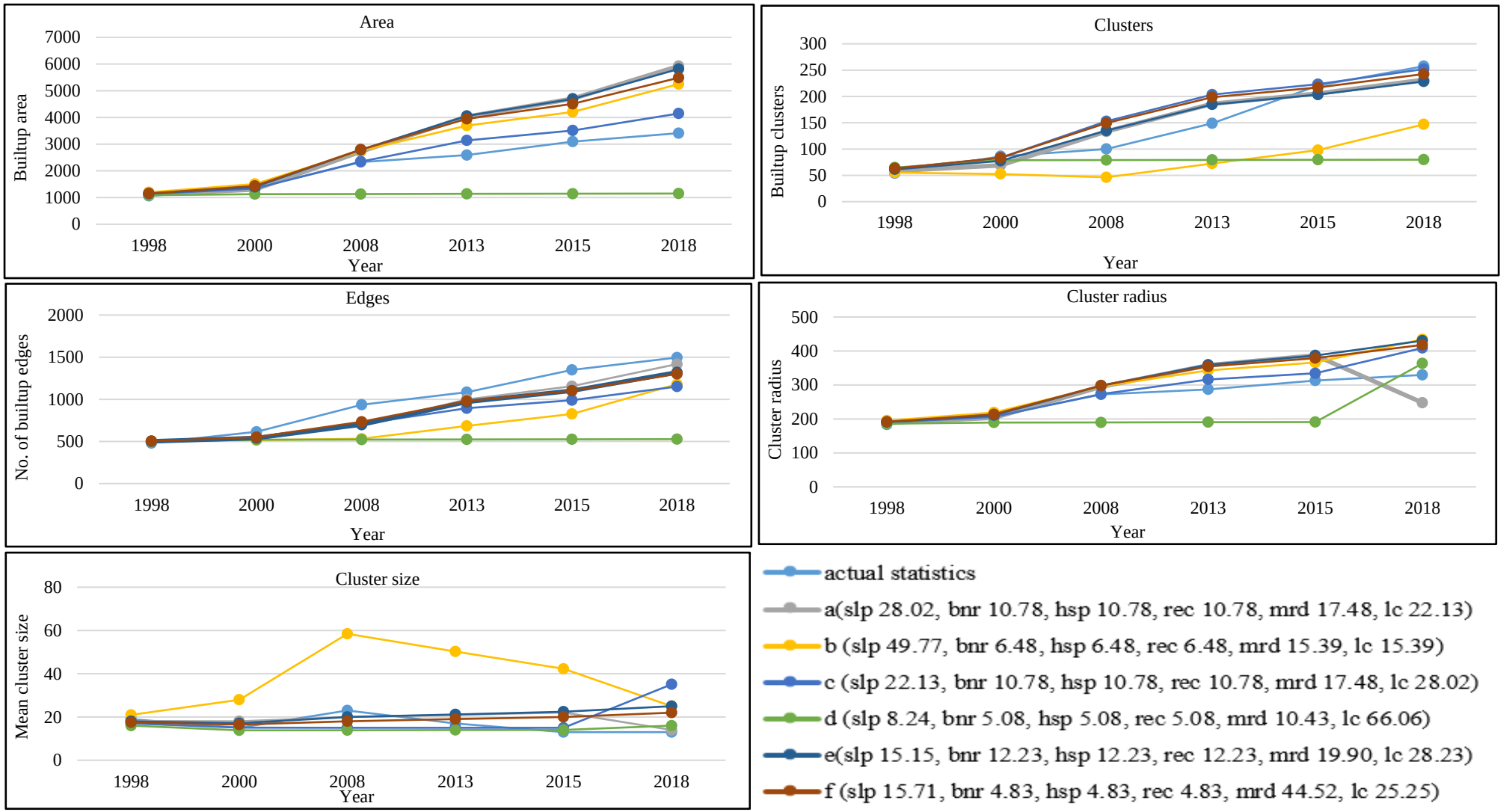

Figure 7.22: Comparison of statistical measures computed from actual and modeled with different suitability layers outcomes (a)

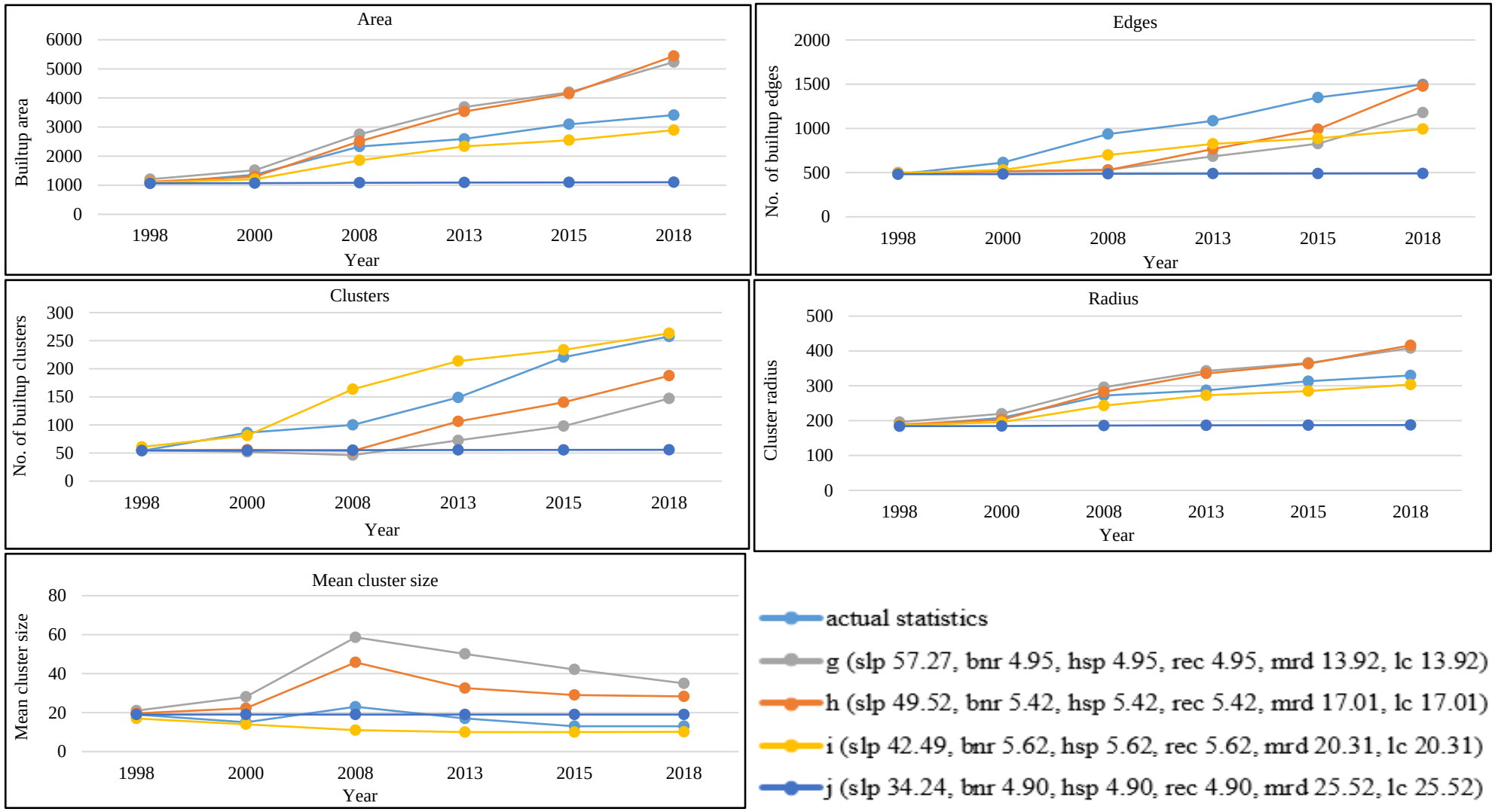

Figure 7.23: Comparison of statistical measures computed from actual and modeled (with different suitability methods) outcomes (b)

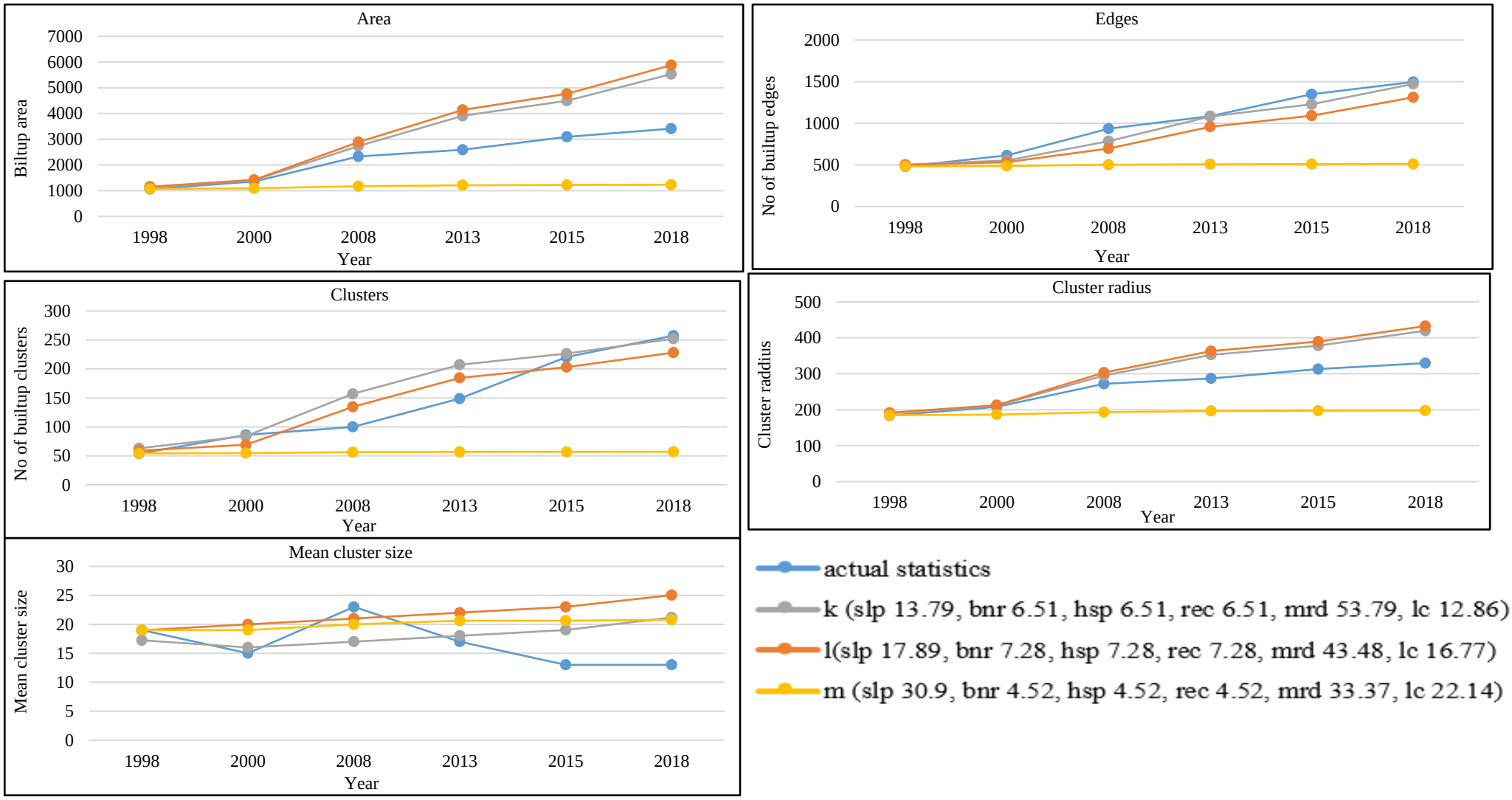

Figure 7.24: Comparison of statistical measures computed from actual and modeled (with different suitability methods) outcomes (c)

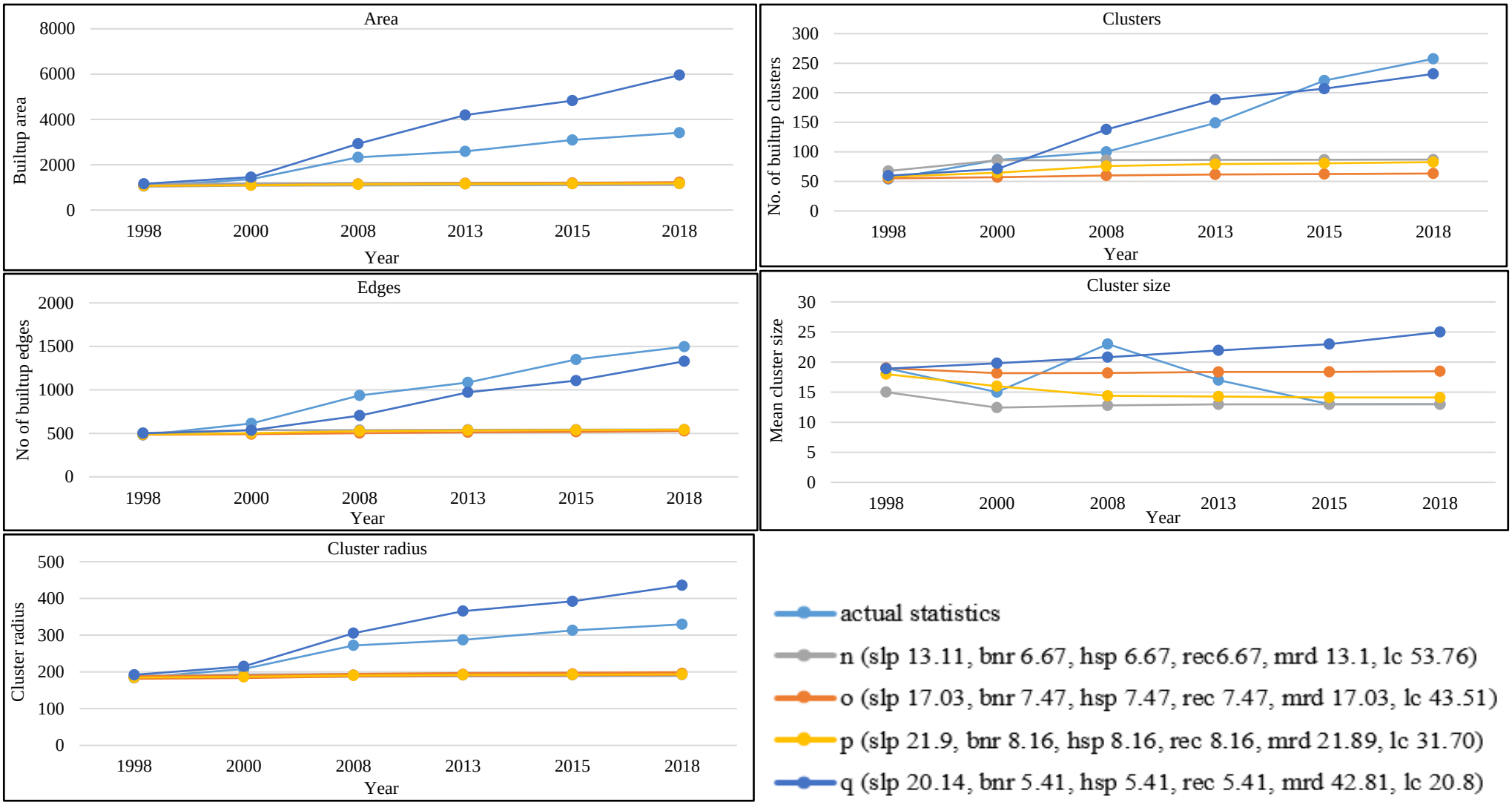

Figure 7.25: Comparison of statistical measures computed from actual and modeled (with different suitability methods) outcomes (d)

The comparison of statistical measures obtained from modelling outcomes of suitability scenarios k to m and actual data is presented in Figure 7.24. The urban area has not been found as close with the reference urban area in any of the scenarios i.e. scenario k to m that may be due to the inappropriate weight combinations of the individual explanatory variable in these scenarios. The no. of urban edges and clusters, however, captured well for the scenario 'k' as it is showing a closer match with the actual no. of edges and clusters respectively as compared to scenario 'l', and'. The mean cluster size and radius have also shown much variation between reference urban area and modeled urban area for all the scenarios i.e. k-m in almost all years.

For suitability scenarios from n to q statistical measures have been compared with the measures calculated from the reference area as given in Figure 7.25. The comparison between actual urban area (reference) and modeled statistics indicates variations for urban area, mean cluster size and radius. Only the no. of urban clusters and edges are found to be closely matched with the reference urban area.

Important inferences can be drawn from the above-discussed results of the sensitivity analysis of SLEUTH-Suitability as a function of AHP weights assigned to individual urbanization drivers in the land suitability decision variable.

- Year wise trend has not been observed in statistical measures for different years for different suitability scenarios. Model performance inferences have been drawn corresponding to the year 2018 to judge the prediction performance.
- It can be concluded that a particular combination of weights to the urbanization drivers in land suitability layer may not be appropriate in capturing all the forms of the urban growth. So, further suitable weights assigned to the urbanization drivers can be identified or refined to capture a particular type of urban growth in a better way.
- Thus, it is required to further refine the weights of different explanatory variables in the land suitability decision layer.

As discussed above a few new weight combinations based on the understanding achieved from the sensitivity analysis may be explored to arrive at better model performance. Three new suitability layer combinations have been prepared to identify more refined weights for the selected urbanization drivers (i.e., suitability_r, suitability_s and suitability_t). The model was calibrated and urban growth was predicted for these three suitability scenarios keeping other model inputs the same.

In suitability_r, slope driver was assigned the highest weight i.e 32.93. The land cost and slope variables were assigned weights of 24.29 and 32.93, respectively. Weights assigned to different drivers are presented in Table 7.30.

Table 7.30: Pairwise comparison matrix and weights for Suitability_r scenario

Urbanization expl. variables	Slope	DBR	DH	DRP	DMR	Land cost	Final weights
Slope	1						32.932
DBR	0.2	1					8.182
DH	0.2	1	1				8.182
DRP	0.199	1	1	1			8.176
DMR	0.9	2.2	2.2	2.2	1		18.229
Land cost	0.9	2.2	2.2	2.2	2.3	1	24.299
CR = 0.027							

In the suitability_s scenario higher weight was assigned to the slope as 44.7. The DMR and land cost variables were the same weights as 20.0.5. The remaining three variables were the same weight as 5.06, as presented in Table 7.31.

Table 7.31: Pairwise comparison matrix and weights for Suitability_s scenario

Urbanization expl. variables	Slope	DBR	DH	DRP	DMR	Land cost	Final weights
Slope	1						44.709
DBR	0.1	1					5.06
DH	0.1	1	1				5.06
DRP	0.1	1	1	1			5.06
DMR	0.55	3.7	3.7	3.7	1		20.056
Land cost	0.55	3.7	3.7	3.7	1	1	20.056
CR = 0.004							

The suitability_t scenario 8.4 has been assigned as a weight to distance from bus & railway station, distance from recreational places and hospital variables. The weight for the slope was assigned 22.18 and distance from main roads and land cost variables were assigned weights of 24.53 and 28.08, respectively (Table 7.32).

The newly formulated pairwise comparison matrix has given final weights for respective suitability weight scenario and land suitability layers are prepared for all control years as presented in Figure 7.20 for the year 2015, as a sample. Furthermore, the SLEUTH-Suitability model was calibrated and urban growth was simulated for each suitability scenario independently. The model has produced similar statistical metrics as already

discussed in the above sections and these metrics are compared to determine the best weight combination scenario.

Table 7.32: Pairwise comparison matrix and weights for Suitability_t scenario

Urbanization expl. variables	Slope	DBR	DH	DRP	DMR	Land cost	Final weights
Slope	1						22.182
DBR	0.7	1					8.401
DH	0.7	1	1				8.401
DRP	0.7	1	1	1			8.401
DMR	0.6	4	4	4	1		24.535
Land cost	0.65	4	4	4	1.5	1	28.08
CR = 0.067							

A good value of Compare, Pop, Edges, Clusters, Xmean and Radius have been obtained (0.94) for the suitability_s scenario. In addition, an improved LeeSallee value of 0.52 has been achieved which is quite good for urban growth modelling applications using SLEUTH (Rafiee et al., 2009; Hui-Hui et al., 2012; Akın et al., 2014; Dezhkam et al., 2014). The OSM achieved as 0.17 for set 's' that is far improved from the other two combinations i.e. 'r' and 't'. The goodness of fit measure favors the suitability weight combinations of set's' (please refer to Figure 7.26).

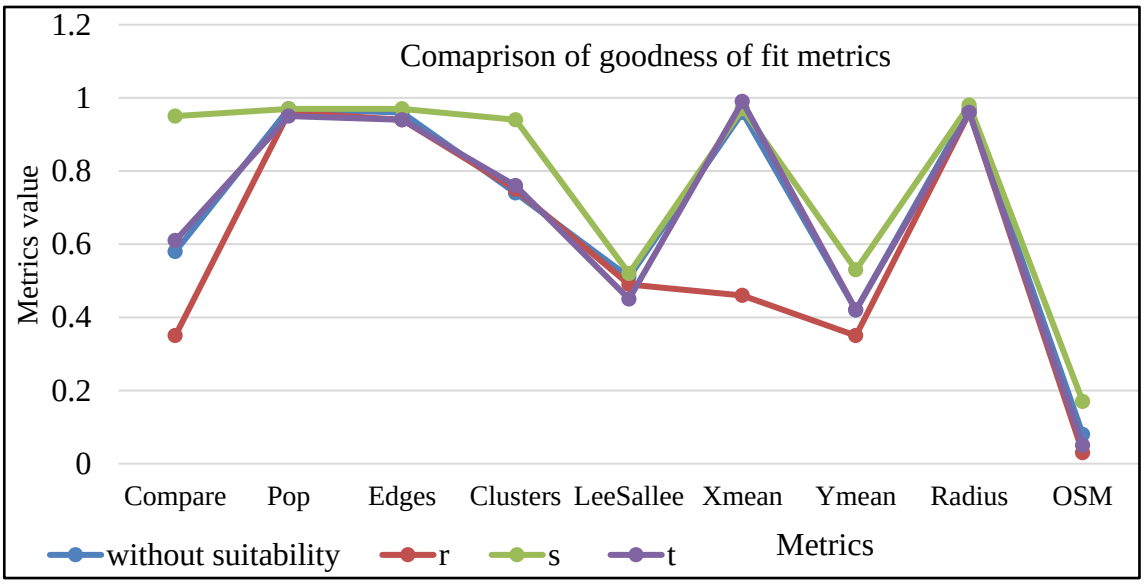

Figure 7.26: Comparison of different spatial and statistical goodness of fit metrics

In addition, the statistical measures have also been compared with respect to the actual data as discussed in the above sections. The urban area, no. of clusters, edges, radius and

mean cluster size is found to be closely matched with the actual data based respective statistics for set ‘s’ as compared to the set ‘r’ and ’t’ (please refer to Figure 7.27).

The current section dealt with the sensitivity analysis of the combination of weights of different urbanization explanatory variables. The individual combination of suitability weight layers has been introduced into the model as one of the input variable layers and the model is calibrated and simulated for each combination independently. The above discussion about the sensitivity analysis of the combination of weights gives an idea about the optimal weights combination which best reflects the socio-economic, bio-physical and topographic characteristics of the study area in modelling outcomes. It is identified that slope weight of 44.709 with highest preference, distance from main roads and land cost with lesser weight of 20.056 and distance from bus n railway, distance from recreational places and hospitals with equal weight as 5.06 are the optimal weights to derive the land suitability decision variable for the cities and towns having Ajmer like socio-economic & topographical characteristics (Table 7.33).

Table 7.33: Optimal weights to urbanization drivers participating in land suitability

Variable	Slope	Land Cost	DMR	DRP	DBR	DH
Weight	44.7	20.05	20.05	5.06	5.06	5.06

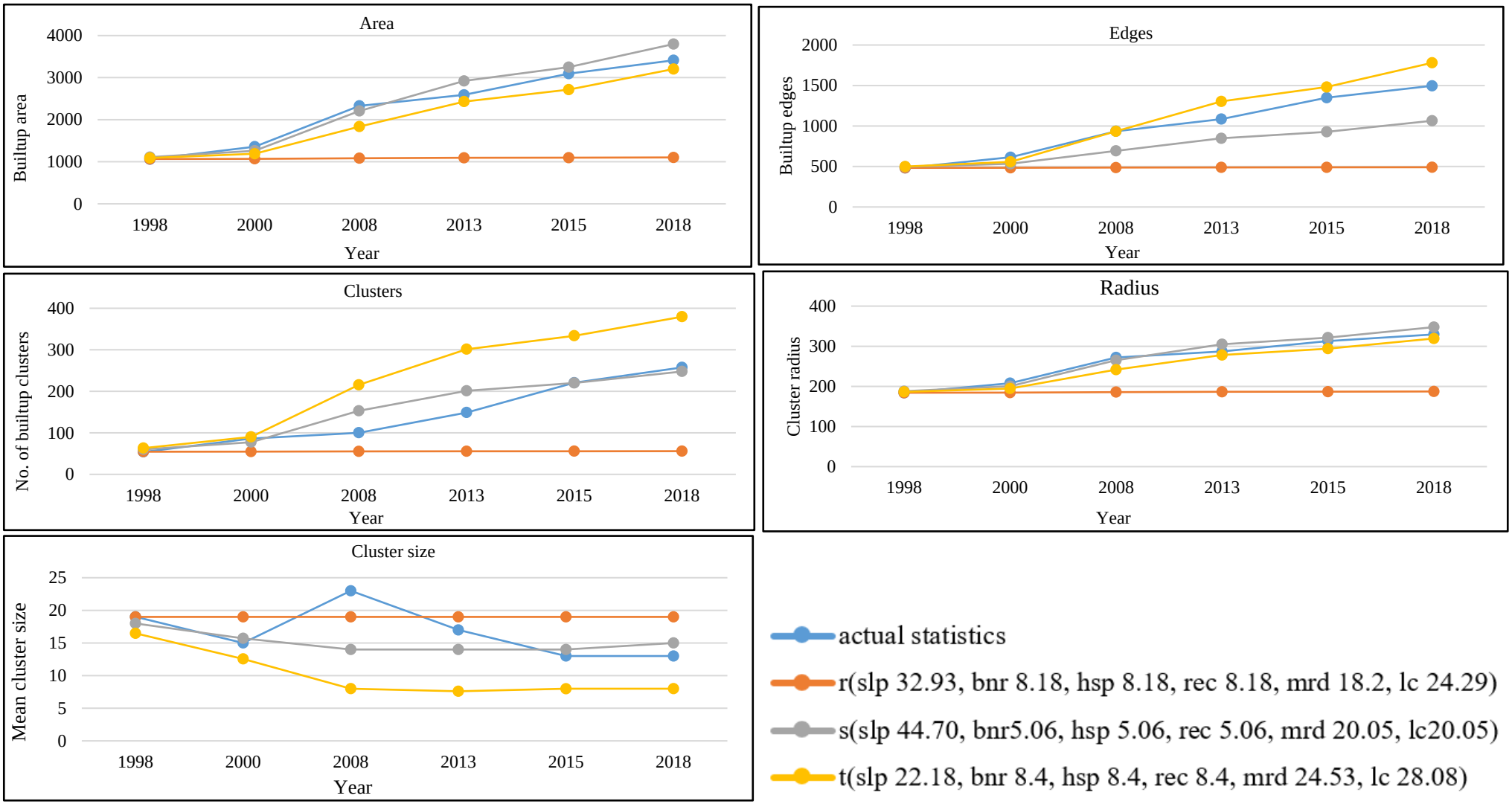

Figure 7.27 Comparison of statistical measures computed from actual and modeled (with different suitability methods) outcome (e)

7.7 Concluding Remarks

The SLEUTH-Suitability model has been successfully developed by developing an algorithm to include the land suitability decision rule in the simulation process, programming code was written and integrated with the existing SLEUTH. SLEUTH-Suitability model was successfully tested on a demo input dataset. Important urbanization drivers and explanatory variables have been identified and land suitability decision variable layer has been derived using AHP based MCE method. SLEUTH-Suitability models sensitivity to the weights of urbanization drivers in land suitability decision layer has been determined by determining the relative change in models calibration and urban growth prediction performance for different suitability scenarios (with different weights to urbanization drivers) in term of the goodness of fit of landscape metrics and spatial & statistical measures. Optimum weights for the different urbanization drivers have been determined as presented in Table 7.33. Improved model performance has been achieved from the SLEUTH-Suitability with a good LeeSallee i.e. 0.52 and OSM i.e. 0.2 values. The new version of the model i.e., SLEUTH-Suitability has performed well as compared to original SLEUTH during calibration as well as in urban growth predictions on account of the inclusion of more urbanization drivers in the simulation process. The new model has been found to be better and satisfactory in capturing the fragmented and small size developments in addition to other forms of urban growth. However, the SLEUTH-Suitability further needs to be tested for modelling of the urban growth of different cities in different socio-economic and geographical conditions.

CHAPTER 8

DEMONSTRATION OF MODEL APPLICATION AND PERFORMANCE COMPARISION

8.1 Prologue

The SLEUTH model works with a strict structure of growth coefficients, rules which operate upon input layers (i.e. slope, land use, exclusion, urban, transportation and hillshade in SLEUTH; plus one additional layer i.e., land suitability in SLEUTH-Suitability) as discussed in detail in Chapter 4. However, the original SLEUTH model has some limitations as discussed in Chapter 4 and 5, which have been improved in the present research work by identifying the appropriate value of model parameters/constants through sensitivity analysis (discussed in Chapter 5) and further by incorporating an additional urbanization decision rule i.e., land suitability, which is a function of important urbanization drivers, into the LULC change and urban growth simulation process, as discussed in Chapter 7. A new improved version of model SLEUTH-Suitability has been successfully developed to incorporate the land suitability urbanization decision variable.

Application of three different versions of the SLEUTH model i.e. base SLEUTH model with default parameters (i.e. version 1), SLEUTH model with optimum model constants & parameters (i.e. version 2) and SLEUTH-Suitability (i.e. version 3) have been demonstrated for Ajmer fringe, a medium-size developing city situated in Rajasthan state of India. Three versions of the model have been parameterized using the same input data of the Ajmer fringe independently, calibrated using the GA based method and urban growth was predicted for up to the year 2040 using the methodology as discussed in Chapter 4.

Further, the performance of three versions of the SLEUTH model has been compared in term of their performance during calibration, in urban growth prediction and in term of their capability in capturing the different type of urban growth. Also, the improvement in performance from original SLEUTH to SLEUTH-Suitability has been determined in terms of different metrics, measures, and accuracy. The overall comparison was done on the basis of several criteria i.e., criteria 1: goodness of fit landscape metrics to compare calibration performance; criteria 2: spatial and statistical measures i.e. urban area, no. of edges and clusters, mean cluster size and cluster radius to judge the performance of urban growth prediction; criteria 3: growth coefficients; criteria 4: hit-miss-false alarm method; criteria 5: accuracy assessment on the basis of random sample points overlaid on

high resolution Geo-eye satellite image; criteria 6: accuracy assessment on the basis of GCP's collected from field and criteria 7: visual analysis.

8.2 Application Demonstration

8.2.1 The base version of SLEUTH model with default parameters

The application of the base SLEUTH model with default parameter/ constant (i.e. *boom* 1.01, *bust* 0.09, *critical low* 0.97 and *critical high* 1.3, *diffusive value parameter* 0.005, *critical slope* 15, *Monte Carlo* 10, *game of life critical threshold* 2 cells and *cellular neighborhood size* 8 cells) settings has been demonstrated for Ajmer fringe including Pushkar town. The model has been parameterized for the prerequisite conditions and calibrated satisfactorily to obtain the optimal growth coefficient values utilized in simulating the urban growth up to the year 2040 using the methodology discussed in detail in Chapter 4. Model performance in calibration and urban growth prediction has been assessed in terms of different metrics, measures, and accuracy as discussed in section 8.1. After successful model calibration in phases, optimum growth coefficients (Table 8.1) have been obtained corresponding to the goodness of fit landscape metrics and one composite metric i.e., OSM (Table 8.1). The model calibration has been found to be satisfactory in terms of goodness of fit metrics i.e. compare, pop, edges, clusters, LeeSallee, Xmean, Ymean, Radius and OSM (Table 8.1). The optimal growth coefficients have been obtained as 16, 98, 100, 36 and 52 for diffusion (diff), breed (brd), spread (sprd), slope resistance (slp) and road gravity (rg) coefficients, respectively. The major contributing coefficients are breed and spread coefficients indicating more new spreading center and organic/ spread growth for the study area. The simulated urban growth maps of the year 1998, 2000, 2008, 2013, 2015 and 2018 are presented in Figure 8.1. The trend of urban growth of Ajmer has been presented in Figure 8.2. Urban growth for control years (i.e. the year 2000, 2008, 2013 and 2015) has been simulated as 1260.42, 1602.89, 1793.63 and 1872.71 (in km^2) respectively while actual urban growth obtained from the classified satellite images of respective years as 1358.38, 2328.68, 2589.73 and 3093.72 (in km^2). For the predicted urban growth in the year 2018, it has been simulated as 1996.86 km^2 while actually, it is 3411.53 km^2 (extracted from the classified image of the year 2018). Urban growth map for Ajmer in the year 2040 has been presented in Figure 8.3. Urban growth of Ajmer may reach to 3176.18 km^2 up to the year 2040. Urban growth will increase exponentially in the near future in the urban fringe.

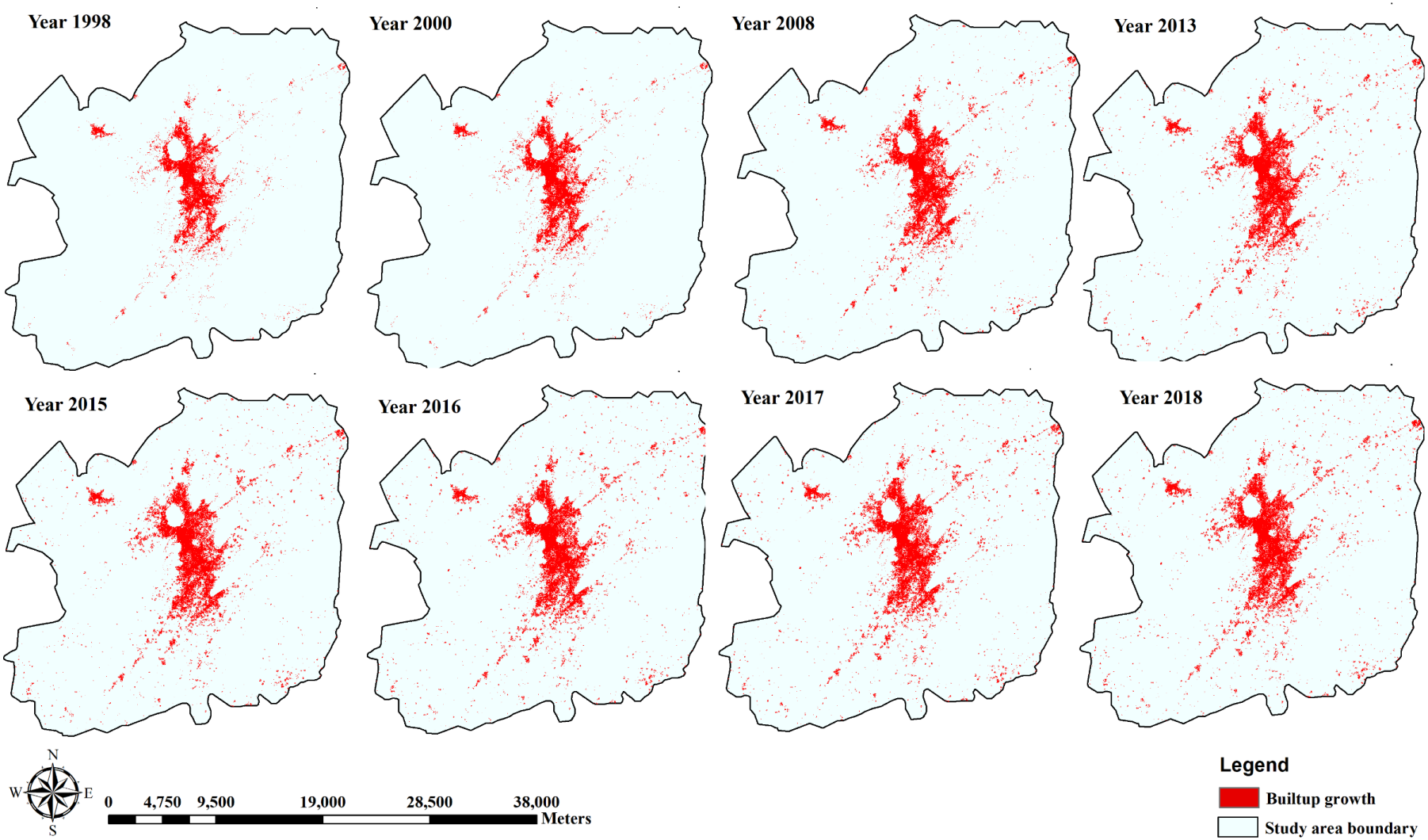

Figure 8.1: Simulated urban growth for year 1997. 2000, 2008, 2013, 2015, 2016, 2017 and 2018 using base version 1 of SLEUTH

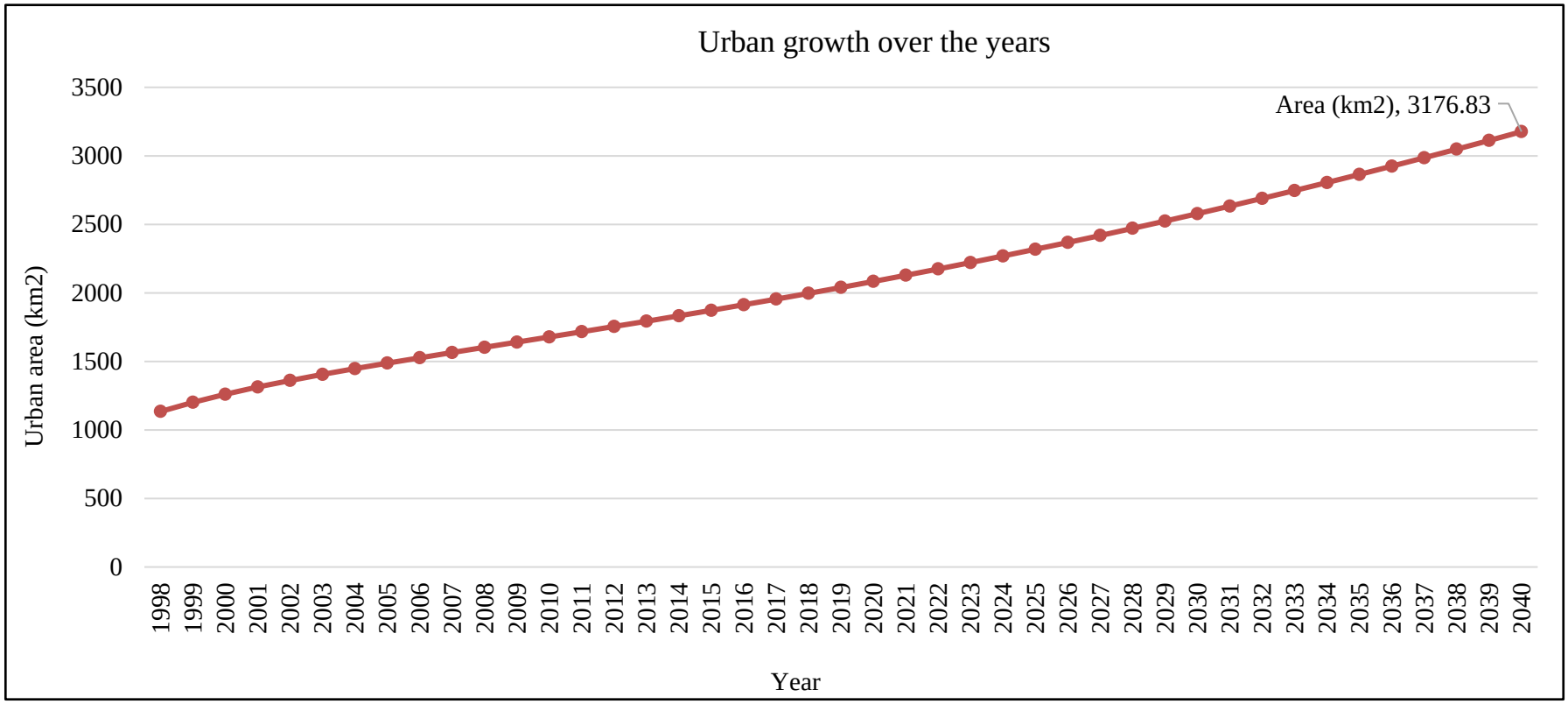

Figure 8.2: Predicted urban growth area for a period (1998-2040) using base SLEUTH version1

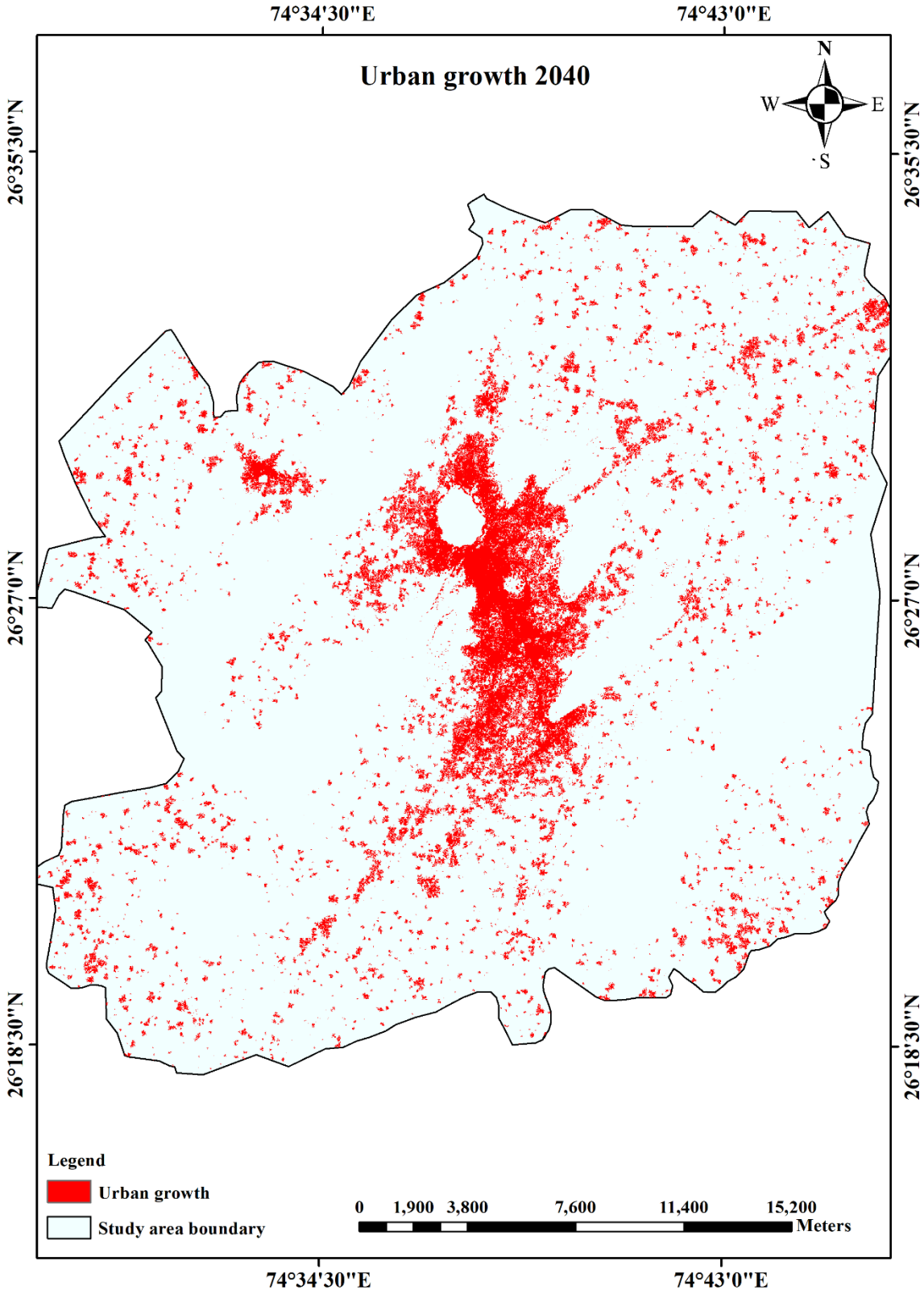

Figure 8.3: Predicted urban growth area for year 2040 using base SLEUTH version 1

The study shows that rapid urban growth is taking place in Ajmer along the Jaipur road (NH8), the area near the highway has grown more rapidly through the years (Figure 8.3). The area around Ana Sagar Lake has urbanized at a faster rate in the past few years as

population density of that area has grown rapidly. The area nearby Foy Sagar depicted very high urban growth which may be due to the development of new colonies in relatively flat areas. Pushkar bypass Road is showing road influenced growth as new development has taken place recently and is likely to further grow in the near future. Madar area which is in a North-East direction to Ana Sagar Lake is also showing growth as new railway colonies have been developed and more are likely to get developed in the future. Beawar Road which is in the south direction is also showing road influenced growth. Many educational institutes are developing along highways due to which nearby development is also taking place. So, the study area will be developing at a faster rate in upcoming years. Nasirabad Road is in the east direction also showing urban growth at a faster rate in the past few years. The area around Bisal Sagar has grown rapidly as a huge amount of population is shifting to earn their livelihood. Areas nearby Khanpura Pond is also likely to get developed at a smaller pace as many industrial activities are taking place at this region. The Pushkar region is one of the most important places in Ajmer fringe which is depicting higher growth in upcoming years. Pushkar region is a religious and popular place, commercialization is being increased and also the urban density is getting higher at this place. In upcoming years it will be growing at large.

8.2.2 SLEUTH model with optimum model constants & parameters

The SLEUTH model's sensitivity to a few selected model parameters and constants have been determined and their optimum values are estimated (i.e. *boom* 1.3, *bust* 0.10, *critical low* 0.90 and *critical high* 1.25, *diffusive value parameter* 0.0055, *critical slope* 15, *Monte Carlo* 60, *game of life critical threshold* 1 cells and *cellular neighborhood size* 12 cells). Sensitivity analysis has been discussed and presented in Chapter 5 in detail. Improvement in the base SLEUTH model with optimum model parameters has been further examined by simulating urban growth of Ajmer fringe which also includes Pushkar town using the same input data as used in application demonstration of SLEUTH with default model parameters. The model has been parameterized for the prerequisite conditions and calibrated using the GA based calibration process to obtain the optimal growth coefficient values corresponding to optimal model fitness measure i.e. OSM using the methodology discussed in Chapter 4. The goodness of fit metrics obtained from the calibration are found to be 0.57, 0.98, 0.97, 0.93, 0.51, 0.95, 0.52, 0.98 and 0.08 for compare, pop, edges, clusters, LeeSallee, Xmean, Ymean, Radius and OSM respectively. In this case, optimal growth coefficients have been obtained as 87, 100, 100, 60 and 44 for diffusion, breed,

spread, slope resistance, and road gravity coefficients, respectively. The major contributing growth coefficients are found to be breed and spread coefficients indicating more new spreading centers and organic/ spread growth. In addition, higher values of diffusion, slope resistance, and road gravity coefficients are also indicating greater diffusive/ spontaneous and road influenced growth in the study area. Further, optimum growth coefficient values (as presented in Table 8.2) utilized in simulating the real urban growth patterns and based on the existing growth scenario urban growth is predicted for up to the year 2040. The simulated growth from this version of the model for a different year like 1998, 2000, 2008, 2013, 2015 and 2018 has been presented in Figure 8.4. Urban growth for the control years (i.e. the year 2000, 2008, 2013 and 2015) has been simulated as 1298.3, 1910.78, 2417.05 and 2652.2 (in km^2) respectively while actual urban growth obtained from the classified satellite images of respective years as 1358.38, 2328.68, 2589.73 and 3093.72 (in km^2). For the predicted urban growth in the year 2018, it has been simulated as 3037.45 km^2 while actually, it is 3411.53 km^2 (extracted from the classified image of the year 2018). The trend of urban growth area (km^2) and urban growth map for Ajmer in the year 2040 are presented in Figure 8.5 & 8.6 respectively. Urban growth of Ajmer may reach to 6486.8 km^2 up to the year 2040. Urban growth will increase exponentially in the near future in the urban fringe.

The study shows that rapid urban growth is taking place in Ajmer along the Jaipur road (NH8), area nearby highway has grown more rapidly through the years (Figure 8.6). The area around Ana Sagar Lake has urbanized at a faster rate in the past few years as population density of that area has grown rapidly. The area nearby Foy Sagar depicted very high future urban growth as compared to the growth predicted by the base version of the SLEUTH model. Small size development has been captured well from this version of the model (Figure 8.6). The area along the Jaipur road and Pushkar bypass will be developed rapidly up the year 2040. Large amounts of growth may take place in this area on account of various factors like the establishment of two universities on the Pushkar bypass road, better road connectivity with the surrounding areas and availability of flat land. Another locality which may develop significantly is the Beawer and Nasirabad Road on account of favorable conditions like good roads and flat land availability.

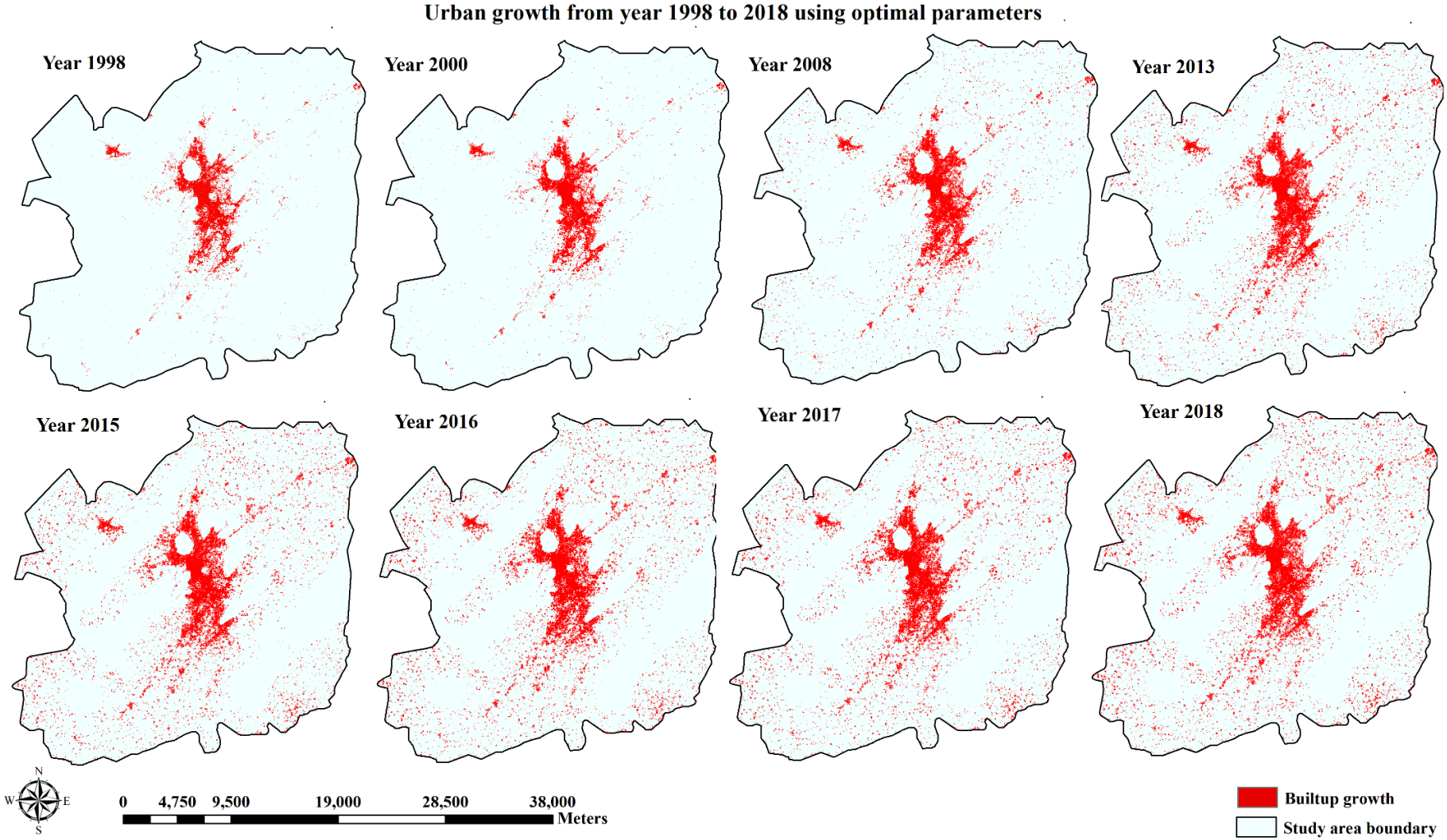

Figure 8.4: Simulated urban growth for year 1997. 2000, 2008, 2013, 2015, 2016, 2017 and 2018 using version 2

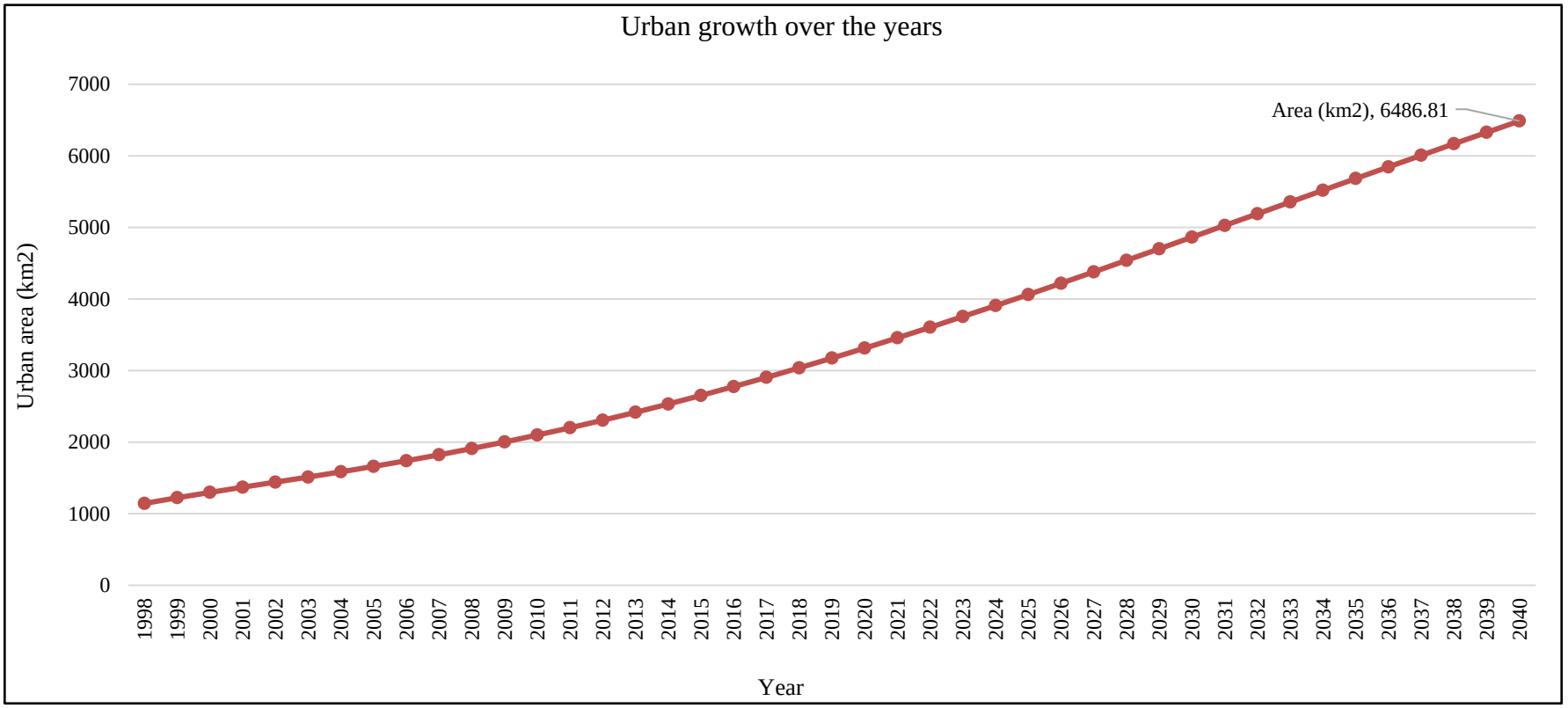

Figure 8.5: Predicted urban growth area for a period from 1998-2040 using optimum model parameters i.e. version 2

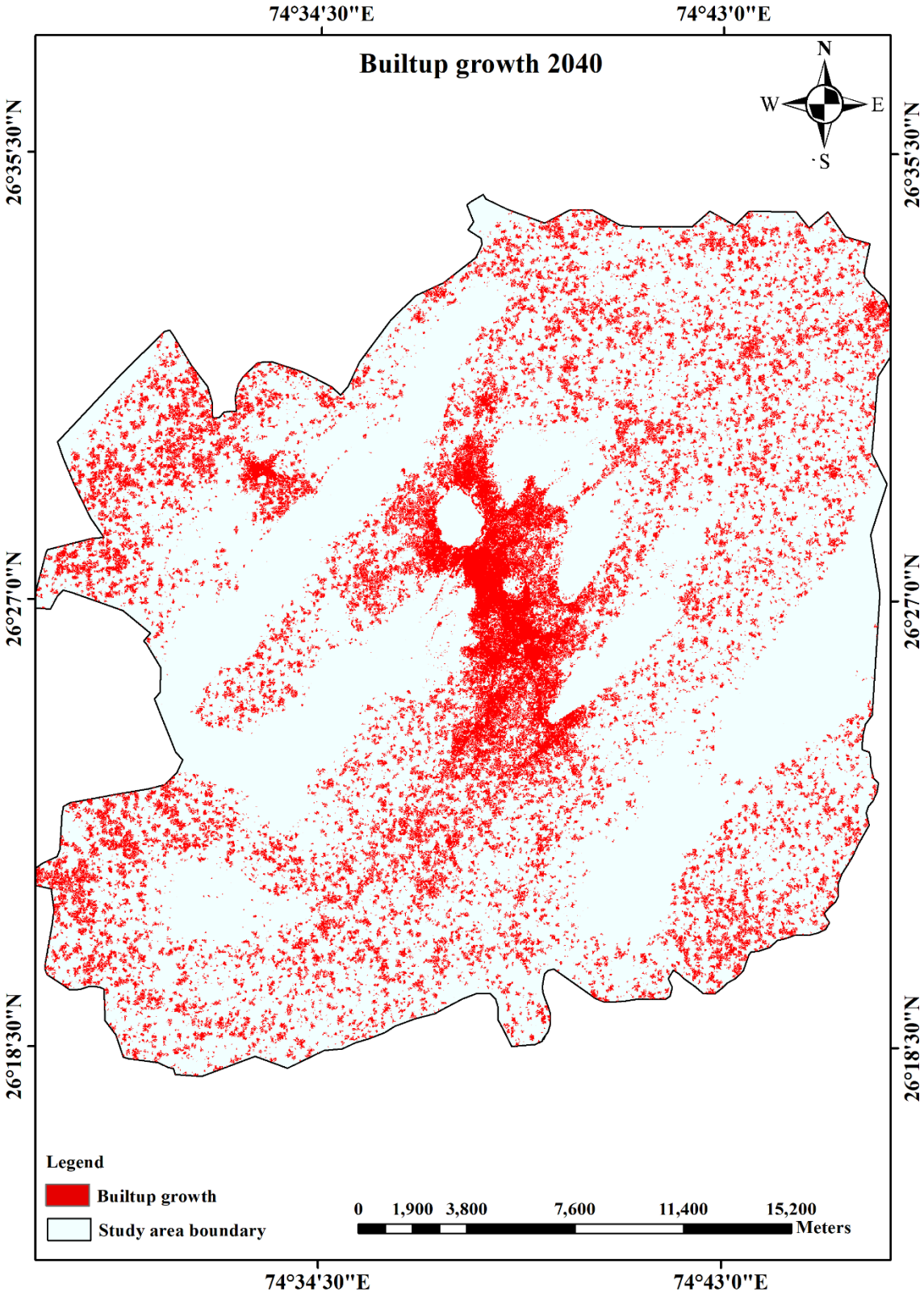

Figure 8.6: Predicted urban growth area for the year 2040 using version 2

8.2.3 SLEUTH-Suitability

As discussed in Chapter 5, SLEUTH model performance can be improved by incorporating the effect of other important urbanization drivers/ explanatory variables into urban growth simulation process to simulate urban growth more accurately and simulating small size development and fragmented growth in a better way, in different socio-economic conditions. Thus, an attempt has been made in the present study to develop a newer version of SLEUTH i.e., SLEUTH-Suitability by adding one more urban growth decision rule i.e., land suitability in the simulation process. The methodology adopted in developing SLEUTH-Suitability has been discussed in detail in Chapter 4 and Chapter 7. Further, application of the SLEUTH-Suitability has been demonstrated by simulating the urban growth of Ajmer fringe. Also, improvement in performance of SLEUTH-Suitability as compared to the base SLEUTH model performance has also been quantified as discussed in subsequent sections.

The SLEUTH-Suitability model was parameterized for the prerequisite conditions with the required input dataset including a land suitability decision variable layer and optimum model parameters/ constants obtained from sensitivity analysis. SLEUTH-Suitability was calibrated using the GA based algorithm and urban growth was simulated up to the year 2040 using the methodology discussed in Chapter 4 and 7. Optimum growth coefficients have been obtained corresponding to the optimal model fitness measure i.e., OSM. Further model accuracy in simulating urban growth and different forms of urbanization has been tested using different methods as explained in Chapter 4. Model performance has been found to be good and improved as compared to the base version of SLEUTH. The accuracy assessment of the modelling outcomes has been performed in many ways that validate the model performance.

After calibrating SLEUTH-Suitability optimal growth coefficients have been obtained as 51, 6, 26 and 74 for diffusion, breed, spread, and road gravity coefficients, respectively. The major contributing coefficients are diffusion and road gravity coefficients indicate more spontaneous and road influenced growth as compared to the clustered and new spreading center growth. the goodness of fit metrics obtained from the calibration are found to be 0.95, 0.97, 0.97, 0.94, 0.52, 0.97, 0.53, 0.98 and 0.2 for compare, pop, edges, clusters, LeeSallee, Xmean, Ymean, radius and OSM respectively.

Table 8.1: Optimal values of model growth coefficients corresponding to different goodness of fit metrics for base SLEUTH case

Metrics/ coefficient	Compare	Pop	Edges	Clusters	LeeSallee	Xmean	Ymean	Radius	OSM	diff	brd	sprd	slp	rg
Values	0.57	0.98	0.97	0.93	0.51	0.95	0.52	0.98	0.08	87	100	100	60	44

Table 8.2: Optimal values of model growth coefficients corresponding to different goodness of fit metrics for SLEUTH-Sensitivity

Metrics/ coefficients	Compare	Pop	Edges	Clusters	LeeSallee	Xmean	Ymean	Radius	OSM	diff	brd	sprd	slp	rg
Values	0.59	0.97	0.95	0.8	0.5	0.95	0.52	0.98	0.07	16	98	100	36	52

Table 8.3: Optimal values of model growth coefficients corresponding to different goodness of fit metrics for SLEUTH-Suitability

Metrics/ coefficients	Compare	Pop	Edges	Clusters	LeeSallee	Xmean	Ymean	Radius	OSM	diff	brd	sprd	rg
Values	0.95	0.97	0.97	0.94	0.52	0.97	0.53	0.98	0.2	51	6	26	74

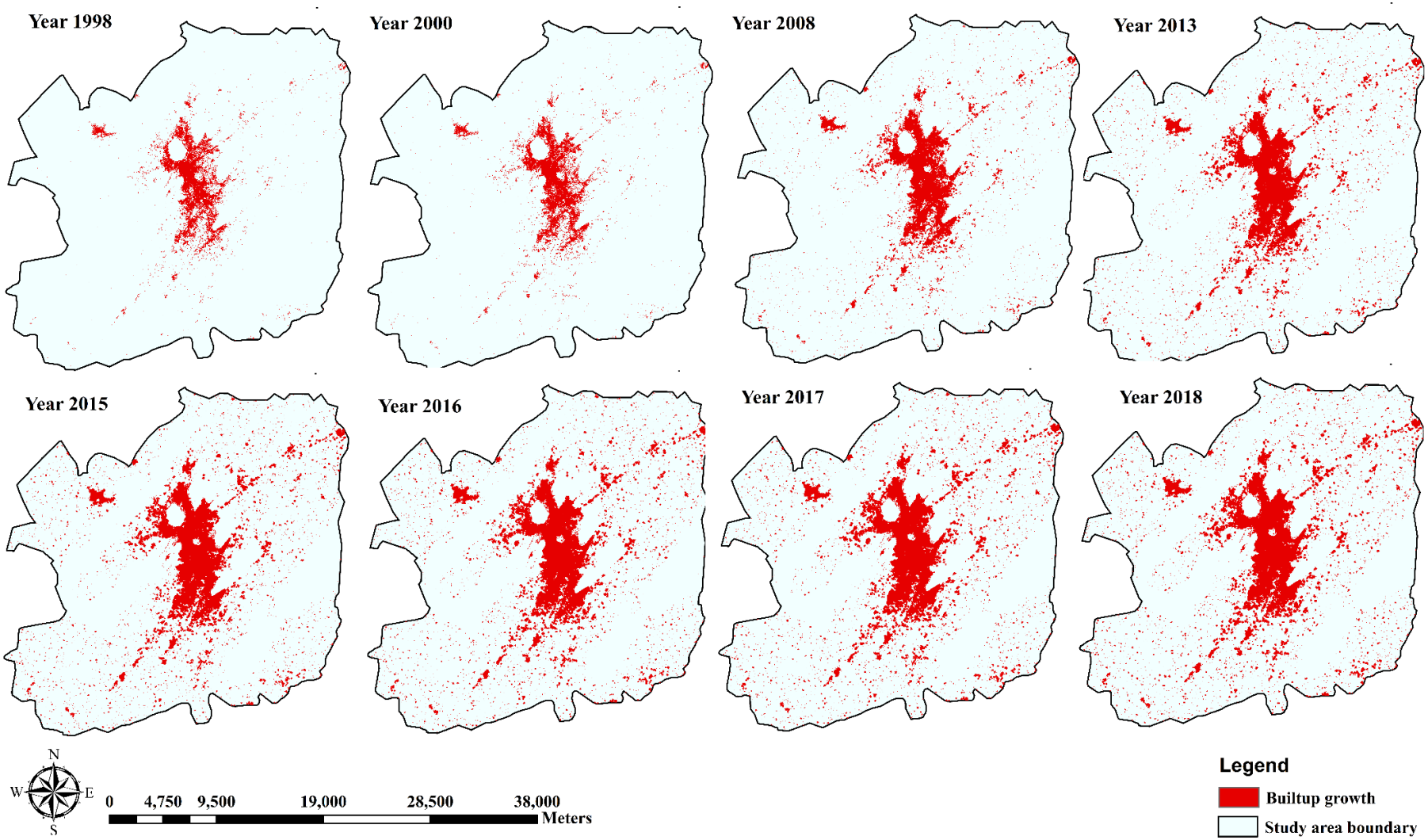

Figure 8.7: Simulated urban growth s for year 1997, 2000, 2008, 2013, 2015, 2016, 2017 and 2018 using SLEUTH-Suitability i.e. version 3

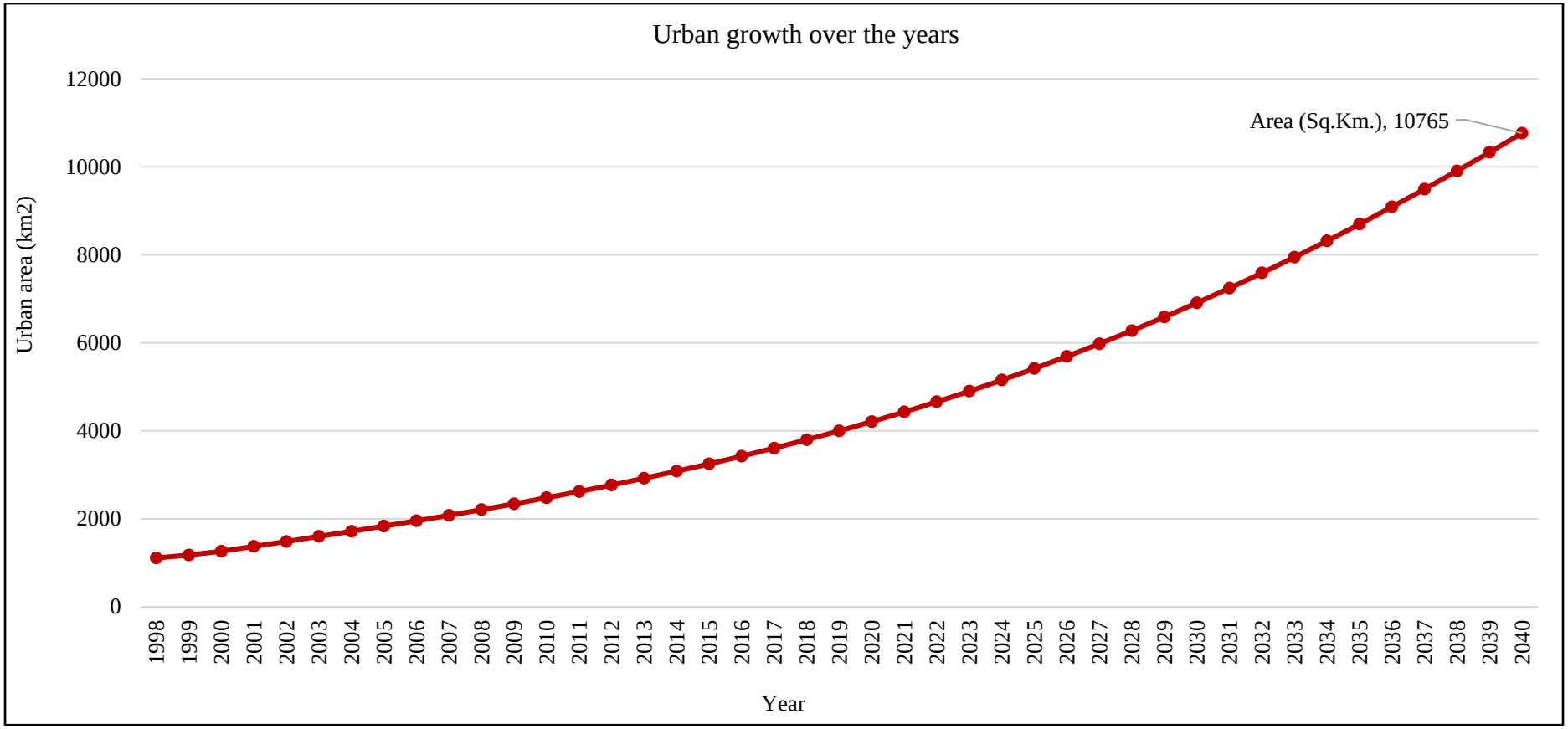

Figure 8.8: Predicted urban growth for Ajmer fringe up to the year 2040 using SLEUTH-Suitability i.e. version 3

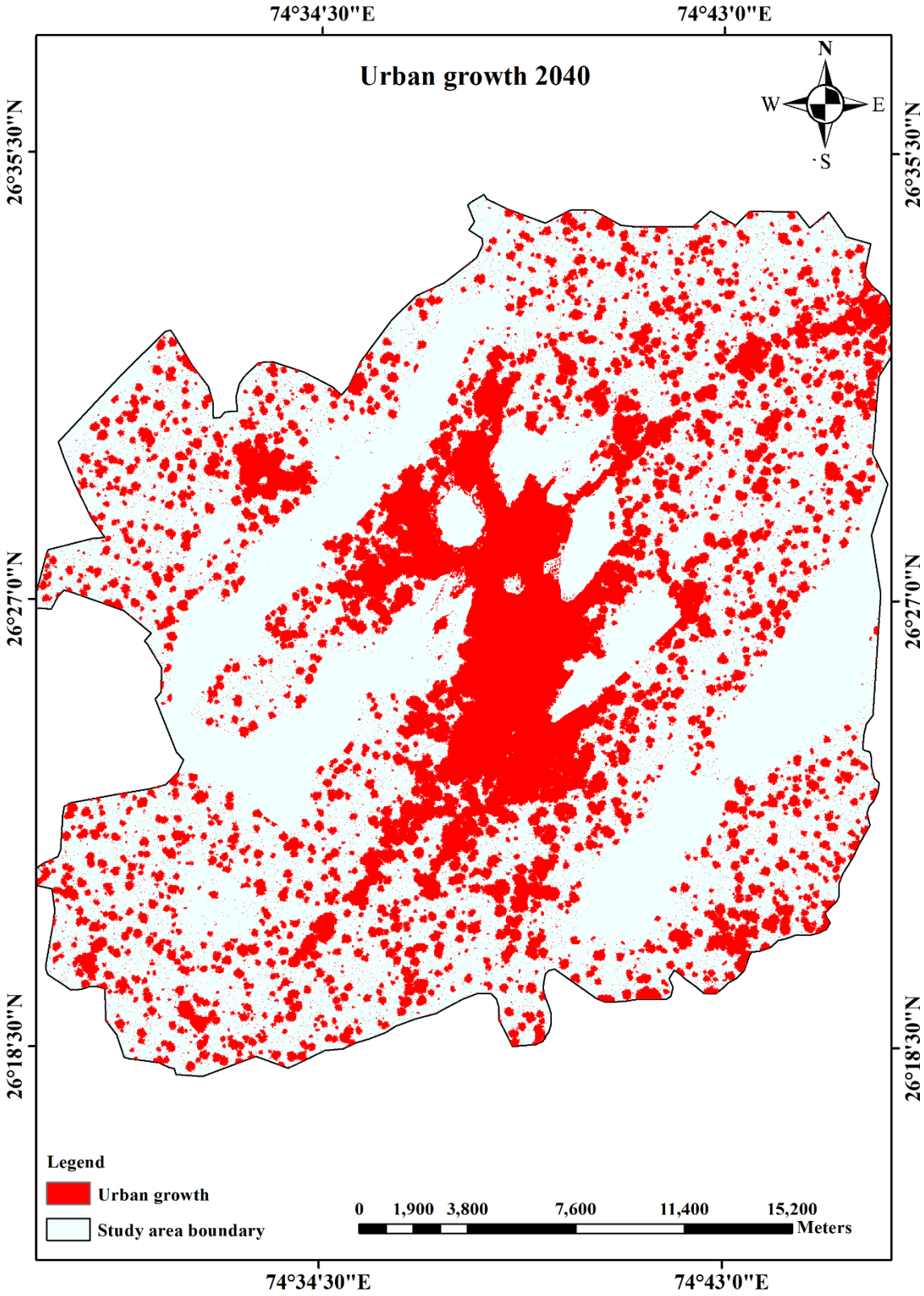

Figure 8.9: Predicted urban growth for Ajmer in the year 2040 using SLEUTH-Suitability

The simulated urban growth for different years i.e., 1998, 2000, 2008, 2013, 2015 and 2018 has been presented in Figure 8.7. Urban growth for control years (i.e. the year 2000, 2008, 2013 and 2015) has been simulated as 1261.64, 2207.15, 2921.39 and 3248.81 (in km^2)

respectively while actual urban growth obtained from the classified satellite images of respective years as 1358.38, 2328.68, 2589.73 and 3093.72 (in km^2). For the predicted urban growth in the year 2018, it has been simulated as 3798.26 km^2 while actually, it is 3411.53 km^2 (extracted from the classified image of the year 2018). The urban growth has been predicted up to the year 2040 and it is indicating exponential urban growth in the coming years as presented in Figure 8.8. Urban growth map for Ajmer in the year 2040 has been presented in Figure 8.9. The urban growth of Ajmer may reach 10765 km^2 up to the year 2040. Urban growth results obtained from this version of the model have been found to be consistent as per the actual growth available on the ground for the year 2018. Ajmer will develop significantly along the main roads like Pushkar bypass, Jaipur road, Jaipur bypass, Beawar road. More development has been predicted for the year 2040 in areas where land suitability is better like flat land in Foy Sagar area, Pancheel area and Pushkar bypass, which indicates land suitability representing urbanization drivers are playing a significant role in urban growth simulation.

8.3 Comparison of Performance of Different Versions of SLEUTH Model

8.3.1 Methodology for performing a model performance comparison

A comparative analysis of three versions of the SLEUTH model has been made to understand how the performance of the SLEUTH model has been improved from one version of a model to another. The base SLEUTH model with default parameters (i.e. version 1) has been first parameterized and calibrated to reach out to the optimal growth coefficient values which are called as best fit coefficient values. These optimal set of coefficient values are used for the simulation and prediction of urban growth up to the year 2040 using the methodology as discussed in Chapter 4. Further, to identify the appropriate range of crucial model constants and parameters rigorous sensitivity testing has been performed and the obtained optimal values of parameters have been used to again parametrize and calibrate the model i.e., version 2. The more refined growth coefficient values against the improved OSM and LeeSallee values have been used to simulate urban growth up to the year 2040. Further, a newer version of model i.e. SLEUTH-Suitability (version 3) has been developed to incorporate an additional LULC change and urban growth decision variable i.e. land suitability which incorporates the influence of important urbanization driver into the simulation process. A suitable framework has also been developed to derive land suitability decision variables using AHP based MCE technique.

In addition, SLEUTH-Suitability model sensitivity testing with respect to the combination of weights assigned to different selected urbanization drivers participating in the land suitability variable has been performed to obtain the appropriate weights for the individual explanatory variable at which the land suitability decision variable is appropriate and model performance improves for simulating the different urban growth forms and patterns.

Performance of three versions of the SLEUTH has been compared using the methodology presented in Figure 8.10. The red, green and blue color lines are showing the work flow for version 1, version 2 and version 3, respectively while black lines are indicating the common flow for each version of SLEUTH model. Comparison of the models has been made for their performance in calibration measured in terms of the goodness of fit landscape metrics, model prediction performance was compared in terms of spatial and statistical measures and overall performance of the model versions in terms of percentage accuracy, kappa statistics, Hit-Miss-False alarm method, ground truthing and visual analysis. Seven criteria are conceptualized to compare the performance of different versions of the model, as discussed in subsequent sections of the chapter.

8.3.1.1 Criteria 1: a Model comparison in term of the goodness of fit metrics

All three versions of the model (base SLEUTH model, SLEUTH with optimum parameters and SLEUTH-Suitability) were parameterized using the required input data of the same study area i.e. Ajmer fringe and calibrated independently. The calibration performance of three model versions has been assessed based on several goodnesses of fit metrics i.e. Compare, Pop, Edges, Clusters, LeeSallee, Xmean, Y mean, Radius and OSM. Details of the metrics have been presented in Table 4.1 in Chapter 4. The metrics value closer to '1' is indicative of a better model fit during calibration. The Compare metrics showing the ratio of simulated urban population for a final year over actual urban (seed urban area) population in the respective year has been found to be the highest for the SLEUTH-Suitability (Figure 8.11 as 'suit') i.e. version3. In figures, three versions of the model are referred *def* for as base SLEUTH with default parameters (referred as version 1), *sens* for base SLEUTH with optimum constant/ parameters (referred as version 2), and *suit* for SLEUTH-Suitability (referred as version 3), (Figure 8.11). It is evident from Figure 8.11 that the calibration performance has gradually improved from the base version (referred as version 1) to SLEUTH –Suitability (referred as version 3).

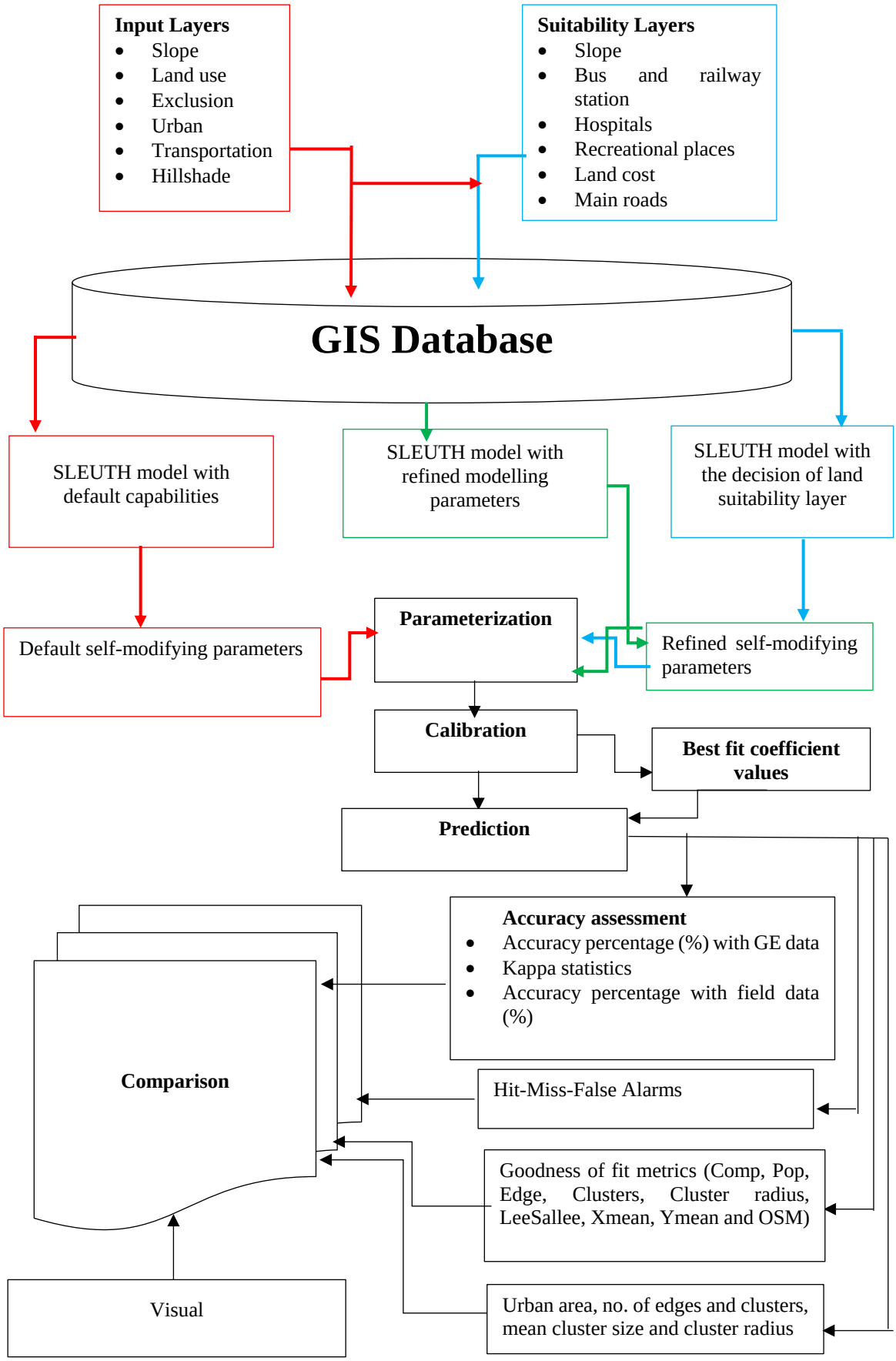

Figure 8.10: Methodology used for the comparison of two improved version of SLEUTH model with respect to the default version i.e. version 1

The performance of model version 1 and 2 are almost the same in capturing the urban population but not as good as version 3, Urban population metrics value has been found to be around 0.6 for version 1 and version 2 however, it has improved to 0.96 for version 3 which is quite good. The Pop metric showing the least square regression score for modelled urbanization as compared to reference urban area provided as seed urban area for the control years has been found to be almost similar in all the three versions of SLEUTH model i.e. 0.97, which is quite good. The higher value of Pop indicates that all the three version of SLEUTH have the capability to imitating the historical urban growth for the controlling years. However, it is difficult to say that all the three versions can predict urban growth equally well. To analyze the capability of all the three versions of the model in urban growth prediction, some other spatial and statistical measures (discussed in later sections) have also been considered. The Edge metric showing the least square regression score for modelled urban edges count as compared to the edge count estimated from the seed urban area for each control year. The edge metric has been found to be the highest for version 3 (0.97) as compared to version 1 (0.95) and 2 (0.96). The difference in performance of the model in term of edge metric has not been so significant however, version 3 has produced marginally better urban edges means it is better in capturing the small size development and fragmented growth. The Clusters metric showing the least square regression score for modelled urban clusters as compared to the known urban clusters for the controlling years estimated from the seed urban area has been found to be quite good in case of version 2 i.e. 0.96 as compared to other versions.

The LeeSallee metric which represents a spatial fit between the model simulated urban growth and the known urban extent for the control years (seed urban area obtained from LULC maps) has found to be improving from 0.5 to 0.51 and 0.52 respectively for version 1, 2 and 3. Getting such higher LeeSallee values is quite difficult in urban growth modelling. The value of LeeSalle more than 0.30 has found to be acceptable in urban growth modelling applications. A higher value of LeeSaalee indicates that all versions of the SLEUTH are capable of simulating the urban growth satisfactorily and version 3 has been found to be better. The Xmean and Ymean metrics are the least square regression of average x and y values for modelled urbanized cells as compared to average x and y values estimated from the seed urban area for different control years. Version 3 has been found to be better in terms of Xmean and Ymean metrics as shown in Figure 8.11. The Radius metric showing the least square regression of standard radius of the urban distribution i.e. normalized standard deviation in x and y has been found to be 0.98 in all the three versions

of the SLEUTH model. The OSM metric is a multiplication of seven metrics (Dietzel and Clarke, 2007) which is used to select the optimum growth coefficients during the model calibration. Calibration performance of version 3 has been found to be better with 0.20 OSM value as compared to OSM value of 0.07 and 0.08 for version 1 and 2, respectively. Better OSM for version 3 i.e. SLEUTH-Suitability model indicates better model calibration performance which may have improved because of the inclusion of important urbanization drivers in the simulation process in the form of the land suitability variable.

Moreover, the calibration statistics obtained from the calibration of an individual version of SLEUTH model are the indicators of success in simulating urban growth for the controlling years. The SLEUTH-Suitability has been found to be comparatively better in the calibration stage in term of the goodness of fit landscape metrics like Compare, Pop, Edges, LeeSallee, Xmean, Ymean Radius and OSM (Figure 8.11). Version 3 is imitating the historical growth of the control years well.

8.3.1.2 Criteria 2: a Model comparison in term of spatial and statistical measures

Performance of three versions of the SLEUTH model have been further compared in term of relative differences among spatial and statistical measures which indicate the capability of a model to capture the different forms of urban growth, calculated from predicted urban growth and from reference urban area obtained from LULC maps prepared from classification of satellite data for control years as well as for year 2018. Comparison of spatial and statistical measures corresponding to simulated growth and reference urban area is presented in Figure 8.12. The capability of capturing different urban forms has been consistently improved from version 1 to 2 to 3. It is evident from Figure 8.12 that modeled urban area is closely matching to the reference urban area for version 3. The performance of SLEUTH with optimum parameters i.e. version 1 has been found to be better than base i.e. version 1 of the model. Urban growth predicted for years other than seed years has been found to be better for version 3 as compared to the other two versions. Performance of the version 2 model has also been found better as compared to version 1. In term of urban growth predicted for the year 2018, version 1 has been found to be closer to the actual growth in the year 2018 obtained from a classified satellite image. The no. of urban edges captured from version 2 was found closer to actual no. of urban edges as compared to the other two version of models.

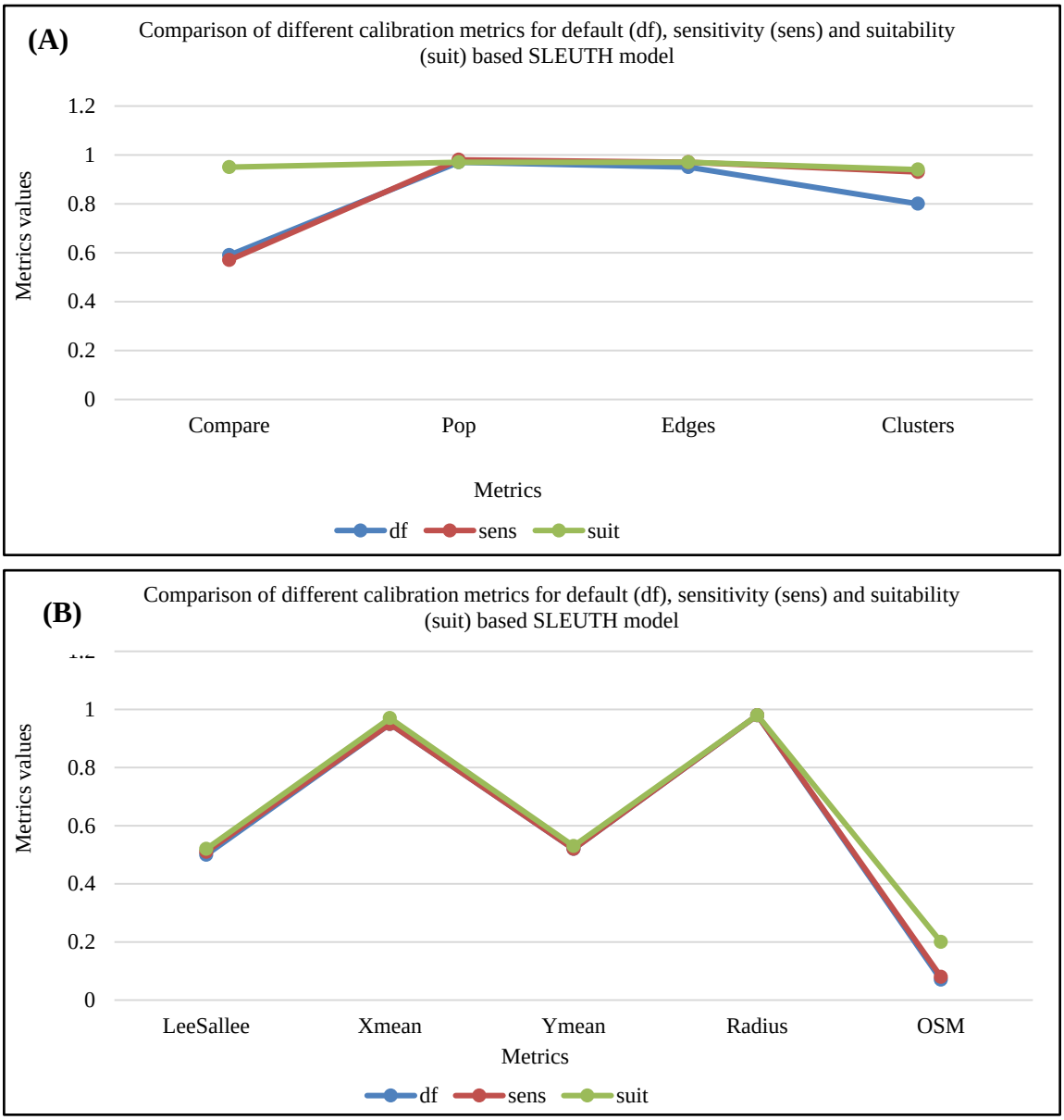

Figure 8.11: Comparison of three versions of SLEUTH model using spatial and statistical metrics. A: compare, pop, edges, clusters; B: Lee Sallee, Xmean, Ymean, Radius and OSM

For capturing urban edges in the sensitivity based SLEUTH model i.e. version 2 is found to be more reliable than the remaining two. The number of urban clusters is most appropriately captured by the case of version 2 and 3 of SLEUTH model as it shows the closest match with the urban clusters calculated from reference urban area. The cluster radius captured for version 3 (SLEUTH-Suitability) has been found to be better and in close agreement with the cluster radius obtained from reference urban area for different years as compared to the other two versions. The mean cluster size is captured a little greater than that obtained from reference urban area in case of SLEUTH-Suitability, however, better than the two other versions.

It can be concluded from the comparative analysis of spatial and statistical measures that SLEUTH-Suitability is able to simulate urban growth better and it is also capable of capturing the different forms of urban growth. A continuous improvement in the model has been observed from base version 1 to optimal constant/ parameter based version 2 and SLEUTH-Suitability i.e. version 3.

8.3.1.3 Criteria 3: a Model comparison in term of growth coefficients

As discussed earlier each version of the model was calibrated independently and optimum growth coefficients have been obtained corresponding to optimum model fitness (OSM). Urban growth coefficients affect overall model performance in the prediction phase. Optimum growth coefficients obtained for different versions of the model are presented in Figure 8.13. The breed and spread coefficients are the major controllers of the urban growth in the case of version 1 and 2. However, the road gravity coefficient seems to be controlling the urban growth in SLEUTH-Suitability. In addition, along with road gravity, diffusive and spread coefficients are also contributing to the growth in term of disaggregated and organic growth. It has observed that SLEUTH-Suitability is able to capture fragmented growth in a better way with a diffusive value of 51 for which goodness of fit metrics are also found to be better than other versions of the model (as discussed above).

8.3.1.4 Criteria 4: Comparison of the models using Hit-Miss-False alarm method

Hit-Miss-False Alarm method has also been used to determine the performance of the different versions of the model in simulating the urban growth. A number of hits indicates correctly captured urban pixels in percentage, miss indicates urban pixels which were left out and false alarm are the pixels wrongly captured by the model as urban pixels. This method has been discussed in detail in Chapter 4. The component of correctness, error, ratio indices and statistical measures for version1 (def), version2 (sens) and version3 (suit) of SLEUTH (% landscape) obtained from Hit-Miss-False alarm method are presented in Table 8.4. Results presented in Table 8.4 indicates a better spatial match between simulated urban growth and reference urban area for respective years for the SLEUTH-Suitability version of the model.

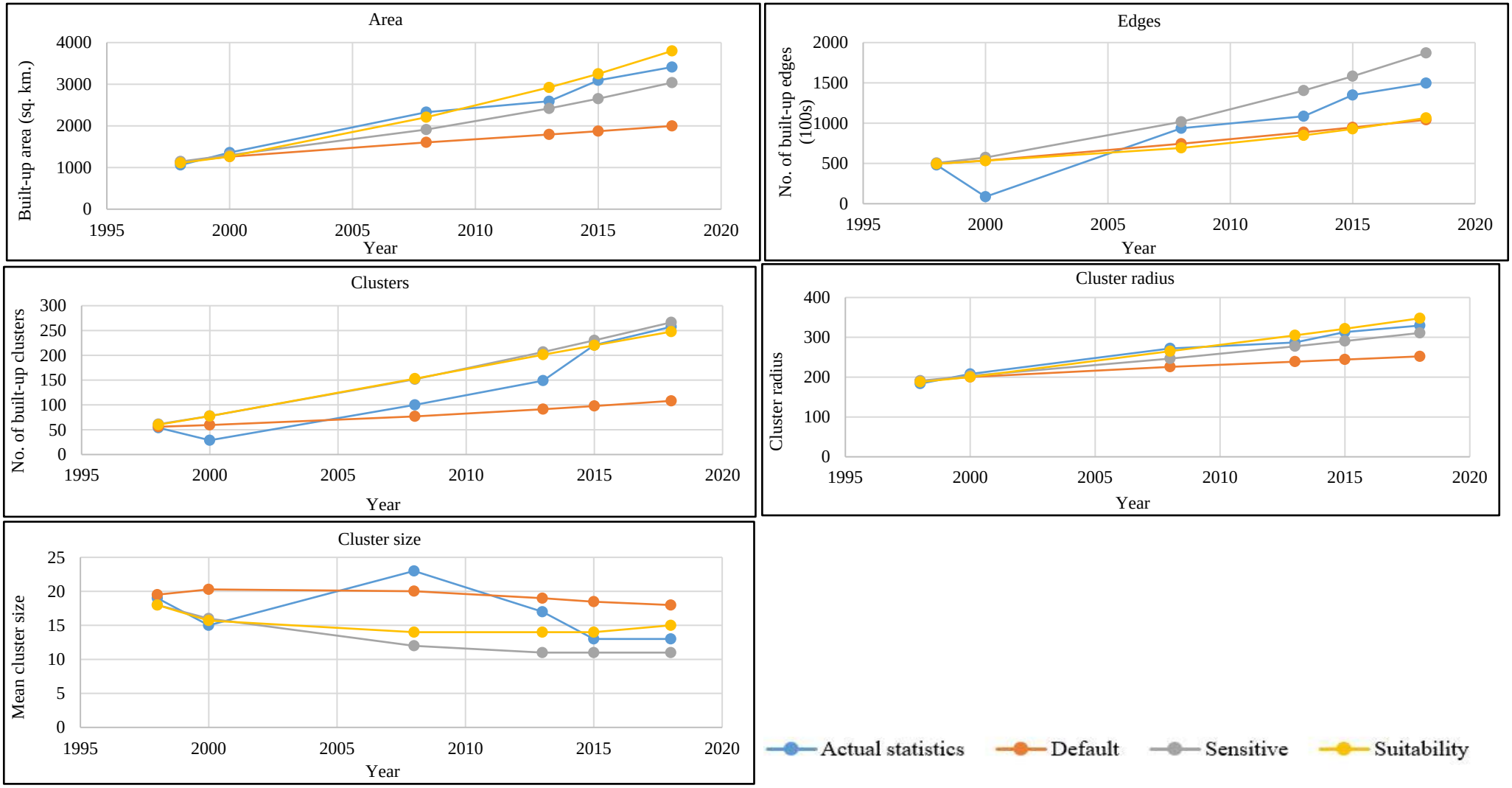

Figure 8.12: Comparison of three versions of SLEUTH model using spatial and statistical measures

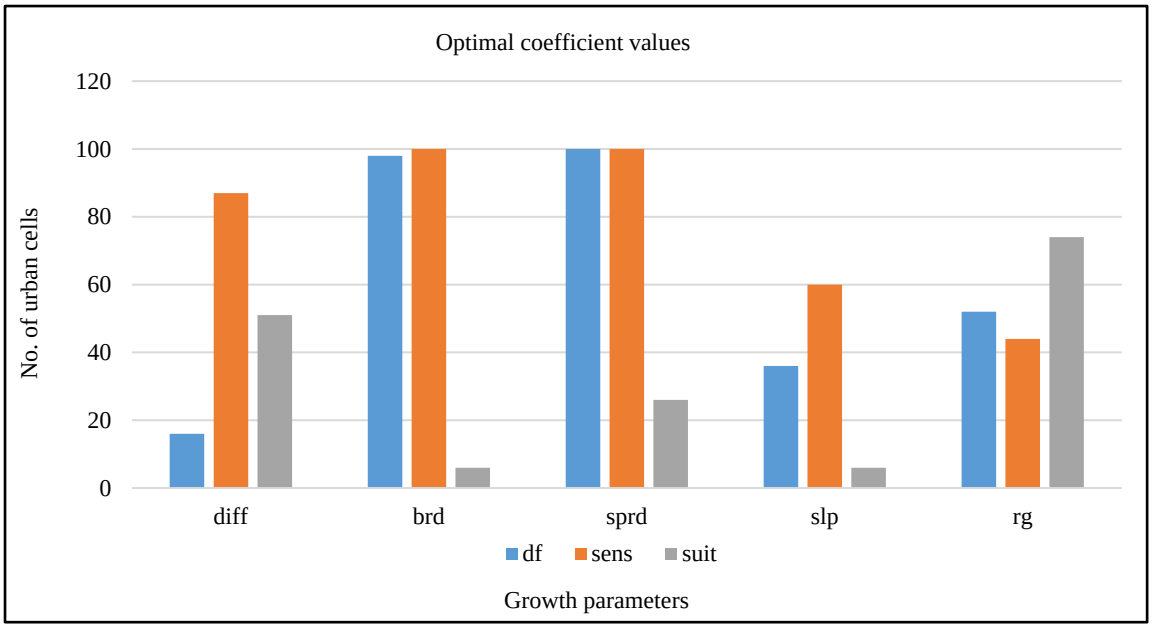

Figure 8.13: Urban growth behavior in terms of growth coefficients for different versions of SLEUTH model

Table 8.4: Comparison of components of correctness, error, ratio indices and statistical measures for different versions of the SLEUTH model (% landscape)

	2000			2008			2013			2015			2018		
	def	Sens	suit	def	sens	suit	def	sens	suit	def	sens	suit	def	sens	suit
H	3.8	3.8	3.8	4.4	4.4	5	4.5	4.6	5.6	4.7	4.9	6.2	4.9	5.1	6.8
M	0.2	0.9	0.9	3.4	3.4	2.7	4.1	4.1	3	5.6	5.5	4.2	6.4	6.3	4.6
F	0.5	0.6	0.5	0.9	1.7	2.2	1.3	2.7	3.8	1.3	3.1	4.1	1.5	3.8	5.2
HOC	0.9	0.8	0.8	0.6	0.6	0.6	0.5	0.5	0.7	0.5	0.5	0.6	0.4	0.4	0.6
MOC	0.1	0.2	0.2	0.4	0.4	0.4	0.5	0.5	0.3	0.5	0.5	0.4	0.6	0.6	0.4
FOC	0.1	0.1	0.1	0.1	0.2	0.3	0.1	0.3	0.4	0.1	0.3	0.4	0.1	0.3	0.5
FOM	84.3	71.4	72.5	50.1	46.5	50.6	45.5	40.4	45.4	40.5	36.1	42.8	38.1	33.5	41.1

Model performance has been found to be improving from base version 1 to version 2 and further it has improved in SLEUTH-Suitability i.e. version 3, which means that the land suitability decision rule has improved the model performance. More hits i.e. 6.8 and a lesser misses i.e. 4.6 have been observed for the year 2018 from the SLEUTH-Suitability as compared to two other versions of the SLEUTH. However, A greater false alarms have also been observed for version 3 model as compared to version 1and 2.

The HOC metric has improved from 0.4 in version 1 and 2 to 0.6 in version 3 for the year 2018. The MOC metric also showed improvement from 0.6 in version 1 and 2 to

0.4 in version 3. The overall FOM metric for the year 2018 has shown improvement from 38.1 in version 1 to 41.1 in version 3 i.e., SLEUTH-Suitability.

In addition to these, the present study has also tried to visually analyze the locations of urban growth which are successfully captured by the individual version of the SLEUTH model. Also, the locations which either missed out from capturing or were falsely captured by the individual version of the model have also been identified as presented in Figure 8.14- 8.16. Lesser no. of hits and false alarms can be seen from Figure 8.14 from the base SLEUTH model as compared to version 2 and 3. However, the no. of hits are increased especially at the edges and road side areas in the SLEUTH_Suitability i.e. version 3 indicates better capturing of fragmented and diffusive growth as compared to the growth obtained from version 1 and 2. Version 2 is found to be better in term of no. of hits than version 1, though, not as good as version 3. Moreover, fewer misses are noticed in the case of version 3 than version 1 and 2. But, again version 2 is found better than version 1 in term of misses. Therefore, it can be concluded from the results of Hit-Miss-False Alarm method that SLEUTH-Suitability has performed better in simulating the urban growth as compared to the other two versions. The base SLEUTH model with optimum model constants/parameters (version 1) has been found to be better as compared to SLEUTH with default parameters (version 2).

8.3.1.5 Criteria 5: a Model comparison in term of accuracy assessment using Geo-Eye (GE) image as reference data

Performance of three versions of SLEUTH has also been compared in term of percentage accuracy and kappa statistics for simulated urban growth. Accuracy assessment of simulation growth from three versions was tested by determining the number of urban test pixels correctly captured. Land use of more than 100 randomly selected test pixels was checked with the correct land use of the same pixels in the reference data i.e., a high resolution satellite image of Geo-eye satellite obtained from Google Earth for model results of all three versions for the year 2018. The test pixel locations were overlaid on the GE image and the correct ground feature information in terms of binary numbers has been collected. The classification is done for urban and non-urban pixels/ points as ‘1’ and ‘0’ respectively.

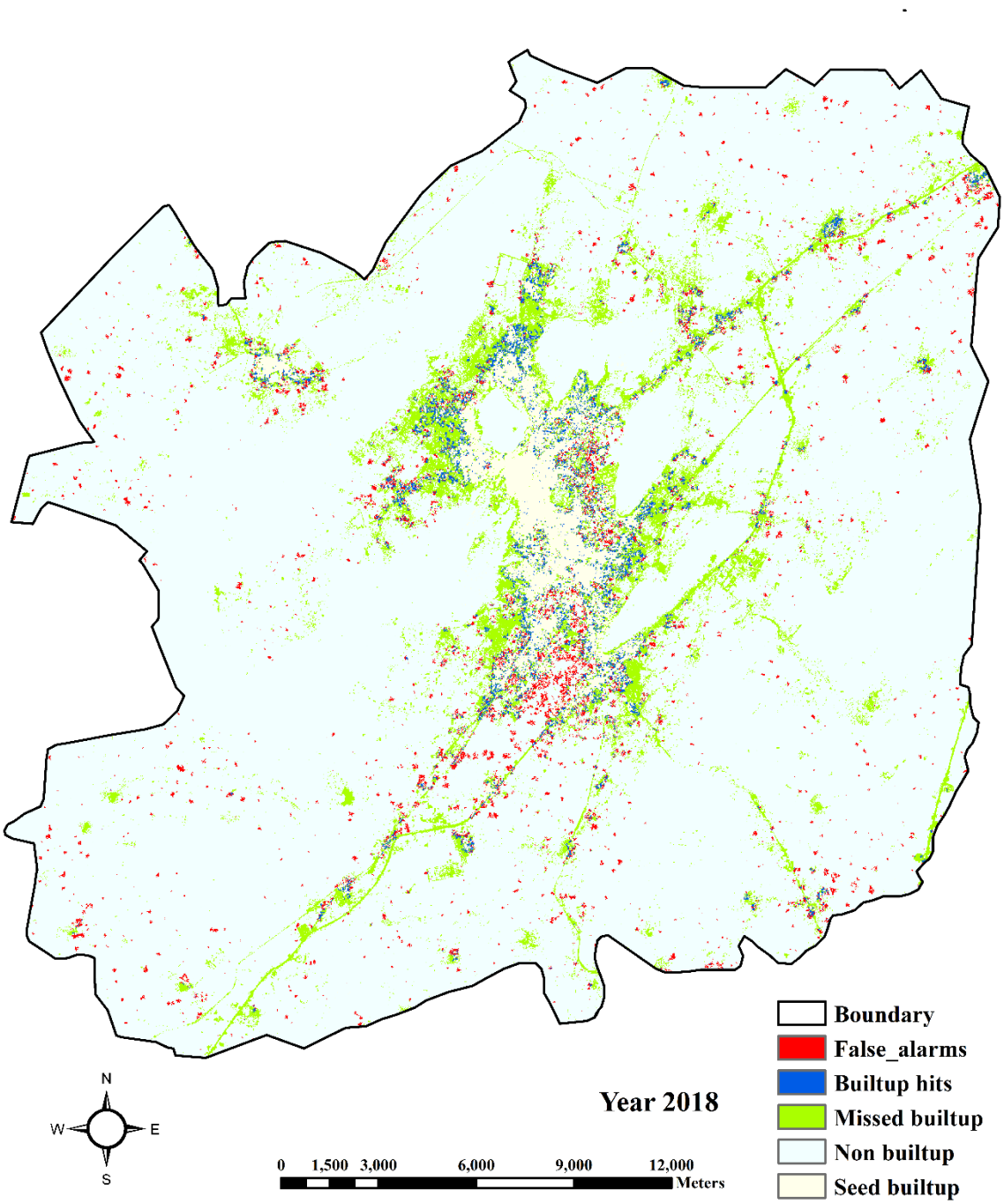

Figure 8.14: Urban growth map showing urban hits, misses and false alarms for default SLEUTH model i.e. version1

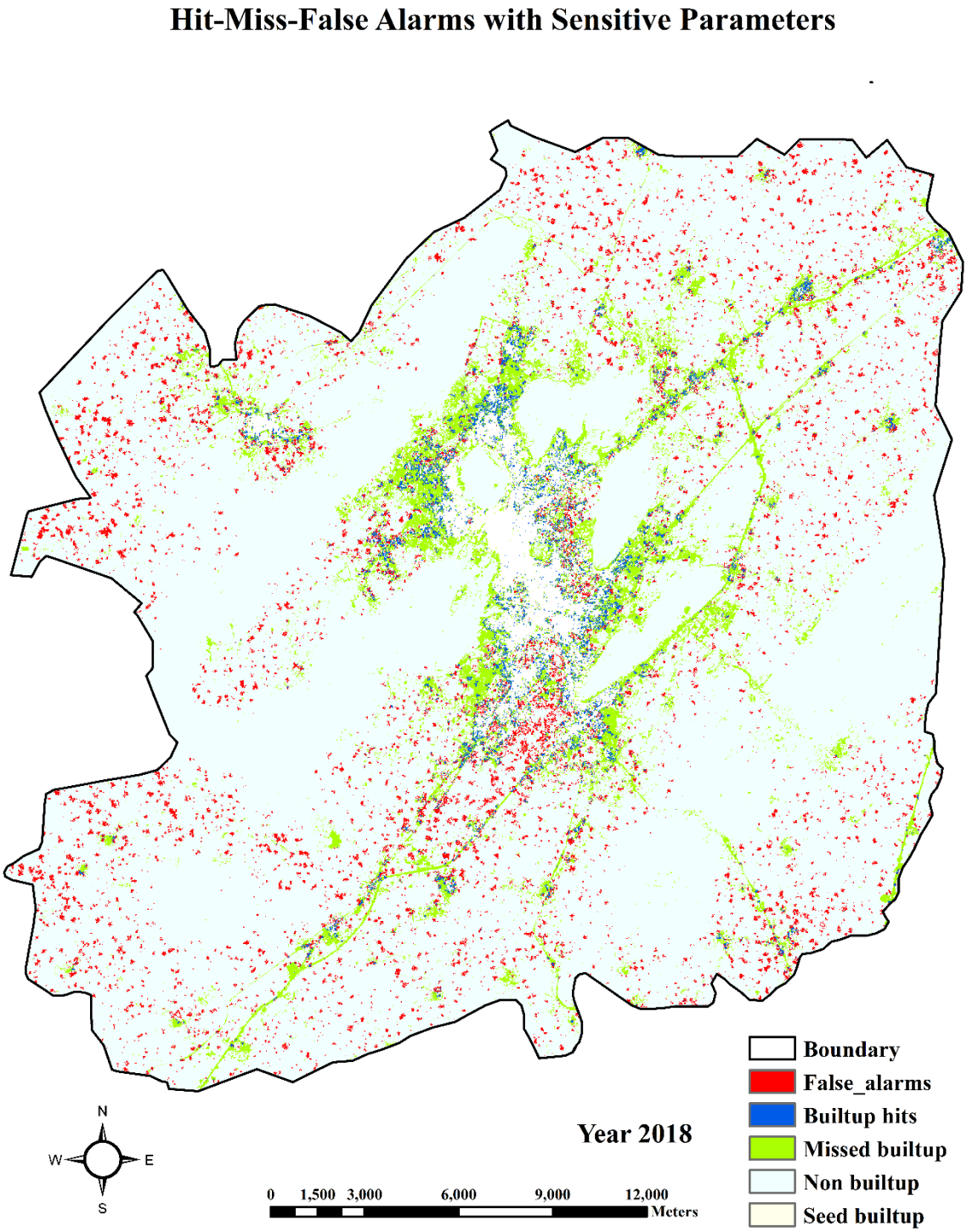

Figure 8.15: Urban growth map showing urban hits, misses and false alarms for sensitive parameters based SLEUTH model i.e. version2

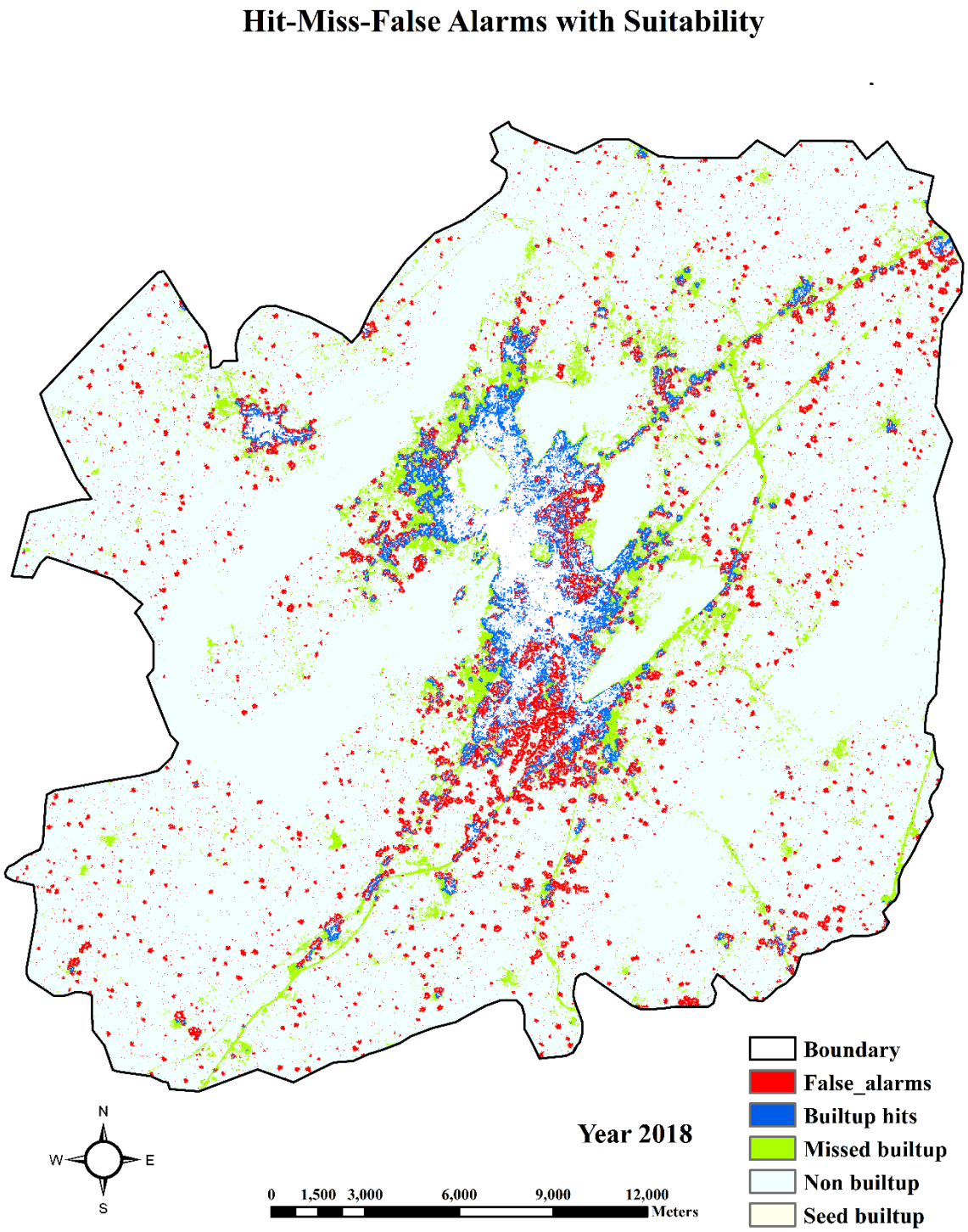

Figure 8.16: Urban growth map showing urban hits, misses and false alarms for suitability based SLEUTH model i.e. version3

The confusion matrix is prepared in between observed and modeled urban pixels for the year 2018 to calculate the users and producers accuracy. The kappa statistics and accuracy percentage have been computed for all the three versions of the SLEUTH model by following the same process. The percentage accuracy achieved with respect to reference

GE data (which is considered as quite good) has shown improvement from version 1 to 2 to 3. The model accuracy has improved from 79% for version 1 to 80% for version 2 to 83% for SLEUTH-Suitability i.e. version 3. Moreover, the kappa statistics has also found to be improving from version 1 to 2 to 3 i.e. 0.55, 0.57 and 0.61, respectively. SLEUTH-Suitability has been found to be better in term of percentage accuracy and kappa statistics, as indicated by the results in Table 8.5. Model simulated growth with more than 80% percentage accuracy and 0.61 kappa statistics have been quite satisfactory and acceptable (Table 8.5).

Table 8.5: Accuracy percentage and kappa statistics for different versions of the SLEUTH model using GE data as reference

The year 2018	Accuracy (%)	Kappa coefficient
Version 1	79	0.55
Version 2	80	057
Version 3	83	0.61

8.3.1.6 Criteria 6: a Model comparison in term of % accuracy on the basis of field observations

Performance of the three versions of SLEUTH has also been compared in term of percentage accuracy and kappa statistics achieved through ground truthing. Status of urbanization of a number of randomly selected locations collected through field survey was compared with land use obtained from the model results for the year 2018. The accuracy assessment on the basis of field observations has also been performed for the year 2018 in two ways i.e. accuracy with respect to the pixels urbanized in the year 2017-18 means newly constructed locations in the year 2017-18 and percentage of locations which are correctly identified by the model that were urbanized up to the year 2018. During field visits, it was planned to capture only those sites which seem to be under construction or newly constructed sites in the year 2018 for the first case so that they can be validated with the simulated urban growth which have taken place only in the year 2018. Percentage accuracy achieved with reference to field verification for three versions of the model has been presented in Table 8.6. Accuracy was assessed using the urbanization status of ground control points which are presented in Table 8.7.

Table 8.6: Sample sites selected for the accuracy assessment based on field observation

S.no.	Sites	X_cordinate	Y_cordinate
1	new multistoreydevelopmnt pushrd	74° 39' 45.786" E	74° 39' 45.786" E
2	kanas village near push needevdl	74° 35' 29.784" E	74° 35' 29.784" E
3	multistorey pushar road	74° 39' 41.816" E	74° 39' 41.816" E
4	new construction aradhna colonry	74° 40' 58.601" E	74° 40' 58.601" E
5	sai jyoti nagar newddvelopmnt	74° 40' 51.739" E	74° 40' 51.739" E
6	sai jyoti nagarnew const	74° 40' 46.387" E	74° 40' 46.387" E
7	new development gfeen colony	74° 40' 55.136" E	74° 40' 55.136" E
8	vidya vihar coloney new develop	74° 40' 50.126" E	74° 40' 50.126" E
9	new developmng near kayad road	74° 40' 47.097" E	74° 40' 47.097" E
10	boodhapushakar	74° 35' 10.947" E	74° 35' 10.947" E
11	new construction saraswati naga	74° 41' 6.956" E	74° 41' 6.956" E
12	new construction sarswati road	74° 40' 58.305" E	74° 40' 58.305" E
13	nee construction near jaipur roa	74° 41' 0.021" E	74° 41' 0.021" E
14	multi storey construction jaipur	74° 41' 0.608" E	74° 41' 0.608" E
15	panchsheel nagar5	74° 38' 26.799" E	74° 38' 26.799" E
16	construction point1	74° 38' 6.717" E	74° 38' 6.717" E
17	near globl public school	74° 38' 56.465" E	74° 38' 56.465" E
18	new consgfunctuon mds road	74° 40' 58.341" E	74° 40' 58.341" E
19	castle royal vaishli ngr	74° 37' 35.901" E	74° 37' 35.901" E
20	ganpati nagarpushjar	74° 33' 50.792" E	74° 33' 50.792" E
21	ganpati nagar multistoreypushkar	74° 33' 51.332" E	74° 33' 51.332" E
22	vaishli nagar 2	74° 37' 23.449" E	74° 37' 23.449" E
23	vaishali nagar3	74° 37' 22.362" E	74° 37' 22.362" E
24	newconstru tionpush	74° 33' 13.799" E	74° 33' 13.799" E
25	vaishali ngar two storey	74° 37' 1.458" E	74° 37' 1.458" E
26	haribhau nagar new constryctiin	74° 36' 35.049" E	74° 36' 35.049" E
27	new development haribhau	74° 35' 54.573" E	74° 35' 54.573" E
28	pragati nagar multistprey constr	74° 35' 29.907" E	74° 35' 29.907" E
29	foysagar road multi,storey	74° 36' 48.674" E	74° 36' 48.674" E
30	mehu road underconstrionmultistr	74° 39' 9.731" E	74° 39' 9.731" E
31	bihari gnjmultistorey	74° 38' 57.124" E	74° 38' 57.124" E
32	adarshnaar multistorey	74° 39' 4.823" E	74° 39' 4.823" E
33	adarshngr construction multistor	74° 39' 3.615" E	74° 39' 3.615" E
34	adarsh nad new,constrmulistiry	74° 39' 11.311" E	74° 39' 11.311" E
35	single stories bewar road	74° 39' 5.642" E	74° 39' 5.642" E
36	bewar road	74° 38' 22.953" E	74° 38' 22.953" E

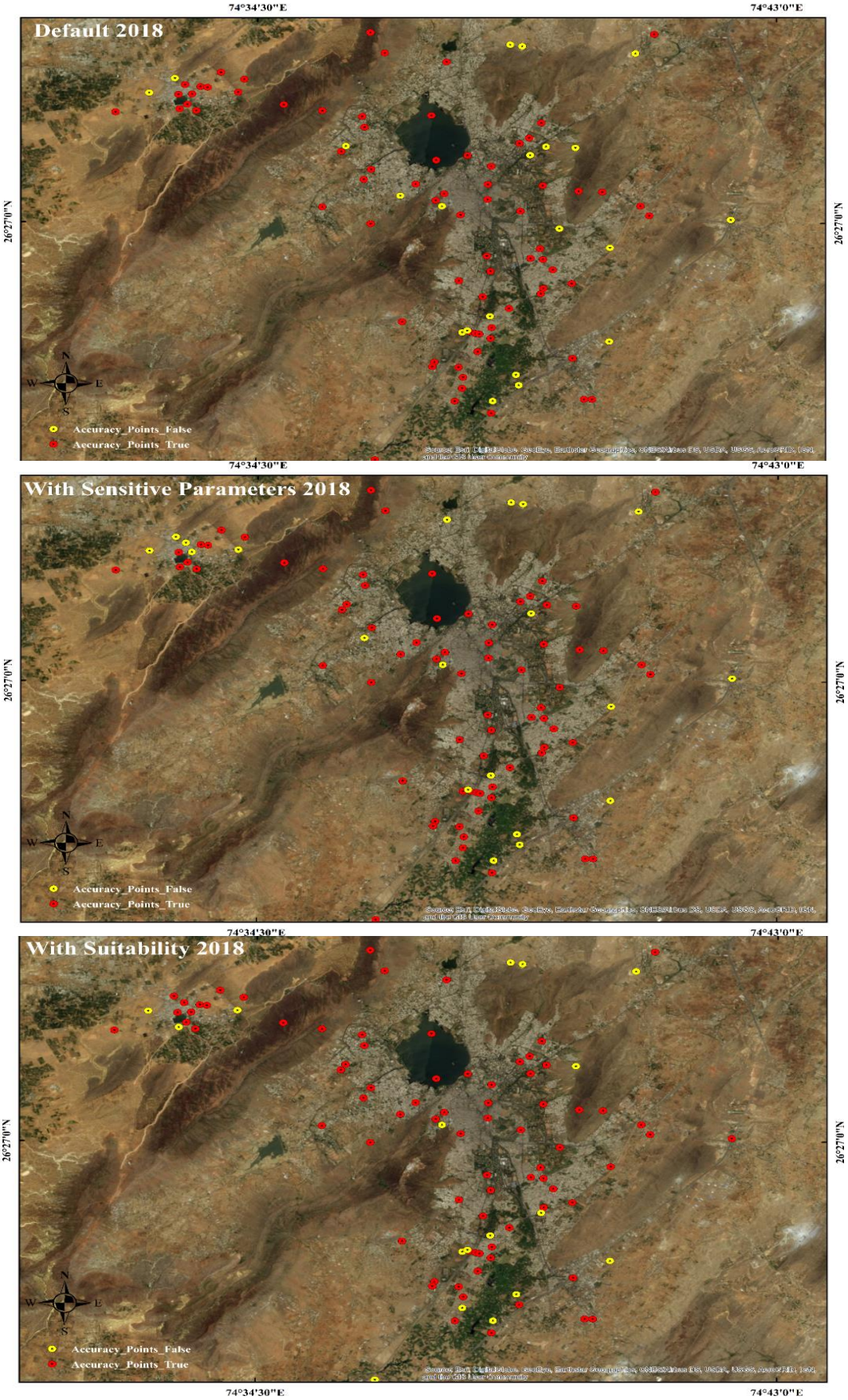

Figure 8.17: Comparison among three versions of SLEUTH model

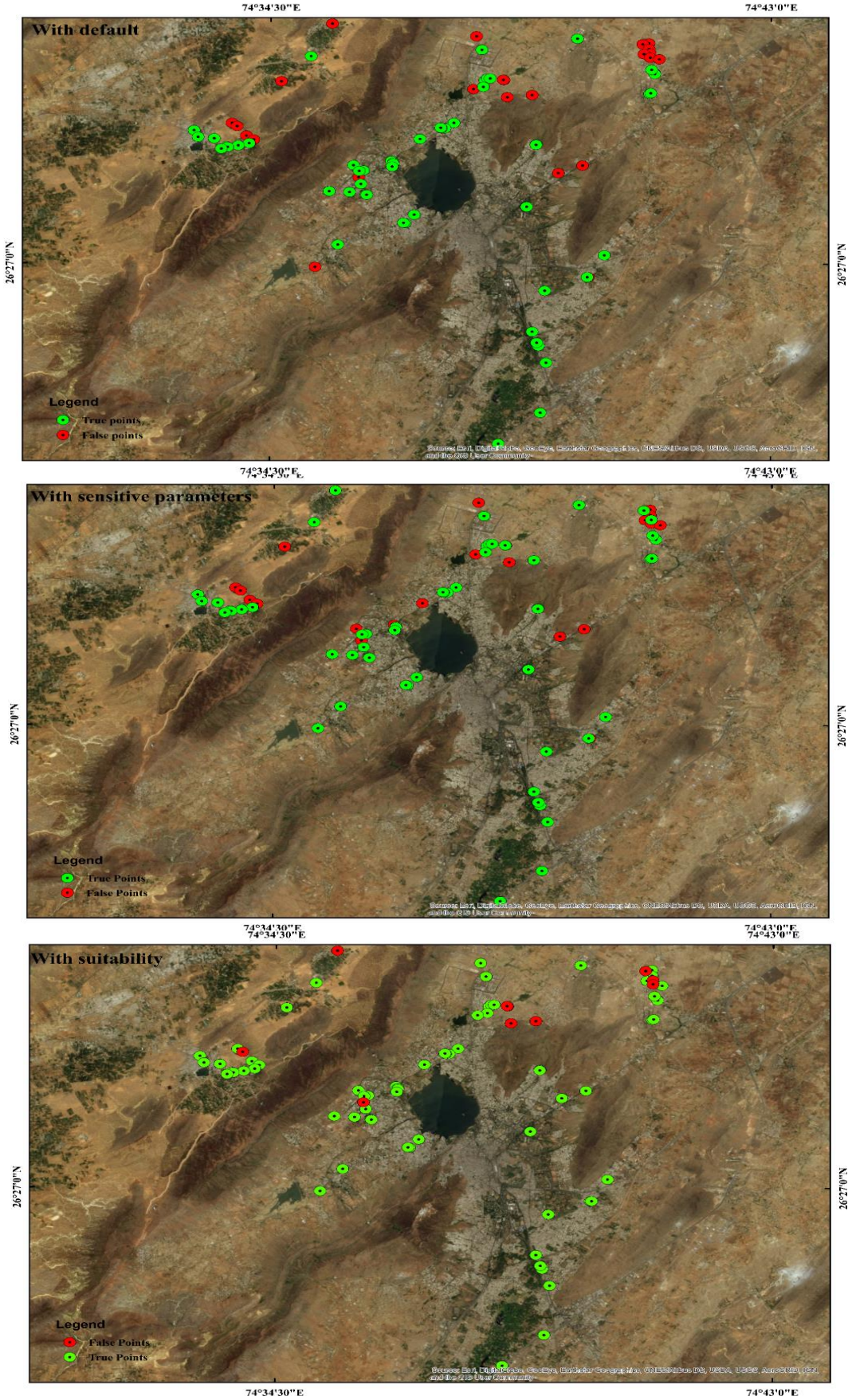

Figure 8.18: Comparison among three versions of SLEUTH model

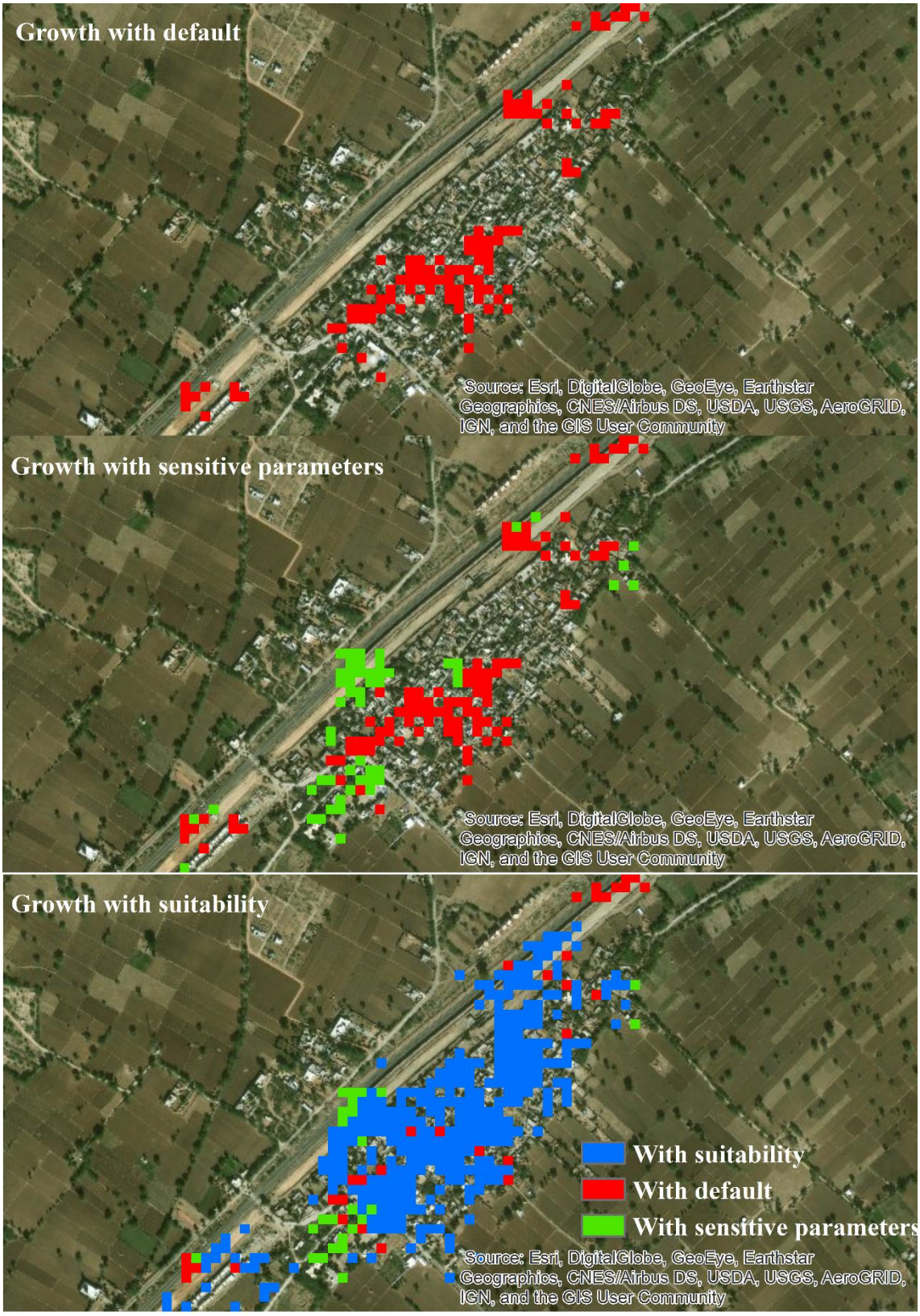

Figure 8.19: Visual comparison of modeled urban growth in year 2018

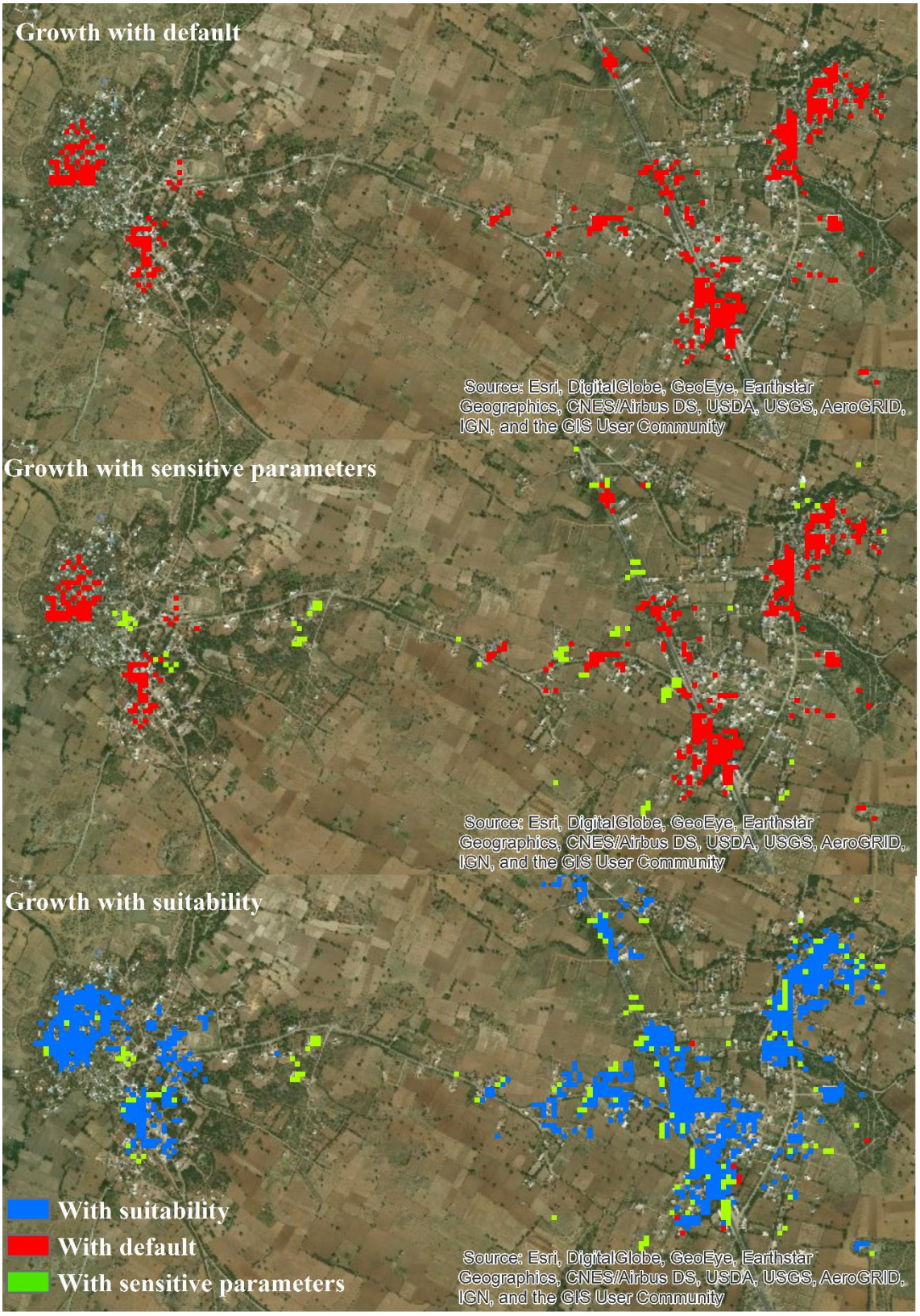

Figure 8.20: Visual comparison of modeled urban growth in year 2018

Highest accuracy has been achieved for the SLEUTH-Suitability (83%) in capturing the urban growth that took place only in the year 2017-18 as compared to moderate accuracy achieved from version 2 (67%) and base version 1 of SLEUTH (58%) (Table 8.7).

Table 8.7: Accuracy percentage for newly constructed locations in the year 2017-18 for different versions of the SLEUTH model using field observations

Year 2018	Accuracy (%)
Version 1	58
Version 2	67
Version 3	83

With respect to overall urban growth (till the year 2018), again highest accuracy has been achieved for SLEUTH-Suitability i.e. version 3 (68%), as compared to version 2 (56%) and base SLEUTH model i.e. version 1 (56%). The accuracy is found to be improving from version 1 (52%) to version 2 (56%) to version 3 (68%) as presented in Table 8.8. It is quite clear from Figure 8.17 & 8.18 that the no. of GCP's correctly captured has gradually increased from base SLEUTH model i.e. version 1 to SLEUTH-Suitability i.e. version 3 for predicted growth of the year 2018 for which reference data is available and captured from the field.

Table 8.8: Accuracy percentage for overall urban growth in year 2018 for different versions of the SLEUTH model using field observations

Year 2018	Accuracy (%)
Version 1	52
Version 2	56
Version 3	68

8.3.1.7 Crieteria7: Visual comparison

Further, visual analysis was carried out to determine the relative difference in the performance of the three versions of the SLEUTH model as presented in Figure 8.19- 8.20. Visual comparison of a few locations indicates that the default version of the SLEUTH model is not able to capture the roadside development which is better captured in case of version 2 and even more accurately captured by the SLEUTH-Suitability. In addition, fragmented urban growth at a few places is also better captured by the SLEUTH-Suitability as compared to base version 1 of SLEUTH with default parameters and version 2, base SLEUTH with optimum model parameters.

8.4 Concluding Remarks

Application of three versions of the SLEUTH model has been successfully demonstrated in modelling the urban growth of Ajmer fringe. The performance of three versions of the SLEUTH model i.e. default, improved model with sensitivity analysis based optimal parameters and land suitability based improved version i.e., SLEUTH-Suitability are compared in term goodness of fit landscape metrics, spatial and statistical measures, Hit-Miss-False alarm method and accuracy assessment with respect to reference data obtained from Geo-Eye satellite and ground truthing obtained from field visit. Performance of the SLEUTH-Suitability has been found to be better and satisfactory as compared to base version 1 of the SLEUTH. Better performance of SLEUTH-Suitability also indicates the role of selected urbanization drivers incorporated into urban growth simulation through a new land suitability decision rule. The inclusion of a land suitability decision rule further enhanced the model capability in capturing of the small size development, fragmented and roadside growth.

CHAPTER 9
CONCLUSIONS AND FUTURE RECOMMENDATIONS

The present chapter includes the conclusions of the present study and the recommendations for future research.

9.1. Conclusions

The present study has been successful in accomplishing its research objectives. The proposed research was aimed to understand and study the LULC change and urbanization processes, drivers, different modelling approaches and models to develop an appropriate model which is suitable in simulating realistic urban growth considering different LULC change and urbanization drivers using Cellular Automata and geospatial techniques. Possible reasons of the lower performance of the available SLEUTH model have been identified as unsuitable values of a few model constants and parameters for which model sensitivity was not tested earlier and the non-inclusion of a few important explanatory variables of LULC change and urban growth in the model algorithm. Rigorous sensitivity testing of various crucial model parameters/ constants has been performed to identify the appropriate optimal values of those parameters at which the model has produced more realistic and accurate urban growth. An improved version of SLEUTH i.e. SLEUTH-Suitability has been developed incorporating land suitability decision growth rule in model simulation that further improved the accuracy of simulated urban growth including smaller size built-up and fragmented growth. In another effort, the capability of the SLEUTH model has been improved to estimate the built-up density. A new version of the model i.e., SLEUTH-Density has been developed, tested which is capable of simulating the built-up density/ intensity as a function of few selected geo-spatial urbanization drivers. SLEUTH-Density application has been successfully demonstrated for Ajmer and Pushkar cities and found to be very useful in determining the future needs of urban services, infrastructure facilities, investment to be made and other optimum land use policy decisions. The study has been successful in finding out the answers to the research questions as presented below.

- The understanding of the present state of knowledge of LULC change and urban growth phenomenon has been improved by reviewing literature extensively (please refer to Appendix II). The important LULC change and urban growth explanatory variables were identified.

- Different approaches, methods, and models capable of simulating LULC changes and urban growth were studied thoroughly to know the intricacy of individual models and identify the suitable method and model to simulate complex phenomenon of LULC change and urbanization for socio-economic conditions of developing countries. The CA-based SLEUTH model has been found to be more robust and widely used in many cities worldwide and was selected for carrying out the present research.
- A suitable GIS database at required spatial and temporal resolutions was prepared for the parameterization of the SLEUTH model and improved versions.
- The SLEUTH model was conceptualized for the selected study area and successfully calibrated. Various limitations of the SLEUTH were determined, which include overestimation of urban areas at some places, unable to capture fragmented growth especially of smaller size built-up features, unable to capture all forms of the urban growth leading to lower accuracy and more false positives and negatives.
- Possible reasons of the lower performance of the available SLEUTH model have been identified as unsuitable values of a few model constants/ parameters for which model sensitivity was not tested earlier and non-inclusion of a few important explanatory variables of LULC change and urban growth in the model simulation.
- Rigorous model sensitivity testing of crucial model constants/ parameters has been performed to determine the optimal values/ ranges of those parameters i.e. *self-modifying parameters, diffusion value, no. of Monte-Carlo iterations, critical slope, a game of life rule* and *cellular neighborhood size*. The model performance has been found to be better with the optimum model constants in term of capturing fragmented urban growth and smaller built-up features more accurately, more no. of hits, accuracy percentage and kappa statistics than the base model with default parameters.
- A new version of the model i.e., SLEUTH-Suitability has been developed to include the land suitability decision variable rule into the simulation process. The SLEUTH code has been modified and a land suitability decision variable has been integrated with the existing SLEUTH model to incorporate the effect of land cost, distance from the road, distance from the railway stations, bus stands and distance from recreational places as urbanization drivers. The program of SLEUTH-Suitability was successfully tested for a demo input dataset and the application of SLEUTH-Suitability was demonstrated for Ajmer fringe including Pushkar town by utilizing the input dataset of Ajmer and optimal parameters/ constant values obtained from the sensitivity

analysis. Performance of the SLEUTH-suitability has been found to be better as compared to conventional SLEUTH model with default model constants and with optimum parameters obtained from sensitivity analysis. The new version of the model has also been found to be capable of capturing the different forms of urban growth, small size fragmented growth and also results are more realistic and near to the actual growth. Therefore, the SLEUTH Model has been improved successfully in the present work and performance of the newly developed model (SLEUTH-Suitability) has been found to be significantly better.

- A new version of the model i.e., SLEUTH-Density has been developed which is capable of simulating and predicting the urban intensity or built-up density. The new algorithm has been developed and program code has been modified to include the simulation and prediction of built-up density. The built-up density was successfully validated with the field data and various statistical and other metrics of built-up density estimation.

Salient findings and inferences of the present research work have been explained below;

1. Different issues related to LULC change and urban growth modelling and simulation using the SLEUTH model were identified.
2. Historical LULC maps have been generated for different years i.e. 1997, 2000, 2004, 2008, 2013 and 2015 and a GIS database was created and raster layers were generated for model parameterization which includes urban maps, road layer, slope, restricted areas, distance to main roads, hospitals, railway & bus stations, recreational places, slope, and land cost.
3. Input dataset for Pushkar has been used for the development and testing of newly developed SLEUTH versions and application of the models have been demonstrated for Ajmer fringe (which itself includes Pushkar town). The SLEUTH model with default constants/ parameters values has been calibrated and the optimal growth coefficient values were obtained as 49, 45, 25, 68 and 46 for diffusion, breed, spread, slope resistance, and road gravity coefficients respectively corresponding to 0.28 as OSM fitness measure for Pushkar town. For Ajmer fringe optimum growth coefficient from the base SLEUTH model have been found to be as 16, 98, 100, 36 and 52 for diffusion, breed spread, slope resistance, and road gravity coefficients, respectively with a lower OSM fitness measure i.e. 0.07. However, the spatial pattern index i.e. LeeSallee was achieved as 0.3 and 0.5 for Pushkar town and Ajmer fringe, respectively.

4. The model calibration performance was evaluated on the basis of different goodness of fit metrics for both the study areas. For Pushkar town Compare, Pop, Edges, Clusters, LeeSallee, Slope, Xmean, Ymean, Radius and OSM have been obtained as 0.9, 0.9, 0.88, 0.7, 0.27, 0.57, 0.96, 0.89, 0.91 and 0.28 respectively while for Ajmer fringe values of landscape metrics were 0.59, 0.97, 0.95, 0.8, 0.5, 0.32, 0.95, 0.52, 0.98 and 0.07 respectively.
5. The performance of the base version of the SLEUTH was found to be lower in capturing different forms of urban growth like fragmented and scattered growth. The Model has underestimated the urban growth of Ajmer for the year 2018. Simulated growth (1996.86 Km^2) for the year 2018 has been found to be significantly less as compared to the actual urban area (3411.53 Km^2).
6. It has been observed that model performance can be improved by using an appropriate range of model constants/ parameters for which model sensitivity was tested. Performance of the SLEUTH model can further be improved by considering different LULC change and urbanization explanatory variables in the simulation process.
7. The model sensitivity for selected critical model constants/ parameters has been tested using an iterative procedure. The optimal values for *self-modifying parameters* such as for *boom, bust, critical low* and *critical high* have been obtained as 1.3, 0.10, 0.90, and 1.25, respectively. The optimum value of diffusive *value parameter* has been found to be as 0.0055. Sixty (60) *Monte Carlo runs*, a range of 15-19 for *critical slope*, a *game of life rule* threshold value of 1 and extended Moore Neighborhood of 12 *cell size* have been found to be the optimum.
8. SLEUTH simulates LULC change and urban growth as a function of four urbanization drivers like slope, urban area, road, and restricted areas. However, it was revealed from a literature review that there are some crucial urban growth explanatory variables which should be included in SLEUTH to improve its performance. The new version of SLEUTH i.e., SLEUTH-Suitability has been developed by integrating the land suitability decisions variable in the urban growth simulation. Land suitability decision variable includes the influence of other important urban growth explanatory variables like slope, land cost, distance to main roads, hospitals, railway and bus stations, and recreational places. The land suitability decision layer has been developed based on considering relative weight of each explanatory variable in the land suitability value arrived using the Analytical Hierarchy Process (AHP) based on Multi-Criteria Evaluation (MCE) techniques.

9. The appropriate weights for the new explanatory variables have been determined by sensitivity testing for a range of weights for each explanatory variable. The optimal weights achieved for new explanatory variables considered were 44.7 for the slope, 5.06 for the distance from bus and railway stations, hospitals & recreational places and 20.05 for the distance from the main roads.
10. Application of the SLEUTH-Suitability was demonstrated for both Ajmer city and Pushkar Town. Performance of the SLEUTH-Suitability was examined through accuracy assessment and by comparing results with the results obtained from the conventional SLEUTH model with default parameters and optimum parameters. The optimal growth coefficient values obtained for Ajmer are 51, 6, 26 and 74 for diffusion, breed, spread, and road gravity coefficients, respectively corresponding to the goodness of fit metrics like Compare Pop, Edges, Clusters, Xmean, Ymean and Radius which were achieved as 0.95, 0.97, 0.97, 0.94, 0.97, 0.53 and 0.98, respectively.
11. The improved SLEUTH-Suitability version has performed better in simulating the different forms of urban growth in term of overall accuracy with respect to different statistical metric, ground truthing, and reference information as compared to conventional SLEUTH model with default model parameters and with optimum model coefficients obtained from sensitivity analysis.
12. The SLEUTH performance has improved in capturing more hits i.e. from 4.9 in base SLEUTH model with default parameters/ constant to 5.1 in SLEUTH with optimal/ constant values to 6.8 in SLEUTH-Suitability. The overall figure of merit (FOM) has improved from 38.1 in SLEUTH with default settings to 41.1 from the SLEUTH-Suitability. The accuracy percentage obtained with respect to reference data of 100 stratified random sampling GCPs for the year 2018 has improved from 79% (SLEUTH with default settings) to 80% (SLEUTH with optimal parameters/ constants) to 83% (SLEUTH-Suitability). The kappa statistics has improved from 0.55(SLEUTH with default settings) to 0.57 (SLEUTH with optimal parameters/ constants) to 0.61 (SLEUTH-Suitability). The accuracy percentage with respect to the ground truthing (randomly field observation sites) has improved from 52% (SLEUTH default settings) to 56% (SLEUTH with optimal parameters/ constants) to 68% (SLEUTH-Suitability). In addition, the accuracy percentage for newly constructed locations for the year 2018 with respect to the ground truthing (using filed observation data) has improved from 58% (SLEUTH default settings) to 67% (SLEUTH with optimal parameters/ constants) to 83% from SLEUTH-Suitability.

13. A new version of the SLEUTH model has been developed to estimate built-up intensity or density. The model has been demonstrated for Ajmer fringe for simulating built-up density from the year 1997 to 2040. Application of the built-up density version was validated and accuracy assessment was performed with respect to spectral band indices, built-up density indices, LST, population density, actual vertical growth at different locations. Built-up density has been found to be proportional with LST and other urban indices & population density. Accuracy assessment has also been done by comparing simulated normalized built-up density and actual built-up density in term of vertical growth (multistory built-up activities) obtained from field data. Performance and accuracy of built-up density estimated from SLEUTH-Density have been found to be satisfactory. The R^2 value of 0.79 has been found for the relationship between simulated built-up density and observed no. of floors and the accuracy was found to be 75%. The built-up density/ intensity for different future years may help urban planners, development authorities in making of appropriate services provision like parking requirements, roads, and transportation requirement, water supply & sanitation services, open spaces corresponding to increased density in future.
14. The present study has been successful in improving the existing SLEUTH model and new SLEUTH versions have been developed i.e. SLEUTH-density and SLEUTH-Suitability.

9.2. Limitations and Future recommendations of the study

9.2.1 Limitations

1. Optimum values of self-modifying parameters obtained from sensitivity testing may be suitable only for the urban growth forms in similar socio-economic conditions as of Ajmer. This set of the coefficient may not be suitable to capture all the forms of urban growth.
2. To capture different forms of urban growth the optimum value of diffusivity coefficient may be different. However, for the overall performance of the model one value has been arrived as 0.0055.
3. To reach out to the near optimal solution of modeling relying only on the model fitness may not be suitable, as it only gives an idea about urban growth form. How well a model captures different urban forms may not be answered on the basis of one optimal fitness of model criteria i.e. OSM only.

4. It may not be possible to identify all the urban forms for the same parametric settings. One parametric setting may be appropriate for capturing one type of urban form but may not be able to capture all other urban forms.
5. The SLEUTH-Density model does not incorporate the additional land suitability decision variable.
6. The developed new versions of SLEUTH need to be tested for urban areas having different socio-economic conditions.
7. Model results have uncertainties of misclassification in land use land cover information extracted from satellite images.
8. The model still requires large computational resources and CPU hours.

9.2.2 Future recommendations of the study

1. The sensitivity of the model parameters should be tested for the different urban areas having different socio-economic conditions.
2. Influence of the spatial resolution of the input data may be further studied on model performance.
3. A suitable range of model coefficients can be determined which is suitable to capture a different type of urban form.
4. SLEUTH-Density version may be further improved to incorporate a few more urban growth explanatory variables as a decision variable in the simulation process like land suitability.
5. SLEUTH-Suitability and SLEUTH-Density versions should be further tested for the urban areas/ cities and towns of different size and having different socio-economic conditions.
6. Other important urban growth explanatory variables may be included in the SLEUTH and their influences may be studied.
7. Urban growth is based on historical information of urban growth assuming same land use policies and developmental decisions will be followed in future as well, future road networks, infrastructure level of facilities like roads, built-up zonation restrictions have been assumed at the level of year of 2015.

REFERENCES

1. Agarwal, C., Green, G. M., Grove, J. M., Evans, T. P., Schweik, C. M., 2002. A review and assessment of land-use change models: dynamics of space, time, and human choice.
2. Akın, A., Clarke, K. C., Berberoglu, S., 2014. The impact of historical exclusion on the calibration of the SLEUTH urban growth model. International Journal of Applied Earth Observation and Geoinformation, 27, 156-168.
3. Alkimim, A., Sparovek, G., Clarke, K. C., 2015. Converting Brazil's pastures to cropland: An alternative way to meet sugarcane demand and to spare forestlands. Applied Geography, 62, 75-84.
4. Al-shalabi, M., Billa, L., Pradhan, B., Mansor, S., Al-Sharif, A. A., 2013. Modelling urban growth evolution and land-use changes using GIS based cellular automata and SLEUTH models: the case of Sana'a metropolitan city, Yemen. Environmental earth sciences, 70(1), 425-437.
5. Al-sharif, A. A., Pradhan, B., 2014. Monitoring and predicting land use change in Tripoli Metropolitan City using an integrated Markov chain and cellular automata models in GIS. Arabian Journal of Geosciences, 7(10), 4291-4301.
6. Alberti, M., Waddell, P., 2000. An integrated urban development and ecological simulation model. Integrated Assessment, 1(3), 215-227.
7. Alig, R., Adams, D., McCarl, B., Callaway, J. M., Winnett, S., 1997.
8. Berry, M., Minser, K., 1997. Distributed land-cover change simulation using PVM and MPI. Paper presented at the Land use modeling workshop.
9. Alig, R., Adams, D., McCarl, B., Callaway, J. M., Winnett, S., 1997. Assessing effects of mitigation strategies for global climate change with an intertemporal model of the US forest and agriculture sectors. Environmental and Resource Economics, 9(3), 259-274.
10. Asgarian, A., Amiri, B. J., Sakieh, Y., 2015. Assessing the effect of green cover spatial patterns on urban land surface temperature using landscape metrics approach. Urban Ecosystems, 18(1), 209-222.
11. Aspinall, R., 2004. Modelling land use change with generalized linear models—a multi-model analysis of change between 1860 and 2000 in Gallatin Valley, Montana. Journal of environmental management, 72(1-2), pp.91-103.
12. Bajracharya, B., Uddin, K., Chettri, N., Shrestha, B., Siddiqui, S. A., 2010. Understanding land cover change using a harmonized classification system in the Himalaya: a case study from Sagarmatha National Park, Nepal. Mountain Research and Development, 30(2), 143-156.
13. Batty, M., Xie, Y., 1994. From cells to cities. Environment and planning B: Planning and design, 21(7), S31-S48.
14. Batty, M., Couclelis, H., Eichen, M., 1997. Urban systems as cellular automata. Environment and Planning B: Planning and Design, 24(2), 159-164.
15. Batty, M., Xie, Y., 1997. Possible urban automata. Environment and planning B: Planning and design, 24(2), 175-192.

16. Batty, M., 1997. Cellular automata and urban form: a primer. Journal of the American Planning Association, 63(2), 266-274.
17. Batty, M., Xie, Y., Sun, Z., 1999. Modeling urban dynamics through GIS-based cellular automata. Computers, environment and urban systems, 23(3), 205-233.
18. Batty, M., 2000. Geocomputation using cellular automata. In Geocomputation.(pp. 95-126). New York: Taylor & Francis.
19. Batty, M., 2005. Agents, cells, and cities: new representational models for simulating multiscale urban dynamics. Environment and Planning A, 37(8), 1373-1394.
20. Batty, M., 2007. Cities and complexity: understanding cities with cellular automata, agent-based models, and fractals. The MIT press.
21. Brown, D. G., Pijanowski, B. C., Duh, J., 2000. Modeling the relationships between land use and land cover on private lands in the Upper Midwest, USA. Journal of environmental management, 59(4), 247-263.
22. Beekhuizen, J., Clarke, K. C., 2010. Toward accountable land use mapping: Using geocomputation to improve classification accuracy and reveal uncertainty. International Journal of Applied Earth Observation and Geoinformation, 12(3), 127-137.
23. Berry, M.W., Flamm, R.O., Hazen, B.C., MacIntyre, R.L., 1994. The Land-use Change Analysis System (LUCAS) for evaluating landscape management decisions. Knoxville: University of Tennessee.
24. Berry, M.W., Hazen, B.C., MacIntyre, R.L., Flamm, R.O., 1996. LUCAS: a system for modeling land-use change. IEEE Computational Science and Engineering, 3(1), 24-35.
25. Bihamta, N., Soffianian, A., Fakheran, S., Gholamalifard, M., 2015. Using the SLEUTH urban growth model to simulate future urban expansion of the Isfahan metropolitan area, Iran. Journal of the Indian Society of Remote Sensing, 43(2), 407-414.
26. Bisht, B., Kothyari, B., 2001. Land-cover change analysis of Garur Ganga watershed using GIS/remote sensing technique. Journal of the Indian Society of Remote Sensing, 29(3), 137-141.
27. Bockstael, N.E., 1996. Modeling economics and ecology: the importance of a spatial perspective. American Journal of Agricultural Economics, 78(5), 1168-1180.
28. Borning, A., Waddell, P., Förster, R., 2008. UrbanSim: Using simulation to inform public deliberation and decision-making Digital government. Springer, Boston, MA, 439-464.
29. Brown, D.G., 2006. Agent-based models. The Earth's Changing Land.
30. Buffum, B., Gratzer, G., Tenzin, Y., 2009. Forest grazing and natural regeneration in a late successional broadleaved community forest in Bhutan. Mountain Research and Development, 29(1), 30-35.
31. Bürgi, M., Turner, M. G., 2002. Factors and processes shaping land cover and land cover changes along the Wisconsin River. Ecosystems, 5(2), 184-201.
32. Caglioni, M., Pelizzoni, M., Rabino, G. A., 2006. Urban sprawl: A case study for project gigalopolis using SLEUTH model. In International Conference on Cellular Automata ,Springer Berlin Heidelberg, 436-445.
33. Candau, J., 2000. Calibrating a cellular automaton model of urban growth in a timely manner. Paper presented at the Proceedings of the 4th international conference on

integrating geographic information systems and environmental modeling: problems, prospects, and needs for research.
34. Candau, J.T., 2002. Temporal calibration sensitivity of the SLEUTH urban growth model (Doctoral dissertation, University of California, Santa Barbara).
35. Carlson, T.N. and Arthur, S.T., 2000. The impact of land use—land cover changes due to urbanization on surface microclimate and hydrology: a satellite perspective. Global and planetary change, 25(1-2), 49-65.
36. Carruthers, J.I. and Ulfarsson, G.F., 2003. Urban sprawl and the cost of public services. Environment and Planning B: Planning and Design, 30(4), 503-522.
37. Chang, J.S., 2006. Models of the relationship between transport and land-use: A review. Transport Reviews, 26(3), 325-350.
38. Chao, T., Yihua, T., Huajie, C., Bo, D.U. and Jinwen, T.I.A.N., 2016. Object-oriented method of hierarchical urban building extraction from high-resolution remote-sensing imagery. Acta Geodaetica et Cartographica Sinica, 39(1), 39-45.
39. Chaudhuri, G., Clarke, K., 2013. The SLEUTH land use change model: A review. Environmental Resources Research, 1(1), 88-105.
40. Chaudhuri, G., Clarke, K. C., 2014. Temporal accuracy in urban growth forecasting: A study using the SLEUTH model. Transactions in GIS, 18(2), 302-320.
41. Chaudhuri, G., Clarke, K. C., 2015. On the spatiotemporal dynamics of the coupling between land use and road networks: does political history matter? Environment and Planning B: Planning and Design, 42(1), 133-156.
42. Chomitz, K. and Gray, A.D., 1995. Roads, lands, markets, and deforestation (Vol. 1444). World Bank Publications.
43. Chu, H.-J., Lin, Y.P., & Wu, C.F., 2010. Forecasting space-time land use change in the Paochiao Watershed of Taiwan using demand estimation and empirical simulation approaches Computational Science and Its Applications–ICCSA 2010 Springer, 116-130.
44. Clark, W. A., 1991. Residential preferences and neighborhood racial segregation: A test of the Schelling segregation model. Demography, 28(1), 1-19.
45. Clarke, K. C., Hoppen, S., Gaydos, L., 1996. Methods and techniques for rigorous calibration of a cellular automaton model of urban growth. Paper presented at the Third International Conference/Workshop on Integrating GIS and Environmental Modeling, Santa Fe, New Mexico.
46. Clarke, K. C., Hoppen, S., Gaydos, L., 1997. A self-modifying cellular automaton model of historical urbanization in the San Francisco Bay area. Environment and Planning B: Planning and Design, 24(2), 247-261.
47. Clarke, K. C., 1997. Land transition modeling with deltatrons. In Proc. The Land Use Modeling Conference.
48. Clarke, K. C., Gaydos, L. J., 1998. Loose-coupling a cellular automaton model and GIS: long-term urban growth prediction for San Francisco and Washington/Baltimore. International Journal of Geographical Information Science, 12(7), 699-714.
49. Clarke, K. C., Gazulis, N., Dietzel, C., Goldstein, N. C., 2007. A decade of SLEUTHing: Lessons learned from applications of a cellular automaton land use

change model. Classics in IJGIS: twenty years of the international journal of geographical information science and systems, 413-427.
50. Clarke, K. C., 2008. Cellular Automata. In Kemp, K. (2008) Encyclopedia of Geographic Information Science. Sage: Thousand Oaks, CA., 29-30.
51. Clarke, K. C., 2008. Mapping and modelling land use change: an application of the SLEUTH model. In Landscape Analysis and Visualisation (pp. 353-366). Springer Berlin Heidelberg.
52. Clarke, K. C., 2014. Why simulate cities? GeoJournal, 79(2), 129-136.
53. Clarke, K. C., 2014. Cellular automata and agent-based models. In Handbook of regional science (pp. 1217-1233). Springer Berlin Heidelberg.
54. Clarke, K.C., 2017. Improving SLEUTH Calibration with a Genetic Algorithm. In GISTAM (pp. 319-326).
55. Clarke, K.C., 2018. Land use change modeling with sleuth: Improving calibration with a genetic algorithm. In Geomatic Approaches for Modeling Land Change Scenarios (pp. 139-161). Springer, Cham.
56. Cohen, B., 2004. Urban growth in developing countries: a review of current trends and a caution regarding existing forecasts. World development, 32(1), 23-51.
57. Congalton, R.G. and Green, K., 1999. Assessing the accuracy of remotely sensed data: principles and applications. Lewis Pub-Lishers: Boca Raton, FL, USA.
58. Couclelis, H., 2002. Modeling frameworks, paradigms, and approaches. Geographic information systems and environmental modelling, Prentice Hall, London.
59. Cousins, S. A., 2001. Analysis of land-cover transitions based on 17th and 18th century cadastral maps and aerial photographs. Landscape ecology, 16(1), 41-54.
60. Couclelis, H., 2005. "Where has the future gone?" Rethinking the role of integrated land-use models in spatial planning. Environment and planning A, 37(8), 1353-1371.
61. Coutts, A.M., Beringer, J. and Tapper, N.J., 2007. Impact of increasing urban density on local climate: spatial and temporal variations in the surface energy balance in Melbourne, Australia. Journal of Applied Meteorology and Climatology, 46(4), 477-493.
62. Deadman, P., Robinson, D., Moran, E., Brondizio, E., 2004. Colonist household decisionmaking and land-use change in the Amazon Rainforest: an agent-based simulation. Environment and planning B: Planning and design, 31(5), 693-709.
63. Deep, S., Saklani, A., 2014. Urban sprawl modeling using cellular automata. The Egyptian Journal of Remote Sensing and Space Science, 17(2), 179-187.
64. Dezhkam, S., Amiri, B.J., Darvishsefat, A.A., Sakieh, Y., 2014. Simulating the urban growth dimensions and scenario prediction through sleuth model: A case study of Rasht County, Guilan, Iran. GeoJournal, 79(5), 591-604.
65. Dietzel, C., Clarke, K. C., 2004. Replication of spatio-temporal land use patterns at three levels of aggregation by an urban cellular automata Cellular automata (pp. 523-532): Springer.
66. Dietzel, C., Clarke, K. C., 2004. Spatial Differences in Multi-Resolution Urban Automata Modeling. Transactions in GIS, 8(4), 479-492.

67. Dietzel, C., Oguz, H., Hemphill, J. J., Clarke, K. C., Gazulis, N., 2005. Diffusion and coalescence of the Houston Metropolitan Area: evidence supporting a new urban theory. Environment and Planning B: Planning and Design, 32(2), 231-246.
68. Dietzel, C., Herold, M., Hemphill, J. J., Clarke, K. C., 2005. Spatio-temporal dynamics in California's Central Valley: Empirical links to urban theory. International Journal of Geographical Information Science, 19(2), 175-195.
69. Dietzel, C., Clarke, K., 2006. The effect of disaggregating land use categories in cellular automata during model calibration and forecasting. Computers, Environment and Urban Systems, 30(1), 78-101.
70. Dietzel, C., Clarke, K. C., 2006. Decreasing computational time of urban cellular automata through model portability. Geoinformatica, 10(2), 197-211.
71. Dietzel, C., Clarke, K. C., 2007. Toward optimal calibration of the SLEUTH land use change model. Transactions in GIS, 11(1), 29-45.
72. Ding, W. J., Wang, R. Q., Wu, D. Q., Liu, J., 2013. Cellular automata model as an intuitive approach to simulate complex land-use changes: an evaluation of two multi-state land-use models in the Yellow River Delta. Stochastic environmental research and risk assessment, 27(4), 899-907.
73. Dovey, K. and Pafka, E., 2014. The urban density assemblage: Modelling multiple measures. Urban design international, 19(1), 66-76.
74. Duthie, J., Kockelman, K., Valsaraj, V. and Zhou, B., 2007. Applications of integrated models of land use and transport: A comparison of ITLUP and UrbanSim land use models. In 54th Annual North American Meetings of the Regional Science Association International, Savannah, Ga.
75. Ewing, R., Pendall, R. and Chen, D., 2003. Measuring sprawl and its transportation impacts. Transportation Research Record: Journal of the Transportation Research Board, (1831), 175-183.
76. Ewing, R., Bartholomew, K., Winkelman, S., Walters, J. and Anderson, G., 2008. Urban development and climate change. Journal of Urbanism, 1(3), 201-216.
77. Foody, G.M., 2002. Status of land cover classification accuracy assessment. Remote sensing of environment, 80(1), 185-201.
78. Fallah, B., Partridge, M., Olfert, M. R., 2012. Uncertain economic growth and sprawl: evidence from a stochastic growth approach. The Annals of Regional Science, 49(3), 589-617.
79. Fan, F., Wang, Y., Wang, Z., 2008. Temporal and spatial change detecting (1998–2003) and predicting of land use and land cover in Core corridor of Pearl River Delta (China) by using TM and ETM+ images. Environmental Monitoring and Assessment, 137(1-3), 127-147.
80. Feng, Y., Liu, Y., 2013. A heuristic cellular automata approach for modelling urban land-use change based on simulated annealing. International Journal of Geographical Information Science, 27(3), 449-466.
81. Fitz, H., DeBellevue, E., Costanza, R., Boumans, R., Maxwell, T., Wainger, L., Sklar, F., 1996. Development of a general ecosystem model for a range of scales and ecosystems. Ecological modelling, 88(1), 263-295.

82. García, A., Santé, I., Boullón, M., Crecente, R., 2013. Calibration of an urban cellular automaton model by using statistical techniques and a genetic algorithm. Application to a small urban settlement of NW Spain. International Journal of Geographical Information Science, 27(8), 1593-1611.
83. Gaunt, C., Jackson, L., 2003. Models for assessing the effects of community change on land use patterns. In Planning support systems in practice (pp. 351-371). Springer, Berlin, Heidelberg.
84. Gautam, A. P., Webb, E. L., Eiumnoh, A., 2002. GIS assessment of land use/land cover changes associated with community forestry implementation in the Middle Hills of Nepal. Mountain Research and Development, 22(1), 63-69.
85. Gazulis, N., Clarke, K. C., 2006. Exploring the DNA of our regions: Classification of outputs from the SLEUTH model. In International Conference on Cellular Automata (pp. 462-471). Springer Berlin Heidelberg.
86. Georgiadou, Y., Puri, S.K., Sahay, S., 2005. Towards a potential research agenda to guide the implementation of Spatial Data Infrastructures—A case study from India. International Journal of Geographical Information Science, 19(10), pp.1113-1130.
87. Gharbia, S. S., Alfatah, S. A., Gill, L., Johnston, P., Pilla, F., 2016. Land use scenarios and projections simulation using an integrated GIS cellular automata algorithms. Modeling Earth Systems and Environment, 2(3), 151.
88. Gilani, H., Shrestha, H. L., Murthy, M., Phuntso, P., Pradhan, S., Bajracharya, B., Shrestha, B., 2015. Decadal land cover change dynamics in Bhutan. Journal of environmental management, 148, 91-100.
89. Gimblett, H.R., 2002. Integrating geographic information systems and agent-based modeling techniques for simulating social and ecological processes. Oxford University Press.
90. Godefroid, S. and Koedam, N., 2007. Urban plant species patterns are highly driven by density and function of built-up areas. Landscape Ecology, 22(8), pp.1227-1239.
91. Goldstein, N. C., Dietzel, C., Clarke, K. C., 2005. Don't stop 'til you get enough–sensitivity testing of Monte Carlo iterations for model calibration. In Proceedings of the 8th International Conference on Geo-Computation (pp. 1-3).
92. Gottmann, J., 1957. Megalopolis or the Urbanization of the Northeastern Seaboard. Economic geography, 189-200.
93. Gould, W. A., Martinuzzi, S., Parés-Ramos, I. K., 2012. Land use, population dynamics, and land-cover change in eastern Puerto Rico.
94. Guan, Q. G., 2008. Getting started with pSLEUTH.
95. Guan, Q., Clarke, K. C., 2010. A general-purpose parallel raster processing programming library test application using a geographic cellular automata model. International Journal of Geographical Information Science, 24(5), 695-722.
96. Han, H., Hwang, Y., Ha, S. R., Kim, B. S., 2015. Modeling Future Land Use Scenarios in South Korea: Applying the IPCC Special Report on Emissions Scenarios and the SLEUTH Model on a Local Scale. Environmental management, 55(5), 1064-1079.

97. Han-qiu, X.U., 2005. Fast information extraction of urban built-up land based on the analysis of spectral signature and normalized difference index. 地理研究, 24(2), 311-320.
98. Hatna, E. and Benenson, I., 2012. The Schelling model of ethnic residential dynamics: Beyond the integrated-segregated dichotomy of patterns. Journal of Artificial Societies and Social Simulation, 15(1), p.6.
99. Harrison Jr, D. and Kain, J.F., 1974. Cumulative urban growth and urban density functions. Journal of Urban Economics, 1(1), 61-98.
100. Hart, S.L. 1997. Beyond greening: strategies for a sustainable world. Harvard business review, 75(1), pp.66-77.
101. He, C., Shi, P., Chen, J., Li, X., Pan, Y., Li, J., Li, J., 2005. Developing land use scenario dynamics model by the integration of system dynamics model and cellular automata model. Science in China Series D: Earth Sciences, 48(11), 1979-1989.
102. He, C., Zhang, D., Huang, Q., & Zhao, Y., 2016. Assessing the potential impacts of urban expansion on regional carbon storage by linking the LUSD-urban and InVEST models. Environmental Modelling & Software, 75, 44-58.
103. He, C., Okada, N., Zhang, Q., Shi, P. and Zhang, J., 2006. Modeling urban expansion scenarios by coupling cellular automata model and system dynamic model in Beijing, China. Applied Geography, 26(3-4), 323-345.
104. Hepinstall, J.A., Alberti, M. and Marzluff, J.M., 2008. Predicting land cover change and avian community responses in rapidly urbanizing environments. Landscape ecology, 23(10), 1257-1276.
105. Hepinstall-Cymerman, J., Coe, S., & Hutyra, L. R., 2013. Urban growth patterns and growth management boundaries in the Central Puget Sound, Washington, 1986–2007. Urban Ecosystems, 16(1), 109-129.
106. Herold, M., Couclelis, H., & Clarke, K. C., 2005. The role of spatial metrics in the analysis and modeling of urban land use change. Computers, Environment and Urban Systems, 29(4), 369-399.
107. Hilbert, D.W. and Ostendorf, B., 2001. The utility of artificial neural networks for modelling the distribution of vegetation in past, present and future climates. Ecological modelling, 146(1-3), 311-327.
108. Houet, T., Aguejdad, R., Doukari, O., Battaia, G., Clarke, K., 2016. Description and validation of a “non-path-dependent” model for projecting contrasting urban growth futures. Cybergeo: European Journal of Geography.
109. Hu, X., Tao, C.V. and Hu, Y., 2004. Automatic road extraction from dense urban area by integrated processing of high resolution imagery and lidar data. International Archives of Photogrammetry, Remote Sensing and Spatial Information Sciences. Istanbul, Turkey, 35, p.B3.
110. Hu, Z., Lo, C., 2007. Modeling urban growth in Atlanta using logistic regression. Computers, Environment and Urban Systems, 31(6), 667-688.
111. Hui-Hui, F.E.N.G., Hui-Ping, L.I.U., Ying, L.Ü., 2012. Scenario prediction and analysis of urban growth using SLEUTH model. Pedosphere, 22(2), 206-216.

112. Huang, B., Xie, C., Tay, R., 2010. Support vector machines for urban growth modeling. Geoinformatica, 14(1), 83-99.
113. Hurtt, G.C., Frolking, S., Fearon, M.G., Moore, B., Shevliakova, E., Malyshev, S., Pacala, S.W., Houghton, R.A., 2006. The underpinnings of land-use history: Three centuries of global gridded land-use transitions, wood-harvest activity, and resulting secondary lands. Global Change Biology, 12(7), 1208-1229.
114. Hurtt, G.C., Chini, L.P., Frolking, S., Betts, R.A., Feddema, J., Fischer, G., Fisk, J.P., Hibbard, K., Houghton, R.A., Janetos, A., Jones, C.D., 2011. Harmonization of land-use scenarios for the period 1500–2100: 600 years of global gridded annual land-use transitions, wood harvest, and resulting secondary lands. Climatic change, 109(1-2), p.117.
115. Irwin, E. G., 2010. New directions for urban economic models of land use change: incorporating spatial dynamics and heterogeneity. Journal of Regional Science, 50(1), 65-91.
116. Jabareen, Y. R., 2006. Sustainable urban forms their typologies, models, and concepts. Journal of planning education and research, 26(1), 38-52.
117. Jaiswal, R. K., Saxena, R., Mukherjee, S., 1999. Application of remote sensing technology for land use/land cover change analysis. Journal of the Indian Society of Remote Sensing, 27(2), 123-128.
118. Jantz, C. A., Goetz, S. J., 2005. Analysis of scale dependencies in an urban land-use-change model. International Journal of Geographical Information Science, 19(2), 217-241.
119. Jantz, C.A., Goetz, S.J., Donato, D., Claggett, P., 2010. Designing and implementing a regional urban modeling system using the SLEUTH cellular urban model. Computers, Environment and Urban Systems, 34(1), 1-16.
120. Jantz, C., Drzyzga, S., Maret, M., 2014. Calibrating and Validating a Simulation Model to Identify Drivers of Urban Land Cover Change in the Baltimore, MD Metropolitan Region. Land, 3(3), 1158-1179. In this study, urban growth has been determined using SLEUTH model.
121. Jat, M.K., Choudhary, M., Saxena, A., 2017. Application of geo-spatial techniques and cellular automata for modelling urban growth of a heterogeneous urban fringe. The Egyptian Journal of Remote Sensing and Space Science, 20(2), 223-241.
122. Jat, M.K., Saxena, A., 2018. Sustainable Urban Growth using Geoinformatics and CA based Modelling. In Proceedings of the 11th International Conference on Theory and Practice of Electronic Governance (pp. 499-508). ACM.
123. Jat, M. K., Garg, P. K., Khare, D., 2008. Monitoring and modelling of urban sprawl using remote sensing and GIS techniques. International journal of Applied earth Observation and Geoinformation, 10(1), 26-43.
124. Jat, M. K., Garg, P. K., Khare, D., 2008. Modelling of urban growth using spatial analysis techniques: a case study of Ajmer city (India). International Journal of Remote Sensing, 29(2), 543-567.
125. Jha, C., Dutt, C., Bawa, K. S., 2000. Deforestation and land use changes in Western Ghats, India. CURRENT SCIENCE-BANGALORE-, 79(2), 231-237.

126. Irwin, E. G., Geoghegan, J., 2001. Theory, data and methods: developing spatially explicit economic models of land use change. Agriculture, Ecosystems & Environment, 85(1), 7-24.
127. Irwin, E.G., Bockstael, N.E., 2002. Interacting agents, spatial externalities and the evolution of residential land use patterns. Journal of economic geography, 2(1), 31-54.
128. Kanta Kumar, L. N., Sawant, N. G., Kumar, S., 2011. Forecasting urban growth based on GIS, RS and SLEUTH model in Pune metropolitan area. International journal of geomatics and geosciences, 2(2), 568.
129. Keshtkar, H., Voigt, W., 2016. A spatiotemporal analysis of landscape change using an integrated Markov chain and cellular automata models. Modeling Earth Systems and Environment, 2(1), 1-13.
130. Kim, D., Batty, M., 2011. Calibrating Cellular Automata Models for Simulating Urban Growth: Comparative Analysis of SLEUTH and Metronamica. Centre for Advanced Spatial Analysis, Paper, 176.
131. Knox, P. L., 1991. The restless urban landscape: economic and sociocultural change and the transformation of metropolitan Washington, DC. Annals of the Association of American Geographers, 81(2), 181-209.
132. Kok, K., 2001. Scaling the land use system: A modelling approach with case studies for Central America: Wageningen University, Wageningen.
133. Kumar, A., Pandey, A.C., Jeyaseelan, A.T., 2012. Built-up and vegetation extraction and density mapping using WorldView-II. Geocarto International, 27(7), 557-568.
134. Kumar, M., Shaikh, V.R. 2013. Site suitability analysis for urban development using GIS based multicriteria evaluation technique. Journal of the Indian Society of Remote Sensing, 41(2), pp.417-424.
135. Kuang, W., Liu, J., Shao, Q., He, J., Sun, C., Tian, H., Ban, Y., 2011. Dynamic urban growth model at regional scale and its application. Acta Geographica Sinica, 66(2), 178-188.
136. Lambin, E. F., Rounsevell, M., Geist, H., 2000. Are agricultural land-use models able to predict changes in land-use intensity? Agriculture, Ecosystems & Environment, 82(1), 321-331.
137. Lambin, E. F., Turner, B. L., Geist, H. J., Agbola, S. B., Angelsen, A., Bruce, J. W., Folke, C., 2001. The causes of land-use and land-cover change: moving beyond the myths. Global environmental change, 11(4), 261-269.
138. Lambin, E. F., Meyfroidt, P., 2011. Global land use change, economic globalization, and the looming land scarcity. Proceedings of the National Academy of Sciences, 108(9), 3465-3472.
139. Landis, J. D., 1994. The California Urban Futures Model: a new generation of metropolitan simulation models. Environment and planning B: planning and design, 21(4), 399-420.
140. Landis, J., Zhang, M., 1998. The second generation of the California urban futures model. Part 1: Model logic and theory. Environment and Planning B: Planning and Design, 25(5), 657-666.

141. Lang, T., 2012. How do cities and regions adapt to socio-economic crisis? Towards an institutionalist approach to urban and regional resilience. Raumforschung und Raumordnung, 70(4), 285-291.
142. Lewis, C.M., Lloyd-Sherlock, P., 2009. Social policy and economic development in South America: an historical approach to social insurance. Economy and Society, 38(1), 109-131.
143. Lewis, D.J., 2010. An economic framework for forecasting land-use and ecosystem change. Resource and Energy Economics, 32(2), 98-116.
144. Liao, J., Tang, L., Shao, G., Qiu, Q., Wang, C., Zheng, S., Su, X., 2014. A neighbor decay cellular automata approach for simulating urban expansion based on particle swarm intelligence. International Journal of Geographical Information Science, 28(4), 720-738.
145. Li, F., Wang, L., Chen, Z., Clarke, K.C., Li, M., Jiang, P. 2018. Extending the SLEUTH model to integrate habitat quality into urban growth simulation. Journal of environmental management, 217, pp.486-498.
146. Li, X., Yeh, A. G.O., 2002. Neural-network-based cellular automata for simulating multiple land use changes using GIS. International Journal of Geographical Information Science, 16(4), 323-343.
147. Li, X., Liu, X., 2006. An extended cellular automaton using case-based reasoning for simulating urban development in a large complex region. International Journal of Geographical Information Science, 20(10), 1109-1136.
148. Li, X., Liu, X., Yu, L., 2014. A systematic sensitivity analysis of constrained cellular automata model for urban growth simulation based on different transition rules. International Journal of Geographical Information Science, 28(7), 1317-1335.
149. Li, X., Liu, X., Gong, P., 2015. Integrating ensemble-urban cellular automata model with an uncertainty map to improve the performance of a single model. International Journal of Geographical Information Science, 29(5), 762-785.
150. Lin, J., Huang, B., Chen, M., Huang, Z., 2014. Modeling urban vertical growth using cellular automata—Guangzhou as a case study. Applied geography, 53, 172-186.
151. Liu, X., Li, X., Liu, L., He, J., Ai, B., 2008. A bottom-up approach to discover transition rules of cellular automata using ant intelligence. International Journal of Geographical Information Science, 22(11-12), 1247-1269.
152. López, E., Bocco, G., Mendoza, M., Duhau, E., 2001. Predicting land-cover and land-use change in the urban fringe: a case in Morelia city, Mexico. Landscape and Urban Planning, 55(4), 271-285.
153. Lu, Y., Kawamura, K., Zellner, M., 2008. Exploring the influence of urban form on work travel behavior with agent-based modeling. Transportation Research Record: Journal of the Transportation Research Board (2082), 132-140.
154. Lu, Y., Cao, M., Zhang, L., 2015. A vector-based Cellular Automata model for simulating urban land use change. Chinese Geographical Science, 25(1), 74-84.
155. Magarotto, M. G., da Costa, M. F., Tenedório, J. A., Silva, C. P., 2016. Vertical growth in a coastal city: an analysis of Boa Viagem (Recife, Brazil). Journal of Coastal Conservation, 20(1), 31-42.

156. Mahiny, A.S., Gholamalifard, M. 2011, June. Linking SLEUTH urban growth modeling to multi-criteria evaluation for a dynamic allocation of sites to landfill. In International Conference on Computational Science and Its Applications (pp. 32-43). Springer, Berlin, Heidelberg.
157. Mahiny, A. S., Clarke, K. C., 2012. Guiding SLEUTH land-use/land-cover change modeling using multicriteria evaluation: towards dynamic sustainable land-use planning. Environment and planning B: planning and design, 39(5), 925-944.
158. Mahiny, A.S. Clarke, K.C. 2013. Simulating Hydrologic Impacts of Urban Growth Using SLEUTH, Multi-Criteria Evaluation and Runoff Modeling. Journal of Environmental Informatics, 22(1).
159. Makse, H. A., Havlin, S., Stanley, H. E. 1995. Modelling urban growth patterns. Nature, 377(1912), 779-782.
160. Manca, G., Clarke, K. C., 2012. Waiting to Know the Future: A SLEUTH Model Forecast of Urban Growth with Real Data. Cartographica: The International Journal for Geographic Information and Geovisualization, 47(4), 250-258.
161. Mao, X., Meng, J., Xiang, Y., 2013. Cellular automata-based model for developing land use ecological security patterns in semi-arid areas: a case study of Ordos, Inner Mongolia, China. Environmental earth sciences, 70(1), 269-279.
162. Martellozzo, F., Clarke, K. C., 2011. Measuring urban sprawl, coalescence, and dispersal: a case study of Pordenone, Italy. Environment and Planning B: Planning and Design, 38(6), 1085-1104.
163. Mas, J. F., Pérez-Vega, A., Clarke, K. C., 2012. Assessing simulated land use/cover maps using similarity and fragmentation indices. Ecological Complexity, 11, 38-45.

164. Nolè, G., Murgante, B., Calamita, G., Lanorte, A., Lasaponara, R., 2015. Evaluation of Urban Sprawl from space using open source technologies. Ecological Informatics, 26, 151-161.
165. Matthews, R. B., Gilbert, N. G., Roach, A., Polhill, J. G., Gotts, N. M., 2007. Agent-based land-use models: a review of applications. Landscape Ecology, 22(10), 1447-1459.
166. Millington, J.D., Perry, G.L., Romero-Calcerrada, R., 2007. Regression techniques for examining land use/cover change: a case study of a Mediterranean landscape. Ecosystems, 10(4), 562-578.
167. Mills, E.S., 1970. Urban density functions. Urban Studies, 7(1), 5-20.
168. Morabito, M., Crisci, A., Messeri, A., Orlandini, S., Raschi, A., Maracchi, G., Munafò, M., 2016. The impact of built-up surfaces on land surface temperatures in Italian urban areas. Science of the Total Environment, 551, 317-326.
169. Mills, E.S., Tan, J.P., 1980. A comparison of urban population density functions in developed and developing countries. Urban studies, 17(3), 313-321.
170. Niazi, M., Hussain, A., 2011. Agent-based computing from multi-agent systems to agent-based models: a visual survey. Scientometrics, 89(2), p.479.
171. Nong, Y., Du, Q., 2011. Urban growth pattern modeling using logistic regression. Geo-spatial Information Science, 14(1), 62-67.

172. Nelson, G.C., Hellerstein, D., 1997. Do roads cause deforestation? Using satellite images in econometric analysis of land use. American Journal of Agricultural Economics, 79(1), 80-88.
173. Newburn, D.A., Berck, P., 2011. Growth management policies for exurban and suburban development: theory and an application to Sonoma County, California. Agricultural and Resource Economics Review, 40(3), 375-392.
174. Nouri, J., Gharagozlou, A., Arjmandi, R., Faryadi, S., Adl, M., 2014. Predicting urban land use changes using a CA–Markov model. Arabian Journal for Science and Engineering, 39(7), 5565-5573.
175. Onsted, J., Clarke, K. C., 2012. The inclusion of differentially assessed lands in urban growth model calibration: a comparison of two approaches using SLEUTH. International Journal of Geographical Information Science, 26(5), 881-898.
176. Otukei, J. R., Blaschke, T., 2010. Land cover change assessment using decision trees, support vector machines and maximum likelihood classification algorithms. International Journal of Applied Earth Observation and Geoinformation, 12, S27-S31.
177. Page, S. E., 2008. Agent-based models. The new Palgrave dictionary of economics, 47-51.
178. Palatnik, R.R., Roson, R., 2009. Climate change assessment and agriculture in general equilibrium models: Alternative modeling strategies.
179. Palme, M., Ramírez, J.G., 2013. A critical assessment and projection of urban vertical growth in Antofagasta, Chile. Sustainability, 5(7), 2840-2855.
180. Pan, X.Z., Zhao, Q.G., Chen, J., Liang, Y., Sun, B., 2008. Analyzing the variation of building density using high spatial resolution satellite images: the example of Shanghai City. Sensors, 8(4), 2541-2550.
181. Pandey, A. C., Kumar, A., Jeyaseelan, A. T., 2013. Urban built-up area assessment of Ranchi township using Cartosat-I stereopairs satellite images. Journal of the Indian Society of Remote Sensing, 41(1), 141-155.
182. Park, S., Wagner, D. F., 1997. Incorporating cellular automata simulators as analytical engines in GIS. Transactions in GIS, 2(3), 213-231.
183. Park, S., Jeon, S., Kim, S., Choi, C., 2011. Prediction and comparison of urban growth by land suitability index mapping using GIS and RS in South Korea. Landscape and urban planning, 99(2), 104-114.
184. Park, S., Jeon, S., Choi, C., 2012. Mapping urban growth probability in South Korea: comparison of frequency ratio, analytic hierarchy process, and logistic regression models and use of the environmental conservation value assessment. Landscape and ecological engineering, 8(1), 17-31.
185. Parker, D.C., Manson, S.M., Janssen, M.A., Hoffmann, M.J., Deadman, P., 2003. Multi-agent systems for the simulation of land-use and land-cover change: a review. Annals of the association of American Geographers, 93(2), 314-337.
186. Parker, D.C., Meretsky, V., 2004. Measuring pattern outcomes in an agent-based model of edge-effect externalities using spatial metrics. Agriculture, Ecosystems & Environment, 101(2-3), 233-250.

187. Pathiranage, I.S.S., Kantakumar, L.N., Sundaramoorthy, S., 2018. Remote Sensing Data and SLEUTH Urban Growth Model: As Decision Support Tools for Urban Planning. Chinese Geographical Science, 28(2), 274-286.
188. Perini, K., Magliocco, A., 2014. Effects of vegetation, urban density, building height, and atmospheric conditions on local temperatures and thermal comfort. Urban Forestry & Urban Greening, 13(3), 495-506.
189. Petit, C., Lambin, E., 2002. Impact of data integration technique on historical land-use/land-cover change: comparing historical maps with remote sensing data in the Belgian Ardennes. Landscape ecology, 17(2), 117-132.
190. Petrov, A. N., Sugumaran, R., 2005. Monitoring and modeling cropland loss in rapidly growing urban and depopulating rural counties using remotely sensed data and GIS. Geocarto International, 20(4), 45-52.
191. Pingale, S.M., Jat, M.K., Khare, D., 2014. Integrated urban water management modelling under climate change scenarios. Resources, Conservation and Recycling, 83, 176-189.
192. Prakash, A., Gupta, R., 1998. Land-use mapping and change detection in a coal mining area-a case study in the Jharia coalfield, India. International Journal of Remote Sensing, 19(3), 391-410.
193. Pontius, R. G., Cornell, J. D., Hall, C. A., 2001. Modeling the spatial pattern of land-use change with GEOMOD2: application and validation for Costa Rica. Agriculture, Ecosystems & Environment, 85(1), 191-203.
194. Pontius, R. G., Schneider, L. C., 2001. Land-cover change model validation by an ROC method for the Ipswich watershed, Massachusetts, USA. Agriculture, Ecosystems & Environment, 85(1), 239-248.
195. Pontius Jr, R. G., Boersma, W., Castella, J. C., Clarke, K., de Nijs, T., Dietzel, C., Koomen, E., 2008. Comparing the input, output, and validation maps for several models of land change. The Annals of Regional Science, 42(1), 11-37.
196. Portugali, J., Benenson, I., 1995. Artificial planning experience by means of a heuristic cell-space model: simulating international migration in the urban process. Environment and Planning A, 27(10), 1647-1665.
197. Price, A., Jones, E. C., Jefferson, F., 2015. Vertical Greenery Systems as a Strategy in Urban Heat Island Mitigation. Water, Air, & Soil Pollution, 226(8), 1-11.
198. Qiang, Y., Lam, N. S., 2015. Modeling land use and land cover changes in a vulnerable coastal region using artificial neural networks and cellular automata. Environmental monitoring and assessment, 187(3), 1-16.
199. Quartulli, M., Datcu, M., 2004. Stochastic geometrical modeling for built-up area understanding from a single SAR intensity image with meter resolution. IEEE Transactions on geoscience and remote sensing, 42(9), 1996-2003.
200. Qin, J., Fang, C., Wang, Y., Li, G., Wang, S., 2015. Evaluation of three-dimensional urban expansion: a case study of Yangzhou City, Jiangsu Province, China. Chinese Geographical Science, 25(2), 224-236.
201. Rafiee, R., Mahiny, A.S., Khorasani, N., Darvishsefat, A.A., Danekar, A., 2009. Simulating urban growth in Mashad City, Iran through the SLEUTH model (UGM). Cities, 26(1), 19-26.

202. Ray, D.K., Pijanowski, B.C., 2010. A backcast land use change model to generate past land use maps: application and validation at the Muskegon River watershed of Michigan, USA. Journal of Land Use Science, 5(1), 1-29.
203. Riccioli, F., El Asmar, T., El Asmar, J. P., Fratini, R., 2013. Use of cellular automata in the study of variables involved in land use changes. Environmental monitoring and assessment, 185(7), 5361-5374.
204. Rimal, B., 2011. APPLICATION OF REMOTE SENSING AND GIS, LAND USE/LAND COVER CHANGE IN KATHMANDU METROPOLITAN CITY, NEPAL. Journal of Theoretical & Applied Information Technology, 23(2).
205. Rimal, D. B., 2012. Spatiotemporal dynamics of land use pattern response to urbanization in Biratnagar Sub-Metropolitan City, Nepal. IRACST, Vol, 2.
206. Romano, G., Dal Sasso, P., Liuzzi, G.T., Gentile, F., 2015. Multi-criteria decision analysis for land suitability mapping in a rural area of Southern Italy. Land Use Policy, 48, pp.131-143.
207. Rottensteiner, F., Briese, C., 2002. A new method for building extraction in urban areas from high-resolution LIDAR data. International Archives of Photogrammetry Remote Sensing and Spatial Information Sciences, 34(3/A), 295-301.
208. Rottensteiner, F., Briese, C., 2003. Automatic generation of building models from LIDAR data and the integration of aerial images. na.
209. Ryavec, K., 2001. Land use/cover change in central Tibet, c. 1830–1990: devising a GIS methodology to study a historical Tibetan land decree. The Geographical journal, 167(4), 342-357.
210. Salvati, L., Zitti, M., Sateriano, A., 2013. Changes in city vertical profile as an indicator of sprawl: Evidence from a Mediterranean urban region. Habitat International, 38, 119-125.
211. Sankhala, S., Singh, B., 2014. Evaluation of urban sprawl and land use land cover change using remote sensing and GIS techniques: a case study of Jaipur City, India. International Journal of Emerging Technology and Advanced Engineering, 4(1), 66-72.
212. Sar, N., Chatterjee, S., Adhikari, M. D., 2015. Integrated remote sensing and GIS based spatial modelling through analytical hierarchy process (AHP) for water logging hazard, vulnerability and risk assessment in Keleghai river basin, India. Modeling Earth Systems and Environment, 1(4), 1-21.
213. Satty, T.L. 1986. Axiomatic foundation of the analytic hierarchy process. Management Science, 32(7), pp.841-855.
214. Svoray, T., Bar, P., Bannet, T., 2005. Urban land-use allocation in a Mediterranean ecotone: Habitat Heterogeneity Model incorporated in a GIS using a multi-criteria mechanism. Landscape and Urban Planning, 72(4), pp.337-351.
215. Saxena, A., Jat, M.K., 2018. Analyzing Performance of SLEUTH Model Calibration using Brute Force and Genetic Algorithm based Methods. Geocarto International, (just-accepted), 1-38.
216. Schelling, T. C., 1971. Dynamic models of segregation†. Journal of mathematical sociology, 1(2), 143-186.

217. Serra, P., Pons, X., Saurí, D., 2008. Land-cover and land-use change in a Mediterranean landscape: a spatial analysis of driving forces integrating biophysical and human factors. Applied Geography, 28(3), 189-209.
218. Serneels, S., Lambin, E. F., 2001. Proximate causes of land-use change in Narok District, Kenya: a spatial statistical model. Agriculture, Ecosystems & Environment, 85(1), 65-81.
219. Shen, J.-r., Chen, S., Yao, S.-m., 2001. Study on urban land saving in the economic developed coastal region of China. Chinese Geographical Science, 11(1), 11-16.
220. Silva, E. A., Clarke, K. C., 2002. Calibration of the SLEUTH urban growth model for Lisbon and Porto, Portugal. Computers, Environment and Urban Systems, 26(6), 525-552.
221. Silva, E.M.A., 2003. The CVCA model: A cellular automaton model of landscape ecological strategies.
222. Silva, E.A., Ahern, J., Wileden, J., 2008. Strategies for landscape ecology: An application using cellular automata models. Progress in Planning, 70(4), 133-177.
223. Silva, E. A., Clarke, K. C., 2005. Complexity, emergence and cellular urban models: lessons learned from applying SLEUTH to two Portuguese metropolitan areas. European Planning Studies, 13(1), 93-115.
224. Silva, E., Wu, N., 2012. Surveying models in urban land studies. Journal of Planning Literature, 27(2), 139-152.
225. Singh, A., 1989. Review article digital change detection techniques using remotely-sensed data. International Journal of Remote Sensing, 10(6), 989-1003.
226. Sohn, G., Dowman, I., 2007. Data fusion of high-resolution satellite imagery and LiDAR data for automatic building extraction. ISPRS Journal of Photogrammetry and Remote Sensing, 62(1), 43-63.
227. Solecki, W. D., Oliveri, C., 2004. Downscaling climate change scenarios in an urban land use change model. Journal of environmental management, 72(1), 105-115.
228. Srinivasan, V., Seto, K. C., Emerson, R., Gorelick, S. M., 2013. The impact of urbanization on water vulnerability: a coupled human–environment system approach for Chennai, India. Global Environmental Change, 23(1), 229-239.
229. Su, D. Z., 1998. GIS-based urban modelling: practices, problems, and prospects. International Journal of Geographical Information Science, 12(7), 651-671.
230. Su, D. Z., 1998. GIS-based urban modelling: practices, problems, and prospects. International Journal of Geographical Information Science, 12(7), 651-671.
231. Syphard, A. D., Clarke, K. C., Franklin, J., 2005. Using a cellular automaton model to forecast the effects of urban growth on habitat pattern in southern California. Ecological Complexity, 2(2), 185-203.
232. Syphard, A. D., Clarke, K. C., Franklin, J., 2007. Simulating fire frequency and urban growth in southern California coastal shrublands, USA. Landscape ecology, 22(3), 431-445.
233. Syphard, A. D., Clarke, K. C., Franklin, J., Regan, H. M., Mcginnis, M., 2011. Forecasts of habitat loss and fragmentation due to urban growth are sensitive to source of input data. Journal of Environmental Management, 92(7), 1882-1893.

234. Takeyama, M., Couclelis, H., 1997. Map dynamics: integrating cellular automata and GIS through Geo-Algebra. International Journal of Geographical Information Science, 11(1), 73-91.
235. Thapa, R. B., Murayama, Y., 2011. Urban growth modeling of Kathmandu metropolitan region, Nepal. Computers, Environment and Urban Systems, 35(1), 25-34.
236. Thapa, R. B., Murayama, Y., 2012. Scenario based urban growth allocation in Kathmandu Valley, Nepal. Landscape and Urban Planning, 105(1), 140-148.
237. Towe, C.A., Nickerson, C.J., Bockstael, N., 2008. An empirical examination of the timing of land conversions in the presence of farmland preservation programs. American Journal of Agricultural Economics, 90(3), 613-626.
238. Turner, M. G., O'Neill, R. V., Gardner, R. H., Milne, B. T., 1989. Effects of changing spatial scale on the analysis of landscape pattern. Landscape ecology, 3(3-4), 153-162.
239. Van der Werf, E., Peterson, S., 2009. Modeling linkages between climate policy and land use: an overview. Agricultural Economics, 40(5), 507-517.
240. Van Tongeren, F., Van Meijl, H., Surry, Y., 2001. Global models applied to agricultural and trade policies: a review and assessment. Agricultural economics, 26(2), 149-172.
241. Van Niel, K., Laffan, S.W., 2003. Gambling with randomness: the use of pseudo-random number generators in GIS. International Journal of Geographical Information Science, 17(1), 49-68.
242. van Vliet, J., Bregt, A. K., Brown, D. G., van Delden, H., Heckbert, S., Verburg, P. H., 2016. A review of current calibration and validation practices in land-change modeling. Environmental Modelling & Software, 82, 174-182.
243. Veldkamp, A., Lambin, E. F., 2001. Predicting land-use change. Agriculture, ecosystems & environment, 85(1), 1-6.
244. Verburg, P. H., Soepboer, W., Veldkamp, A., Limpiada, R., Espaldon, V., Mastura, S. S., 2002. Modeling the spatial dynamics of regional land use: the CLUE-S model. Environmental management, 30(3), 391-405.
245. Verburg, P. H., Schulp, C., Witte, N., Veldkamp, A., 2006. Downscaling of land use change scenarios to assess the dynamics of European landscapes. Agriculture, ecosystems & environment, 114(1), 39-56.
246. Voinov, A., Costanza, R., Wainger, L., Boumans, R., Villa, F., Maxwell, T., Voinov, H., 1999. Patuxent landscape model: integrated ecological economic modeling of a watershed. Environmental Modelling & Software, 14(5), 473-491.
247. Vu, T.T., Yamazaki, F., Matsuoka, M., 2009. Multi-scale solution for building extraction from LiDAR and image data. International Journal of Applied Earth Observation and Geoinformation, 11(4), 281-289.
248. Waddell, P., 2002. UrbanSim: Modeling urban development for land use, transportation, and environmental planning. Journal of the American Planning Association, 68(3), 297-314.
249. Wagner, D. F., 1997. Cellular automata and geographic information systems. Environment and planning B: Planning and design, 24(2), 219-234.

250. Wang, Y., Kockelman, K., Wang, X., 2011. Anticipation of land use change through use of geographically weighted regression models for discrete response. Transportation Research Record: Journal of the Transportation Research Board, (2245), 111-123.
251. Weber, C., Puissant, A., 2003. Urbanization pressure and modeling of urban growth: example of the Tunis Metropolitan Area. Remote sensing of environment, 86(3), 341-352.
252. Weng, Q., 2002. Land use change analysis in the Zhujiang Delta of China using satellite remote sensing, GIS and stochastic modelling. Journal of environmental management, 64(3), 273-284.
253. Weng, Q., Lu, D., Schubring, J., 2004. Estimation of land surface temperature–vegetation abundance relationship for urban heat island studies. Remote sensing of Environment, 89(4), 467-483.
254. Wegener, M., 1995. Current and future land use models. Paper presented at the Travel Model Improvement Program Land Use Model Conference, Dallas, Texas.
255. Weidner, U., Förstner, W., 1995. Towards automatic building extraction from high-resolution digital elevation models. ISPRS journal of Photogrammetry and Remote Sensing, 50(4), 38-49.
256. Wentz, E.A., York, A.M., Alberti, M., Conrow, L., Fischer, H., Inostroza, L., Jantz, C., Pickett, S.T., Seto, K.C., Taubenböck, H., 2018. Six fundamental aspects for conceptualizing multidimensional urban form: A spatial mapping perspective. Landscape and Urban Planning, 179, pp.55-62.
257. White, R. W., 1989. The artificial intelligence of urban dynamics: Neural network modeling of urban structure. In Papers of the Regional Science Association (Vol. 67, No. 1, pp. 43-53). Springer-Verlag.
258. White, R., Engelen, G., 1993. Cellular automata and fractal urban form: a cellular modelling approach to the evolution of urban land-use patterns. Environment and planning A, 25(8), 1175-1199.
259. Wilson, A. G., 1971. A family of spatial interaction models, and associated developments. Environment and Planning A, 3(1), 1-32.
260. Wolfram, S., 1984. Cellular automata as models of complexity. Nature, 311(5985), 419-424.
261. White, R., Engelen, G., Uljee, I., 1997. The use of constrained cellular automata for high-resolution modelling of urban land-use dynamics. Environment and Planning B: Planning and Design, 24(3), 323-343.
262. Wu, F., 1998. SimLand: a prototype to simulate land conversion through the integrated GIS and CA with AHP derived transition rules. International Journal of Geographical Information Science, 12(1), 63-82.
263. Wu, F., 1998. SimLand: a prototype to simulate land conversion through the integrated GIS and CA with AHP-derived transition rules. International Journal of Geographical Information Science, 12(1), 63-82.
264. Wu, X., Hu, Y., He, H. S., Bu, R., Onsted, J., Xi, F., 2009. Performance evaluation of the SLEUTH model in the Shenyang metropolitan area of northeastern China. Environmental modeling & assessment, 14(2), 221-230.

265. Waddell, P., 2000. A behavioral simulation model for metropolitan policy analysis and planning: residential location and housing market components of UrbanSim. Environment and planning B: planning and design, 27(2), 247-263.
266. Waddell, P., Borning, A., Noth, M., Freier, N., Becke, M., Ulfarsson, G., 2003. Microsimulation of urban development and location choices: Design and implementation of UrbanSim. Networks and spatial economics, 3(1), 43-67.
267. Wang, Q., Zhang, P.Z., Freymueller, J.T., Bilham, R., Larson, K.M., Lai, X.A., You, X., Niu, Z., Wu, J., Li, Y., Liu, J., 2001. Present-day crustal deformation in China constrained by global positioning system measurements. science, 294(5542), 574-577.
268. White, R., Engelen, G., 2000. High-resolution integrated modelling of the spatial dynamics of urban and regional systems. Computers, environment and urban systems, 24(5), 383-400.
269. Wilson, E. H., Hurd, J. D., Civco, D. L., Prisloe, M. P., Arnold, C., 2003. Development of a geospatial model to quantify, describe and map urban growth. Remote Sensing of Environment, 86(3), 275-285.
270. Wolfram, S., 1986. Theory and applications of cellular automata: including selected papers 1983-1986. World scientific.
271. Wrenn, D., Irwin, E., 2012. Time is money: An empirical examination of the dynamic effects of regulatory uncertainty on residential subdivision development. Job Market Paper, The Ohio State University, http://deepblue. lib. umich. edu/bitstream/handle/2027.42/69247/WestbrookThesis2010.
272. Wu, F., Webster, C.J., 1998. Simulation of land development through the integration of cellular automata and multicriteria evaluation. Environment and Planning B: Planning and design, 25(1), 103-126.
273. Wu, J., Hobbs, R., 2002. Key issues and research priorities in landscape ecology: an idiosyncratic synthesis. Landscape ecology, 17(4), 355-365.
274. Wu, F., 2002. Calibration of stochastic cellular automata: the application to rural-urban land conversions. International Journal of Geographical Information Science, 16(8), 795-818.
275. Wu, X., Hu, Y., He, H.S., Bu, R., Onsted, J., Xi, F., 2009. Performance evaluation of the SLEUTH model in the Shenyang metropolitan area of northeastern China. Environmental modeling & assessment, 14(2), 221-230.
276. Wu, H., Zhou, L., Chi, X., Li, Y., Sun, Y., 2012. Quantifying and analyzing neighborhood configuration characteristics to cellular automata for land use simulation considering data source error. Earth Science Informatics, 5(2), 77-86.
277. Xian, G., Crane, M., 2005. Assessments of urban growth in the Tampa Bay watershed using remote sensing data. Remote Sensing of Environment, 97(2), 203-215.
278. Xiang, W. N., Clarke, K. C., 2003. The use of scenarios in land-use planning. Environment and planning B: planning and design, 30(6), 885-909.
279. Xinchang, Z., Qiong, P., Yuan, Z., 2004. Research on spatial calculating analysis model of landuse change. Journal of Geographical Sciences, 14(3), 359-365.
280. Xu, H., 2007. Extraction of urban built-up land features from Landsat imagery using a thematic oriented index combination technique. Photogrammetric Engineering & Remote Sensing, 73(12), 1381-1391.

281. Xu, H., 2008. A new index for delineating built-up land features in satellite imagery. International Journal of Remote Sensing, 29(14), 4269-4276.
282. Xu, L., Li, Z., Song, H., Yin, H., 2013. Land-use planning for urban sprawl based on the clue-s model: A Case study of Guangzhou, China. Entropy, 15(9), 3490-3506.
283. Yagoub, M. M., Al Bizreh, A. A., 2014. Prediction of land cover change using Markov and cellular automata models: case of Al-Ain, UAE, 1992-2030. Journal of the Indian Society of Remote Sensing, 42(3), 665-671.
284. Yin, H., Kong, F., Hu, Y., James, P., Xu, F., Yu, L., 2015. Assessing growth scenarios for their landscape ecological security impact using the SLEUTH urban growth model. Journal of Urban Planning and Development, 142(2), p.05015006.
285. Youssef, A.M., Pradhan, B., Tarabees, E., 2011. Integrated evaluation of urban development suitability based on remote sensing and GIS techniques: contribution from the analytic hierarchy process. Arabian Journal of Geosciences, 4(3-4), pp.463-473.
286. Yu, B., Liu, H., Wu, J., Hu, Y., Zhang, L., 2010. Automated derivation of urban building density information using airborne LiDAR data and object-based method. Landscape and Urban Planning, 98(3-4), 210-219.
287. Zeng, C., Liu, Y., Stein, A., Jiao, L., 2015. Characterization and spatial modeling of urban sprawl in the Wuhan Metropolitan Area, China. International journal of Applied earth Observation and Geoinformation, 34, 10-24.
288. Zha, Y., Gao, J., Ni, S., 2003. Use of normalized difference built-up index in automatically mapping urban areas from TM imagery. International journal of remote sensing, 24(3), 583-594.
289. Zhang, Q., Wang, J., Peng, X., Gong, P., Shi, P., 2002. Urban built-up land change detection with road density and spectral information from multi-temporal Landsat TM data. International Journal of Remote Sensing, 23(15), 3057-3078.

ANNEXURE - I

S.no.	Model's Name	Model's structure	Driving Factors	Relation with Urban Growth	In what way the driving forces have been included in the method	The relative contribution of driving factors
1	CLUE (Verburg et al., 2006; Xu et al., 2013)	Dynamic, Spatially explicit model	Socio-economic, Bio-physical drivers	The relation between land use and its driving factors are evaluated using step-wise logistic regression.	In the form of independent variables in a logistic regression equation, it has been included.	Relative influence of driving factors on land use change is determined thereafter probability of land use change in probabilistic terms has determined.
2	CURBA (Landis et al., 1998)	A detailed Spatially explicit model	Demographic factors, topographic factors, socio-economic factors site-specific factors, distance to road factors	The relation between land use and drivers has been analyzed by developing logit models under statistical packages.	Construction and development of various logit models are done under statistical packages like SPSS or SAS.	By including driving forces various landscape metrics are calculated which thereafter use to predict future urban growth.
3	LUCAS (Berry et al., 1994, 1996;Irwin et al., 2001)	A spatially explicit stochastic model	Ecological, Socio-economic factors, Demographic, Topographic factors	The relation between drivers and land use change in the form of transition probabilities are determined.	The transition probabilities were determined using multinomial logit models.	This research has not provided prediction results yet, like how much change is likely to occur in near future. Also, it can be well implemented for urban growth only by including some driving forces and also by applying some

S.no.	Model's Name	Model's structure	Driving Factors	Relation with Urban Growth	In what way the driving forces have been included in the method	The relative contribution of driving factors
						restrictions like development away from the drainage area would be preferred etc. The LUCAS model can include both type of transition pixel based (grid-based) and cluster (patch based transition). The study has been made for pixel-based transition only. However, the patch-based transition is more difficult because of the task of patch identification.
4	DINAMICA (Wang and Zhang, 2001; Mas et al., 2012)	Spatially explicit model	Socio-economic factors, Infrastructure factors	The relationship between driving factors and land use change is analyzed by overlaying the driving factors maps over the land use maps.	The driving factors have been included in the form of weighted evidence. Thereafter Bayesian empirical methods are adopted to find the land use change probability.	In this model implementation, the main focus has been given to compute transition probabilities by assigning weights to the variables. Also, this study can give stochastic as well as deterministic results by integrating CA with SPRING GIS.

S.no.	Model's Name	Model's structure	Driving Factors	Relation with Urban Growth	In what way the driving forces have been included in the method	The relative contribution of driving factors
5	UrbanSim (Waddell, 2000, 2002; Waddell et al., 2003; Duthie et al., 2007; Hepinstall et al., 2008; Wang et al., 2011)	Spatially explicit model	Economic factors, Demographic factors, Employment factors, Household mobility, Location choice factors	The relationship between driving forces and land use change is analyzed in the form of probabilistic terms.	In the form of independent variables, the driving forces have been included.	Adopts an equilibrium formulation in which the market price is endogenous and determined by the highest bid for each site among all consumers. The multinomial logit model is used to predict the probability.
6	SimLand (Wu, 1998;)	The spatially explicit transition model	Socio-economic factors, Topographic factors	The relationship between land use and driving factors are determined using variables in multinomial logit models that determine the suitability of land use change.	In the form of transition rules of land use change, it has been included.	AHP the method of MCE is used to include behavioral decision making that transition rules can be implied in a more realistic way. The limitation of a CA-based model; Since the form and function are linked through a nonlinear, dynamic process, it is still not clear to what extent the two correspond with each other. Sensitivity is also an issue which is worth exploring. Statistical

S.no.	Model's Name	Model's structure	Driving Factors	Relation with Urban Growth	In what way the driving forces have been included in the method	The relative contribution of driving factors
						methods can be introduced as a method for defining transition rules, which calibrates the simulation on the basis of past development paths. All these issues need to be addressed in future applications of CA to spatial analysis.
7	DUEM (Batty et al., 1998; Kuang et al., 2011)	CA-based dynamically spatially explicit	Distance, population density, direction and mutation probabilities	The drivers have been included in the form of CA-based transition rules.	In the form of transition probabilities.	The transition rules help in simulation the urban growth.
8	FASOM (Alig et al., 1997)	Dynamic optimization model	Economic factors	Optimization techniques have been used.	Nonlinear mathematical programming methods that maximize the problem functions.	This perfect Knowledge and assumptions regarding economics allow optimal selection of resource management actions.
9	GEM (Fitz et al., 1996)	The explicit spatial simulation model	Biological, physical and/or biotic and abiotic factors.	Rule-based transition algorithms are used to simulate the changes	The GEM requires a large number (~ 100) of parameters that may change with ecosystem	The range of scales and ecosystems for which the model is suitable depends upon the questions being addressed, but this version

S.no.	Model's Name	Model's structure	Driving Factors	Relation with Urban Growth	In what way the driving forces have been included in the method	The relative contribution of driving factors
					(habitat) type, and ongoing sensitivity analyses indicate which parameters are most important to quantify for application to particular systems.	is being applied to wetland and upland terrestrial sites to evaluate basic system dynamics.
10	PLM (Vinov et al., 1999)	Spatially explicit	Ecological, economic factors	The economic model allows human decisions in the form of economic and ecological functional variables.	These are based on empirically estimated parameters and spatially heterogeneous probabilities of land use change.	Based on empirically estimated parameters, spatially heterogeneous probabilities of land conversion are modeled as functions of predicted land values
11	PRISM (Alberti and Waddell, 2000)	Process-based and Spatially explicit dynamic model	Demographic, economic, environmental and policy scenarios	In the form of economic models thereafter the output of this is taken as input to find out the land use transition probabilities.	Produced land use maps were used to analyze the impact of land use change on habitat species etc.	The proposed models aim to improve the existing urban models also improves the ability to represent biophysical factors into the model.

S.no.	Model's Name	Model's structure	Driving Factors	Relation with Urban Growth	In what way the driving forces have been included in the method	The relative contribution of driving factors
12	CUF (Landis and Zhang, 1998; Silva and Wu, 2012)	Multinomial logit model	Site characteristics, site accessibility, community characteristics, policy factors, relationship to neighboring sites	These contributing factors to urban growth determine the real pattern of urban dynamics.	In the form of multinomial logit variables.	The model efficiently replicates the urban dynamics and helpful in predicting future landscape patterns. Binomial logit model later extended to the multinomial logit model which improves the efficiency of the CUF model. However, a multinomial logit model is very complex as each variable includes multiple coefficients and difficult to interpret the outputs of the model.
13	CVCA (Sliva, 2003; Silva et al., 2008)	The spatially explicit transition model	Nearest neighboring conditions and the CVCA model requires the same input files as the SLEUTH model requires such as slope, land use, urban, transportation,	It uses a set of landscape ecological strategies to counteract the urban growth at good to grow areas.	Cellular automata based transition rules are applied	The outputs of CVCA are the same as in SLEUTH model but four more output classes are generated in CVCA such as protective, offensive, defensive, opportunistic and let it grow that matches five landscape planning strategies.

S.no.	Model's Name	Model's structure	Driving Factors	Relation with Urban Growth	In what way the driving forces have been included in the method	The relative contribution of driving factors
			and hillshade and excluded map.			
14	LOV (White, R. and Engelen, G., 2000)	CA-based Dynamic, spatially explicit model	Demographic, economic	The model generates regional demands for population and a number of economic activities. These demands are translated into demands for cell space, which the CA then attempts to locate.	Cellular automata based transition rules are applied	Helps in designing Planning Support System (PSS)
15	LUCITA (Deadman et al., 2004)	Agent-Based Model, spatially explicit	Social interaction, decision making, and environmental factors	Driving factors are used in the form of regression variables.	Heuristic decision making	The urban heterogeneity effects have been monitored by including ecological effects such as soil and burn qualities into this model which shows the realism of the simulation of urban growth.

S.no.	Model's Name	Model's structure	Driving Factors	Relation with Urban Growth	In what way the driving forces have been included in the method	The relative contribution of driving factors
16	LUCIM (Matthews et al., 2007)	Agent-Based Model, spatially explicit	Transportation variables, Social interaction, decision making, and environmental factors	Driving factors are used in the form of regression variables.	Heuristic decision making	The urban heterogeneity effects have been monitored by including ecological effects such as soil and burn qualities into this model which shows the realism of the simulation of urban growth.
17	LUSD (He et al., 2005, 2016)	Integration of CA and system dynamics, spatially explicit	Interaction of Capital, population, socio-economic factors.	Driving factors are used in the form of regression variables.	Regression method is used for the prediction of urban growth as it is simpler and requires fewer variables. Allocation module of LUSD model uses CA-based neighboring transitions rules.	Regression method is used for the prediction of urban growth as it is simpler and requires fewer variables. And gives the better utilization of driving factors for urban growth modelling and prediction.
18	GEOMOD2 (Pontius et al., 2001;)	Empirical-based	biogeophysical factors	GEOMOD2 uses digital raster maps of biogeophysical attributes, as well as digital maps of existing land-use, to extrapolate the	To incorporate this rule into the model, GEOMOD2 creates a "suitability" map empirically, by using several attribute maps and	GEOMOD2 creates the suitability map by computing for each grid cell a weighted sum of all the reclassified attribute maps.

S.no.	Model's Name	Model's structure	Driving Factors	Relation with Urban Growth	In what way the driving forces have been included in the method	The relative contribution of driving factors
				known pattern of land-use from one point in time to other points in time.	one land-use map. The suitability map has high values at locations that have biogeophysical attributes similar to those of disturbed land and has low values at locations that have biogeophysical attributes similar to those of undisturbed closed-cover forest.	
19	SLEUTH (Clarke et al., 1997; Clarke and Gaydos, 1998; Jeannette, 2000; Silva and Clarke, 2002; Xiang and Clarke, 2003; Dietzel and Clarke, 2004; Solecki et al., 2004; Jantz et al., 2005; Xian and Crane, 2005; Silva and Clarke, 2005; Dietzel et al., 2005; Goldstein et al., 2005;	Cellular automata model	The extent of urban areas, Elevation, Slope Roads	SLEUTH is a cellular automaton (CA) model that predicts the spatial extent of urban expansion based on repeated application of growth rules and weighted probabilities that encourage or inhibit growth.	In the form of growth rules applied on a cellular basis.	Each cell acts independently, but according to rules that take spatial properties of neighboring locations into account.

S.no.	Model's Name	Model's structure	Driving Factors	Relation with Urban Growth	In what way the driving forces have been included in the method	The relative contribution of driving factors
	Caglioni et al., 2006; Dietzel and Clarke, 2006; Gazulis and Clarke, 2006; Clarke et al., 2007; Dietzel and Clarke, 2007; Hu and Lo, 2007; Clarke, 2008; Guan, 2008; Silva et al., 2008; Wu et al., 2009; Guana and Clarke, 2010; Nong and Du, 2011; KantaKumar et al., 2011; Kim and Batty, 2011; Martellozzo and Clarke, 2011; Syphard et al., 2011; Mahiny and Clarke, 2012; Manca and Clarke, 2012; Onsted and Clarke, 2012; Wu et al., 2012; Chaudhuri and Clarke, 2013; Al-shalabi et al., 2013; Akın et al., 2014; Clarke, 2014; Chaudhuri and Clarke, 2014; Jantz et al., 2014;					

S.no.	Model's Name	Model's structure	Driving Factors	Relation with Urban Growth	In what way the driving forces have been included in the method	The relative contribution of driving factors
	Han et al., 2015; Houet et al., 2016)					

ANNEXURE-II

S. no.	Location	Research Group/ Affiliation	Application	Reference
1	Albuquerque, NM	USGS/GD/RMMC	Urban Change	Hester 1999; Hester and Feller 2002
2	Alexandria, Egypt	Newcastle University	Urban Change	Azaz 2004
3	Atlanta, GA	Florida State University, Tallahassee, Department of	Urban Change	Yang and Lo 2003; Yang 2004
4	Austin,TX	USGS/GD/RMMC*	Urban and land use change	USGS/RMMC 2004
5	Chester County, PA	Penn State Meteorology and Atmospheric Science	Coupled modelling	Arthur et al. 200; Arthur 2001
6	Chicago, IL	USGS Urban Dynamics	Urban Change	Xian et al. 2000
7	Colorado Front range	USGS/GD/RMMC*	Urban and land use change	USGS/ RMMC 2004
8	Detroit, MI	USGS Eros Data Center	Urban Change	Richards 2003
9	Houston, TX	Texas A&M University	Urban Change	Oguz et al. 2004
10	Lisbon, Portugal	University of Massachusetts	Urban Change	Silva 2001; Silvaa and Clarke 2002
11	Mexico City, Mexico	Paola Gomez, UCSB Bren School	Urban Change	UCIME 2001
12	Modeling Monterey Bay, California	UC Santa Cruz Environmental Studies	Biodiversity loss/ model integration	Cogan et al. 2001
13	Netherlands	Beriage Institute	Urban Change	Tack 2000
14	New York, NY	Montclair state university	New York Climate and Health Project	Olveri 2003; Soleckl and Ollveri 2004
15	New York City, NY	USGS/GD/RMMC*	Urban Change	USGS/RMMC 2004
16	Oahu, HI	University of Hawaii at Manoa	Urban Change	James 2004

17	Phoenix, AZ	Arizona State University, school of Life Sciences	Urban Change	Brelling-wolf and Wu 2004
18	Porto, Portugal	University of Massachusetts, University of Santa Barbara	Urban Change	Silva 2001; Silva and Clarke 2002
19	Porto Alegre, Brazil	The University of Melbourne Department of Geomatics	Coupled clustering	Leao et al 2001, 2004
20	San Antonio, TX	USGS/GD/RMMC*	Urban and land sue change	USGS/RMMC, 2004
21	San Francisco, CA	UCSB Geography/ USGS Urban Dynamics	Urban Change	Clarke et al. 1997
22	San Joaquin Valley, CA	UCSB Geography	Urban Change/ Calibration testing	Dietz and Clarke 2004 a; Dietzal et al. In press
23	Santa Barbara, CA	UCSB Geography	Urban Change/ coupled modelling	Canadau and Clarke 2000; Goldstein et al. 2000,2004: Herold et al. 2002, 2003
24	Santa Monica Mountains, CA	San Diego State University	Vegetation successin	Syphard et al, in press
25	Seattle, WA	USGS/GD/RMMC*	Urban Change	USGS/RMMC 2004
26	Sioux Falls, SD	UCSB Geography	Development of GA	Goldstein 2004a
27	Sydney, Australia	The University of Southern Qeensland	Urban Change	Liu and Phinn 2004
28	Tampa/S. Florida	USGS/GD/RMMC*	Urban Change	USGS/RMMC 2004
29	Tijuana, Mexico	University Paul Valery	Urban Change	Le Page 2000
30	Washington, DC/Baltimor e	University of Maryland, college Park, Department of Geography	Urban Change	Jantz et al. 2003
31	Washington/ Baltimore	USGS/GD/RMMC*/ UCSB Geography	Urban Change/	Acevedo 1997; Clarke et al. 1997

			Change Visualization	
32	Yaounde, Cameroon	University of Melbourne, School of Anthrology	Urban Change	Stechiping 2004
33	Santa Barbara	University of California, Santa Barbara, Santa Barbara	Urban Change	Gazulis, N. et al 2006
34	San Joaquin County (CA)	University of California—Santa Barbara	Land use and urban change	Dietzel, C., & Clarke, K. (2006)
35	Palermo, Italy	piazza Leonardo da Vinci	Urban Change	Caglioni, M. et al 2006
36	Demo City	University of California – Santa Barbara	Land use change and urban change	Dietzel, C., & Clarke, K. C. 2007
37	Santa Barbara	University of California, Santa Barbara	Land use change and urban change	Guan, Q. G. (2008)
38	Demo City	University of California, Santa Barbara	Land use change and urban change	Clarke, K. C. (2008)
39	Santa Barbara	University of Nebraska-Lincoln, University of California, Santa Barbara	Land use change and urban change	Guan, Q., & Clarke, K. C. (2010)
40	Pune City, India	Institute of Environment Education and Research, Bharati Vidyapeeth University	Urban change	KantaKumar, L. N. et al (2011)
41	Italy	McGill University,	Urban change	Martellozzo, F., & Clarke, K. C. (2011)
42	Gorgan Township	Gorgan University of Agricultural Sciences and Natural Resources, Beheshti Avenue; UC Santa Barbara ,	Land use change	Mahiny, A. S., & Clarke, K. C. (2012)

43	United States	Florida International University , Miami; UC Santa Barbara ,	Urban Change	Onsted, J., & Clarke, K. C. (2012)
44	Sardinia	George Mason University; University of California, Santa Barbara	Urban Change	Manca, G., & Clarke, K. C. (2012)
45	Unite States and other nations	University of Wisconsin-La Crosse; University of California Santa Barbara	Land use change and urban change: a review	Chaudhuri, G., & Clarke, K. (2013)
46	Gorizia-Nova Gorica	University of Wisconsin-La Crosse; University of California Santa Barbara	Urban Change	Chaudhuri, G., & Clarke, K. C. (2014)
47	Adana, Turkey	Bursa Technical University, University of California, Cukurova University,	Urban Change	Akın, A. et al (2014)
48	Toulouse	Université Toulouse le Mirail; Université de Strasbourg; Ecole Spéciale des Travaux Publics; Toulouse Tech Transfer, Maison de la Recherche et de la Valorisation; University of California, Santa Barbara	Land use change and urban change	Houet, T. et al (2016)

LIST OF PUBLICATIONS

International Journals

1. **Saxena, A.** and Jat, M. K., 2018. Analysing Performance of SLEUTH Model Calibration using Brute Force and Genetic Algorithm based Methods. *Geocarto International*, (just-accepted), pp.1-38. (SCI Indexed)

2. **Saxena, A.** and Jat, M. K., 2018. An Integrated Approach for Natural Resources Monitoring Using Geo-Informatics and CA. *Journal of Rural Development*, *37*(2), pp.341-354. (Scopus Indexed)

3. **Saxena, A**. Pradhan, B. and Anurag, 2018. Land Use/Land Cover Change Modelling: Issues and Challenges. *Journal of Rural Development*, *37*(2), pp.413-424. (Scopus Indexed)

4. Jat, M. K., Choudhary, M. and **Saxena, A.,** 2017. Application of geo-spatial techniques and cellular automata for modelling urban growth of a heterogeneous urban fringe. *The Egyptian Journal of Remote Sensing and Space Science*, *20*(2), pp.223-241. (SCI Indexed)

5. **Saxena, A.,** Jat, M. K., & Choudhary, M.., 2016. Analysis of Urban Growth using Geospatial Techniques. *International Journal of Earth Sciences and Engineering*, *09*(06), 2855-2861. (Scopus Indexed)

6. **Saxena**, A. and Jat, M.K., 2018. Capturing Heterogeneous Urban Growth using SLEUTH Model. *Remote Sensing Applications: Society and Environment*, vol 13, 426-434.

International Conferences

1. **Saxena, A**. and Jat, M. K., 2017, March. Integration of geo-spatial technologies and CA for urban growth assessment and prediction. In *Urban Remote Sensing Event (JURSE), 2017 Joint* (pp. 1-4). IEEE.

2. Jat, M. K. and **Saxena, A.,** 2018, April. Sustainable Urban Growth using Geoinformatics and CA based Modelling. In *Proceedings of the 11th International Conference on Theory and Practice of Electronic Governance* (pp. 499-508). ACM.